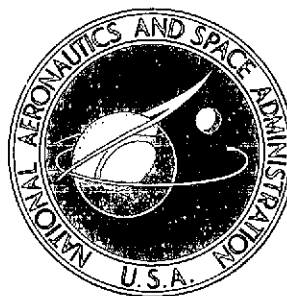


NASA TECHNICAL NOTE



NASA TN D-7752

NASA TN D-7752

CACI FILE
COPY

PROGRAM AND CHARTS FOR DETERMINING
SHOCK TUBE, EXPANSION TUBE, AND
EXPANSION TUNNEL FLOW QUANTITIES
FOR REAL AIR

by Charles G. Miller III and Sue E. Wilder

Langley Research Center

Hampton, Va. 23665

NATIONAL AERONAUTICS AND SPACE ADMINISTRATION • WASHINGTON, D. C. • FEBRUARY 1975

1. Report No. NASA TN D-7752		2. Government Accession No.		3. Recipient's Catalog No.	
4. Title and Subtitle PROGRAM AND CHARTS FOR DETERMINING SHOCK TUBE, EXPANSION TUBE, AND EXPANSION TUNNEL FLOW QUANTITIES FOR REAL AIR				5. Report Date February 1975	
				6. Performing Organization Code	
7. Author(s) Charles G. Miller III and Sue E. Wilder				8. Performing Organization Report No. L-9700	
				10. Work Unit No. 502-27-02-01	
9. Performing Organization Name and Address NASA Langley Research Center Hampton, Va. 23665				11. Contract or Grant No.	
				13. Type of Report and Period Covered Technical Note	
12. Sponsoring Agency Name and Address National Aeronautics and Space Administration Washington, D.C. 20546				14. Sponsoring Agency Code	
15. Supplementary Notes					
16. Abstract A computer program written in FORTRAN IV language is presented which determines shock tube, expansion tube, and expansion tunnel flow quantities for real-air test gas. This program permits, as input data, a number of possible combinations of flow quantities generally measured during a test. The versatility of the program is enhanced by the inclusion of such effects as a standing or totally reflected shock at the secondary diaphragm, thermochemical-equilibrium flow expansion and frozen flow expansion for the expansion tube and expansion tunnel, attenuation of the flow in traversing the acceleration section of the expansion tube, real air as the acceleration gas, and the effect of wall boundary layer on the acceleration section air flow. Charts which provide a rapid estimation of expansion tube performance prior to a test are included.					
17. Key Words (Suggested by Author(s)) Shock tube Expansion tube Expansion tunnel Unsteady expansion Real air				18. Distribution Statement Unclassified -- Unlimited STAR Category 12	
19. Security Classif. (of this report) Unclassified	20. Security Classif. (of this page) Unclassified	21. No. of Pages 278	22. Price* \$8.75		

PROGRAM AND CHARTS FOR DETERMINING SHOCK TUBE,
EXPANSION TUBE, AND EXPANSION TUNNEL
FLOW QUANTITIES FOR REAL AIR

By Charles G. Miller III and Sue E. Wilder
Langley Research Center

SUMMARY

A computer program written in FORTRAN IV language is presented which determines shock tube, expansion tube, and expansion tunnel flow quantities for real-air test gas. For the shock tube phase of the program, flow conditions behind the incident shock into the quiescent test gas are determined from the pressure and temperature of the quiescent test gas in conjunction with (1) incident-shock velocity, (2) static pressure immediately behind the incident shock, or (3) pressure and temperature of the driver gas (imperfect hydrogen or helium). The effect of shock reflection at the secondary diaphragm of the expansion tube, resulting in a standing or a totally reflected shock, is included. Expansion tube test-section flow conditions are obtained by performing an isentropic unsteady expansion from conditions behind the incident shock, standing shock, or totally reflected shock to either the test region velocity or static pressure. Expansion tunnel test-section flow conditions are obtained by performing an isentropic steady expansion from expansion tube free-stream conditions to either the nozzle test region velocity or static pressure. Both a thermochemical-equilibrium expansion and a frozen expansion for the expansion tube and expansion tunnel are included. The effect of flow attenuation along the acceleration section of the expansion tube is included for an equilibrium expansion. Flow conditions immediately behind the bow shock of a model positioned at the test section of a shock tube, expansion tube, or expansion tunnel are determined. A listing of the computer program is presented along with a description of inputs required and samples of the data printout. Charts which provide a rapid estimation of expansion tube performance prior to a test are included.

INTRODUCTION

Experimental studies using air as the test gas have been initiated in the Langley 6-inch expansion tube, and a number of studies are expected to be performed in the Langley expansion tunnel. Prior to performing studies in these facilities, it is essential for the investigator to ascertain the theoretical performance of the facility because of the

wide range of flow conditions which may be generated and the very short test times (less than 300 μ sec or so) which place stringent requirements on facility instrumentation. Thus, a knowledge of the magnitude of physical quantities to be measured is required. After a test, a convenient means for determining expansion tube and expansion tunnel flow conditions from measured quantities is desirable. Although a number of theoretical studies have been directed toward prediction of expansion tube and expansion tunnel performance with air as the test gas (for example, refs. 1 to 4), these studies were primarily concerned with simulation or duplication of conditions experienced by high-velocity, earth-entry vehicles.

The primary purposes of the present study are (1) to furnish a convenient, versatile, accurate computer program for determining shock tube, expansion tube, and expansion tunnel flow quantities in real air from combinations of measured flow quantities and (2) to provide charts for rapid estimation of facility performance prior to a test. This program is similar to the real-gas mixture study of reference 5; however, a number of differences exist between these two programs. The present program requires much less computer time, with no appreciable sacrifice in accuracy, than the program of reference 5. Such a reduction in computer time is a significant factor in data reduction, since most of the testing in the Langley 6-inch expansion tube is performed with air as the test gas.

Operating experience with the Langley 6-inch expansion tube and operation of this expansion tube as a shock tube demonstrated the desirability for options other than those presented in reference 5. Results included herein, but not in reference 5, are (1) charts illustrating predicted shock tube performance with hydrogen and helium driver gases for a range of driver gas pressure and temperature, (2) a totally reflected shock, as well as a standing shock, at the secondary diaphragm, (3) real air as the acceleration gas, (4) the effect of wall boundary layer on shock tube and acceleration section air flow for laminar (ref. 6) and/or turbulent (ref. 7) boundary layers, (5) the effect of flow attenuation along the acceleration section, (6) imperfect (intermolecular) air effects permitting calculations at higher pressures than permissible with reference 5, (7) determination of expansion tunnel test-section flow conditions from measured nozzle free-stream velocity or static pressure, and (8) charts which provide a convenient means for properly preparing facility instrumentation and determining the level of quiescent test gas and acceleration gas pressures for a test.

The procedures for determining shock tube, expansion tube, and expansion tunnel flow quantities for real air are incorporated into a single computer program written in FORTRAN IV language. Required program inputs are listed and described in appendix A. A flow chart and a listing of the program are also presented in appendix A along with sample data printouts.

SYMBOLS

The International System of Units (SI) is used for all physical quantities in the present study. Conversion factors relating SI Units to U.S. Customary Units are given in reference 8.

A	cross-sectional area, m^2
a	speed of sound, m/sec
d	shock tube or expansion tube inside diameter, m
h	specific enthalpy, m^2/sec^2 (J/kg)
L_a	length of acceleration section, m
L_s	distance measured downstream from secondary diaphragm, m
ℓ	distance between incident shock in region ① and test-air—driver-gas interface, m (see fig. 1)
M	Mach number, U/a
M_s	incident shock Mach number, U_s/a
N_{Re}	unit Reynolds number, $\rho U/\mu$, m^{-1}
p	pressure, N/m^2
\dot{q}	stagnation point convective heat-transfer rate, W/m^2
R	universal gas constant, 8.31434 $kJ/kmol-K$
r	radius, m
s	specific entropy, $kJ/kg-K$
sW_u/R	nondimensional specific entropy

T	temperature, K
t	test time, sec
U	velocity, m/sec
U_I	interface velocity, m/sec
U_R	reflected shock velocity, m/sec
U_S	incident shock velocity, m/sec
W	molecular weight, kg/kmol
W_u	molecular weight of undissociated air, 28.967 kg/kmol
X	distance between primary diaphragm station and incident shock in region ①, m (see fig. 1)
X_S	distance behind incident shock in region ①, m (see fig. 1)
x	mole fraction
Z	compressibility factor, $pW_u/\rho RT$
Z^*	number of kmol of dissociated air per number of kmol of undissociated air, W_u/W
γ	ratio of specific heats
γ_E	isentropic exponent, $\left(\frac{\partial \log p}{\partial \log \rho}\right)_{SW_u/R}$
α	defined by $Z^* = 1 + \alpha$
δ^*	nozzle boundary-layer displacement thickness, m
μ	coefficient of viscosity, N-sec/m ²

ρ	density, kg/m ³
τ	time interval between arrival of incident shock and interface, sec
Subscripts:	
A	denotes region (2) for no standing shock at secondary diaphragm, region (2s) for standing shock, and region (2r) for reflected shock (see fig. 1)
a	atom
eff	effective (based on mass flow considerations)
f	frozen
geo	geometric
i	ideal
k	k = 2 denotes shock tube flow, k = 5 denotes expansion tube flow, and k = 6 denotes expansion tunnel flow
m	molecule
max	maximum
n	model nose
t,2	stagnation conditions behind normal bow shock at shock tube test section
t,5	stagnation conditions behind normal bow shock at expansion tube test section
t,6	stagnation conditions behind normal bow shock at expansion tunnel test section
w	wall
X_s	distance behind incident shock in region (1), m (see fig. 1)

- 1 state of quiescent air in front of incident shock in shock tube (intermediate section of expansion tube)
 - 2 state of air behind incident shock in shock tube
 - 2s state of air behind standing shock at secondary diaphragm or normal bow shock at shock tube test section
 - 2r state of air behind reflected shock at secondary diaphragm
 - 3 state of expanded driver gas
 - 4 initial driver gas conditions
 - 5 state of test air in expansion tube test section
 - 5s static conditions behind normal bow shock at expansion tube test section
 - 6 state of test air in expansion tunnel test section
 - 6s static conditions behind normal bow shock at expansion tunnel test section
 - 10 state of quiescent acceleration gas in front of incident normal shock in acceleration section
 - 20 state of acceleration gas behind incident normal shock in acceleration section
- Superscript:
- * conditions at nozzle throat

FACILITIES, ANALYSIS, AND PROCEDURE

Before the procedures for determining shock tube, expansion tube, and expansion tunnel flow quantities are discussed, a brief description of these facilities is given. Next, the source of imperfect real-air thermodynamic properties is briefly discussed. After these discussions, the procedures for determining free-stream and post-normal-shock flow conditions for the shock tube, expansion tube, and expansion tunnel are presented.

Description of Shock Tube, Expansion Tube, and Expansion Tunnel

Shock tube. - The shock tube is a tube, generally cylindrical, divided by a high-pressure diaphragm into two sections. The upstream section is the driver or high-pressure section. This section is pressurized with a gas having a high speed of sound, such as unheated or heated hydrogen or helium. (Greater operation efficiency is realized with gases having a high speed of sound.) The downstream section is referred to as the driven or low-pressure section and the cross section is constant and generally circular. The driven section is usually evacuated and then filled with the test gas at ambient temperature. As illustrated in figure 1(a), the driver gas at time of diaphragm rupture is designated as region (4) and the quiescent test gas is designated as region (1). Upon rupture of the diaphragm, an incident shock wave propagates into region (1) with velocity $U_{s,1}$. Flow conditions immediately behind this shock are denoted as region (2) (fig. 1(b)), and shock tube testing takes place in the flow region from immediately behind this incident shock wave to the test-gas—driver-gas interface. For a blunt model positioned in the driven section, a standing shock is formed at the model, provided flow in region (2) is supersonic. (See fig. 1(c).) The flow conditions immediately behind this standing shock are designated as region (2s); the model stagnation conditions, as region (t2). When the incident shock wave reaches the end wall (or secondary diaphragm of the expansion tube, to be discussed subsequently), it is reflected back into region (2). (See fig. 1(d).) Flow conditions behind this reflected shock are designated as region (2r).

Expansion tube and expansion tunnel. - The expansion tube is basically a shock tube with a section of constant cross section attached to the downstream end. A weak low-pressure diaphragm (secondary diaphragm) separates this section, denoted as the expansion or acceleration section, from the driven section, which is commonly referred to as the intermediate section of the expansion tube. The acceleration section is evacuated and filled with the acceleration gas at a low pressure and ambient temperature. The expansion tunnel is simply an expansion tube with a nozzle added to the downstream end.

The operating sequence of the expansion tunnel includes that for an expansion tube, which, in turn, includes that for a shock tube; the sequence for an expansion tunnel is shown schematically in figure 2. The sequence begins with the rupture of the primary or high-pressure diaphragm separating the driver and driven sections. An incident shock wave propagates into the static test gas and an expansion wave propagates into the driver gas. The shock wave encounters and ruptures the secondary diaphragm. Flow energy lost in rupturing this diaphragm results in an upstream-facing shock wave reflected from the diaphragm. If this shock wave is assumed to be a standing shock, flow conditions behind this standing shock are denoted as region (2s); if a totally reflected shock at the secondary diaphragm is assumed, flow conditions behind this reflected shock are

denoted as region (2r). (See fig. 1(d).) A second incident shock wave propagates into the acceleration gas while an upstream expansion wave moves into the test gas. In passing through this upstream expansion wave, the test gas undergoes an isentropic unsteady expansion that results in an increase in flow velocity. Expansion tube testing occurs in the flow that has passed through the expansion and is denoted as region (5) in figure 2. Thus, for the expansion tunnel, the test gas is processed first by an incident shock into the quiescent test gas in region (1), second, by a shock wave resulting from shock reflection at the secondary diaphragm, third, by an unsteady expansion in the acceleration section, and finally, by an isentropic steady expansion in the nozzle. Expansion tunnel testing takes place in region (6) of figure 2.

Thermodynamic Properties for Real Air

Thermodynamic properties for imperfect real air in thermochemical equilibrium are obtained from a magnetic tape furnished to the Langley Research Center by the Arnold Engineering Development Center (AEDC). The thermodynamic properties obtained from this tape correspond to the properties tabulated in reference 9 for various values of entropy sW_u/R . The temperature range of the AEDC tape is 100 K to 15 000 K and the sW_u/R range is 15.6 to 133. A subroutine for searching the real-air tape was also obtained from AEDC and is designated herein as SLOW. An interpolation procedure allowing pressure p and enthalpy h as inputs was derived for the study of reference 10 and is referred to herein as SEARCH.

The relations derived in reference 11 for predicting thermodynamic properties of real air in thermochemical equilibrium are also employed in the present study. These relations were obtained from curve fits and cover a temperature range of 90 K to 15 000 K and an sW_u/R range of 26 to 126. Imperfect air (intermolecular force) effects are neglected in reference 11. These relations are incorporated into a subroutine designated as SAVE. The sources of thermodynamic properties are discussed in more detail in reference 10 and appendix B.

Calculation Procedure for Shock Tube

As in reference 5, three combinations of inputs are considered for determining flow quantities in region (2). In all three combinations, the quiescent test air pressure p_1 and temperature T_1 are assumed to be known. The quantities (1) incident-shock velocity $U_{s,1}$, (2) pressure behind the incident shock in the driven section p_2 , or (3) the driver gas pressure p_4 and temperature T_4 are used in conjunction with p_1 and T_1 to determine conditions in region (2).

The conservation relations, in a laboratory coordinate system, for mass, momentum, and energy for a normal shock wave moving through region (1) are

$$\rho_1 U_{s,1} = \rho_2 (U_{s,1} - U_2) \quad (1)$$

$$p_1 + \rho_1 U_{s,1}^2 = p_2 + \rho_2 (U_{s,1} - U_2)^2 \quad (2)$$

$$h_1 + \frac{1}{2} U_{s,1}^2 = h_2 + \frac{1}{2} (U_{s,1} - U_2)^2 \quad (3)$$

These relations are solved in conjunction with the equation of state (that is, source of real-air thermodynamic properties) in the form

$$\rho_2 = \rho_2(p_2, h_2) \quad (4)$$

for the unknown quantities ρ_2 , h_2 , U_2 , and p_2 or $U_{s,1}$. For the Langley shock tube and expansion tube, T_1 is ambient and p_1 is generally less than 1 MN/m^2 . At these conditions in region (1), imperfect air effects are negligible and corresponding thermodynamic quantities appearing on the left-hand side of equations (1) to (3) are obtained from perfect air ($Z_1 = 1$, $\gamma_1 = 7/5$) relations.

Equations (1) to (4) are solved by iteration. The iterative schemes used for inputs $U_{s,1}$, p_2 , or p_4 and T_4 are discussed in detail in reference 5. For all three combinations of inputs, the air flow in region (2) is assumed to be in thermochemical equilibrium.

The procedure for determining shock tube performance where p_4 and T_4 are inputs is commonly referred to as "simple shock tube theory," since it is based on a simplified one-dimensional, inviscid flow model which assumes instantaneous diaphragm rupture, no shock wave attenuation, and a driver to driven cross-sectional area ratio of unity. Imperfect gas effects in region (4) for helium at $200 \text{ K} \leq T_4 \leq 15\,000 \text{ K}$ and hydrogen at $273 \text{ K} \leq T_4 \leq 600 \text{ K}$ are included.

Two additional shock tube flow regions of interest (fig. 1) are the result of a standing shock in region (2) (region (2s)) and a totally reflected shock into region (2) (region (2r)). Because of shock reflection at the secondary diaphragm of the expansion tube, these two regions are also considered in the calculation of expansion tube flow quantities and are discussed subsequently.

Effect of boundary layer on test time.— Shock tube wall boundary-layer growth behind the incident shock introduces departures from ideal shock tube flow. (See refs. 6

and 7.) The presence of this boundary layer causes the incident shock to decelerate, the interface to accelerate, and the flow between the incident shock and interface to be non-uniform. When the wall boundary-layer displacement thickness is large in comparison with the tube diameter, the separation distance between the incident shock and the interface and the test time approach limiting maximum values. (Test time is defined as the time interval between arrival of incident shock in region ① and arrival of the test-gas—driver-gas interface at a given station.) Actual shock tube test times may be considerably less than the values predicted by use of idealized theory. Thus, shock tube test time and flow nonuniformity are considered in the present calculations. Since these flow phenomena are dependent on the character of the shock tube wall boundary layer behind the incident shock, the effect of both laminar and turbulent wall boundary layers are included.

Shock tube test times have been treated analytically in reference 6 for laminar boundary layers and in reference 7 for turbulent boundary layers. For a laminar boundary layer, the test time t is obtained from the relation (ref. 6)

$$2\ell_{\max}\left(\frac{\rho_2}{\rho_1}\right)\left[\log_e\left(1 - \sqrt{\frac{U_{s,1}t}{\ell_{\max}}}\right) + \sqrt{\frac{U_{s,1}t}{\ell_{\max}}}\right] + U_{s,1}t = -X \quad (5)$$

where the separation distance between the incident shock in region ① and the test-gas—driver-gas interface ℓ for a given distance X downstream of the diaphragm station is given by (ref. 6)

$$2\ell_{\max}\left(\frac{\rho_2}{\rho_1}\right)\left[\log_e\left(1 - \sqrt{\frac{\ell}{\ell_{\max}}}\right) + \sqrt{\frac{\ell}{\ell_{\max}}}\right] = -X \quad (6)$$

Simple expressions for the maximum separation distance ℓ_{\max} in terms of known quantities were obtained from curve fits applied to the real-air results of reference 6 and yielded the expressions

$$\ell_{\max} = p_1 d^2 \left(2.060 - 2.056 \times 10^{-1} M_{s,1} + 8.095 \times 10^{-3} M_{s,1}^2 \right) \quad (4 < M_{s,1} \leq 14) \quad (7a)$$

$$\ell_{\max} = p_1 d^2 \left(8.723 \times 10^{-1} - 7.488 \times 10^{-3} M_{s,1} \right) \quad (14 < M_{s,1} < 30) \quad (7b)$$

The results of figure 6 of reference 6 were extrapolated to a value of $M_{s,1}$ equal to 30 to obtain equation (7b). As the separation distance approaches this limiting value ℓ_{\max} , the interface velocity approaches the incident shock velocity and is essentially equal to $U_{s,1}$ at ℓ_{\max} .

The test time for a turbulent boundary layer is obtained from the relation (ref. 7)

$$\frac{5\ell_{\max}}{4} \left(\frac{\rho_2}{\rho_1} \right) \left\{ \log_e \left[\frac{1 + \left(\frac{U_{s,1}t}{\ell_{\max}} \right)^{0.2}}{1 - \left(\frac{U_{s,1}t}{\ell_{\max}} \right)^{0.2}} \right] + 2 \tan^{-1} \left(\frac{U_{s,1}t}{\ell_{\max}} \right)^{0.2} - 4 \left(\frac{U_{s,1}t}{\ell_{\max}} \right)^{0.2} \right\} - U_{s,1}t = X \quad (8)$$

where ℓ is obtained from the relation (ref. 7)

$$\frac{5\ell_{\max}}{4} \left(\frac{\rho_2}{\rho_1} \right) \left\{ \log_e \left[\frac{1 - \left(\frac{\ell}{\ell_{\max}} \right)^{0.2}}{1 + \left(\frac{\ell}{\ell_{\max}} \right)^{0.2}} \right] - 2 \tan^{-1} \left(\frac{\ell}{\ell_{\max}} \right)^{0.2} + 4 \left(\frac{\ell}{\ell_{\max}} \right)^{0.2} \right\} = -X \quad (9)$$

Curve fits to the real-air results of reference 7 yielded the following expressions for ℓ_{\max} :

$$\ell_{\max} = p_1^{0.25} d^{1.25} \left(5.273 - 7.514 \times 10^{-1} M_{s,1} + 3.435 \times 10^{-2} M_{s,1}^2 \right) \quad (4 < M_{s,1} < 10) \quad (10a)$$

$$\ell_{\max} = p_1^{0.25} d^{1.25} \left(1.546 - 3.017 \times 10^{-2} M_{s,1} \right) \quad (10 \leq M_{s,1} < 30) \quad (10b)$$

For the inviscid case, the "ideal" test time is given by the relation (ref. 12)

$$t_{i,2} = \frac{\rho_1}{\rho_2} \frac{X}{U_2} \quad (11)$$

Effect of boundary layer on flow nonuniformity.- A method for estimating flow non-uniformity (axial variation of flow quantities) between the incident shock and interface after maximum separation distance is reached is presented in references 6 and 13. In these references, the concept of an equivalent inviscid channel is employed and yields the following continuity equation:

$$\rho_{2,X_S} (U_{s,1} - U_{2,X_S}) = \rho_{2,X_S=0} (U_{s,1} - U_{2,X_S=0}) \left[1 - \left(\frac{X_S}{\ell_{\max}} \right)^n \right] \quad (12)$$

where $n = 0.5$ for a laminar boundary layer and $n = 0.8$ for a turbulent boundary layer. Additional relations required for solution of flow conditions in the region between the incident shock and interface are the isentropic condition for equivalent inviscid channel flow

$$\left(\frac{s_2 W_u}{R} \right)_{X_S} = \left(\frac{s_2 W_u}{R} \right)_{X_S=0} \quad (13)$$

and either the energy relation

$$h_{2,X_S} + \frac{1}{2} (U_{s,1} - U_{2,X_S})^2 = h_{2,X_S=0} + \frac{1}{2} (U_{s,1} - U_{2,X_S=0})^2 \quad (14a)$$

if the AEDC real-air tape is used as the source of thermodynamic properties ($\rho = \rho(h, sW_u/R)$), or the momentum relation

$$p_{2,X_S} + \rho_{2,X_S} (U_{s,1} - U_{2,X_S})^2 = p_{2,X_S=0} + \rho_{2,X_S=0} (U_{s,1} - U_{2,X_S=0})^2 \quad (14b)$$

if the AEDC real-air curve fit expressions are used ($\rho = \rho(p, sW_u/R)$). This system of equations is solved for the unknowns ρ_{2,X_S} , U_{2,X_S} , and p_{2,X_S} , in conjunction with the equation of state, by iteration on ρ_{2,X_S} for a given value of X_S/ℓ_{\max} . As discussed in reference 6, equation (12) is less accurate for the case where the maximum separation distance has not been obtained. This inaccuracy is due to entropy variations (associated with nonuniform shock motion) and the unsteady nature of the flow between the incident shock and the interface. Since the accuracy of equation (12) decreases as ℓ/ℓ_{\max} decreases from its limiting value near unity, the effect of flow nonuniformity is determined herein only when the condition $\ell/\ell_{\max} \geq 0.9$ is satisfied.

Calculation Procedure for Expansion Tube

As discussed in reference 14, the flow energy lost in rupture of the secondary diaphragm must result in an upstream-facing shock wave reflected from this diaphragm. When the diaphragm ruptures, the resulting expansion fan overtakes and weakens the reflected shock. It is sometimes assumed that the reflected shock has been weakened to a standing shock by the time it processes the flow which eventually becomes the test flow. Therefore, the possible existence of a standing normal shock at the secondary diaphragm (region (2s)) was considered in reference 5.

Recently, tests were performed in the Langley expansion tube with helium as the test gas. (See ref. 15.) The primary reason for employing helium was to divorce possible effects of flow chemistry on test-section flow quantities from the gas dynamics or fluid mechanics of the flow and, thereby, to provide an approximate model of the expansion tube fluid mechanics. These helium tests indicated the existence of a totally reflected shock at the secondary diaphragm (region (2r)). Hence, the effects of a reflected shock, as well as those of a standing shock, at the secondary diaphragm are considered herein. As in region (2), flow quantities in regions (2s) and (2r) are assumed to be in thermochemical equilibrium. In computing flow quantities in regions (2s) and (2r), flow quantities in region (2) are assumed to be uniform.

Standing shock at secondary diaphragm. - The conservation relations for a standing shock at the secondary diaphragm are

$$\rho_2 U_2 = \rho_{2s} U_{2s} \quad (15)$$

$$p_2 + \rho_2 U_2^2 = p_{2s} + \rho_{2s} U_{2s}^2 \quad (16)$$

$$h_2 + \frac{1}{2} U_2^2 = h_{2s} + \frac{1}{2} U_{2s}^2 \quad (17)$$

Since the conditions in region (2) are assumed to be known (that is, calculated previously), equations (15) to (17) are solved in conjunction with the equation of state, by iteration, to yield conditions behind the standing shock (region (2s)). (It should be noted that the flow conditions in region (2s) are the same as those immediately behind a normal bow shock wave on a model positioned in the shock tube test section.)

Totally reflected shock at secondary diaphragm. - For a totally reflected shock wave at the secondary diaphragm, the conservation relations are

$$\rho_2 (U_2 + U_r) = \rho_{2r} U_r \quad (18)$$

$$p_2 + \rho_2 (U_2 + U_r)^2 = p_{2r} + \rho_{2r} U_r^2 \quad (19)$$

$$h_2 + \frac{1}{2} (U_2 + U_r)^2 = h_{2r} + \frac{1}{2} U_r^2 \quad (20)$$

Again, the conditions in region (2) are assumed to be known. Equations (18) to (20) are solved by iteration for the thermodynamic properties in region (2r) and the reflected shock velocity U_r .

Thermochemical-equilibrium unsteady expansion. - Region (A) is defined as being region (2) for the case of no shock reflection at the secondary diaphragm, region (2s) for a standing shock, and region (2r) for a totally reflected shock. As discussed previously, the expansion tube flow undergoes an isentropic, unsteady expansion from region (A) to region (5). Across an upstream-facing unsteady expansion wave, the velocity increment is related to the thermodynamic properties by the integral expression (ref. 1)

$$\Delta U = U_5 - U_A = - \int_{h_A}^{h_5} \left(\frac{dh}{a} \right) s_A W_u / R \quad (21)$$

Either free-stream pressure or test-air—acceleration-gas interface velocity U_5 is considered, individually, as inputs necessary for the solution of equation (21). As is typical of high-enthalpy facilities, the assumption of thermochemical-equilibrium air flow is subject to question. Hence, limiting cases are obtained by performing both a thermochemical equilibrium expansion and a frozen expansion.

For an equilibrium expansion where the quantity U_5 is an input, the ΔU of equation (21) is known. If the AEDC real-air tape is to be used as the source of thermodynamic properties, the enthalpy is decreased from a maximum value of h_A in given increments. Since an isentropic ($s_A W_u / R = s_5 W_u / R$) expansion is assumed, subroutine SLOW (inputs h and $s_A W_u / R$) is used to generate corresponding values of the inverse of the speed of sound a^{-1} . If the AEDC real-air curve-fit relations are to be used instead of the AEDC tape, pressure is decreased in given increments from a maximum value of p_A . These values of pressure are used in the subroutine SAVE with constant entropy $s_A W_u / R$ to generate corresponding values of enthalpy (the maximum value being h_A) and the inverse of the speed of sound. Equation (21) is integrated numerically between the known limit h_A and the unknown limit h_5 . The value of h which equates the integral of equation (21) to ΔU is the desired value of h_5 . Corresponding thermodynamic quantities in region (5) are obtained from the real-air source, since the quantities $s_5 W_u / R$

and h_5 or p_5 are now known. When p_5 is an input, the thermodynamic quantities in region (5) are obtained directly from the real-air source since $s_5 W_u / R$ and p_5 are known. With the limits of integration known, the integral in equation (21) is evaluated numerically to give ΔU , and hence U_5 .

Additional conditions in region (5) that are of interest are free-stream Mach number M_5 and free-stream unit Reynolds number $N_{Re,5}$. For values of T_5 less than or equal to 1500 K, the free-stream viscosity μ_5 required in determining $N_{Re,5}$ is calculated from Sutherland's viscosity law (ref. 10), whereas for values of T_5 greater than 1500 K, μ_5 is obtained by use of the results of reference 16.

Frozen unsteady expansion. - Frozen flow is defined herein as flow in which the vibrational energy and chemistry remain unchanged during the expansion of the test air. For the expansion tube, this freezing of the vibrational energy and chemistry is assumed to occur in region (A). Hence, the energy in region (A) may be viewed as consisting of an active or available part which provides the energy for flow expansion and a frozen or nonavailable part. Since the energy associated with vibration and chemistry is constant for a frozen expansion, the ratio of specific heats γ will be constant and the test air behaves as a perfect gas. To obtain an estimate of the ratio of frozen specific heats γ_f for dissociated but unionized air, it is assumed that the dissociated air may be modeled by atoms (O and N) and molecules (N_2 , O_2 , and NO). It is further assumed that the atoms are not distinguishable and the molecules are not distinguishable. This is a reasonable assumption since W_O is approximately equal to W_N , and W_{O_2} , W_{N_2} , and W_{NO} are approximately equal. The molecular weight for this composition is given by the relation

$$W = x_a W_a + x_m W_m \approx W_a (2 - x_a) \quad (22)$$

where the sum of the mole fractions is unity ($x_a + x_m = 1$) and the molecular weight of a molecule (O_2 , N_2 , NO) is approximately twice that of an atom (O, N). From the relation Z^* equal to W_u / W , where W_u is approximately W_m , the expression

$$Z^* = \frac{2}{2 - x_a} \quad (23)$$

is obtained. By letting the quantity Z^* be defined as $1 + \alpha$, it can be shown that

$$\gamma_f = \frac{7 + 3\alpha}{5 + \alpha} \quad (24)$$

Since the quantity Z_A^* is assumed to be known, values of α , and hence γ_f , may be obtained.

For a frozen (perfect) gas, equation (21) may be evaluated in closed form to yield

$$U_{5,f} - U_A = \frac{2}{\gamma_f - 1} (a_{A,f} - a_{5,f}) \quad (25)$$

If a value of $U_{5,f}$ is known, the frozen free-stream speed of sound $a_{5,f}$ follows from equation (25) and the corresponding frozen thermodynamic quantities in region (5) are determined from the isentropic perfect gas relations of reference 17. (See ref. 5.) For the case where a value of $p_{5,f}$ is known, the quantity $a_{5,f}$ is determined from the isentropic perfect gas relation (ref. 17)

$$a_{5,f} = a_{A,f} \left(\frac{p_{5,f}}{p_A} \right)^{\frac{\gamma_f - 1}{2\gamma_f}} \quad (26)$$

Corresponding frozen quantities in region (5) are determined similarly, and $U_{5,f}$ is obtained from equation (25).

The ideal test time for the expansion tube (test time is defined as the time interval between arrival of the acceleration-gas—test-air interface and the expansion fan (ref. 1) is given by the relation

$$t_{i,5} = L_a \left(\frac{1}{U_5 - a_5} - \frac{1}{U_5} \right) \quad (27)$$

The actual test time may be somewhat less than this ideal test time because of the early arrival of a downstream expansion wave. (See ref. 14.) The time of arrival of this downstream expansion wave for real air is not determined in the present study.

Flow attenuation.— The air-test-gas—helium-acceleration-gas interface velocity in the acceleration section of the Langley pilot model expansion tube was observed (ref. 14) to decrease in traversing the acceleration section. A decrease in flow velocity along the acceleration section was also observed in recent tests (ref. 15) performed in the Langley 6-inch expansion tube with air test gas and air acceleration gas. Thus, the effect of flow attenuation on calculated flow quantities in region (5) and on the post-normal-shock region of a test model subjected to flow in region (5) is considered herein.

A method for determining the effect of flow attenuation on thermodynamic quantities in region (5) is discussed in reference 14. To illustrate this method, consider a thermodynamic quantity in region (5), such as p_5 , plotted as a function of interface velocity U_5

at the exit of the acceleration section. Application of the method of reference 14 is equivalent to a shift of point p_5, U_5 for no flow attenuation to point $p_5, U_5 - 2\Delta U_5$ with flow attenuation. The quantity ΔU_5 is the difference between the maximum and minimum (that is, acceleration section exit) values of interface velocity observed along the acceleration section. In the present program, the unsteady expansion is performed to the acceleration section exit (region (5)) and the interface velocity U_5 changed to $U_5 - 2\Delta U_5$ to account for flow attenuation. Post-normal-shock flow quantities (regions (5s) and (t5)) are calculated by the shock crossing procedure to be discussed subsequently, where the free-stream velocity is equal to $U_5 - 2\Delta U_5$. The effect of flow attenuation is included for an equilibrium expansion only.

Acceleration-gas flow quantities and quiescent pressure. - An important parameter in the operation of an expansion tube is the initial pressure of the acceleration gas p_{10} . This pressure is the controlling factor in determining the degree of expansion in the acceleration section. In reference 5, a range of p_{10} was determined for each U_5 with helium acceleration gas. Only helium was considered in reference 5, since helium was used exclusively as the acceleration gas in the Langley pilot model expansion tube. (See ref. 14.) However, more recent tests in the Langley 6-inch expansion tube (ref. 15) have indicated the desirability of using the same gas for both test gas and acceleration gas.

In the present study, the conditions in region (5) are determined prior to calculating the corresponding value of p_{10} required. Since the values of p_{10} are relatively low and since the quiescent acceleration air temperature T_{10} is ambient, thermodynamic conditions in region (10) obey ideal air relations. At the interface of the acceleration air and test air, it is required that p_{20} equal p_5 and U_{20} equal U_5 . Hence, the conservation relations for an incident shock wave into region (10), excluding the effect of boundary-layer growth along the tube wall, are

$$\frac{W_{10}}{RT_{10}} p_{10} U_{s,10} = \rho_{20} (U_{s,10} - U_5) \quad (28)$$

$$p_{10} \left(1 + \frac{W_{10}}{RT_{10}} U_{s,10}^2 \right) = p_5 + \rho_{20} (U_{s,10} - U_5)^2 \quad (29)$$

$$\frac{7}{2} \frac{R}{W_{10}} T_{10} + \frac{1}{2} U_{s,10}^2 = h_{20} + \frac{1}{2} (U_{s,10} - U_5)^2 \quad (30)$$

where the unknowns are p_{10} , ρ_{20} , h_{20} , and $U_{s,10}$. The equation of state represents the required fourth relation. These relations are solved by iteration. An initial guess

of the quantity $U_{s,10}$ is made, this being 1.11 times U_5 (corresponding to ρ_{20}/ρ_{10} equal to 10), and h_{20} is obtained from equation (30). The quantity p_{20} (which is equal to p_5) and this initial estimate of h_{20} are used as inputs to the source of thermodynamic properties and a value of ρ_{20} is obtained. This value of ρ_{20} is used in equation (29) to obtain a value of p_{10} . A new (up-dated) value of $U_{s,10}$ is determined from equation (28), and if not within 0.1 percent of the initial guess of $U_{s,10}$, the procedure is repeated. Iteration on the quantity $U_{s,10}$ is continued until successive values of $U_{s,10}$ are within the desired tolerance.

If helium is to be used as the acceleration gas, as in the experimental study of reference 14, the corresponding value of p_{10} for helium may be estimated from that for air. Combining equations (28) and (29) yields the expression

$$p_5 = p_{10} + \rho_{10} U_{s,10} U_5$$

For a strong incident shock, p_{10} is small compared with the product $\rho_{10} U_{s,10} U_5$; hence, p_5 is approximately equal to $\rho_{10} U_{s,10} U_5$. Equating p_5 and U_5 for both acceleration gases gives

$$(\rho_{10} U_{s,10})_{\text{He}} \approx (\rho_{10} U_{s,10})_{\text{air}}$$

For the same value of U_5 , the incident shock velocities in air and helium are relatively close; in the limit of maximum separation distance between the shock and interface, these $U_{s,10}$ values are equal. Thus, $\rho_{10,\text{He}}$ is approximately equal to $\rho_{10,\text{air}}$ and $p_{10,\text{He}}$ is equal to 7.24 times $p_{10,\text{air}}$.

An often employed method of measuring the velocity of a moving gas is the microwave interferometer technique (refs. 14 and 15). If helium is used as the acceleration gas, the helium behind the incident shock into region (10) is generally not ionized and thus is transparent to the microwave signal. Hence, the flow being tracked by the signal is the helium-acceleration-gas-air-test-gas interface and the quantity U_5 is inferred from measurement. When air is used as the acceleration gas, the microwave signal tracks the incident shock into region (10) and not the interface. For this reason, the laminar theory of reference 6 (discussed previously) is used in the present program to determine the U_5 from measured values of $U_{s,10}$, known thermodynamic conditions in region (10), and acceleration-section diameter and length. At the acceleration-section station where l/l_{max} is nearly unity, the quantity U_5 is equal to $U_{s,10}$ and may be inferred directly from measurement.

Calculation Procedure for Expansion Tunnel

Thermochemical-equilibrium steady expansion.- The entrance conditions at the nozzle of the expansion tunnel correspond to the conditions in region (5). As discussed previously, the expansion tunnel flow is assumed to undergo an isentropic steady expansion from region (5) to region (6). The basic differential equation for this expansion is (ref. 1)

$$dU = - \left(\frac{dh}{U} \right)_{sW_u/R} \quad (31)$$

which may be integrated between regions (5) and (6) to give

$$h_5 + \frac{1}{2} U_5^2 = h_6 + \frac{1}{2} U_6^2 \quad (32)$$

The left-hand side of equation (32) is considered to be known. Inputs considered (individually) for determining expansion tunnel flow conditions are p_6 and U_6 . For an equilibrium nozzle expansion in which the quantity U_6 is known, h_6 is obtained from equation (32) and the corresponding thermodynamic quantities in region (6) are determined from the source of thermodynamic properties with the quantities h_6 and $s_6 W_u/R$ (which is equal to $s_A W_u/R$) as input. For the case where a value of p_6 is known, the thermodynamic quantities in region (6) follow from the source of thermodynamic properties with the quantities p_6 and $s_6 W_u/R$ as input, and the corresponding value of U_6 is obtained from equation (32).

Frozen steady expansion.- For a frozen nozzle expansion, it is assumed that the flow in region (5) is in equilibrium, and the assumption is made that freezing occurs at the nozzle throat. The procedure for calculating frozen flow conditions in region (6) is similar to that discussed previously for region (5) of the expansion tube, whereby the equilibrium conditions in region (5) correspond to those of region (A) and the frozen conditions of region (6) correspond to those of region (5). The difference is that equation (32) for a steady expansion replaces equation (25) which applies to an unsteady expansion.

Nozzle boundary-layer displacement thickness.- A quantity of interest is the nozzle boundary-layer displacement thickness. This quantity, with one-dimensional flow assumed, is given by the relation

$$\delta^* = r_{\text{geo}} - r_{\text{eff}} \quad (33)$$

where the radius of the inviscid core is given by

$$r_{\text{eff}} = r_{\text{eff}}^* \left(\frac{A}{A^*} \right)_{\text{eff}}^{1/2} \quad (34)$$

and r_{geo} is the nozzle wall radius. The ratio $(A/A^*)_{\text{eff}}$ is determined from the continuity equation for one-dimensional, steady flow

$$\left(\frac{A}{A^*} \right)_{\text{eff}} = \frac{\rho_5 U_5}{\rho_6 U_6} \quad (35)$$

where quantities appearing on the right-hand side have been calculated previously. With the assumption that the displacement thickness at the nozzle entrance (throat) is zero ($r_{\text{geo}}^* = r_{\text{eff}}^*$), equation (33) becomes

$$\delta^* = r_{\text{geo}} - r_{\text{geo}}^* \left(\frac{\rho_5 U_5}{\rho_6 U_6} \right)^{1/2} \quad (36)$$

Calculation of Flow Quantities Behind Normal Bow Shock at Test Model

For some tests in the shock tube and most tests in the expansion tube or expansion tunnel, a test model is positioned in the test section. Hence, it is desirable to determine the flow quantities behind the normal part of the bow shock of a blunt test model. The conservation relations for a standing normal shock at a blunt body are given in equations (15) to (17), where the subscripts 2 and 2s are now replaced by 5 and 5s for the expansion tube and 6 and 6s for the expansion tunnel. For an equilibrium expansion, the flow behind the normal bow shock is assumed to be in equilibrium; for a frozen expansion, the flow behind the normal bow shock is assumed to be either in equilibrium or frozen. For the case of equilibrium post-bow-shock flow, the conservation relations are solved, in conjunction with the equation of state, by iteration to obtain the static conditions immediately behind the shock. Stagnation-point properties are determined by using the assumption that the flow region from immediately behind the bow shock to the stagnation point is isentropic (that is, $s_{\text{ks}} W_u/R = s_{\text{t,k}} W_u/R$, where k is equal to 2 for shock tube, 5 for expansion tube, and 6 for expansion tunnel) and the energy relation for an equilibrium expansion to the test section is ($k = 2, 5$, or 6)

$$h_{\text{t,k}} = h_{\text{k}} + \frac{1}{2} U_{\text{k}}^2 \quad (37)$$

and for a frozen expansion is ($k = 5$ or 6)

$$h_{t,k} = h_{k,f} + h_{A,f} + \frac{1}{2} U_{k,f}^2 \quad (38)$$

This procedure, in which $s_{t,k} W_u/R$ and $h_{t,k}$ are known, requires usage of the AEDC tape. A second procedure considered, which makes use of the AEDC curve fits, is to estimate $p_{t,k}$ from the relation (ref. 5)

$$p_{t,k} = p_{ks} \left(1 + \frac{\gamma_{E,ks} - 1}{2} M_{ks}^2 \right)^{\frac{\gamma_{E,ks}}{\gamma_{E,ks} - 1}} \quad (39)$$

This value of $p_{t,k}$ is used in conjunction with $s_{t,k} W_u/R$ as input to the subroutine SAVE. If the value of $h_{t,k}$ obtained from SAVE is not within 0.1 percent of the value obtained from equation (37) or (38), $p_{t,k}$ is up-dated by the relation

$$(p_{t,k})_{\text{new}} = \frac{(p_{t,k})_{\text{previous}} (h_{t,k})_{\text{known}}}{(h_{t,k})_{\text{previous}}} \quad (40)$$

(where $(h_{t,k})_{\text{known}}$ was obtained from eq. (37) or (38)) and the iterative procedure repeated until the desired criteria on $h_{t,k}$ is obtained. The stagnation-point heat-transfer rate for a spherical body positioned in the shock tube ($k = 2$), expansion tube ($k = 5$), or expansion tunnel ($k = 6$) is determined from the expression (ref. 18)

$$\dot{q}_{t,k} = 3.88 \times 10^{-4} \sqrt{\frac{p_{t,k}}{r_n}} (h_{t,k} - h_w) \quad (41)$$

For the case of frozen post-bow-shock flow, normal-shock crossing relations for perfect air (ref. 17) are used to obtain conditions immediately behind the shock and isentropic, perfect air relations are used to obtain stagnation-point conditions.

It should be noted that flow properties behind the normal part of the bow shock wave of an entry body at high velocity are equivalent to the properties behind an incident shock in a shock tube traveling at that velocity. In free flight, the free-stream conditions and flight velocity correspond to the initial conditions in region ① and the incident shock

velocity $U_{s,1}$, respectively, whereas static and stagnation conditions behind the bow shock correspond to conditions in regions (2) and (t2), respectively.

RESULTS AND DISCUSSION

Description of the inputs necessary to utilize the present computer program is presented in appendix A along with a flow chart, listing of the program, brief description of basic subroutines, and sample printout. The accuracy and limitations of the program are discussed in appendix B. Results of calculations illustrating the application of the program to shock tube and expansion tube flows are presented in figures 3 to 20, with figures 3, 4, 5, and 18 for the shock tube and figures 6 to 17, 19, and 20 for the expansion tube.

Flow quantities in region (2) may be obtained by using the basic measured inputs in the following combinations:

Case (1): p_1 , T_1 , and $U_{s,1}$

Case (2): p_1 , T_1 , and p_2

Case (3): p_1 , T_1 , p_4 , T_4 , and W_4

Case (3) is useful in ascertaining the theoretical performance prior to a test and in comparison of measured quantities $U_{s,1}$ and p_2 with predicted values from simple shock tube theory. The computational method for case (3) is illustrated in figure 3 where velocity-pressure (U_3, p_3) curves for perfect and imperfect, isentropic unsteady expansion of helium and hydrogen driver gases are shown in conjunction with velocity-pressure (U_2, p_2) curves for incident normal shocks in equilibrium, real air. In figure 3, the value of p_4 was 68.95 MN/m² for both driver gases and T_4 is varied from 300 K to 10 000 K for helium (figs. 3(a) to 3(c)) and from 300 K to 600 K for hydrogen (figs. 3(d) and 3(e)). The ambient air temperature T_1 was 300 K and p_1 was varied from 6.9 N/m² to 6.9 MN/m². Solutions for case (3) are the intersections of the U_2, p_2 air curves (generated by using 20 values of $U_{s,1}$ for each value of p_1 and the AEDC curve-fit expressions as a source of thermodynamic properties) and U_3, p_3 helium or hydrogen curves. (That is, the solution is obtained when $U_2 = U_3$ and $p_2 = p_3$.) For a helium driver gas and the conditions in region (4) of figure 3, no appreciable imperfect helium effects on the predicted isentropic expansion are observed. A small effect of imperfect hydrogen is observed in figures 3(d) and 3(e).

Shock tube performance for real air with helium and hydrogen driver gases is shown in figure 4, where incident shock velocity $U_{s,1}$ is plotted as a function of pressure

ratio p_4/p_1 . These results were generated by two methods. First, two values of p_1 (6.9 N/m² and 6.9 kN/m²) were used in conjunction with various values of p_4 to obtain the range of p_4/p_1 shown. Compressibility factors for the higher values of p_4 for helium and hydrogen driver gases are given in the following table:

p_4 , MN/m ²	T_4 , K	Z_4 for -	
		Helium	Hydrogen
0.69	600	1.001	1.002
3.45	600	1.007	1.012
6.90	600	1.015	1.024
13.79	600	1.029	1.051
34.47	600	1.071	1.135
68.95	600	1.139	1.282
137.90	600	1.264	1.566

Second, p_4 was held constant at 68.95 MN/m² and p_1 varied from 6.9 N/m² to 6.9 MN/m². In both cases, T_1 was equal to 300 K and T_4 was equal to 600 K. The curves from these two methods were found to be identical for both the helium driver gas and the hydrogen driver gas. Differences between perfect hydrogen ($Z_4 = 1.0$) and imperfect hydrogen driver gas are observed (fig. 4) to be small, and the perfect hydrogen driver gas yields somewhat higher values of $U_{s,1}$ for a given p_4/p_1 in agreement with reference 19. The improved performance expected with hydrogen driver gas, in comparison with helium driver gas, is evident in figure 4.

Simple shock tube predictions for real air are shown for helium (figs. 5(a) and 5(b)) and hydrogen (fig. 5(c)) driver gases at p_4 equal to 68.95 MN/m². The T_4 for helium is varied in 50 K increments from 300 K to 700 K (fig. 5(a)) and in 1000 K increments from 1000 K to 12 000 K (fig. 5(b)) and for hydrogen (fig. 5(c)) is varied in 50 K increments from 300 K to 600 K. The value $T_4 = 700$ K for helium represents the maximum value obtainable in the Langley expansion tube with resistance heating and the value $T_4 = 600$ K for hydrogen represents the limit of curve fitting as applied to virial coefficients in reference 5. For an arc-driven shock tube or expansion tube using helium driver gas, much higher T_4 values than presented in figure 5(a) are realized; hence, figure 5(b) represents an extension in range of T_4 to figure 5(a). At the maximum T_4 of 12 000 K, ionization of the helium driver gas is essentially negligible. (See ref. 20.) Values of p_1 , p_4 , and T_4 being known, a theoretical value of $U_{s,1}$ in real air may be obtained from figure 5.

Combinations of measured input for obtaining stagnation-point conditions in the expansion tube test section (region (t5)), when it is assumed that thermochemical equilibrium flow conditions in region (A) are known (previously calculated), are summarized in the following table:

Case	Measured input	Unsteady expansion	Post normal shock
(1)	U_5 or p_5	Equilibrium	Equilibrium
(2)	U_5 or p_5	Frozen	Equilibrium
(3)	U_5 or p_5	Frozen	Frozen

Similarly, combinations of measured input for obtaining stagnation-point conditions in the expansion tunnel test section (region (t6)), when thermochemical equilibrium flow conditions in region (5) are known, are summarized in the following table:

Case	Measured input	Steady expansion	Post normal shock
(1)	U_6 or p_6	Equilibrium	Equilibrium
(2)	U_6 or p_6	Frozen	Equilibrium
(3)	U_6 or p_6	Frozen	Frozen

The first consideration in performing a test in an expansion tube or expansion tunnel is to determine theoretical flow quantities for the chosen mode of operation. Such a procedure is necessary in order to obtain approximate magnitudes of quantities to be measured in the various flow regions. Because of the wide range of flow conditions that may be generated in the expansion tube and the long computer times associated with the program of reference 5, the program of reference 5 was not exercised to generate a family of working plots illustrating expansion tube performance. However, the provision of such plots would be a worthwhile convenience to the experimenter and would also illustrate the versatility of such a facility. Since the present program requires much less computer time than that of reference 5 (present program is approximately 60 to 80 times faster than the program of reference 5 with a 10 species air model), working plots were generated for real-air expansion tube flows and are presented in figures 6 to 17.

Various flow quantities in region (5) (p_5 , ρ_5 , T_5 , M_5 , and $N_{Re,5}$), region (5s) (ρ_{5s}/ρ_5), and region (t5) ($p_{t,5}$, $\rho_{t,5}$, $T_{t,5}$, $h_{t,5}$, and $\dot{q}_{t,5}$ for $r_n = 2.54$ cm) are

plotted as a function of input U_5 for values of p_1 equal to 0.7, 3.45, 6.9, 34.47, 68.95, and 344.7 kN/m² in figures 6 to 11, respectively. In figures 6 to 11, the flow in region (5) is assumed to be in equilibrium and there is no shock reflection at the secondary diaphragm. These results are shown for a range of $U_{s,1}$ from 2.1 to 4.5 km/sec. The upper limit on $U_{s,1}$ represents the highest value obtained to date in the Langley expansion tube using arc-heated helium as the driver gas. Also shown in figures 6 to 11 are values of p_{10} required to produce the corresponding flow conditions. Figures 12 to 17 correspond to figures 6 to 11, respectively, except that a totally reflected shock at the secondary diaphragm is included. Thus, limiting cases for these shock-wave reflection phenomena are provided. The results of figures 6 to 17 were obtained by using the AEDC real-air curve-fit expressions to determine conditions in regions (2), (2r), (5s), and (t5) and the AEDC real-air tape for determination of the unsteady expansion quantities of region (5). (The reader is referred to appendix B for discussion of the computational procedures incorporated in the present program. For these results, method (2) (ISAV = 2, IEXP = 1) was employed, JAC being 100.) These figures were generated by machine and linear line segments were used to connect adjacent data points.

For purposes of illustration, let it be assumed that a study is to be performed in the expansion tube at U_5 equal to 5.4 km/sec and M_5 equal to 10. Both the case of no shock reflection at the secondary diaphragm and the existence of a totally reflected shock are considered. The driver gas is unheated helium ($T_4 = 300$ K) and a value of p_1 equal to 3.45 kN/m² is selected. From figures 7 and 13, flow conditions and the required p_{10} for this example are as follows:

Condition	No shock reflection	Totally reflected shock
$U_{s,1}$, km/sec	2.48	2.25
p_5 , kN/m ²	0.78	0.45
T_5 , kK	0.76	0.75
ρ_5 , g/m ³	3.6	2.1
$N_{Re,5}$, m ⁻¹	5.6×10^5	3.2×10^5
ρ_{5s}/ρ_5	11.85	12.1
$p_{t,5}$, kN/m ²	100.0	57.7
$T_{t,5}$, kK	6.0	5.9
$\rho_{t,5}$, g/m ³	44.5	25.7
$h_{t,5}$, MJ/kg	15.5	15.3
$\dot{q}_{t,5}$, MW/m ²	11.6	8.8
p_{10} , N/m ²	1.9	1.2

The value of $U_{s,1}$ corresponding to the chosen values of U_5 and M_5 is obtained from figure 7(d) for no shock reflection and from figure 13(d) for a totally reflected shock. These $U_{s,1}$ values are, in turn, used to obtain the remaining flow quantities presented in figures 7 and 13. At this point the range of p_{10} required to generate the desired values of U_5 and M_5 for p_1 equal to 3.45 kN/m² is known. The corresponding range of p_4 required to produce this range of $U_{s,1}$, for a given p_1 , is obtained from figure 5. The pressure in region (2) is obtained from figure 18, where the quantities p_2/p_1 , ρ_2/ρ_1 , T_2/T_1 , h_2/h_1 , and s_2W_u/R (predicted by using the AEDC real-air tape) are plotted as a function of $U_{s,1}$ for the values of p_1 considered in figures 6 to 17.

Figure 19 illustrates the effect of frozen expansion, in comparison with a thermochemical equilibrium expansion, for several sample cases. These cases show a large effect of shock reflection at the secondary diaphragm on predicted frozen flow quantities. Such large differences are the result of the increase in dissociation in region (A) from the case of no shock reflection to the case of a standing shock or totally reflected shock, coupled with the assumption that the flow freezes in region (A).

As discussed previously, it is often necessary to infer the test-air—acceleration-air interface velocity U_I from measured $U_{s,10}$ by using the theory of reference 6. Figure 20 shows flow quantities τ_i , τ , ℓ/ℓ_{\max} , and $U_{s,10}/U_I$ as a function of non-dimensionalized distance downstream of the secondary diaphragm for a representative expansion tube test. For the results of figure 20, p_1 is equal to 3.45 kN/m², $U_{s,1}$ is equal to 2.85 km/sec, and L_a is equal to 17 m. From figure 20(b), the time a model positioned at the test section (tube exit) is subjected to acceleration-air flow diminishes with increasing U_5 . The separation distance between the incident shock in region (10) and the test-air—acceleration-air interface approaches the maximum separation distance ℓ_{\max} more rapidly with increasing U_5 (fig. 20(c)). When the value of ℓ is essentially equal to ℓ_{\max} , the interface velocity U_I is essentially equal to the incident shock velocity $U_{s,10}$, as illustrated in figure 20(d). For this sample case, the interface velocity is equal to the incident shock velocity (measured) at the tube exit for values of U_5 in excess of 5.0 km/sec.

Several expansion tunnel flow quantities (p_6 , T_6 , U_6 , M_6 , $N_{Re,6}$, ρ_{6s}/ρ_6 , and $p_{t,6}$) are shown in figure 21 as a function of effective area ratio $(A/A^*)_{\text{eff}}$. Nozzle entrance conditions (conditions at $(A/A^*)_{\text{eff}}$ of unity) correspond to a representative expansion tube test (ref. 15) with unheated helium driver gas and air test gas having a value of p_1 of 3.45 kN/m². These entrance conditions were determined by assuming no shock reflection at the secondary diaphragm, no flow attenuation in the acceleration section, and a thermochemical equilibrium expansion to region (5). The tunnel results were generated, assuming quasi one-dimensional flow, by increasing input U_6 from

5.3 to 5.5 km/sec in increments of 50 m/sec and from 5.50 to 5.57 km/sec in increments of 10 m/sec. These tunnel predictions also assume a thermochemical equilibrium expansion.

The results of figure 21 may be used to obtain a rough estimate of inviscid test core diameter and corresponding nozzle exit flow quantities for given entrance conditions. For example, use the dimensions of the Langley expansion tunnel configuration and assume that the conical nozzle has an entrance diameter of 7.62 cm, an exit diameter of 63.75 cm, and a length of 1.59 m. Hence, the geometric area ratio $(A/A^*)_{\text{geo}}$ is 70 and the nozzle half angle is 10° . Now, let $(A/A^*)_{\text{eff}}$ be equal to $(A/A^*)_{\text{geo}}$, corresponding to zero tunnel wall boundary-layer displacement thickness. The quantities M_6 and $N_{\text{Re},6}$ corresponding to this first estimate of $(A/A^*)_{\text{eff}}$ may be obtained from figure 21. From these quantities, the displacement thickness at the nozzle exit may be estimated by using simple expressions in terms of M_6 and $N_{\text{Re},6}$ based on nozzle axial distance from the nozzle apex. (See ref. 21.) (Eq. (7) of ref. 21 was used to predict δ^* for this example, where $\gamma_{E,6}$ was equal to 1.4.) Having determined an initial estimate of δ^* at the nozzle exit, a new value of $(A/A^*)_{\text{eff}}$ is calculated where the effective exit diameter is the nozzle (geometric) exit diameter minus $2\delta^*$. At the nozzle entrance, the effective entrance diameter is assumed equal to the geometric entrance diameter and hence a constant. From figure 21, M_6 and $N_{\text{Re},6}$ corresponding to this new value of $(A/A^*)_{\text{eff}}$ are obtained and a second value of δ^* is calculated. This iterative procedure is continued until successive values of $(A/A^*)_{\text{eff}}$ are within a desired tolerance. For this particular example, iteration to within 2 percent on $(A/A^*)_{\text{eff}}$ (three iterations required) showed that the inviscid test core diameter is approximately 48.5 cm. The corresponding values of M_6 and $N_{\text{Re},6}$ are 13.2 and 7.4×10^4 per meter, respectively.

CONCLUDING REMARKS

A computer program written in FORTRAN IV language which determines shock tube, expansion tube, and expansion tunnel flow quantities for real-air test gas is presented. This program permits, as input data, a number of possible combinations of flow quantities generally measured during a test. The versatility of the program is enhanced by the inclusion of such effects as a standing or totally reflected shock at the secondary diaphragm, thermochemical-equilibrium flow expansion and frozen flow expansion for the expansion tube and expansion tunnel, flow attenuation in traversing the acceleration section of the expansion tube, real air as the acceleration gas, and the effect of wall boundary layer on the acceleration section air flow. The effects of several of these phenomena are demonstrated by sample calculations.

The usage of the program in preparing the shock tube and expansion tube for testing is illustrated from working charts. These charts, which were generated with the present program, cover a wide range of flow conditions and should prove to be a convenience for the experimenter in such facilities. The expansion tunnel phase of the program is demonstrated by a sample calculation. This program is similar to, but more comprehensive than, the real-gas mixture program previously available for air test gas. The present program requires approximately 1/70 the computer time of the gas-mixture program with no appreciable sacrifice in accuracy.

Langley Research Center,
National Aeronautics and Space Administration,
Hampton, Va., September 4, 1974.

APPENDIX A

COMPUTER-PROGRAM INPUTS, FLOW CHART, AND LISTING WITH SAMPLE DATA PRINTOUTS

The present program is written in FORTRAN IV language for Control Data series 6000 computer systems. Minimum machine requirements are 110000 octal locations of core storage. The FORTRAN NAMELIST capability is used for data input with INP as the NAMELIST name. The units for the inputs which are physical quantities are given in the section entitled "Symbols." The program symbols and a brief description of the inputs necessary to utilize the computer program are listed as follows:

<u>Program symbol</u>	<u>Description</u>
P1	Pressure of quiescent test air in region ①
T1	Temperature of quiescent test air in region ①
US1	Incident-shock velocity into region ①
P2	Static pressure in region ②
P4	Driver-gas pressure in region ④
T4	Driver-gas temperature in region ④
U5	Velocity in region ⑤
P5	Static pressure in region ⑤
U6	Velocity in region ⑥
P6	Static pressure in region ⑥
DIA	Shock tube or expansion tube diameter
DIAT	Nozzle entrance diameter
DIAN	Nozzle test-section diameter

APPENDIX A

XIS	Distance downstream of primary diaphragm
XAS	Distance downstream of secondary diaphragm
TW	Model surface temperature
BNR	Model nose radius
RUN	Facility test number
NDRIV	NDRIV = 0 denotes helium driver gas NDRIV = 1 denotes hydrogen driver gas
LB	LB = 0 denotes inputs p_1 , T_1 , and $U_{s,1}$ used to find region ② quantities LB = 1 denotes inputs p_1 , T_1 , and p_2 used to find region ② quantities LB = 2 denotes inputs p_1 , T_1 , p_4 , and T_4 used to find region ② quantities
ISTET	ISTET = 0 denotes only quantities in regions ②, ②s, and ②r determined ISTET = 1 denotes shock tube and expansion tube flow quantities determined ISTET = 2 denotes shock tube, expansion tube, and expansion tunnel flow quantities determined
LF	LF = 1 denotes U_5 is basic input in region ⑤ LF = 2 denotes p_5 is basic input in region ⑤
LG	LG = 1 denotes U_6 is basic input in region ⑥ LG = 2 denotes p_6 is basic input in region ⑥
ISAV	ISAV = 1 denotes use of AEDC real-air tape (subroutines SLOW and SEARCH) ISAV = 2 denotes use of AEDC real-air curve fits (subroutine SAVE)

APPENDIX A

INU	INU = 1 denotes use of AEDC real-air tape in determining flow nonuniformities in region (2) INU = 2 denotes use of AEDC real-air curve fits in determining flow nonuniformities in region (2)
IEXP	IEXP = 1 denotes use of AEDC real-air tape in determining unsteady expansion process for expansion tube IEXP = 2 denotes use of AEDC real-air curve fits in determining unsteady expansion process for expansion tube
JAC	Number of enthalpy increments used in unsteady expansion from region (A) for IEXP = 1 (300 maximum)
IAC	Number of pressure increments used in unsteady expansion from region (A) for IEXP = 2 (100 maximum)
IREP	IREP = 1 denotes only a single value of U_5 is of interest for given region (A) quantities IREP = 2 denotes several U_5 of interest for given region (A) quantities
U5I	Velocity increment for IREP = 2
NVEL	Total number of U_5 of interest for IREP = 2 (10 maximum)
DELU5	Difference between maximum and minimum interface velocity along acceleration section
LREP	LREP = 1 denotes only a single value of U_6 is of interest for given region (5) quantities LREP = 2 denotes several U_6 values of interest for given region (5) quantities
NUMU6	Total number of U_6 of interest for LREP = 2 (10 maximum)
U6I	Velocity increment for LREP = 2

APPENDIX A

LD

LD = 1 denotes no shock reflection at secondary diaphragm

LD = 2 denotes existence of standing shock at secondary diaphragm for ISTET = 1; for ISTET = 0, LD = 2 denotes conditions in regions (2), (2s), (t2), and (2r) determined

LD = 3 denotes existence of totally reflected shock from secondary diaphragm

LD = 4 denotes all three cases (LD = 1, LD = 2, and LD = 3) are performed

To minimize the number of inputs required for running cases on the computer, inputs are assigned values within the program. These assigned values, which represent values most commonly used for data reduction in the Langley 6-inch expansion tube, are as follows:

<u>Program symbol</u>	<u>Assigned value</u>
T1	300.
DIA	0.1524
DIAT	0.0762
DIAN	0.6452
XIS	4.65
XAS	16.98
TW	300.
RUN	1.0
BNR	0.0254
NDRIV	0
LB	0
ISTET	1
LF	1
LG	1
ISAV	2
IEXP	1
JAC	50
IAC	50

APPENDIX A

<u>Program symbol</u>	<u>Assigned value</u>
IREP	2
NVEL	8
U5I	400.
LD	4
INU	2
DELU5	0.
LREP	2
NUMU6	5
U6I	50.

Each of these values may be changed from its assigned value by a card change or inclusion in the NAMELIST INP. For a given LB, only the basic parameters p_1 , T_1 , and $U_{s,1}$ (LB = 0), p_2 (LB = 1), or p_4 and T_4 (LB = 2) need be included in INP. Similarly, for a given LF, only U_5 (LF = 1) or p_5 (LF = 2) need be included in INP; for a given LG, only U_6 (LG = 1) or p_6 (LG = 2) need be included in INP.

Three options exist for determining flow conditions in region (5) for LF equal to 1 or LF equal to 2. These options, in terms of inputs ISAV and IEXP, are

Option	ISAV	IEXP
(1)	1	1
(2)	2	1
(3)	2	2

Thus, for option (1), the AEDC real-air tape is used as the source of real-air thermodynamic properties necessary to generate tables of h as a function of a^{-1} required for numerical integration. Corresponding flow properties in region (5) are also obtained from the tape. For option (2), the tape is used for the numerical integration and for obtaining conditions in region (5), whereas real-air curve-fit expressions are used to obtain corresponding flow properties for the other flow regions (that is, regions (2), (2s), (2r), (5s), and (t5)). Curve-fit expressions are used in option (3) for the integration and determination of corresponding properties. Option (1) will provide the highest accuracy (appendix B) in calculated flow parameters and demand the most computer time, whereas option (3) will have the lowest accuracy but fastest computational time.

APPENDIX A

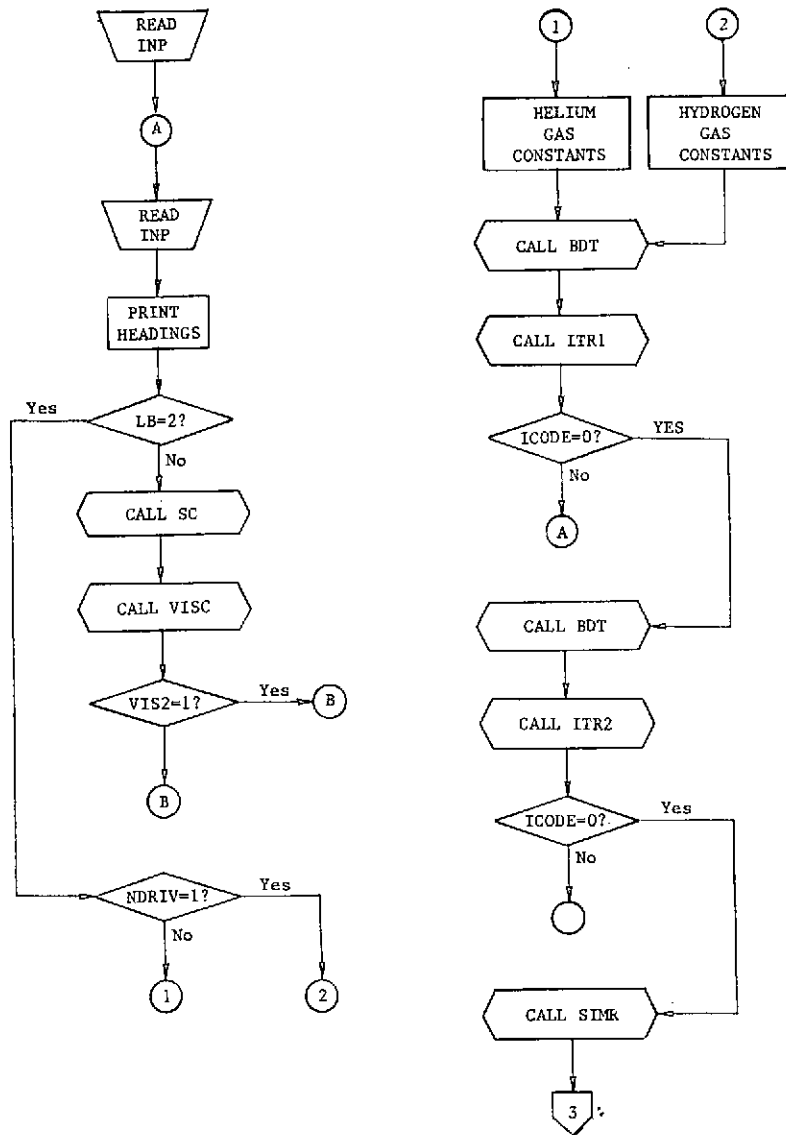
The basic subroutines of this program are as follows:

- (1) SLOW – determines imperfect, real-air thermodynamic quantities p , ρ , h , T , a , Z , γ_E , and Z^* from AEDC real-air tape for given sw_u/R and any one of the thermodynamic quantities
- (2) SEARCH – determines imperfect, real-air thermodynamic quantities ρ , sw_u/R , T , a , Z , γ_E , and Z^* from AEDC real-air tape for given p and h
- (3) SAVE – determines real-air thermodynamic quantities from AEDC real-air curve-fit expressions with combinations
 - (1) p and sw_u/R
 - (2) p and ρ
 - (3) p and h
 - (4) ρ and h
 - (5) p and T
- (4) VISC – computes real-air μ for given p and T
- (5) BDT – computes virial coefficients for helium or hydrogen for given T
- (6) SOLUT – given (p_2, U_2) array and (p_3, U_3) array, finds solution to curves
- (7) SC – iterative procedure for solving conservation relations for a moving normal shock
- (8) SNS – iterative procedure for solving conservation relations for a standing shock at secondary diaphragm or a normal bow shock at a model, including stagnation-point conditions
- (9) SIMR – computes $\int \left(\frac{dh}{a} \right)_{sw_u/R}$ by Simpson's rule

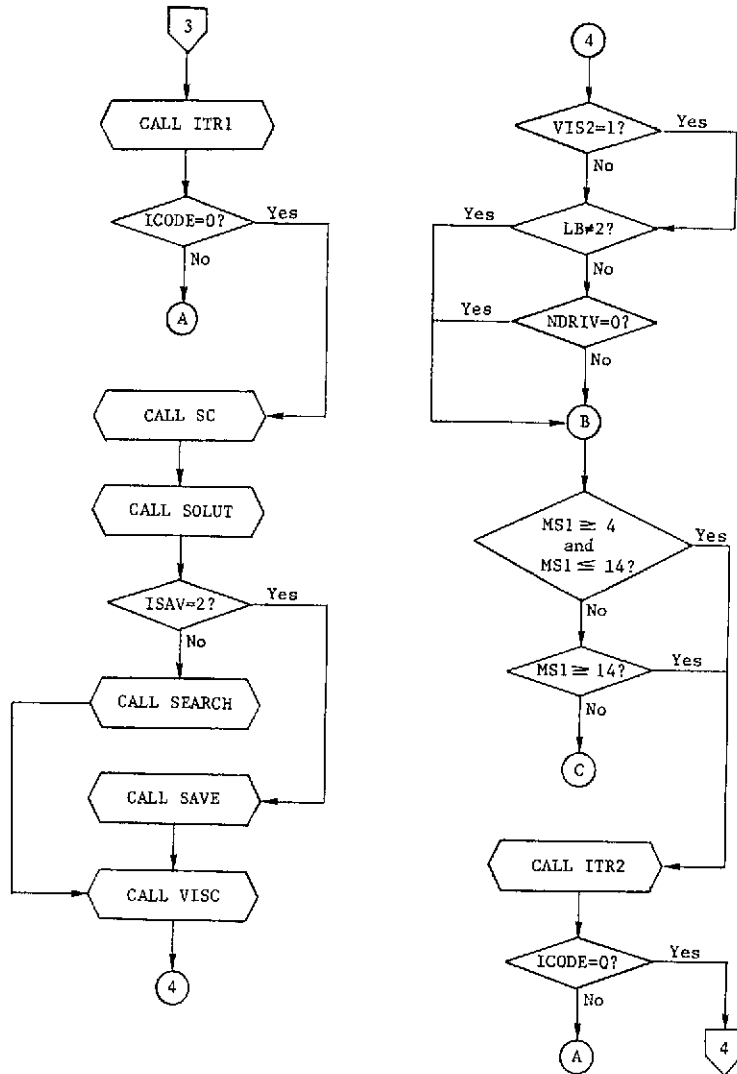
Langley Library Subroutines ITR1, ITR2, FTLUP, and DISCOT are used with this program and are presented as appendixes C, D, E, and F.

A flow chart of this program is given on the following pages.

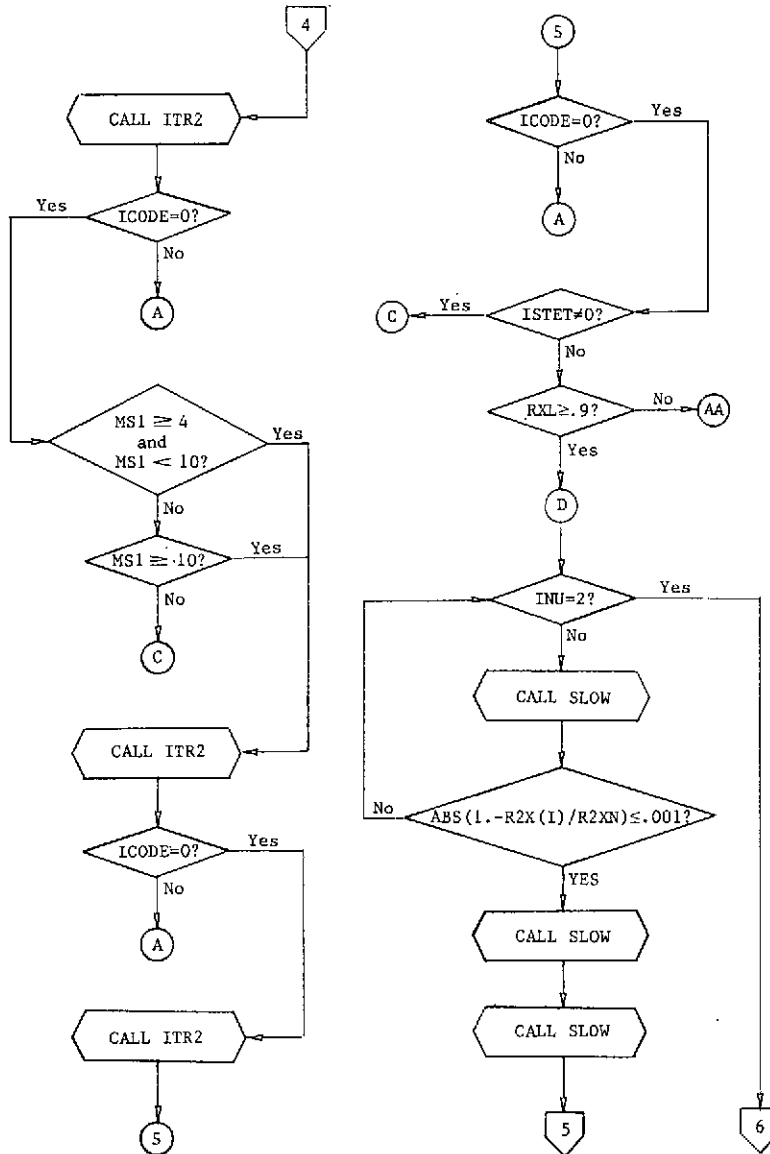
APPENDIX A



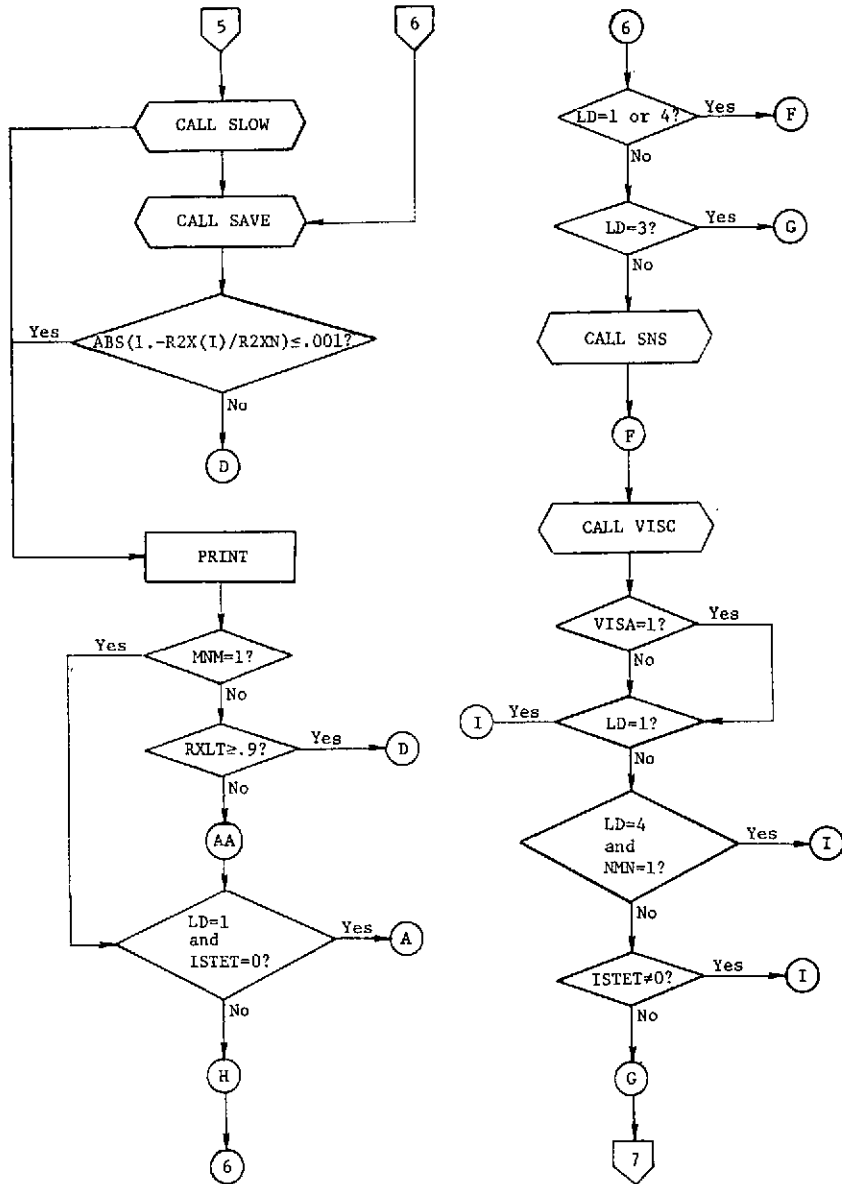
APPENDIX A



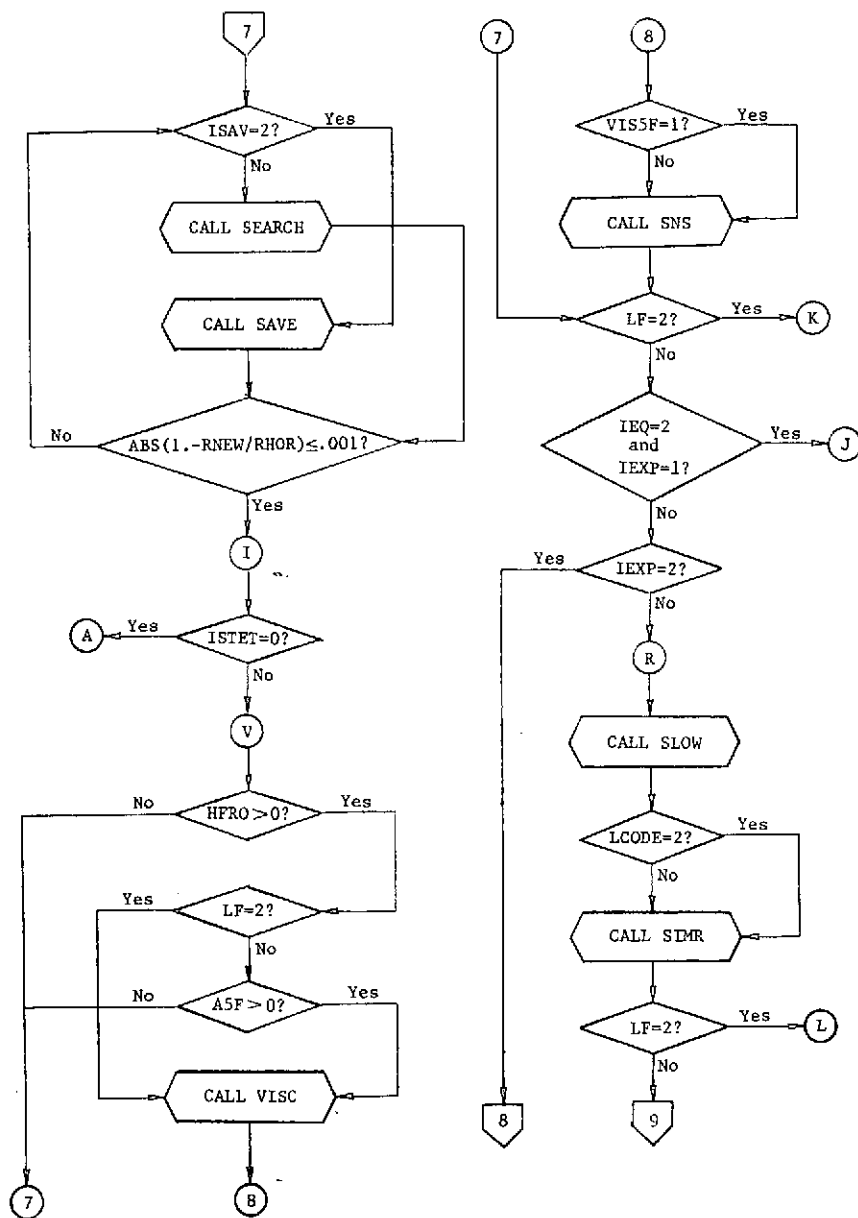
APPENDIX A



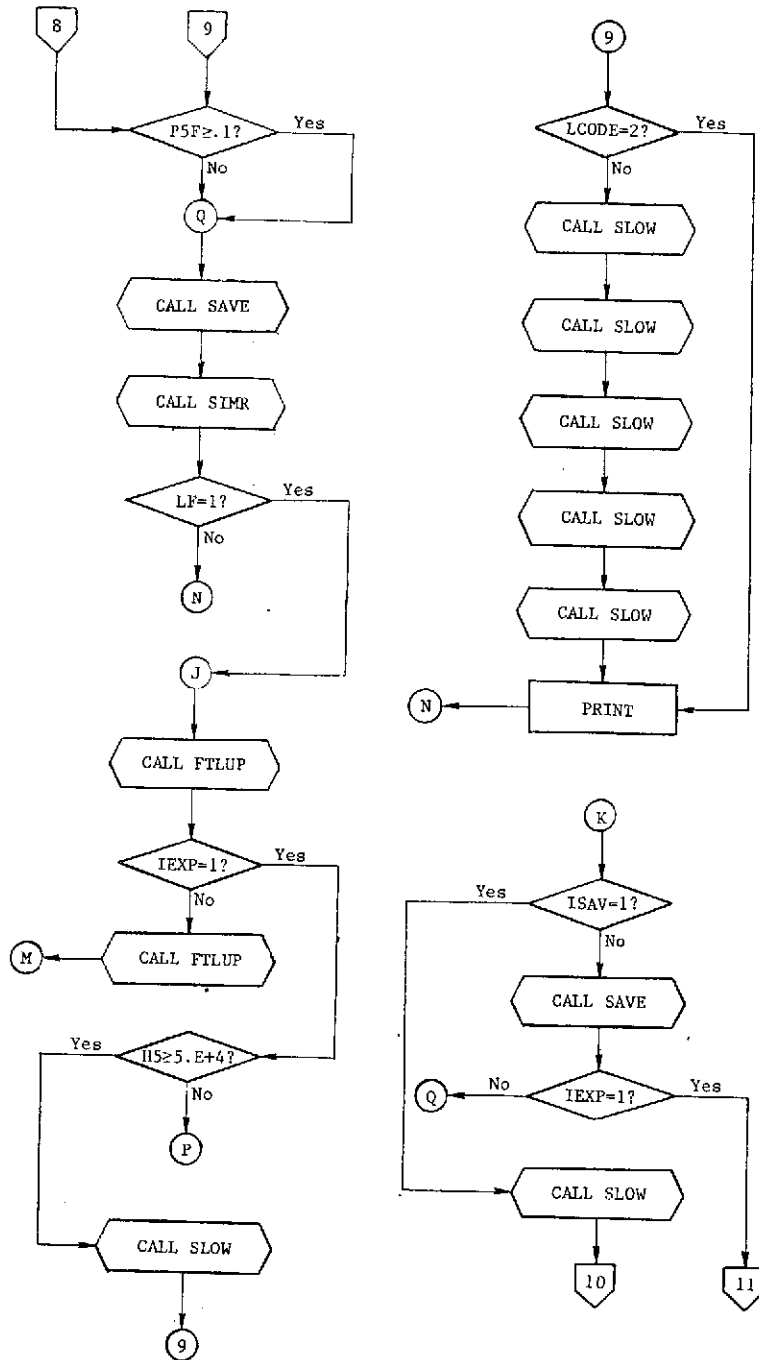
APPENDIX A



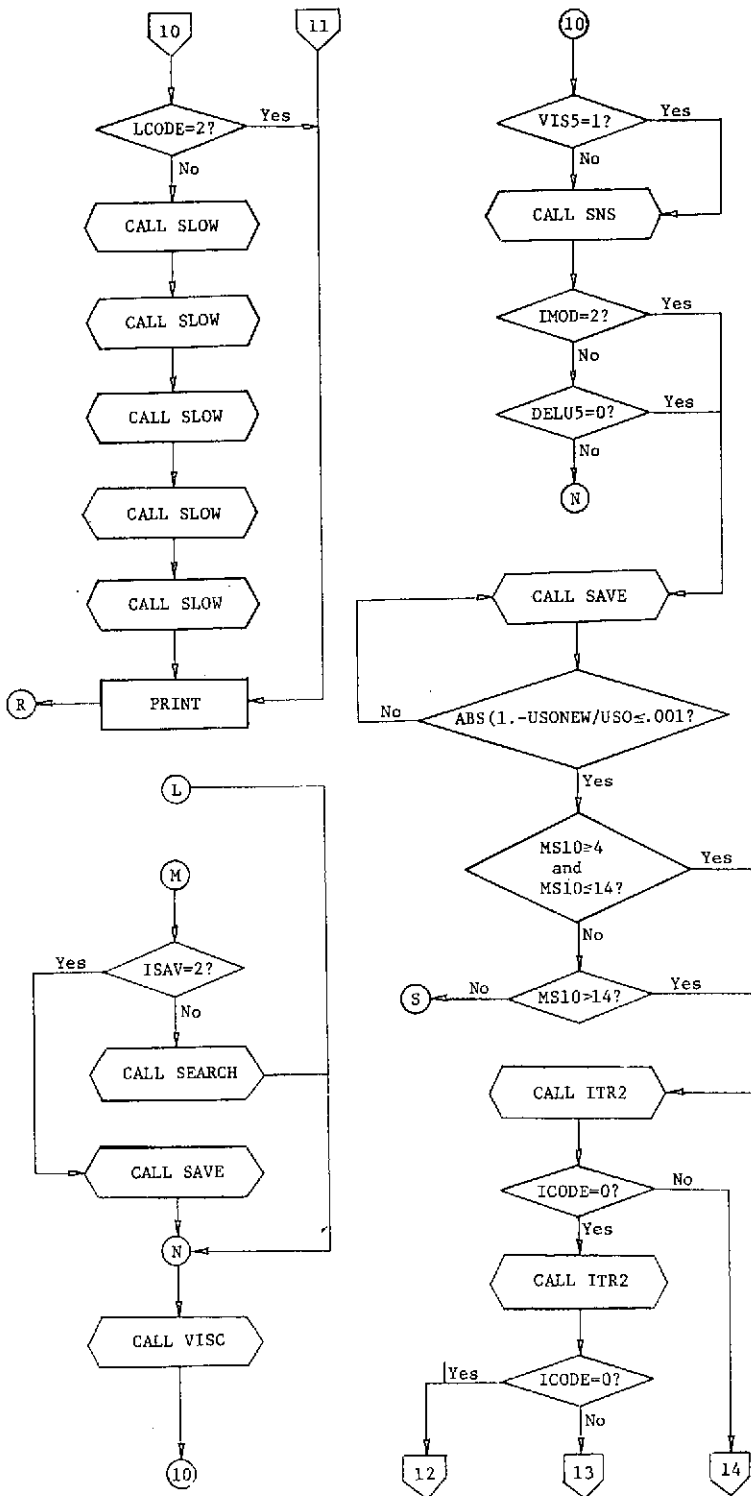
APPENDIX A



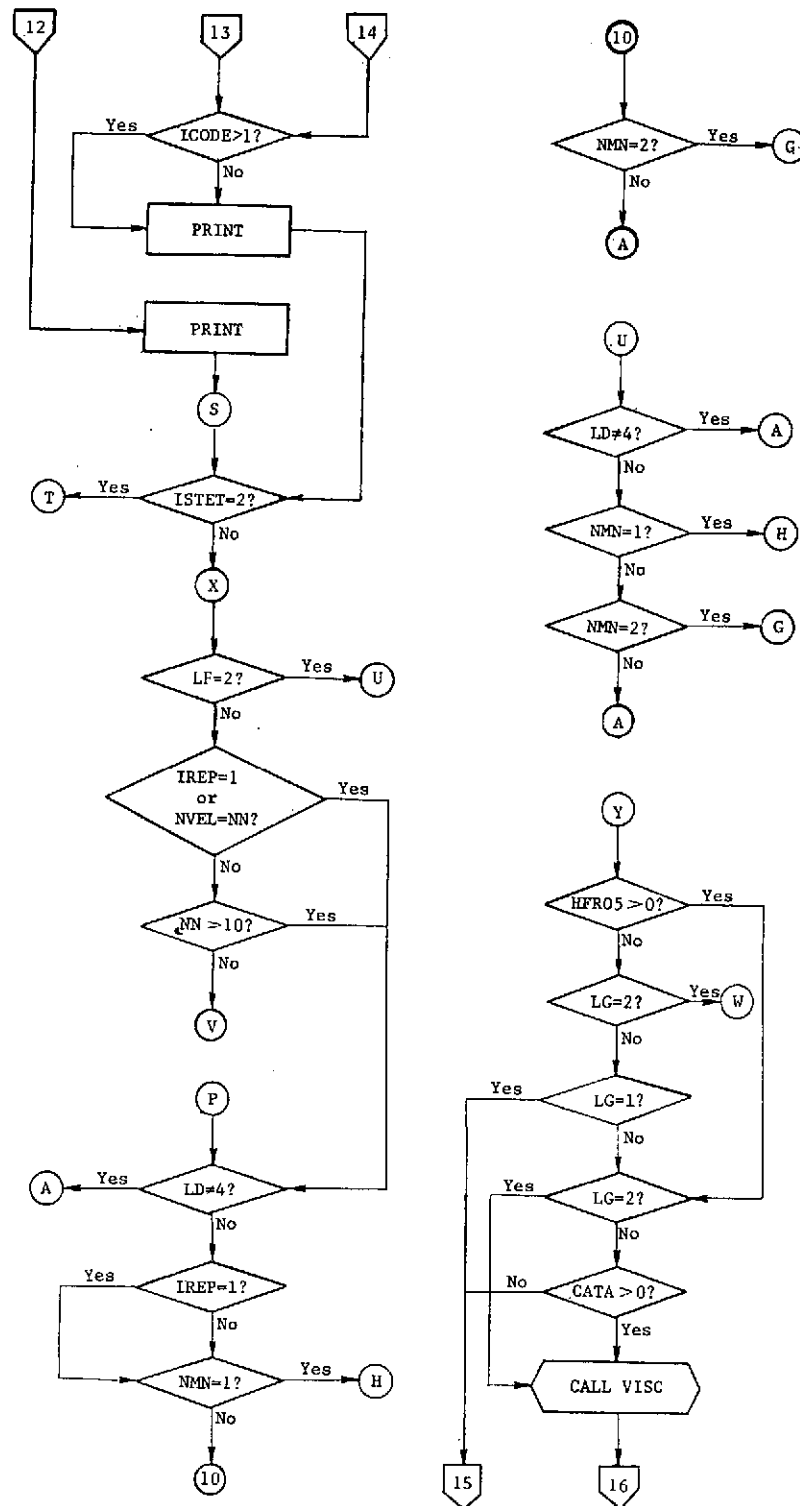
APPENDIX A



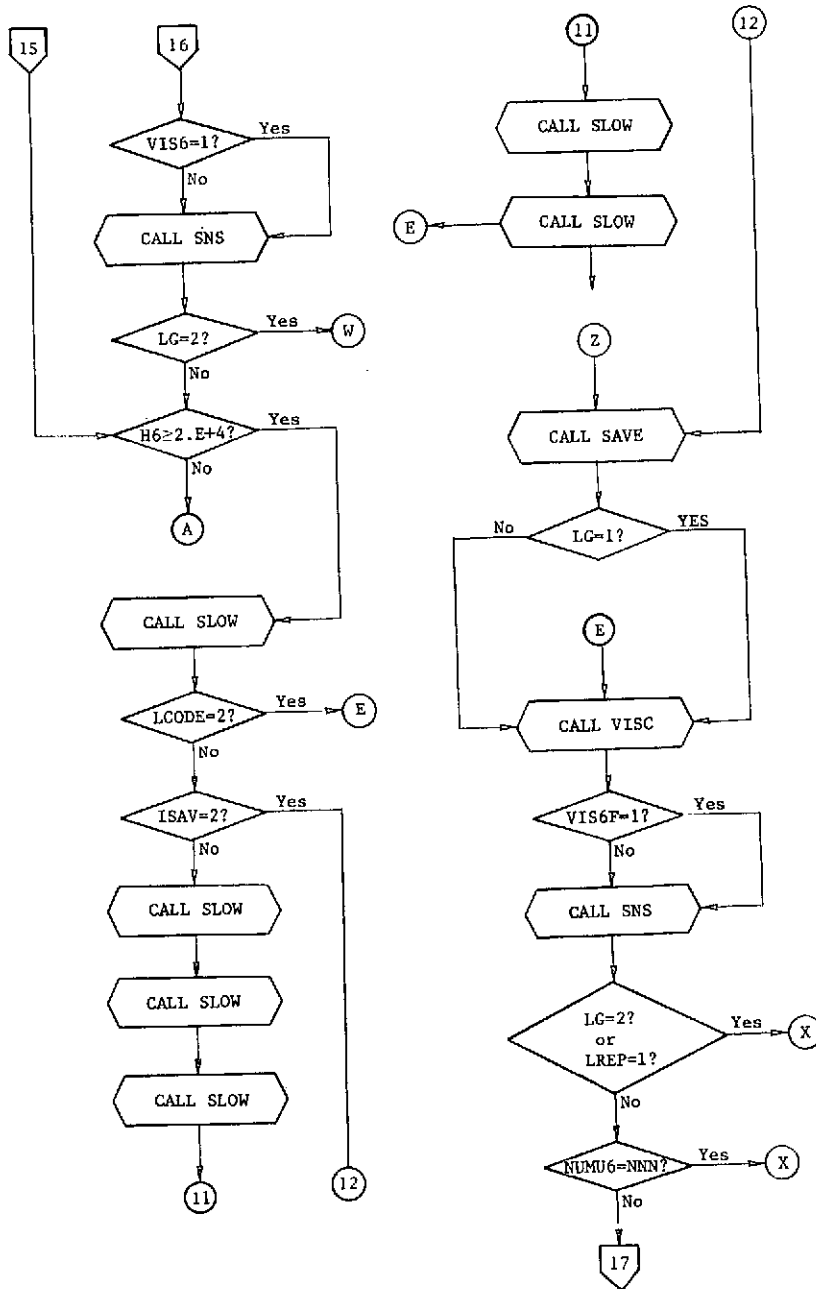
APPENDIX A



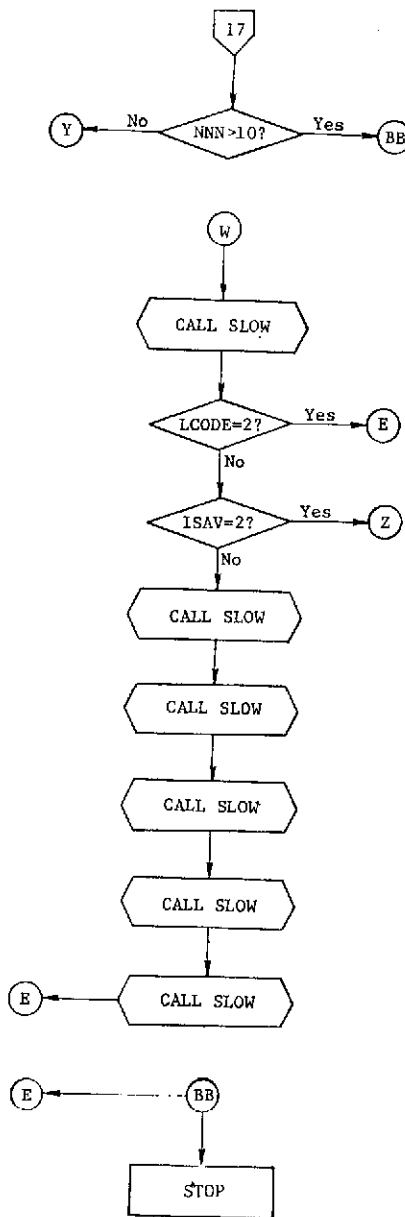
APPENDIX A



APPENDIX A



APPENDIX A



APPENDIX A

A listing of this program, including subroutines and comments, is reproduced on the following pages.

```

JOB.1.0700.115000.20000.      A3187  D3348      100690      1250      CENT
USER:MILLER, CHARLES G III      000605575N 64720
LINECNT(20000).
RUN(S).
REQUEST,TAPF8,HY,X.      716011,R0L
REWIND(TAPF8).
SETINDF. .
LGO. .
SPPRINT(OUTPUT,3).
UNLOAD(TAPF8).
EXIT..
SPPRINT(OUTPUT,3).
UNLOAD(TAPF8).
- .
PROGRAM LFT(INPUT,OUTPUT,TAPF5=INPUT,TAPF6=OUTPUT,TAPF8)
DIMENSION X(4), Y(4,9,150), Z(9), U(4), V(4), W(4), NP(4)
DIMENSION TAPHR(300), TARA(300), TABANS(300), TARR(100), P5G(100)
DIMENSION RESULT(2), IN(4), P5K(100)
DIMENSION TARTI(50), TARRI(50), TARRI(50), TAPZI(50), TAPHI(50)
DIMENSION TAPAI(50), TAPUI(50), YA(10)
DIMENSION US1I(20), U2I(20), P2I(20), H2I(20), PH2I(20)
DIMENSION XSLM(5), BNON(5), P2X(5), U2X(5), H2X(5), T2X(5), P2Y(5)
1. A2X(5), QXR(5), PYH(5), RXU(5), PXR(5), PXT(5), PYA(5)
REAL MS1,M2,M5,M55,MX,MN,MNS,MS,MA,M5F,M55F,M555F,MP,M20
REAL M6,M65,M6F,M65F,M655F,M510
EXTERNAL FOFX,FOFX,FOFMS,FOFAX,FOFXY,FOFAXT,FOFXT
COMMON ICOUNT,IMET(2),NP,ARAP,ME,ME,SAP,LCODE,DELU,ISAV
COMMON /BLK1/ PT4,CT4,RHOG
COMMON /BLK2/ RT1,CT1,T1,CVR1,SAP,SRFF,ORT1,OPT1
COMMON /BLK3/ T1,GAM4,W4,T4,P4,P1
COMMON /BLK4/ LF,NON,LU,NDRIV,LR,LD,LG
COMMON /BLK5/ SR,T11,AT,ZI,CI,K,P2,ISP
COMMON /BLK6/ BETA1,BETA2
NAMELIST /INP/ T1,P1,US1,P2,LR,LD,LF,LG,U5,P5,P6,U6,P4,T4,IAC,RUN,
11STET,DIA,NDRIV,XIS,XAS,TW,BMP,ISAV,IFXD,US1,1REF,NVCL,INU,DIAT,OT
2AN,LREP,NUMU6,U61,JAC,DELU5
CALL DAYTIM (RESULT)
C
C SHOCK TUBE PHASE
C
C NDRIV=0 DENOTES IMPERFECT HELIUM DRIVER GAS
C NDRIV=1 DENOTES IMPERFECT HYDROGEN GAS
C
C LR=0 DENOTES SHOCK TUBE INPUTS P1,T1,US1
C LR=1 DENOTES SHOCK TUBE INPUTS P1,T1,P2
C LR=2 DENOTES SHOCK TUBE INPUTS P1,T1,P4,T4
C
C XIS IS DISTANCE DOWNSTREAM FROM PRIMARY DIAPHRAGM
C XAS IS DISTANCE DOWNSTREAM FROM SECONDARY DIAPHRAGM
C
C DIA IS SHOCK TUBE OR EXPANSION TUBE DIAMETER
C DIAT IS NOZZLE THROAT DIAMETER
C DIAN IS NOZZLE TEST SECTION DIAMETER
C
C 1STET DENOTES PHASE(S) CALCULATED
C 1STET=0 DENOTES SHOCK TUBE PHASE ONLY
C 1STET=1 DENOTES EXPANSION TUBE PHASE
C 1STET=2 DENOTES EXPANSION TUNNEL PHASE
C
C ISAV=1 DENOTES USE OF REAL AIR TAPE (SLOW SEARCH)
C ISAV=2 DENOTES USE OF AEDC CURVE FITS (SAVE)
C

```

APPENDIX A

C		A	48
C	INU=1 DENOTES USE OF TAPE FOR FLOW NONUNIFORMITY CALC IN REGION 2	A	49
C	INU=2 DENOTES USE OF CURVE FITS FOR FLOW NONUNIFORMITY IN REGION 2	A	50
C		A	51
C	LD=1 DENOTES INCIDENT SHOCK ONLY	A	52
C	LD=2 DENOTES STANDING SHOCK ONLY	A	53
C	LD=3 DENOTES REFLECTED SHOCK ONLY	A	54
C	LD=4 DENOTES INCIDENT, STANDING, AND REFLECTED SHOCKS	A	55
C		A	56
C	FOR ISTET=0 AND LD=2, CONDITIONS IN REGIONS 2, 2S, 2T, 2B DETERMINED	A	57
C		A	58
C	IFXP=1 DENOTES USE OF TAPE FOR UNSTEADY EXPANSION	A	59
C	IFXP=2 DENOTES USE OF CURVE FITS FOR UNSTEADY EXPANSION	A	60
C		A	61
C	JAC IS NUMBER OF INCREMENTS USED IN UNSTEADY EXPANSION FOR IXP=1	A	62
C	JAC HAS MAXIMUM VALUE OF 300	A	63
C		A	64
C	IAC IS NUMBER OF INCREMENTS USED IN UNSTEADY EXPANSION FOR IXP=2	A	65
C	IAC HAS MAXIMUM VALUE OF 100	A	66
C		A	67
C	DELUS IS ATTENUATION IN INTERFACE VELOCITY US, M/SEC	A	68
C		A	69
C	IREP=1 DENOTES SINGLE VALUE OF US OF INTEREST	A	70
C	IREP=2 DENOTES SEVERAL US OF INTEREST	A	71
C		A	72
C	US1 IS US INCREMENT FOR IREP=2	A	73
C	NVEL IS TOTAL NUMBER OF US OF INTEREST FOR IREP=2	A	74
C		A	75
C	LRFP=1 DENOTES SINGLE VALUE OF U6 OF INTEREST	A	76
C	LRFP=2 DENOTES SEVERAL U6 OF INTEREST	A	77
C		A	78
C	U61 IS U6 INCREMENT FOR LRFP=2	A	79
C	NUMU6 IS TOTAL NUMBER OF U6 OF INTEREST FOR LRFP=2	A	80
C		A	81
	IT=8	A	82
	NV=0	A	83
	RU=9.71434E+3	A	84
	W=28.967	A	85
	MM=0	A	86
	READ (5,234) IN	A	87
1	US1=P2=P4=T4=US=P5=U6=P6=DELUS=0.0	A	88
	NN=NNN=LB=NDPRIV=0	A	89
	NMN=RU=ISTET=LF=IFXP=LG=ISP=1	A	90
	ISAV=IREP=LRFP=INU=2	A	91
	LD=4	A	92
	NVEL=8	A	93
	NUMU6=5	A	94
	JAC=IAC=50	A	95
	T1=TW=300.	A	96
	DIA=.1524	A	97
	DIA7=.0762	A	98
	DIA8=.6452	A	99
	XIS=4.65	A	100
	XAS=16.08	A	101
	BNR=.0254	A	102
	USI=400.	A	103
	U6I=50.	A	104
	READ (5,INP)	A	105
	IF (ENDFILE 5) 144,2	A	106
2	CONTINUE	A	107
	PRINT 235, RESULT(1)	A	108
	PRINT 234, IN	A	109
	PRINT 148	A	110
	PRINT 149	A	111
	PRINT 150	A	112
	PRINT 151	A	113

APPENDIX A

	PRINT 152	A 114
	PRINT 153, RUN, P1, T1, US1, P2, P4, T4, X15, DIA, ISAV, INU, LD	A 115
	IMET(1)=IMET(2)=0	A 116
	LCODE=1	A 117
	SSUM=0.	A 118
	LU=0	A 119
	K=3	A 120
	HW=1.0046E+3*TW	A 121
	RHO1=(P1*W)/(RU*T1)	A 122
	H1=3.49*(RU/W)*T1	A 123
	A1=SQRT(1.4*(RU/W)*T1)	A 124
	IF (LB.EQ.2) GO TO 4	A 125
C		A 126
C	INPUTS P1, T1, AND US1(LB=0)	A 127
C	INPUTS P1, T1, AND P2(LB=1)	A 128
C		A 129
	CALL SC (RHO2, U2, P2, H2, RHO1, US1, P1, H1, ISAV)	A 130
	S2R=SR	A 131
	T2=T11	A 132
	A2=A1	A 133
	Z2=Z1	A 134
	GAM2=G1	A 135
	M2=U2/A2	A 136
	MS1=US1/A1	A 137
	RF2=0.0	A 138
	CALL VISC (T2, P2, VIS2)	A 139
	IF (VIS2.EQ.1.0) GO TO 3	A 140
	RF2=RHO2*U2/VIS2	A 141
3	CONTINUE	A 142
	GO TO 31	A 143
C		A 144
C	INPUTS P4, T4, P1, AND T1(LB=2)	A 145
C		A 146
4	LU=20	A 147
	R=8.31434E+3	A 148
	IF (NDRIV.EQ.1) GO TO 5	A 149
C		A 150
C	HELIUM DRIVER GAS(NDRIV=0)	A 151
C		A 152
	HWRT=2.5	A 153
	CVR1=1.5	A 154
	SREF=4.8024	A 155
	GAM4=1.66667	A 156
	W4=4.003	A 157
	RHOG=(P4*W4)/(R*T4)	A 158
	ALOW=.70*RHOG	A 159
	GO TO 6	A 160
C		A 161
C	HYDROGEN DRIVER GAS(NDRIV=1)	A 162
C		A 163
5	HWRT=3.5	A 164
	CVR1=2.5	A 165
	SREF=-1.0363	A 166
	GAM4=1.4	A 167
	W4=2.016	A 168
	RHOG=(P4*W4)/(R*T4)	A 169
	ALOW=.50*RHOG	A 170
6	AUP=1.05*RHOG	A 171
	DELTIX=(AUP-ALOW)/100.	A 172
	E1=.1E-6	A 173
	CALL BDT (BT4, CT4, DBT4, DCT4, D2BT4, D2CT4, T4)	A 174
	RHO4=1.2*RHOG	A 175
	CALL ITR1 (RHO4, DELTIX, FOFX, F1, E1, 200, ICODE)	A 176
	IF (ICODE) 7, 10, 7	A 177
7	GO TO (8, 9, 9, 9), ICODE	A 178
8	PRINT 154	A 179
	GO TO 1	A 180

APPENDIX A

```

9      PRINT 155, ICODE                                A 181
      GO TO 1                                            A 182
10     Z4=1.+RH04*BT4+RH04**2*CT4                      A 183
      H4=(R*T4/W4)*(HWRT+RH04*(BT4-T4*DBT4)+(RH04**2/2.)*(2.*CT4-T4*DCT4
11     ))                                              A 184
      S4R=CVRI*ALOG(T4)-ALOG(RH04)-RH04*(BT4+T4*DBT4)-(RH04**2/2.)*(CT4+
12     T4*DCT4)+SRFF                                  A 185
      CVR=CVRI-T4*(RH04*(2.*DBT4+T4*D2BT4)+(RH04**2/2.)*(2.*DCT4+T4*D2CT
13     ))                                              A 186
      PPTR=(RH04*R/W4)*(1.+RH04*(BT4+T4*DBT4)+(RH04**2)*(CT4+T4*DCT4))
      PPRT=(T4*R/W4)*(1.+2.*RH04*BT4+3.*RH04**2*CT4)
      A4=SQRT(PPRT+((T4*W4)/(CVR*R*RH04**2))*PPTR**2)
      TABTI(1)=T4                                     A 187
      TABPI(1)=P4                                     A 188
      TABRI(1)=RH04                                  A 189
      TABZI(1)=Z4                                     A 190
      TABHI(1)=H4                                     A 191
      TABAI(1)=1./A4                                  A 192
      TSC=ALOG10(T4)                                  A 193
      DELT=TSC/50.                                    A 194
      NU=1                                             A 195
      DO 11 I=2,50                                    A 196
      TABTI(I)=TSC-FLOAT(I-1)*DELT                    A 197
      TABTI(I)=10.**TABTI(I)                          A 198
11     CONTINUE                                       A 199
      AUP=1.1*RH04                                    A 200
      ALLOW=1.E-6                                     A 201
      DELR=(AUP-ALLOW)/200.                          A 202
      RI=RH04                                         A 203
      DO 17 I=2,50                                    A 204
      TI=TABTI(I)                                     A 205
      IF (TI.LT.3.) GO TO 18                          A 206
      CALL BDT (BTI,CTI,DBTI,DCTI,D2BTI,D2CTI,TI)
      CALL ITR2 (RI,ALLOW,AUP,DEL,R,FOFR,F1,F1,400,ICODE)
      IF (ICODE) 12,16,12                             A 207
12     GO TO (13,14,14,15), ICODE                    A 208
13     PRINT 154                                     A 209
      GO TO 1                                          A 210
14     PRINT 155, ICODE                               A 211
      GO TO 1                                          A 212
15     PRINT 156, ICODE,RI,DEL,R                     A 213
      GO TO 1                                          A 214
16     TABRI(I)=RI                                    A 215
      TABZI(I)=1.+RI*BTI+RI**2*CTI                    A 216
      TABPI(I)=TI*(R/W4)*RI*TABZI(I)                  A 217
      TABHI(I)=(R*TI/W4)*(HWRT+RI*(BTI-TI*DBTI)+(RI**2/2.)*(2.*CTI-TI*DCT
17     ))                                              A 218
      CVIR=CVRI-TI*(RI*(2.*DBTI+TI*D2BTI)+(RI**2/2.)*(2.*DCTI+TI*D2CTI))
      PPTRI=(RI*R/W4)*(1.+RI*(BTI+TI*DBTI)+(RI**2)*(CTI+TI*DCTI))
      PPRTI=(TI*R/W4)*(1.+2.*RI*BTI+3.*RI**2*CTI)
      TABAI(I)=1./(SQRT(PPRTI+((TI*W4)/(CVIR*R*RI**2))*PPTRI**2))
      NU=NU+1                                         A 219
17     CONTINUE                                       A 220
18     CALL SIMR (TABHI,TABAI,NU,NU,TABANS)            A 221
      PRINT 157                                       A 222
      DO 19 I=1,NU                                    A 223
      PRINT 158, TABPI(I),TABTI(I),TABRI(I),TABZI(I),TABHI(I),TABAI(I),T
19     TABANS(I)                                       A 224
      CONTINUE                                       A 225
      MS=1.4                                          A 226
      DELS=.2                                         A 227
      CALL ITR1 (MS,DELS,FOFMS,F1,E1,200,ICODE)
      IF (ICODE) 20,23,20                             A 228
20     GO TO (21,22,22), ICODE                       A 229
21     PRINT 154                                     A 230
      GO TO 1                                          A 231

```

APPENDIX A

22	PRINT 155, ICODE	A 247
	GO TO 1	A 248
23	A1=SQRT(401.839*TI)	A 249
	USMAX=.1*A1*MS	A 250
	USMIN=.65*USMAX	A 251
	US1(I)=USMAX	A 252
	DFL1=(USMAX-USMIN)/20.	A 253
	PRINT 159	A 254
	DO 24 I=1,20	A 255
	US1(I)=USMAX-FLOAT(I-1)*DFL1	A 256
	CALL SC (RH2(I),U2(I),P2(I),H2(I),RH01,US1(I),P1,H1,ISAV)	A 257
	PRINT 160, P2(I),RH2(I),H2(I),U2(I),US1(I)	A 258
24	CONTINUE	A 259
	CALL SOLUT (TABANS,TABPI,U2,P2,NU,20,UR,P)	A 260
	P2=P	A 261
	U2=UP	A 262
	US1=(P2-P1)/(RH01*U2)	A 263
	MS1=US1/A1	A 264
	H2=H1+.5*US1**2-.5*(US1-U2)**2	A 265
	GO TO (25,26), ISAV	A 266
25	CALL SEARCH (P2,RH02,H2,S2R,T2,A2,Z2,GAM2,ZS2,ISP)	A 267
	GO TO 27	A 268
26	CALL SAVE (P2,RH02,H2,S2R,T2,A2,Z2,GAM2,Z)	A 269
	ZS2=Z2	A 270
27	M2=U2/A2	A 271
	RF2=0.0	A 272
	CALL VISC (T2,P2,VIS2)	A 273
	IF (VIS2.EQ.1.0) GO TO 28	A 274
	RF2=RHO2*U2/VIS2	A 275
28	CONTINUE	A 276
	IF (LB.NE.2) GO TO 31	A 277
	IF (NDRIV.EQ.0) GO TO 29	A 278
	PRINT 161	A 279
	GO TO 30	A 280
29	PRINT 162	A 281
30	PRINT 163	A 282
	PRINT 164	A 283
	PRINT 165, P4,RH04,T4,H4,S4R,Z4,A4,W4	A 284
31	PRINT 147	A 285
	PRINT 166	A 286
	PRINT 147	A 287
	PRINT 167	A 288
	PRINT 168, P2,RH02,T2,H2,S2R,Z2,GAM2,A2,U2,M2,RF2	A 289
	RAP=P2/P1	A 290
	RAPHO=RHO2/RHO1	A 291
	RAT=T2/T1	A 292
	RAH=H2/H1	A 293
	RAA=A2/A1	A 294
	PRINT 169	A 295
	PRINT 170	A 296
	PRINT 171, RAP,RAPHO,RAT,RAH,RAA,MS1,US1	A 297
C		A 298
C	SHOCK TUBE TEST TIME-REFERENCE MIRELS(PHYS OF FLUIDS,SEPT 1963)	A 299
C		A 300
	PRINT 172	A 301
	PRINT 173	A 302
	IF (MS1.GE.4.0.AND.MS1.LE.14.0) GO TO 32	A 303
	IF (MS1.GT.14.0) GO TO 33	A 304
	PRINT 174	A 305
	GO TO 55	A 306
C		A 307
C	XLMAX IS MAXIMUM SEPARATION DISTANCE-SHOCK TO INTERFACE	A 308
C	XL IS SEPARATION DISTANCE-SHOCK TO INTERFACE	A 309
C		A 310
C	LAMINAR CASE	A 311
C		A 312

APPENDIX A

32	XLMAX=P1*DIA**2*(2.06-.2056*MS1+8.095E-3*MS1**2)	A 313
	GO TO 34	A 314
33	XLMAX=P1*DIA**2*(.8723-7.488E-3*MS1)	A 315
34	BETA1=XIS*RHO1/(2.*XLMAX*RHO2)	A 316
	BETA2=2.*RHO2/RHO1	A 317
	AXUP=.999999999	A 318
	AXLOW=.00001	A 319
	DELTAX=(AXUP-AXLOW)/100.	A 320
	E1=.1E-6	A 321
	AX=.5	A 322
	CALL ITR2 (AX,AXLOW,AXUP,DELTAX,FOFAX,E1,E1,200,ICODE)	A 323
	IF (ICODE) 7,35,7	A 324
C		A 325
C	RXL IS RATIO OF XL TO XLMAX	A 326
C		A 327
35	RXL=AX**2	A 328
	XL=RXL*XLMAX	A 329
C		A 330
C	TAUI IS IDEAL TEST TIME	A 331
C		A 332
	TAUI=RHO1*XIS/(RHO2*U2)	A 333
C		A 334
C	BX IS SQRT OF US1*TAU/XLMAX	A 335
C		A 336
	BXUP=.999999999	A 337
	BXLOW=.00001	A 338
	DELTBX=(BXUP-BXLOW)/100.	A 339
	BX=.5	A 340
	CALL ITR2 (BX,BXLOW,BXUP,DELTBX,FOFBX,E1,E1,200,ICODE)	A 341
	IF (ICODE) 7,36,7	A 342
36	TAU=BX**2*XLMAX/US1	A 343
	UI=XL/TAU	A 344
C		A 345
C	TURBULENT CASE	A 346
C		A 347
	IF (MS1.GE.4..AND.MS1.LT.10.) GO TO 37	A 348
	IF (MS1.GE.10.) GO TO 38	A 349
	PRINT 174	A 350
	GO TO 55	A 351
37	XLMAXT=(P1**25)*(DIA**1.25)*(5.2729-.751385*MS1+.03435*MS1**2)	A 352
	GO TO 39	A 353
38	XLMAXT=(P1**25)*(DIA**1.25)*(1.5464-.030174*MS1)	A 354
39	DELA XT=DELTAX	A 355
	AXT=.5	A 356
	BETA1=XIS*RHO1/(2.*XLMAXT*RHO2)	A 357
	CALL ITR2 (AXT,AXLOW,AXUP,DELA XT,FOFAXT,E1,E1,200,ICODE)	A 358
	IF (ICODE) 7,40,7	A 359
C		A 360
C	RXLT IS RATIO OF XLT TO LTMXT(TURBULENT CASE)	A 361
C		A 362
40	RXLT=AXT**5	A 363
	XLT=RXLT*XLMAXT	A 364
	BXTUP=.999999999	A 365
	BXTLOW=.00001	A 366
	DELBXT=(BXTUP-BXTLOW)/100.	A 367
	BXT=.5	A 368
	CALL ITR2 (BXT,BXTLOW,BXTUP,DELBXT,FOFBXT,E1,E1,200,ICODE)	A 369
	IF (ICODE) 7,41,7	A 370
41	TAUT=BXT**5*XLMAXT/US1	A 371
"	UIT=XLT/TAUT	A 372
	PRINT 175, XLMAX,XL,RXL,TAU,UI,XLMAXT,XLT,RXLT,TAUT,UIT,TAUI	A 373
	IF (ISTET.NF.0) GO TO 55	A 374
C		A 375
C	SHOCK TUBE FLOW NONUNIFORMITY-LAMINAR CASE	A 376
C		A 377

APPENDIX A

	IF (RXL.GE.0.9) GO TO 42	A 378
	PRINT 176	A 379
	GO TO 50	A 380
42	PRINT 177	A 381
	PRINT 178	A 382
	PRINT 179	A 383
C		A 384
C	FUD IS RATIO OF X5 TO XL	A 385
		A 386
	MNM=0	A 387
	FUD=.2	A 388
	XSLM(1)=FUD*RXL	A 389
	DO 49 I=1.5	A 390
	BNON(1)=RH02*(US1-U2)*(1.-SQRT(XSLM(1)))	A 391
43	CNON=H2+.5*(US1-U2)**2	A 392
	DNON=P2+RH02*(US1-U2)**2	A 393
	R2X(1)=1.01*RH02	A 394
44	U2X(1)=US1-BNON(1)/R2X(1)	A 395
	GO TO (45,47). INU	A 396
45	H2X(1)=CNON-.5*(US1-U2X(1))**2	A 397
	Z(4)=ALOG10(H2X(1)/287.0245)	A 398
	IMFT(1)=IMFT(2)=0	A 399
	CALL SLOW (S2R,Z,4.2,1T,NV,NERR,Y,X)	A 400
	R2XN=(10.**Z(2))*1.2914889	A 401
	IF (ABS(1.-R2X(1)/R2XN).LF..001) GO TO 46	A 402
	R2X(1)=R2XN	A 403
	GO TO 44	A 404
46	Z(2)=ALOG10(R2X(1)/1.2914889)	A 405
	CALL SLOW (S2R,Z,2.1,1T,NV,NERR,Y,X)	A 406
	T2X(1)=Z(1)	A 407
	CALL SLOW (S2R,Z,2.3,1T,NV,NERR,Y,X)	A 408
	P2X(1)=(10.**Z(3))*1.013245F+5	A 409
	CALL SLOW (S2R,Z,2.6,1T,NV,NERR,Y,X)	A 410
	A2X(1)=Z(6)*331.4193	A 411
	GO TO 48	A 412
C		A 413
C	INU=1 BASED ON ENERGY EQ. AND INU=2 BASED ON MOMENTUM EQ.	A 414
C		A 415
47	P2X(1)=DNON-R2X(1)*(US1-U2X(1))**2	A 416
	CALL SAVE (P2X(1),R2XN,H2X(1),S2R,T2X(1),A2X(1),Z2X,GAM2X,1)	A 417
	IF (ABS(1.-R2X(1)/R2XN).LF..001) GO TO 48	A 418
	R2X(1)=R2XN	A 419
	GO TO 44	A 420
48	RXR(1)=R2X(1)/RH02	A 421
	RXH(1)=H2X(1)/H2	A 422
	RXU(1)=U2X(1)/U2	A 423
	RXP(1)=P2X(1)/P2	A 424
	RXT(1)=T2X(1)/T2	A 425
	RXA(1)=A2X(1)/A2	A 426
	PRINT 180, XSLM(1),RXR(1),RXH(1),RXT(1),RXU(1),RXA(1),RXU(1)	A 427
	IF (MNM.EQ.1) GO TO 52	A 428
	FUD=FUD+.2	A 429
	XSLM(I+1)=FUD*RXL	A 430
49	CONTINUE	A 431
C		A 432
C	SHOCK TUBE FLOW NONUNIFORMITIES-TURBULENT CASE	A 433
C		A 434
50	IF (RXLT.GE.0.9) GO TO 51	A 435
	PRINT 181	A 436
	GO TO 54	A 437
51	PRINT 182	A 438
	PRINT 178	A 439
	PRINT 179	A 440
	FUD=.2	A 441
	XSLM(1)=FUD*RXLT	A 442
	DO 53 I=1.5	A 443

APPENDIX A

```

      BNON(1)=RH02*(U51-U2)*(1.-(XSLM(1))**.8)
      MNM=1
      GO TO 43
52    FUD=FUD+.2
      XSLM(1+1)=FUD*RXLT
53    CONTINUE
      C
      C    STANDING OR REFLECTED SHOCK AT SECOND DIAPHRAGM
      C
54    IF (LD.EQ.1.AND.1STET.EQ.0) GO TO 1
55    GO TO (57,56,60,57), LD
      C
      C    STANDING SHOCK PHASE
      C
56    CALL SNS (RHOA,UA,PA,HA,SAR,TA,AA,ZA,GAMA,ZSTARA,MA,RH02,U2,P2,H2,
1HT2,PT2,RT2,ST2R,TT2,AT2,ZT2,GT2,ZSTART2)
      HUP=HA
      NMN=2
      GO TO 58
      C
      C    CONDITIONS IN REGION A FOR NO STANDING SHOCK
      C
57    PA=P2
      RHOA=RH02
      TA=T2
      SAR=S2R
      HA=H2
      HUP=HA
      AA=A2
      UA=U2
      ZA=Z2
      GAMA=GAM2
      ZSA=ZS2
58    MA=UA/AA
      IFQ=1
      REA=0.0
      CALL VISC (TA,PA,VISA)
      IF (VISA.EQ.1.0) GO TO 59
      REA=RHOA*UA/VISA
59    CONTINUE
      IF (LD.EQ.1) GO TO 66
      IF (LD.EQ.4.AND.NMN.EQ.1) GO TO 66
      PRINT 147
      PRINT 183
      PRINT 147
      PRINT 167
      PRINT 168, PA,RHOA,TA,HA,SAR,ZA,GAMA,AA,UA,MA,REA
      IF (1STET.NE.0) GO TO 66
      C
      C    STAGNATION CONDITIONS BEHIND STANDING SHOCK IN SHOCK TUBE
      C
      OT2=3.8798E-4*SQRT(PT2/BNR)*(HT2-HW)
      PRINT 184
      PRINT 185
      PRINT 212, PT2,RT2,TT2,HT2,SAR,ZT2,GT2,AT2,OT2,BNR
      C
      C    REFLECTED SHOCK PHASE
      C
60    RHOR=10.*RH02
      NMN=3
61    UR=U2/(RHOR/RH02-1.)
      PR=P2+RH02*((U2+UR)**2)-RHOR*UR**2
      HR=H2+.5*((U2+UR)**2)-.5*UR**2
      GO TO (62,63), ISAV

```

A 444
 A 445
 A 446
 A 447
 A 448
 A 449
 A 450
 A 451
 A 452
 A 453
 A 454
 A 455
 A 456
 A 457
 A 458
 A 459
 A 460
 A 461
 A 462
 A 463
 A 464
 A 465
 A 466
 A 467
 A 468
 A 469
 A 470
 A 471
 A 472
 A 473
 A 474
 A 475
 A 476
 A 477
 A 478
 A 479
 A 480
 A 481
 A 482
 A 483
 A 484
 A 485
 A 486
 A 487
 A 488
 A 489
 A 490
 A 491
 A 492
 A 493
 A 494
 A 495
 A 496
 A 497
 A 498
 A 499
 A 500
 A 501
 A 502
 A 503
 A 504
 A 505
 A 506
 A 507

APPENDIX A

62	CALL SEARCH (PR,RNEW,HR,SARR,TR,AR,7R,GAMR,ZSR,ISP)	A 508
	GO TO 64	A 509
63	CALL SAVE (PR,RNEW,HR,SARR,TR,AR,7R,GAMR,3)	A 510
	ZSR=7R	A 511
64	IF (ABS(1.-RNEW/RHOR).LE.0.001) GO TO 65	A 512
	RHOR=RNEW	A 513
	GO TO 61	A 514
65	RHOR=RNEW	A 515
	MR=REAR=UR=0.0	A 516
	PRINT 147	A 517
	PRINT 186	A 518
	PRINT 147	A 519
	PRINT 167	A 520
	PRINT 168, PR,RHOR,TR,HR,SARR,ZR,GAMR,AR,UR,MR,REAR	A 521
	PA=PR	A 522
	RHOA=RHOR	A 523
	TA=TR	A 524
	HA=HR	A 525
	HUP=HR	A 526
	SAR=SARR	A 527
	ZA=ZR	A 528
	GAMA=GAMR	A 529
	AA=AR	A 530
	UA=0.0	A 531
	ZSA=ZSR	A 532
	MA=0.0	A 533
	IFQ=1	A 534
66	IF (ISTET.EQ.0) GO TO 1	A 535
C		A 536
C	EXPANSION TURF PHASE	A 537
C		A 538
C	LF=1 DENOTES U5 IS BASIC INPUT	A 539
C	LF=2 DENOTES P5 IS BASIC INPUT	A 540
C		A 541
C		A 542
C	FROZEN FLOW- EXPANSION TURF	A 543
C		A 544
	PRINT 147	A 545
	PRINT 187	A 546
	PRINT 146	A 547
	PRINT 188	A 548
	PRINT 189	A 549
	IF (LF.EQ.1) P5=0.0	
	IF (LF.EQ.2) U5=0.0	
	PRINT 190, U5,P5,XAS,DELU5,ISAV,IFXP,IREP,NVEL,IAC,JAC	A 550
67	ALPHA=ZA-1.	A 551
	GAMACT=(7.+3.*ALPHA)/(5.+ALPHA)	A 552
	AACT=SQRT(GAMACT*ZA*RU*TA/W)	A 553
	HACT=AACT**2/(GAMACT-1.)	A 554
	HFRQ=HA-HACT	A 555
	IF (HFRQ.GT.0.) GO TO 68	A 556
	PRINT 191	A 557
	P5F=0.1	A 558
	GO TO 74	A 559
68	GO TO (69,71), LF	A 560
69	U5F=U5	A 561
	A5F=AACT+((GAMACT-1.)/2.)*(UA-U5F)	A 562
	IF (A5F.GT.0.) GO TO 70	A 563
	PRINT 192	A 564
	P5F=0.1	A 565
	GO TO 74	A 566
70	P5F=PA*((A5F/AACT)**(2.*GAMACT/(GAMACT-1.)))	A 567
	GO TO 72	A 568
71	P5F=P5	A 569
	A5F=AACT*(P5F/PA)**((GAMACT-1.)/(2.*GAMACT))	A 570
	U5F=2.*(AACT-A5F)/(GAMACT-1.)+UA	A 571

APPENDIX A

72	M5F=U5F/A5F	A 572
	T5F=TA*(A5F/A6T)**2	A 573
	RH05F=P5F*W/(RU*ZA*T5F)	A 574
	S5RF=SAR	A 575
	H5F=HACT*(T5F/TA)	A 576
	Z5FF=ZSA	A 577
	Z5F=ZA	A 578
	GAM5F=GAMACT	A 579
	RE5F=0.0	A 580
	CALL VISC (T5F,P5F,VIS5F)	A 581
	IF (VIS5F.EQ.1.0) GO TO 73	A 582
	RE5F=RH05F*U5F/VIS5F	A 583
73	CONTINUE	A 584
	T15F=XAS*((1.0/(U5F-A5F))-(1.0/U5F))	A 585
	PRINT 193	A 586
	PRINT 167	A 587
	PRINT 168, P5F,RH05F,T5F,H5F,S5RF,Z5F,GAM5F,A5F,U5F,M5F,RE5F	A 588
C		A 589
C	SHOCK CROSSING - FROZEN EXPANSION - EQUILIBRIUM POST SHOCK	A 590
C		A 591
	H5FSC=H5F+HFR0	A 592
	CALL SNS (R55F,U55F,P55F,H55F,S55RF,T55F,A55F,Z55F,G55F,Z55FF,M55F	A 593
	1,RH05F,U5F,P5F,H5FSC,HT5F,PT5F,RT5F,ST5F,T15F,AT5F,ZT5F,GT5F,Z55F	A 594
	2F)	A 595
	RAT5F=R55F/RH05F	A 596
	PRINT 203	A 597
	PRINT 194	A 598
	PRINT 205	A 599
	PRINT 206, P55F,R55F,T55F,H55F,S55RF,Z55F,G55F,A55F,U55F,M55F,RAT5	A 600
1E		A 601
	PRINT 207	A 602
	PRINT 194	A 603
	PRINT 208	A 604
	QTZOF=3.8798E-4*SQR(T15F/RNR)*(HT5F-HW)	A 605
	PRINT 212, PT5F,RT5F,T15F,HT5F,ZT5F,GT5F,AT5F,QTZOF,RNR,T15F	A 606
	PRINT 203	A 607
	PRINT 195	A 608
	PRINT 205	A 609
	P55FF=P5F*(2.*GAMACT*M5F**2-GAMACT+1.)/(GAMACT+1.)	A 610
	R55FF=(RH05F*(GAMACT+1.)*M5F**2)/((GAMACT-1.)*M5F**2+2.)	A 611
	T55FF=P55FF*W/(R55FF*RU*ZA)	A 612
	H55FF=H5F*T55FF/T5F	A 613
	Z55FF=ZA	A 614
	G55FF=GAMACT	A 615
	A55FF=A5F*SQR(T55FF/T5F)	A 616
	U55FF=RH05F*U5F/P55FF	A 617
	M55FF=U55FF/A55FF	A 618
	S55RFF=(ALOG(P55FF/P5F)-GAMACT*ALOG(R55FF/RH05F))/(GAMACT-1.)+S5RF	A 619
	RAT5F=R55FF/RH05F	A 620
	PRINT 206, P55FF,R55FF,T55FF,H55FF,S55RFF,Z55FF,G55FF,A55FF,U55FF,	A 621
1M55FF,RAT5F		A 622
	PRINT 207	A 623
	PRINT 195	A 624
	PRINT 208	A 625
	HT5FF=H5F+.5*U5F**2	A 626
	T15FF=T55FF*HT5FF/H55FF	A 627
	PT5FF=P55FF*(HT5FF/H55FF)**(GAMACT/(GAMACT-1.))	A 628
	RT5FF=PT5FF*W/(T15FF*ZA*R11)	A 629
	ZT5FF=ZA	A 630
	GT5FF=GAMACT	A 631
	AT5FF=A55FF*SQR(T15FF/T55FF)	A 632
	QTZOFF=3.8798E-4*SQR(T15FF/RNR)*(HT5FF-HW)	A 633
	PRINT 212, PT5FF,RT5FF,T15FF,HT5FF,ZT5FF,GT5FF,AT5FF,QTZOFF,RNR,T1	A 634
15F		A 635
C		A 636
C	EQUILIBRIUM EXPANSION-EXPANSION TIME	A 637

APPENDIX A

C		A 638
74	IF (LF.EQ.2) GO TO 93	A 639
C		A 640
C	LF=1 CASE	A 641
C		A 642
	IF (IEQ.EQ.2.AND.IEXP.EQ.1) GO TO 87	A 643
	DFLU=U5-UA	A 644
	GO TO (75,82), IEXP	A 645
75	HMIN=1.0E+5	A 646
76	DELH=(HUP-HMIN)/(FLOAT(JAC)-1.0)	A 647
	PRINT 196	A 648
	IMET(1)=IMET(2)=0	A 649
	LCODE=1	A 650
	DO 80 J=1,JAC	A 651
	Z(4)=(HUP-FLOAT(J-1)*DELH)/287.0245	A 652
	Z(4)=ALOG10(Z(4))	A 653
	CALL SLOW (SAR,Z,4,6,IT,NV,NERR,Y,X)	A 654
	GO TO (79,77), LCODE	A 655
77	L=J	A 656
	DO 78 K=L,JAC	A 657
	TABHR(K)=HUP-FLOAT(K-1)*DELH	A 658
	TARA(K)=1.5766/SQRT(TABHR(K))	A 659
78	CONTINUE	A 660
	PRINT 197	A 661
	GO TO 81	A 662
79	TABHR(J)=(10.**Z(4))*287.0245	A 663
	TARA(J)=1./(Z(6)*3.314193E+2)	A 664
80	CONTINUE	A 665
81	CALL SIMR (TABHR,TARA,JAC,JAC,TABANS)	A 666
	IF (LF.EQ.2) GO TO 99	A 667
	GO TO 86	A 668
82	IF (P5F.GF.0.1) GO TO 83	A 669
	P5F=0.1	A 670
83	DELPG=ALOG10(PA/P5F)/(FLOAT(IAC)-1.0)	A 671
84	P5G(1)=ALOG10(PA)	A 672
	PRINT 198	A 673
	P5K(1)=PA	A 674
	TABHR(1)=HA	A 675
	TARA(1)=1./AA	A 676
	TARP(1)=PA	A 677
	DO 85 J=2,IAC	A 678
	P5G(J)=P5G(J-1)-DELPG	A 679
	P5K(J)=10.**P5G(J)	A 680
	CALL SAVE (P5K(J),RK,HK,SAR,TK,AK,7K,6K,1)	A 681
	TABHR(J)=HK	A 682
	TARA(J)=1./AK	A 683
	TARP(J)=P5K(J)	A 684
85	CONTINUE	A 685
	CALL SIMR (TABHR,TARA,IAC,IAC,TABANS)	A 686
86	IF (LF.EQ.1) GO TO 87	A 687
	U5=(IA+TABANS(IAC)	A 688
	GO TO 103	A 689
87	CALL FTLUP (DELU,H5,2,NON,TABANS,TABHR)	A 690
	IMOD=1	A 691
	GO TO (89,88), IEXP	A 692
88	CALL FTLUP (DELU,P5,2,NON,TABANS,TARP)	A 693
	GO TO 100	A 694
89	IF (H5.GF.5.E+4) GO TO 90	A 695
	PRINT 199	A 696
	GO TO 120	A 697
90	XX=SAR	A 698
	Z(4)=ALOG10(H5/287.0245)	A 699
	IMET(1)=IMET(2)=0	A 700
	LCODE=1	A 701
	CALL SLOW (XX,Z,4,1,IT,NV,NERR,Y,X)	A 702
	GO TO (91,92), LCODE	A 703

APPENDIX A

91	CALL SLOW (XX,Z,4,2,IT,NV,NERR,Y,X)	A 704
	CALL SLOW (XX,Z,4,3,IT,NV,NERR,Y,X)	A 705
	CALL SLOW (XX,Z,4,5,IT,NV,NERR,Y,X)	A 706
	CALL SLOW (XX,Z,4,6,IT,NV,NERR,Y,X)	A 707
	CALL SLOW (XX,Z,4,7,IT,NV,NERR,Y,X)	A 708
	T5=Z(1)	A 709
	R5=(10.**Z(2))*1.2014889	A 710
	P5=(10.**Z(3))*1.013246E+5	A 711
	GAM5=Z(5)	A 712
	A5=7(6)*331.4193	A 713
	ZZ5=7(7)	A 714
	GO TO 103	A 715
92	PRINT 200	A 716
	PRINT 201	A 717
	P5=1.01325E+5*(H5/2.99657E+5)**3.5*EXP(23.919-SAR)	A 718
	T5=H5/998.857	A 719
	R5=3.48398E-3*P5/T5	A 720
	A5=20.046*SQRT(T5)	A 721
	ZZ5=ZST5=1.0	A 722
	GAM5=1.4	A 723
	GO TO 103	A 724
C		A 725
C	LF=2 CASE	A 726
C		A 727
93	GO TO (95,94), ISAV	A 728
94	CALL SAVE (P5,R5,H5,SAR,T5,A5,ZZ5,GAM5,1)	A 729
	IF (IEXP,FQ,1) GO TO 98	A 730
	DFLPG=ALOG10(PA/P5)/(FLOAT(IAC)-1.)	A 731
	GO TO 84	A 732
95	Z(3)=ALOG10(P5/1.013246E+5)	A 733
	IMET(1)=IMET(2)=0	A 734
	LCONF=1	A 735
	CALL SLOW (SAR,Z,3,1,IT,NV,NERR,Y,X)	A 736
	GO TO (96,97), LCONF	A 737
96	CALL SLOW (SAR,Z,3,2,IT,NV,NERR,Y,X)	A 738
	CALL SLOW (SAR,Z,3,4,IT,NV,NERR,Y,X)	A 739
	CALL SLOW (SAR,Z,3,5,IT,NV,NERR,Y,X)	A 740
	CALL SLOW (SAR,Z,3,6,IT,NV,NERR,Y,X)	A 741
	CALL SLOW (SAR,Z,3,7,IT,NV,NERR,Y,X)	A 742
	T5=Z(1)	A 743
	R5=(10.0**Z(2))*1.2914889	A 744
	H5=(10.0**Z(4))*287.0245	A 745
	GAM5=Z(5)	A 746
	A5=7(6)*331.4193	A 747
	ZZ5=7(7)	A 748
	GO TO 98	A 749
97	PRINT 200	A 750
	PRINT 201	A 751
	H5=2.99657E+5*((P5/1.01325E+5)/(EXP(23.919-SAR)))*0.2857	A 752
	T5=H5/998.857	A 753
	R5=3.48398E-3*P5/T5	A 754
	A5=20.046*SQRT(T5)	A 755
	ZZ5=ZST5=1.0	A 756
	GAM5=1.4	A 757
98	HMIN=H5	A 758
	GO TO 76	A 759
99	U5=(14+TABANS(JAC)	A 760
	GO TO 103	A 761
100	GO TO (101,102), ISAV	A 762
101	CALL SEARCH (P5,R5,H5,SAR,T5,A5,ZZ5,GAM5,ZST5,ISP)	A 763
	GO TO 103	A 764
102	CALL SAVE (P5,R5,H5,SAR,T5,A5,ZZ5,GAM5,1)	A 765
	ZST5=ZZ5	A 766
103	M5=U5/A5	A 767
	REF=0.0	A 768
	CALL VISC (T5,P5,VIS5)	A 769

APPENDIX A

```

104 IF (V1SS.EQ.1.0) GO TO 104
REF=R5*U5/V1SS
CONTINUE
T15=XAS*((1.0/(U5-A5))-(1.0/U5))
PRINT 202
PRINT 167
PRINT 168, P5,R5,T5,H5,SAR,Z75,GAM5,A5,U5,M5,RF5
CALL SNS (RH05S,U5S,P5S,H5S,S5SR,T5S,A5S,Z5S,GAMF5S,ZSTAR5S,M5S,R5
1,U5,P5,H5,HT5,PT5,RT5,ST5R,TT5,AT5,ZT5,GAMET5,ZSTART5)
RATEF=RH05S/R5
PRINT 203
PRINT 204
PRINT 205
PRINT 206, P5S,RH05S,T5S,H5S,S5SR,Z5S,GAMF5S,A5S,U5S,M5S,DATEF
PRINT 207
PRINT 204
PRINT 208

C
C HEAT TRANSFER RELATION OF NASA TN D-4799
C
QTZO=3.8798E-4*SQR(T5/BNR)*(HT5-HW)
PRINT 209, PT5,RT5,TT5,HT5,ZT5,GAMET5,AT5,QTZO,BNR,T15
IF (IMOD.EQ.2) GO TO 105
IF (DFLUS.EQ.0.0) GO TO 106
IMOD=2
PRINT 147
PRINT 145
PRINT 146
U5=U5-2.0*DFLUS
GO TO 103
105 U5=U5+2.0*DFLUS
C
C COMPUTING ACCELERATION GAS (AIR) CONDITIONS
C
106 US0=1.1*U5
107 H20=1004.598*T1+0.5*US0**2-0.5*(US0-U5)**2
CALL SAVE (P5,RH020,H20,SR20,T20,A20,Z20,GAM20,3)
P10=(P5+RH020*(US0-U5)**2)/(1.+(.003484*(US0**2)/T1))
US0NEW=U5/(1.-(.003484*P10)/(T1*RH020))
IF (ABS(1.-US0NEW/US0).LE.0.0010) GO TO 108
US0=US0NEW
GO TO 107
108 M20=U5/A20
MS10=US0/A1
RH010=(P10*W)/(RU*T1)
R20R=RH020/RH010
PRINT 210
PRINT 211
PRINT 212, P5,RH020,T20,H20,Z20,M20,P10,U50,MS10,R20R
PRINT 213
PRINT 214

C
C ACCELERATION TEST TIME- MIRELS THEORY (LAMINAR)
C
XA(1)=.1*XAS
IF (MS10.GT.4.0.AND.MS10.LE.14.0) GO TO 109
IF (MS10.GT.14.0) GO TO 110
PRINT 215
GO TO 118
109 XXMAX=P10*DIA**2*(2.06-.2056*MS10+.095E-3*MS10**2)
GO TO 111
110 XXMAX=P10*DIA**2*(.8723-7.488E-3*MS10)
C
C XAS IS DIVIDED INTO 10 INTERVALS XA
C
111 DO 117 J=1,10
BETA1=XA(1)*RH010/(2.*XXMAX*RH020)

```

APPENDIX A

BETA2=2.*RH020/RH010	A 837
AXUP=.99999	A 838
AXLOW=.00001	A 839
DELTAX=(AXUP-AXLOW)/100.	A 840
F1=.1F-6	A 841
AX=.5	A 842
CALL ITR2 (AX,AXLOW,AXUP,DELTAX,F0FAX,F1,F1,200,ICODE)	A 843
IF (ICODE) 113,112,113	A 844
112 RXL=AX**2	A 845
XL=RXL*XXMAX	A 846
TAU1=RH010*XA(1)/(RH020*U5)	A 847
BXUP=.99999	A 848
BXLOW=.00001	A 849
DELTBX=(BXUP-BXLOW)/100.	A 850
BX=.5	A 851
CALL ITR2 (BX,BXLOW,BXUP,DELTBX,F0FBX,F1,F1,200,ICODE)	A 852
IF (ICODE) 113,116,113	A 853
113 GO TO (114,115,115,115), ICODE	A 854
114 PRINT 154	A 855
GO TO 118	A 856
115 PRINT 155, ICODE	A 857
GO TO 118	A 858
116 TAU=RX**2*XXMAX/U50	A 859
U1=XL/TAU	A 860
URAT=U1/U5	A 861
URA=U50/U1	A 862
PRINT 216, XAS,XA(1),XXMAX,XL,RXL,TAU,U1,URAT,URA,TAU1	A 863
XA(1+1)=XA(1)+.1*XAS	A 864
117 CONTINUE	A 865
118 IF (ISTET.EQ.2) GO TO 122	A 866
119 IF (LF.EQ.2) GO TO 121	A 867
NN=NN+1	A 868
IF (IREP.EQ.1.OR.NVEL.EQ.NN) GO TO 120	A 869
IF (NN.GT.10) GO TO 120	A 870
U5=U5+U51	A 871
DELU=U5-UA	A 872
IF0=2	A 873
GO TO 67	A 874
120 IF (LD.NE.4) GO TO 1	A 875
IF (IREP.EQ.1) GO TO 250	
U5=U5-(FLOAT(NVEL)-1.)*U51	A 876
250 NN=0	A 877
IMET(1)=IMET(2)=0	A 878
LCODE=1	A 879
IF (NMN.EQ.1) GO TO 56	A 880
IF (NMN.EQ.2) GO TO 60	A 881
GO TO 1	A 882
121 IF (LD.NE.4) GO TO 1	A 883
IF0=2	A 884
IMET(1)=IMET(2)=0	A 885
LCODE=1	A 886
IF (NMN.EQ.1) GO TO 56	A 887
IF (NMN.EQ.2) GO TO 60	A 888
GO TO 1	A 889
C	A 890
C EXPANSION TUNNEL - EQUILIBRIUM EXPANSION	A 891
C	A 892
122 PRINT 147	A 893
PRINT 217	A 894
PRINT 146	A 895
PRINT 218	A 896
PRINT 219	A 897
IF (LG.EQ.1) P6=0.0	
IF (LG.EQ.2) U6=0.0	
PRINT 220, U6,P6,DIAT,DIAN,ISAV	A 898
C	A 899

APPENDIX A

C	FROZEN FLOW- EXPANSION TUNNEL	A 900
C		A 901
123	ALP5=ZZ5-1.	A 902
	GACT5=(7.+3.*ALP5)/(5.+ALP5)	A 903
	AACT5=SQRT(GACT5*ZZ5*RU*TS/W)	A 904
	HACT5=AACT5**2/(GACT5-1.)	A 905
	HERO5=H5-HACT5	A 906
	IF (HERO5.GT.0.0) GO TO 124	A 907
	PRINT 221	A 908
	GO TO (130,140). LG	A 909
124	GO TO (125,127). LG	A 910
125	U6F=U6	A 911
	CATA=(GACT5-1.0)*(U5**2-U6**2)+AACT5**2	A 912
	IF (CATA.GT.0.0) GO TO 126	A 913
	PRINT 222	A 914
	GO TO 130	A 915
126	A6F=SQRT(CATA)	A 916
	P6F=P5*((A6F/AACT5)**(2.*GACT5/(GACT5-1.0)))	A 917
	GO TO 128	A 918
127	P6F=P6	A 919
	A6F=AACT5*(P6F/P5)**((GACT5-1.)/(2.*GACT5))	A 920
	U6F=SQRT(U5**2+(AACT5**2-A6F**2)/(GACT5-1.0))	A 921
128	M6F=U6F/A6F	A 922
	T6F=T5*(A6F/AACT5)**2	A 923
	RH06F=P6F*W/(RU*ZZ5*T6F)	A 924
	H6F=HACT5*(T6F/T5)	A 925
	Z6F=ZZ5	A 926
	GAM6F=GACT5	A 927
	S6RF=SAR	A 928
	RF6F=0.0	A 929
	CALL VISC (T6F,P6F,VIS6F)	A 930
	IF (VIS6F.EQ.1.0) GO TO 129	A 931
	RF6F=RH06F*U6F/VIS6F	A 932
129	PRINT 223	A 933
	PRINT 167	A 934
	PRINT 168, P6F,RH06F,T6F,H6F,SAR,Z6F,GAM6F,A6F,U6F,M6F,RF6F	A 935
	H6FSC=H6F+HERO5	A 936
	CALL SNS (R6SF,U6SF,P6SF,H6SF,S6SRF,T6SF,A6SF,Z6SF,G6SF,Z66SF,M6SF	A 937
	1,RH06F,U6F,P6F,H6FSC,HT6F,PT6F,RT6F,ST6F,TT6F,AT6F,ZT6F,GT6F,ZST6	A 938
	2F)	A 939
	RATF6=R6SF/RH06F	A 940
	PRINT 224	A 941
	PRINT 194	A 942
	PRINT 205	A 943
	PRINT 206, P6SF,R6SF,T6SF,H6SF,S6SRF,Z6SF,G6SF,A6SF,U6SF,M6SF,RATF	A 944
16		A 945
	PRINT 225	A 946
	PRINT 194	A 947
	PRINT 208	A 948
	QTF6=3.8798E-4*SQRT(PT6F/RNR)*(HT6F-HW)	A 949
	T16F=0.0	A 950
	PRINT 212, PT6F,RT6F,TT6F,HT6F,ZT6F,GT6F,AT6F,QTF6,RNR,T16F	A 951
	PRINT 224	A 952
	PRINT 195	A 953
	PRINT 205	A 954
	P6SFF=P6F*(2.*GACT5*M6F**2-GACT5+1.)/(GACT5+1.)	A 955
	R6SFF=(RH06F*(GACT5+1.)*M6F**2)/((GACT5-1.)*M6F**2+2.)	A 956
	T6SFF=P6SFF*W/(R6SFF*RU*ZZ5)	A 957
	H6SFF=H6F*T6SFF/T6F	A 958
	Z6SFF=ZZ5	A 959
	G6SFF=GACT5	A 960
	A6SFF=A6F*SQRT(T6SFF/T6F)	A 961
	U6SFF=RH06F*U6F/R6SFF	A 962
	M6SFF=U6SFF/A6SFF	A 963
	S6SRFF=(ALOG(P6SFF/P6F)-GACT5*ALOG(R6SFF/RH06F))/(GACT5-1.)*S6RF	A 964
	RATFF6=R6SFF/RH06F	A 965
	PRINT 206, P6SFF,R6SFF,T6SFF,H6SFF,S6SRFF,Z6SFF,G6SFF,A6SFF,U6SFF,	A 966

APPENDIX A

	1M6SFF,RATFF6	A 967
	PRINT 225	A 968
	PRINT 195	A 969
	PRINT 208	A 970
	HT6FF=H6F+.5*U6F**2	A 971
	TT6FF=T6SFF*HT6FF/H6SFF	A 972
	PT6FF=P6SFF*(HT6FF/H6SFF)**(GACT5/(GACT5-1.))	A 973
	RT6FF=PT6FF*W/(TT6FF*ZZ5*RU)	A 974
	ZT6FF=ZZ5	A 975
	GT6FF=GACT5	A 976
	AT6FF=A6SFF*SQRT(TT6FF/T6SFF)	A 977
	OTFF6=3.8798E-4*SQRT(PT6FF/BNR)*(HT6FF-HW)	A 978
	PRINT 212, PT6FF,RT6FF,TT6FF,HT6FF,ZT6FF,GT6FF,AT6FF,OTFF6,BNR,TI6	A 979
	IF	A 980
	GO TO (130,140), LG	A 981
C		A 982
C	LG=1 DENOTES U6 IS INPUT	A 983
C		A 984
130	H6=H5+.5*(U5**2-U6**2)	A 985
	IF (H6,GF,2,E+4) GO TO 131	A 986
	PRINT 226	A 987
	GO TO 1	A 988
131	Z(4)=ALOG10(H6/287.0245)	A 989
	IMET(1)=IMET(2)=0	A 990
	LCODE=1	A 991
	CALL SLOW (SAR,Z,4,3,IT,NV,NERR,Y,X)	A 992
	GO TO (132,135), LCODE	A 993
132	P6=(10.0**Z(3))*1.01325E+5	A 994
	GO TO (133,134), ISAV	A 995
133	CALL SLOW (SAR,Z,4,1,IT,NV,NERR,Y,X)	A 996
	CALL SLOW (SAR,Z,4,2,IT,NV,NERR,Y,X)	A 997
	CALL SLOW (SAR,Z,4,5,IT,NV,NERR,Y,X)	A 998
	CALL SLOW (SAR,Z,4,6,IT,NV,NERR,Y,X)	A 999
	CALL SLOW (SAR,Z,4,7,IT,NV,NERR,Y,X)	A1000
	T6=Z(1)	A1001
	R6=(10.0**Z(2))*1.2914889	A1002
	GAM6=Z(5)	A1003
	A6=Z(6)*231.4193	A1004
	ZZ6=Z(7)	A1005
	PRINT 227	A1006
	GO TO 137	A1007
134	CALL SAVF (P6,R6,H6,SAR,T6,A6,ZZ6,GAM6,1)	A1008
	PRINT 228	A1009
	IF (LG,EQ,1) GO TO 137	A1010
	U6=SQRT(2.0*(H5-H6)+U5**2)	A1011
	GO TO 137	A1012
135	P6=1.01325E+5*(H6/2.99657E+5)**3.5*EXP(23.019-SAR)	A1013
136	T6=H6/998.857	A1014
	R6=3.48398E-3*P6/T6	A1015
	A6=20.046*SQRT(T6)	A1016
	GAM6=1.4	A1017
	ZZ6=7ST6=1.0	A1018
	PRINT 229	A1019
137	M6=U6/A6	A1020
	RF6=0.0	A1021
	CALL VISC (T6,P6,VIS6)	A1022
	IF (VIS6,EQ,1.0) GO TO 138	A1023
	RE6=P6*U6/VIS6	A1024
138	PRINT 230	A1025
	PRINT 167	A1026
	PRINT 168, P6,R6,T6,H6,SAR,ZZ6,GAM6,A6,U6,M6,RF6	A1027
	CALL SNS (RH06S,U6S,P6S,H6S,S6SR,T6S,A6S,Z6S,GAMFAS,7STAR6S,M6S,P6	A1028
	I,U6,P6,H6,HT6,PT6,RT6,ST6R,TT6,AT6,ZT6,GAMET6,ZSTART6)	A1029
	RAT6E=RH06S/R6	A1030
	QT6=3.8798E-4*SQRT(PT6/BNR)*(HT6-HW)	A1031
	AA6=(R5*U5)/(R6*U6)	A1032

APPENDIX A

DELT6=0.5*(DIAN-DIAT*SQRT(AA6))	A1033
PRINT 231	A1034
PRINT 204	A1035
PRINT 205	A1036
PRINT 206, P6S,RH06S,T6S,H6S,S6SR,76S,GAMF6S,A6S,U6S,W6S,DAT6F	A1037
PRINT 232	A1038
PRINT 204	A1039
PRINT 233	A1040
PRINT 206, PT6,RT6,TT6,HT6,7T6,GAMFT6,AT6,QT6,BNP,AA6,DELT6	A1041
IF (LG.EQ.2.OR.LREP.EQ.1) GO TO 119	A1042
NNN=NNN+1	A1043
IF (NUMU6.EQ.NNN) GO TO 139	A1044
IF (NNN.GT.10) GO TO 119	A1045
U6=U6+U61	A1046
GO TO 123	A1047
139 U6=U6-(FLOAT(NUMU6)-1.)*U61	A1048
NNN=0	A1049
GO TO 119	A1050
C	A1051
C LG=2 DENOTES P6 IS INPUT	A1052
C	A1053
140 IMFT(1)=IMFT(2)=0	A1054
LCONF=1	A1055
Z(3)=ALOG10(P6/1.013246F+5)	A1056
CALL SLOW (SAR,Z.3.1,IT,NV,NERR,Y,X)	A1057
GO TO (141,143), LCONF	A1058
141 GO TO (142,134), ISAV	A1059
142 CALL SLOW (SAR,Z.3.2,IT,NV,NERR,Y,X)	A1060
CALL SLOW (SAR,Z.3.4,IT,NV,NERR,Y,X)	A1061
CALL SLOW (SAR,Z.3.5,IT,NV,NERR,Y,X)	A1062
CALL SLOW (SAR,Z.3.6,IT,NV,NERR,Y,X)	A1063
CALL SLOW (SAR,Z.3.7,IT,NV,NERR,Y,X)	A1064
T6=Z(1)	A1065
R6=(10.**Z(2))*1.2914889	A1066
H6=(10.**Z(4))*287.0245	A1067
GAM6=Z(5)	A1068
A6=Z(6)*331.4193	A1069
ZZ6=Z(7)	A1070
PRINT 227	A1071
U6=SQRT(2.*(H5-H6)+U5**2)	A1072
GO TO 137	A1073
143 H6=2.99657F+5*((P6/1.01325F+5)/(EXP(23.919-SAR)))*C.2857	A1074
U6=SQRT(2.*(H5-H6)+U5**2)	A1075
GO TO 136	A1076
144 STOP	A1077
C	A1078
C	A1079
C	A1080
145 FORMAT (/51H FOLLOWING EQUILIBRIUM CONDITIONS INCLUDE FLOW ATTN)	A1081
146 FORMAT (/55H XX	A1082
1X)	A1083
147 FORMAT (/55H XX	A1084
1XX)	A1085
148 FORMAT (/46H EXPANSION TUBE PROGRAM OF MILLER FOR REAL AIR)	A1086
149 FORMAT (51H ALL PHYSICAL QUANTITIES IN MKS UNITS- NASA SP-7012)	A1087
150 FORMAT (/28H SHOCK TUBE PHASE OF PROGRAM)	A1088
151 FORMAT (/37H MEASURED INPUTS FOR SHOCK TUBE PHASE)	A1089
152 FORMAT (/105H RUN P1 T1 US1 P2	A1090
1P4 T4 X1S DIA ISAV INU LD)	A1091
153 FORMAT (9E10.3,315)	A1092
154 FORMAT (20H MAX COUNT EXCEEDED)	A1093
155 FORMAT (17H DERIVATIVE = 0. ,15)	A1094
156 FORMAT (7H ICODE=.15,5H RI=.E12.3,7H DFLR=.F12.3)	A1095
157 FORMAT (/65H P3 T3 RH03 73 H3 1/	A1096
1A3 U3)	A1097
158 FORMAT (7F10.3)	A1098

APPENDIX A

159	FORMAT (/46H P2 RH02 H2 U2 US1)	A1100
160	FORMAT (5E10.3)	A1100
161	FORMAT (/30H IMPERFECT HYDROGEN DRIVER GAS)	A1101
162	FORMAT (/28H IMPERFECT HELIUM DRIVER GAS)	A1102
163	FORMAT (/13H 4 CONDITIONS)	A1103
164	FORMAT (/75H P RH0 T H S/P 7	A1104
1	A W)	A1105
165	FORMAT (8F10.3)	A1106
166	FORMAT (/44H CONDITIONS BEHIND INCIDENT SHOCK - REGION 2)	A1107
167	FORMAT (/106H P RH0 T H S/P	A1108
1Z	GAME A U M NRE)	A1109
168	FORMAT (11E10.3)	A1110
169	FORMAT (/44H RATIO- 2 TO 1 CONDITIONS AND SHOCK VELOCITY)	A1111
170	FORMAT (/66H P RH0 T H A M	A1112
1S1	US1)	A1113
171	FORMAT (7F10.3)	A1114
172	FORMAT (/47H SHOCK TUBE FLOW PARAMETERS USING MIRELS THEORY)	A1115
173	FORMAT (/107H LMAX L L/LMAX TIM UIT	A1116
1LMAXT	LT LT/LMAXT TIMT UIT TIMI)	A1117
174	FORMAT (/45H SHOCK TUBE TEST TIME NOT COMPUTED - MS1 LT 4)	A1118
175	FORMAT (11F10.3)	A1119
176	FORMAT (/51H SHOCK TUBE LAMINAR FLOW NONUNIFORMITY NOT COMPUTED)	A1120
177	FORMAT (/45H SHOCK TUBE FLOW NONUNIFORMITIES-LAMINAR CASE)	A1121
178	FORMAT (/44H RATIOS-PARAMETER AT XS TO PARAMETER AT XS=0)	A1122
179	FORMAT (/65H XS/L P RH0 T H A	A1123
1	U)	A1124
180	FORMAT (7F10.3)	A1125
181	FORMAT (/53H SHOCK TUBE TURBULENT FLOW NONUNIFORMITY NOT COMPUTED	A1126
1)		A1127
182	FORMAT (/47H SHOCK TUBE FLOW NONUNIFORMITIES-TURBULENT CASE)	A1128
183	FORMAT (/52H CONDITIONS BEHIND STANDING SHOCK AT SECONDARY DIAPH)	A1129
184	FORMAT (/54H STAGNATION CONDITIONS BEHIND STANDING SHOCK-REGION T	A1130
12)		A1131
185	FORMAT (/98H P RH0 T H S/P 7	A1132
1	GAME A QT RN)	A1133
186	FORMAT (/53H CONDITIONS BEHIND REFLECTED SHOCK AT SECONDARY DIAPH	A1134
1)		A1135
187	FORMAT (/32H EXPANSION TUBE PHASE OF PROGRAM)	A1136
188	FORMAT (/32H INPUTS FOR EXPANSION TUBE PHASE)	A1137
189	FORMAT (/72H US P5 XAS DELU5 ISAV IEXP I	A1138
1REP NVEL	IAC JAC)	A1139
190	FORMAT (4F10.3,615)	A1140
191	FORMAT (40H FROZEN ENTHALPY IN REGION A IS NEGATIVE)	A1141
192	FORMAT (/16H ASE IS NEGATIVE)	A1142
193	FORMAT (/34H 5 CONDITIONS FOR FROZEN EXPANSION)	A1143
194	FORMAT (41H FROZEN EXPANSION--EQUILIBRIUM POST SHOCK)	A1144
195	FORMAT (37H FROZEN EXPANSION-- FROZEN POST SHOCK)	A1145
196	FORMAT (/54H AEDC REAL-AIR TAPE USED FOR UNSTEADY EXPANSION-IFXP=1	A1146
1)		A1147
197	FORMAT (/53H PERFECT AIR RELATIONS USED FOR NUMERICAL INTEGRATION)	A1148
198	FORMAT (/55H AEDC CURVE FIT EXPRESSIONS USED FOR UNSTEADY EXPANSIO	A1149
1N)		A1150
199	FORMAT (/50H H5 LT 5F+4- EQUILIBRIUM 5 CONDITIONS NOT COMPUTED)	A1151
200	FORMAT (/37H QUANTITIES IN REGION 5 OFF AEDC TAPE)	A1152
201	FORMAT (53H THESE QUANTITIES DETERMINED FROM IDEAL AIR RELATIONS)	A1153
202	FORMAT (/39H 5 CONDITIONS FOR EQUILIBRIUM EXPANSION)	A1154
203	FORMAT (/47H STATIC CONDITIONS BEHIND BOW SHOCK - REGION 5S)	A1155
204	FORMAT (46H EQUILIBRIUM EXPANSION--EQUILIBRIUM POST SHOCK)	A1156
205	FORMAT (/108H P RH0 T H S/R	A1157
1Z	GAME A U M RATIO)	A1158
206	FORMAT (11E10.3)	A1159
207	FORMAT (/49H STAGNATION CONDITIONS BEHIND BOW SHOCK-REGION 1S)	A1160
208	FORMAT (/97H P RH0 T H 7 C	A1161
1AME	A QT RN TIMI)	A1162
209	FORMAT (10E10.3)	A1163
210	FORMAT (/48H ACCELERATION AIR CONDITIONS (REGION 20) AND P10)	A1164

APPENDIX A

211	FORMAT (101H P20 RH020 T20 H20 Z20	A1165
	1M20 P10 US10 MS10 RATIO 1	A1166
212	FORMAT (10E10.3)	A1167
213	FORMAT (//53H ACCELERATION AIR FLOW PARAMETERS USING MIRELS THEORY	A1168
	1)	A1169
214	FORMAT (//97H XAS XA LMAX L L/LMAX	A1170
	1TIM UI UI/US US20/UI TIM1)	A1171
215	FORMAT (//50H ACCELERATION AIR LEAKY PISTON EFFECT NOT COMPUTED)	A1172
216	FORMAT (10E10.3)	A1173
217	FORMAT (//34H EXPANSION TUNNEL PHASE OF PROGRAM)	A1174
218	FORMAT (//34H INPUTS FOR EXPANSION TUNNEL PHASE)	A1175
219	FORMAT (//47H U6 P6 D-THROAT D-NOZZLE ISAV)	A1176
220	FORMAT (4E10.3,115)	A1177
221	FORMAT (//40H FROZEN ENTHALPY IN REGION 5 IS NEGATIVE)	A1178
222	FORMAT (//46H A6F NEGATIVE - FROZEN CONDITIONS NOT COMPUTED)	A1179
223	FORMAT (//41H 6 CONDITIONS FOR FROZEN NOZZLE EXPANSION)	A1180
224	FORMAT (//47H STATIC CONDITIONS BEHIND BOW SHOCK - REGION 6S)	A1181
225	FORMAT (//51H STAGNATION CONDITIONS BEHIND BOW SHOCK - REGION T6)	A1182
226	FORMAT (//44H H6 LESS THAN 2.0E+4- T6 LESS THAN 20 DEG K)	A1183
227	FORMAT (//43H AEDC TAPE USED FOR STEADY NOZZLE EXPANSION)	A1184
228	FORMAT (//53H AEDC CURVE FIT EXPRESSIONS USED FOR NOZZLE EXPANSION)	A1185
229	FORMAT (//54H REGION 6 QUANTITIES OFF TAPE - PERFECT RELATIONS USED	A1186
	1)	A1187
230	FORMAT (//46H 6 CONDITIONS FOR EQUILIBRIUM NOZZLE EXPANSION)	A1188
231	FORMAT (//45H STATIC CONDITIONS BEHIND BOW SHOCK-REGION 6S)	A1189
232	FORMAT (//49H STAGNATION CONDITIONS BEHIND BOW SHOCK-REGION T6)	A1190
233	FORMAT (//109H P RHO T H Z	A1191
	1GAME A QT RN A/ASTAR DELSTAR)	A1192
234	FORMAT (4A10)	A1193
235	FORMAT (1H1,A10/)	A1194
	END	A1195-
	SUBROUTINE VISC (T,P,VIS)	R 1
	DIMENSION TAPY(4), TABTY(13), TABNUY(52)	R 2
C		R 3
C	TABLE OF VISCOSITY FROM YOS(AVCO RAD-TM-63-7)	R 4
C		R 5
	DATA TAPY/1.01325E+5,3.03975E+5,1.01325E+6,3.03975E+6/	R 6
	DATA TABTY/1000.,2000.,3000.,4000.,5000.,6000.,7000.,8000.,9000.,1	R 7
	10000.,12000.,14000.,16000./	R 8
	DATA TABNUY/.418E-4,.648E-4,.858E-4,1.08E-4,1.30E-4,1.54E-4,1.86E-	R 9
	14.2E-4,2.04E-4,2.63E-4,2.63E-4,1.77E-4,.96E-4,.418E-4,.648E-4,.8	R 10
	2857E-4,1.07E-4,1.30E-4,1.52E-4,1.80E-4,2.14E-4,2.45E-4,2.66E-4,2.8	R 11
	35E-4,2.34E-4,1.53E-4,.418E-4,.648E-4,.857E-4,1.07E-4,1.30E-4,1.51E-	R 12
	4-4,1.76E-4,2.06E-4,2.4E-4,2.67E-4,3.00E-4,2.82E-4,2.24E-4,.418E-4,	R 13
	5.648E-4,.856E-4,1.06E-4,1.27E-4,1.50E-4,1.73E-4,2.00E-4,2.32E-4,2.	R 14
	663E-4,3.06E-4,3.10E-4,2.66E-4/	R 15
	IF (T.LE.1500.) GO TO 2	R 16
	IF (T.GT.16000. OR P.GT.3.04E+06) GO TO 1	R 17
	CALL DISCOT (T,P,TABTY,TABNUY,TAPY,11.52,4,VIS)	R 18
	GO TO 3	R 19
1	VIS=1.0	R 20
	GO TO 3	R 21
2	VIS=1.462E-6*SQRT(T)/(1.+112./T)	R 22
3	RETURN	R 23
	END	R 24-
	SUBROUTINE SHOCK (RN,CN,DN,RN,UN,PN,HN)	C 1
	BN=RN*UN	C 2
	CN=PN+RN*UN**2	C 3
	DN=HN+.5*UN**2	C 4
	RETURN	C 5
	END	C 6-
	FUNCTION FOFAXT (AXT)	D 1
	COMMON /BLK6/ BETA1,BETA2	D 2
	FOFAXT=-.4*BETA1-.25*ALOG((1.-AXT)/(1.+AXT))+.5*ATAN(AXT)-AXT	D 3
	RETURN	D 4
	END	D 5-

APPENDIX A

```

FUNCTION FOFBXT (RXT)
COMMON /BLK6/ BETA1,BETA2
FOFBXT=-.4*BETA1+.25*ALOG((1.+RXT)/(1.-RXT))+.5*ATAN(RXT)-.4*RXT**
15/BETA2-RXT
RETURN
END
FUNCTION FOFAX (AX)
COMMON /BLK6/ BETA1,BETA2
FOFAX=-BETA1-ALOG(1.-AX)-AX
RETURN
END
FUNCTION FOFBX (RX)
COMMON /BLK6/ BETA1,BETA2
FOFBX=-BETA1-ALOG(1.-RX)-RX**2/BETA2-RX
RETURN
END
FUNCTION FOFX (RN)
COMMON /BLK1/ BT4,CT4,RHOG
FOFX=RHOG-(BT4*RN**2+CT4*RN**3)
RETURN
END
FUNCTION FOFR (RNI)
COMMON /BLK2/ BT1,CT1,T1,CVR1,S4P,SREF,DBT1,DCT1
A=CVR1*ALOG(T1)
R=BT1+T1*DBT1
C=CT1+T1*DCT1
1 FOFR=A-ALOG(RNI)-(RNI*R)-(RNI**2/2.)*C+SREF-S4P
RETURN
END
FUNCTION FOEMS (MSN)
COMMON /BLK3/ T1,GAM4,W4,T4,P4,P1
REAL MSN
A=P4/P1
B=(GAM4-1.)/2.4
C=SQRT(.04833*((T1*W4)/(GAM4*T4)))
D=2.*GAM4/(GAM4-1.)
DEN=(1.-B*C*(MSN-1./MSN))**D
FOEMS=SQRT(((A*DEN)+.1667)/1.1667)
RETURN
END
SUBROUTINE SIMP (TABX,TARY,N,NMAX,TABANS)
DIMENSION TABX(NMAX), TARY(NMAX), TABANS(NMAX)
DIMENSION NP(4)
COMMON ICOUNT,IMFT(2),NP,APAR,ME,ME,SAP,LCODE,DELU
COMMON /BLK4/ LF,NON,LU,NDRIV,LR,LQ,LG
TABANS(1)=0
DEN=2.
K=2
C
TABX(THAT IS TABHR) IN DECREASING ORDER - DELX THIS NEGATIVE
DO I J=K,N
NON=J
DELX=(TABX(J)-TABX(J-1))/DEN
X=TABX(J-1)+DELX
CALL FTLUP (X,Y,-2,N,TABX,TARY)
SUM=(TARY(J-1)+4.*Y+TARY(J))*(ABS(DELX))/3.
TABANS(J)=TABANS(J-1)+SUM
I
CONTINUE
RETURN
END
SUBROUTINE SNS (RX,UX,PX,HX,SX,TX,AX,ZY,GX,ZSX,MX,PSX,USX,PSY,H5X,
1 HTX,PTX,RTX,STX,TTX,ATX,ZTX,GTU,ZTSX)
DIMENSION X(4), Y(4,9,150), Z(9), U(4), V(4), W(4), NO(4)
REAL M51,M2,M5,M55,MX,MN,MNS
COMMON ICOUNT,IMFT(2),NP,APAR,ME,ME,SAP,LCODE,DELU,ISAV
CALL SHOCK (BSN,CSN,DSN,PSX,USX,PSY,H5X)
IMFT(1)=IMFT(2)=0

```

APPENDIX A

	IT=8	L	0
	NV=0	L	0
	ISP=1	L	10
	RX=12.*R5X	L	11
	HTX=DSN	L	12
1	UX=PSN/RX	L	13
	PX=PSN-PSN*UX	L	14
	HX=DSN-.5*UX**2	L	15
	GO TO (2,3), ISAV	L	16
2	CALL SEARCH (PX,RNEW,HX,SX,TX,AX,ZX,GX,ZSX,ISP)	L	17
	GO TO 4	L	18
3	CALL SAVE (PX,RNEW,HX,SX,TX,AX,ZX,GX,Z)	L	19
	ZSX=ZX	L	20
4	IF (ABS(1.-RX/RNEW).LE.0.001) GO TO 5	L	21
	RX=RNEW	L	22
	GO TO 1	L	23
5	RX=RNEW	L	24
	MX=IX/AX	L	25
	STX=SX	L	26
	GO TO (6,7), ISAV	L	27
6	HTX=HX+.5*UX**2	L	28
	Z(4)=HTX/287.024F	L	29
	Z(4)=ALOG10(Z(4))	L	30
	CALL SLOW (SX,Z(4),3,IT,NV,NFPR,Y,X)	L	31
	PTX=(10.0**Z(3))*1.013246F+5	L	32
	CALL SEARCH (PTX,RTX,HTX,STX,TTX,ATX,ZTX,GTZ,7TSX,ISP)	L	33
	STX=GX	L	34
	GO TO 9	L	35
7	PTX=PX*(1.+(GX-1.)/2.)*MX**2)**(GX/(GX-1.))	L	36
8	CALL SAVE (PTX,RTX,HTX,STX,TTX,ATX,ZTX,GTZ,1)	L	37
	ZTSX=ZTX	L	38
	IF (ABS(1.-HTX/(HX+.5*UX**2)).LE.0.001) GO TO 9	L	39
	PTX=(PTX*(HX+.5*UX**2))/HTX	L	40
	GO TO 8	L	41
9	RETURN	L	42
	END	L	43-
	SUBROUTINE RDT (RTM,CTM,DBM,DCM,D2RM,D2CM,TM)	M	1
	COMMON /BLK4/ LF,NDN,LU,NDRIV,LR,LD,LG	M	2
	IF (NDRIV.EQ.1) GO TO 1	M	3
C		M	4
C	HFLJHM USED AS DRIVER GAS	M	5
C		M	6
	AMT1=15.8922-ALOG(TM)	M	7
	AMT2=-3.7156F-3*TM	M	8
	RTM=3.3565F-6*AMT1**3-2.0085F-3*EXP(AMT2)	M	9
	CTM=5.637F-12*AMT1**6	M	10
	DBM=(-1.00695F-5/TM)*AMT1**2+7.4628F-6*EXP(AMT2)	M	11
	DCM=(-3.3798F-11/TM)*AMT1**5	M	12
	D2RM=(2.0139E-5/TM**2)*AMT1+(1.00695F-5/TM**2)*AMT1**2-2.7729F-8*F	M	13
	EXP(AMT2)	M	14
	D2CM=(1.6899F-10/TM**2)*AMT1**4+(3.3798F-11/TM**2)*AMT1**5	M	15
	GO TO 2	M	16
C	HYDROGEN USED AS DRIVER GAS	M	17
1	RTM=1.6994F-3*TM**0.25	M	18
	CTM=2.1E-4	M	19
	DBM=4.2485F-4*TM**(-.75)	M	20
	DCM=0.2CM=0.	M	21
	D2RM=-3.1864F-4*TM**(-1.75)	M	22
2	RETURN	M	23
	END	M	24-
	SUBROUTINE SEARCH (P,RHO,H1,SOR,T1,A1,Z1,GAM,ZS,ISP)	N	1
	DIMENSION G(4), Y1(4), Y2(4), Y3(4), Y4(4), Y5(4), Y6(4), Y7(4)	N	2
	DIMENSION ICOUNT(25), JFLAG(25), V(9,150), P(25), RHO(25)	N	3
	DIMENSION SAVEH(25,4), SAVEP(25,4), SAVET(25,4), SAVEA(25,4)	N	4
	DIMENSION SAVEZ(25,4), SAVES(25,4), SAVEC(25,4), SAVE7S(25,4)	N	5
	DIMENSION H1(25), T1(25), A1(25), Z1(25), SOR(25), GAM(25), ZS(25)	N	6

APPENDIX A

	DIMENSION TART(150), TARR(150), TARP(150), TAPH(150)	N	7
	DIMENSION TABA(150), TARZ(150), TARG(150), TAPZS(150)	N	8
	DO 1 I=1,150	N	9
	ICOUNT(I)=1	N	10
	JFLAG(I)=0	N	11
1	CONTINUE	N	12
	JUMP=0	N	13
	IT=8	N	14
	REWIND IT	N	15
2	READ (IT) X,NV,((Y(I,L),I=1,9),L=1,NV)	N	16
	IF (ENDFILE IT) 3,6	N	17
3	CONTINUE	N	18
	WRITE (6,16)	N	19
	DO 5 I=1,ISP	N	20
	IF (JFLAG(I).EQ.0) GO TO 4	N	21
	GO TO 5	N	22
4	CONTINUE	N	23
	RHO(I)=0.	N	24
	T1(I)=0.	N	25
	A1(I)=0.	N	26
	Z1(I)=0.	N	27
	SOR(I)=0.	N	28
	GAM(I)=0.	N	29
	ZS(I)=0.	N	30
5	CONTINUE	N	31
	GO TO 15	N	32
6	CONTINUE	N	33
	DO 14 J=1,ISP	N	34
	IF (JFLAG(J).EQ.1) GO TO 14	N	35
	NN=ICOUNT(J)	N	36
	PP=ALOG10(P(J)/1.21325E+5)	N	37
	HH=ALOG10(H1(J)/287.0245)	N	38
	IF ((PP-Y(3,1))*(PP-Y(3,NV)).LT.0.) GO TO 7	N	39
	SAVEH(J,1)=0.	N	40
	SAVER(J,1)=0.	N	41
	SAVET(J,1)=0.	N	42
	SAVEA(J,1)=0.	N	43
	SAVEZ(J,1)=0.	N	44
	SAVES(J,1)=0.	N	45
	SAVEG(J,1)=0.	N	46
	SAVEZS(J,1)=0.	N	47
	NN=2	N	48
	GO TO 10	N	49
7	DO 8 I=1,NV	N	50
	TART(I)=Y(1,I)	N	51
	TARR(I)=Y(2,I)	N	52
	TARP(I)=Y(3,I)	N	53
	TAPH(I)=Y(4,I)	N	54
	TARG(I)=Y(5,I)	N	55
	TABA(I)=Y(6,I)	N	56
	TARZ(I)=Y(7,I)	N	57
	TAPZS(I)=Y(9,I)	N	58
8	CONTINUE	N	59
	CALL DISCOT (PP,PP,TARP,TAPH,TARH,-130,NV,0,ANS1)	N	60
	CALL DISCOT (PP,PP,TARP,TARR,TABR,-130,NV,0,ANS2)	N	61
	CALL DISCOT (PP,PP,TARP,TART,TART,-130,NV,0,ANS3)	N	62
	CALL DISCOT (PP,PP,TARP,TABA,TABA,-130,NV,0,ANS4)	N	63
	CALL DISCOT (PP,PP,TARP,TARZ,TARZ,-130,NV,0,ANS5)	N	64
	CALL DISCOT (PP,PP,TARP,TARG,TARG,-130,NV,0,ANS6)	N	65
	CALL DISCOT (PP,PP,TARP,TAPZS,TAPZS,-130,NV,0,ANS7)	N	66
	SAVES(J,NN)=X	N	67
	SAVEH(J,NN)=ANS1	N	68
	SAVER(J,NN)=ANS2	N	69
	SAVET(J,NN)=ANS3	N	70
	SAVEA(J,NN)=ANS4	N	71
	SAVEZ(J,NN)=ANS5	N	72

APPENDIX A

	SAVEG(J,NN)=ANS6	N	73
	SAVEZS(J,NN)=ANS7	N	74
	IF (SAVEH(J,NN).GT.HH) GO TO 11	N	75
	IF (NN.EQ.3) GO TO 9	N	76
	NN=NN+1	N	77
	GO TO 10	N	78
9	SAVER(J,1)=SAVER(J,2)	N	79
	SAVEH(J,1)=SAVEH(J,2)	N	80
	SAVET(J,1)=SAVET(J,2)	N	81
	SAVEA(J,1)=SAVEA(J,2)	N	82
	SAVEZ(J,1)=SAVEZ(J,2)	N	83
	SAVES(J,1)=SAVES(J,2)	N	84
	SAVEG(J,1)=SAVEG(J,2)	N	85
	SAVEZS(J,1)=SAVEZS(J,2)	N	86
	SAVER(J,2)=SAVER(J,3)	N	87
	SAVEH(J,2)=SAVEH(J,3)	N	88
	SAVET(J,2)=SAVET(J,3)	N	89
	SAVEA(J,2)=SAVEA(J,3)	N	90
	SAVER(J,2)=SAVER(J,3)	N	91
	SAVES(J,2)=SAVES(J,3)	N	92
	SAVEG(J,2)=SAVEG(J,3)	N	93
	SAVEZS(J,2)=SAVEZS(J,3)	N	94
10	ICOUNT(J)=NN	N	95
	GO TO 14	N	96
11	IF (NN.EQ.4) GO TO 12	N	97
	NN=NN+1	N	98
	ICOUNT(J)=NN	N	99
	GO TO 14	N	100
12	JFLAG(J)=1	N	101
	DO 13 M=1,4	N	102
	G(M)=SAVEH(J,M)	N	103
	Y1(M)=SAVER(J,M)	N	104
	Y2(M)=SAVET(J,M)	N	105
	Y3(M)=SAVEA(J,M)	N	106
	Y4(M)=SAVEZ(J,M)	N	107
	Y5(M)=SAVES(J,M)	N	108
	Y6(M)=SAVEG(J,M)	N	109
	Y7(M)=SAVEZS(J,M)	N	110
13	CONTINUE	N	111
	CALL INTRP (4,G,Y1,HH,R)	N	112
	CALL INTRP (4,G,Y2,HH,T)	N	113
	CALL INTRP (4,G,Y3,HH,A)	N	114
	CALL INTRP (4,G,Y4,HH,Z)	N	115
	CALL INTRP (4,G,Y5,HH,SR1)	N	116
	CALL INTRP (4,G,Y6,HH,GAM1)	N	117
	CALL INTRP (4,G,Y7,HH,ZS1)	N	118
	RHO(J)=(10.*R)*1.291489	N	119
	T1(J)=T	N	120
	A1(J)=A*331.4184	N	121
	Z1(J)=Z	N	122
	SOR(J)=SR1	N	123
	GAM(J)=GAM1	N	124
	ZS(J)=ZS1	N	125
	JUMP=JUMP+1	N	126
	IF (JUMP.EQ.15) GO TO 15	N	127
14	CONTINUE	N	128
	GO TO 2	N	129
15	CONTINUE	N	130
	RETURN	N	131
C		N	132
C		N	133
C		N	134
16	FORMAT (1H1,60X,7HWARNING////)	N	135
	END	N	136
	SUBROUTINE SLOW (XX,Z,I1,J1,IT,NV,NPR,Y,X)	C	1
C	TAPE IS WRITTEN WITH LINES OF CONSTANT XX	C	2

APPENDIX A

C	Z(11) AND XX ARE INDEPENDENT VARIABLES	3
C	Z(J1) IS THE DEPENDENT VARIABLE	4
C	AK= +1. IF XX INCREASES MONOTONICALLY ON TAPE	5
C	AK= -1. IF XX DECREASES MONOTONICALLY ON TAPE	6
C	IT= TAPE UNIT	7
C	NV= NO. OF VARIABLES ON TAPE FOR EACH XX (NOT GREATER THAN 9)	8
C	NO. OF POINTS FOR EACH XX NOT GREATER THAN 150	9
C	BEGIN EXECUTION	10
	DIMENSION X(4), Y(4,9,150), Z(9), U(4), V(4), W(4), NP(4)	11
	COMMON ICOUNT,IMET(2),NP,ABAR,MF,MF,SAR,LCODE,DELU	12
	REAL MF,MF	13
	ICOUNT=ICOUNT+1	14
	IF (IMET(1)) 3,1,3	15
1	BACKSPACE IT	16
	READ (IT) DUM	17
	REWIND IT	18
	DO 2 K=1,3	19
	READ (IT) X(K),J,((Y(K,I,L),I=1,NV),L=1,J)	20
2	NP(K)=J	21
	XW=X(2)-X(1)	22
	AK=ABS(XW)/XW	23
	DIR1=1.	24
	IMET(1)=1	25
	XXX=YX	26
	NERR=0	27
	IM=3	28
	GO TO 18	29
3	NERR=0	30
C	EXCEPT FOR FIRST TIME THROUGH	31
	IF ((XX-X(M1))*(XX-X(M2))) 25,25,4	32
4	TEMP=(XX-XXX)*AK	33
	DIR2=ABS(TEMP)/TEMP	34
	GO=DIR1*DIR2	35
	XXY=YX	36
	DIR1=DIR2	37
	IF (DIR2) 5,35,16	38
C		39
C	NEGATIVE DIRECTION	40
5	IF (GO) 6,35,7	41
6	BACKSPACE IT	42
	BACKSPACE IT	43
	BACKSPACE IT	44
	GO TO 9	45
7	IM=IM-1	46
	IF (IM) 8,8,9	47
8	IM=4	48
9	M1=IM+1	49
	BACKSPACE IT	50
	BACKSPACE IT	51
	IF (M1-4) 11,11,10	52
10	M1=1	53
11	M2=M1+1	54
	IF (M2-4) 13,13,12	55
12	M2=1	56
13	READ (IT) X(IM),J,((Y(IM,I,L),I=1,NV),L=1,J)	57
	NP(IM)=J	58
	IF ((XX-X(M1))*(XX-X(M2))) 25,25,14	59
14	IF (X(M1)-X(M2)) 7,15,7	60
C	ERROR, VARIABLE OFF FRONT END OF TAPE	61
15	CONTINUE	62
	NERR=1	63
	GO TO 36	64
C		65
C	POSITIVE DIRECTION	66
16	IF (GO) 17,35,18	67

APPENDIX A

```

17 READ (IT) DUM
   READ (IT) DUM
   READ (IT) DUM
   GO TO 20
18 IM=IM+1
   IF (IM-4) 20,20,19
19 IM=1
20 M1=IM-1
   IF (M1) 21,21,22
21 M1=4
22 M2=M1-1
   IF (M2) 23,23,24
23 M2=4
24 READ (IT) X(IM),J,((Y(IM,I,L),I=1,NV),L=1,J)
   NP(IM)=J
   IF ((XX-X(M1))*(XX-X(M2))) 25,25,18
C
C   TAPE SEARCH COMPLETE & DO CROSS FOUR POINT
25 DO 34 K=1,4
   NPK=NP(K)-1
   DO 26 I=1,NPK
   IF ((Y(K,I,1)-Z(I1))*(Y(K,I,1+1)-Z(I1))) 27,27,26
26 CONTINUE
   NFRR=1
   GO TO 36
27 IF (I-1) 29,28,29
28 J=0
   GO TO 32
29 IF (I-NPK) 31,30,31
30 J=NPK-3
   GO TO 32
31 J=1-2
32 DO 33 L=1,4
   MX=L+J
   U(L)=Y(K,I,MX)
33 V(L)=Y(K,J,MX)
34 CALL INTRP (4,U,V,Z(I1),W(K))
   CALL INTRP (4,X,W,XX,Z(J1))
   RETURN
35 CONTINUE
36 NFRR=1
   IF (IMET(2)) 38,37,38
37 IMET(2)=1
   LODE=2
   WRITE (6,39) XX,J1,Z(I1),J1
38 RETURN
C
C
C
39 FORMAT (///39H NO SOLUTION ON TAPE FOR THE CONDITIONS//5X,6H S/R=
1F12.6,37X,9H EVALUATE/6X,2HZ(11,2H)=F16.8,38X,3H Z(11,1H)///)
END
SUBROUTINE SAVE (P,RHO,H,SP,T,AM,Z,GAME,K)
C
C   SAVE OBTAINS THERMODYNAMIC PROPERTIES FOR REAL AIR
C   IS BASED ON CURVE FIT EXPRESSIONS OF AEDC-TOR-63-138
C   EXPRESSIONS OF AEDC-TOR-63-138 APPLICABLE FOR T=90 TO 15000
C   MAXIMUM PERCENT ERRORS- T=2000 TO 15000, AND P=1E+4 TO 1E+6
C
C   RHO      H      T      A      Z      GAME
C   2.42     1.96     2.24     2.78     0.75     5.68
C
C   INPUTS ARE PRESSURE(N/SQ METER) AND-
C   (1) ENTROPY,S/R (K=1)
C   (2) DENSITY, KG/CUBIC METER (K=2)
C   (3) ENTHALPY, SQ METER/SQ SEC (K=3)

```

APPENDIX A

C			P	16
C	ALSO, INPUTS DENSITY AND ENTHALPY ARE INCLUDED (K=4)		P	17
C			P	18
C			P	19
C	MODIFIED 9/7/71 FOR INPUTS P AND T (K=5)		P	20
C			P	21
	DIMENSION TABSR(6), TARR(6), TABH(6)		P	22
	DIMENSION TARP(13), TAPHM(13), TAPSRM(13), PM(13)		P	23
	DIMENSION TARTR(17), TARRR(17), TABSR(17), TAPHR(17), TABZR(17)		P	24
	W0=28.967		P	25
	RUNIV=8314.34		P	26
	NN=0		P	27
	MM=0		P	28
	IF (K.NE.5) GO TO 3		P	29
	ZZ=.8		P	30
	DO 2 I=1,17		P	31
	RHO=P*W0/(RUNIV*ZZ*T)		P	32
	TABRR(I)=RHO		P	33
	GO TO 6		P	34
1	TABSR(I)=SR		P	35
	TAPHR(I)=HA		P	36
	TABZR(I)=Z		P	37
	TARTR(I)=TA		P	38
	ZZ=ZZ+.2		P	39
	MM=0		P	40
	NN=0		P	41
2	CONTINUE		P	42
	CALL FTLUP (T,SR,2,17,TARTR,TABSR)		P	43
	CALL FTLUP (T,H,2,17,TAPTR,TAPHR)		P	44
	CALL FTLUP (T,Z,2,17,TABTR,TABZR)		P	45
	CALL FTLUP (T,RHO,2,17,TARTR,TABRR)		P	46
	MM=3		P	47
	GO TO 8		P	48
3	IF (K.NE.4) GO TO 6		P	49
	CONS=.03		P	50
	DO 5 J=1,13		P	51
	PM(J)=RHO*H*CONS		P	52
	TARPM(J)=PM(J)		P	53
	P=PM(J)		P	54
	GO TO 6		P	55
4	TAPHM(J)=HA		P	56
	TAPSRM(J)=SR		P	57
	CONS=CONS+.03		P	58
	MM=0		P	59
	NN=0		P	60
5	CONTINUE		P	61
	CALL FTLUP (H,P,2,13,TAPHM,TARPM)		P	62
	CALL FTLUP (H,SR,2,13,TAPHM,TAPSRM)		P	63
	MM=3		P	64
6	PLOG=ALOG10(P/1.01325E+5)		P	65
	A=PLOG*PLOG		P	66
	C=A*PLOG		P	67
	IF (K.EQ.1) GO TO 8		P	68
	IF (K.EQ.4.AND.MM.EQ.3) GO TO 8		P	69
	SRUP=142.		P	70
	SRLOW=14.		P	71
	SR=(SRUP-SRLOW)/2.+14.		P	72
7	DFLSR=(SRUP-SRLOW)/2.		P	73
	IF (NN.EQ.0) GO TO 8		P	74
	SR=SRUP-DFLSR		P	75
8	SRLOG=ALOG10(SR)		P	76
	B=SRLOG*SRLOG		P	77
	D=B*SRLOG		P	78
	X15=-39.1442+83.0558*SRLOG-38.2842*SRLOG*SRLOG		P	79
	X151=-10.*(PLOG-X15)		P	80
	IF (X151-40.) 10,9,9		P	81

APPENDIX A

9	TI5=0.0	D	82
	GO TO 13	D	83
10	IF (X151+40.) 11,12,12	D	84
11	TI5=1.0	D	85
	GO TO 13	D	86
12	TI5=1./(1.+EXP(X151))	D	87
13	IF (K.FQ.3.AND.MM.NF.2) GO TO 39	D	88
	IF (K.FQ.2.AND.MM.FQ.2) GO TO 39	D	89
	IF (K.FQ.4.AND.MM.FQ.3) GO TO 61	D	90
	IF (K.FQ.4.AND.MM.FQ.2) GO TO 39	D	91
	IF (K.FQ.5.AND.MM.FQ.2) GO TO 39	D	92
	IF (K.FQ.5.AND.MM.FQ.3) GO TO 83	D	93
C		D	94
C	COMPUTING RHO AS A FUNCTION OF P AND S/P	D	95
C		D	96
14	XR12=-16.5527+57.45*SRLOG-30.8036*B	D	97
	XR23=499.544-938.91*SRLOG+609.028*B-135.995*B	D	98
	XR34=360.507-634.538*SRLOG+389.174*B-82.4653*B	D	99
	XR45=489.628-458.5*SRLOG+106.25*B	D	100
	XR121=-10.*(PLOG-XR12)	D	101
	XR231=-10.*(PLOG-XR23)	D	102
	XR341=-10.*(PLOG-XR34)	D	103
	XR451=-10.*(PLOG-XR45)	D	104
	IF (XR121-40.) 15,18,18	D	105
15	IF (XR121+40.) 16,17,17	D	106
16	TR12=1.0	D	107
	GO TO 19	D	108
17	TR12=1./(1.+EXP(XR121))	D	109
	GO TO 19	D	110
18	TR12=0.0	D	111
19	IF (XR231-40.) 20,23,23	D	112
20	IF (XR231+40.) 21,22,22	D	113
21	TR23=1.0	D	114
	GO TO 24	D	115
22	TR23=1./(1.+EXP(XR231))	D	116
	GO TO 24	D	117
23	TR23=0.0	D	118
24	IF (XR341-40.) 25,28,28	D	119
25	IF (XR341+40.) 26,27,27	D	120
26	TR34=1.0	D	121
	GO TO 29	D	122
27	TR34=1./(1.+EXP(XR341))	D	123
	GO TO 29	D	124
28	TR34=0.0	D	125
29	IF (XR451-40.) 30,33,33	D	126
30	IF (XR451+40.) 31,32,32	D	127
31	TR45=1.0	D	128
	GO TO 34	D	129
32	TR45=1./(1.+EXP(XR451))	D	130
	GO TO 34	D	131
33	TR45=0.0	D	132
34	RHCL1=15.951867-0.00228295*PLOG-15.994242*SRLOG+.0065187267*A+.530	D	133
	179685*PLOG*SRLOG+3.175974*B	D	134
	RHCL2=1541.1666-63.93035*PLOG-2993.1662*SRLOG+.935437*A+84.30375*B	D	135
	1RLOG*PLOG+1938.7061*B-.004746016*C-.6128404*A*SRLOG-27.422666*B*OL	D	136
	2OG-419.0881*B	D	137
	RHCL3=427.4745-18.126622*PLOG-765.47626*SRLOG+.29343169*A+22.92687	D	138
	17*PLOG*SRLOG+456.717*B-.0017033404*C-.18068309*A*SRLOG-6.9143617*B	D	139
	2*PLOG-91.131851*B	D	140
	RHCL4=206.23144-8.2270278*PLOG-329.54655*SRLOG+.1324191*A+9.8884165	D	141
	1*PLOG*SRLOG+175.03931*B-.0010178454*C-.07654371*A*SRLOG-2.6920144*	D	142
	2B*PLOG-31.237824*B	D	143
	RHCL5=-399.52358+12.899477*PLOG+411.64144*SRLOG-.097694919*A-6.220	D	144
	14477*PLOG*SRLOG-106.6733*B	D	145
	RHCL1=(RHCL2-RHCL1)*TR12+(RHCL3-RHCL2)*TR23+(RHCL4-RHCL3)*TR	D	146
	134+(RHCL5-RHCL4)*TR45	D	147
	RH15=-79.282533+6.3537078*PLOG+179.22721*SRLOG-.12607098*A-8.40131	D	148

APPENDIX A

```

122*PLOG*SRL0G-129.95269*B+.0010037437*C+.004185511*A*SRL0G+3.12569 P 149
266*PLOG*B+30.203862*D P 150
RHCAL=RH15+(RHCAL-RH15)*T15 P 151
RHOA=(10.**RHCAL)*1.29233 P 152
IF (K.EQ.1) GO TO 39 P 153
IF (K.EQ.3) GO TO 61 P 154
IF (K.EQ.2.AND.MM.EQ.1) GO TO 59 P 155
IF (K.EQ.4.AND.MM.EQ.1) GO TO 59 P 156
IF (K.EQ.5.AND.MM.EQ.1) GO TO 59 P 157
C P 158
C CONVERGENCE TEST FOR K=2 P 159
C P 160
IF (ABS(1.-RHO/RHOA).LE..001) GO TO 39 P 161
NN=NN+1 P 162
IF (RHO.GT.RHOA) GO TO 37 P 163
35 SRLOW=SR P 164
SRUP=SR+DELSR P 165
IF (DELSR.GT.1.) GO TO 7 P 166
TAPSR(1)=SRLOW P 167
TAPSR(6)=SRUP P 168
IF (K.EQ.2.OR.K.EQ.4) GO TO 36 P 169
IF (K.EQ.5) GO TO 36 P 170
N=2 P 171
GO TO 52 P 172
36 N=-2 P 173
GO TO 57 P 174
37 SRUP=SR P 175
SRLOW=SR-DELSR P 176
IF (DELSR.GT.1.) GO TO 7 P 177
TAPSR(1)=SRUP P 178
TAPSR(6)=SRLOW P 179
IF (K.EQ.2.OR.K.EQ.4) GO TO 38 P 180
IF (K.EQ.5) GO TO 38 P 181
N=-2 P 182
GO TO 52 P 183
38 N=2 P 184
GO TO 57 P 185
C P 186
C COMPUTING ENTHALPY AS A FUNCTION OF P AND S/R P 187
C P 188
39 IF (SRL0G-1.6) 40,40,41 P 189
40 HRCAL=12.693869+5.3975312*PLOG-48.729217*SRL0G-.14961521*A-5.87887 P 190
174*PLOG*SRL0G+48.19278*B+.00090144132*C+.001151473*A*SRL0G+1.62828 P 191
229*PLOG*B-13.065267*D P 192
GO TO 51 P 193
41 IF (SRL0G-1.76) 42,42,48 P 194
42 HR22=-156.37194+6.6959228*PLOG+269.93097*SRL0G-.097179965*A-7.6379 P 195
1714*PLOG*SRL0G-152.13866*B+.00057029937*C+.058364795*A*SRL0G+2.159 P 196
22755*PLOG*B+28.940926*D P 197
HR21=-84.008522+2.5761318*PLOG+107.06198*SRL0G-.014352904*A-1.5313 P 198
1194*PLOG*SRL0G-32.316439*B P 199
XH=-61.2053+114.103*SRL0G-47.5532*B P 200
XH1=-10.*(PLOG-XH) P 201
IF (XH1-40.) 43,45,46 P 202
43 IF (XH1+40.) 44,45,45 P 203
44 TH=1. P 204
GO TO 47 P 205
45 TH=1./(1.+EXP(XH1)) P 206
GO TO 47 P 207
46 TH=0.0 P 208
47 HRCAL=HR21+(HR22-HR21)*TH P 209
GO TO 51 P 210
48 IF (SRL0G-1.92) 49,49,50 P 211
49 HRCAL=-35.160671+.5366924*PLOG+56.99585*SRL0G-.022661358*A-.484703 P 212
105*SRL0G*PLOG-27.641087*B+.00058568839*C+.016299962*A*SRL0G+.14073 P 213
2606*B*PLOG+4.712261*D P 214
GO TO 51 P 215

```

APPENDIX A

```

50  HRCAL=-114.94796+4.004583*PLOG+180.08427*SRL0G-.041327787*A-4.0366 P 216
    1535*PLOG*SRL0G-90.76006*B+.00040320694*C+.024360248*A*SRL0G+1.0462 P 217
    2299*PLOG*B+15.467804*D P 218
51  HR15=28.160664-2.2339873*PLOG-59.053694*SRL0G+.054973544*A+3.71832 P 219
    157*PLOG*SRL0G+40.986503*B-.0004292698*C-.040726332*A*SRL0G-1.37045 P 220
    205*PLOG*B-8.253645*D P 221
    HRCAL=HR15+(HRCAL-HR15)*T15 P 222
    HA=(10.0*HRCAL)*287.0388 P 223
    IF (K.EQ.1.0R.K.EQ.2) GO TO 61 P 224
    IF (K.EQ.5) GO TO 61 P 225
    IF (K.EQ.3.AND.MM.EQ.1) GO TO 55 P 226
    IF (K.EQ.4) GO TO 4 P 227
C P 228
C CONVERGENCE TEST FOR K=3 P 229
C P 230
    IF (ABS(1.-H/HA).LE.0.001) GO TO 14 P 231
    NN=NN+1 P 232
    IF (HA.GT.H) GO TO 37 P 233
    GO TO 35 P 234
C P 235
C INTERPOLATION FOR DELSR LESS THAN 1 P 236
C P 237
52  TAPR(1)=HA P 238
53  DELSR=(TABSR(6)-TABSR(1))/5. P 239
    DO 54 I=2,5 P 240
    TABSR(I)=TABSR(I-1)+DELSR P 241
54  CONTINUE P 242
    IF (K.EQ.2.0R.K.EQ.4) GO TO 58 P 243
    IF (K.EQ.5) GO TO 58 P 244
    DO 56 I=2,6 P 245
    MM=1 P 246
    SR=TABSR(1) P 247
    GO TO 8 P 248
55  TAPR(1)=HA P 249
56  CONTINUE P 250
    CALL FTLUP (H,SR,N,6,TAPR,TABSR) P 251
    MM=2 P 252
    GO TO 8 P 253
57  TAPR(1)=RHOA P 254
    GO TO 53 P 255
58  DO 60 I=2,6 P 256
    MM=1 P 257
    SR=TABSR(1) P 258
    GO TO 8 P 259
59  TAPR(1)=RHOA P 260
60  CONTINUE P 261
    CALL FTLUP (RHO,SR,N,6,TAPR,TABSR) P 262
    MM=2 P 263
    GO TO 8 P 264
C P 265
C COMPUTING Z P 266
C P 267
61  XZ12=62.91-41.5*SRL0G P 268
    XZ23=72.945-45.75*SRL0G P 269
    XZ34=65.75-37.5*SRL0G P 270
    XZ45=62.92-32.0*SRL0G P 271
    XZ121=-10.0*(PLOG-XZ12) P 272
    XZ231=-10.0*(PLOG-XZ23) P 273
    XZ341=-10.0*(PLOG-XZ34) P 274
    XZ451=-10.0*(PLOG-XZ45) P 275
    ZCAL2=519.80374-27.753514*PLOG-987.00729*SRL0G+.27286957*A+30.0847 P 276
    179*PLOG*SRL0G+620.04168*B-.0021648826*C-.22710079*A*SRL0G-9.496907 P 277
    2*PLOG*B-129.78921*D P 278
    ZCAL3=366.40674-15.517444*PLOG-647.42436*SRL0G+.18701758*A+18.0403 P 279
    183*PLOG*SRL0G+379.59834*B-.00087958438*C-.10580129*A*SRL0G-5.18882 P 280

```

APPENDIX A

```

254*PLOG*B-73.504269*0
ZCAL4=516.07331-16.59277*PLOG-808.49823*SRLOG+.071256235*A+16.5268
113*PLOG*SRLOG+418.45341*B+.00094183347*C-.019727817*A*SRLOG-3.9948
2906*PLOG*B-71.038921*0
IF (XZ121-40.) 62,65,65
62 IF (XZ121+40.) 63,64,64
63 TZ12=1.
GO TO 66
64 TZ12=1./(1.+EXP(X7121))
GO TO 66
65 TZ12=0.0
66 IF (XZ231-40.) 67,70,70
67 IF (XZ231+40.) 68,69,69
68 TZ23=1.
GO TO 71
69 TZ23=1./(1.+EXP(X7231))
GO TO 71
70 TZ23=0.0
71 IF (XZ341-40.) 72,75,75
72 IF (XZ341+40.) 73,74,74
73 TZ34=1.
GO TO 76
74 TZ34=1./(1.+EXP(XZ341))
GO TO 76
75 TZ34=0.0
76 IF (XZ451-40.) 77,80,80
77 IF (XZ451+40.) 78,79,79
78 TZ45=1.
GO TO 81
79 TZ45=1./(1.+EXP(X7451))
GO TO 81
80 TZ45=0.0
81 ZCAL=1.0+(ZCAL2-1.)*TZ12+(ZCAL3-ZCAL2)*TZ23+(ZCAL4-ZCAL3)*TZ34+(4.
10-ZCAL4)*TZ45
ZCAL=1.+(ZCAL-1.)*T15
Z=ZCAL
C
C COMPUTING T(DFG K)
C
IF (K.F0.2.0R.K.F0.4) GO TO 82
IF (K.E0.5) GO TO 82
RHO=RH0A
82 TA=P*W0/(RHO*RUN)V*Z)
IF (K.F0.5) GO TO 1
T=TA
C
C COMPUTING A(M/SEC)
C
83 IF (T-2100.) 84,84,87
84 IF (T-1500.) 86,86,85
85 IF (PLOG+1.) 87,87,86
86 CON1=SQRT(T/273.15)
AOAO=-.0753808+CON1*(1.12644-.0552696*CON1)
AM=331.3115*AOAO
GO TO 108
87 XA12=635.054-1220.46*SRLOG+803.882*B-180.845*0
XA23=373.702-663.358*SRLOG+408.854*B-86.8056*0
XA34=1703.78-2602.97*SRLOG+1337.93*B-231.422*0
XA22=1043.37-1820.34*SRLOG+1076.36*B-215.445*0
XA121=-10.*(PLOG-XA12)
XA231=-10.*(PLOG-XA23)
XA341=-10.*(PLOG-XA34)
XA221=-10.*(PLOG-XA22)
A1=-4409.6241+196.82259*PLOG+8746.4634*SRLOG-3.1650299*A-262.32947
1*PLOG*SRLOG-5786.449*B+.020004186*C+2.1429825*A*SRLOG+87.589029*DL

```


APPENDIX A

20G	R+1277.6718*D	D	346
	A21=-1814.5117+86.094078*PLOG+3315.6099*SRLOG-1.7593034*A-107.2534	D	347
1	*PLOG*SRLOG-2023.201*R+.016287679*C+1.1398134*A*SRLOG+33.659607*P	D	348
20G	R+413.41945*D	D	349
	A22=2651.2944-81.405596*PLOG-3099.0064*SRLOG+.69752668*A+48.062506	D	350
1	*PLOG*SRLOG+907.70889*R	D	351
	IF (XA221-40.) 89.88.88	D	352
88	TA22=0.0	D	353
	GO TO 92	D	354
89	IF (XA221+40.) 90.90.91	D	355
90	TA22=1.0	D	356
	GO TO 92	D	357
91	TA22=1./(1.+EXP(XA221))	D	358
92	A2=A21+(A22-A21)*TA22	D	359
	A3=-3217.8037+195.34964*PLOG+5348.2143*SRLOG-4.6268475*A-221.12705	D	360
1	*PLOG*SRLOG-2970.8649*R+.044614358*C+2.7070177*A*SRLOG+63.042803*P	D	361
2	LOG*R+553.12007*D	D	362
	A4=16976.939-476.10242*PLOG-17445.315*SRLOG+3.6534057*A+246.41125*	D	363
1	PLOG*SRLOG+4486.3118*R	D	364
	IF (XA121-40.) 94.93.93	D	365
93	TA12=0.0	D	366
	GO TO 97	D	367
94	IF (XA121+40.) 95.95.96	D	368
95	TA12=1.0	D	369
	GO TO 97	D	370
96	TA12=1./(1.+EXP(XA121))	D	371
97	IF (XA231-40.) 99.98.98	D	372
98	TA23=0.0	D	373
	GO TO 102	D	374
99	IF (XA231+40.) 100.100.101	D	375
100	TA23=1.0	D	376
	GO TO 102	D	377
101	TA23=1./(1.+EXP(XA231))	D	378
102	IF (XA341-40.) 104.103.103	D	379
103	TA34=0.0	D	380
	GO TO 107	D	381
104	IF (XA341+40.) 105.105.106	D	382
105	TA34=1.0	D	383
	GO TO 107	D	384
106	TA34=1./(1.+EXP(XA341))	D	385
107	A0A0=A1+(A2-A1)*TA12+(A3-A2)*TA23+(A4-A3)*TA34	D	386
	AM=331.3115*A0A0	D	387
C		D	388
C	COMPUTING GAME	D	389
C		D	390
108	GAME=W0*AM**2/(RUNIV*Z*T)	D	391
	IF (K.EQ.2) GO TO 109	D	392
	IF (K.EQ.3.OR.K.EQ.4) GO TO 110	D	393
	IF (K.EQ.5) GO TO 110	D	394
	H=HA	D	395
	GO TO 110	D	396
109	H=HA	D	397
110	RETURN	D	398
C		D	399
	END	D	400-
	SUBROUTINE INTRP (N,X,Y,XINT,YINT)	D	1
	DIMENSION X(N), Y(N)	D	2
	YINT=0.	D	3
	DO 3 J=1,N	D	4
	SUMN=1.	D	5
	SUMD=1.	D	6
	DO 2 J=1,N	D	7
	IF (J-I) 1,2,1	D	8
1	SUMN=SUMN*(XINT-X(J))	D	9
	SUMD=SUMD*(X(I)-X(J))	D	10
2	CONTINUE	D	11

APPENDIX A

3	YINT=YINT+Y(1)*SUMN/SUMD	Q	12
	RETURN	Q	13
	END	Q	14-
	SUBROUTINE SC (R21,UI,PI,HI,R11,US,P,H,ISAV)	Q	1
	COMMON /BLK4/ LF,NON,LU,NDRIV,LB,LD,LG	Q	2
	COMMON /BLK5/ SR,T11,A1,Z1,G1,K,P2,ISP	Q	3
	R21=10.*R11	Q	4
	IF (LB.EQ.1) GO TO 5	Q	5
	CALL SHOCK (B,C,D,R11,US,P,H)	Q	6
1	UI=US*(1.-R11/R21)	Q	7
	PI=C-(R21*(US-UI)**2)	Q	8
	HI=D-.5*(US-UI)**2	Q	9
	IF (LB.EQ.2) GO TO 3	Q	10
	GO TO (2,3), ISAV	Q	11
2	CALL SFARCH (PI,RNEW,HI,SR,T11,A1,Z1,G1,ZS1,ISP)	Q	12
	GO TO 4	Q	13
3	CALL SAVE (PI,RNEW,HI,SR,T11,A1,Z1,G1,3)	Q	14
4	IF (ABS(1.-RNEW/R21),LF,.001) GO TO 9	Q	15
	R21=RNEW	Q	16
	GO TO 1	Q	17
5	US=SQRT((PI-P)/(R11*(1.-R11/R21)))	Q	18
	UI=US*(1.-R11/R21)	Q	19
	HI=H+.5*(US**2-(US-UI)**2)	Q	20
	GO TO (6,7), ISAV	Q	21
6	CALL SFARCH (PI,RNEW,HI,SR,T11,A1,Z1,G1,ZS1,ISP)	Q	22
	GO TO 8	Q	23
7	CALL SAVE (PI,RNEW,HI,SR,T11,A1,Z1,G1,3)	Q	24
8	IF (ABS(1.-RNEW/R21),LF,.001) GO TO 9	Q	25
	R21=RNEW	Q	26
	GO TO 5	Q	27
9	RETURN	Q	28
	END	Q	29-
	SUBROUTINE SOLUT (U3,P3,U2,P2,M,N,MR,P)	S	1
	DIMENSION U3(20), P3(20), U2(10), P2(10), U(2)	S	2
	FUNCD(PP,UU,R)=PP-UU)*R	S	3
	FUNAR(P,PP,U,UU)=(P-PP)/(U-UU)	S	4
C		S	5
C	USE END POINTS FOR FIRST INTERSECTION	S	6
C		S	7
	MR=1	S	8
	NR=1	S	9
	IF (P2(1).GT.P2(2)) NR=-NR	S	10
	IF (P3(1).GT.P3(2)) MR=-MR	S	11
	P31=P3(1)	S	12
	P32=P3(M)	S	13
	P21=P2(1)	S	14
	P22=P2(N)	S	15
	U21=U2(1)	S	16
	U22=U2(N)	S	17
	U31=U3(1)	S	18
	U32=U3(M)	S	19
1	AA=FUNAR(P22,P21,U22,U21)	S	20
	BB=FUNAR(P32,P31,U32,U31)	S	21
	CC=FUNCD(P21,U21,AA)	S	22
	DD=FUNCD(P31,U31,BB)	S	23
	UR=(CC-DD)/(BB-AA)	S	24
	PR=CC+UR*AA	S	25
	CALL FTLUP (PR,U(1),NR,N,P2,U2)	S	26
	CALL FTLUP (PR,U(2),MR,M,P3,U3)	S	27
	IF (ABS((U(1)-U(2))/U(1))-0.001) 3,3,2	S	28
2	P31=P32	S	29

APPENDIX A

```

P32=PR
P21=P22
P22=PR
U31=U32
U32=U(2)
U21=U22
U22=U(1)
GO TO 1
3 P=PR
  RETURN
END
-00
L.E.T. PROGRAM FOR EQUILIBRIUM REAL AIR.
$INP RUN=441,P1=3447.5,US1=2865,US=5500,IREP=1,DELUS=330$
$INP RUN=86,P1=6895,US1=4300,US=7500,IREP=1,DELUS=500$

```

Sample data printouts for representative tests in the Langley 6-inch expansion tube with unheated and arc-heated helium driver gases are presented on the following pages. In most instances, the headings for various flow regions correspond to those in the section entitled "Symbols." Exceptions are UI, which denotes either the test-air—driver-gas interface velocity or acceleration-air—test-air interface velocity, RATIO, which denotes the ratio of density immediately behind an incident or standing shock to free-stream density, and labels ending in T (under heading "Shock Tube Flow Parameters Using Mirels Theory") which denote turbulent flow quantities. The sample printouts are as follows:

Unheated Helium Driver Gas

```

06/19/74
L.E.T. PROGRAM FOR EQUILIBRIUM REAL AIR

EXPANSION TUBE PROGRAM OF MILLER FOR REAL AIR
ALL PHYSICAL QUANTITIES IN MKS UNITS- NASA SP-7012

SHOCK TUBE PHASE OF PROGRAM

MEASURED INPUTS FOR SHOCK TUBE PHASE
  RUN      P1      T1      US1      P2      P4      T4      XIS      DIA      ISAV      INU      LD
4.410E+02  3.447E+03  3.000E+02  2.865E+03  0.      0.      0.      4.650E+00  1.524E-01  2      2      4

XXXXXXXXXXXXXXXXXXXXXXXXXXXXXXXXXXXXXXXXXXXXXXXXXXXXXXXXXXXX

CONDITIONS BEHIND INCIDENT SHOCK - REGION 2

XXXXXXXXXXXXXXXXXXXXXXXXXXXXXXXXXXXXXXXXXXXXXXXXXXXXXXXXXXXX

  P      RHO      T      H      S/R      Z      GAME      A      U      M      NRE
2.895E+05  3.087E-01  3.175E+03  4.336E+06  3.302E+01  1.029E+00  1.151E+00  1.039E+03  2.493E+03  2.400E+00  8.604E+06

RATIO- 2 TO 1 CONDITIONS AND SHOCK VELOCITY

```

APPENDIX A

P	RHO	T	H	A	MSI	US1
8.396E+01	7.710E+00	1.058E+01	1.443E+01	2.992E+00	8.252E+00	2.865E+03

SHOCK TUBE FLOW PARAMETERS USING WIRELS THEORY

LMAX	L	L/LMAX	TH	UT	LMAXT	LT	LT/LMAXT	TMT	UIT	THI
7.324E+01	5.675E-01	7.748E-03	2.245E-04	2.527E+03	1.030E+00	4.235E-01	4.111E-01	1.580E-04	2.681E+03	2.419E-04

XX

EXPANSION TUBE PHASE OF PROGRAM

XX

INPUTS FOR EXPANSION TUBE PHASE

US	PS	XAS	DELUS	ISAV	IEXP	IREF	NVEL	IAC	JAC
5.500E+03	0.	1.698E+01	3.300E+02	2	1	1	8	50	50

5 CONDITIONS FOR FROZEN EXPANSION

P	RHO	T	H	S/R	Z	GAME	A	U	M	NRE
1.481E+03	7.307E-03	6.850E+02	6.979E+05	3.302E+01	1.029E+00	1.409E+00	5.345E+02	5.500E+03	1.029E+01	1.221E+06

STATIC CONDITIONS BEHIND BOW SHOCK - REGION 55 FROZEN EXPANSION--EQUILIBRIUM POST SHOCK

P	RHO	T	H	S/R	Z	GAME	A	U	M	RATIO
2.027E+05	8.157E-02	6.398E+03	1.681E+07	4.243E+01	1.353E+00	1.144E+00	1.686E+03	4.924E+02	2.921E-01	1.116E+01

STAGNATION CONDITIONS BEHIND BOW SHOCK-REGION T5 FROZEN EXPANSION--EQUILIBRIUM POST SHOCK

P	RHO	T	H	Z	GAME	A	QT	RN	TIME
2.128E+05	8.510E-02	6.427E+03	1.693E+07	1.356E+00	1.144E+00	1.691E+03	1.867E+07	2.540E-02	3.323E-04

STATIC CONDITIONS BEHIND BOW SHOCK - REGION 55 FROZEN EXPANSION-- FROZEN POST SHOCK

P	RHO	T	H	S/R	Z	GAME	A	U	M	RATIO
1.832E+05	4.111E-02	1.509E+04	1.535E+07	3.885E+01	1.029E+00	1.409E+00	2.506E+03	9.775E+02	3.900E-01	5.626E+00

STAGNATION CONDITIONS BEHIND BOW SHOCK-REGION T5 FROZEN EXPANSION-- FROZEN POST SHOCK

P	RHO	T	H	Z	GAME	A	QT	RN	TIME
2.036E+05	4.431E-02	1.555E+04	1.582E+07	1.029E+00	1.409E+00	2.545E+03	1.705E+07	2.540E-02	3.323E-04

AEDC REAL-AIR TAPE USED FOR UNSTEADY EXPANSION-IEXP=1

5 CONDITIONS FOR EQUILIBRIUM EXPANSION

P	RHO	T	H	S/R	Z	GAME	A	U	M	NRE
4.457E+03	1.060E-02	1.464E+03	1.596E+06	3.302E+01	1.000E+00	1.306E+00	7.410E+02	5.500E+03	7.423E+00	1.122E+06

STATIC CONDITIONS BEHIND BOW SHOCK - REGION 55 EQUILIBRIUM EXPANSION--EQUILIBRIUM POST SHOCK

P	RHO	T	H	S/R	Z	GAME	A	U	M	RATIO
2.964E+05	1.186E-01	6.484E+03	1.660E+07	4.180E+01	1.342E+00	1.147E+00	1.693E+03	4.910E+02	2.900E-01	1.120E+01

STAGNATION CONDITIONS BEHIND BOW SHOCK-REGION T5 EQUILIBRIUM EXPANSION--EQUILIBRIUM POST SHOCK

P	RHO	T	H	Z	GAME	A	QT	RN	TIME
3.110E+05	1.237E-01	6.514E+03	1.672E+07	1.345E+00	1.147E+00	1.698E+03	2.229E+07	2.540E-02	4.807E-04

XX

FOLLOWING EQUILIBRIUM CONDITIONS INCLUDE FLOW ATTN

XX

APPENDIX A

5 CONDITIONS FOR EQUILIBRIUM EXPANSION

P	RHO	T	H	S/R	Z	GAME	A	U	M	NRE
4.457E+03	1.060E-02	1.464E+03	1.596E+06	3.302E+01	1.000E+00	1.306E+00	7.410E+02	4.840E+03	6.532E+00	9.870E+05

STATIC CONDITIONS BEHIND BOW SHOCK - REGION 55
EQUILIBRIUM EXPANSION--EQUILIBRIUM POST SHOCK

P	RHO	T	H	S/R	Z	GAME	A	U	M	RATIO
2.282E+05	1.074E-01	5.855E+03	1.319E+07	4.019E+01	1.264E+00	1.163E+00	1.572E+03	4.775E+02	3.038E-01	1.013E+01

STAGNATION CONDITIONS BEHIND BOW SHOCK-REGION T5
EQUILIBRIUM EXPANSION--EQUILIBRIUM POST SHOCK

P	RHO	T	H	Z	GAME	A	QT	RN	TIME
2.407E+05	1.124E-01	5.890E+03	1.331E+07	1.266E+00	1.162E+00	1.578E+03	1.553E+07	2.540E-02	6.342E-04

ACCELERATION AIR CONDITIONS (REGION 20) AND P10

P20	RHO20	T20	H20	Z20	M20	P10	US10	MS10	RATIO
4.457E+03	1.986E-03	5.493E+03	1.767E+07	1.423E+00	3.477E+00	1.178E+01	5.908E+03	1.702E+01	1.452E+01

ACCELERATION AIR FLOW PARAMETERS USING MIRELS THEORY

XAS	XA	LMAX	L	L/LMAX	TIM	UI	UI/U5	US20/UI	TIME
1.698E+01	1.698E+00	2.038E-01	6.847E-02	3.359E-01	1.193E-05	5.738E+03	1.043E+00	1.030E+00	2.127E-05
1.698E+01	3.396E+00	2.038E-01	1.080E-01	5.299E-01	1.863E-05	5.798E+03	1.054E+00	1.019E+00	4.253E-05
1.698E+01	5.094E+00	2.038E-01	1.365E-01	6.599E-01	2.306E-05	5.832E+03	1.060E+00	1.013E+00	6.380E-05
1.698E+01	6.792E+00	2.038E-01	1.531E-01	7.509E-01	2.615E-05	5.854E+03	1.064E+00	1.009E+00	8.507E-05
1.698E+01	8.490E+00	2.038E-01	1.664E-01	8.163E-01	2.835E-05	5.869E+03	1.067E+00	1.007E+00	1.063E-04
1.698E+01	1.019E+01	2.038E-01	1.761E-01	8.638E-01	2.995E-05	5.880E+03	1.069E+00	1.005E+00	1.276E-04
1.698E+01	1.189E+01	2.038E-01	1.832E-01	8.987E-01	3.112E-05	5.887E+03	1.070E+00	1.004E+00	1.489E-04
1.698E+01	1.358E+01	2.038E-01	1.884E-01	9.245E-01	3.198E-05	5.892E+03	1.071E+00	1.003E+00	1.701E-04
1.698E+01	1.528E+01	2.038E-01	1.923E-01	9.436E-01	3.262E-05	5.896E+03	1.072E+00	1.002E+00	1.914E-04
1.698E+01	1.698E+01	2.038E-01	1.952E-01	9.578E-01	3.310E-05	5.899E+03	1.073E+00	1.001E+00	2.127E-04

XX

CONDITIONS BEHIND STANDING SHOCK AT SECONDARY DIAPH

XX

P	RHO	T	H	S/R	Z	GAME	A	U	M	NRE
1.751E+06	1.294E+00	4.307E+03	7.267E+06	3.380E+01	1.094E+00	1.201E+00	1.275E+03	5.946E+02	4.665E-01	6.781E+06

XX

EXPANSION TUBE PHASE OF PROGRAM

XX

INPUTS FOR EXPANSION TUBE PHASE

U5	P5	XAS	DELUS	ISAV	TEXP	IREF	NVEL	IAC	JAC
5.500E+03	0.	1.698E+01	3.300E+02	2	1	1	8	50	50

5 CONDITIONS FOR FROZEN EXPANSION

P	RHO	T	H	S/R	Z	GAME	A	U	M	NRE
1.400E+02	1.762E-03	2.529E+02	2.643E+05	3.380E+01	1.094E+00	1.430E+00	3.370E+02	5.500E+03	1.632E+01	6.015E+05

STATIC CONDITIONS BEHIND BOW SHOCK - REGION 55
FROZEN EXPANSION--EQUILIBRIUM POST SHOCK

P	RHO	T	H	S/R	Z	GAME	A	U	M	RATIO
4.868E+04	1.972E-02	6.122E+03	1.803E+07	4.512E+01	1.405E+00	1.131E+00	1.671E+03	4.913E+02	2.941E-01	1.119E+01

STAGNATION CONDITIONS BEHIND BOW SHOCK-REGION T5
FROZEN EXPANSION--EQUILIBRIUM POST SHOCK

P	RHO	T	H	Z	GAME	A	QT	RN	TIME
5.111E+04	2.058E-02	6.166E+03	1.815E+07	1.408E+00	1.131E+00	1.676E+03	9.826E+06	2.540E-02	2.015E-04

APPENDIX A

STATIC CONDITIONS BEHIND BOW SHOCK - REGION 55
FROZEN EXPANSION-- FROZEN POST SHOCK

P	RHO	T	H	S/R	Z	GAME	A	U	M	RATIO
4.385E+04	9.794E-03	1.426E+04	1.490E+07	4.147E+01	1.094E+00	1.430E+00	2.530E+03	9.896E+02	3.911E-01	5.558E+00

STAGNATION CONDITIONS BEHIND BOW SHOCK-REGION T5
FROZEN EXPANSION-- FROZEN POST SHOCK

P	RHO	T	H	Z	GAME	A	QT	RN	TIMI
4.883E+04	1.056E-02	1.472E+04	1.539E+07	1.094E+00	1.430E+00	2.571E+03	8.117E+06	2.540E-02	2.015E-04

4EDC REAL-AIR TAPE USED FOR UNSTEADY EXPANSION-1EXP=1

5 CONDITIONS FOR EQUILIBRIUM EXPANSION

P	RHO	T	H	S/R	Z	GAME	A	U	M	NRE
6.052E+03	1.126E-02	1.870E+03	2.111E+06	3.380E+01	1.000E+00	1.278E+00	8.284E+02	5.500E+03	6.639E+00	1.002E+06

STATIC CONDITIONS BEHIND BOW SHOCK - REGION 55
EQUILIBRIUM EXPANSION--EQUILIBRIUM POST SHOCK

P	RHO	T	H	S/R	Z	GAME	A	U	M	RATIO
3.156E+05	1.236E-01	6.571E+03	1.711E+07	4.200E+01	1.354E+00	1.147E+00	1.711E+03	5.009E+02	2.927E-01	1.097E+01

STAGNATION CONDITIONS BEHIND BOW SHOCK-REGION T5
EQUILIBRIUM EXPANSION--EQUILIBRIUM POST SHOCK

P	RHO	T	H	Z	GAME	A	QT	RN	TIMI
3.315E+05	1.289E-01	6.602E+03	1.725E+07	1.357E+00	1.147E+00	1.717E+03	2.375E+07	2.540E-02	5.475E-04

XX

FOLLOWING EQUILIBRIUM CONDITIONS INCLUDE FLOW ATTN

XX

5 CONDITIONS FOR EQUILIBRIUM EXPANSION

P	RHO	T	H	S/R	Z	GAME	A	U	M	NRE
6.052E+03	1.126E-02	1.870E+03	2.111E+06	3.380E+01	1.000E+00	1.278E+00	8.284E+02	4.840E+03	5.842E+00	8.817E+05

STATIC CONDITIONS BEHIND BOW SHOCK - REGION 55
EQUILIBRIUM EXPANSION--EQUILIBRIUM POST SHOCK

P	RHO	T	H	S/R	Z	GAME	A	U	M	RATIO
2.431E+05	1.113E-01	5.969E+03	1.370E+07	4.041E+01	1.275E+00	1.160E+00	1.592E+03	4.897E+02	3.077E-01	9.882E+00

STAGNATION CONDITIONS BEHIND BOW SHOCK-REGION T5
EQUILIBRIUM EXPANSION--EQUILIBRIUM POST SHOCK

P	RHO	T	H	Z	GAME	A	QT	RN	TIMI
2.568E+05	1.166E-01	6.005E+03	1.382E+07	1.277E+00	1.159E+00	1.598E+03	1.668E+07	2.540E-02	7.245E-04

ACCELERATION AIR CONDITIONS (REGION 20) AND P10

P20	RHO20	T20	H20	Z20	M20	P10	US10	MS10	RATIO
6.052E+03	2.667E-03	5.565E+03	1.769E+07	1.421E+00	3.455E+00	1.599E+01	5.912E+03	1.703E+01	1.436E+01

ACCELERATION AIR FLOW PARAMETERS USING MIRELS THEORY

XAS	XA	LMAX	L	L/LMAX	TIM	UI	UI/U5	US20/UI	TIMI
1.698E+01	1.698E+00	2.765E-01	7.471E-02	2.702E-01	1.307E-05	5.717E+03	1.039E+00	1.034E+00	2.149E-05
1.698E+01	3.396E+00	2.765E-01	1.221E-01	4.414E-01	2.113E-05	5.776E+03	1.050E+00	1.024E+00	4.298E-05
1.698E+01	5.094E+00	2.765E-01	1.562E-01	5.649E-01	2.688E-05	5.812E+03	1.057E+00	1.017E+00	6.448E-05
1.698E+01	6.792E+00	2.765E-01	1.819E-01	6.577E-01	3.116E-05	5.836E+03	1.061E+00	1.013E+00	8.597E-05
1.698E+01	8.490E+00	2.765E-01	2.016E-01	7.289E-01	3.444E-05	5.853E+03	1.064E+00	1.010E+00	1.075E-04
1.698E+01	1.019E+01	2.765E-01	2.169E-01	7.843E-01	3.697E-05	5.866E+03	1.067E+00	1.008E+00	1.290E-04
1.698E+01	1.189E+01	2.765E-01	2.289E-01	8.278E-01	3.896E-05	5.876E+03	1.068E+00	1.006E+00	1.504E-04
1.698E+01	1.358E+01	2.765E-01	2.384E-01	8.622E-01	4.052E-05	5.883E+03	1.070E+00	1.005E+00	1.719E-04
1.698E+01	1.528E+01	2.765E-01	2.460E-01	8.895E-01	4.176E-05	5.889E+03	1.071E+00	1.004E+00	1.934E-04
1.698E+01	1.698E+01	2.765E-01	2.520E-01	9.112E-01	4.275E-05	5.894E+03	1.072E+00	1.003E+00	2.149E-04

XX

APPENDIX A

CONDITIONS BEHIND REFLECTED SHOCK AT SECONDARY DIAPH

XX

P	RHO	T	H	S/R	Z	GAME	A	U	M	NRE
2.654E+06	1.639E+00	4.984E+03	8.887E+06	3.451E+01	1.132E+00	1.225E+00	1.408E+03	0.	0.	0.

XX

EXPANSION TUBE PHASE OF PROGRAM

XX

INPUTS FOR EXPANSION TUBE PHASE

U5	P5	KAS	DELUS	ISAV	IEXP	TREP	NVEL	IAC	JAC
5.500E+03	0.	1.698E+01	3.300E+02	2	1	1	8	50	50

5 CONDITIONS FOR FROZEN EXPANSION

P	RHO	T	H	S/R	Z	GAME	A	U	M	NRE
8.689E+01	1.266E-03	2.112E+02	2.242E+05	3.451E+01	1.132E+00	1.441E+00	3.145E+02	5.500E+03	1.749E+01	5.016E+05

STATIC CONDITIONS BEHIND BOW SHOCK - REGION 55
FROZEN EXPANSION--EQUILIBRIUM POST SHOCK

P	RHO	T	H	S/R	Z	GAME	A	U	M	RATIO
3.491E+04	1.394E-02	6.097E+03	1.882E+07	4.605E+01	1.431E+00	1.127E+00	1.680E+03	4.991E+02	2.971E-01	1.101E+01

STAGNATION CONDITIONS BEHIND BOW SHOCK-REGION T5
FROZEN EXPANSION--EQUILIBRIUM POST SHOCK

P	RHO	T	H	Z	GAME	A	QT	RN	TIMI
3.669E+04	1.457E-02	6.120E+03	1.895E+07	1.433E+00	1.128E+00	1.685E+03	8.694E+06	2.540E-02	1.872E-04

STATIC CONDITIONS BEHIND BOW SHOCK - REGION 55
FROZEN EXPANSION-- FROZEN POST SHOCK

P	RHO	T	H	S/R	Z	GAME	A	U	M	RATIO
3.137E+04	6.904E-03	1.398E+04	1.484E+07	4.232E+01	1.132E+00	1.441E+00	2.559E+03	1.009E+03	3.942E-01	5.453E+00

STAGNATION CONDITIONS BEHIND BOW SHOCK-REGION T5
FROZEN EXPANSION-- FROZEN POST SHOCK

P	RHO	T	H	Z	GAME	A	QT	RN	TIMI
3.502E+04	7.452E-03	1.446E+04	1.535E+07	1.132E+00	1.441E+00	2.602E+03	6.855E+06	2.540E-02	1.872E-04

AEDC REAL-AIR TAPE USED FOR UNSTEADY EXPANSION-IEXP=1

5 CONDITIONS FOR EQUILIBRIUM EXPANSION

P	RHO	T	H	S/R	Z	GAME	A	U	M	NRE
7.729E+03	1.188E-02	2.256E+03	2.676E+06	3.451E+01	1.003E+00	1.225E+00	8.925E+02	5.500E+03	6.163E+00	9.309E+05

STATIC CONDITIONS BEHIND BOW SHOCK - REGION 55
EQUILIBRIUM EXPANSION--EQUILIBRIUM POST SHOCK

P	RHO	T	H	S/R	Z	GAME	A	U	M	RATIO
3.338E+05	1.278E-01	6.656E+03	1.767E+07	4.222E+01	1.367E+00	1.146E+00	1.730E+03	5.111E+02	2.954E-01	1.075E+01

STAGNATION CONDITIONS BEHIND BOW SHOCK-REGION T5
EQUILIBRIUM EXPANSION--EQUILIBRIUM POST SHOCK

P	RHO	T	H	Z	GAME	A	QT	RN	TIMI
3.508E+05	1.334E-01	6.688E+03	1.780E+07	1.370E+00	1.146E+00	1.736E+03	2.523E+07	2.540E-02	5.980E-04

XX

FOLLOWING EQUILIBRIUM CONDITIONS INCLUDE FLOW ATTN

XX

APPENDIX A

5 CONDITIONS FOR EQUILIBRIUM EXPANSTON

P	RHO	T	H	S/R	Z	GAME	A	U	M	NRE
7.729E+03	1.188E-02	2.256E+03	2.676E+06	3.451E+01	1.003E+00	1.225E+00	8.925E+02	4.840E+03	5.423E+00	8.192E+05

STATIC CONDITIONS BEHIND BOW SHOCK - REGION 55 EQUILIBRIUM EXPANSION--EQUILIBRIUM POST SHOCK

P	RHO	T	H	S/R	Z	GAME	A	U	M	RATIO
2.571E+05	1.143E-01	6.085E+03	1.426E+07	4.067E+01	1.298E+00	1.156E+00	1.613E+03	5.029E+02	3.118E-01	9.623E+00

STAGNATION CONDITIONS BEHIND BOW SHOCK-REGION T5 EQUILIBRIUM EXPANSION--EQUILIBRIUM POST SHOCK

P	RHO	T	H	Z	GAME	A	QT	RN	TIMI
2.720E+05	1.200E-01	6.121E+03	1.439E+07	1.290E+00	1.156E+00	1.619E+03	1.788E+07	2.540E-02	7.932E-04

ACCELERATION AIR CONDITIONS (REGION 20) AND P10

P20	RHO20	T20	H20	Z20	M20	P10	US10	MS10	RATIO
7.729E+03	3.375E-03	5.623E+03	1.772E+07	1.419E+00	3.437E+00	2.040E+01	5.916E+03	1.704E+01	1.424E+01

ACCELERATION AIR FLOW PARAMETERS USING WIRELS THEORY

XAS	XA	LMAX	L	L/LMAX	TIM	UI	UI/U5	US20/UI	TIMI
1.698E+01	1.698E+00	3.529E-01	7.945E-02	2.251E-01	1.394E-05	5.700E+03	1.036E+00	1.038E+00	2.167E-05
1.698E+01	3.396E+00	3.529E-01	1.330E-01	3.769E-01	2.310E-05	5.758E+03	1.047E+00	1.028E+00	4.335E-05
1.698E+01	5.094E+00	3.529E-01	1.735E-01	4.916E-01	2.995E-05	5.794E+03	1.053E+00	1.021E+00	6.502E-05
1.698E+01	6.792E+00	3.529E-01	2.053E-01	5.817E-01	3.528E-05	5.819E+03	1.058E+00	1.017E+00	8.670E-05
1.698E+01	8.490E+00	3.529E-01	2.307E-01	6.537E-01	3.952E-05	5.838E+03	1.061E+00	1.013E+00	1.084E-04
1.698E+01	1.019E+01	3.529E-01	2.513E-01	7.122E-01	4.295E-05	5.852E+03	1.064E+00	1.011E+00	1.300E-04
1.698E+01	1.189E+01	3.529E-01	2.682E-01	7.600E-01	4.574E-05	5.864E+03	1.066E+00	1.009E+00	1.517E-04
1.698E+01	1.358E+01	3.529E-01	2.821E-01	7.994E-01	4.804E-05	5.873E+03	1.068E+00	1.007E+00	1.734E-04
1.698E+01	1.528E+01	3.529E-01	2.936E-01	8.320E-01	4.993E-05	5.880E+03	1.069E+00	1.006E+00	1.951E-04
1.698E+01	1.698E+01	3.529E-01	3.032E-01	8.591E-01	5.151E-05	5.886E+03	1.070E+00	1.005E+00	2.167E-04

Arc-Heated Helium Driver Gas

06/19/74

L.E.T. PROGRAM FOR EQUILIBRIUM REAL AIR

EXPANSION TUBE PROGRAM OF MILLER FOR REAL AIR
ALL PHYSICAL QUANTITIES IN MKS UNITS- NASA SP-7012

SHOCK TUBE PHASE OF PROGRAM

MEASURED INPUTS FOR SHOCK TUBE PHASE

RUN	P1	T1	US1	P2	P4	T4	XIS	DIA	ISAV	INU	LD
8.600E+01	6.895E+03	3.000E+02	4.300E+03	0.	0.	0.	4.650E+00	1.524E-01	2	2	4

XX

CONDITIONS BEHIND INCIDENT SHOCK - REGION 2

XX

P	RHO	T	H	S/R	Z	GAME	A	U	M	NRE
1.337E+06	7.865E-01	5.114E+03	9.450E+06	3.566E+01	1.158E+00	1.224E+00	1.442E+03	3.862E+03	2.678E+00	2.302E+07

RATIO- 2 TO 1 CONDITIONS AND SHOCK VELOCITY

P	RHO	T	H	A	MS1	US1
1.939E+02	9.823E+00	1.705E+01	3.144E+01	4.154E+00	1.238E+01	4.300E+03

SHOCK TUBE FLOW PARAMETERS USING WIRELS THEORY

LMAX	L	L/LMAX	TIM	UI	LMAXT	LT	LT/LMAXT	TIMT	UIT	TIMI
1.210E+02	4.540E-01	3.753E-03	1.167E-04	3.890E+03	1.018E+00	3.523E-01	3.462E-01	8.689E-05	4.054E+03	1.226E-04

APPENDIX A

XX

EXPANSION TUBE PHASE OF PROGRAM

XX

INPUTS FOR EXPANSION TUBE PHASE

U5	PS	XAS	DELUS	ISAV	IEXP	IREP	NVEL	IAC	JAC
7.500E+03	0.	1.698E+01	5.000E+02	2	1	1	8	50	50

5 CONDITIONS FOR FROZEN EXPANSION

P	RHO	T	H	S/R	Z	GAME	A	U	M	NRE
1.165E+04	2.980E-02	1.177E+03	1.262E+06	3.566E+01	1.158E+00	1.449E+00	7.527E+02	7.500E+03	9.964E+00	4.882E+06

STATIC CONDITIONS BEHIND BOW SHOCK - REGION 5S
FROZEN EXPANSION--EQUILIBRIUM POST SHOCK

P	RHO	T	H	S/R	Z	GAME	A	U	M	RATIO
1.550E+06	3.613E-01	8.740E+03	3.316E+07	4.687E+01	1.710E+00	1.185E+00	2.254E+03	6.191E+02	2.746E-01	1.212E+01

STAGNATION CONDITIONS BEHIND BOW SHOCK-REGION T5
FROZEN EXPANSION--EQUILIBRIUM POST SHOCK

P	RHO	T	H	Z	GAME	A	QT	RN	TIME
1.620E+06	3.753E-01	8.783E+03	3.336E+07	1.713E+00	1.186E+00	2.262E+03	1.024E+08	2.540E-02	2.526E-04

STATIC CONDITIONS BEHIND BOW SHOCK - REGION 5S
FROZEN EXPANSION-- FROZEN POST SHOCK

P	RHO	T	H	S/R	Z	GAME	A	U	M	RATIO
1.367E+06	1.556E-01	2.644E+04	2.835E+07	4.094E+01	1.158E+00	1.449E+00	3.568E+03	1.437E+03	4.027E-01	5.220E+00

STAGNATION CONDITIONS BEHIND BOW SHOCK-REGION T5
FROZEN EXPANSION-- FROZEN POST SHOCK

P	RHO	T	H	Z	GAME	A	QT	RN	TIME
1.534E+06	1.685E-01	2.740E+04	2.939E+07	1.158E+00	1.449E+00	3.632E+03	8.770E+07	2.540E-02	2.526E-04

AEDC REAL-AIR TAPE USED FOR UNSTEADY EXPANSION-IEXP=1

5 CONDITIONS FOR EQUILIBRIUM EXPANSION

P	RHO	T	H	S/R	Z	GAME	A	U	M	NRE
4.177E+04	4.314E-02	3.184E+03	4.948E+06	3.566E+01	1.058E+00	1.157E+00	1.058E+03	7.500E+03	7.087E+00	3.597E+06

STATIC CONDITIONS BEHIND BOW SHOCK - REGION 5S
EQUILIBRIUM EXPANSION--EQUILIBRIUM POST SHOCK

P	RHO	T	H	S/R	Z	GAME	A	U	M	RATIO
2.269E+06	5.244E-01	8.905E+03	3.288E+07	4.611E+01	1.693E+00	1.187E+00	2.266E+03	6.176E+02	2.726E-01	1.216E+01

STAGNATION CONDITIONS BEHIND BOW SHOCK-REGION T5
EQUILIBRIUM EXPANSION--EQUILIBRIUM POST SHOCK

P	RHO	T	H	Z	GAME	A	QT	RN	TIME
2.371E+06	5.444E-01	8.948E+03	3.308E+07	1.696E+00	1.187E+00	2.274E+03	1.228E+08	2.540E-02	3.719E-04

XX

FOLLOWING EQUILIBRIUM CONDITIONS INCLUDE FLOW ATTN

XX

5 CONDITIONS FOR EQUILIBRIUM EXPANSION

P	RHO	T	H	S/R	Z	GAME	A	U	M	NRE
4.177E+04	4.314E-02	3.184E+03	4.948E+06	3.566E+01	1.058E+00	1.157E+00	1.058E+03	7.500E+03	6.142E+00	3.117E+06

STATIC CONDITIONS BEHIND BOW SHOCK - REGION 5S
EQUILIBRIUM EXPANSION--EQUILIBRIUM POST SHOCK

APPENDIX A

P	RHO	T	H	S/R	Z	GAME	A	U	M	RATIO
1.699E+06	4.748E-01	8.107E+03	2.590E+07	4.375E+01	1.538E+00	1.167E+00	2.044E+03	5.903E+02	2.888E-01	1.100E+01

STAGNATION CONDITIONS BEHIND BOW SHOCK-REGION T5
EQUILIBRIUM EXPANSION--EQUILIBRIUM POST SHOCK

P	RHO	T	H	Z	GAME	A	QT	RN	TIME
1.783E+06	4.950E-01	8.146E+03	2.608E+07	1.541E+00	1.168E+00	2.051E+03	8.379E+07	2.540E-02	5.080E-04

ACCELERATION AIR CONDITIONS (REGION 20) AND P10

P20	RHO20	T20	H20	Z20	M20	P10	US10	MS10	RATIO
4.177E+04	1.156E-02	7.125E+03	3.206E+07	1.768E+00	3.668E+00	6.000E+01	7.984E+03	2.300E+01	1.658E+01

ACCELERATION AIR FLOW PARAMETERS USING MIRELS THEORY

XAS	XA	LMAX	L	L/LMAX	TIM	UT	UT/US	US20/UI	TIME
1.698E+01	1.698E+00	9.757E-01	8.203E-02	8.408E-02	1.073E-05	7.644E+03	1.019E+00	1.045E+00	1.365E-05
1.698E+01	3.396E+00	9.757E-01	1.492E-01	1.529E-01	1.939E-05	7.693E+03	1.026E+00	1.038E+00	2.731E-05
1.698E+01	5.094E+00	9.757E-01	2.078E-01	2.129E-01	2.689E-05	7.727E+03	1.030E+00	1.033E+00	4.096E-05
1.698E+01	6.792E+00	9.757E-01	2.600E-01	2.665E-01	3.353E-05	7.753E+03	1.034E+00	1.030E+00	5.461E-05
1.698E+01	8.490E+00	9.757E-01	3.072E-01	3.148E-01	3.951E-05	7.775E+03	1.037E+00	1.027E+00	6.827E-05
1.698E+01	1.019E+01	9.757E-01	3.501E-01	3.588E-01	4.493E-05	7.793E+03	1.039E+00	1.025E+00	8.192E-05
1.698E+01	1.189E+01	9.757E-01	3.895E-01	3.992E-01	4.988E-05	7.809E+03	1.041E+00	1.022E+00	9.557E-05
1.698E+01	1.358E+01	9.757E-01	4.257E-01	4.363E-01	5.442E-05	7.822E+03	1.043E+00	1.021E+00	1.092E-04
1.698E+01	1.528E+01	9.757E-01	4.591E-01	4.705E-01	5.860E-05	7.835E+03	1.045E+00	1.019E+00	1.229E-04
1.698E+01	1.698E+01	9.757E-01	4.901E-01	5.023E-01	6.247E-05	7.846E+03	1.046E+00	1.018E+00	1.365E-04

XX

CONDITIONS BEHIND STANDING SHOCK AT SECONDARY DIAPH

XX

P	RHO	T	H	S/R	Z	GAME	A	U	M	NRE
1.062E+07	3.761E+00	7.707E+03	1.658E+07	3.709E+01	1.276E+00	1.178E+00	1.824E+03	8.073E+02	4.427E-01	0.

XX

EXPANSION TUBE PHASE OF PROGRAM

XX

INPUTS FOR EXPANSION TUBE PHASE

US	PS	XAS	DELUS	ISAV	IEXP	IREF	NVEL	IAC	JAC
7.500E+03	0.	1.698E+01	5.000E+02	2	1	1	8	50	50

5 CONDITIONS FOR FROZEN EXPANSION

P	RHO	T	H	S/R	Z	GAME	A	U	M	NRE
7.181E+02	5.821E-03	3.368E+02	3.784E+05	3.709E+01	1.276E+00	1.484E+00	4.278E+02	7.500E+03	1.753E+01	2.168E+06

STATIC CONDITIONS BEHIND BOW SHOCK - REGION 55
FROZEN EXPANSION--EQUILIBRIUM POST SHOCK

P	RHO	T	H	S/R	Z	GAME	A	U	M	RATIO
3.006E+05	6.913E-02	8.327E+03	3.623E+07	5.100E+01	1.819E+00	1.176E+00	2.261E+03	6.310E+02	2.791E-01	1.188E+01

STAGNATION CONDITIONS BEHIND BOW SHOCK-REGION T5
FROZEN EXPANSION--EQUILIBRIUM POST SHOCK

P	RHO	T	H	Z	GAME	A	QT	RN	TIME
3.146E+05	7.185E-02	8.371E+03	3.642E+07	1.822E+00	1.176E+00	2.269E+03	4.933E+07	2.540E-02	1.370E-04

STATIC CONDITIONS BEHIND BOW SHOCK - REGION 55
FROZEN EXPANSION-- FROZEN POST SHOCK

P	RHO	T	H	S/R	Z	GAME	A	U	M	RATIO
2.635E+05	2.949E-02	2.439E+04	2.741E+07	4.432E+01	1.276E+00	1.484E+00	3.641E+03	1.480E+03	4.066E-01	5.066E+00

STAGNATION CONDITIONS BEHIND BOW SHOCK-REGION T5
FROZEN EXPANSION-- FROZEN POST SHOCK

APPENDIX A

P	RHO	T	H	Z	GAME	A	QT	RN	TIMI
2.972E+05	3.198E-02	2.537E+04	2.850E+07	1.276E+00	1.484E+00	3.713E+03	3.743E+07	2.540E-02	1.370E-04

AEDC REAL-AIR TAPE USED FOR UNSTEADY EXPANSION-IXP=1

NO SOLUTION ON TAPE FOR THE CONDITIONS

S/R= 37.090681
Z(6)= 2.54208103E+00

EVALUATE
Z(6)

PERFECT AIR RELATIONS USED FOR NUMERICAL INTEGRATION

5 CONDITIONS FOR EQUILIBRIUM EXPANSION

P	RHO	T	H	S/R	Z	GAME	A	U	H	NRE
4.730E+04	4.146E-02	3.559E+03	6.461E+06	3.709E+01	1.115E+00	1.171E+00	1.155E+03	7.500E+03	6.492E+00	3.162E+06

STATIC CONDITIONS BEHIND BOW SHOCK - REGION 5S
EQUILIBRIUM EXPANSION--EQUILIBRIUM POST SHOCK

P	RHO	T	H	S/R	Z	GAME	A	U	M	RATIO
2.181E+06	4.866E-01	9.044E+03	3.438E+07	4.675E+01	1.727E+00	1.189E+00	2.309E+03	6.390E+02	2.768E-01	1.174E+01

STAGNATION CONDITIONS BEHIND BOW SHOCK-REGION TS
EQUILIBRIUM EXPANSION--EQUILIBRIUM POST SHOCK

P	RHO	T	H	Z	GAME	A	QT	RN	TIMI
2.282E+06	5.056E-01	9.090E+03	3.459E+07	1.730E+00	1.190E+00	2.318E+03	1.261E+08	2.540E-02	4.122E-04

XX

FOLLOWING EQUILIBRIUM CONDITIONS INCLUDE FLOW ATTN

XX

5 CONDITIONS FOR EQUILIBRIUM EXPANSION

P	RHO	T	H	S/R	Z	GAME	A	U	M	NRE
4.730E+04	4.146E-02	3.559E+03	6.461E+06	3.709E+01	1.115E+00	1.171E+00	1.155E+03	6.500E+03	5.627E+00	2.740E+06

STATIC CONDITIONS BEHIND BOW SHOCK - REGION 5S
EQUILIBRIUM EXPANSION--EQUILIBRIUM POST SHOCK

P	RHO	T	H	S/R	Z	GAME	A	U	M	RATIO
1.634E+06	4.396E-01	8.222E+03	2.740E+07	4.445E+01	1.575E+00	1.171E+00	2.086E+03	6.125E+02	2.936E-01	1.060E+01

STAGNATION CONDITIONS BEHIND BOW SHOCK-REGION TS
EQUILIBRIUM EXPANSION--EQUILIBRIUM POST SHOCK

P	RHO	T	H	Z	GAME	A	QT	RN	TIMI
1.718E+06	4.591E-01	8.263E+03	2.759E+07	1.578E+00	1.172E+00	2.094E+03	8.708E+07	2.540E-02	5.646E-04

ACCELERATION AIR CONDITIONS (REGION 20) AND P10

P20	RHO20	T20	H20	Z20	M20	P10	US10	MS10	RATIO
4.730E+04	1.301E-02	2.170E+03	3.208E+07	1.766E+00	3.657E+00	6.792E+01	7.987E+03	2.300E+01	1.650E+01

ACCELERATION AIR FLOW PARAMETERS USING MIRELS THEORY

XAS	XA	LMAX	L	L/LMAX	TIM	UI	UI/U5	US20/UI	TIMI
1.698E+01	1.698E+00	1.104E+00	8.353E-02	7.564E-02	1.094E-05	7.637E+03	1.018E+00	1.046E+00	1.372E-05
1.698E+01	3.396E+00	1.104E+00	1.528E-01	1.384E-01	1.988E-05	7.685E+03	1.025E+00	1.039E+00	2.744E-05
1.698E+01	5.094E+00	1.104E+00	2.138E-01	1.936E-01	2.770E-05	7.718E+03	1.029E+00	1.035E+00	4.117E-05
1.698E+01	6.792E+00	1.104E+00	2.686E-01	2.432E-01	3.468E-05	7.743E+03	1.032E+00	1.031E+00	5.489E-05
1.698E+01	8.490E+00	1.104E+00	3.184E-01	2.883E-01	4.101E-05	7.765E+03	1.035E+00	1.029E+00	6.861E-05
1.698E+01	1.019E+01	1.104E+00	3.641E-01	3.297E-01	4.678E-05	7.783E+03	1.038E+00	1.026E+00	8.233E-05
1.698E+01	1.189E+01	1.104E+00	4.062E-01	3.678E-01	5.209E-05	7.798E+03	1.040E+00	1.024E+00	9.605E-05
1.698E+01	1.358E+01	1.104E+00	4.452E-01	4.032E-01	5.699E-05	7.812E+03	1.042E+00	1.022E+00	1.098E-04
1.698E+01	1.528E+01	1.104E+00	4.815E-01	4.360E-01	6.153E-05	7.824E+03	1.043E+00	1.021E+00	1.235E-04
1.698E+01	1.698E+01	1.104E+00	5.152E-01	4.666E-01	6.576E-05	7.835E+03	1.045E+00	1.019E+00	1.372E-04

XX

APPENDIX A

CONDITIONS BEHIND REFLECTED SHOCK AT SECONDARY DIAPH

XX

P	RHO	T	H	S/R	Z	GAME	A	U	M	NRE
1.541E+07	4.721E+00	8.480E+03	1.989E+07	3.806E+01	1.341E+00	1.176E+00	1.959E+03	0.	0.	0.

XX

EXPANSION TUBE PHASE OF PROGRAM

XX

INPUTS FOR EXPANSION TUBE PHASE

US	PS	XAS	DELUS	ISAV	IEXP	IREF	NVEL	IAC	JAC
7.500E+03	0.	1.698E+01	5.000E+02	2	1	1	8	50	50

5 CONDITIONS FOR FROZEN EXPANSION

P	RHO	T	H	S/R	Z	GAME	A	U	M	NRE
1.785E+02	2.444E-03	1.897E+02	2.185E+05	3.806E+01	1.341E+00	1.502E+00	3.312E+02	7.500E+03	2.264E+01	1.448E+06

STATIC CONDITIONS BEHIND BOW SHOCK - REGION 55
FROZEN EXPANSION--EQUILIBRIUM POST SHOCK

P	RHO	T	H	S/R	Z	GAME	A	U	M	RATIO
1.258E+05	2.829E-02	8.234E+03	3.826E+07	5.344E+01	1.881E+00	1.164E+00	2.275E+03	6.477E+02	2.847E-01	1.158E+01

STAGNATION CONDITIONS BEHIND BOW SHOCK-REGION T5
FROZEN EXPANSION--EQUILIBRIUM POST SHOCK

P	RHO	T	H	Z	GAME	A	QT	RN	TIME
1.318E+05	2.943E-02	8.282E+03	3.847E+07	1.884E+00	1.165E+00	2.284E+03	3.374E+07	2.540E-02	1.046E-04

STATIC CONDITIONS BEHIND BOW SHOCK - REGION 55
FROZEN EXPANSION-- FROZEN POST SHOCK

P	RHO	T	H	S/R	Z	GAME	A	U	M	RATIO
1.098E+05	1.208E-02	2.361E+04	2.719E+07	4.607E+01	1.341E+00	1.502E+00	3.696E+03	1.517E+03	4.105E-01	4.944E+00

STAGNATION CONDITIONS BEHIND BOW SHOCK-REGION T5
FROZEN EXPANSION-- FROZEN POST SHOCK

P	RHO	T	H	Z	GAME	A	QT	RN	TIME
1.243E+05	1.312E-02	2.461E+04	2.834E+07	1.341E+00	1.502E+00	3.773E+03	2.407E+07	2.540E-02	1.046E-04

AEDC REAL-AIR TAPE USED FOR UNSTEADY EXPANSION-IEXP=1

NO SOLUTION ON TAPE FOR THE CONDITIONS

S/R= 38.059235
Z(4)= 2.54208103E+00

EVALUATE
Z(6)

PERFECT AIR RELATIONS USED FOR NUMERICAL INTEGRATION

5 CONDITIONS FOR EQUILIBRIUM EXPANSION

P	RHO	T	H	S/R	Z	GAME	A	U	M	NRE
5.576E+04	4.272E-02	3.919E+03	7.698E+06	3.806E+01	1.159E+00	1.205E+00	1.254E+03	7.500E+03	5.981E+00	3.011E+06

STATIC CONDITIONS BEHIND BOW SHOCK - REGION 55
EQUILIBRIUM EXPANSION--EQUILIBRIUM POST SHOCK

P	RHO	T	H	S/R	Z	GAME	A	U	M	RATIO
2.247E+06	4.859E-01	9.196E+03	3.561E+07	4.716E+01	1.752E+00	1.192E+00	2.348E+03	6.591E+02	2.807E-01	1.138E+01

STAGNATION CONDITIONS BEHIND BOW SHOCK-REGION T5
EQUILIBRIUM EXPANSION--EQUILIBRIUM POST SHOCK

APPENDIX A

P	RHO	T	H	Z	GAME	A	QT	RN	TIME
2.355E+06	5.055E-01	9.246E+03	3.583E+07	1.755E+00	1.192E+00	2.357E+03	1.327E+08	2.540E-02	4.545E-04

XX

FOLLOWING EQUILIBRIUM CONDITIONS INCLUDE FLOW ATTN

XX

5 CONDITIONS FOR EQUILIBRIUM EXPANSION

P	RHO	T	H	S/R	Z	GAME	A	U	M	NRE
5.576E+04	4.272E-02	3.919E+03	7.698E+06	3.806E+01	1.159E+00	1.205E+00	1.254E+03	6.500E+03	5.184E+00	2.609E+06

STATIC CONDITIONS BEHIND BOW SHOCK - REGION 5S
EQUILIBRIUM EXPANSION--EQUILIBRIUM POST SHOCK

P	RHO	T	H	S/R	Z	GAME	A	U	M	RATIO
1.685E+06	4.387E-01	8.347E+03	2.862E+07	4.491E+01	1.603E+00	1.174E+00	2.124E+03	6.329E+02	2.980E-01	1.027E+01

STAGNATION CONDITIONS BEHIND BOW SHOCK-REGION T5
EQUILIBRIUM EXPANSION--EQUILIBRIUM POST SHOCK

P	RHO	T	H	Z	GAME	A	QT	RN	TIME
1.775E+06	4.587E-01	8.391E+03	2.883E+07	1.607E+00	1.175E+00	2.132E+03	9.251E+07	2.540E-02	6.244E-04

ACCELERATION AIR CONDITIONS (REGION 20) AND P10

P20	RHO20	T20	H20	Z20	M20	P10	US10	MS10	RATIO
5.576E+04	1.523E-02	7.231E+03	3.210E+07	1.763E+00	3.642E+00	8.004E+01	7.990E+03	2.301E+01	1.639E+01

ACCELERATION AIR FLOW PARAMETERS USING MIRELS THEORY

XAS	XA	LMAX	L	L/LMAX	TIM	UI	UI/U5	US20/UI	TIME
1.698E+01	1.698E+00	1.301E+00	8.546E-02	6.568E-02	1.120E-05	7.629E+03	1.017E+00	1.047E+00	1.381E-05
1.698E+01	3.396E+00	1.301E+00	1.574E-01	1.210E-01	2.051E-05	7.674E+03	1.023E+00	1.041E+00	2.763E-05
1.698E+01	5.094E+00	1.301E+00	2.215E-01	1.702E-01	2.874E-05	7.706E+03	1.027E+00	1.037E+00	4.144E-05
1.698E+01	6.792E+00	1.301E+00	2.796E-01	2.149E-01	3.617E-05	7.731E+03	1.031E+00	1.034E+00	5.525E-05
1.698E+01	8.490E+00	1.301E+00	3.329E-01	2.559E-01	4.295E-05	7.751E+03	1.033E+00	1.031E+00	6.907E-05
1.698E+01	1.019E+01	1.301E+00	3.822E-01	2.937E-01	4.920E-05	7.769E+03	1.036E+00	1.029E+00	8.288E-05
1.698E+01	1.189E+01	1.301E+00	4.280E-01	3.289E-01	5.498E-05	7.784E+03	1.038E+00	1.026E+00	9.669E-05
1.698E+01	1.358E+01	1.301E+00	4.707E-01	3.617E-01	6.036E-05	7.798E+03	1.040E+00	1.025E+00	1.105E-04
1.698E+01	1.528E+01	1.301E+00	5.107E-01	3.925E-01	6.539E-05	7.810E+03	1.041E+00	1.023E+00	1.243E-04
1.698E+01	1.698E+01	1.301E+00	5.482E-01	4.213E-01	7.009E-05	7.821E+03	1.043E+00	1.022E+00	1.381E-04

APPENDIX B

PROGRAM LIMITATIONS AND UNCERTAINTIES

Limitations on the present program are those restrictions on the source of equilibrium, real-air, thermodynamic properties. The temperature range of both the AEDC real-air tape (ref. 9) and AEDC real-air curve-fit expressions (ref. 11) is 100 K to 15 000 K; however, the pressure range of the tape is greater than that of the curve-fit expressions for given values of entropy. Imperfect air (intermolecular force) effects are neglected in the curve-fit expressions; thus, discretion should be exercised in using these expressions at pressures greater than 10 MN/m² or so. If the lower temperature limit of the AEDC real-air tape is exceeded during the unsteady or steady flow expansion computation, perfect air relations are used to determine thermodynamic properties at these low temperatures. For this case, a statement is printed in the printout acknowledging that perfect air relations were used; thereby, the user is cautioned that the temperature-pressure range may be such that air condensation effects (see, for example, ref. 22) are significant and should be considered.

Primary sources of uncertainties are iteration convergence criteria, source of real-air thermodynamic properties, and computational procedure. To reduce uncertainties arising from usage of various iteration convergence tolerances, tolerances were constant for all iterations in the present study, being 0.1 percent. Real-air thermodynamic properties as obtained from the AEDC tape are believed to be representative of the state of the art in calculation of air properties. However, some differences exist between the AEDC tape and the AEDC curve-fit expressions. For a pressure range of 10 to 1000 kN/m² and a temperature range of 2000 K to 15 000 K, the maximum percentage errors in thermodynamic properties obtained from the curve-fit expressions, as compared with those from the AEDC tape, are (ref. 11):

a, percent	2.78
h, percent	1.96
T, percent	2.24
Z*, percent	0.75
γ_E , percent	≈5.00
ρ , percent	2.52

Because of the wide range of possible shock tube and expansion tube flow conditions and the large number of methods (combinations of inputs) contained within the present program for computing these flow conditions, a comprehensive study of program uncertainties is not feasible. Instead, computations for specific cases, representative of tests performed in the Langley expansion tube, are considered. Values of flow quantities in

APPENDIX B

regions (2) and (2s), obtained for various values of input $U_{s,1}$ ($LB = 0$; see appendix A) and using the AEDC real-air tape, were compared with those values calculated by using the program of reference 5. This comparison showed excellent agreement, as expected. For the case where p_2 is an input, the values of p_2 were obtained from the case where $U_{s,1}$ is an input. This cross-check showed exact agreement between the results.

Flow quantities in region (2) where p_4 and T_4 are inputs were also compared with results from reference 5. For these comparisons, p_4 was equal to 34.5 MN/m^2 , T_4 was equal to 300 K and to 600 K, and p_1 was varied from 0.07 to 689.5 kN/m^2 . Both helium and hydrogen driver gases are considered. For the present program, the AEDC real-air curve-fit expressions ($ISAV = 2$; see appendix A) are used and 20 values of $U_{s,1}$ are used in generating the (p_2, U_2) curves. A 10-species (e^- , Ar, N, N^+ , N_2 , O, O^+ , O_2 , NO, and NO^+) air model is employed in reference 5, the air composition by volume being 78.08 percent N_2 , 20.95 percent O_2 , and 0.97 percent Ar. This composition yields an undissociated molecular weight W_u of 28.97 in agreement with references 9 and 11. As expected, thermodynamic properties in region (4) were in perfect agreement between the two programs for both driver gases. The maximum uncertainties observed between flow quantities in region (2) and $U_{s,1}$, as determined from the present program and reference 5, are

p_2 , percent	0.3
ρ_2 , percent	2.3
T_2 , percent	2.6
h_2 , percent	0.5
$s_2 W_u / R$, percent	0.2
a_2 , percent	1.6
U_2 , percent	0.2
$U_{s,1}$, percent	0.5

The ratios of flow conditions in region (2) to conditions in region (1) presented in figure 18 are shown in figure 22 as a function of $U_{s,1}$. The results of figure 18 were calculated by use of the AEDC tape, whereas the results of figure 22 were calculated by use of the AEDC curve-fit expressions. Comparison of figures 18 and 22 shows p_2/p_1 , h_2/h_1 (which are relatively insensitive to variation in p_1), and $s_2 W_u / R$ are in good agreement for the two sources of real-air thermodynamic properties. However, agreement for ρ_2/p_1 and T_2/T_1 is poorer, differences up to approximately 10 percent occurring for the range of $U_{s,1}$ examined. This comparison implies that some shock tube parameters in regions (2s) and (2r) calculated by using the curve-fit expressions

APPENDIX B

may also contain relatively large uncertainties. Thus, the user of the present program should exercise discretion in using these expressions to calculate shock tube flow quantities.

Expansion tube flow quantities in regions (5), (5s), and (t5) are compared for the three methods of the present program and with the results of reference 5. The three methods of the present program, in terms of inputs ISAV and IEXP (see appendix A), are

Method	ISAV	IEXP
(1)	1	1
(2)	2	1
(3)	2	2

where ISAV = 1 denotes that the AEDC real-air tape is used to determine flow quantities in the expansion tube cycle and ISAV = 2 denotes that the AEDC real-air curve-fit expressions are used. For IEXP = 1, the required table of h as a function of a^{-1} for the unsteady expansion calculation is generated from the AEDC tape. This table is generated by using subroutine SLOW with inputs $s_A W_u/R$ and h , where h is varied from a maximum value of h_A to a minimum value chosen to be 0.1 MJ/kg. This range of h is divided into increments (number of increments is input JAC with maximum of 300) and the numerical integration performed beginning with the upper limit h_A . The integration by Simpson's Rule is terminated when a value of h is obtained that equates to ΔU of equation (21). For IEXP = 2, this table is generated by using the curve-fit expressions. The pressure is varied from a maximum value of p_A to a minimum value of either $p_{5,f}$ or 0.1 N/m², whichever is largest. These values of p are inputs to subroutine SAVE, in conjunction with $s_A W_u/R$, and the corresponding values of h and a^{-1} are tabulated. The number of pressure increments used in generating this table is an input (maximum of 100). Method (1) (ISAV = IEXP = 1) is expected to be the most accurate method but requires more computer time primarily because of the time required for tape manipulation. Method (3) (ISAV = IEXP = 2) should contain the greatest uncertainty but has the smallest computer time. Method (2) represents a compromise between methods (1) and (3) and uses the AEDC tape only for the unsteady expansion calculations.

Flow quantities in regions (5), (5s), and (t5) were calculated with these three methods for the following basic inputs:

$$p_1 = 1.724 \text{ kN/m}^2$$

$$T_1 = 300 \text{ K}$$

APPENDIX B

$$U_{s,1} = 2.865 \text{ km/sec}$$

$$U_5 = 4, 5, 6, \text{ and } 7 \text{ km/sec}$$

No shock reflection at the secondary diaphragm is considered. All quantities are based on the assumption of thermochemical-equilibrium flow throughout the expansion tube flow cycle. The results of methods (2) and (3) are compared with the results of method (1) in the following table. Also illustrated in this table is a comparison of method (1) with results from the program of reference 5 for a 10-species air model and with the same inputs as method (1). For methods (1) and (2), input JAC is equal to 300, and for method (3), input IAC is equal to 50. Fifty pressure increments are also used in the program of reference 5. Agreement between method (1) and the results from the program of reference 5 for all flow quantities of table I is good (generally within 0.5 percent). The results of

TABLE I.- PERCENT DIFFERENCE BETWEEN FLOW QUANTITIES IN REGIONS (5), (5s), AND (t5) AS CALCULATED BY METHODS (1), (2), AND (3) AND REFERENCE 5

Flow quantity	Percent difference between methods (1) and (2) for U_5 , km/sec, of -				Percent difference between methods (1) and (3) for U_5 , km/sec, of -				Percent difference between method (1) and reference 5 for U_5 , km/sec, of -			
	4	5	6	7	4	5	6	7	4	5	6	7
P_5	5.47	5.48	5.50	5.54	1.67	7.85	7.47	8.70	0.09	0.15	0.14	0.50
ρ_5	5.43	5.43	5.48	5.49	3.98	7.28	6.45	7.24	.18	.28	.22	.51
T_5	.04	.00	.08	.03	2.77	.45	1.01	1.51	.04	.06	.00	.05
h_5	.03	.05	.00	.03	.49	.30	.71	1.11	.00	.00	.08	.06
Z_5	.00	.00	.00	.00	.30	.00	.00	.00	.00	.00	.00	.00
$\gamma_{E,5}$.00	.00	.00	.00	3.67	6.88	.68	.65	.00	.00	.00	.07
a_5	.05	.01	.01	.00	.60	3.26	.19	.45	.01	.01	.04	.02
M_5	.05	.02	.01	.00	.59	3.26	.19	.43	.02	.02	.04	.00
$N_{Re,5}$	5.44	5.46	5.47	5.44	5.87	7.02	5.88	6.26	.75	.38	.72	.00
P_{5s}	5.32	5.40	5.46	5.47	3.79	7.22	4.28	7.19	.14	.20	.21	.51
ρ_{5s}	4.63	4.61	5.25	5.18	1.96	6.46	.62	6.83	.11	.18	.25	.57
T_{5s}	.87	.88	.53	.93	.74	.93	.59	1.03	.13	.07	.05	.05
h_{5s}	.00	.00	.00	.00	.19	.07	.05	.04	.00	.00	.00	.00
$s_{5s} w_{u/R}$.05	.12	.29	.48	.79	.17	.31	.46	.00	.05	.04	.02
Z_{5s}	.25	.15	.42	.75	.25	.15	.42	.75	.00	.00	.00	.00
$\gamma_{E,5s}$.91	.17	.26	.00	.99	.17	.26	.00	.08	.09	.00	.09
a_{5s}	.86	.31	.23	.16	.80	.37	.29	.22	.00	.00	.00	.05
$P_{t,5}$	5.37	5.42	5.65	5.49	3.85	7.31	6.54	7.24	.15	.23	.21	.50
$\rho_{t,5}$	4.55	4.58	5.27	5.18	3.13	6.43	6.20	6.85	.14	.26	.27	.56
$T_{t,5}$.99	.86	.54	.93	.84	.92	.60	1.02	.13	.06	.03	.05
$h_{t,5}$.00	.00	.00	.00	.09	.07	.05	.04	.00	.00	.00	.00

APPENDIX B

method (3) are within 8 percent or so of those of method (1) for the range of U_5 examined. (It should be noted that for a value of U_5 of 7 km/sec, the corresponding value of p_5 exceeded the range curve fitted in ref. 11.) Differences between method (1) and method (2) or (3) in table I are believed to be representative of the present program as applied to a wide range of practical expansion tube flow conditions.

Uncertainty in flow quantities is expected to be a function of the number of increments used for the numerical integration required for the unsteady expansion. Hence, inputs JAC and IAC for methods (2) and (3), respectively, were varied to examine uncertainties resulting from these inputs. Percentage differences for flow quantities in region (5) are shown for method (3) with various IAC in the following table. These differences were obtained by comparing results for given values of IAC to results obtained with the maximum value of 100. The inputs p_1 , T_1 , and $U_{s,1}$ are those considered in the previous comparison and the input U_5 is 7 km/sec; thereby, the maximum difference between h_A and h_5 or p_A and p_5 for this case is provided. To minimize computer time without sacrificing accuracy in calculated flow quantities, a value of IAC equal to 50 for method (3) is recommended for most cases.

Flow quantity	IAC of -			
	10	20	30	50
p_5	5.74	0.82	0.63	0.00
ρ_5	4.23	.62	.45	.00
T_5	1.58	.22	.17	.00
h_5	1.65	.23	.18	.00
Z_5	.00	.00	.00	.00
$\gamma_{E,5}$.07	.00	.00	.00
a_5	.77	.10	.08	.00
M_5	.07	.14	.07	.00
$N_{Re,5}$	3.29	.39	.39	.00

A similar comparison for method (2) was performed, where the maximum value of input JAC was 300. This comparison showed the maximum difference between flow quantities in region (5) for JAC equal to 25 and the maximum of 300 was less than 0.25 percent for U_5 equal to 7 km/sec. However, extending the velocity to 8 km/sec yielded differences up to 5.5 percent. Increasing input JAC from 25 to 50 diminished this difference to

APPENDIX B

less than 0.2 percent. (It should be noted that for U_5 equal to 8 km/sec, the temperature T_5 was 250 K; hence, these conditions did not exceed the limits of the AEDC real-air tape.) Therefore, for methods (1) and (2), a value of JAC equal to 50 is recommended for most cases. More severe expansions from region (A) to region (5) than for this sample case may require larger values of JAC and IAC than recommended herein.

For the case where p_5 is an input ($LF = 2$; see appendix A), the values of p_5 calculated for methods (1) and (3) are, in turn, used as inputs. (The values from method (1) were used for $LF = 2$ and $ISAV = IEXP = 1$, and the values from method (3) were used for $LF = 2$ and $ISAV = IEXP = 2$.) This cross-check shows excellent agreement between the results.

The present program was run at conditions for which air behaves, approximately, as an ideal gas in all phases of the expansion tube cycle. Inputs for this case are

$$p_1 = 6.895 \text{ kN/m}^2$$

$$T_1 = 300 \text{ K}$$

$$U_{s,1} = 500 \text{ m/sec}$$

$$U_5 = 700, 900, \text{ and } 1100 \text{ m/sec}$$

and the AEDC tape was used for the unsteady expansion. The purpose of this case was to compare flow quantities for a frozen expansion with those for a thermochemical equilibrium expansion. Flow quantities in region (5), (5s), and (t5) were observed to be within 2 percent between the frozen and equilibrium cases. Comparison of frozen flow quantities between the present program and the program of reference 5 showed agreement to worsen with increasing level of dissociation in region (A). Since the composition of the air in region (A) is calculated in reference 5, the corresponding frozen flow calculations of reference 5 are believed to be more accurate than those of the present program.

Flow quantities calculated in region (6) of the expansion tunnel were verified by manual calculations and usage of reference 9. The same subroutine (SNS; see appendix A) was used to obtain conditions in regions (6s) and (t6) as was used to obtain conditions in regions (5s) and (t5).

APPENDIX C

LANGLEY LIBRARY SUBROUTINE ITR1

Language: FORTRAN

Purpose: To solve the single equation of the form $x = f(x)$ for one real root by the Newton-Raphson iteration method.

Use: CALL ITR1 (X, DELTX, FOFX, E1, E2, MAXI, ICODE)

X	An initial guess supplied by the user. On a normal return to the calling program from ITR1, X contains the root.
DELTX	An increment supplied by the user so that $\frac{f(x + \text{DELTX}) - f(x)}{\text{DELTX}}$ is a reasonable approximation to the derivative of $f(x)$.
FOFX	A function subprogram to evaluate $f(x)$.
E1	Relative error criterion.
E2	Absolute error criterion.
MAXI	A maximum iteration count supplied by the user.
ICODE	An integer supplied by ITR1 as an error code. This code should be tested by the user on return to the calling program. ICODE = 0: Normal return. ICODE = 1: Maximum iteration exceeded. ICODE = 2: Derivative = 0.

Restrictions: A function subprogram with a single argument x must be written by the user to evaluate $f(x)$. The name given to the FOFX subprogram must appear in an EXTERNAL statement in the calling program.

Method: The Newton-Raphson iteration technique (ref. (a) of this subroutine) is used where

$$x_{n+1} = q_n + (1 - q) f(x_n)$$

$$q = \frac{a}{a - 1}$$

$$a = \frac{f(x_n) - f(x_{n-1})}{x_n - x_{n-1}}$$

APPENDIX C

Accuracy: The iteration process is continued until either of two convergence criteria is satisfied. These criteria are given as follows:

If

$$\left| f(x_n) \right| \geq \epsilon_1$$

then

$$\left| \frac{f(x_n) - x_n}{f(x_n)} \right| \leq \epsilon_1 \quad (C1)$$

and if

$$\left| f(x_n) \right| < \epsilon_1$$

then

$$\left| f(x_n) - x_n \right| \leq \epsilon_2 \quad (C2)$$

Reference: (a) Scarborough, James B.: Numerical Mathematical Analysis. Fourth ed.
Johns Hopkins Press, 1958, p. 192.

Storage: 137₈ locations.

Subroutine date: August 1, 1968.

APPENDIX D

LANGLEY LIBRARY SUBROUTINE ITR2

Language: FORTRAN

Purpose: Given $F(X) = 0$, to find a value for X within a given epsilon of relative error in a given interval (a,b) .

Use: CALL ITR2 (X, A, B, DELTX, FOFX, E1, E2, MAXI, ICODE)

X	The root.
A	The lower bound on X. This value is used by ITR2 as an initial guess.
B	The upper bound on X. This value is used by ITR2 as a final guess if the entire interval is scanned.
DELTX	ΔX , the size of the scanning interval.
FOFX	The name of a function subprogram to evaluate $F(X)$.
E1	Relative error criterion.
E2	Absolute error criterion.
MAXI	A maximum iteration count supplied by the user.
ICODE	An integer supplied by ITR2 as an error code. This code should be tested by the user on return to the calling program. ICODE = 0: Normal return ICODE = 1: Maximum iterations are exceeded ICODE = 2: DELTX = 0, or negative ICODE = 3: a root cannot be found within the given bounds ICODE = 4: $A > B$

Restrictions: Make $A < B$, ΔX positive. A function subprogram with a single argument X must be written by the user to evaluate $F(X)$. The name of this subprogram, FOFX, must appear in an EXTERNAL statement of the calling program.

APPENDIX D

Method: The given function $F(X)$ is evaluated at a given starting point a and at intervals of a specified ΔX thereafter, up to and including a specified end point b . A change of sign of the function across a ΔX interval indicates a possible root in that interval. The interval is then halved successively toward $F(X) = 0$ until the prescribed accuracy is satisfied. The given function $F(X)$ is evaluated once for each halving step.

If the given function is expected to have more than one root between the prescribed starting and end points, it is suggested that a sufficiently small ΔX be given such that no more than one root be present within a ΔX interval. A normal return is given upon the location of the first root from the starting point a . Additional roots must be located by new entries into the subroutine using a new starting point a which is just beyond the previous root.

Accuracy: The iteration process is continued until either of two convergence criteria is satisfied. These criteria are

If

$$|X_i| > \epsilon_1$$

then

$$\left| \frac{X_i - X_{i-1}}{X_i} \right| \leq \epsilon_1$$

and if

$$|X_i| \leq \epsilon_1$$

then

$$|X_i - X_{i-1}| \leq \epsilon_2$$

Reference: Scarborough, James B.: Numerical Mathematical Analysis. Fourth ed. John Hopkins Press, 1958.

Storage: 260₈ locations.

APPENDIX E

LANGLEY LIBRARY SUBROUTINE FTLUP

Language: FORTRAN

Purpose: Computes $y = F(x)$ from a table of values using first- or second-order interpolation. An option to give y a constant value for any x is also provided.

Use: CALL FTLUP (X, Y, M, N, VARI, VARD)

X	The name of the independent variable x .
Y	The name of the dependent variable $y = f(x)$.
M	The order of interpolation (an integer) M = 0 for y a constant as explained in the note below. M = 1 or 2. First or second order if VARI is strictly increasing (not equal). M = -1 or -2. First or second order if VARI is strictly decreasing (not equal).
N	The number of points in the table (an integer).
VARI	The name of a one-dimensional array which contains the N values of the independent variable.
VARD	The name of a one-dimensional array which contains the N values of the dependent variable.

Note that VARD(I) corresponds to VARI(I) for $I = 1, 2, \dots, N$. For $M = 0$ or $N \leq 1$, $y = F(VARI(1))$ for any value of x . The program extrapolates.

Restrictions: All the numbers must be floating point. The values of the independent variable x in the table must be strictly increasing or strictly decreasing. The following arrays must be dimensioned by the calling program as indicated: VARI(N), VARD(N).

Accuracy: A function of the order of interpolation used.

APPENDIX E

References: (a) Nielson, Kaj L.: Methods in Numerical Analysis. Macmillan Co.,
c.1956, pp. 87-91.

(b) Milne, William Edmund: Numerical Calculus. Princeton Univ. Press,
1949, pp. 69-73.

Storage: 430_8 locations.

Error condition: If the VARI values are not in order, the subroutine will print "TABLE
BELOW OUT OF ORDER FOR FTLUP AT POSITION xxx TABLE IS STORED IN
LOCATION xxxxxx" (absolute). It then prints the contents of VARI and VARD and stops
the program.

Subroutine date: September 12, 1969.

APPENDIX F

LANGLEY LIBRARY SUBROUTINE DISCOT

Language: FORTRAN

Purpose: DISCOT performs single or double interpolation for continuous or discontinuous functions. Given a table of some function y with two independent variables, x and z , this subroutine performs K_x -th- and K_z -th-order interpolation to calculate the dependent variable. In this subroutine all single-line functions are read in as two separate arrays and all multiline functions are read in as three separate arrays; that is,

x_i ($i = 1, 2, \dots, L$)

y_j ($i = 1, 2, \dots, M$)

z_k ($k = 1, 2, \dots, N$)

Use: CALL DISCOT (XA,ZA,TABX,TABY,TABZ,NC,NY,NZ,ANS)

XA The x argument

ZA The z argument (may be the same name as x on single lines)

TABX A one-dimensional array of x values

TABY A one-dimensional array of y values

TABZ A one-dimensional array of z values

NC A control word that consists of a sign (+ or -) and three digits. The control word is formed as follows:

- (1) If $NX = NY$, the sign is negative. If $NX \neq NY$, then NX is computed by DISCOT as $NX = NY/NZ$ and the sign is positive and may be omitted if desired.
- (2) A one in the hundreds position of the word indicates that no extrapolation occurs above z_{\max} . With a zero in this position, extrapolation occurs when $z > z_{\max}$. The zero may be omitted if desired.
- (3) A digit (1 to 7) in the tens position of the word indicates the order of interpolation in the x -direction.

APPENDIX F

(4) A digit (1 to 7) in the units position of the word indicates the order of interpolation in the z-direction

NY	The number of points in y array
NZ	The number of points in z array
ANS	The dependent variable y

Restrictions: See rule (5c) of section "Method" for restrictions on tabulating arrays and discontinuous functions. The order of interpolation in the x- and z-directions may be from 1 to 7. The following subprograms are used by DISCOT: UNS, DISSER, LAGRAN.

Method: Lagrange's interpolation formula is used in both the x- and z-directions for interpolation. This method is explained in detail in reference (a) of this subroutine. For a search in either the x- or z-direction, the following rules are observed:

(1) If $x < x_1$, the routine chooses the following points for extrapolation:

$$x_1, x_2, \dots, x_{k+1} \text{ and } y_1, y_2, \dots, y_{k+1}$$

(2) If $x > x_n$, the routine chooses the following points for extrapolation:

$$x_{n-k}, x_{n-k+1}, \dots, x_n \text{ and } y_{n-k}, y_{n-k+1}, \dots, y_n$$

(3) If $x \leq x_n$, the routine chooses the following points for interpolation:
When k is odd,

$$x_{i-\frac{k+1}{2}}, x_{i-\frac{k+1}{2}+1}, \dots, x_{i-\frac{k+1}{2}+k} \text{ and } y_{i-\frac{k+1}{2}}, y_{i-\frac{k+1}{2}+1}, \dots, y_{i-\frac{k+1}{2}+k}$$

When k is even,

$$x_{i-\frac{k}{2}}, x_{i-\frac{k}{2}+1}, \dots, x_{i-\frac{k}{2}+k} \text{ and } y_{i-\frac{k}{2}}, y_{i-\frac{k}{2}+1}, \dots, y_{i-\frac{k}{2}+k}$$

(4) If any of the subscripts in rule (3) become negative or greater than n (number of points), rules (1) and (2) apply. When discontinuous functions are tabulated, the independent variable at the point of discontinuity is repeated.

(5) The subroutine will automatically examine the points selected before interpolation and if there is a discontinuity, the following rules apply.
Let x_d and x_{d+1} be the point of discontinuity.

APPENDIX F

- (a) If $x \leq x_d$, points previously chosen are modified for interpolation as shown:

$$x_{d-k}, x_{d-k+1}, \dots, x_d \quad \text{and} \quad y_{d-k}, y_{d-k+1}, \dots, y_d$$

- (b) If $x > x_d$, points previously chosen are modified for interpolation as shown:

$$x_{d+1}, x_{d+2}, \dots, x_{d+k} \quad \text{and} \quad y_{d+1}, y_{d+2}, \dots, y_{d+k}$$

- (c) When tabulating discontinuous functions, there must always be $k + 1$ points above and below the discontinuity in order to get proper interpolation.

- (6) When tabulating arrays for this subroutine, both independent variables must be in ascending order.
- (7) In some engineering programs with many tables, it is quite desirable to read in one array of x values that could be used for all lines of a multiline function or different functions. Even though this situation is not always applicable, the subroutine has been written to handle it. This procedure not only saves much time in preparing tabular data, but also can save many locations previously used when every y coordinate had to have a corresponding x coordinate. Another additional feature that may be useful is the possibility of a multiline function with no extrapolation above the top line.

Accuracy: A function of the order of interpolation used.

Reference: (a) Nielsen, Kaj L.: Methods in Numerical Analysis. Macmillan Co., c.1956.

Storage: 555_8 locations.

Subprograms used: UNS 40_8 locations.

DISSER 110_8 locations.

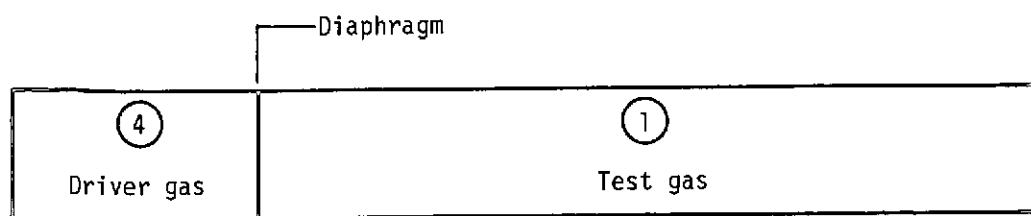
LAGRAN 55_8 locations.

Subroutine date: August 1, 1968.

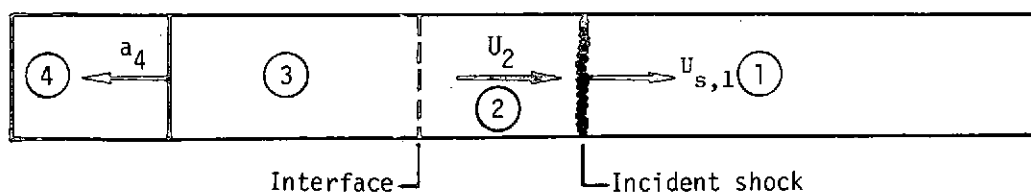
REFERENCES

1. Trimpi, Robert L.: A Preliminary Theoretical Study of the Expansion Tube, A New Device for Producing High-Enthalpy Short-Duration Hypersonic Gas Flows. NASA TR R-133, 1962.
2. Trimpi, Robert L.; and Callis, Linwood B.: A Perfect-Gas Analysis of the Expansion Tunnel, A Modification to the Expansion Tube. NASA TR R-223, 1965.
3. Trimpi, Robert L.: A Theoretical Investigation of Simulation in Expansion Tubes and Tunnels. NASA TR R-243, 1966.
4. Norfleet, Glenn D.; and Loper, F. C.: A Theoretical Real-Gas Analysis of the Expansion Tunnel. AEDC-TR-66-71, U.S. Air Force, June 1966. (Available from DDC as AD 633 656.)
5. Miller, Charles G., III: A Program for Calculating Expansion-Tube Flow Quantities for Real-Gas Mixtures and Comparison With Experimental Results. NASA TN D-6830, 1972.
6. Mirels, Harold: Test Time in Low-Pressure Shock Tubes. Phys. Fluids, vol. 6, no. 9, Sept. 1963, pp. 1201-1214.
7. Mirels, Harold: Shock Tube Test Time Limitation Due to Turbulent-Wall Boundary Layer. AIAA J., vol. 2, no. 1, Jan. 1964, pp. 84-93.
8. Mechtly, E. A.: The International System of Units - Physical Constants and Conversion Factors (Second Revision). NASA SP-7012, 1973.
9. Neel, C. A.; and Lewis, Clark H.: Interpolations of Imperfect Air Thermodynamic Data. I. At Constant Entropy. AEDC-TDR-64-183, U.S. Air Force, Sept. 1964. (Available from DDC as AD 605 471.)
10. Miller, Charles G., III; and Wilder, Sue E.: Real-Air Data Reduction Procedures Based on Flow Parameters Measured in the Test Section of Supersonic and Hypersonic Facilities. NASA TN D-6618, 1972.
11. Lewis, Clark H.; and Burgess, Ernest G., III: Empirical Equations for the Thermodynamic Properties of Air and Nitrogen to 15,000° K. AEDC-TDR-63-138, U.S. Air Force, July 1963.
12. Gaydon, A. G.; and Hurle, I. R.: The Shock Tube in High Temperature Chemical Physics. Reinhold Pub. Corp., 1963.
13. Connor, Laurence N., Jr.; and Andersen, Rolf P.: Real Gas Effects on Shock-Tube Flow Nonuniformity. AIAA J., vol. 8, no. 1, Jan. 1970, pp. 175-177.

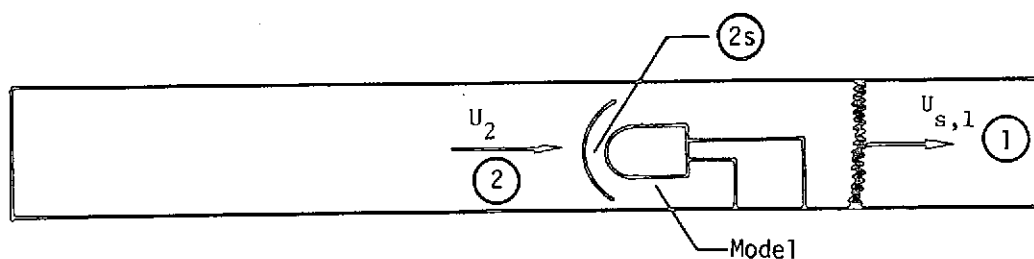
14. Jones, Jim J.; and Moore, John A.: Exploratory Study of Performance of the Langley Pilot Model Expansion Tube With a Hydrogen Driver. NASA TN D-3421, 1966.
15. Miller, Charles G.: Flow Properties in Expansion Tube With Helium, Argon, Air, and CO₂. AIAA J., vol. 12, no. 4, Apr. 1974, pp. 564-566.
16. Yos, Jerrold M.: Transport Properties of Nitrogen, Hydrogen, Oxygen, and Air to 30,000° K. Tech. Mem. RAD-TM-63-7 (Contract AF33(616)-7578), AVCO Corp., Mar. 22, 1963.
17. Ames Research Staff: Equations, Tables, and Charts for Compressible Flow. NACA Rep. 1135, 1953. (Supersedes NACA TN 1428.)
18. Zoby, Ernest V.: Empirical Stagnation-Point Heat-Transfer Relation in Several Gas Mixtures at High Enthalpy Levels. NASA TN D-4799, 1968.
19. Grose, William L.; and Nealy, John E.: Imperfect Gas Effect in Real Hydrogen Drives. AIAA J., vol. 8, no. 6, June 1970, pp. 1164-1165.
20. Olstad, Walter B.; Kemper, Jane T.; and Bengtson, Roger D.: Equilibrium Normal-Shock and Stagnation-Point Properties of Helium for Incident-Shock Mach Numbers From 1 to 30. NASA TN D-4754, 1968.
21. Miller, Charles G., III: Langley Hotshot Tunnel Operations With Helium at Mach Numbers in Excess of 30. NASA TN D-5901, 1970.
22. Daum, Fred L: Air Condensation in a Hypersonic Wind Tunnel. AIAA J., vol. 1, no. 5, May 1963, pp. 1043-1046.



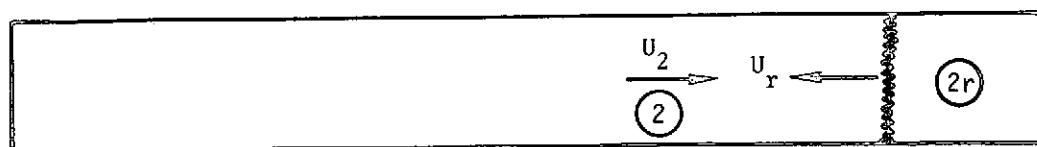
(a) Prior to diaphragm rupture.



(b) Incident (moving) normal shock in test gas.



(c) Standing normal shock at test model.



(d) Reflected normal shock from end wall.

Figure 1.- Sketches illustrating shock-tube regions of interest:
Regions (2), (2s), and (2r).

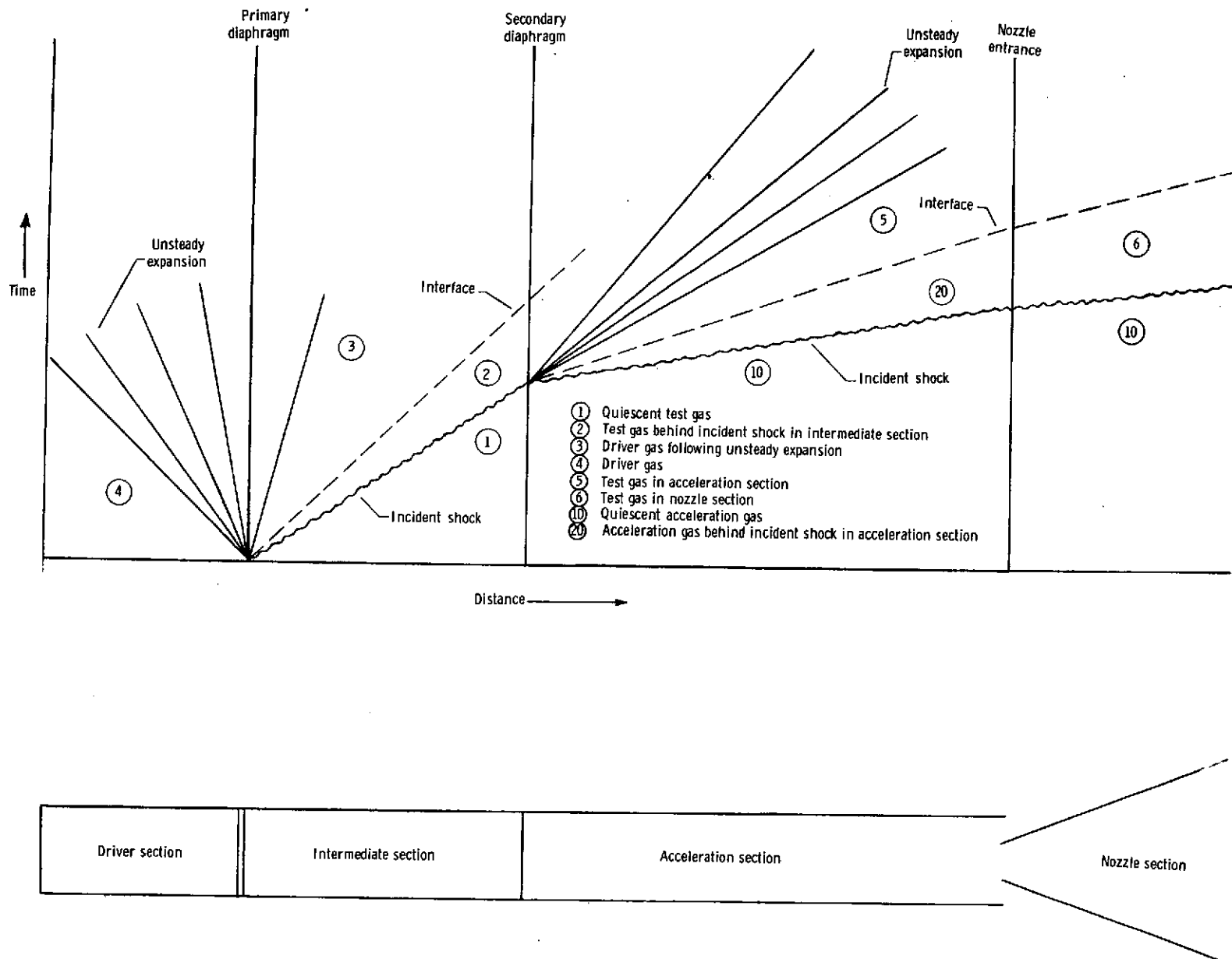
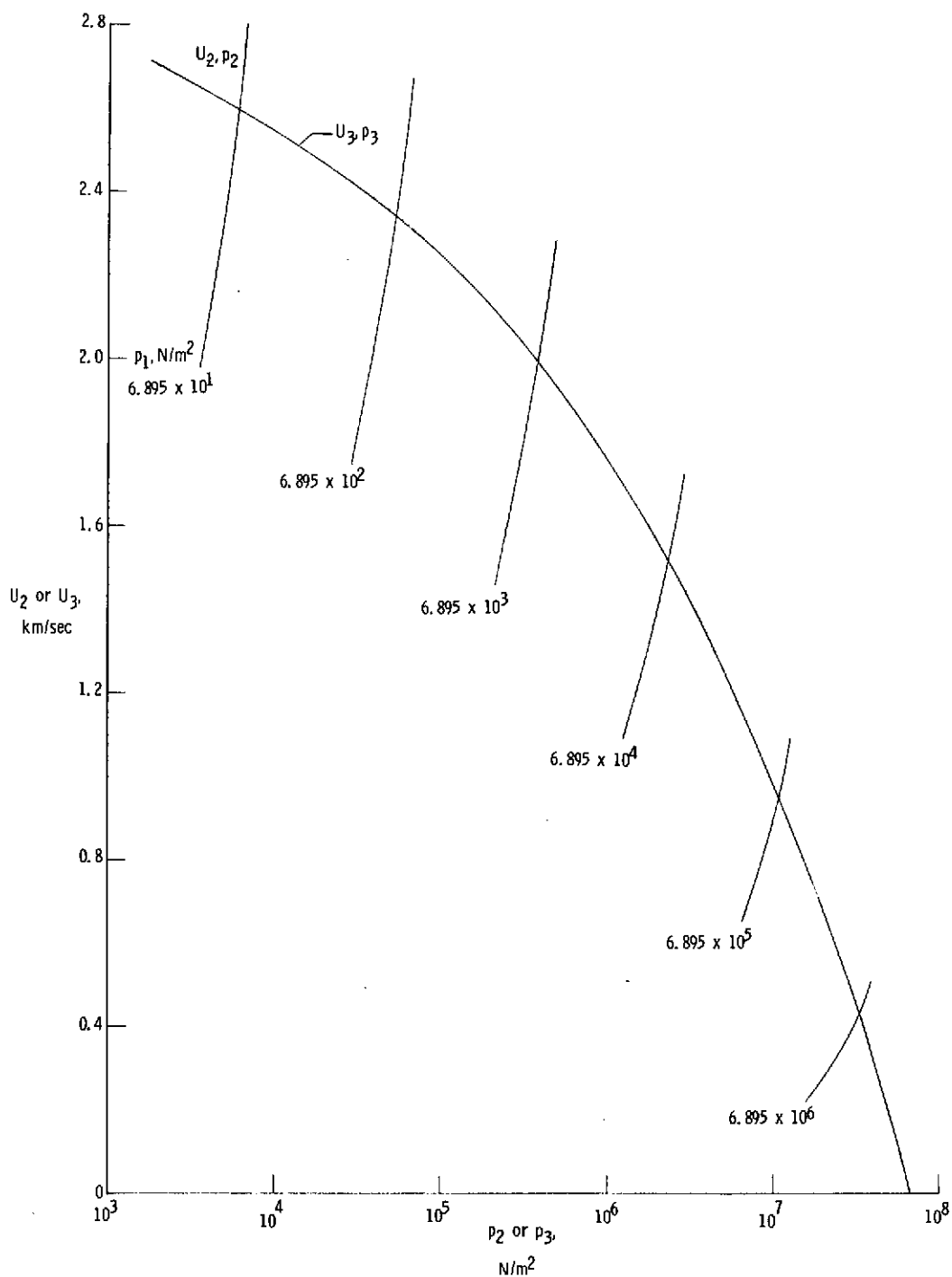
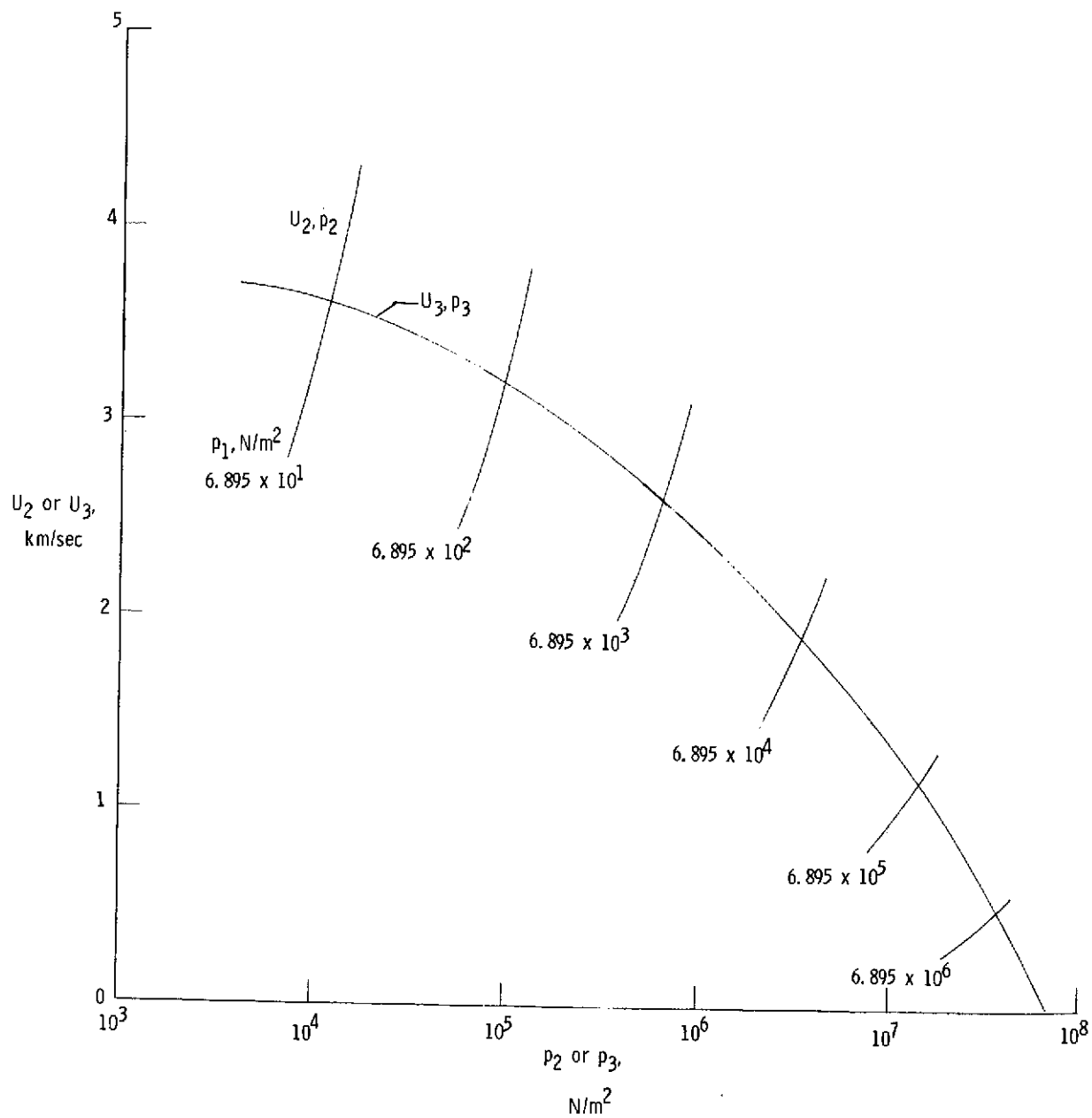


Figure 2.- Schematic diagram of expansion tunnel flow sequence.



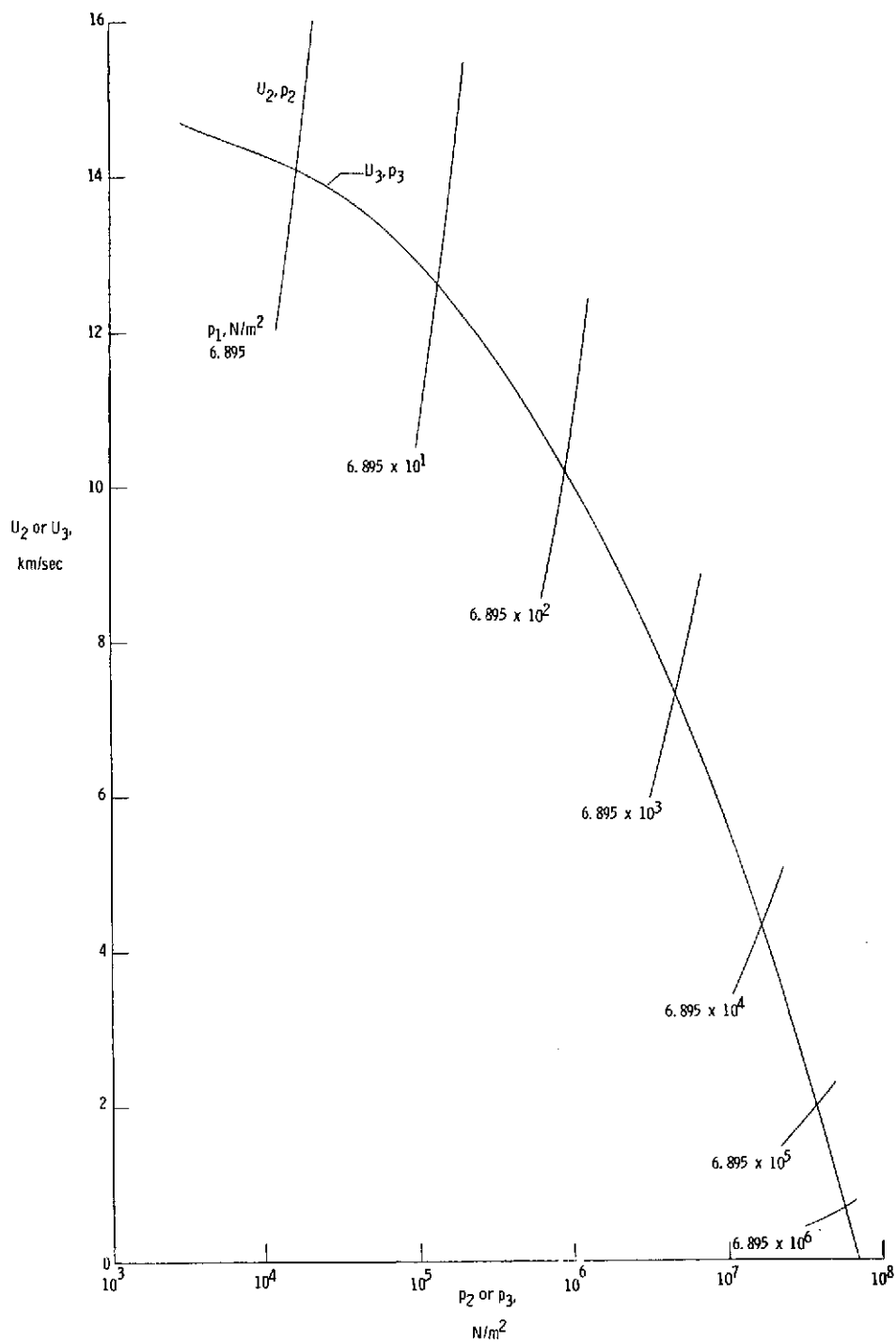
(a) Helium driver gas with $T_4 = 300$ K.

Figure 3.- Velocity U_3 as a function of pressure p_3 for isentropic unsteady expansion of helium and hydrogen driver gases for $p_4 = 68.95$ MN/m² and various T_4 ; velocity U_2 as a function of pressure p_2 for incident normal shock in real air.



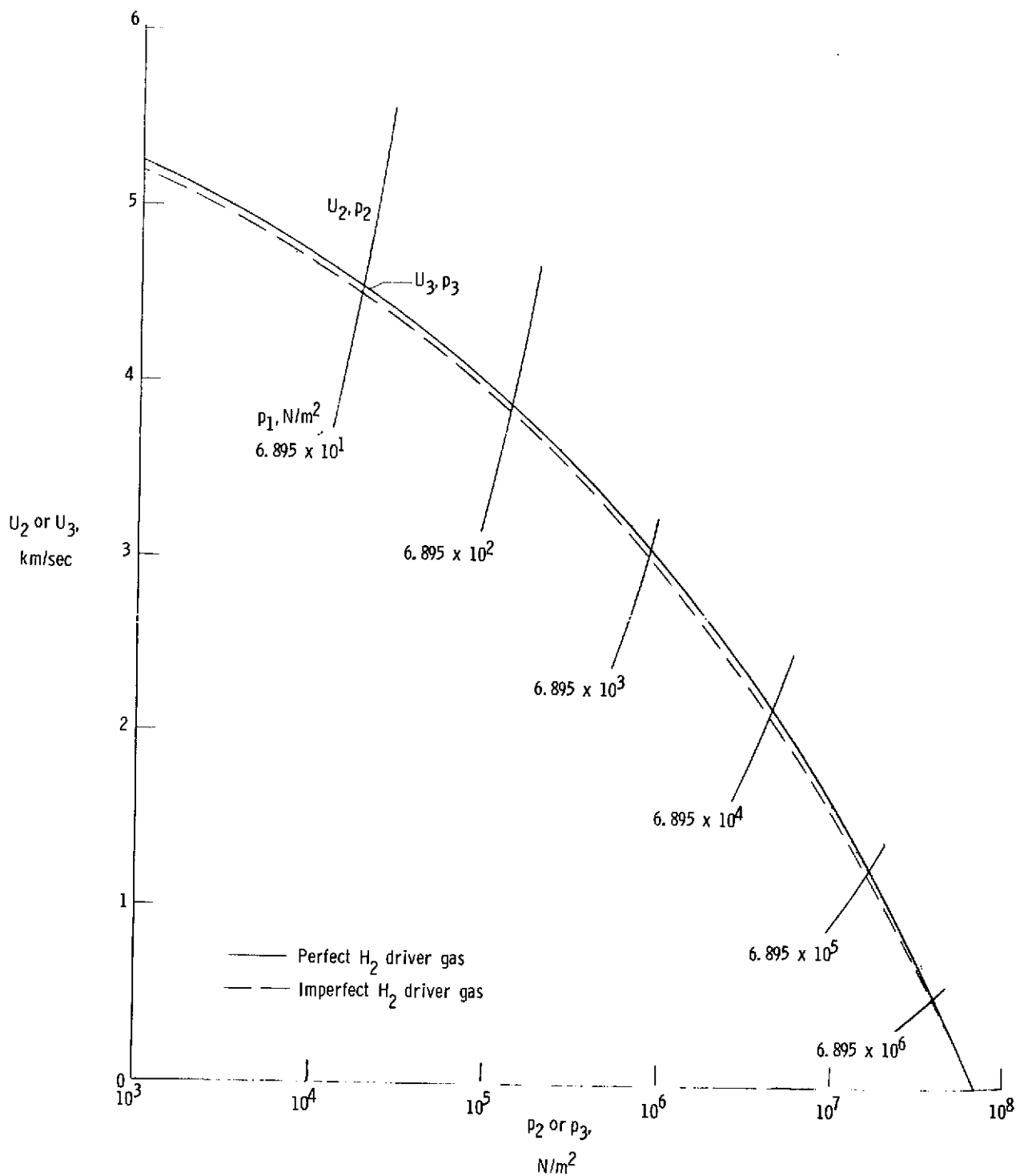
(b) Helium driver gas with $T_4 = 600$ K.

Figure 3.- Continued.



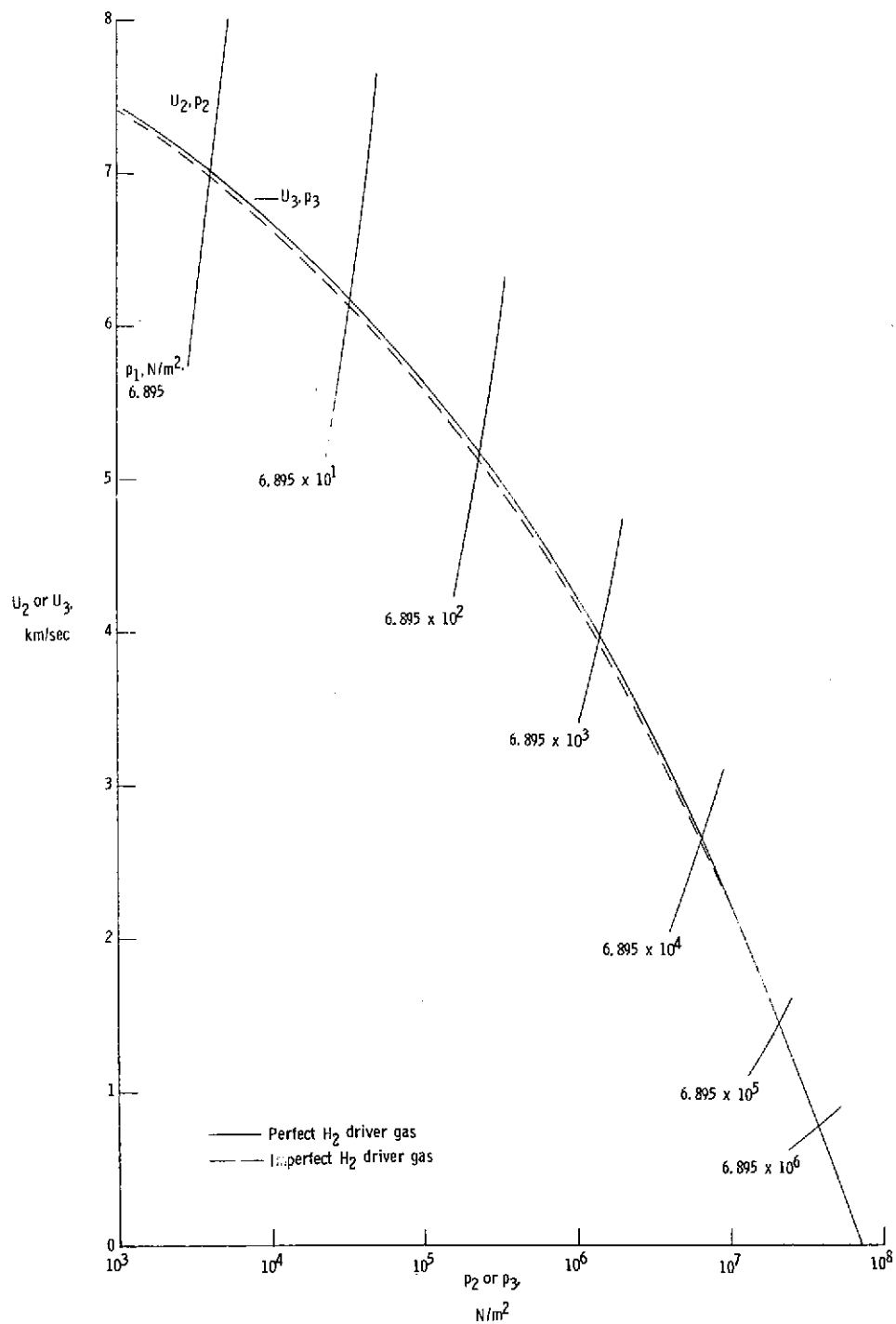
(c) Helium driver gas with $T_4 = 10\,000$ K.

Figure 3.- Continued.



(d) Hydrogen driver gas with $T_4 = 300$ K.

Figure 3.- Continued.



(e) Hydrogen driver gas with $T_4 = 600$ K.

Figure 3.- Concluded.

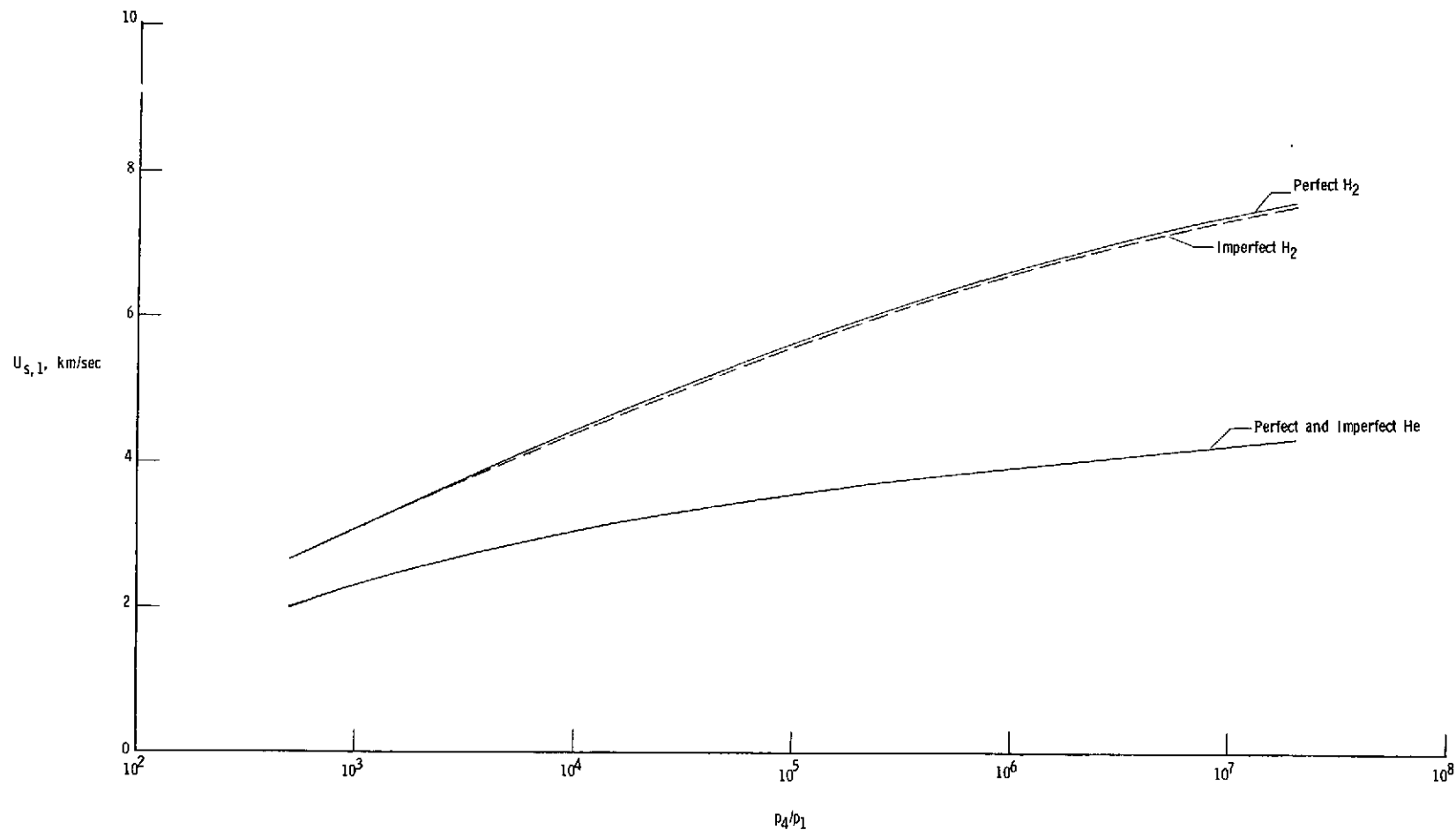
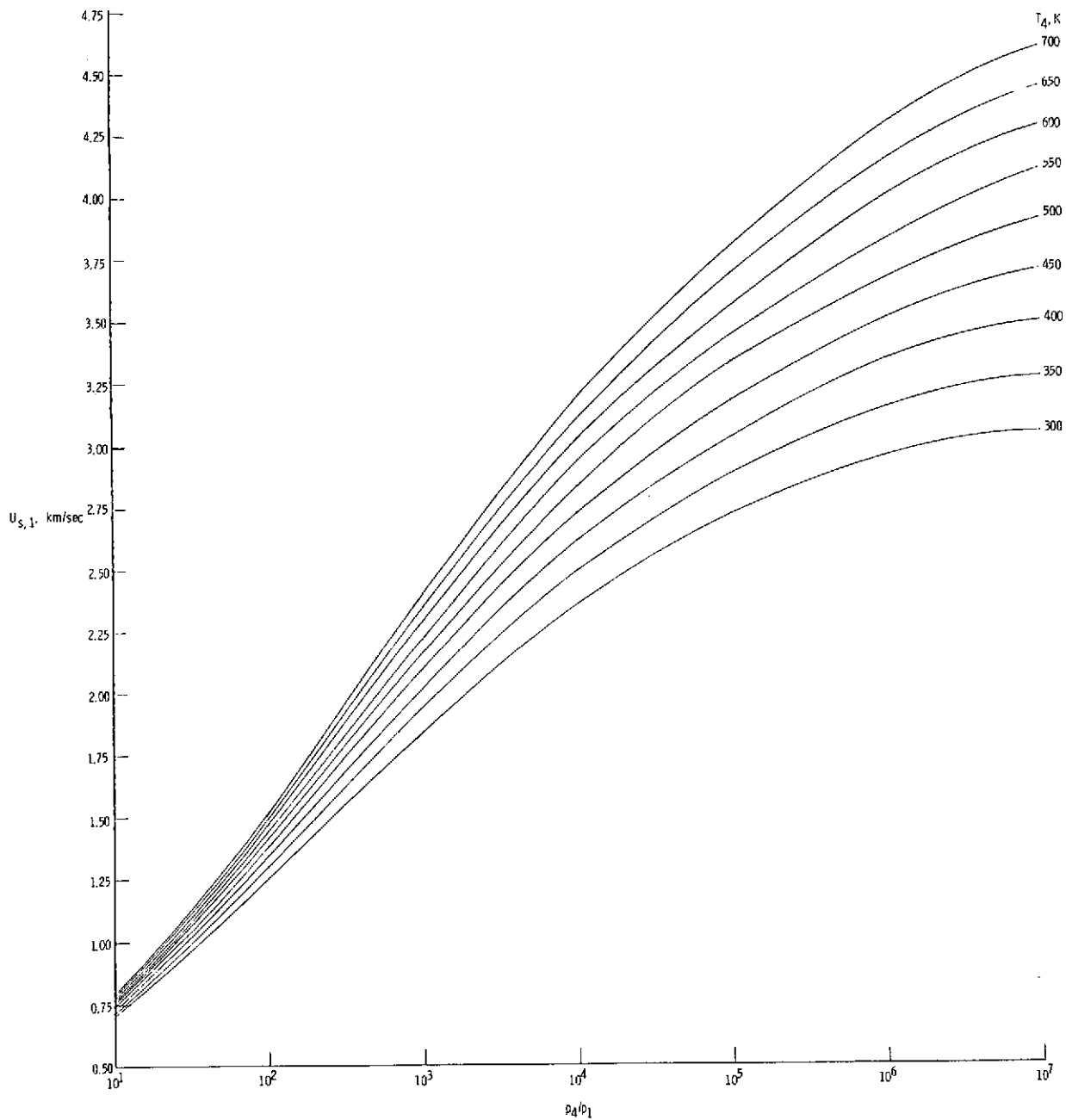
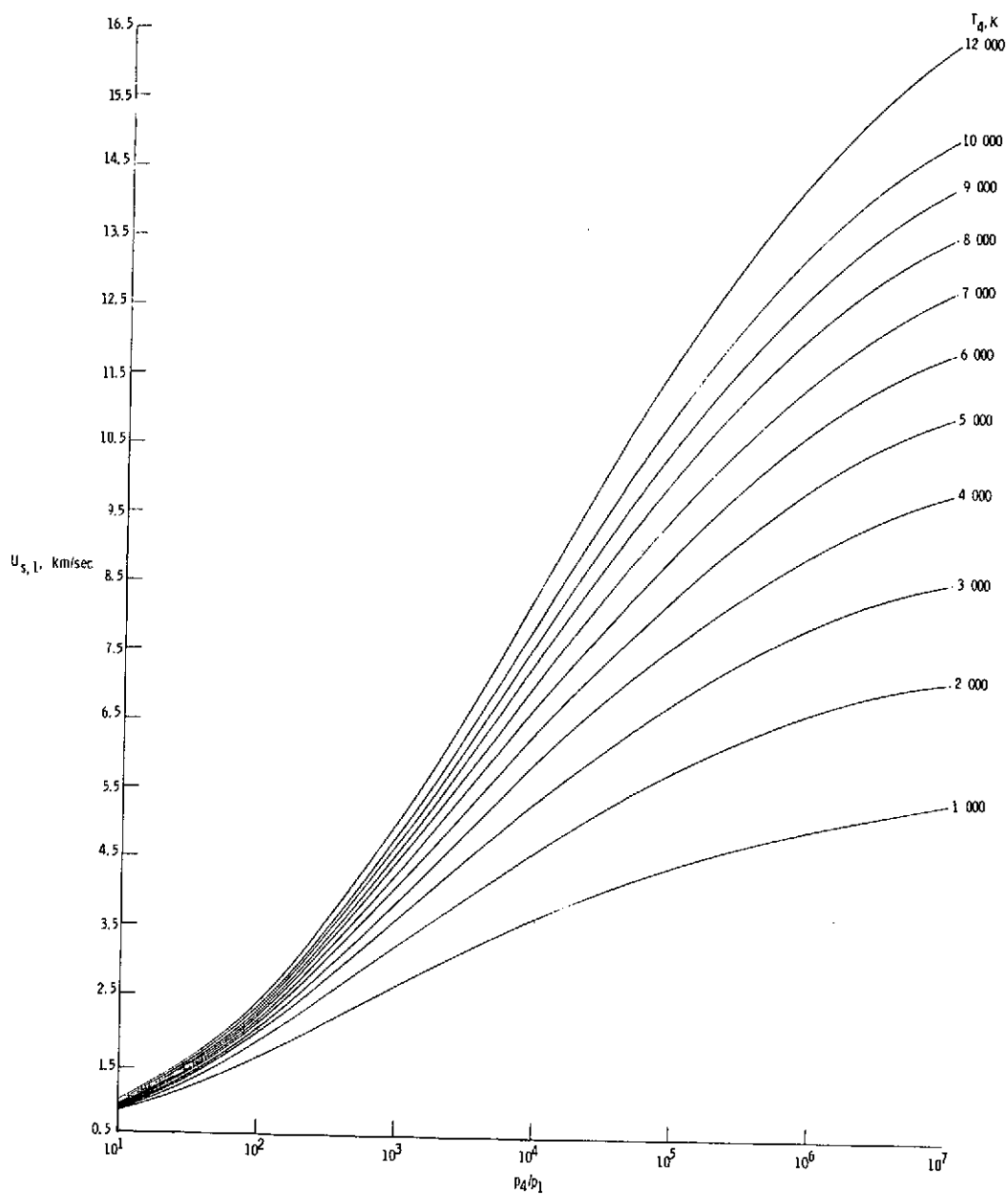


Figure 4.- Incident normal shock velocity as a function of ratio of driver gas pressure to quiescent test air pressure for helium and hydrogen driver gases. $T_4 = 600$ K.



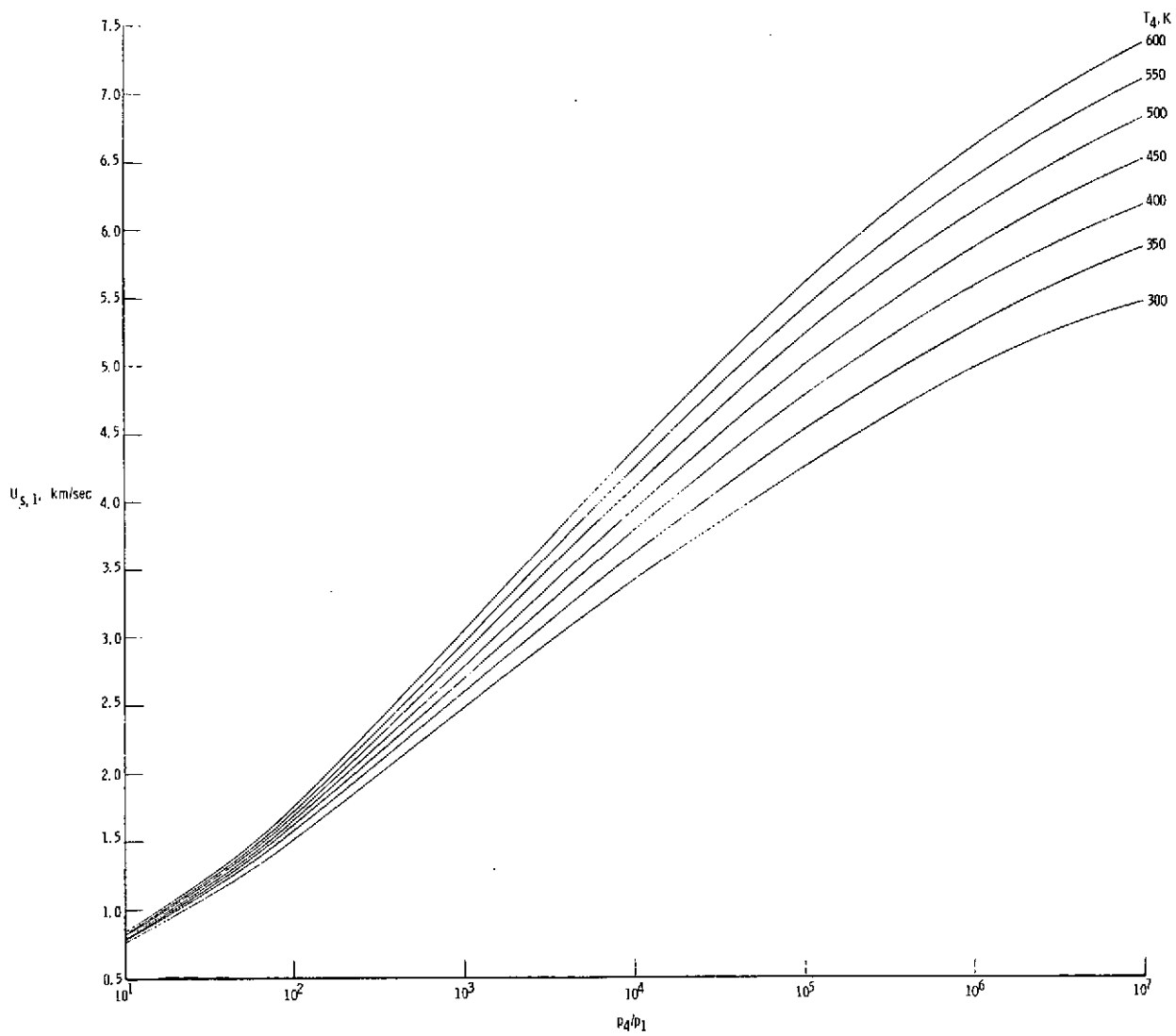
(a) Helium driver gas with $300 \text{ K} \leq T_4 \leq 700 \text{ K}$.

Figure 5.- Shock tube performance for real-air test gas and helium and hydrogen driver gases over range of T_4 . $p_4 = 68.95 \text{ MN/m}^2$.



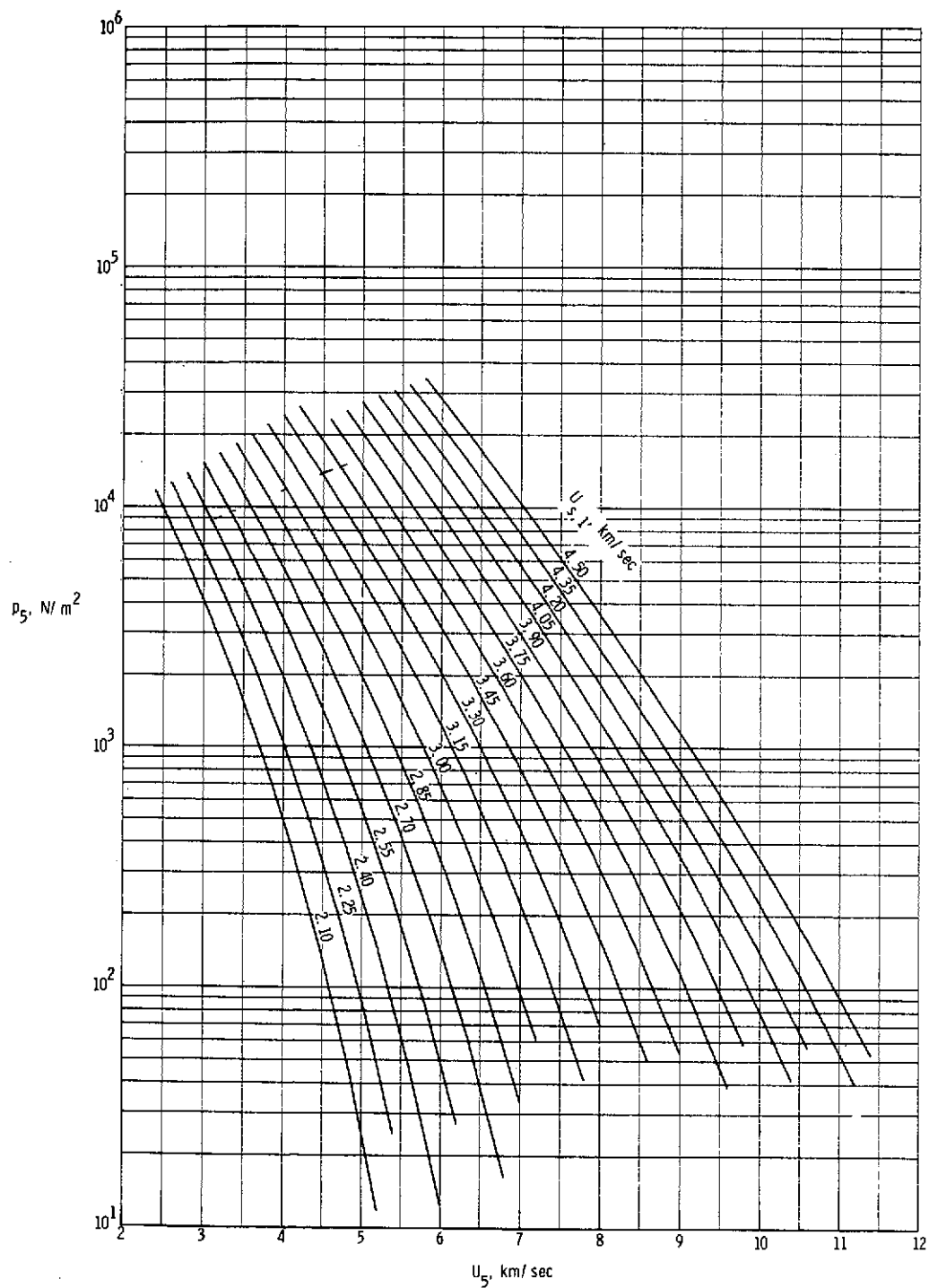
(b) Helium driver gas with $1000 \text{ K} \leq T_4 \leq 12\,000 \text{ K}$.

Figure 5.- Continued.



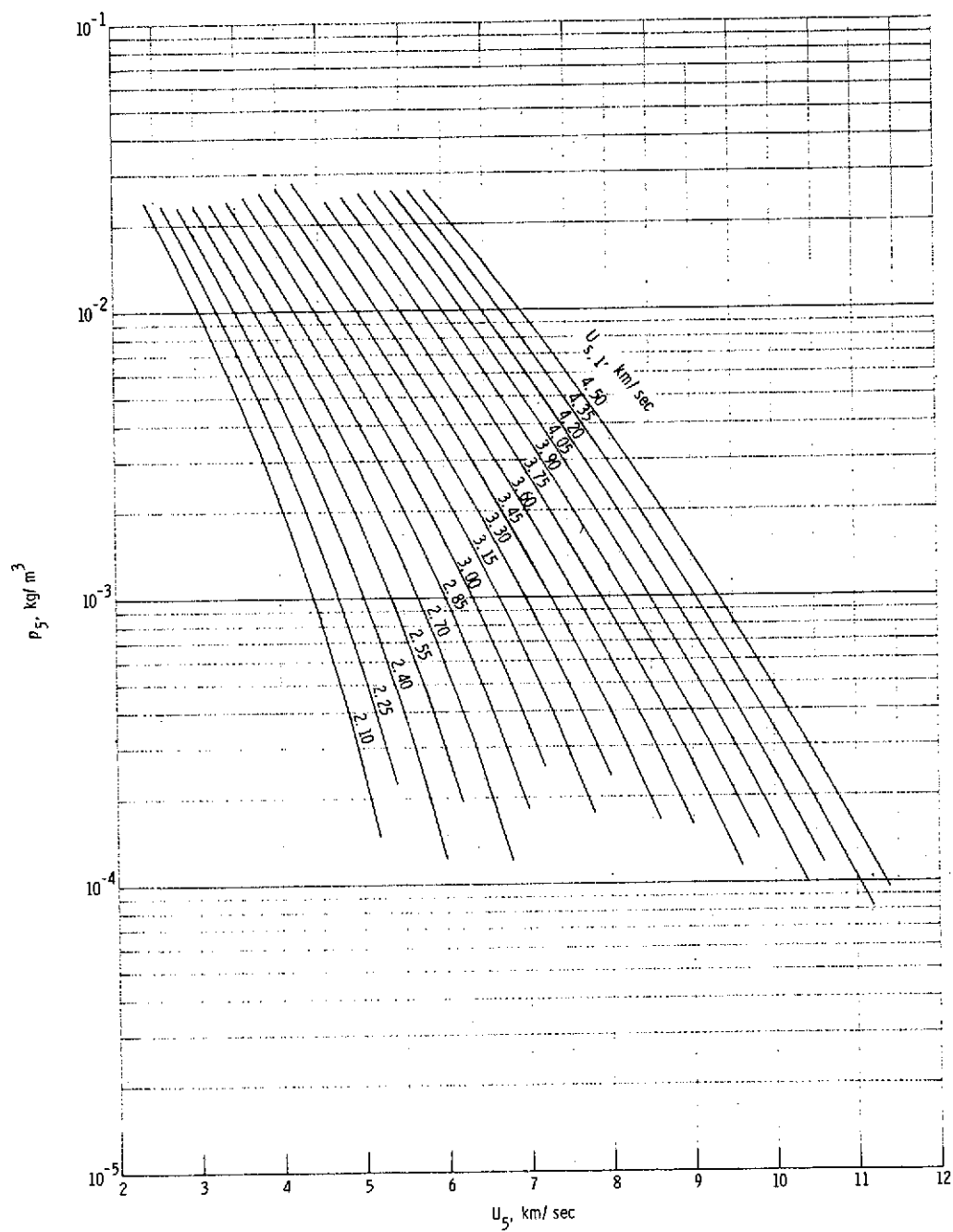
(c) Hydrogen driver gas with $300 \text{ K} \leq T_4 \leq 600 \text{ K}$.

Figure 5.- Concluded.



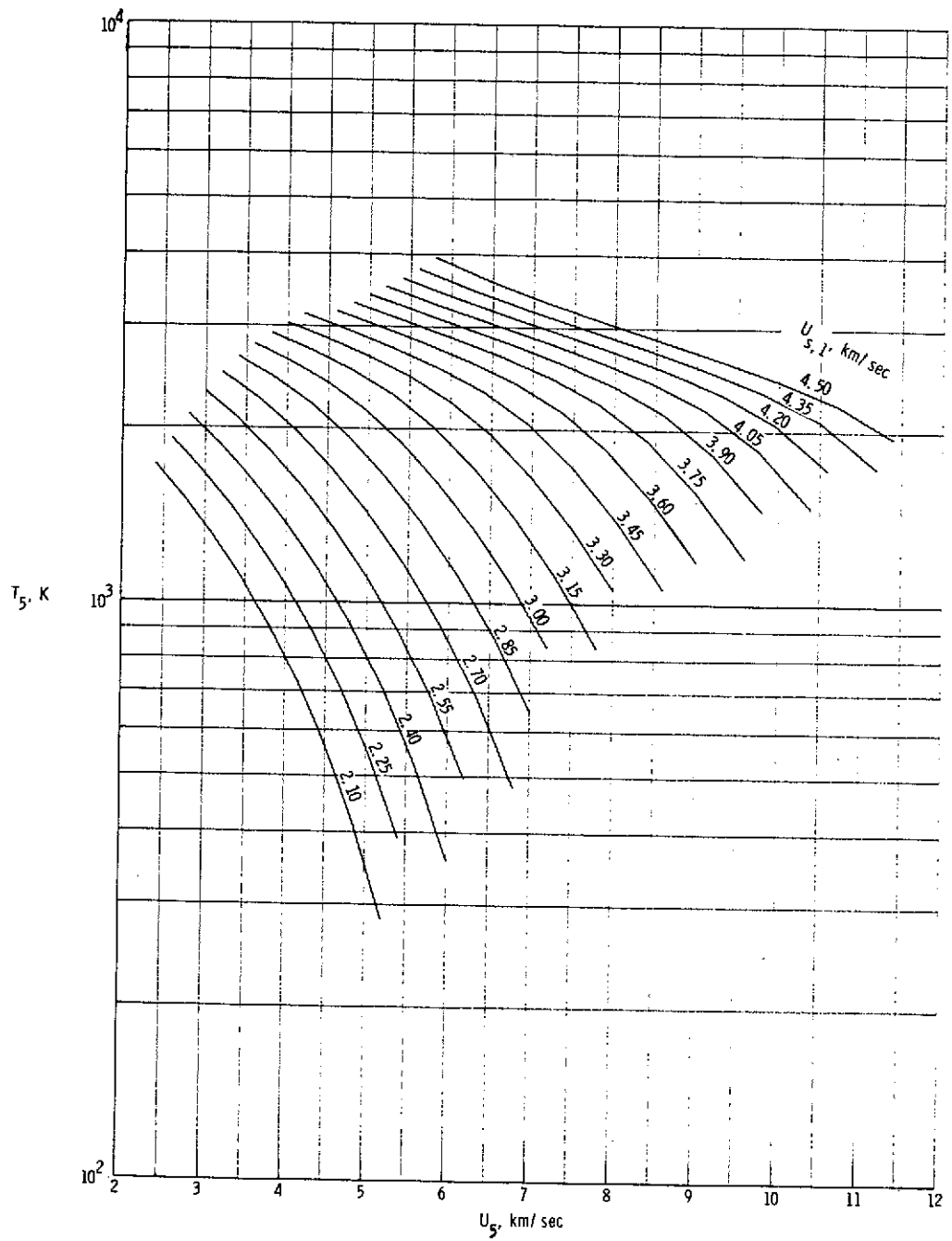
(a) Static pressure in region (5).

Figure 6.- Various expansion tube flow parameters for real air in thermochemical equilibrium as a function of flow velocity and assuming no shock reflection at secondary diaphragm. $p_1 = 0.6895 \text{ kN/m}^2$.



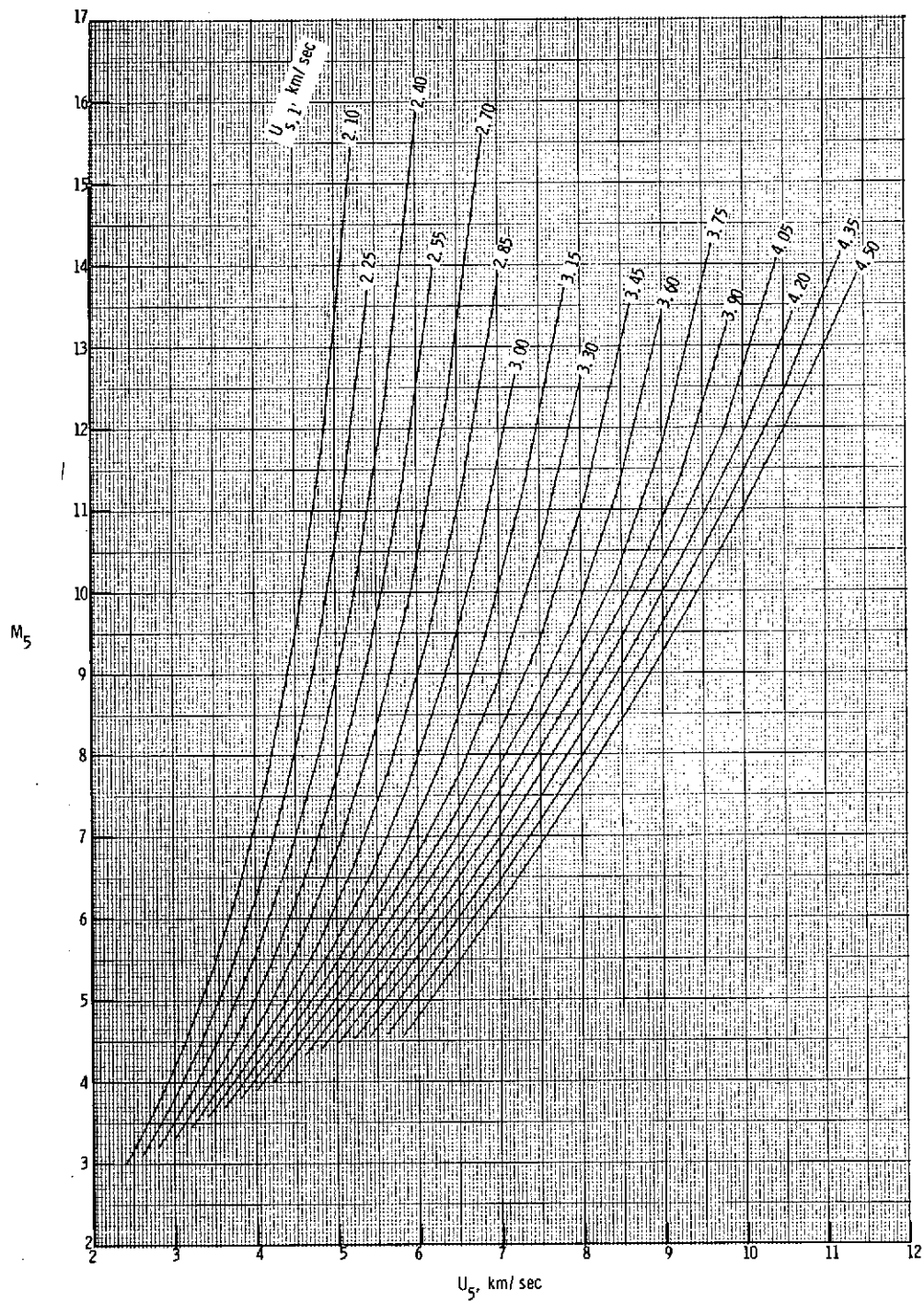
(b) Static density in region (5).

Figure 6.- Continued.



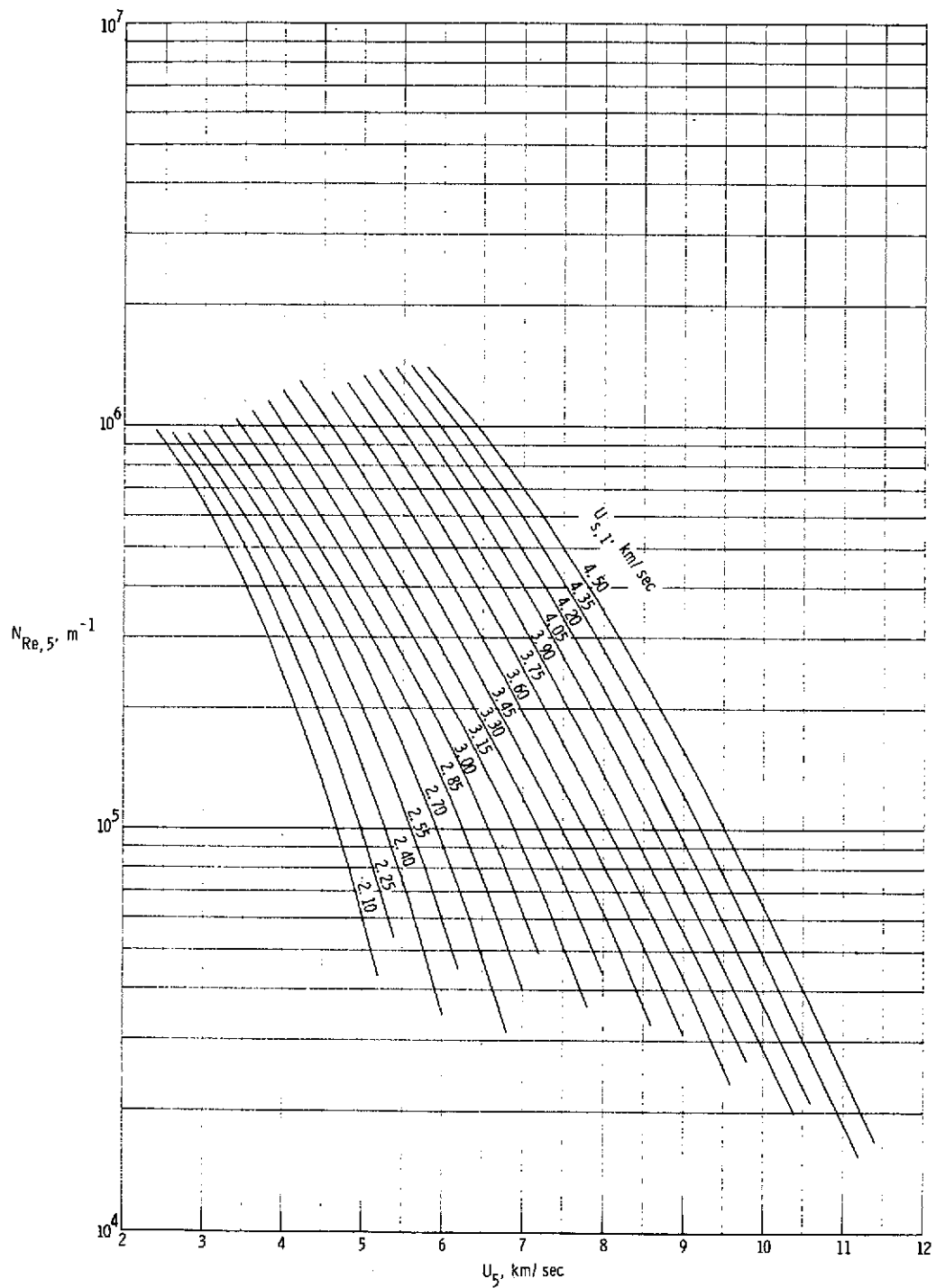
(c) Static temperature in region (5).

Figure 6.- Continued.



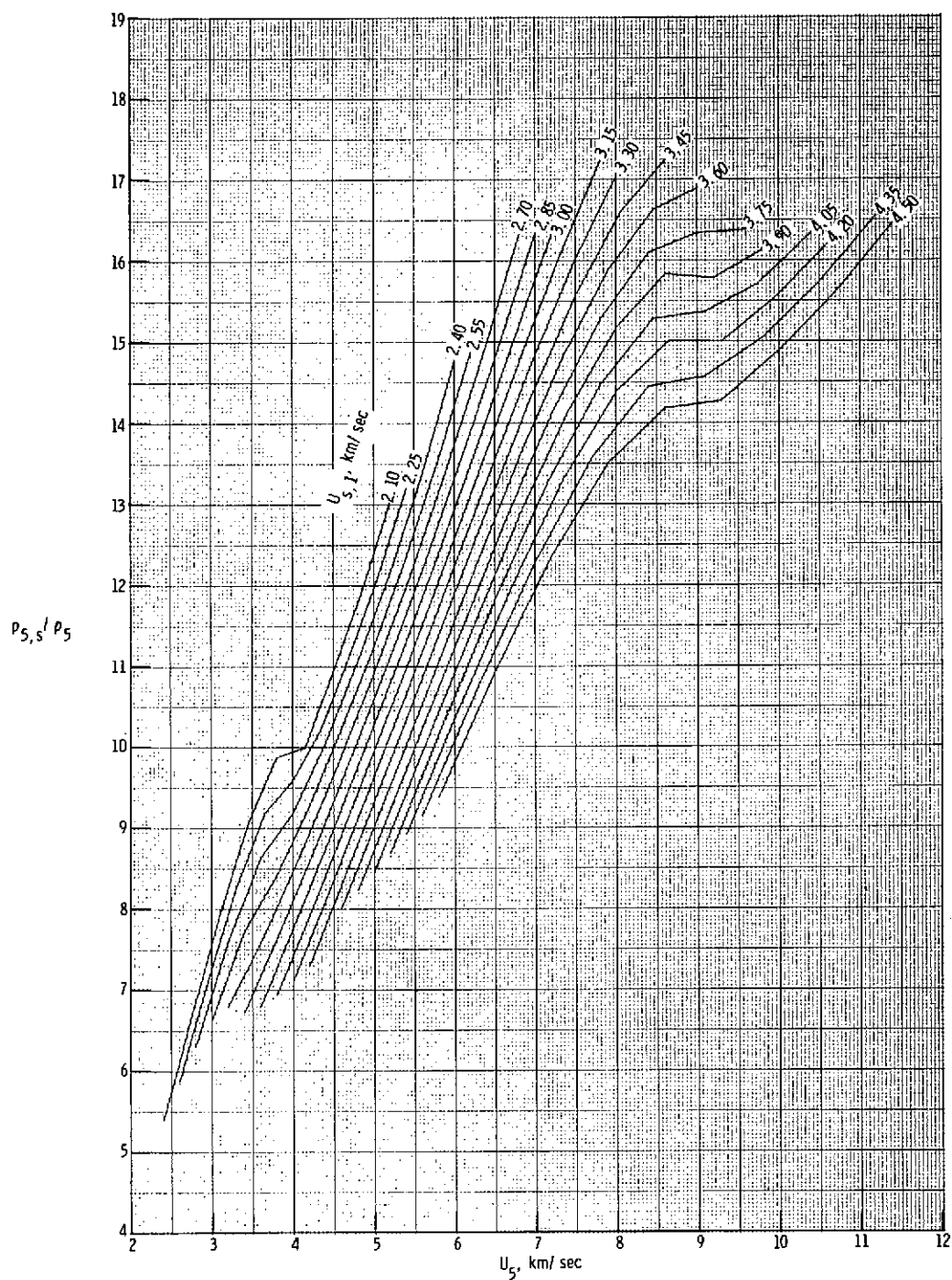
(d) Mach number in region ⑤.

Figure 6.- Continued.



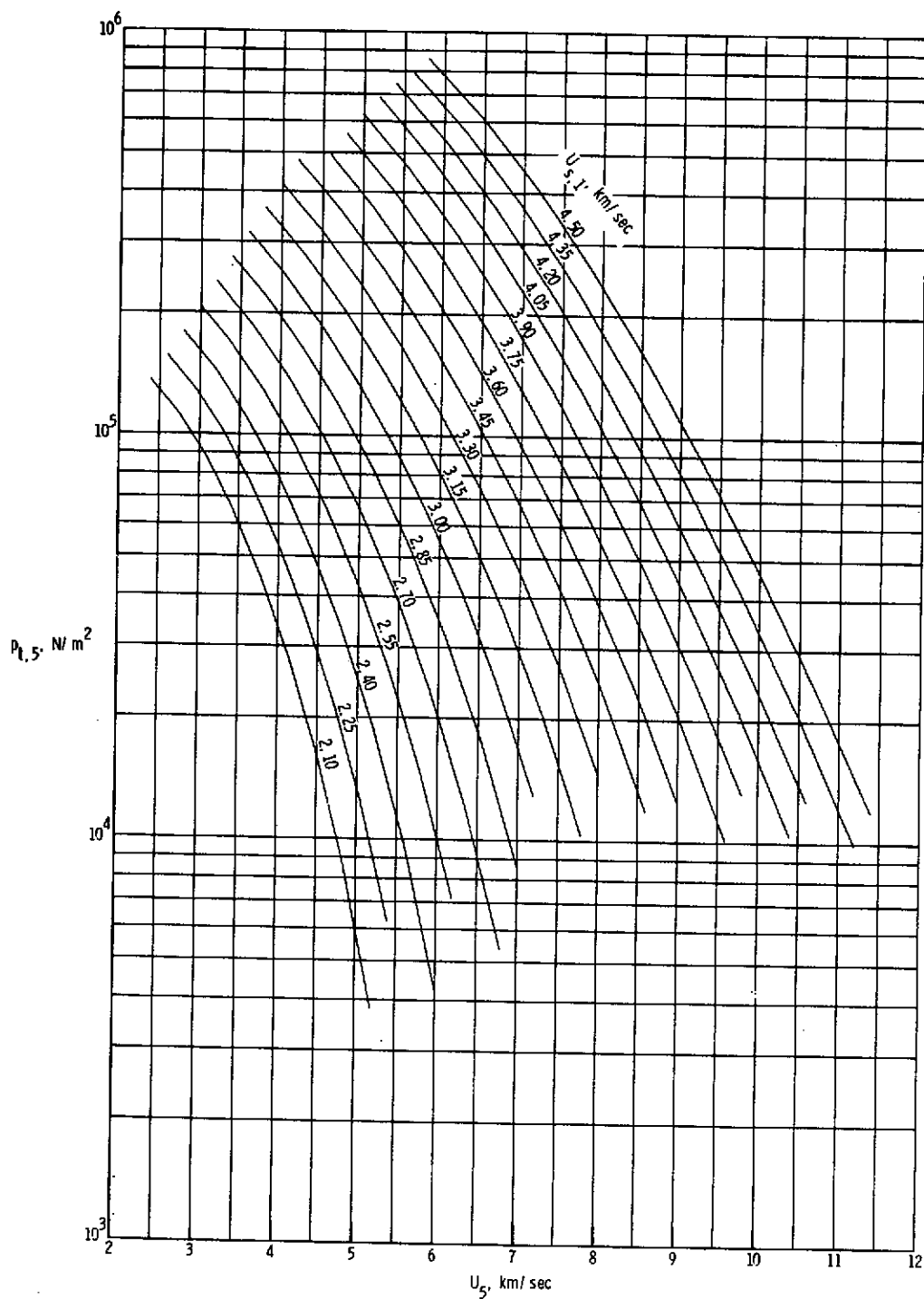
(e) Unit Reynolds number in region (5).

Figure 6.- Continued.



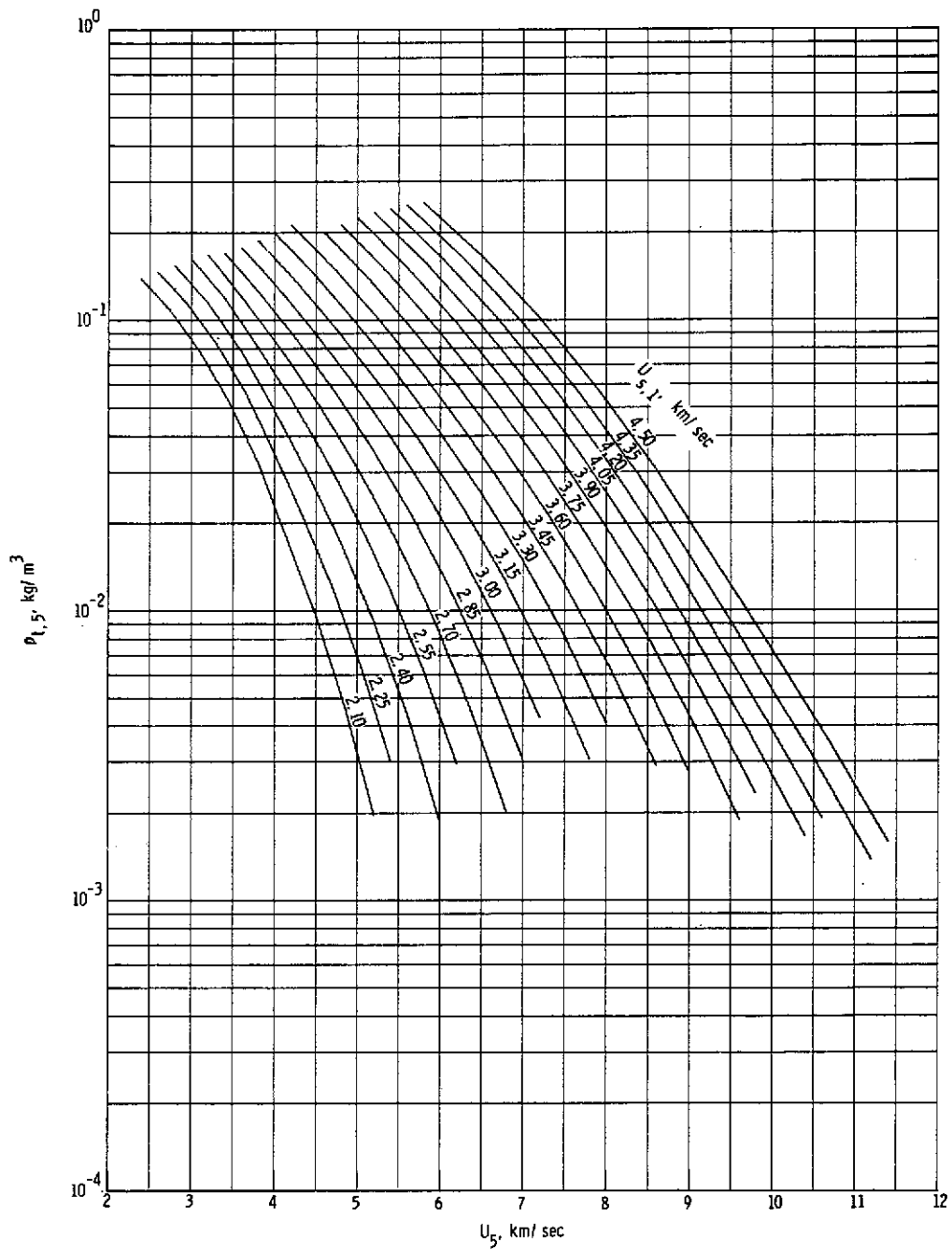
(f) Normal-shock density ratio.

Figure 6.- Continued.



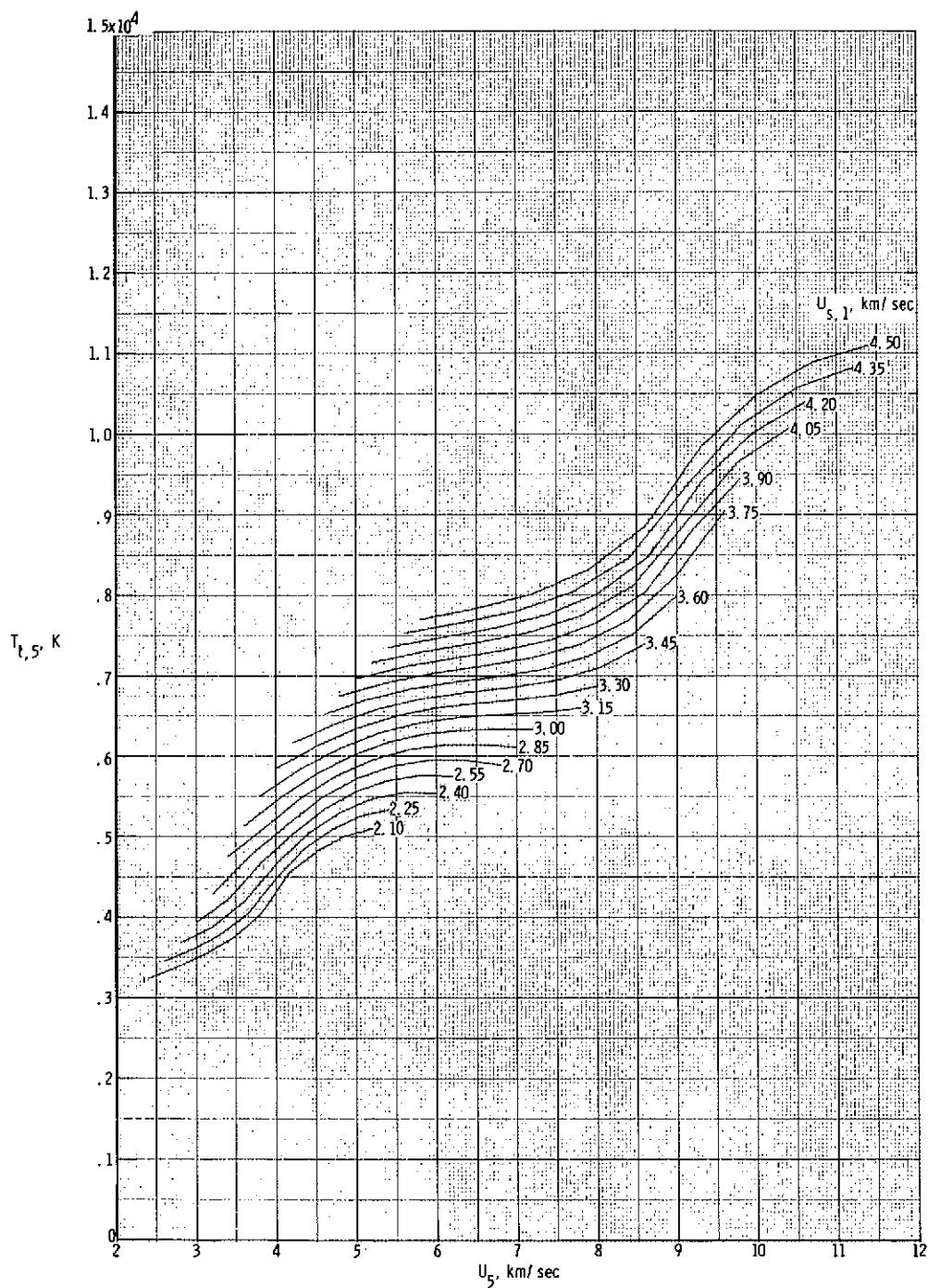
(g) Stagnation pressure behind normal bow shock.

Figure 6.- Continued.



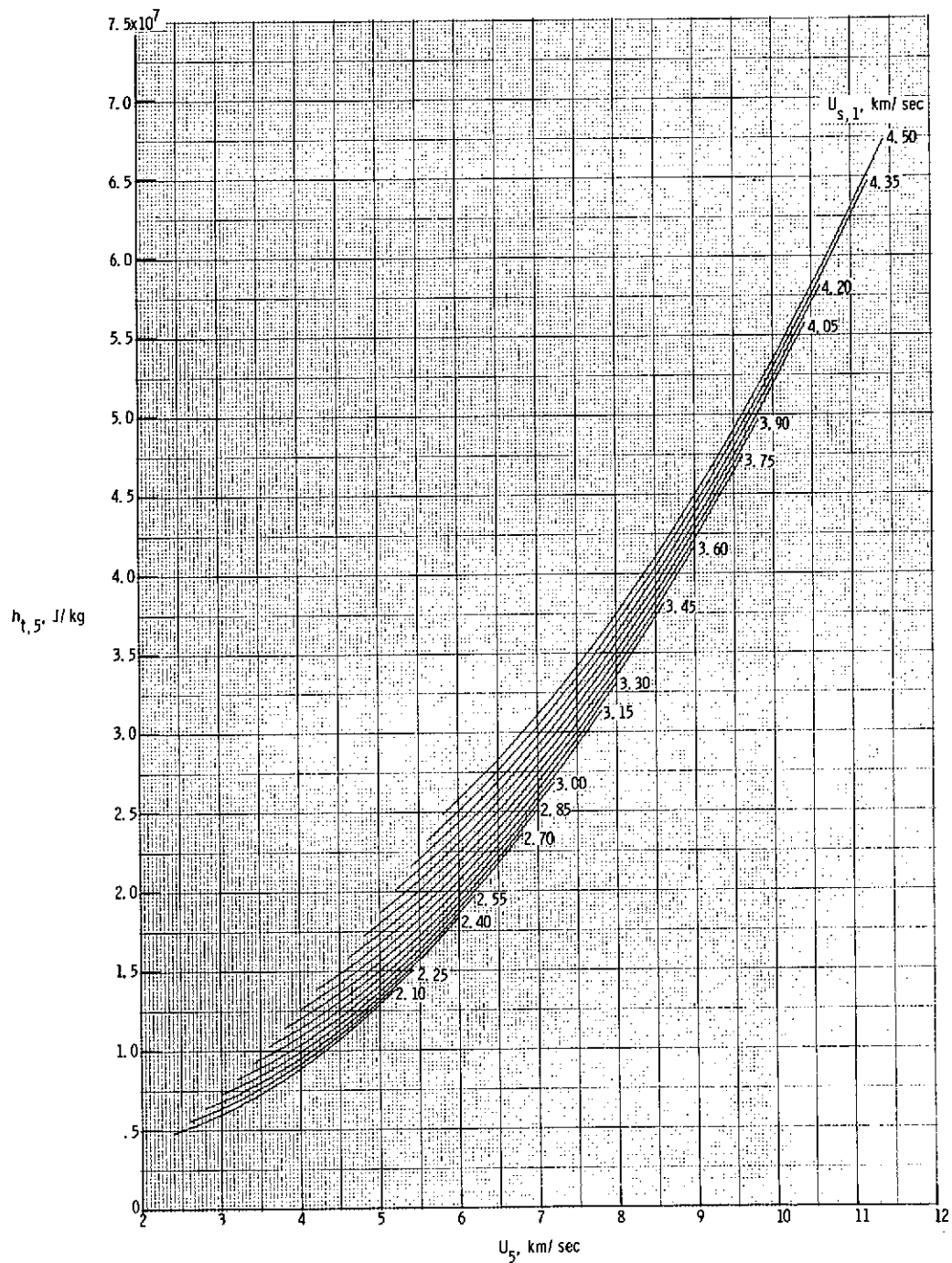
(h) Stagnation density behind normal bow shock.

Figure 6.- Continued.



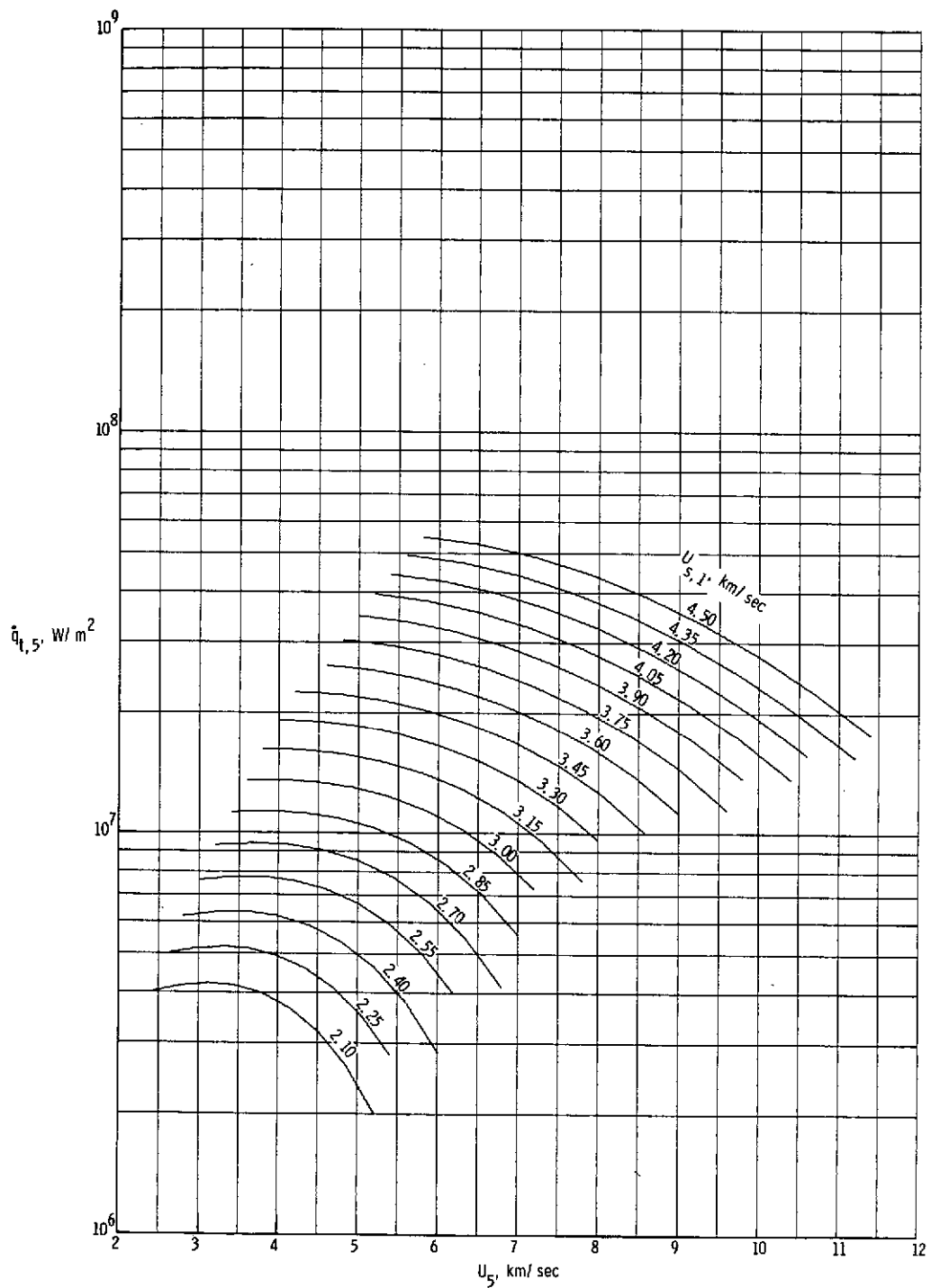
(i) Stagnation temperature behind normal bow shock.

Figure 6.- Continued.



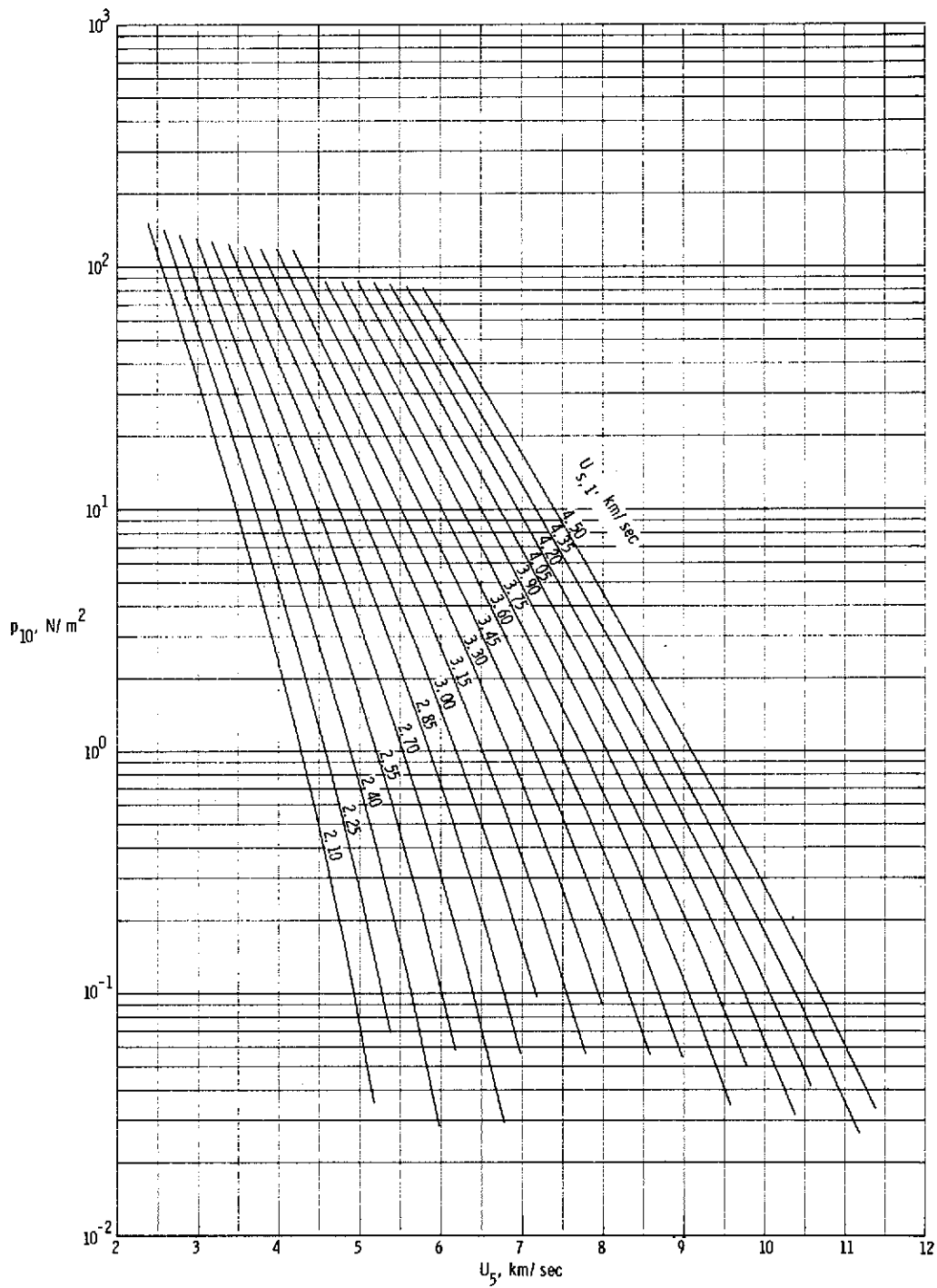
(j) Stagnation enthalpy behind normal bow shock.

Figure 6.- Continued.



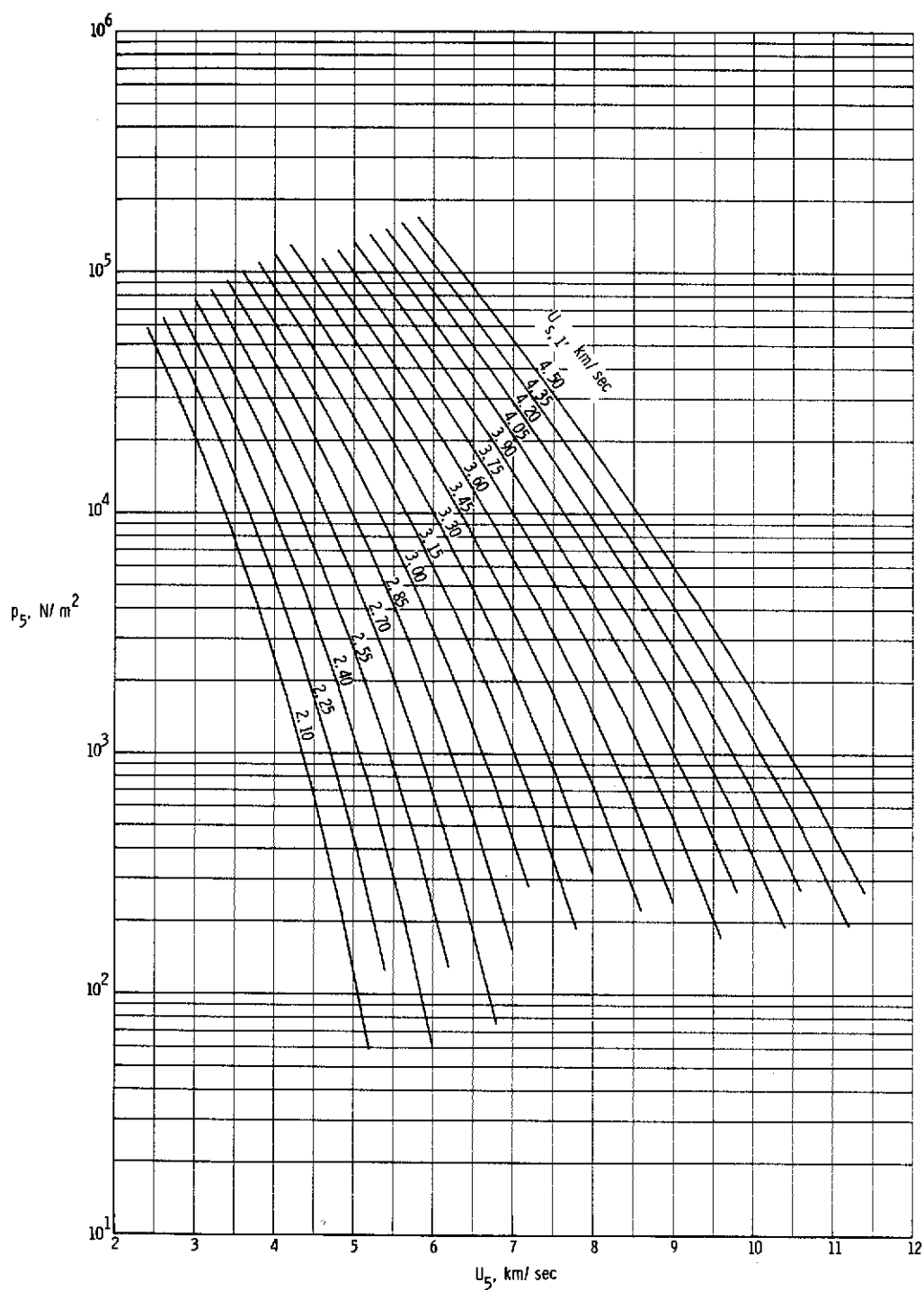
(k) Stagnation-point convective heat-transfer rate to sphere having radius of 2.54 cm.

Figure 6.- Continued.



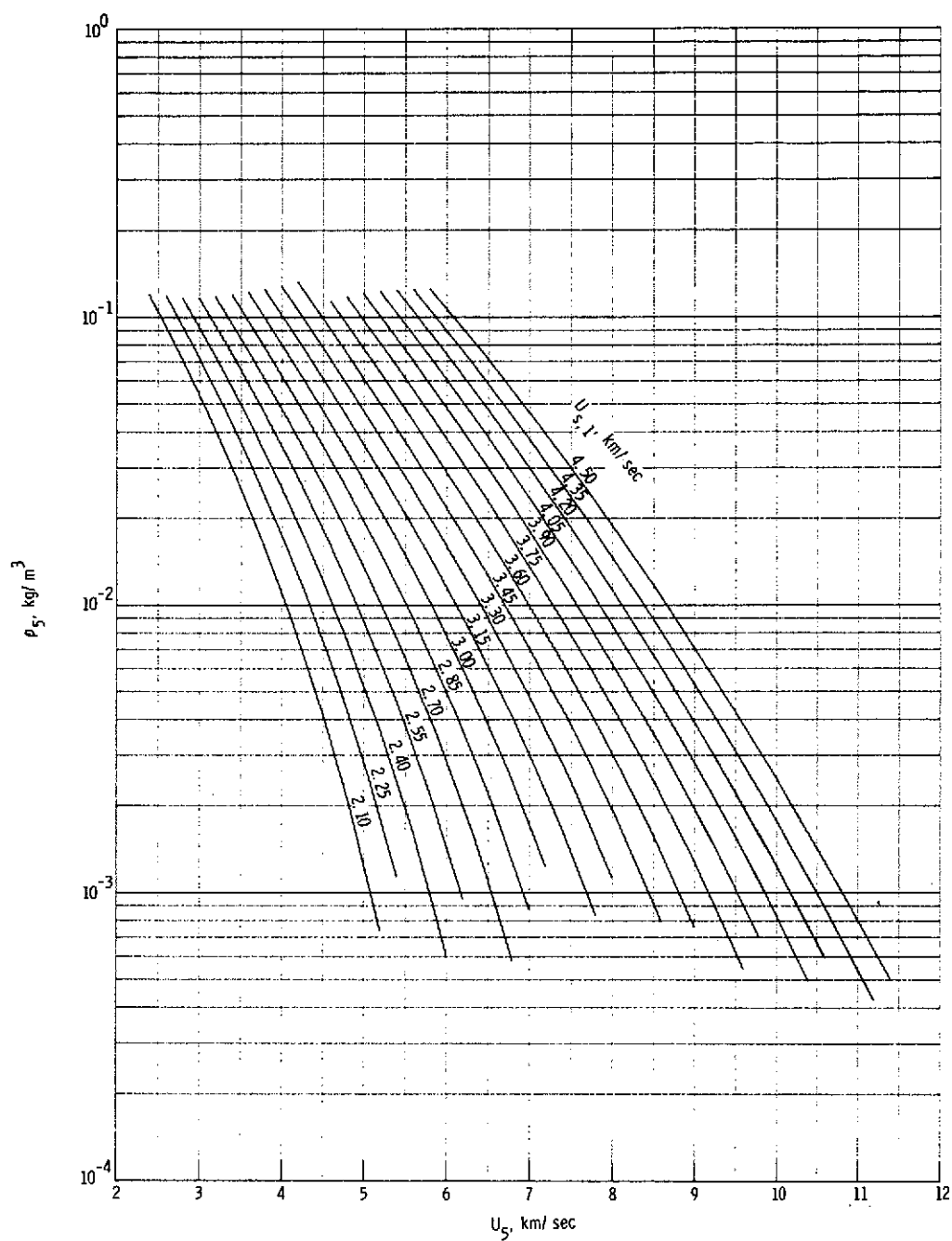
(1) Quiescent acceleration air pressure in region (10).

Figure 6.- Concluded.



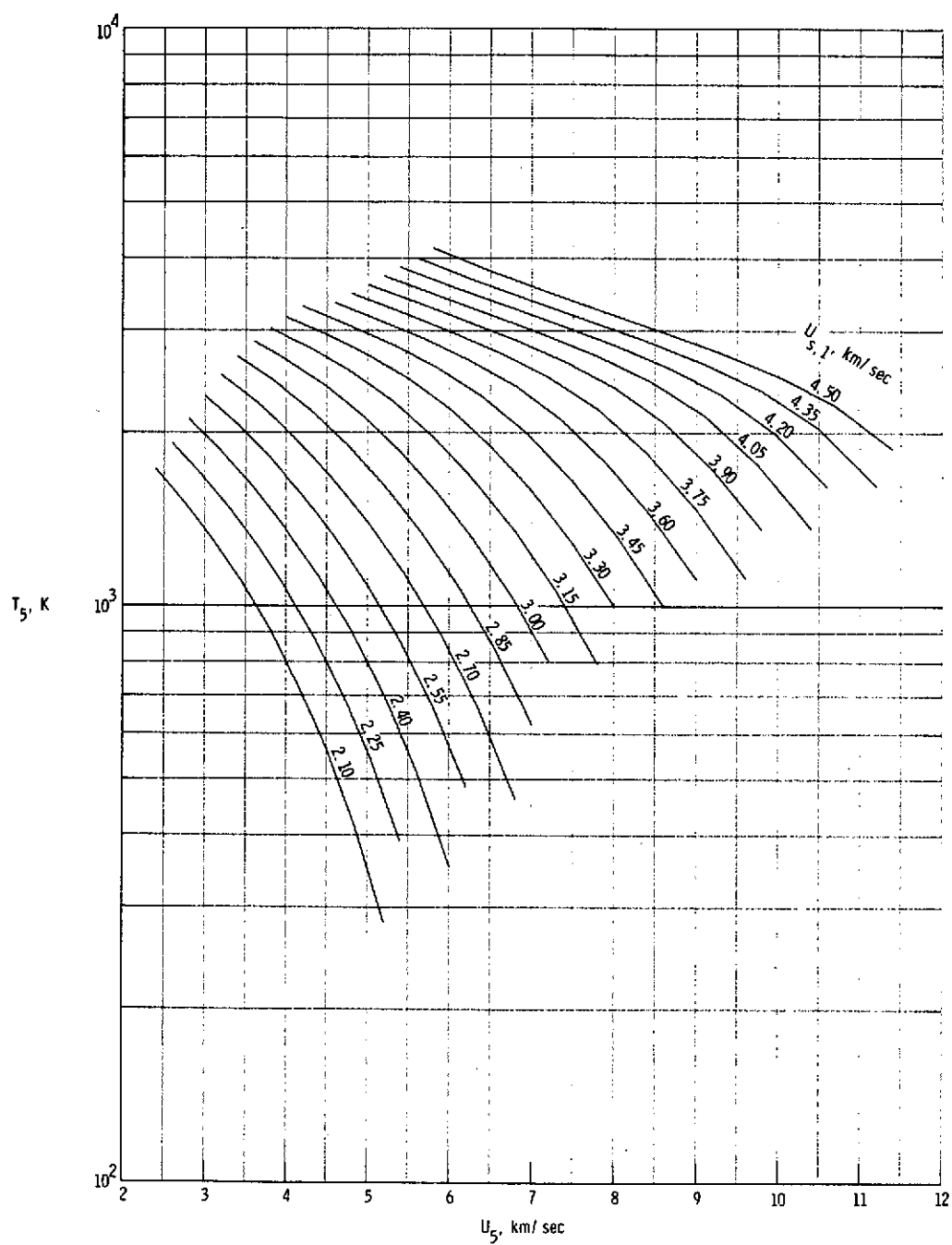
(a) Static pressure in region (5).

Figure 7.- Various expansion tube flow parameters for real air in thermochemical equilibrium as a function of flow velocity and assuming no shock reflection at secondary diaphragm. $p_1 = 3.45 \text{ kN/m}^2$.



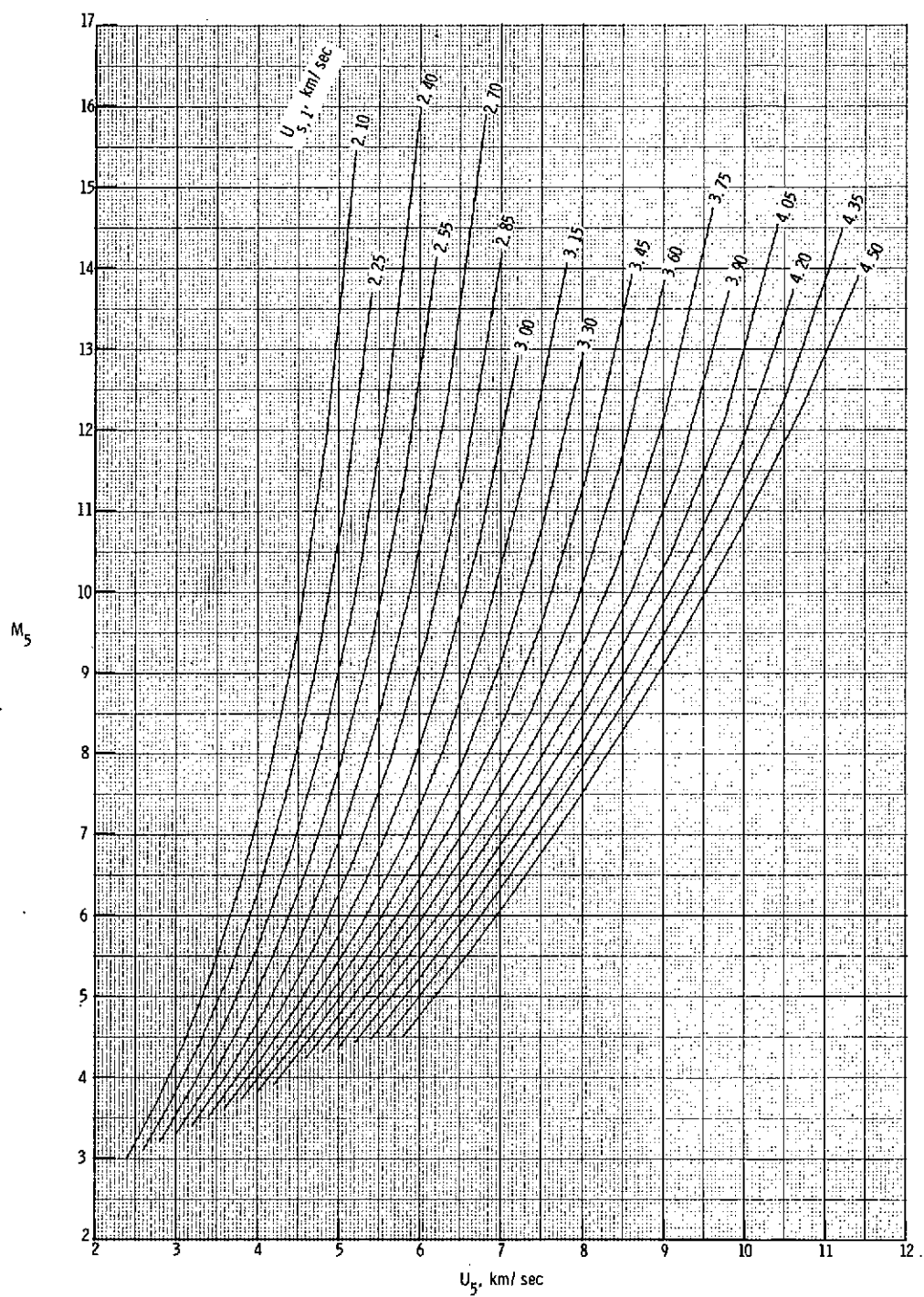
(b) Static density in region (5).

Figure 7.- Continued.



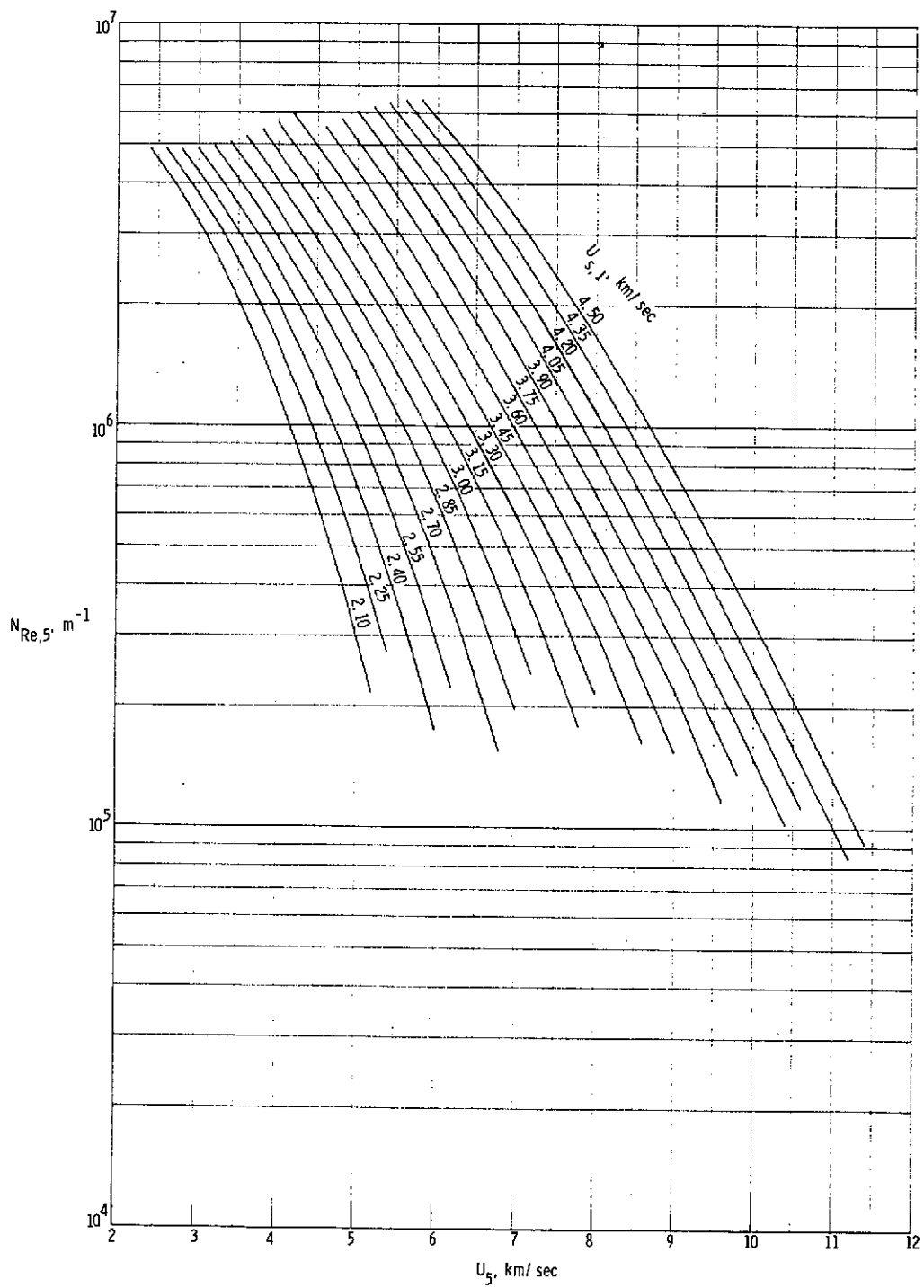
(c) Static temperature in region (5).

Figure 7.- Continued.



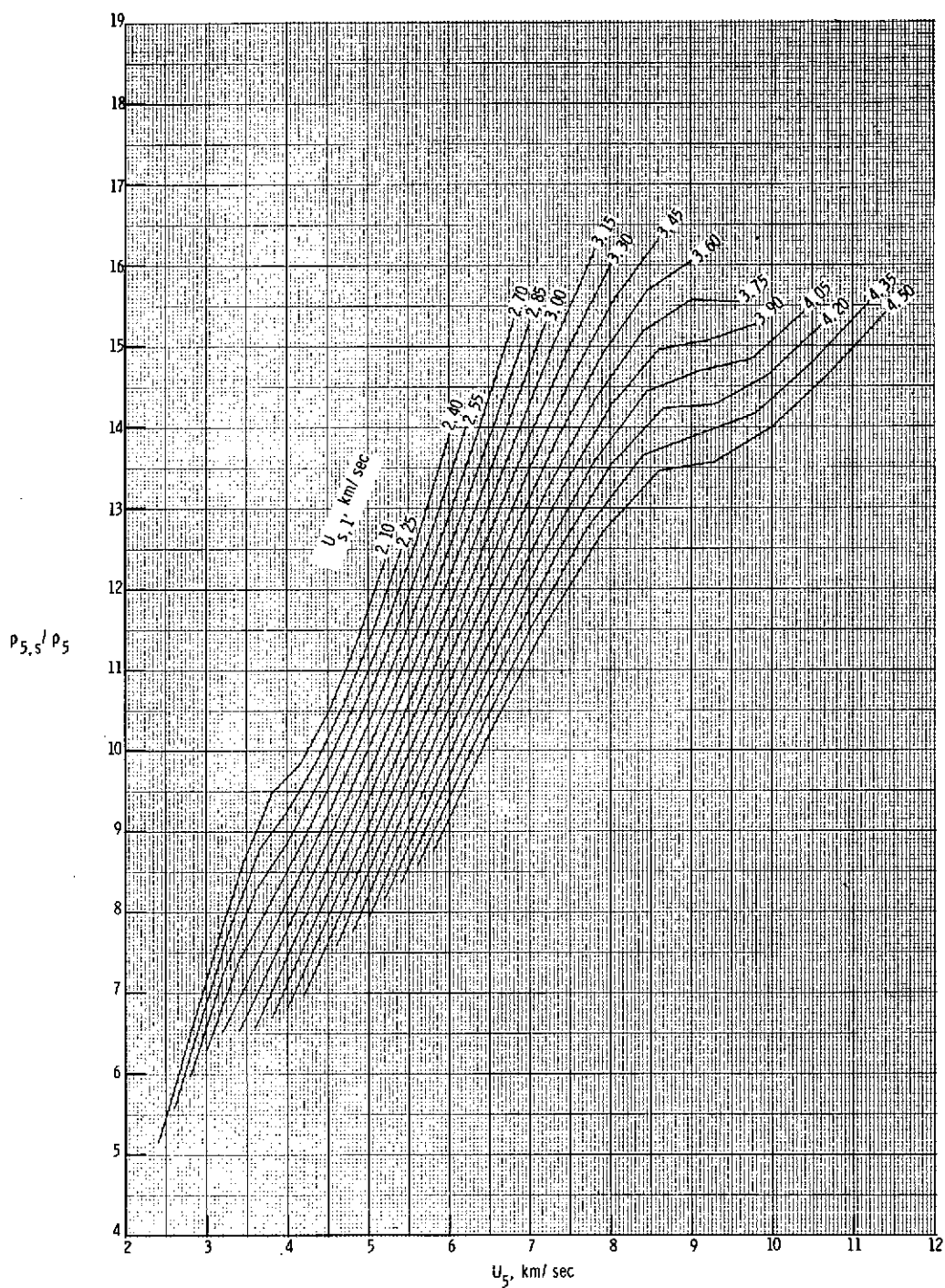
(d) Mach number in region (5).

Figure 7.- Continued.



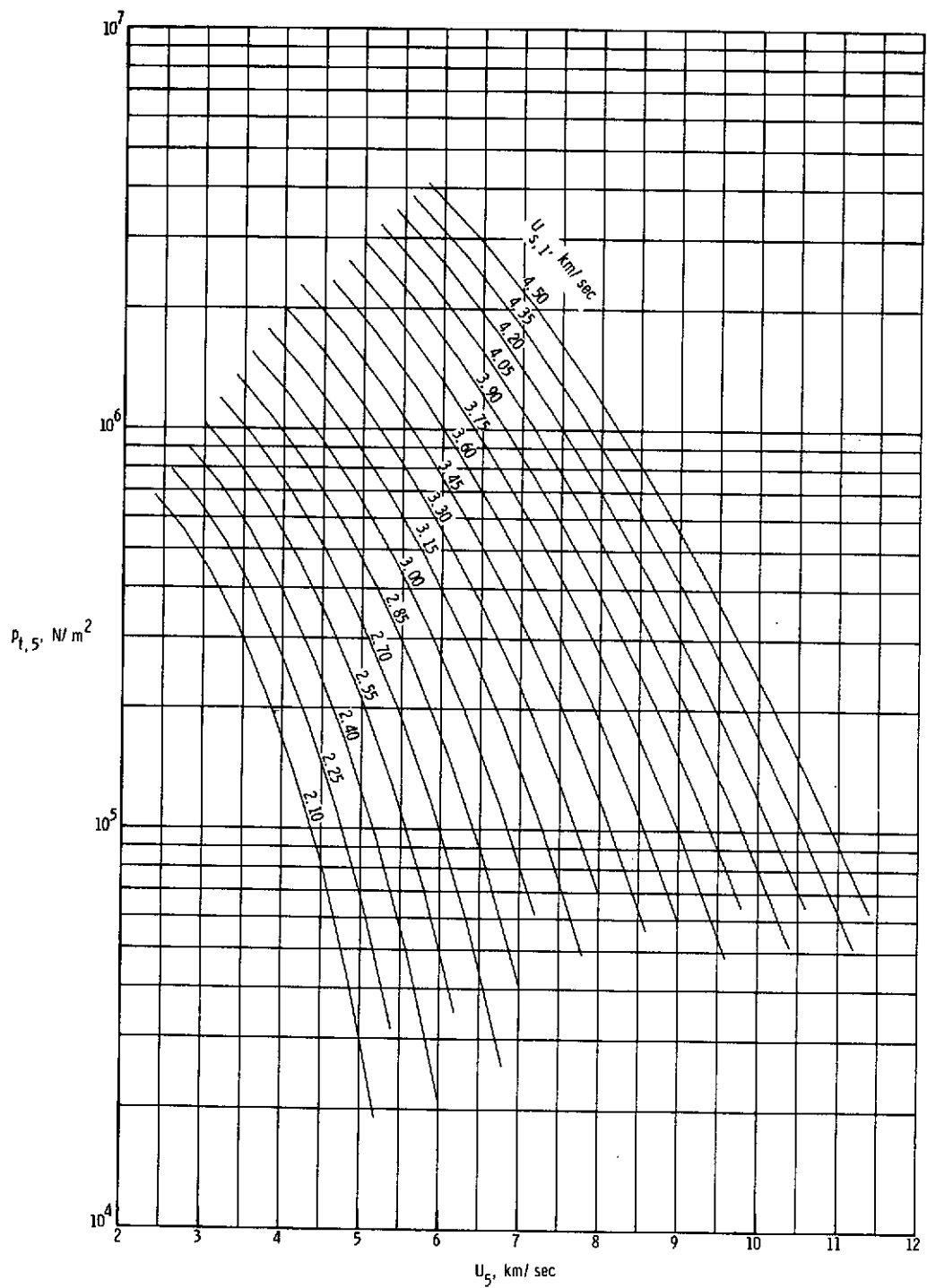
(e) Unit Reynolds number in region (5).

Figure 7.- Continued.



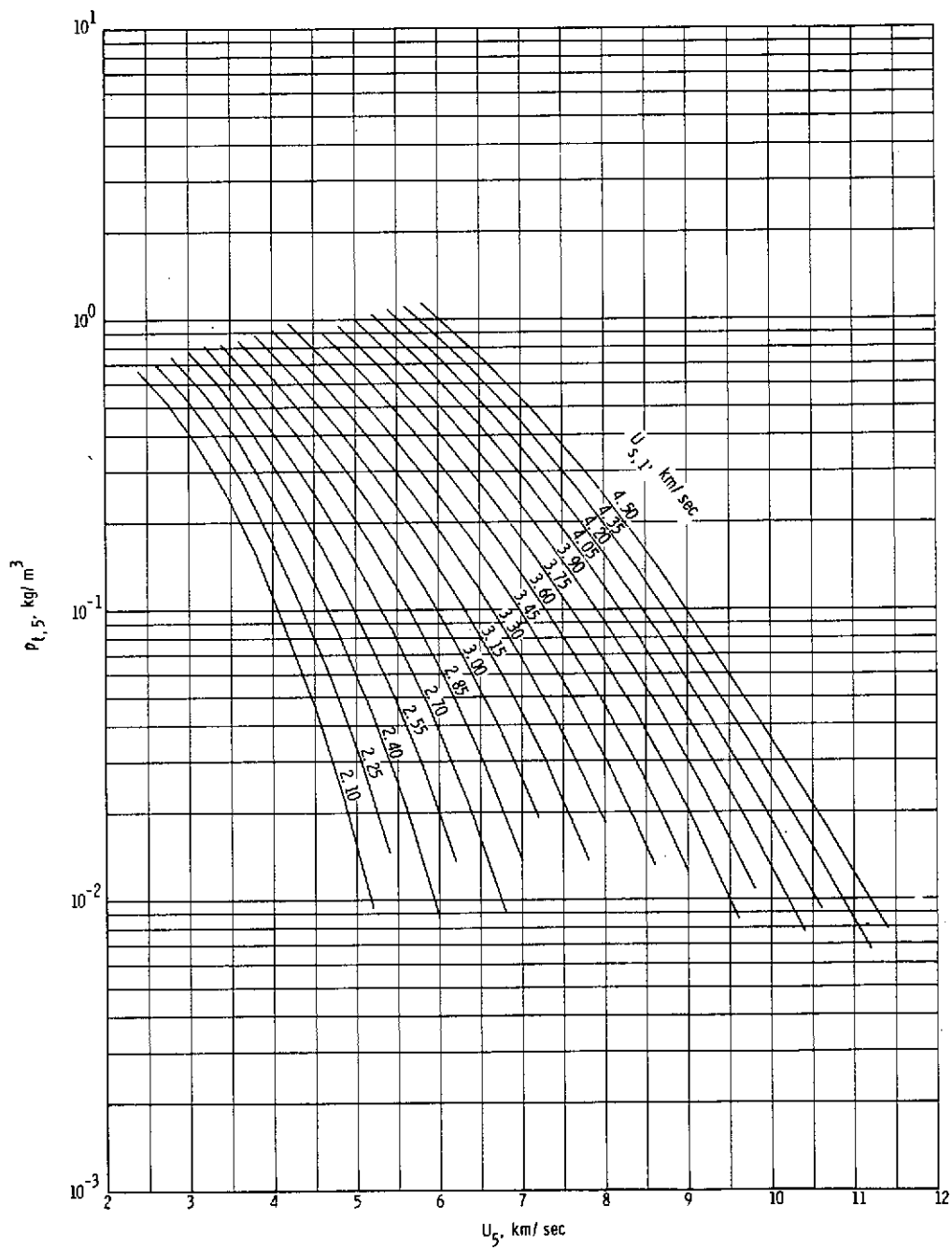
(f) Normal shock density ratio.

Figure 7.- Continued.



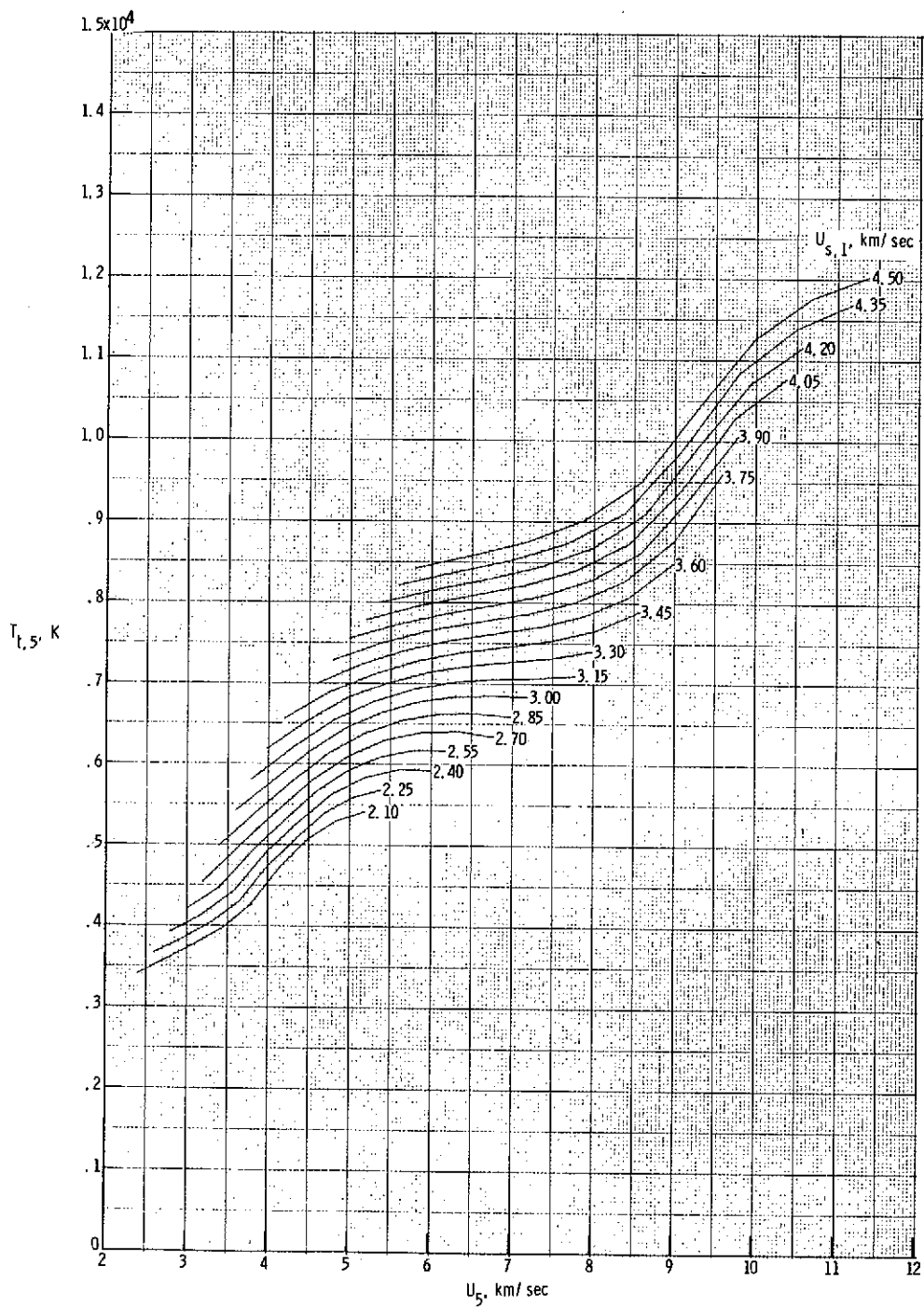
(g) Stagnation pressure behind normal bow shock.

Figure 7.- Continued.



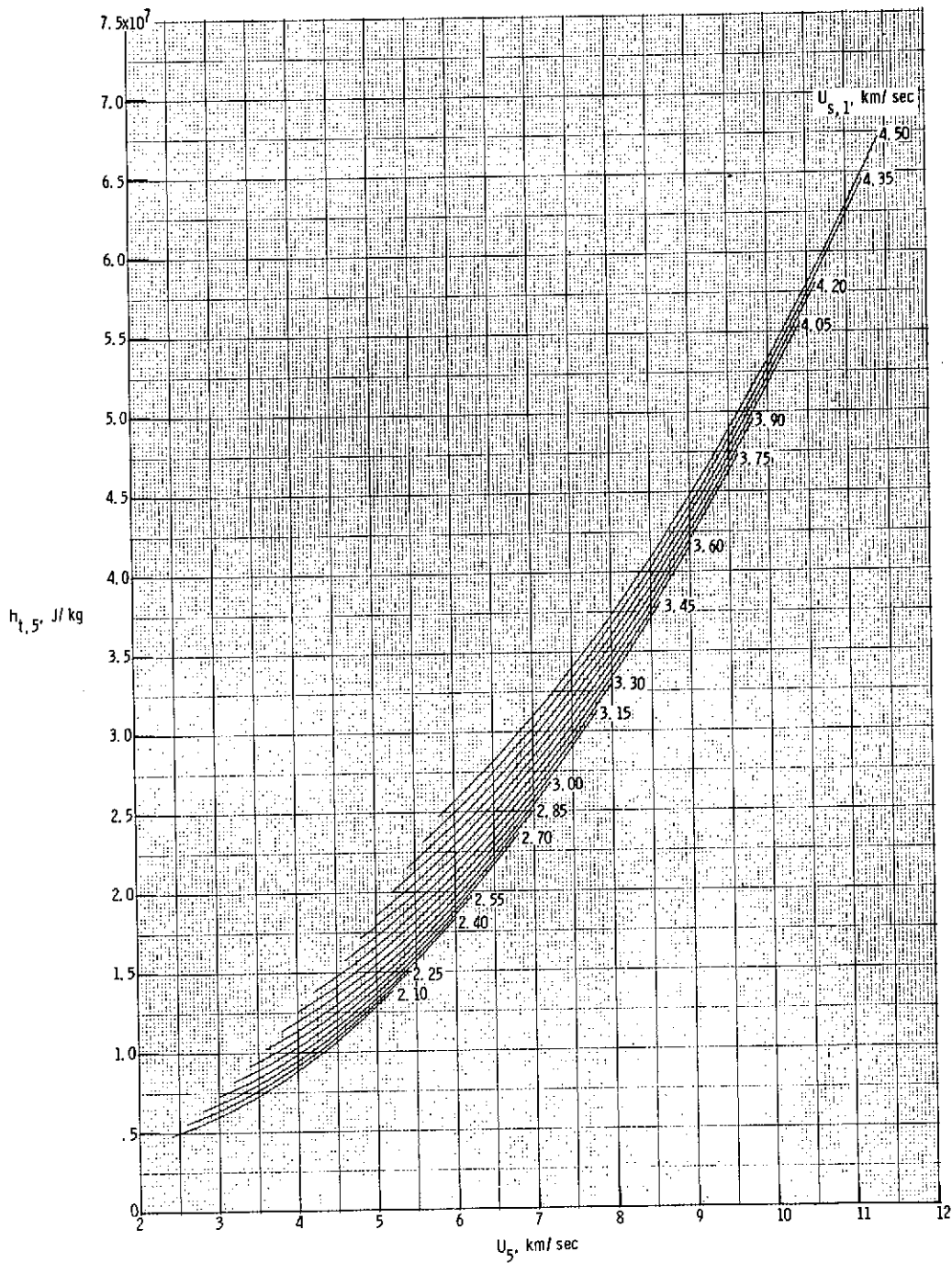
(h) Stagnation density behind normal bow shock.

Figure 7.- Continued.



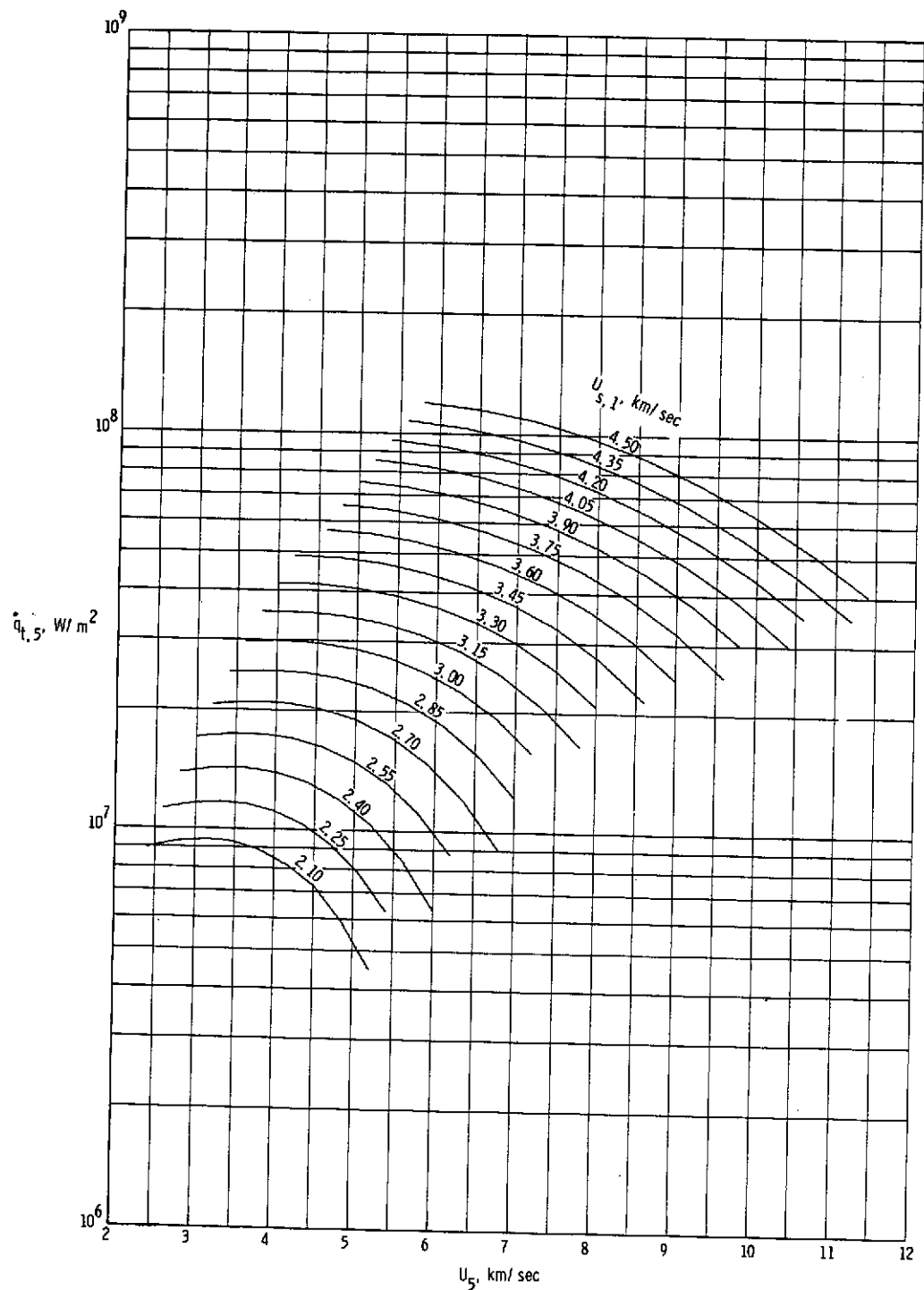
(i) Stagnation temperature behind normal bow shock.

Figure 7.- Continued.



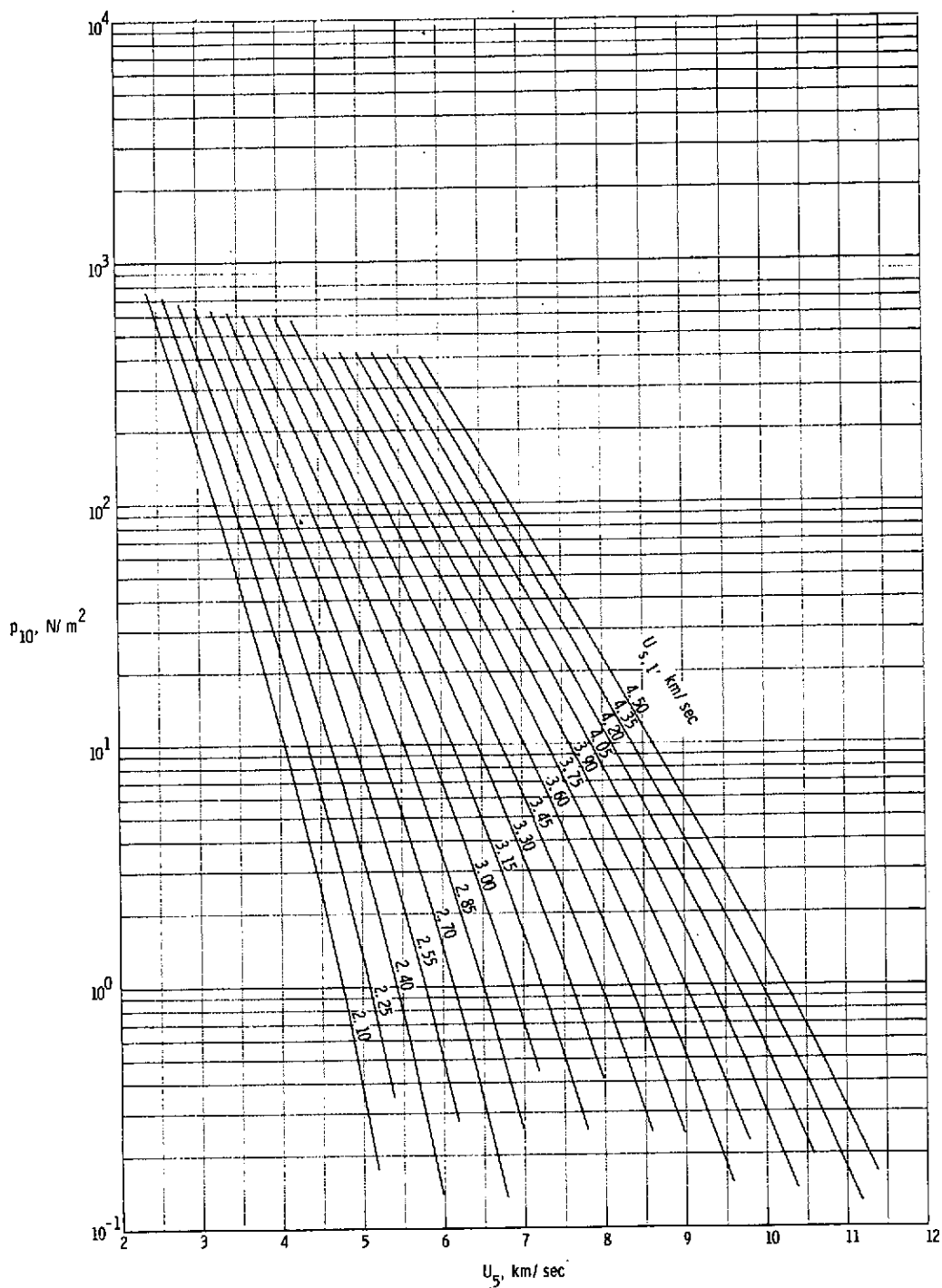
(j) Stagnation enthalpy behind normal bow shock.

Figure 7.- Continued.



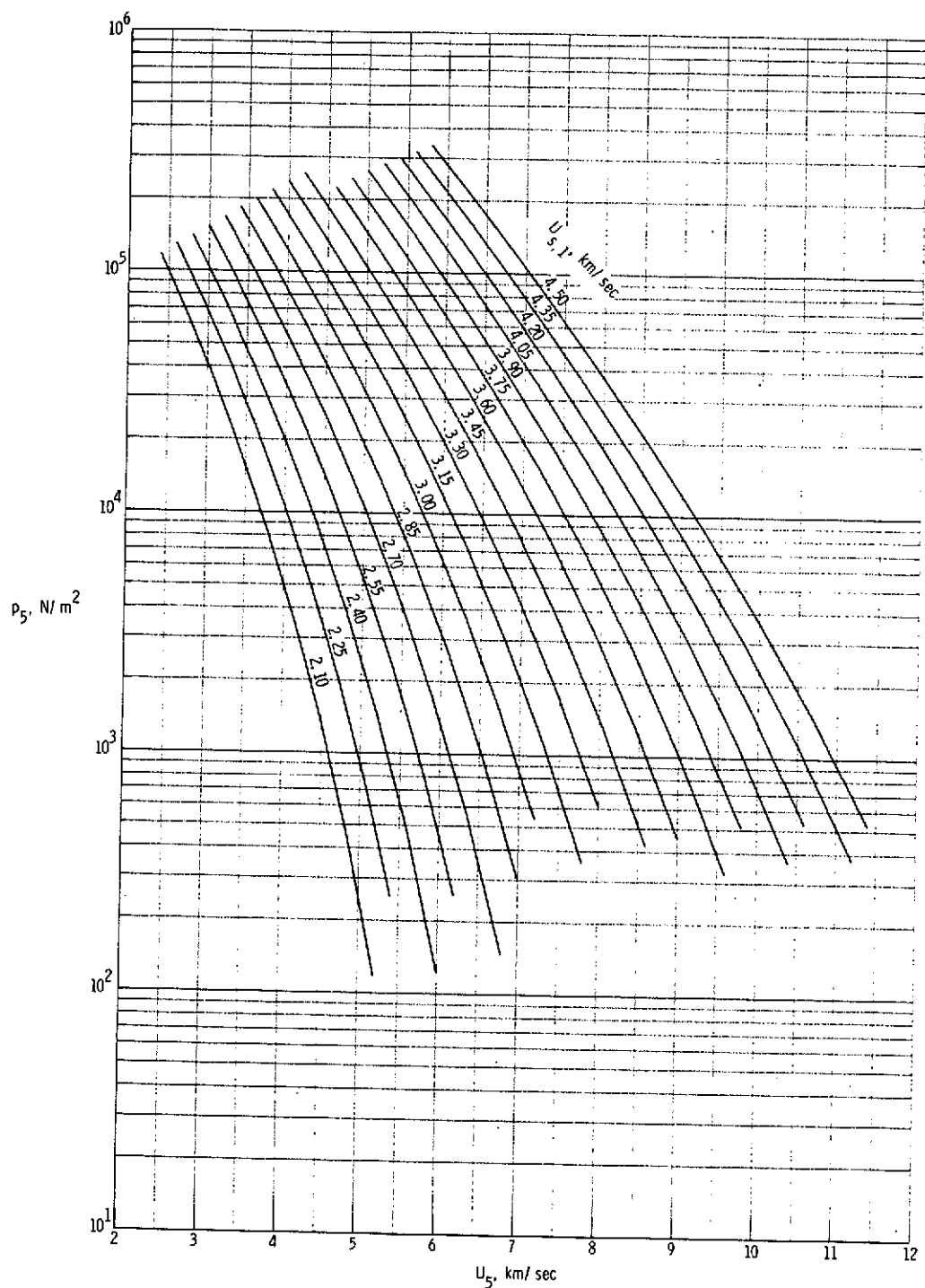
(k) Stagnation-point convective heat-transfer rate to sphere having radius of 2.54 cm.

Figure 7.- Continued.



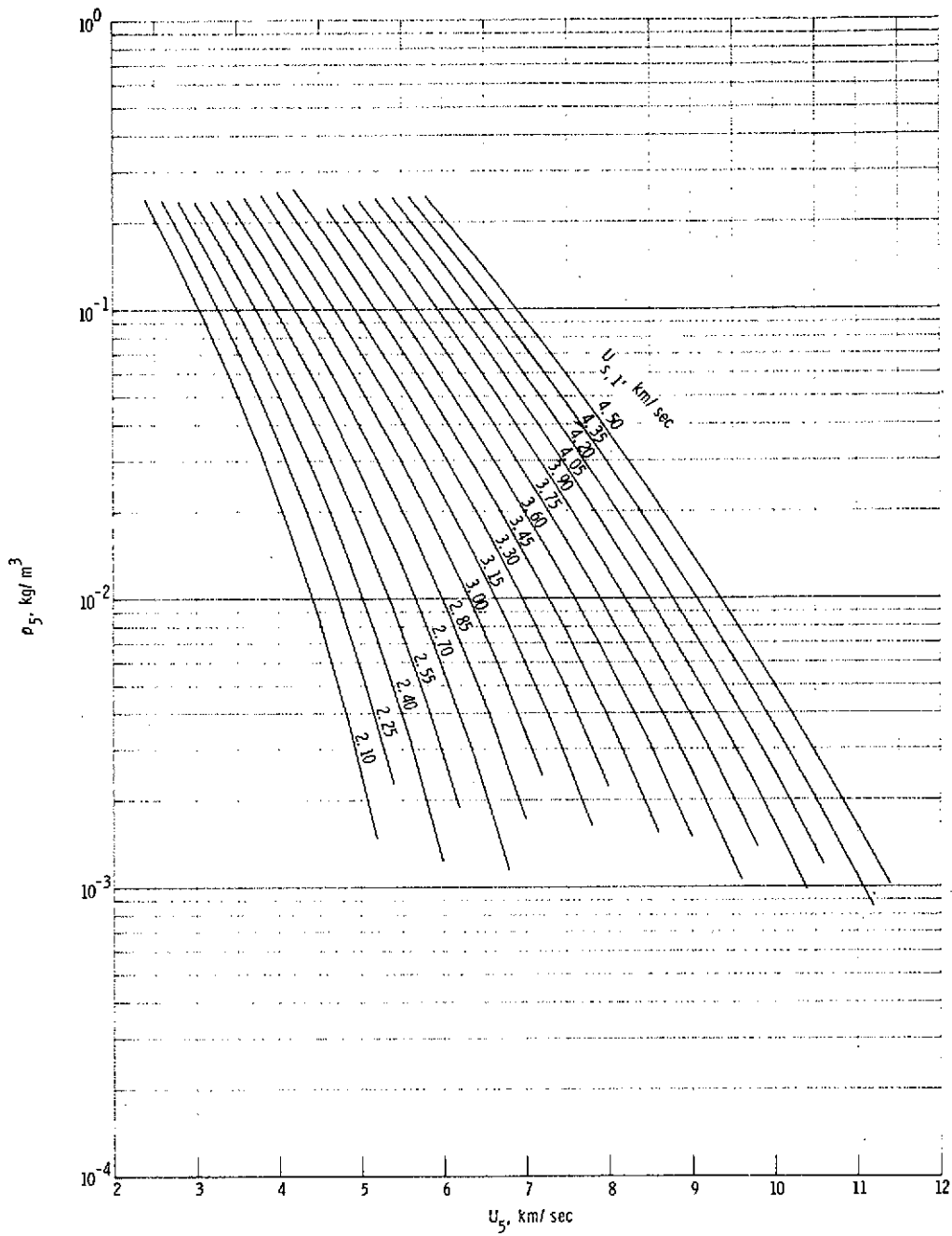
(1) Quiescent acceleration air pressure in region (10).

Figure 7.- Concluded.



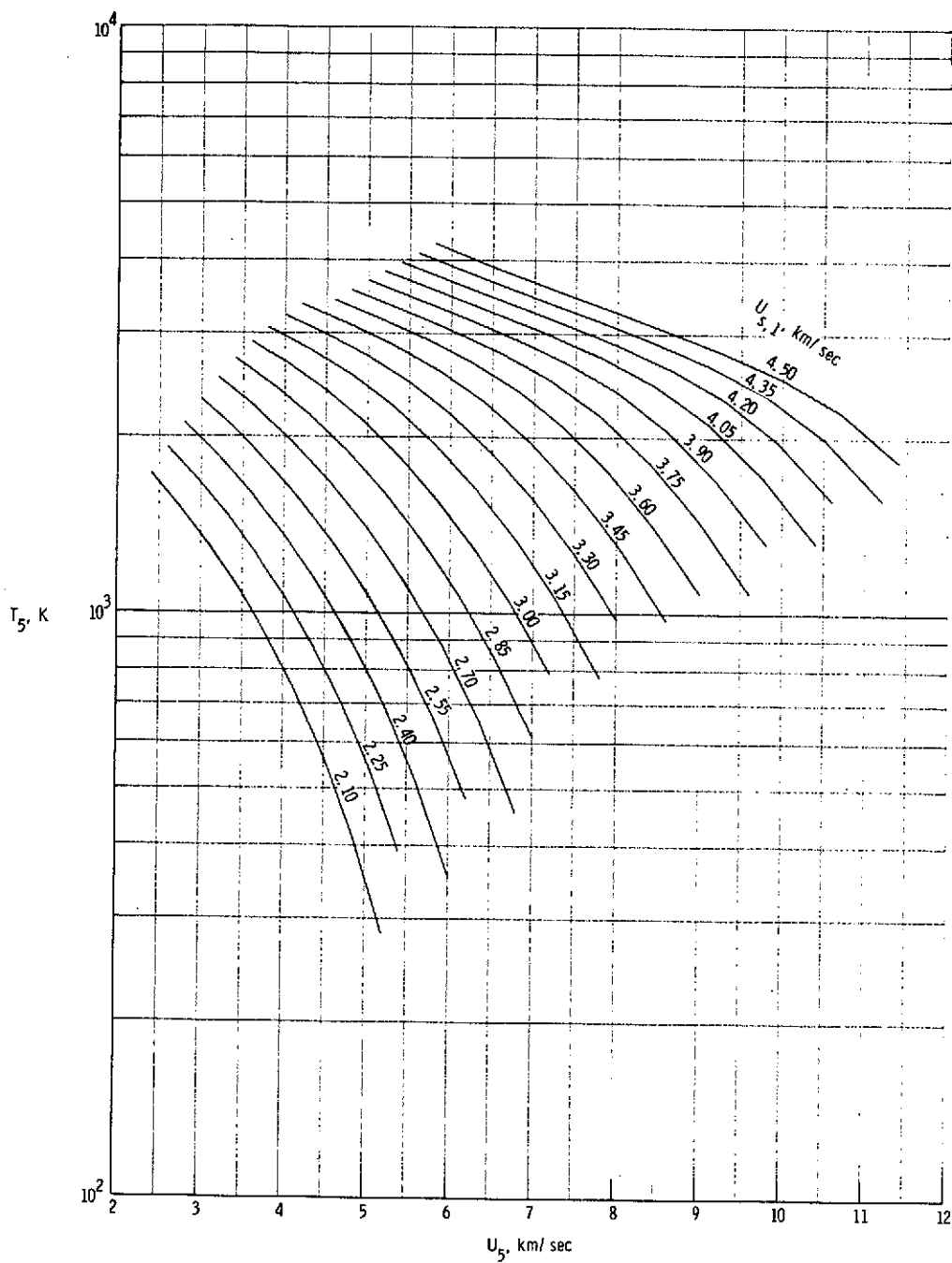
(a) Static pressure in region (5).

Figure 8.- Various expansion tube flow parameters for real air in thermochemical equilibrium as a function of flow velocity and assuming no shock reflection at secondary diaphragm. $p_1 = 6.90 \text{ kN/m}^2$.



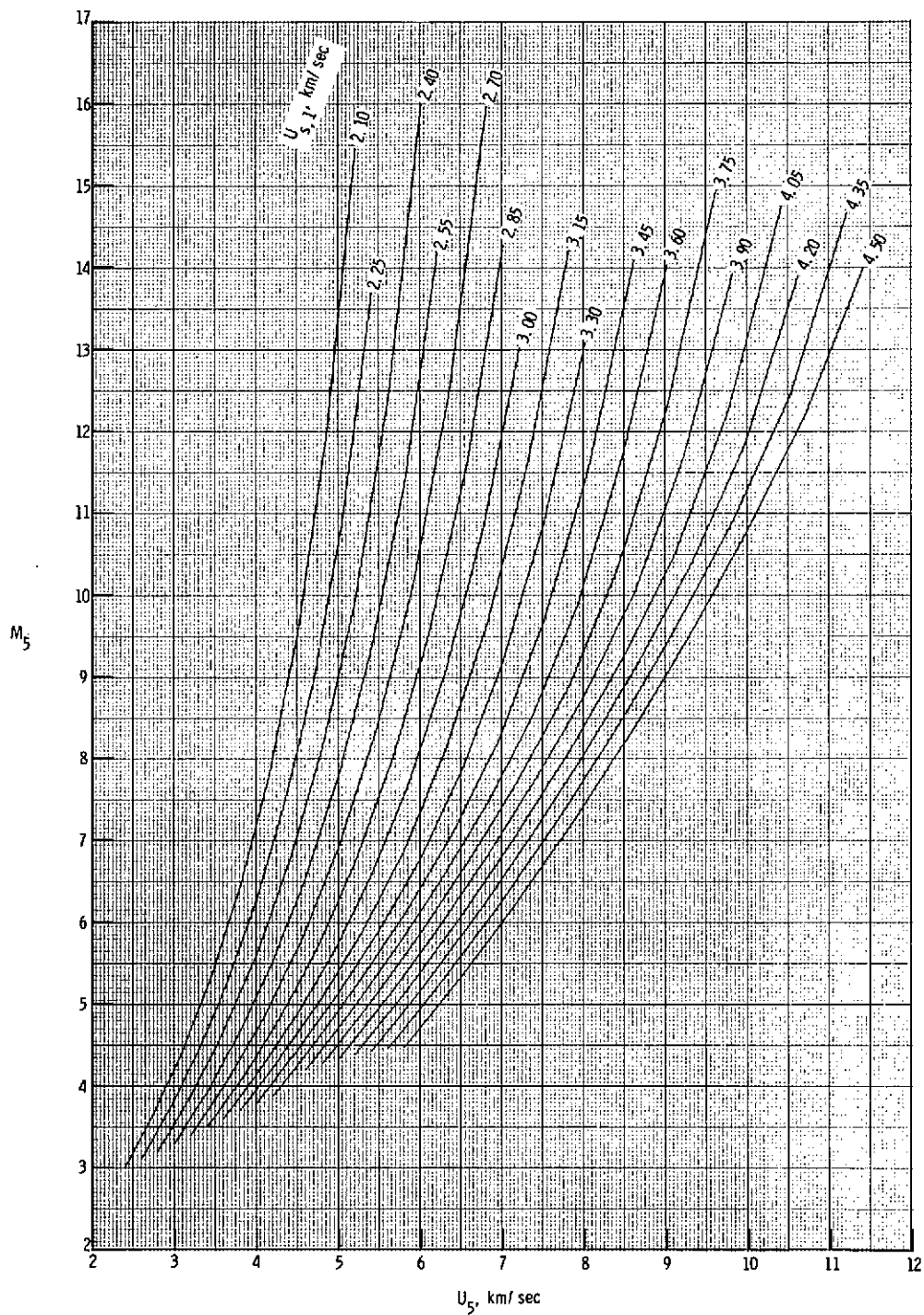
(b) Static density in region (5).

Figure 8.- Continued.



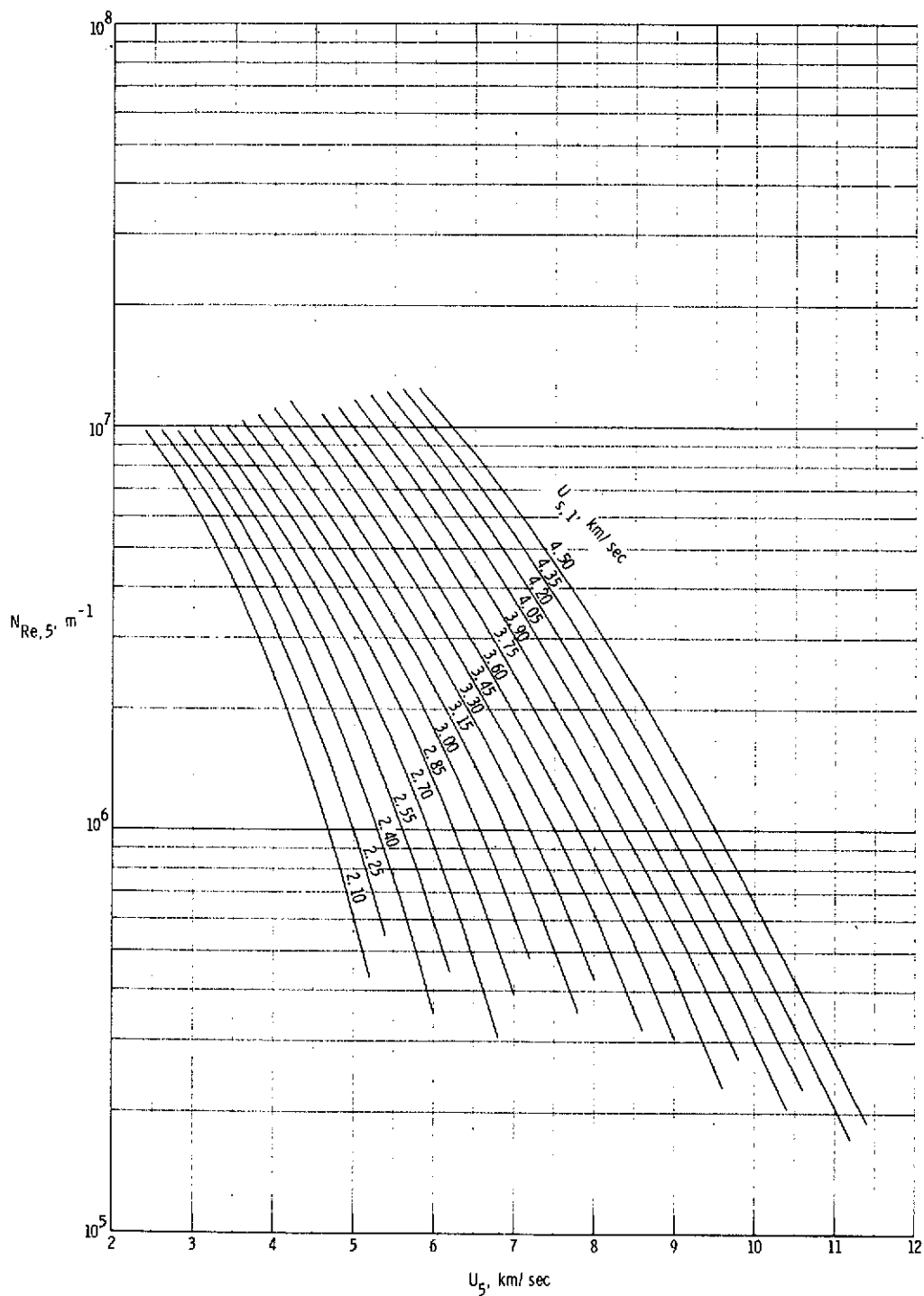
(c) Static temperature in region (5).

Figure 8.- Continued.



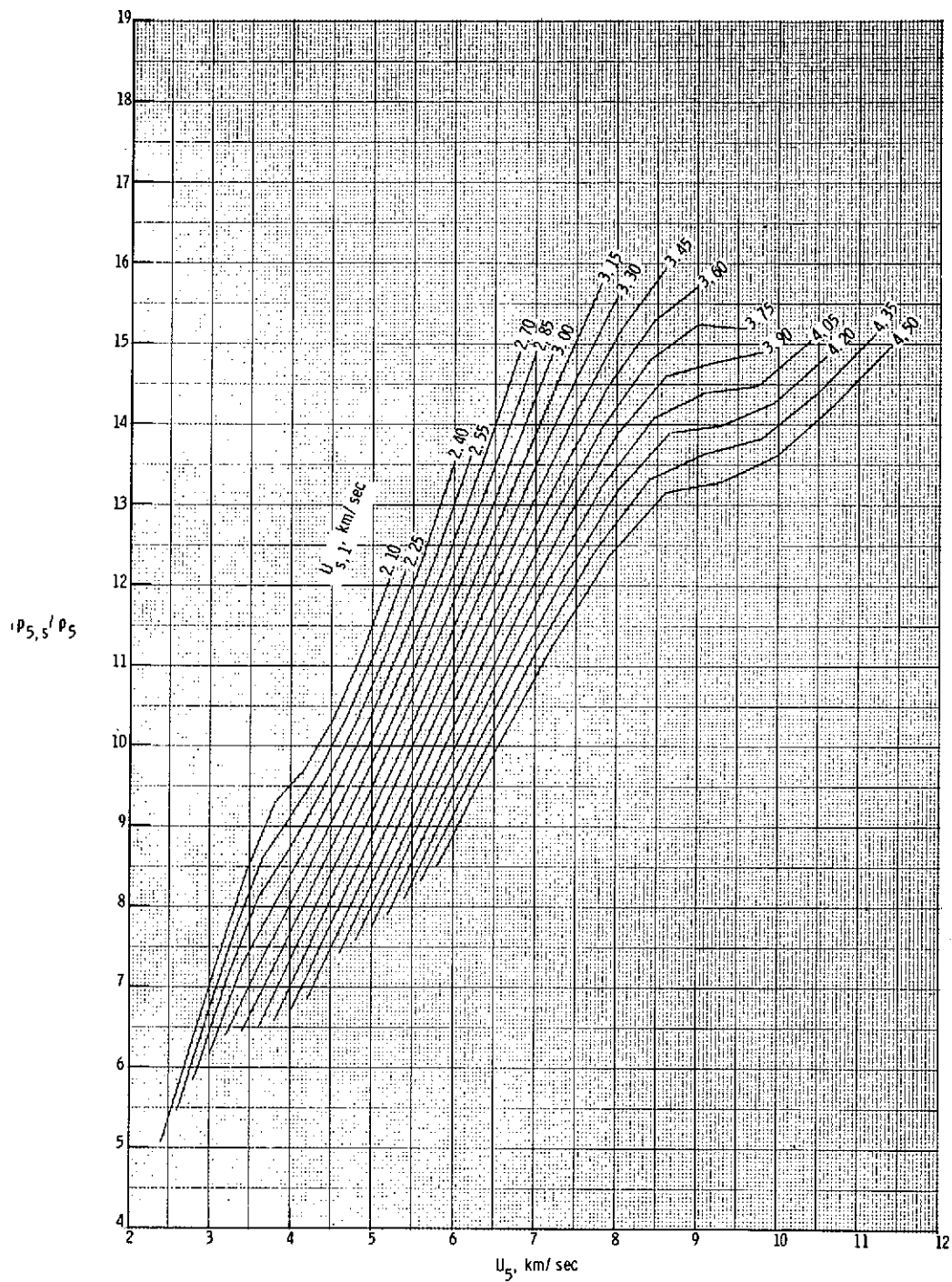
(d) Mach number in region (5).

Figure 8.- Continued.



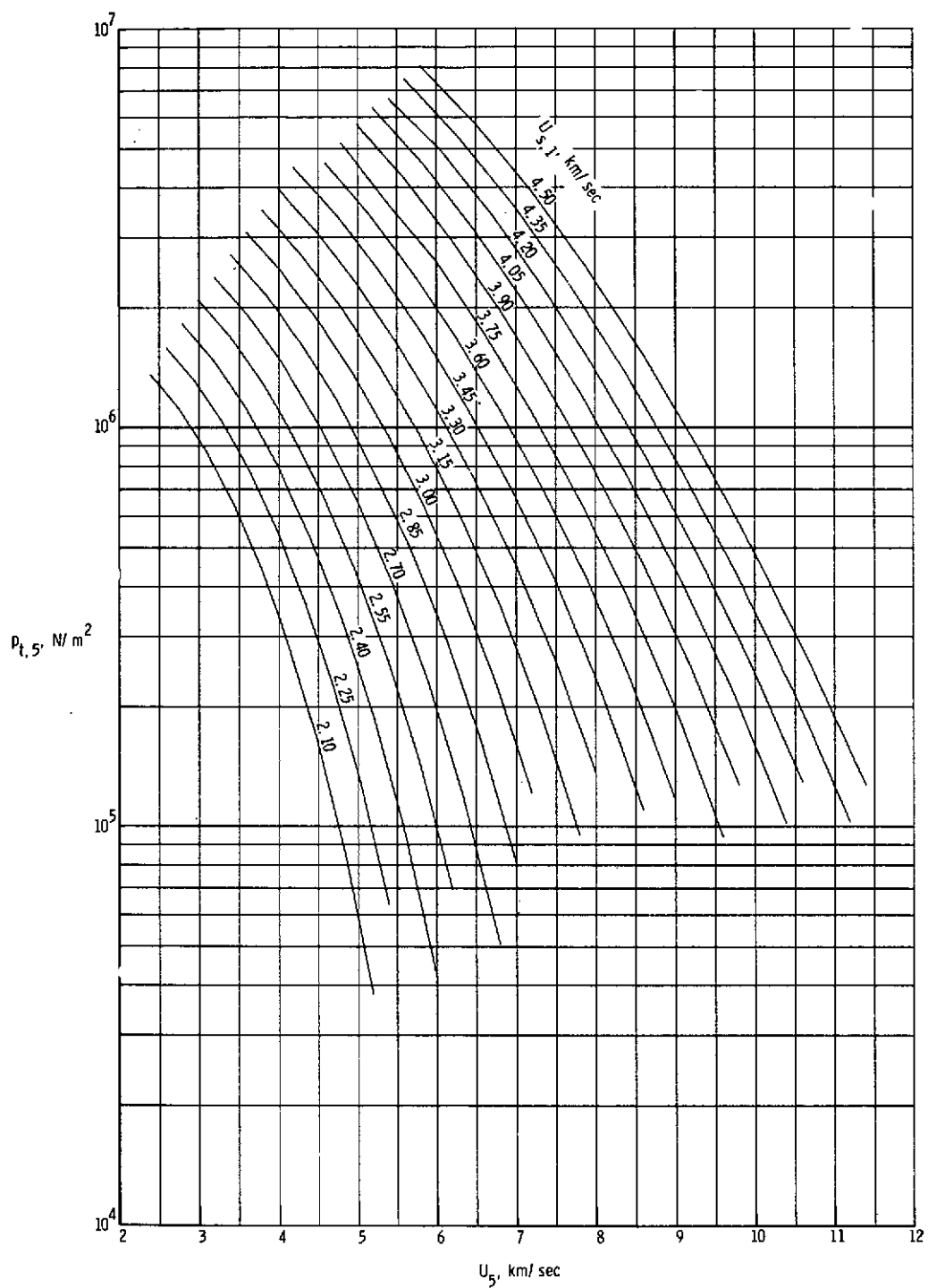
(e) Unit Reynolds number in region (5).

Figure 8.- Continued.



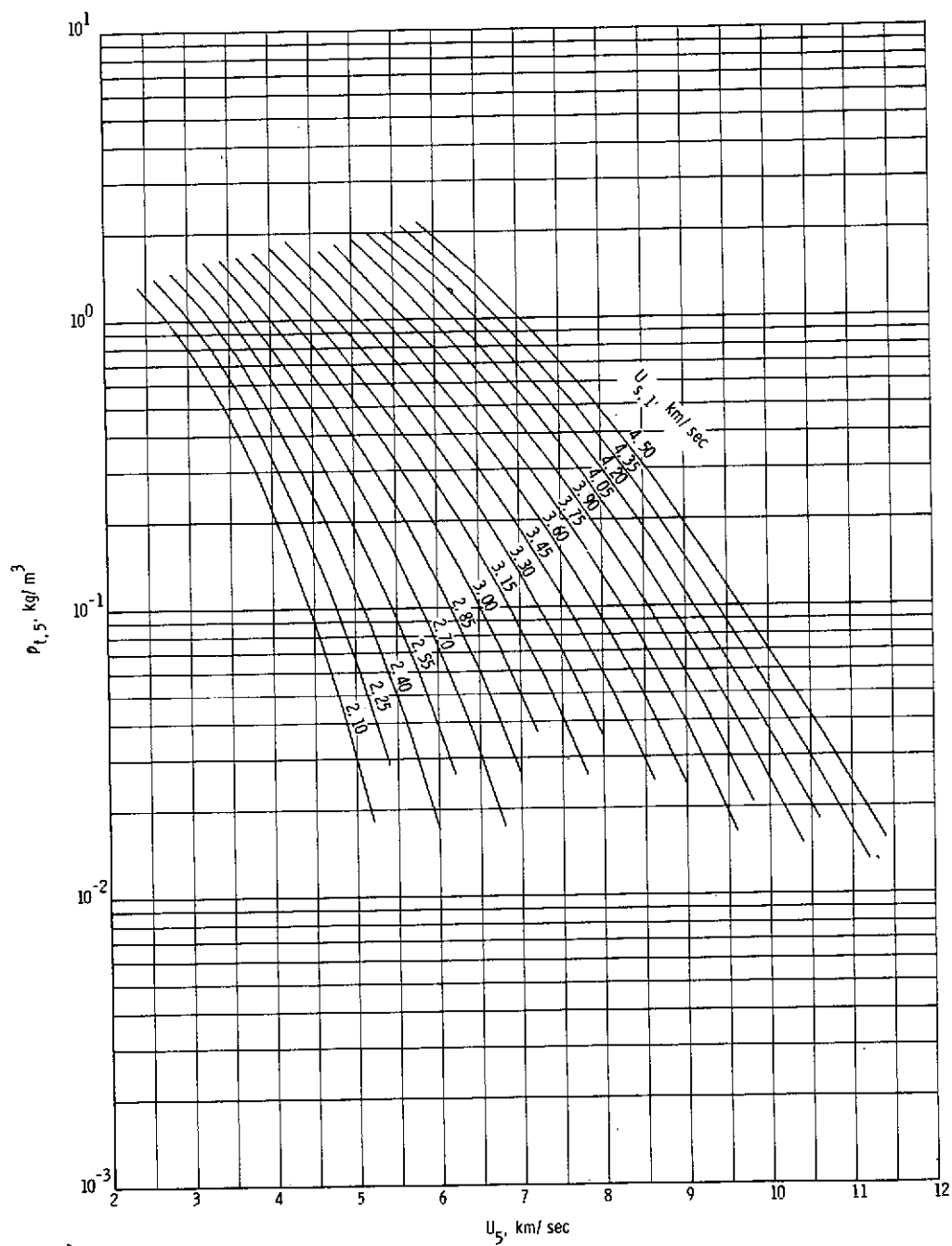
(f) Normal shock density ratio.

Figure 8.- Continued.



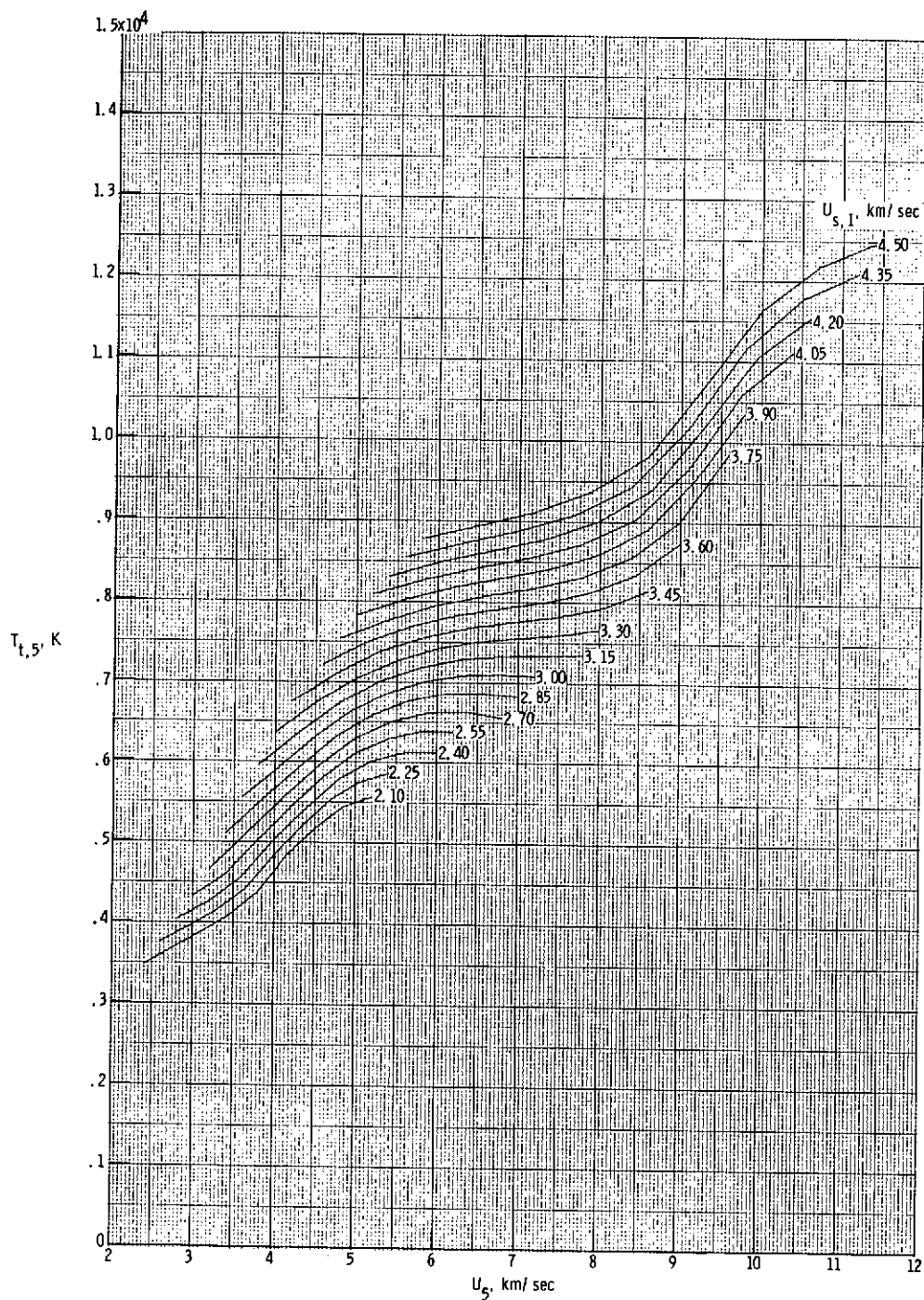
(g) Stagnation pressure behind normal bow shock.

Figure 8.- Continued.



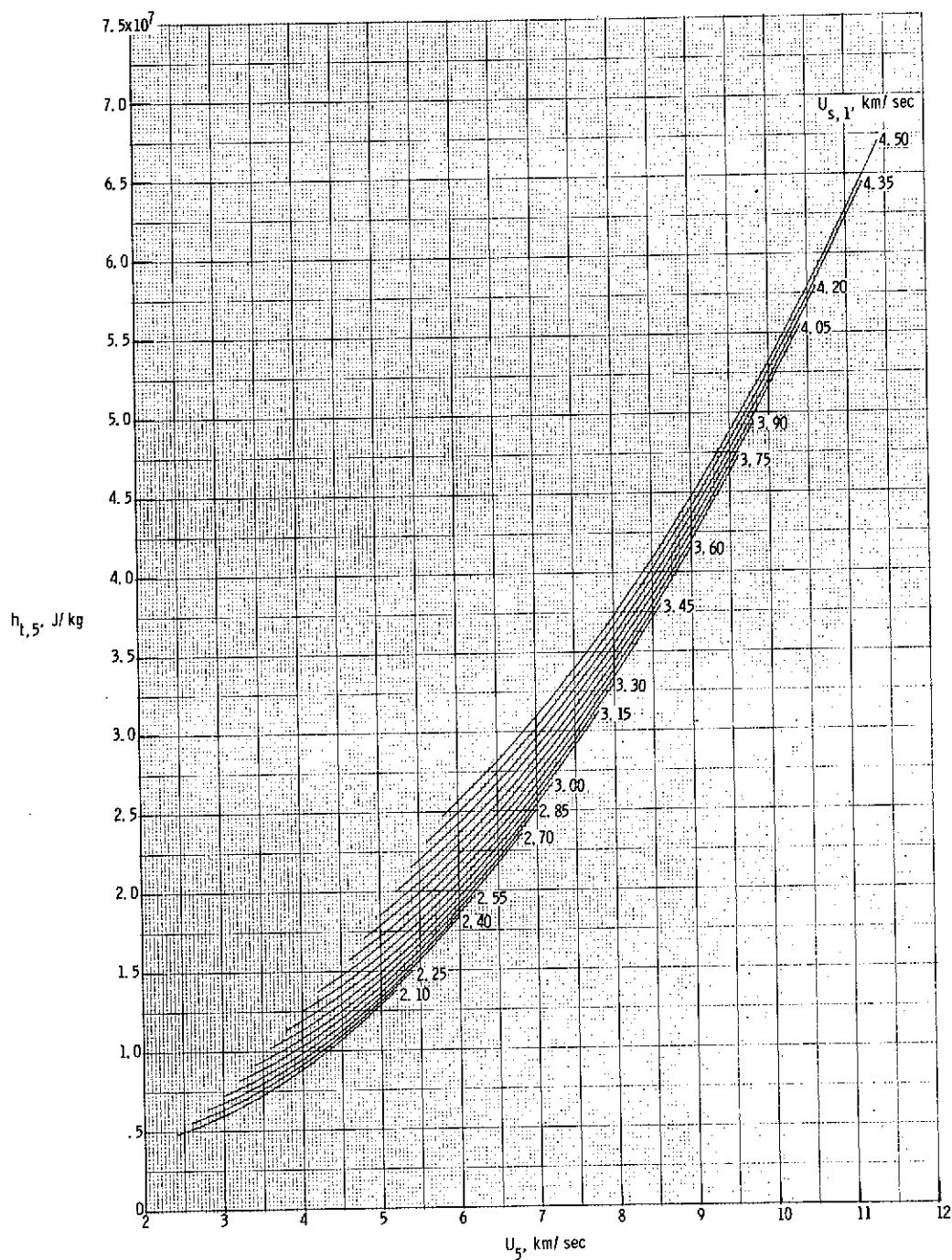
(h) Stagnation density behind normal bow shock.

Figure 8.- Continued.



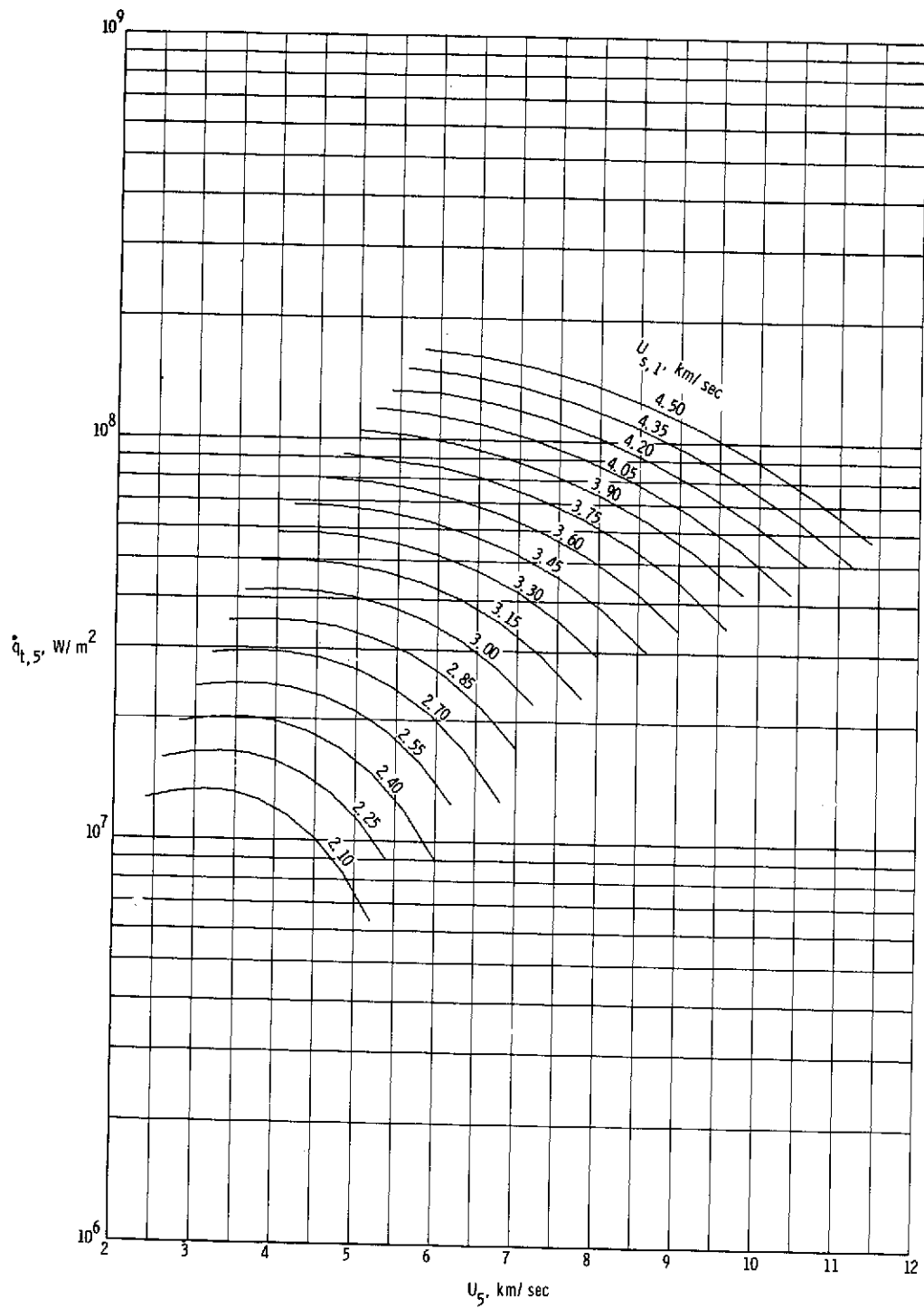
(i) Stagnation temperature behind normal bow shock.

Figure 8.- Continued.



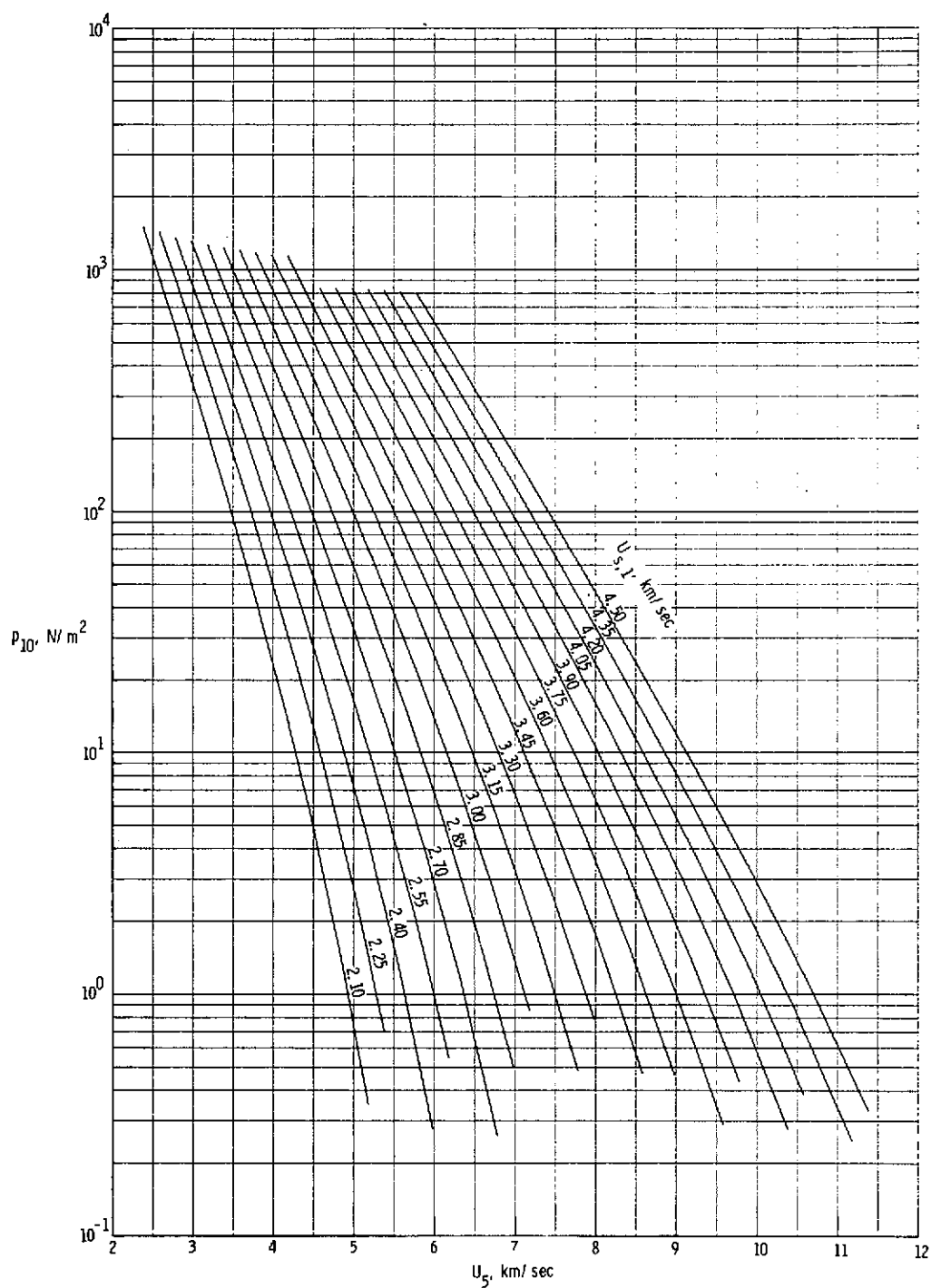
(j) Stagnation enthalpy behind normal bow shock.

Figure 8.- Continued.



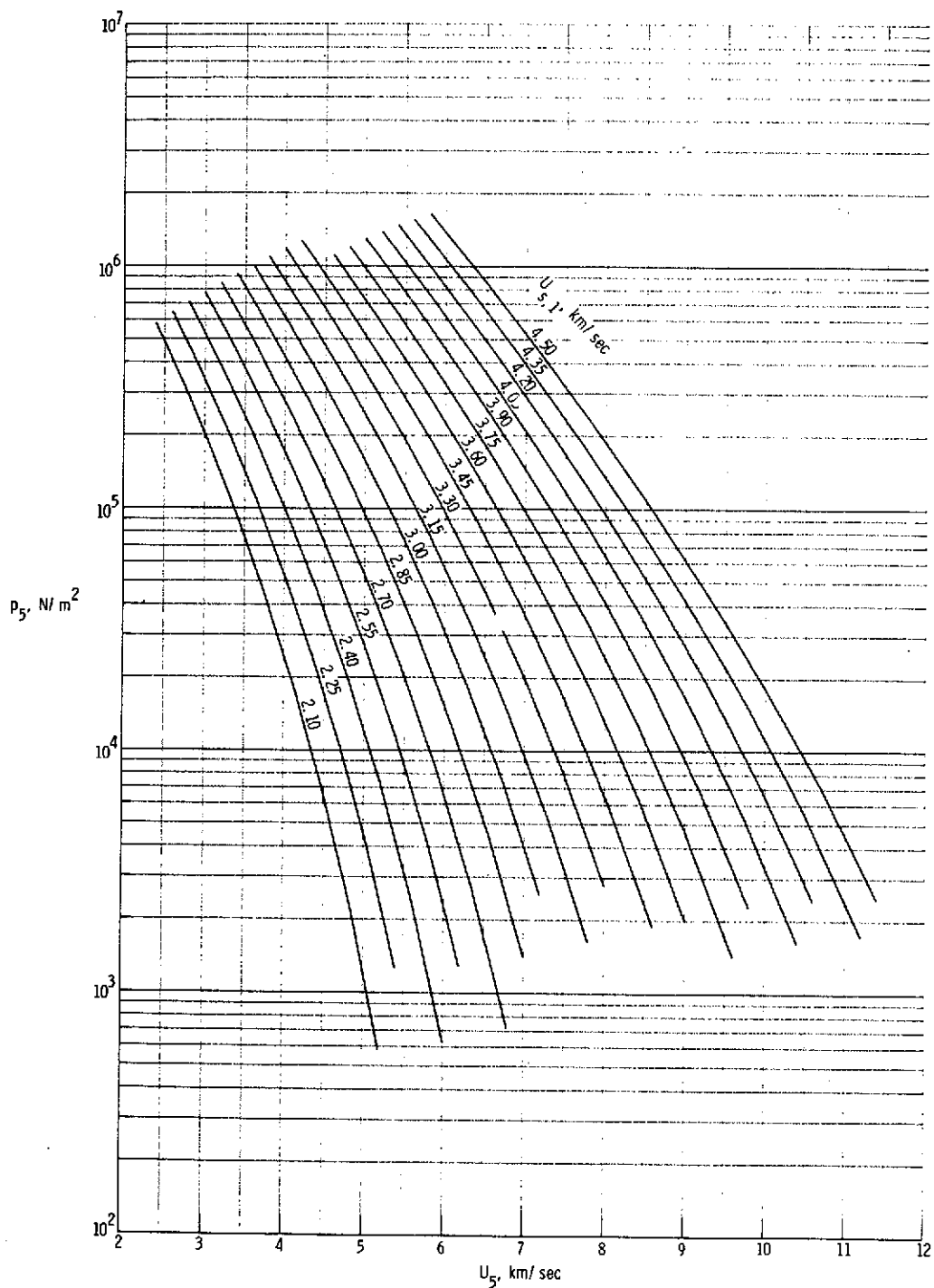
(k) Stagnation-point convective heat-transfer rate to sphere having radius of 2.54 cm.

Figure 8.- Continued.



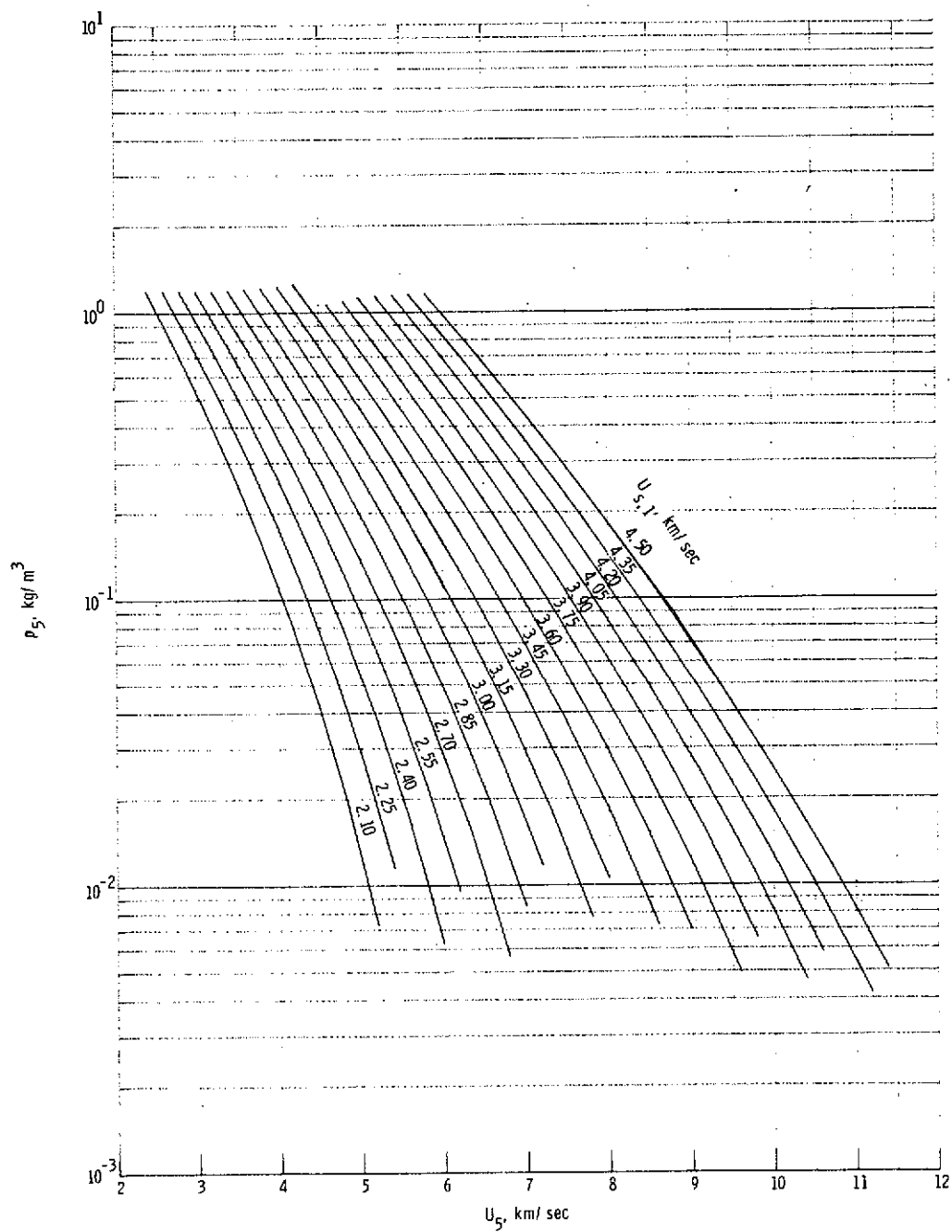
(1) Quiescent acceleration air pressure in region (10).

Figure 8.- Concluded.



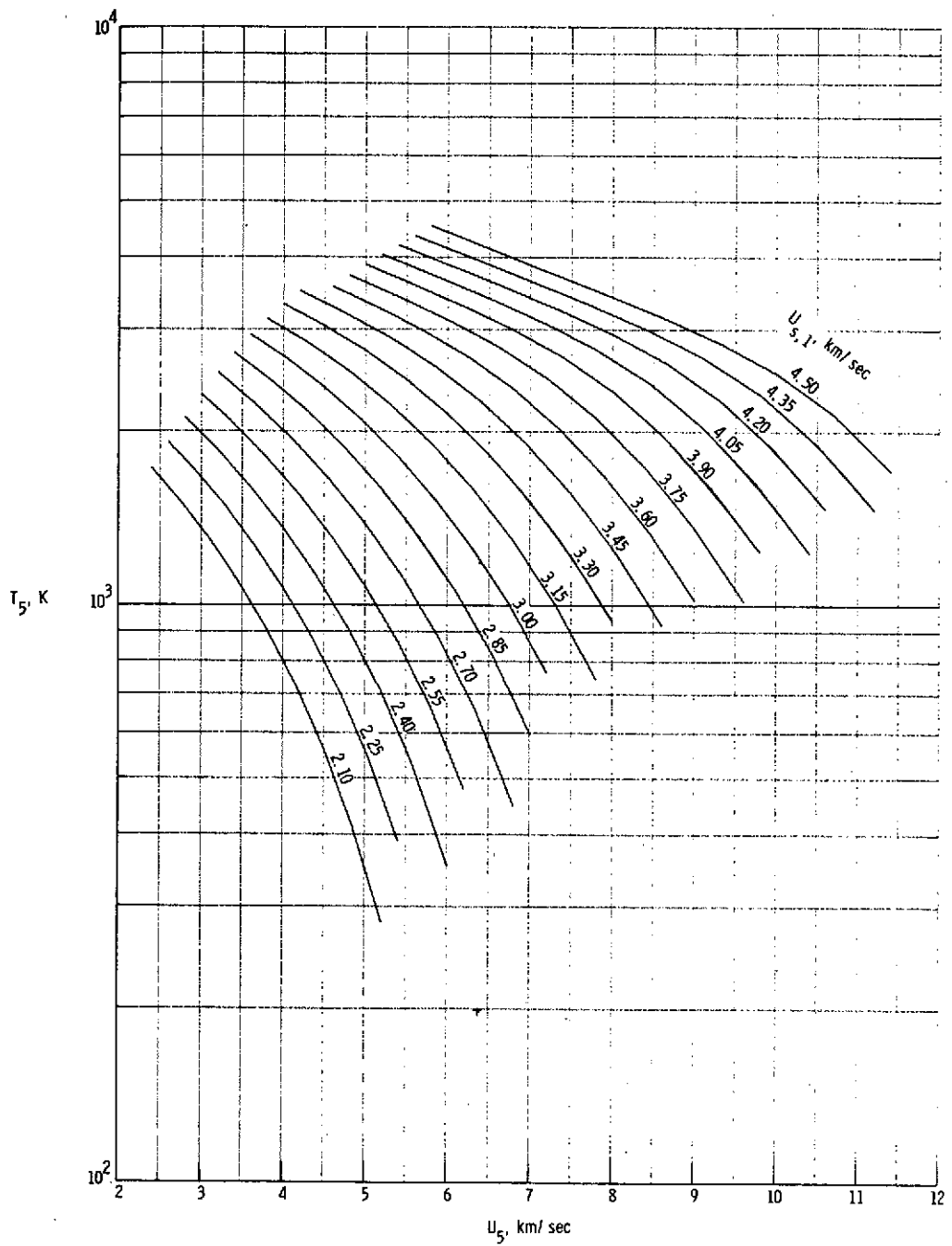
(a) Static pressure in region (5).

Figure 9.- Various expansion tube flow parameters for real air in thermochemical equilibrium as a function of flow velocity and assuming no shock reflection at secondary diaphragm. $p_1 = 34.47 \text{ kN/m}^2$.



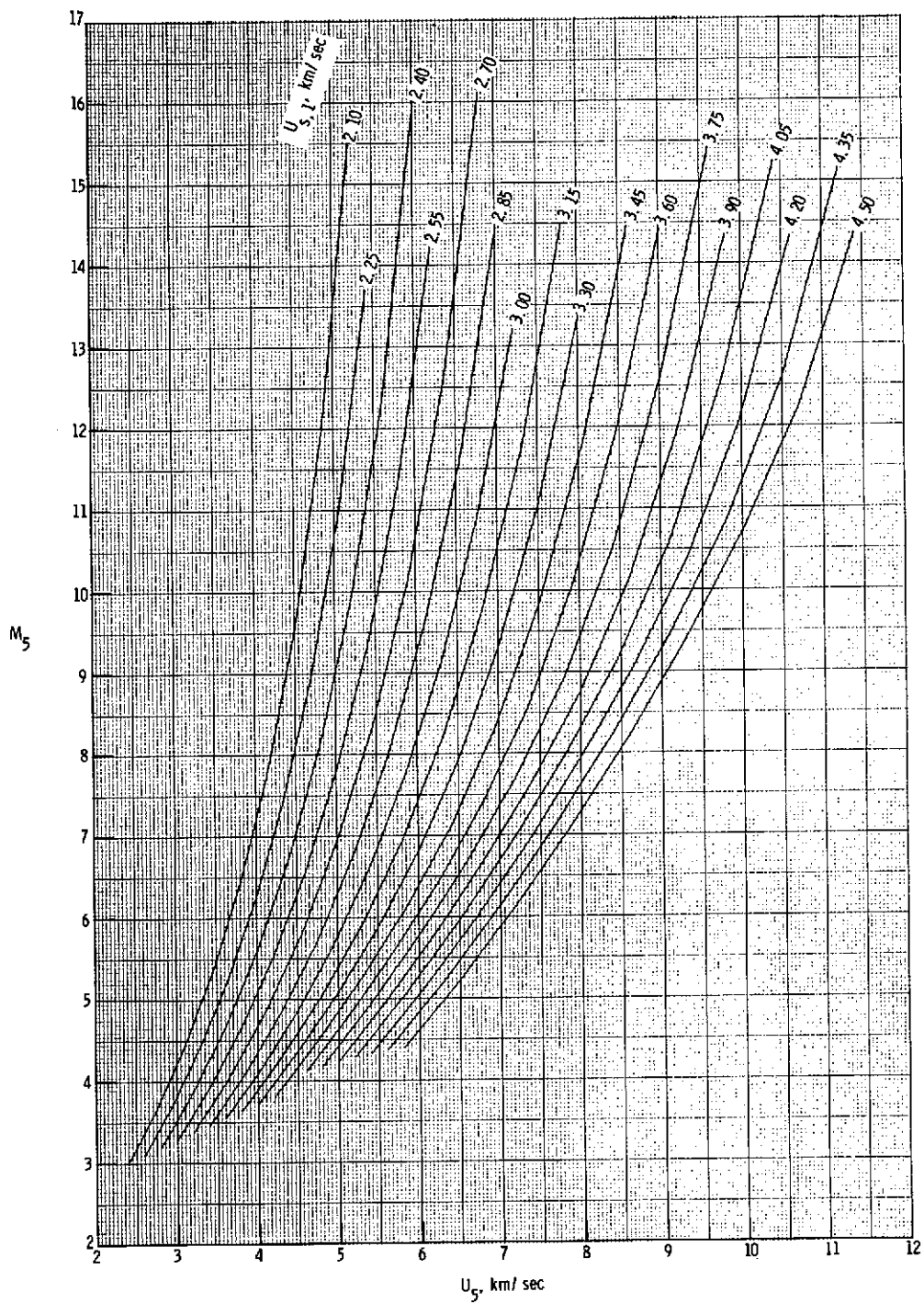
(b) Static density in region (5).

Figure 9.- Continued.



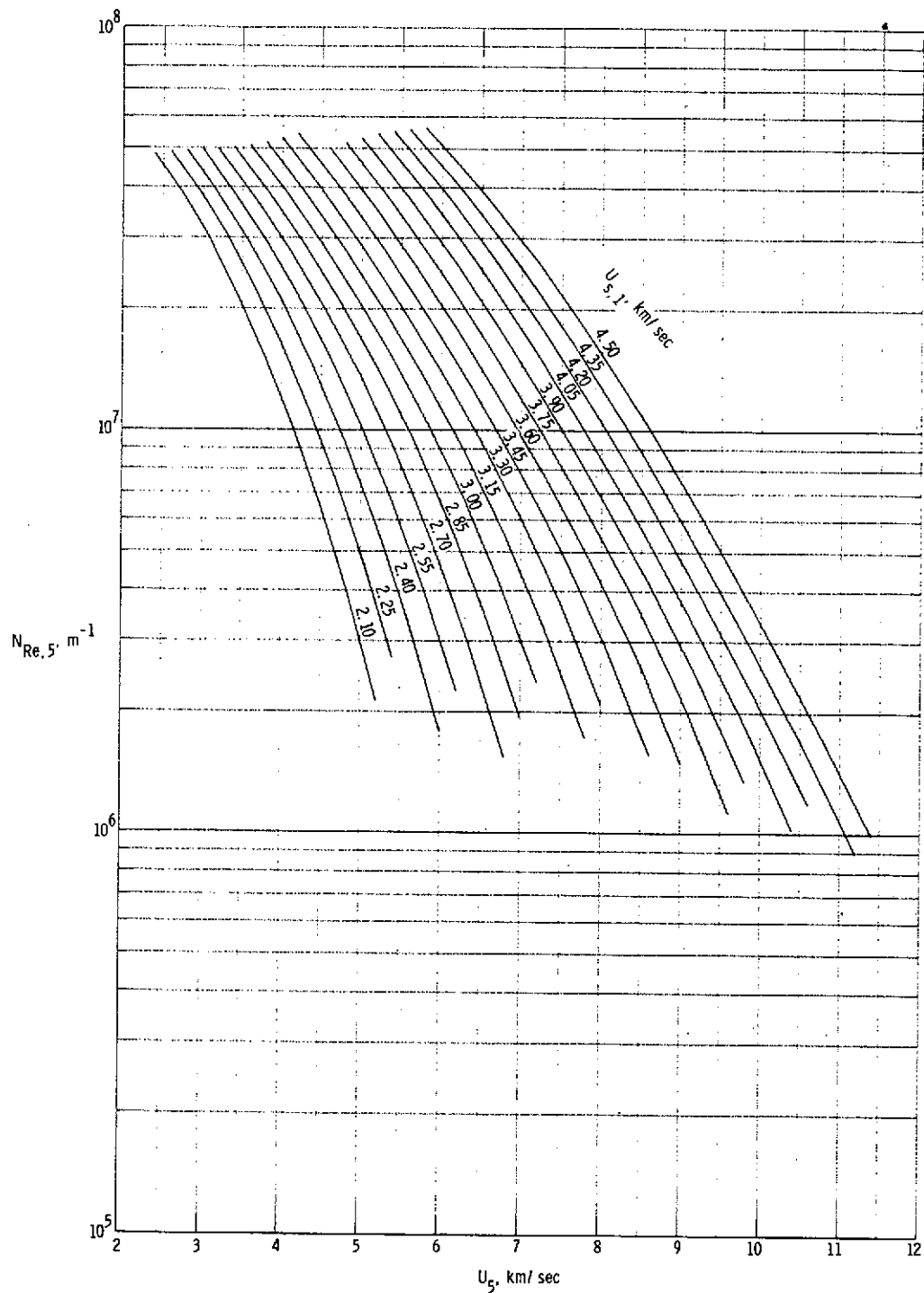
(c) Static temperature in region (5).

Figure 9.- Continued.



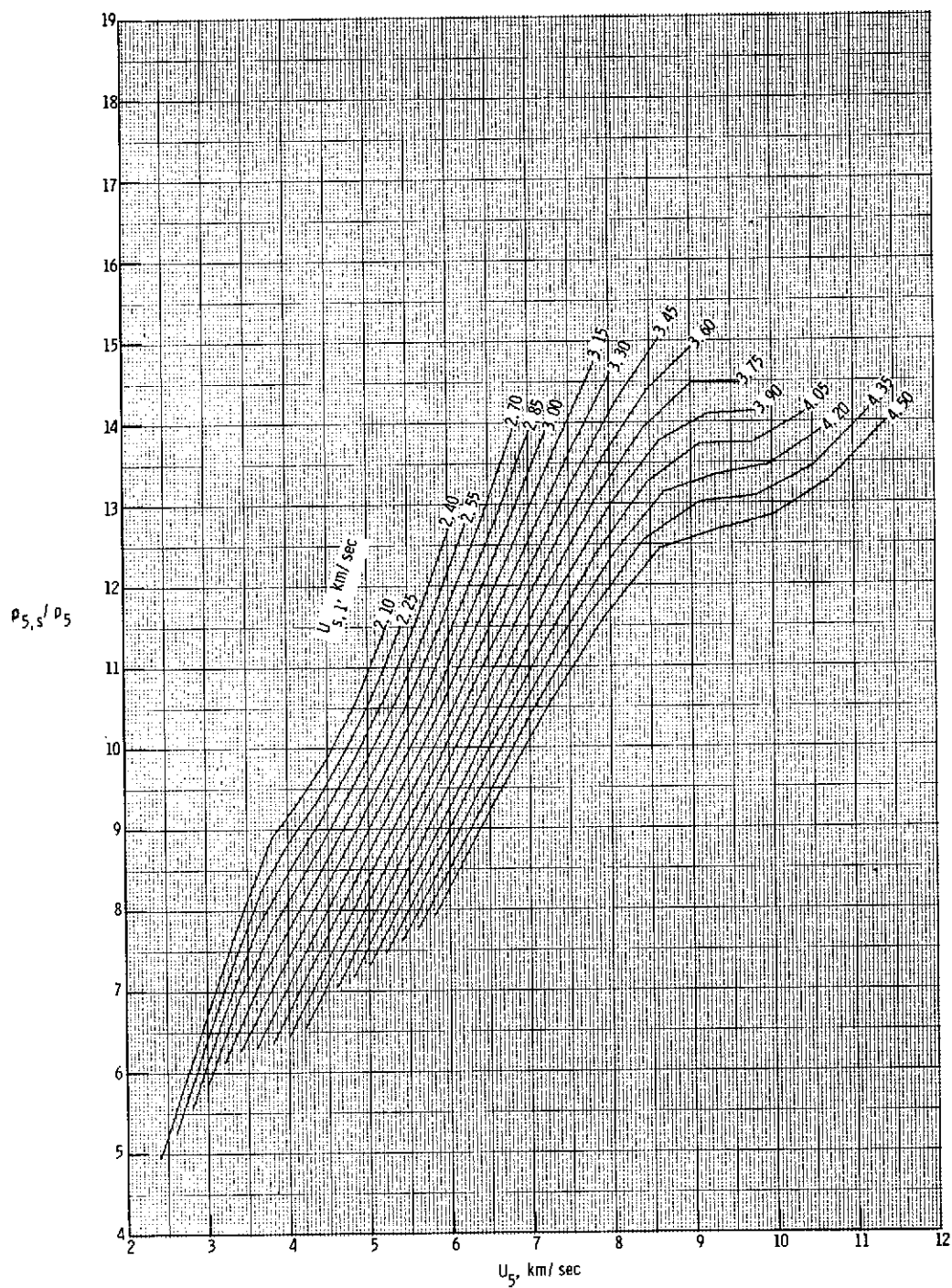
(d) Mach number in region (5).

Figure 9.- Continued.



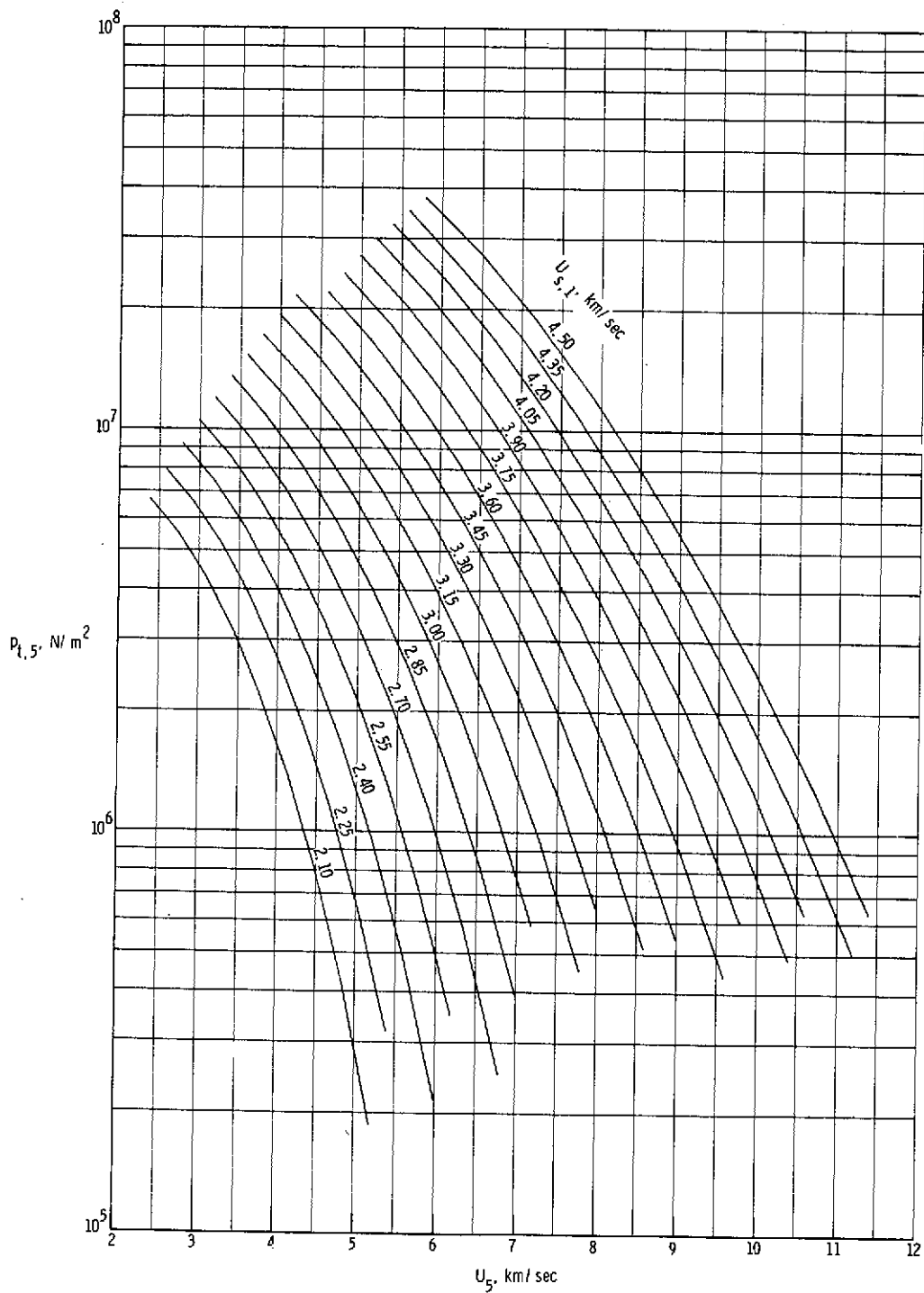
(e) Unit Reynolds number in region (5).

Figure 9.- Continued.



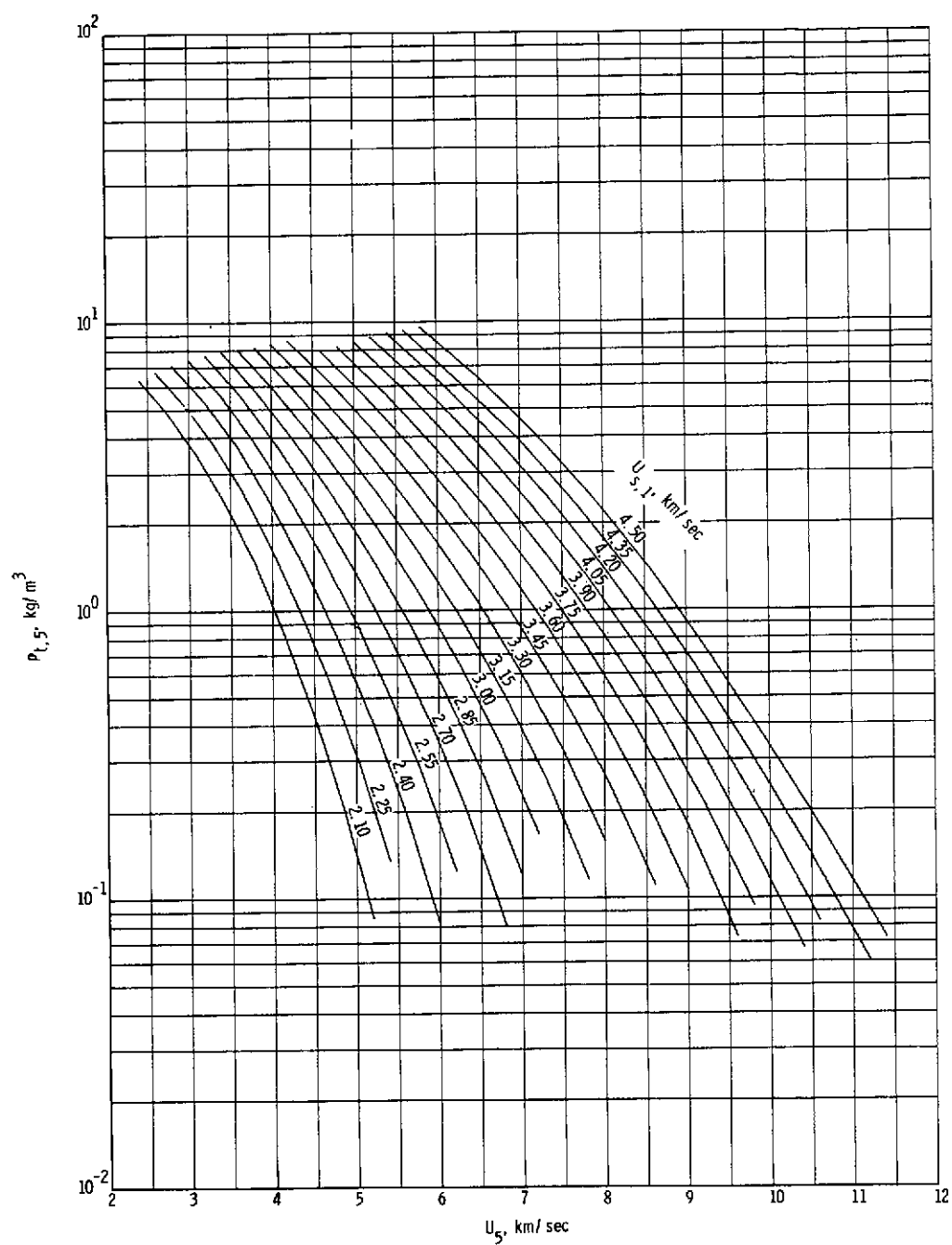
(f) Normal shock density ratio.

Figure 9.- Continued.



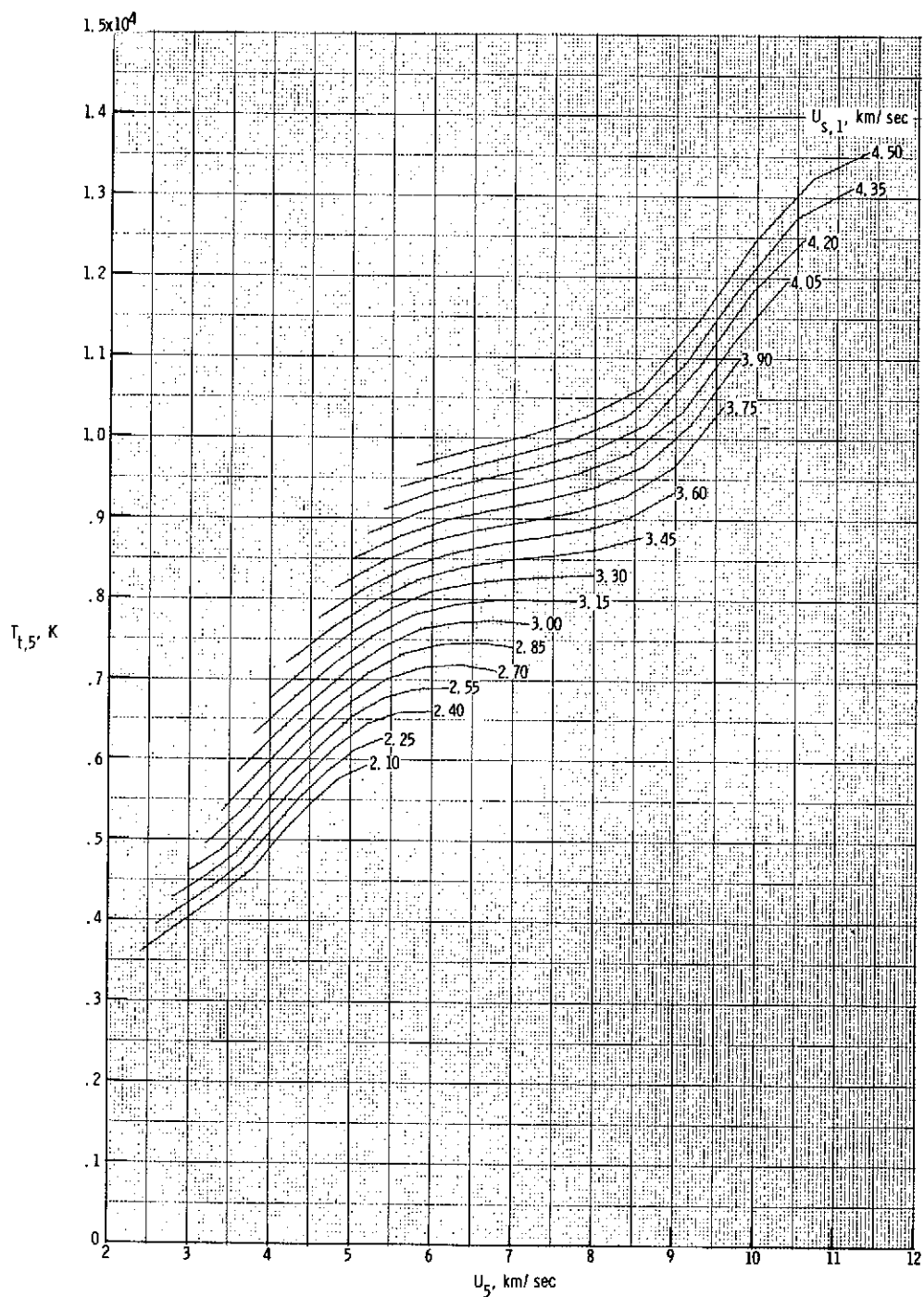
(g) Stagnation pressure behind normal bow shock.

Figure 9.- Continued.



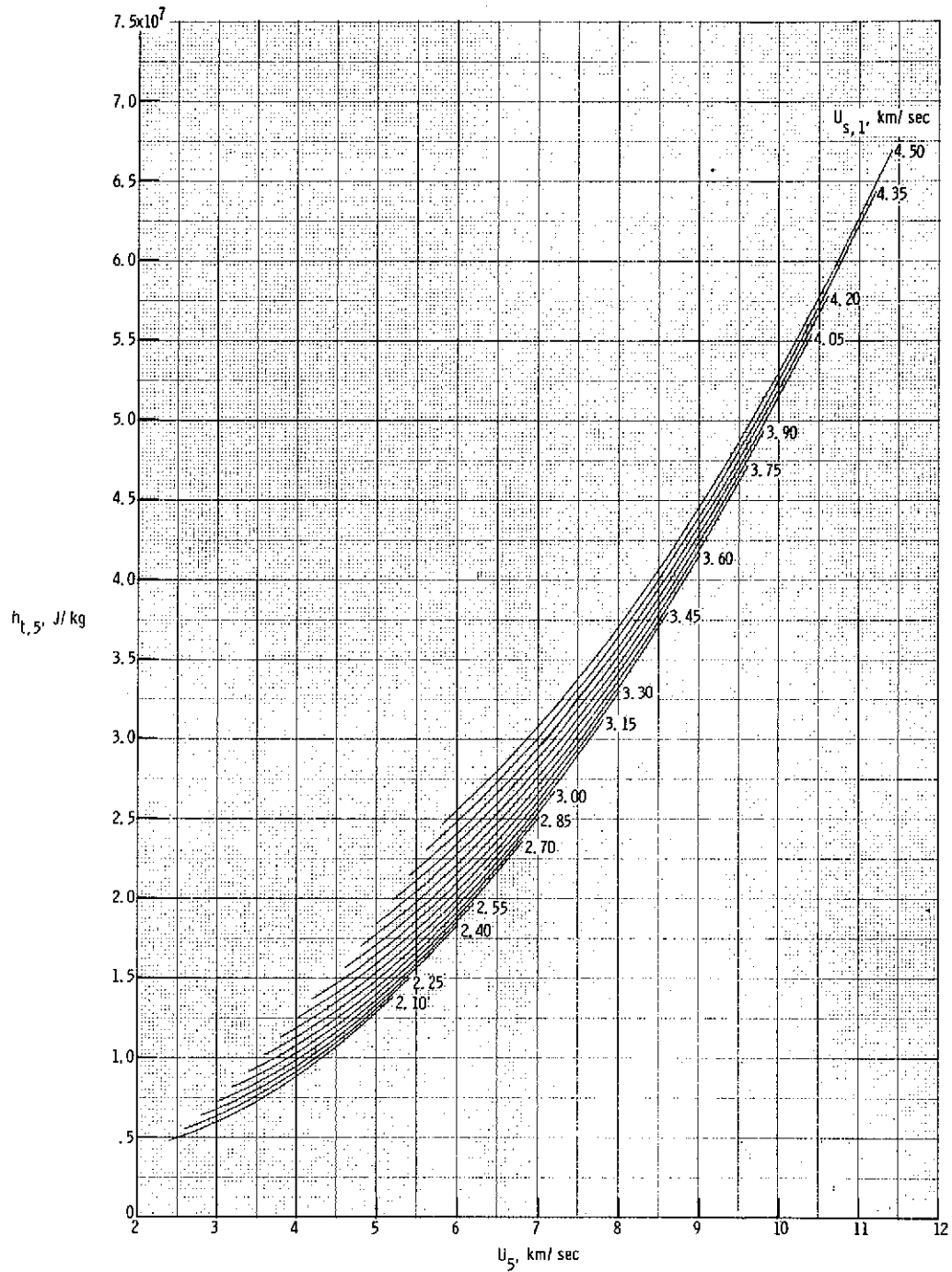
(h) Stagnation density behind normal bow shock.

Figure 9.- Continued.



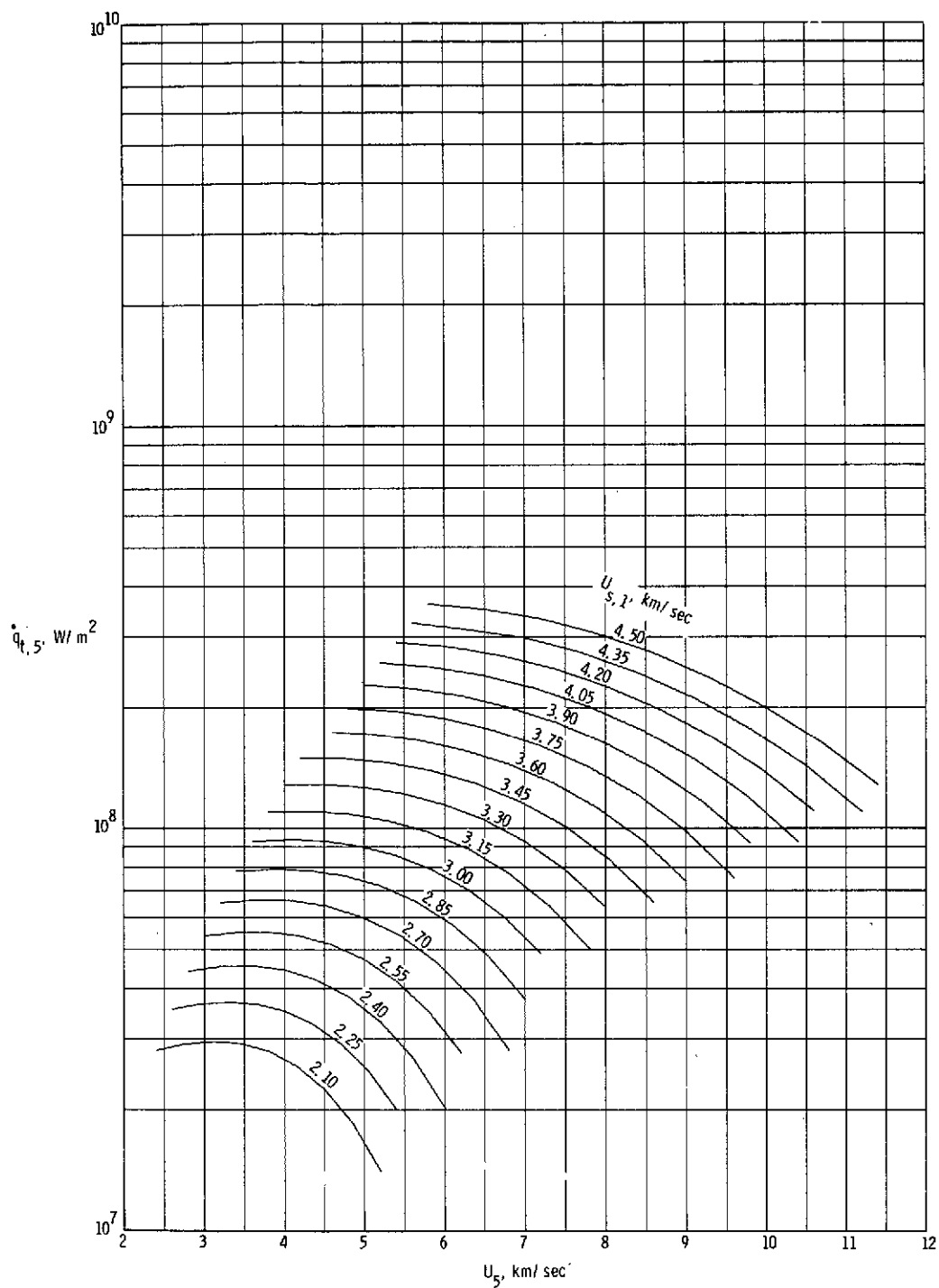
(i) Stagnation temperature behind normal bow shock.

Figure 9.- Continued.



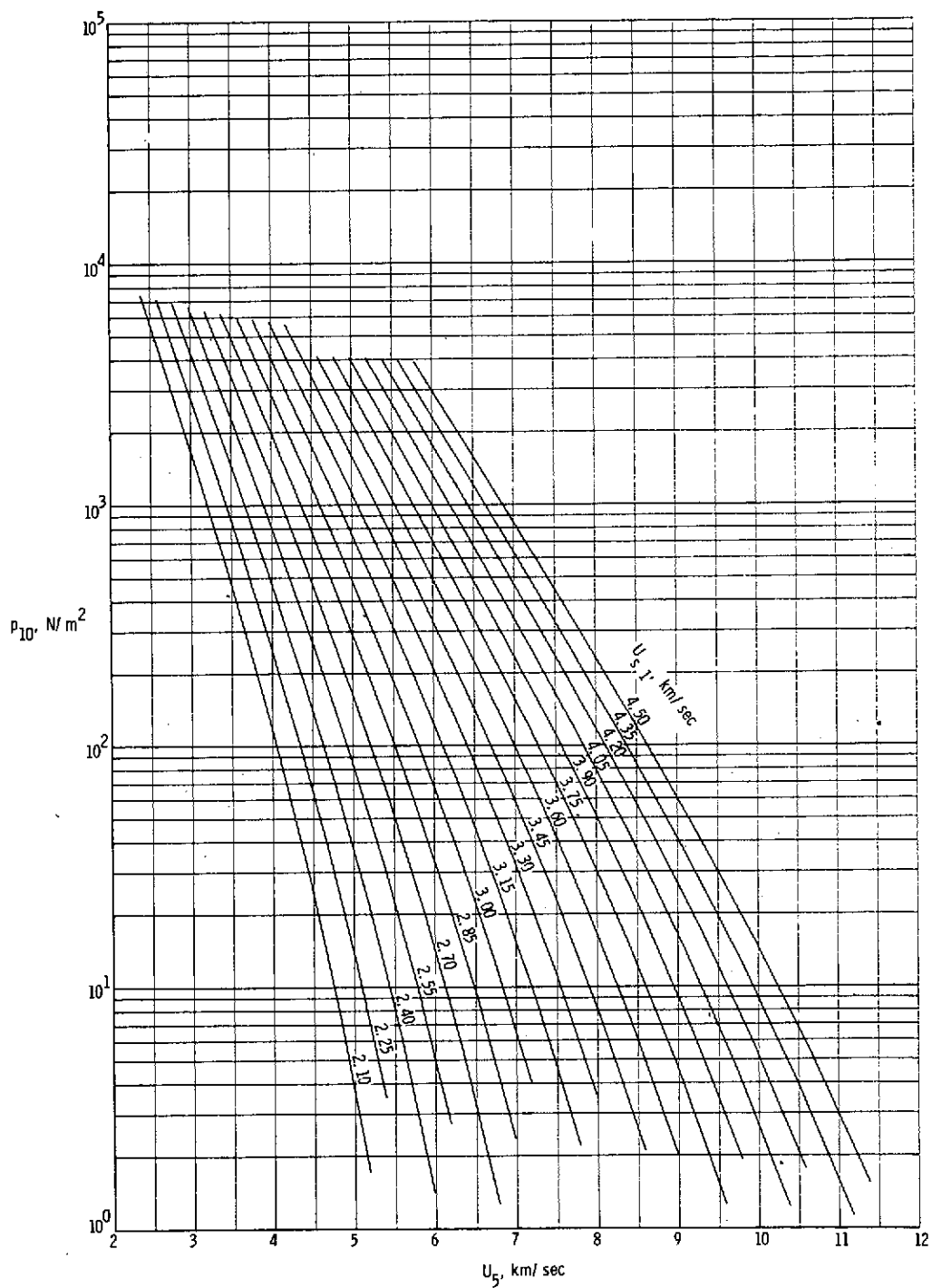
(j) Stagnation enthalpy behind normal bow shock.

Figure 9.- Continued.



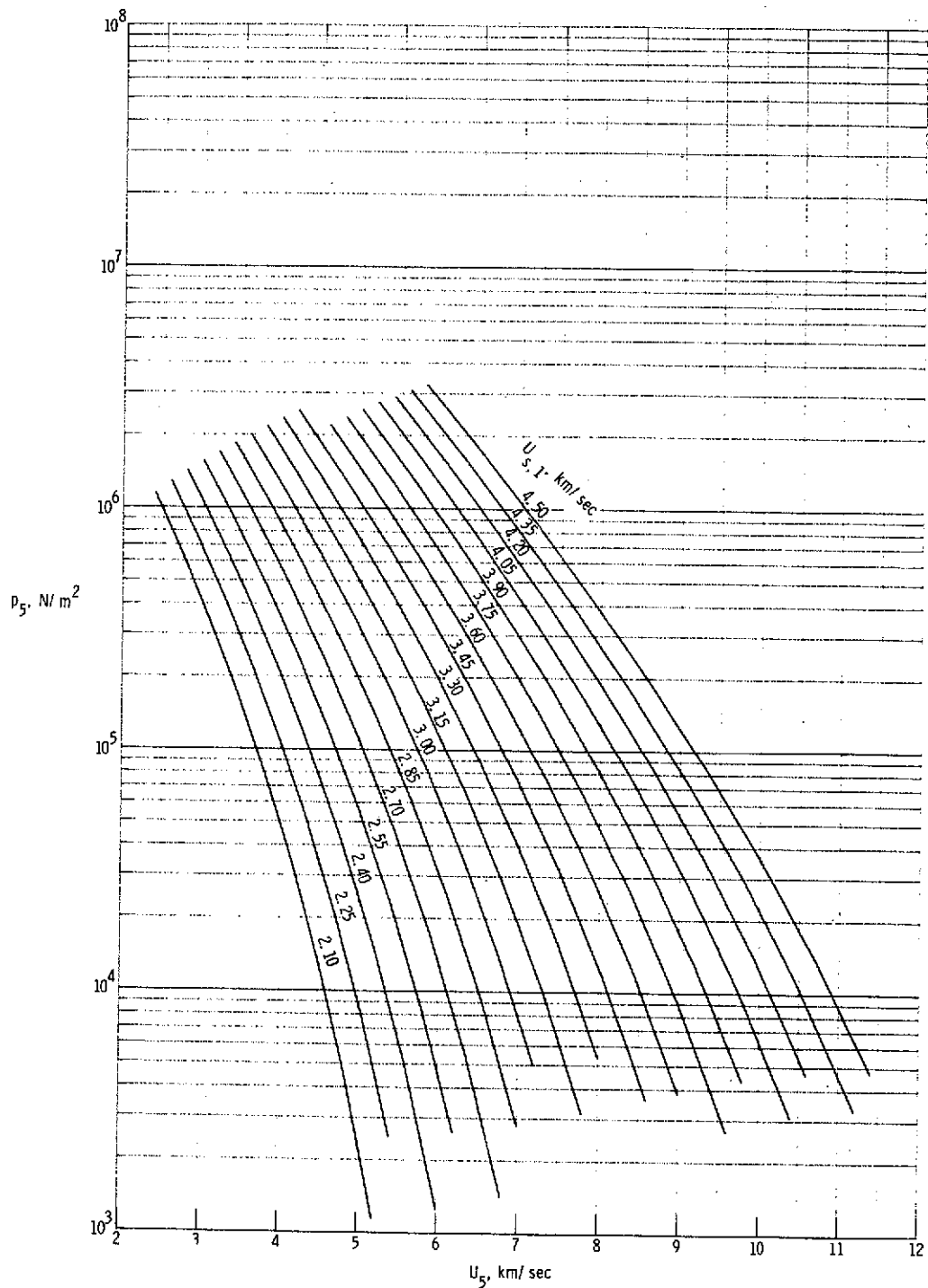
(k) Stagnation-point convective heat-transfer rate to sphere having radius of 2.54 cm.

Figure 9.- Continued.



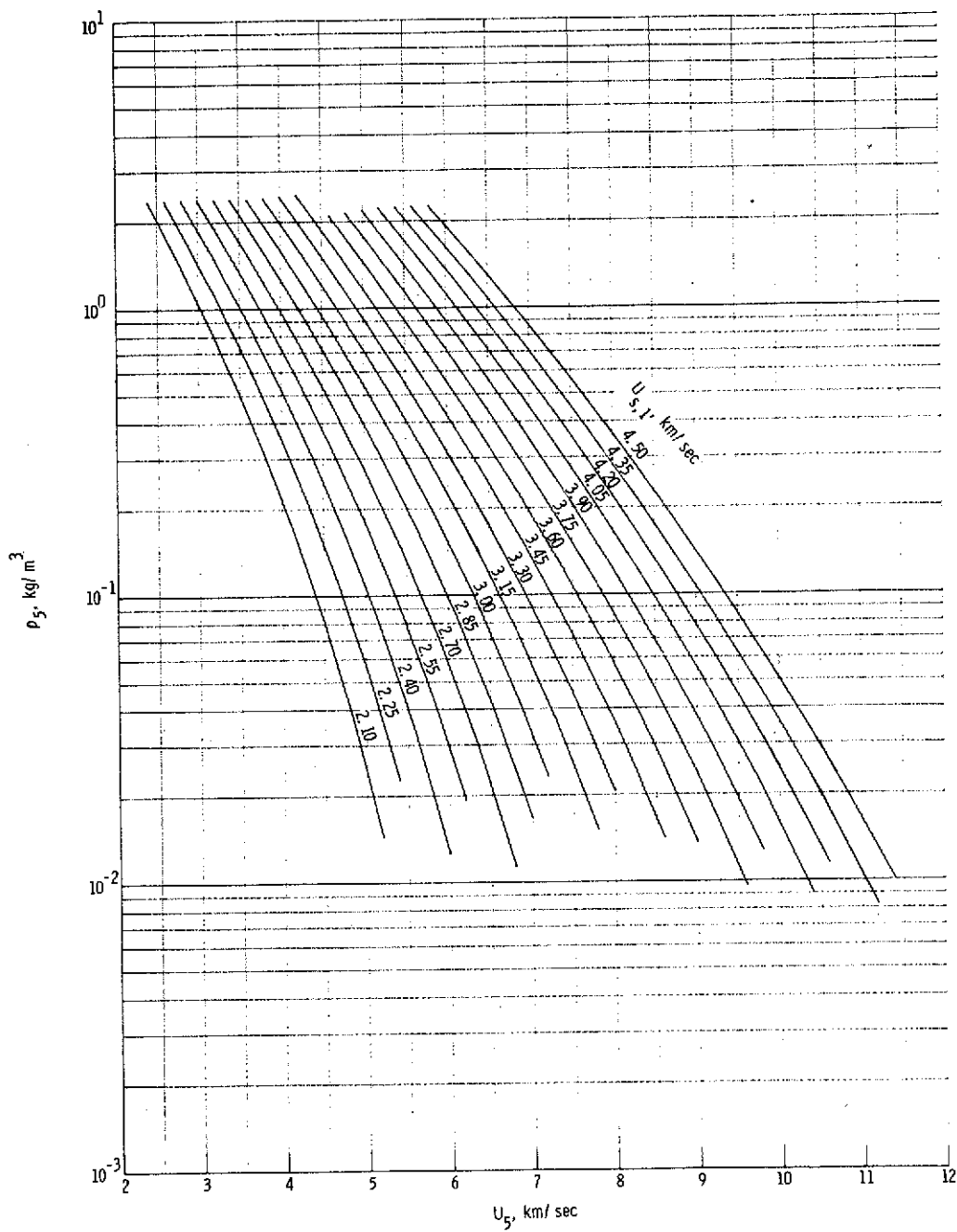
(1) Quiescent acceleration air pressure in region (10).

Figure 9.- Concluded.



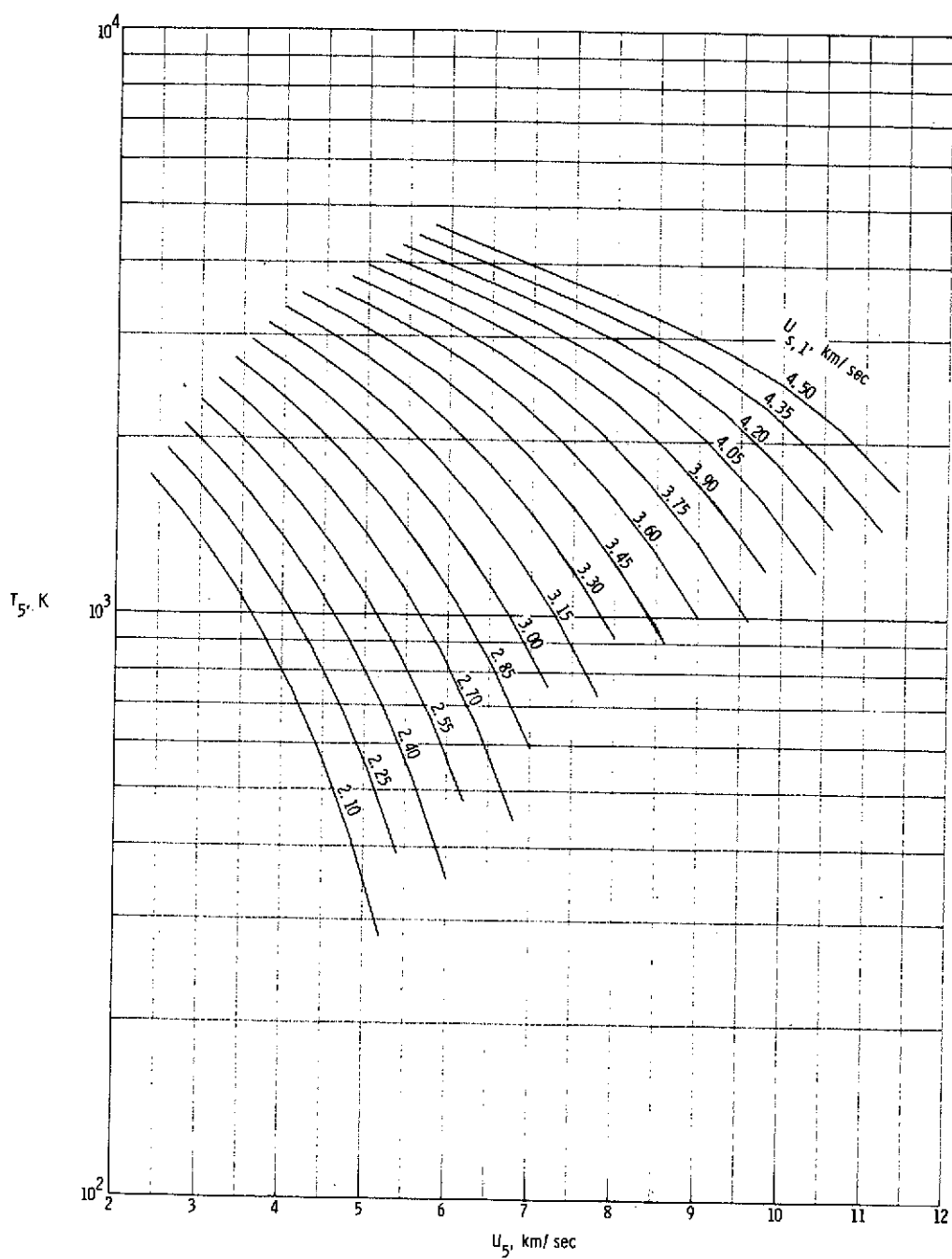
(a) Static pressure in region (5).

Figure 10.- Various expansion tube flow parameters for real air in thermochemical equilibrium as a function of flow velocity and assuming no shock reflection at secondary diaphragm. $p_1 = 68.95 \text{ kN/m}^2$.



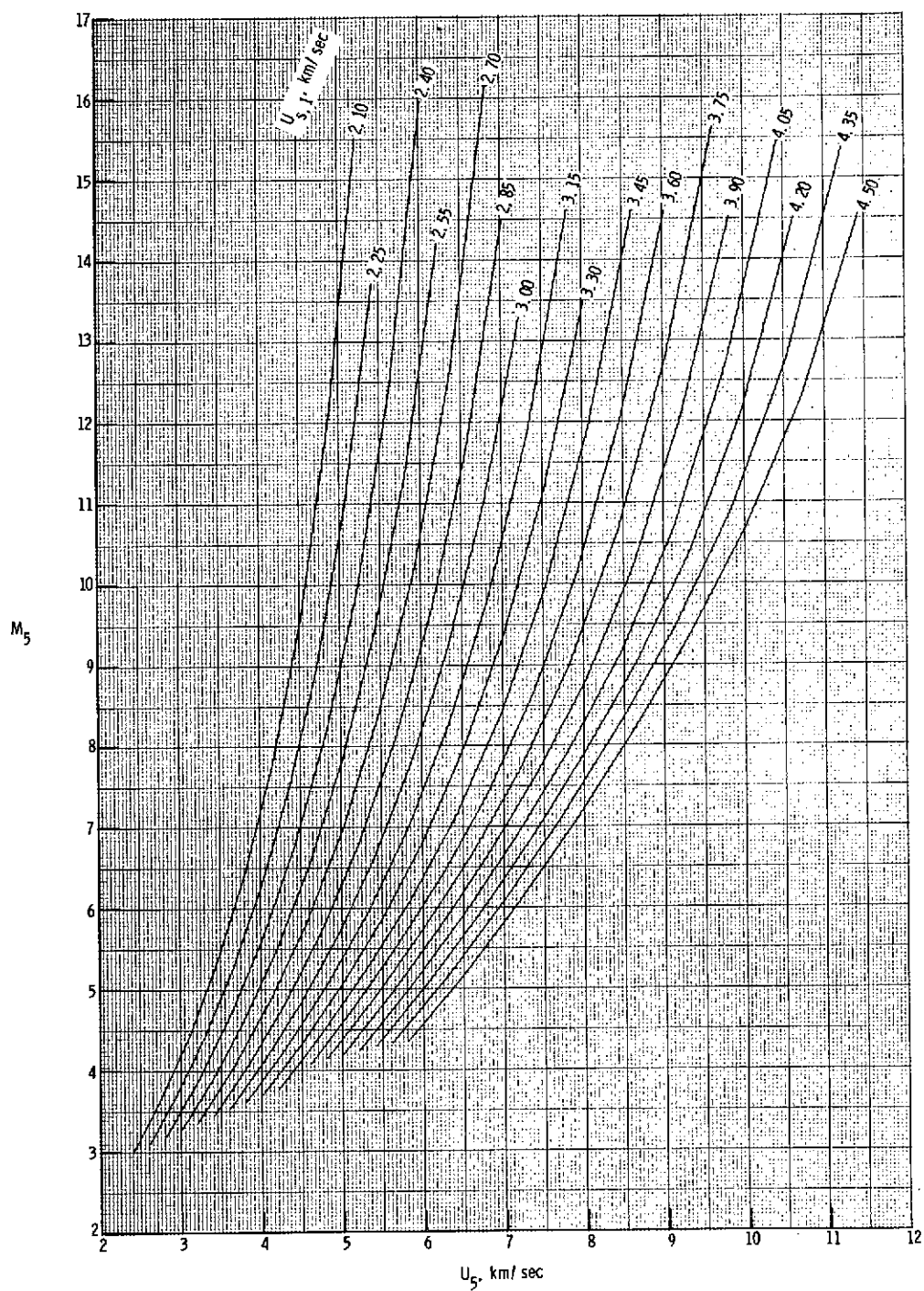
(b) Static density in region (5).

Figure 10.- Continued.



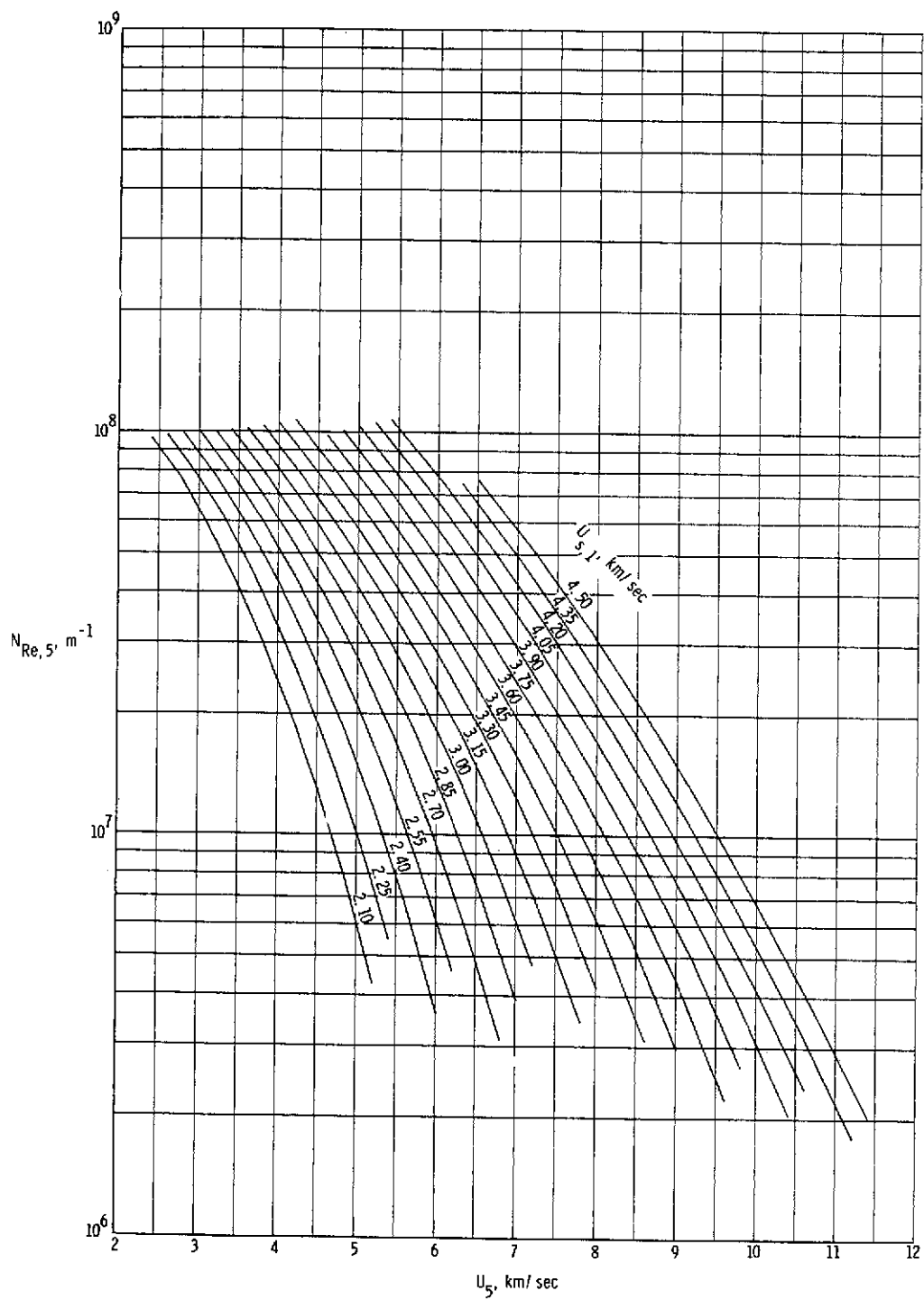
(c) Static temperature in region (5).

Figure 10.- Continued.



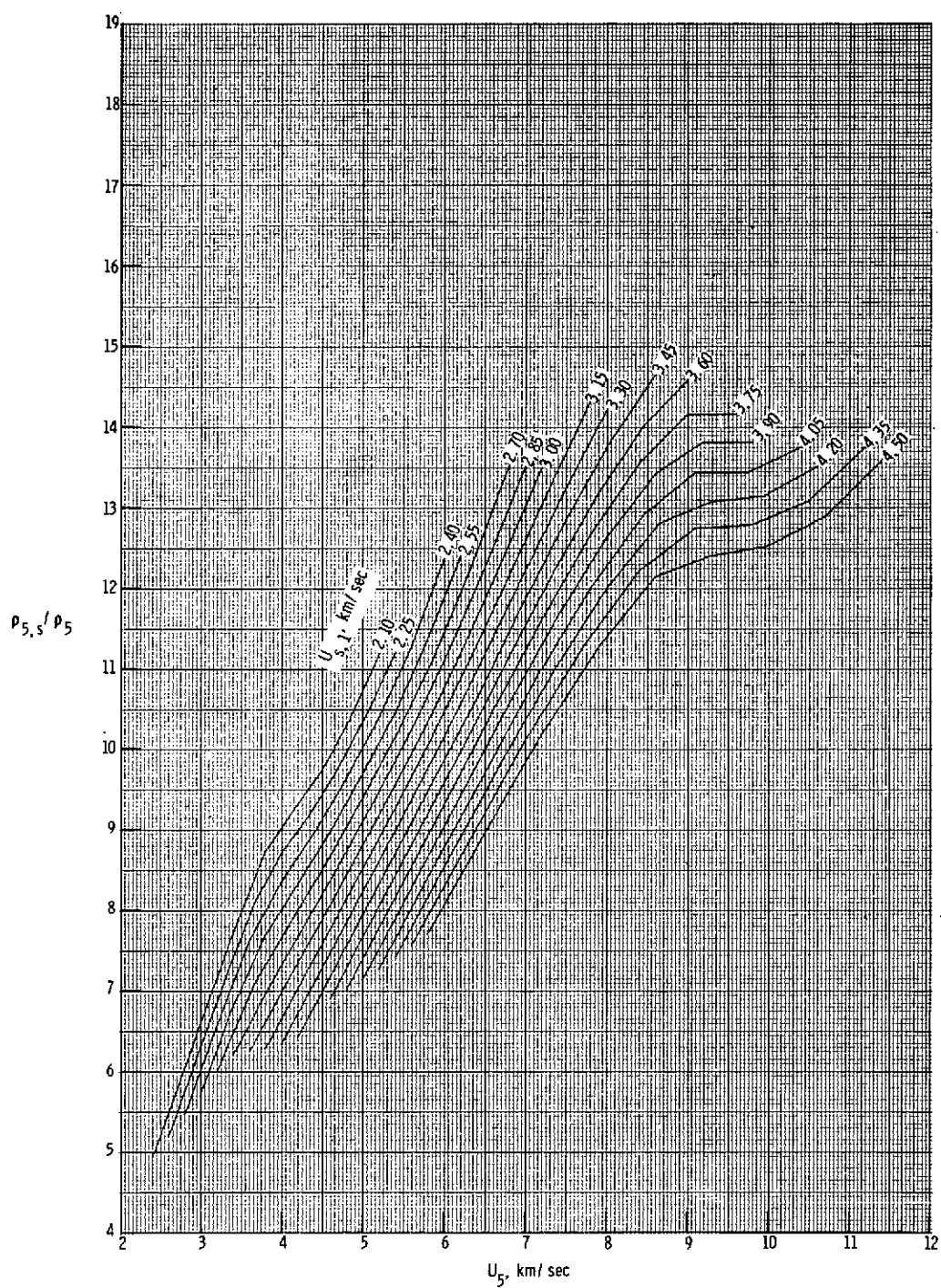
(d) Mach number in region (5).

Figure 10.- Continued.



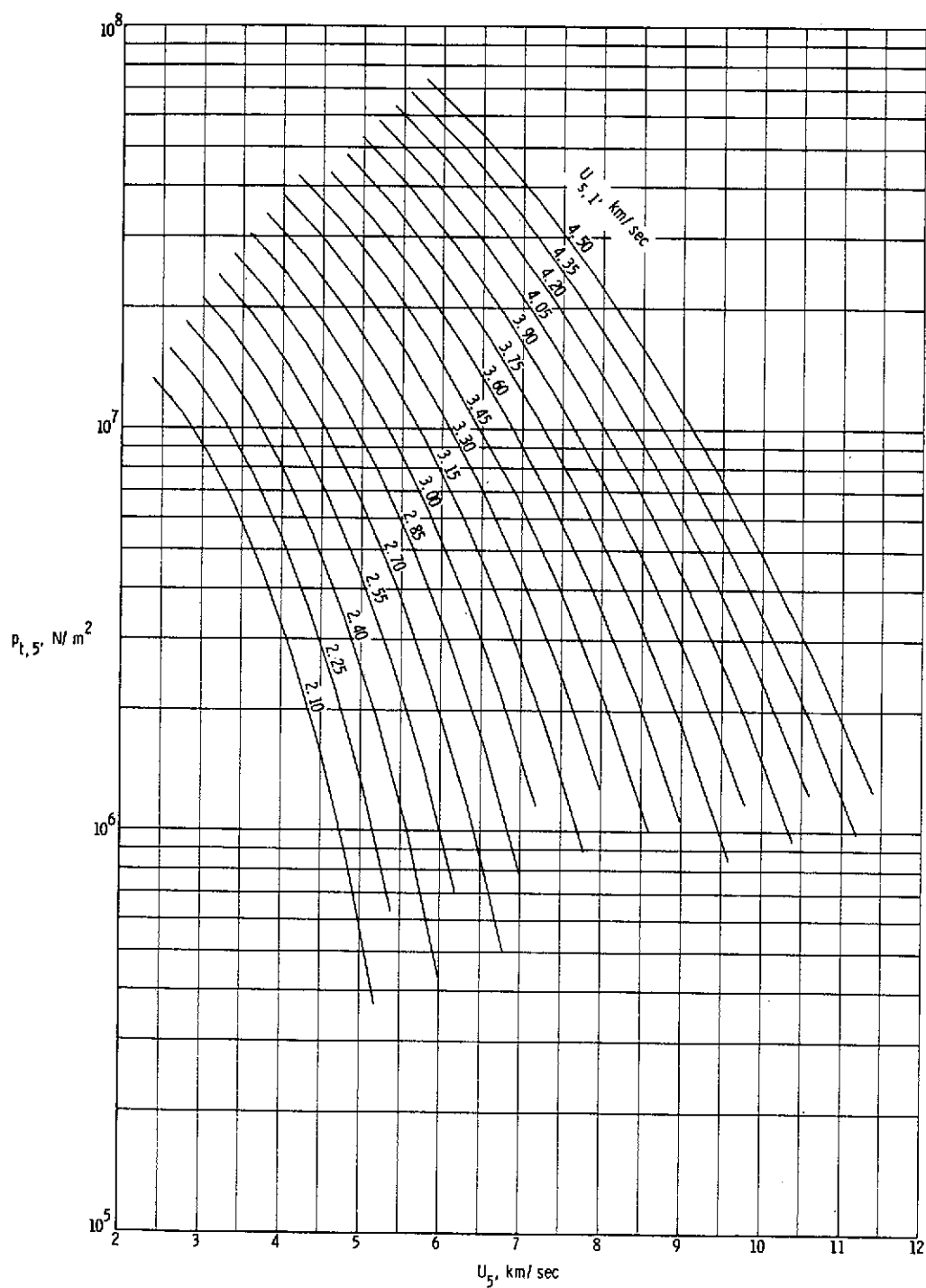
(e) Unit Reynolds number in region (5).

Figure 10.- Continued.



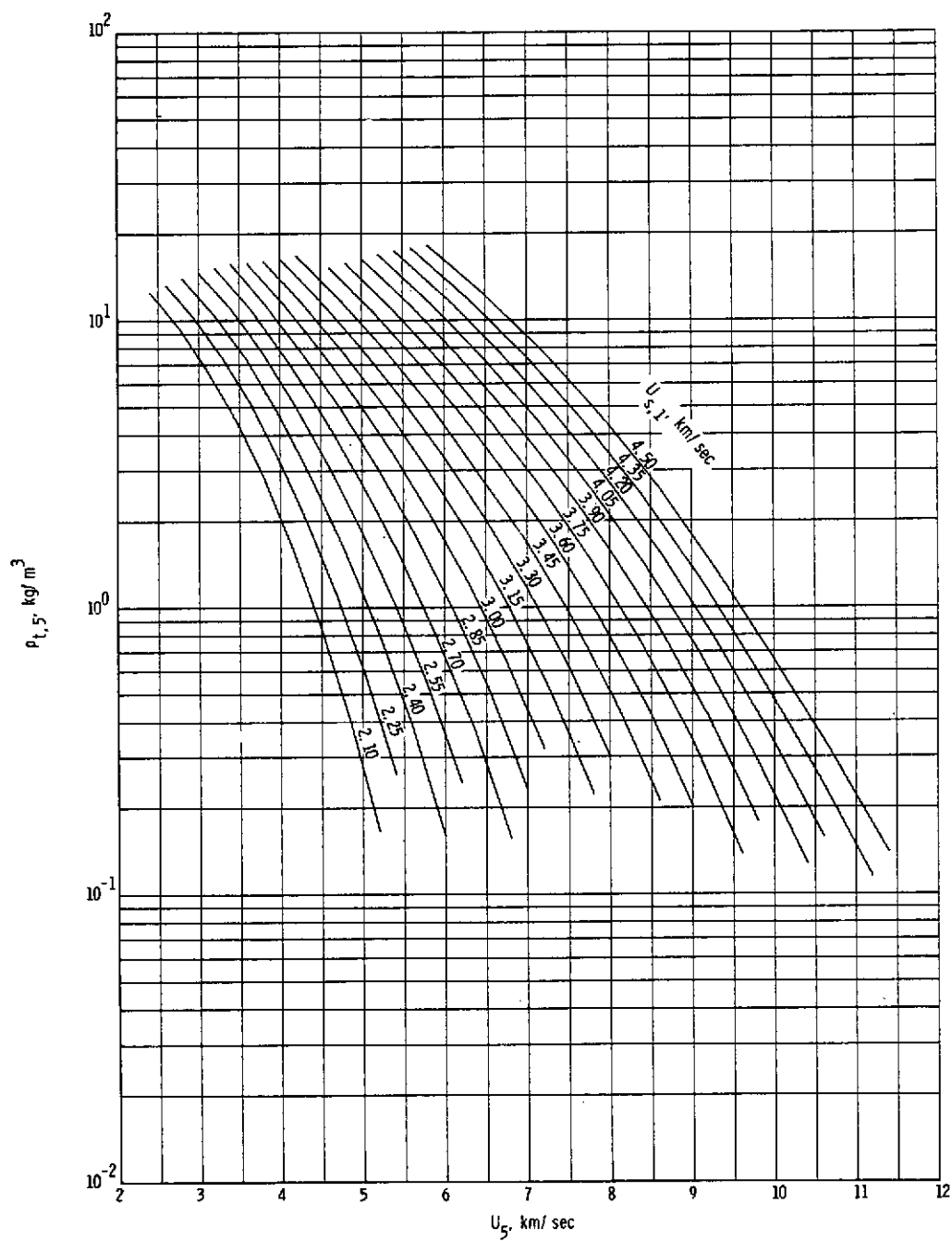
(f) Normal shock density ratio.

Figure 10.- Continued.



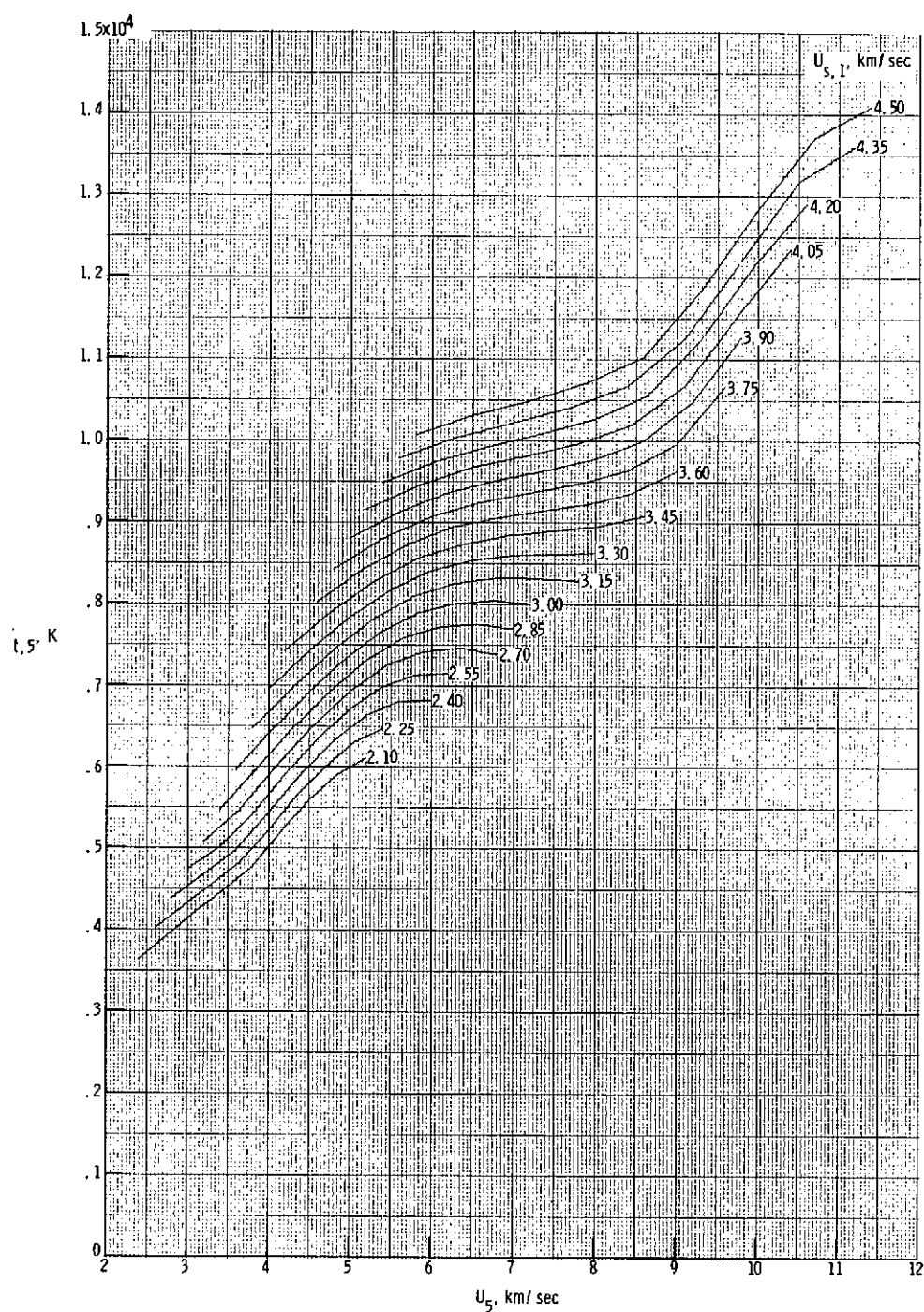
(g) Stagnation pressure behind normal bow shock.

Figure 10.- Continued.



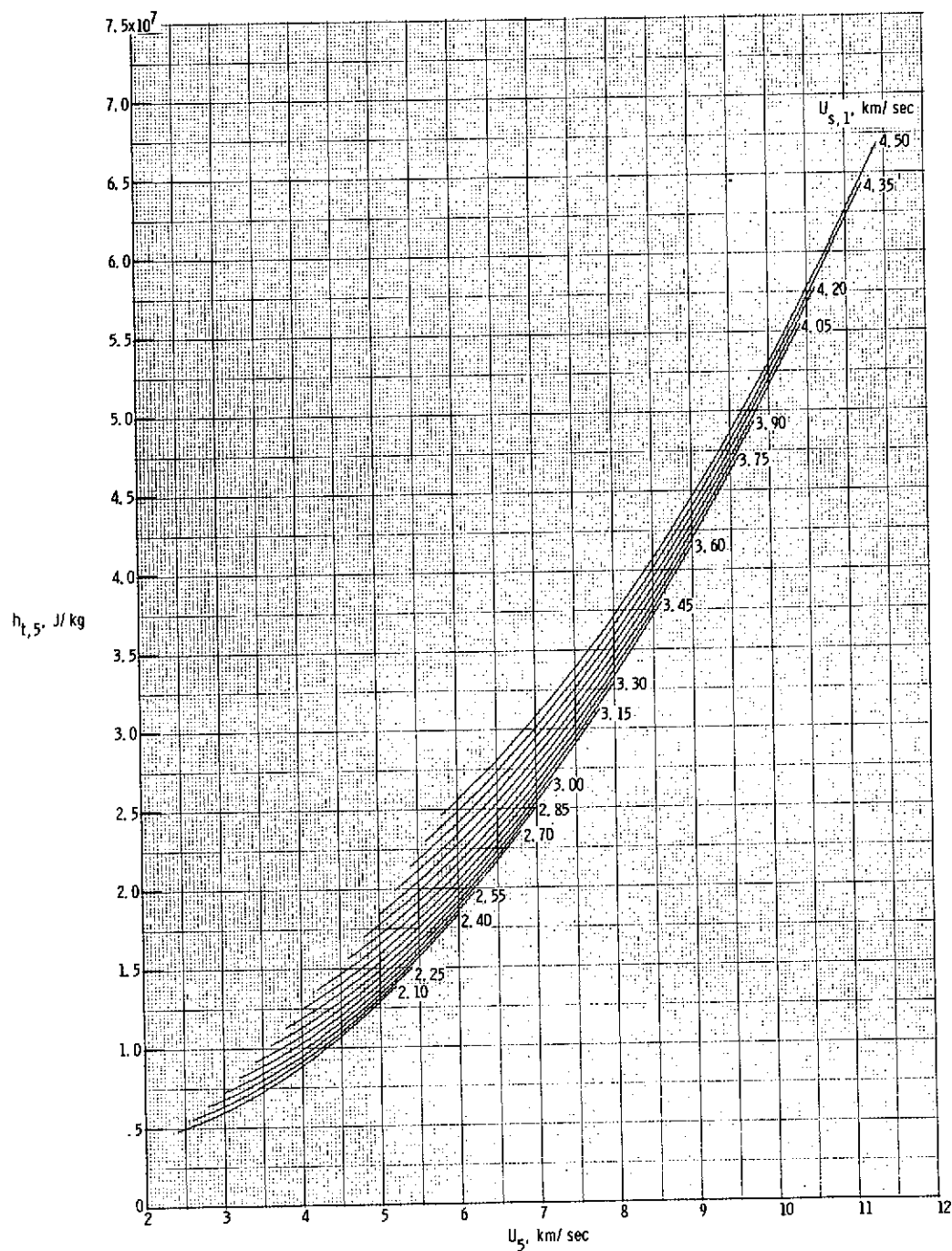
(h) Stagnation density behind normal bow shock.

Figure 10.- Continued.



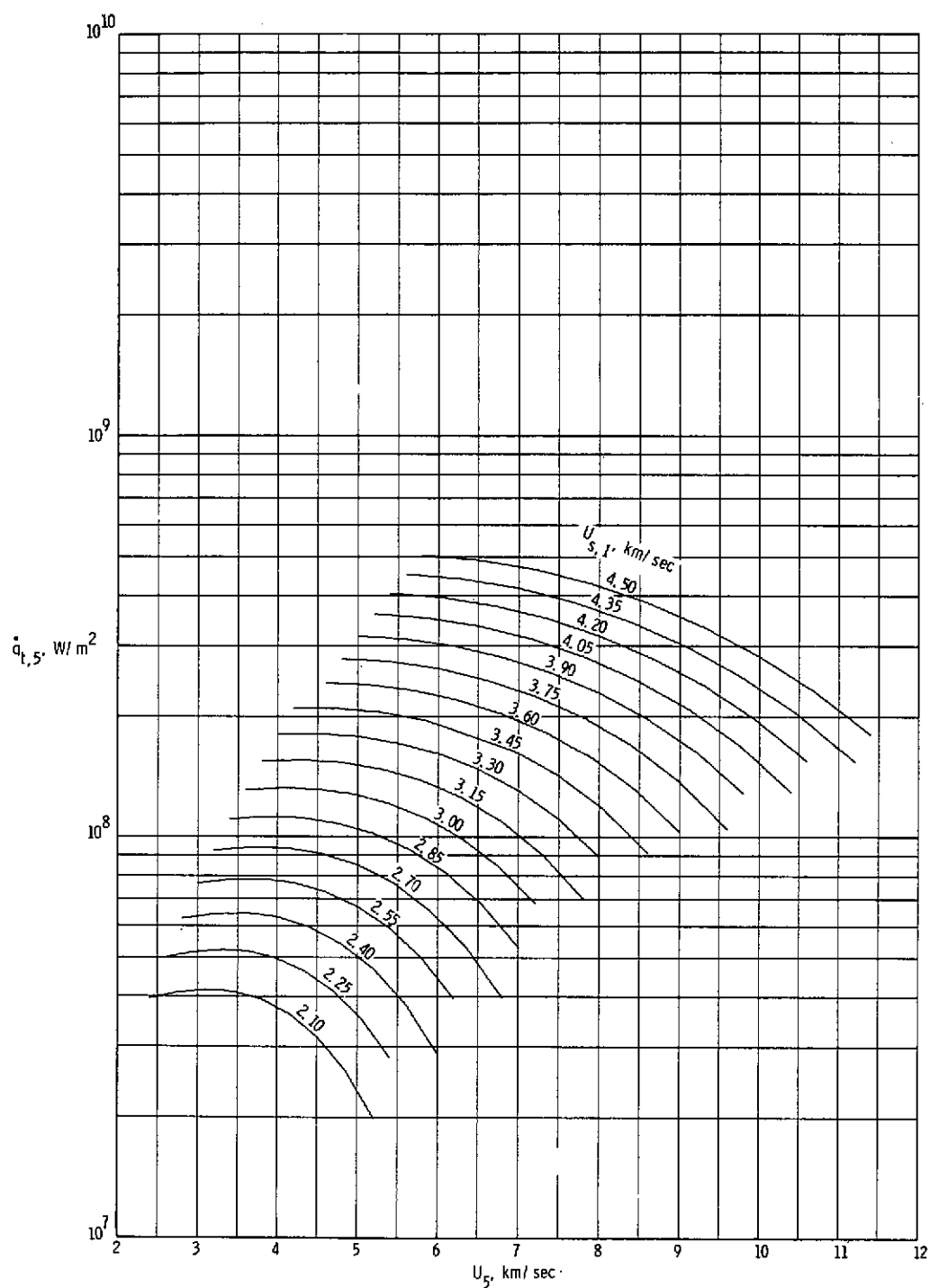
(i) Stagnation temperature behind normal bow shock.

Figure 10.- Continued.



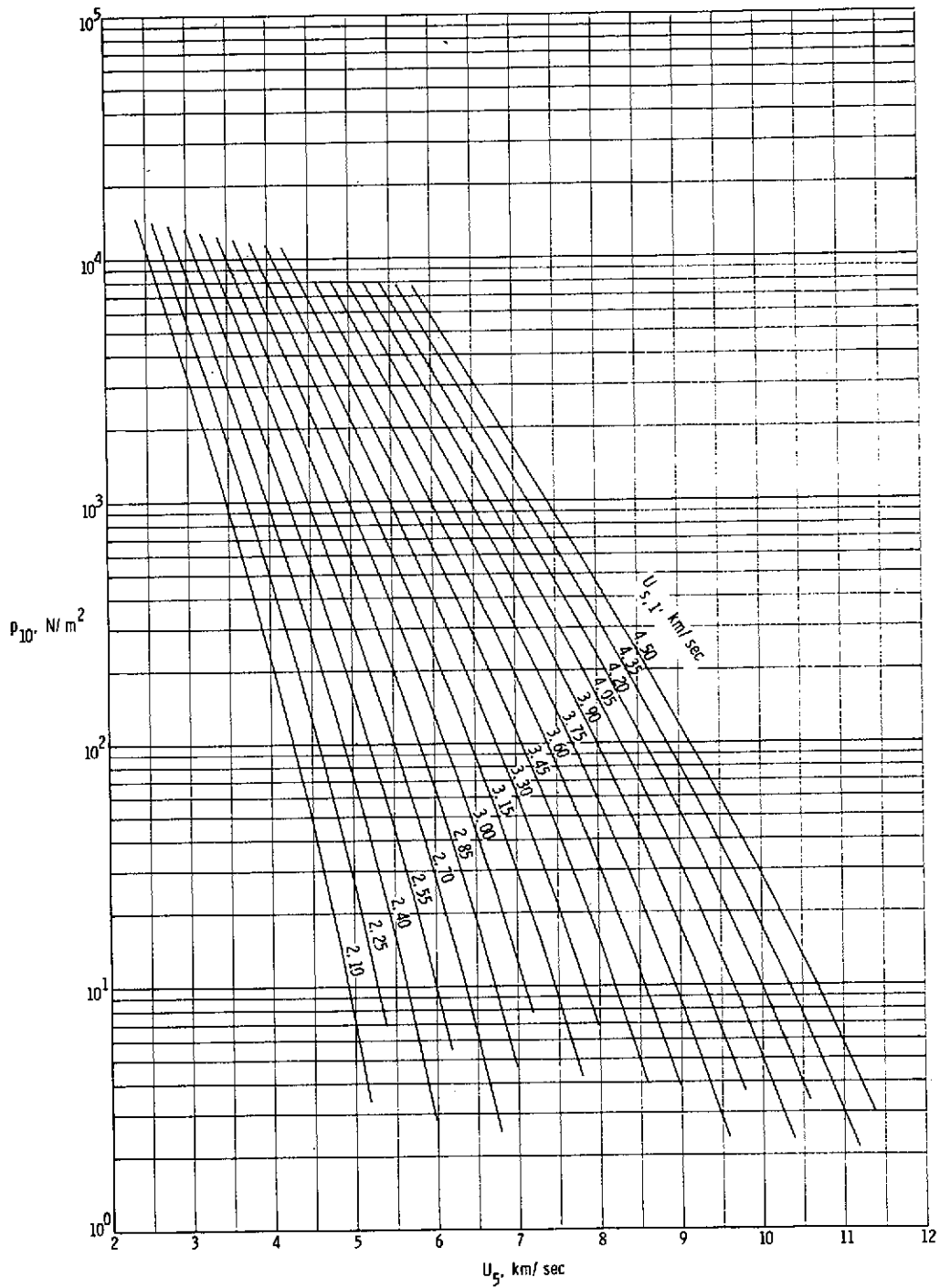
(j) Stagnation enthalpy behind normal bow shock.

Figure 10.- Continued.



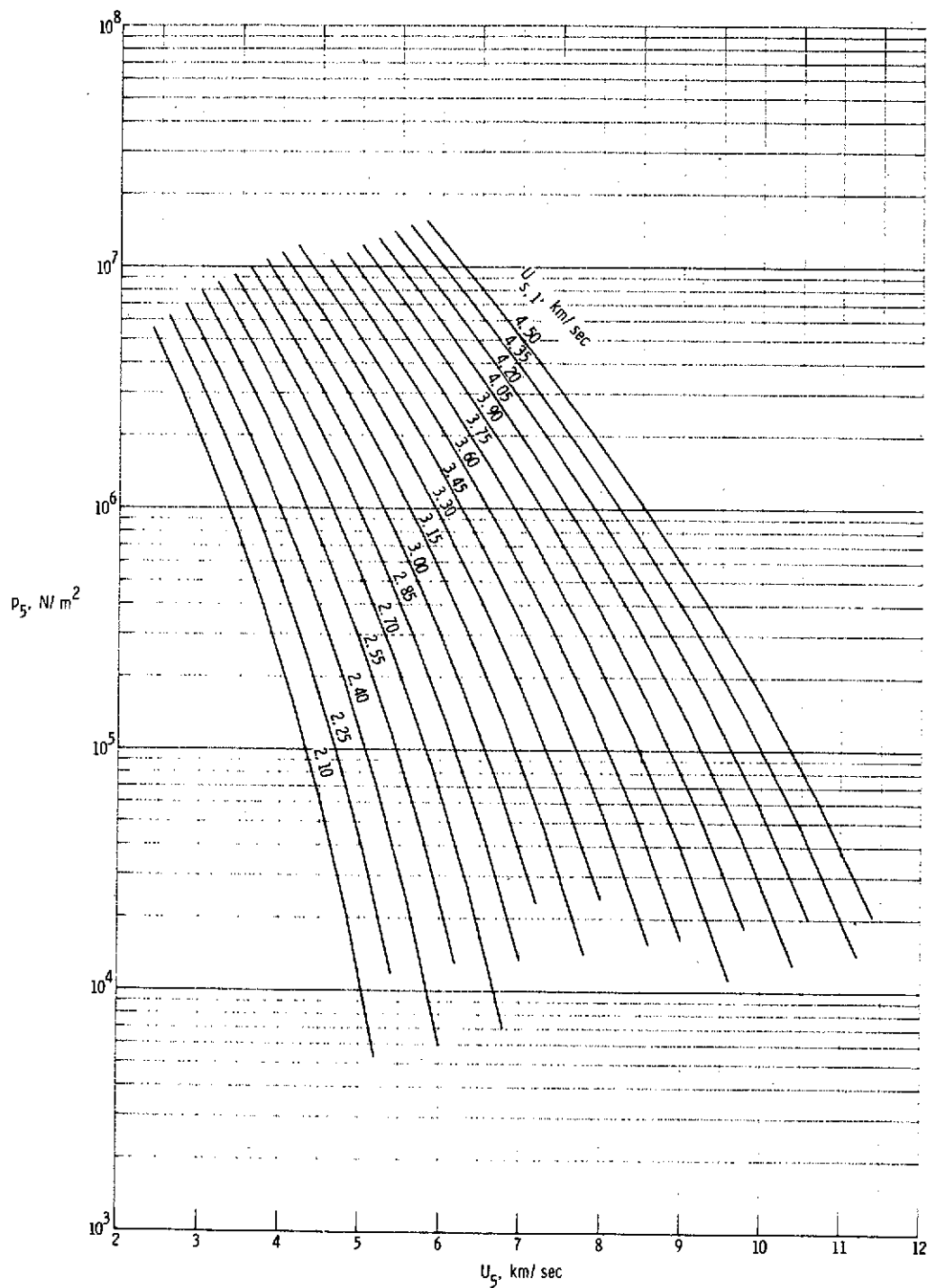
(k) Stagnation-point convective heat-transfer rate to sphere having radius of 2.54 cm.

Figure 10.- Continued.



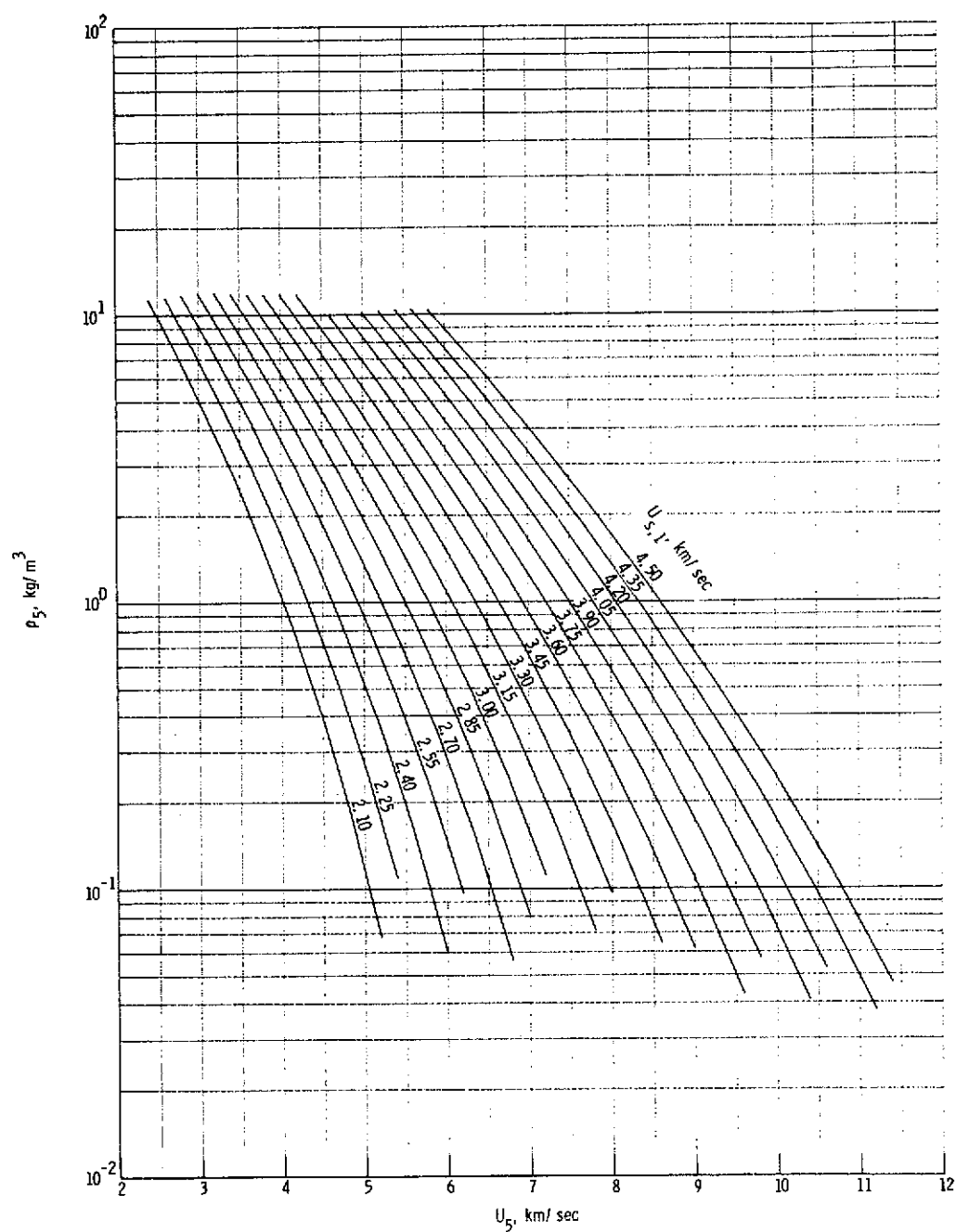
(1) Quiescent acceleration air pressure in region (10).

Figure 10.- Concluded.



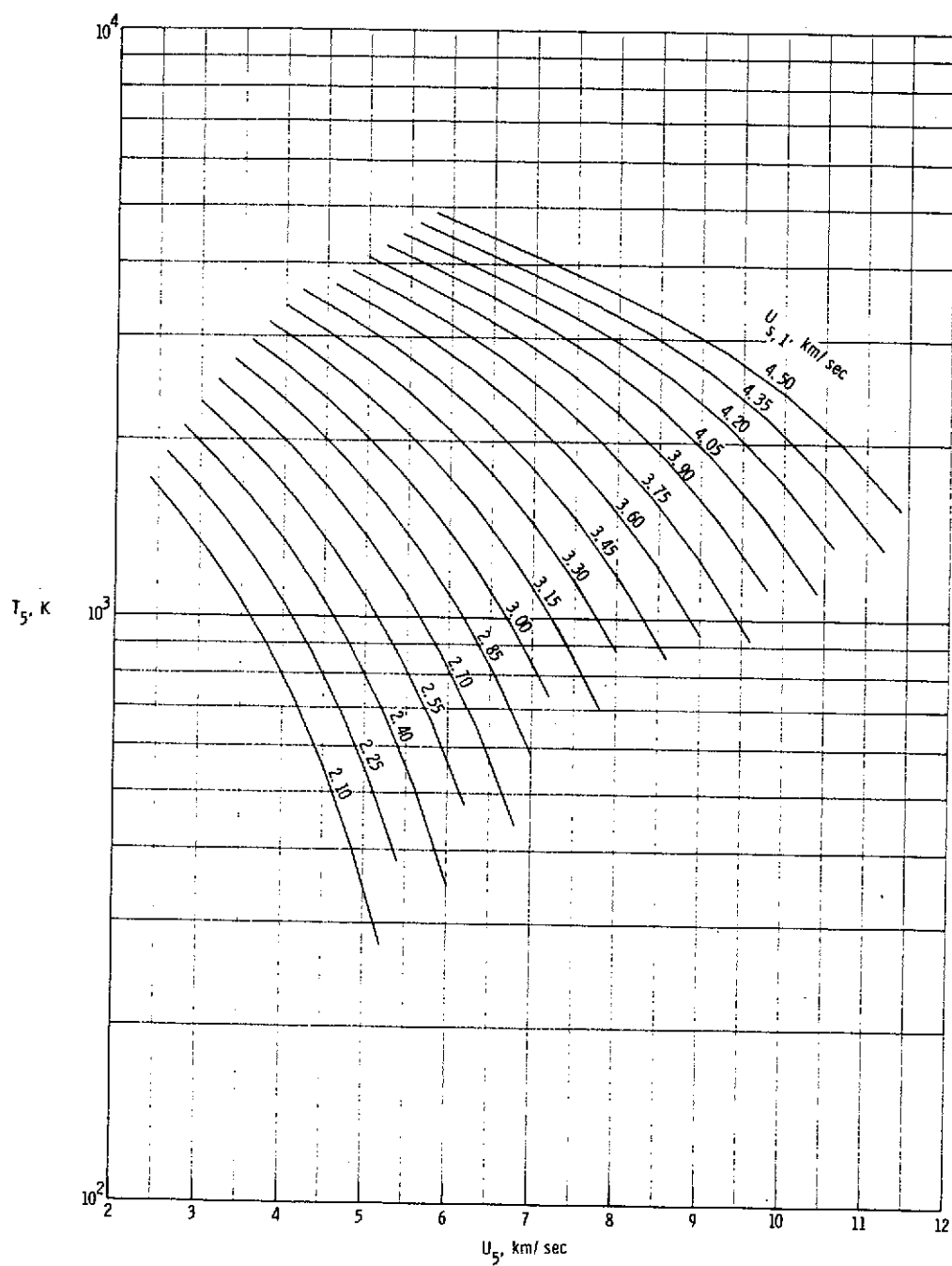
(a) Static pressure in region (5).

Figure 11.- Various expansion tube flow parameters for real air in thermochemical equilibrium as a function of flow velocity and assuming no shock reflection at secondary diaphragm. $p_1 = 344.74 \text{ kN/m}^2$.



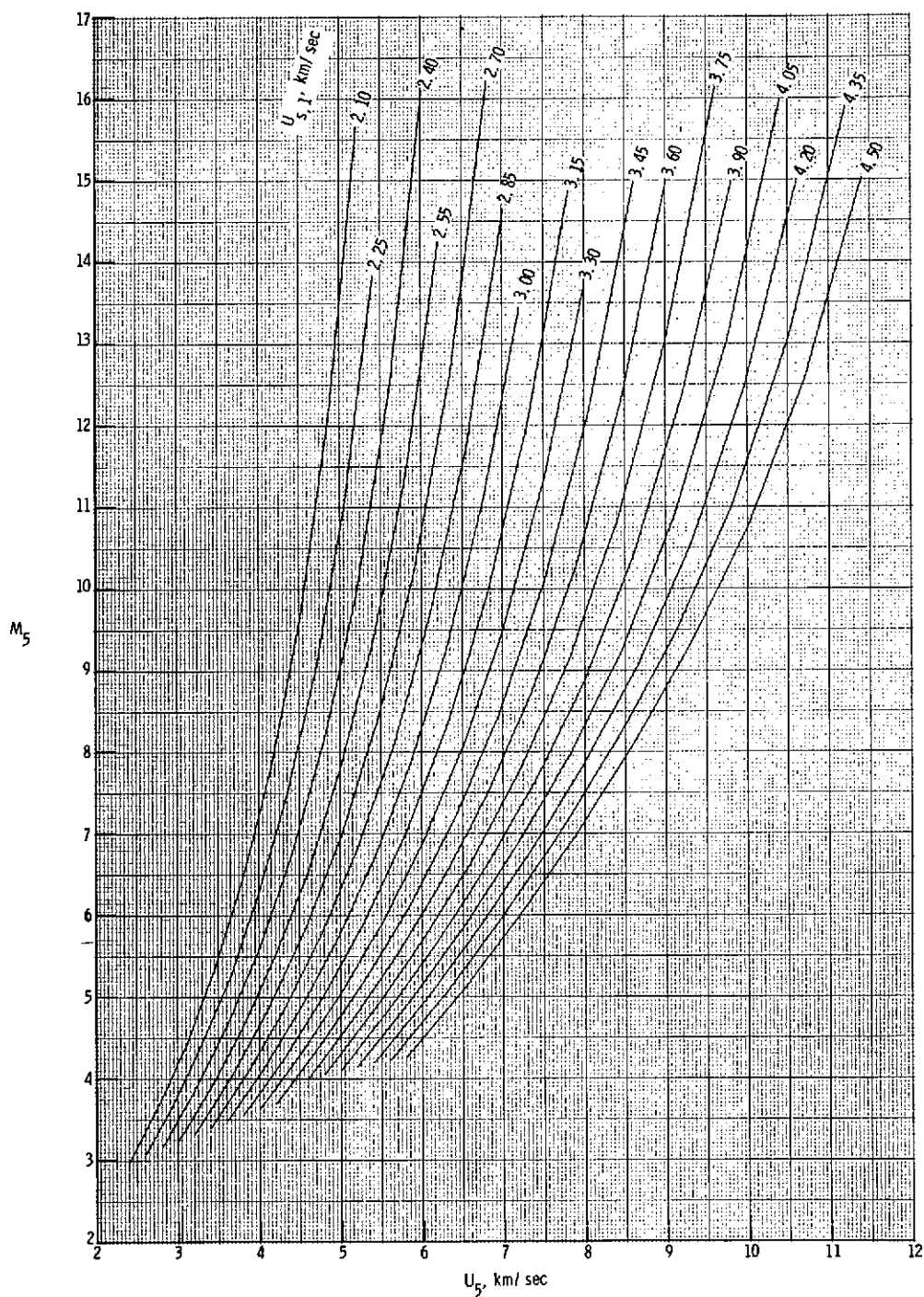
(b) Static density in region (5).

Figure 11.- Continued.



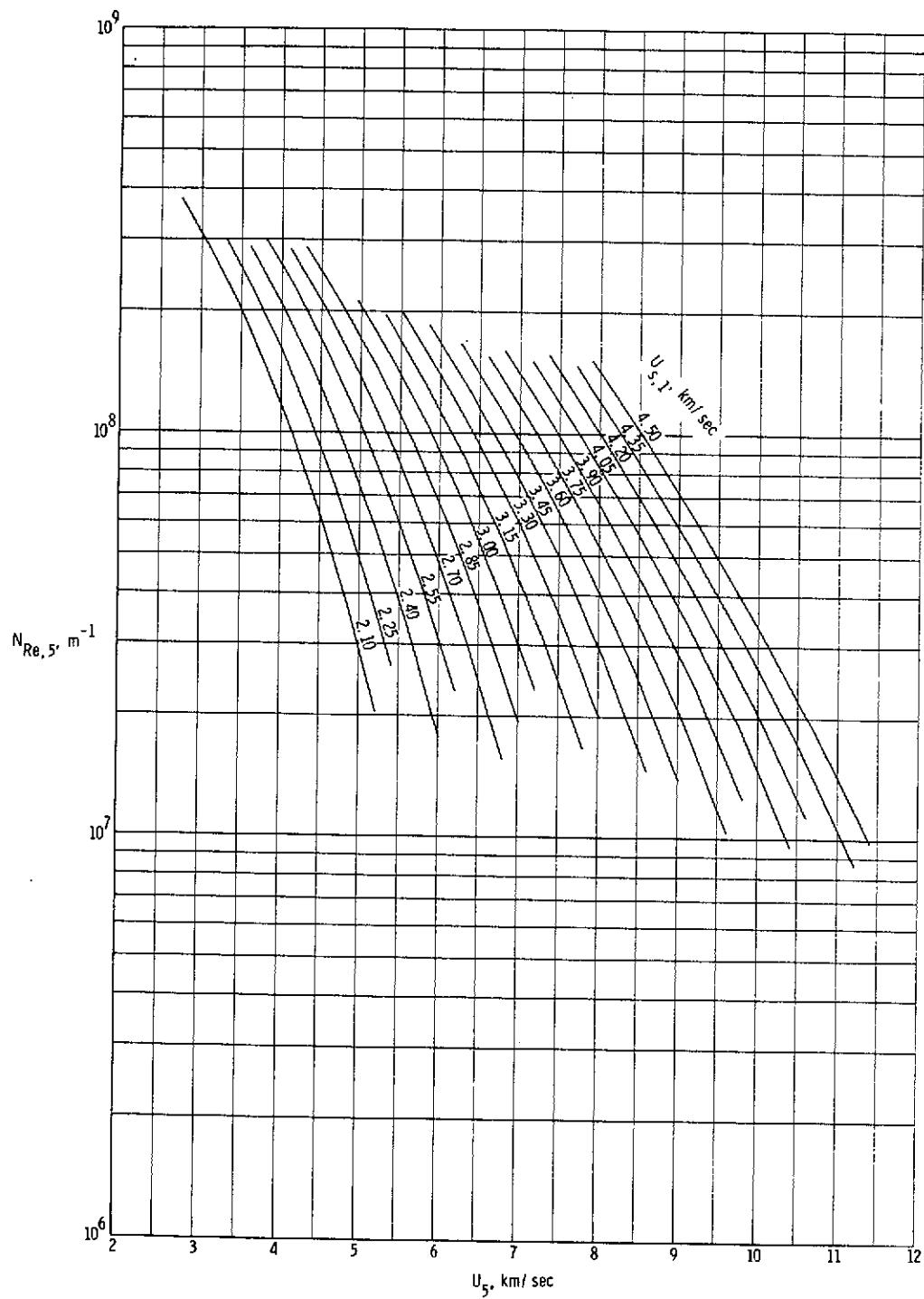
(c) Static temperature in region (5).

Figure 11.- Continued.



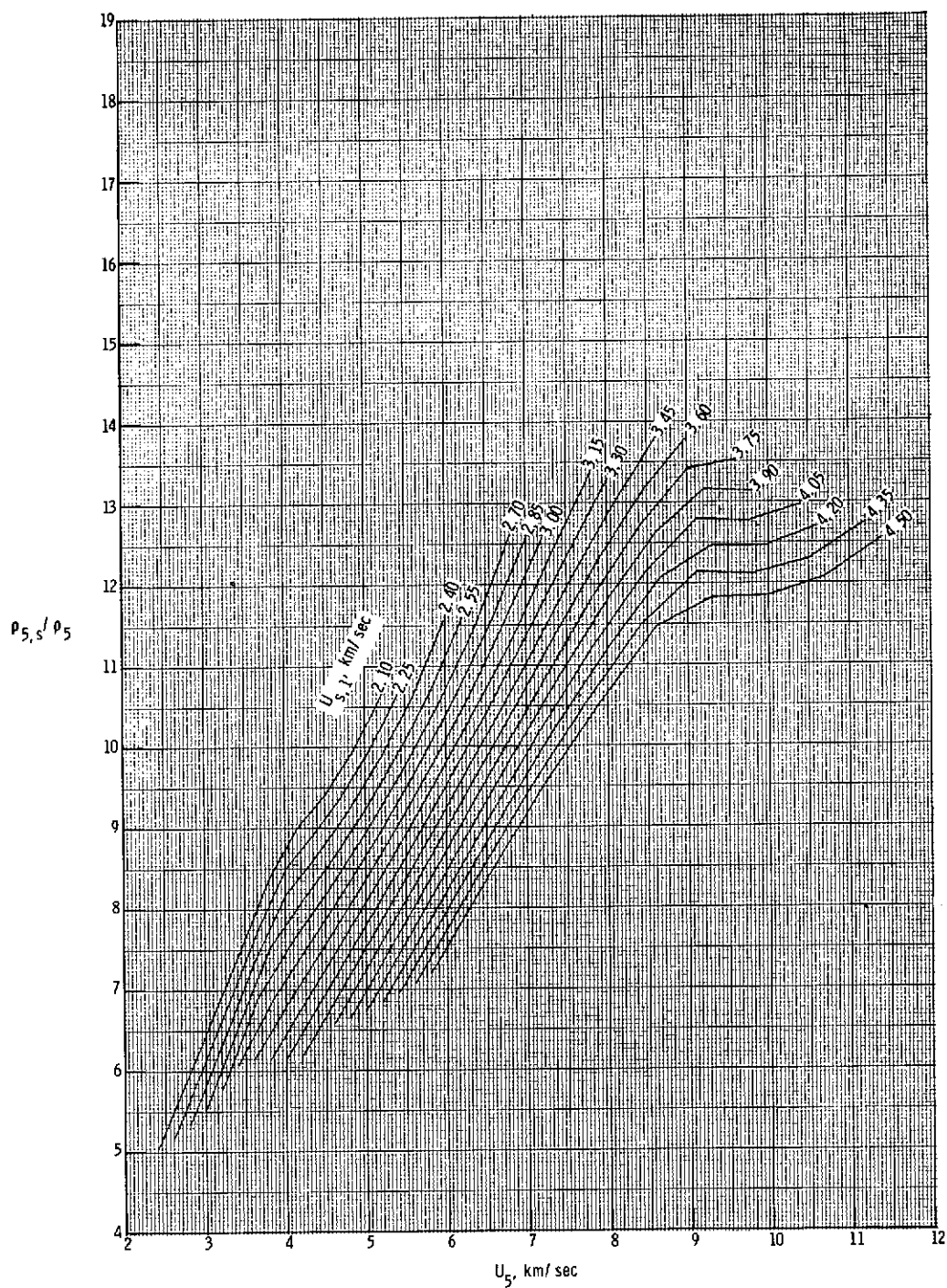
(d) Mach number in region (5).

Figure 11.- Continued.



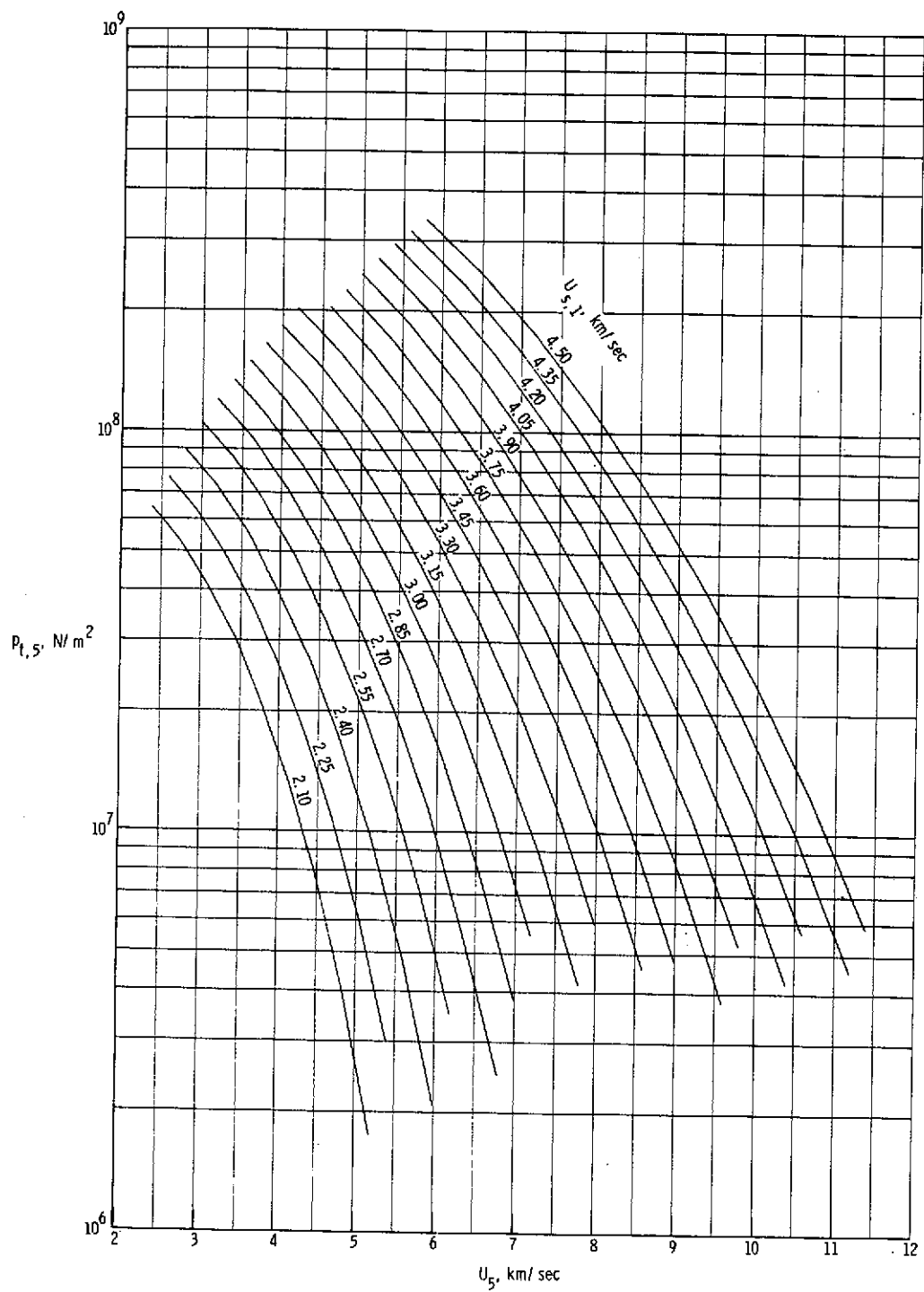
(e) Unit Reynolds number in region (5).

Figure 11.- Continued.



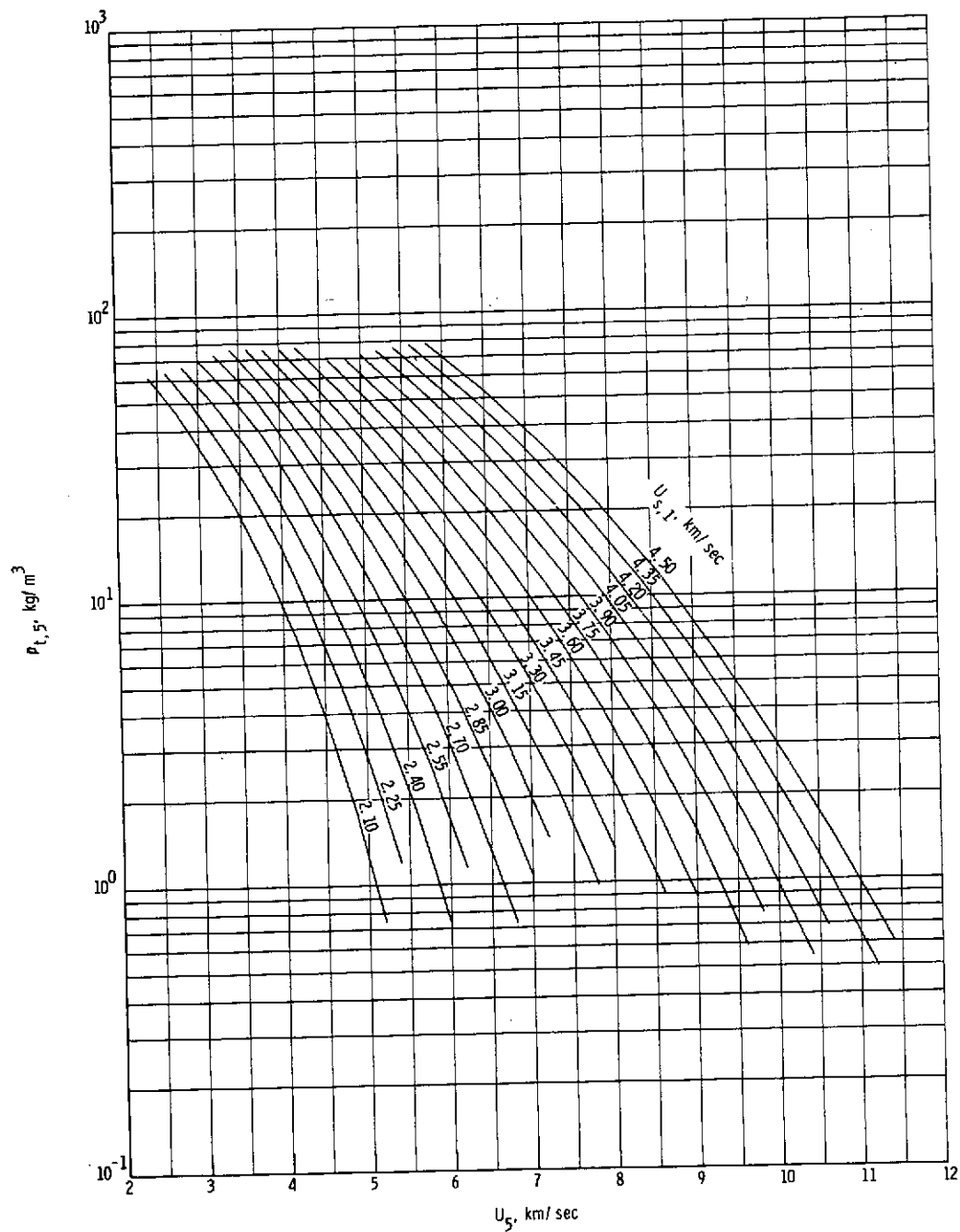
(f) Normal shock density ratio.

Figure 11.- Continued.



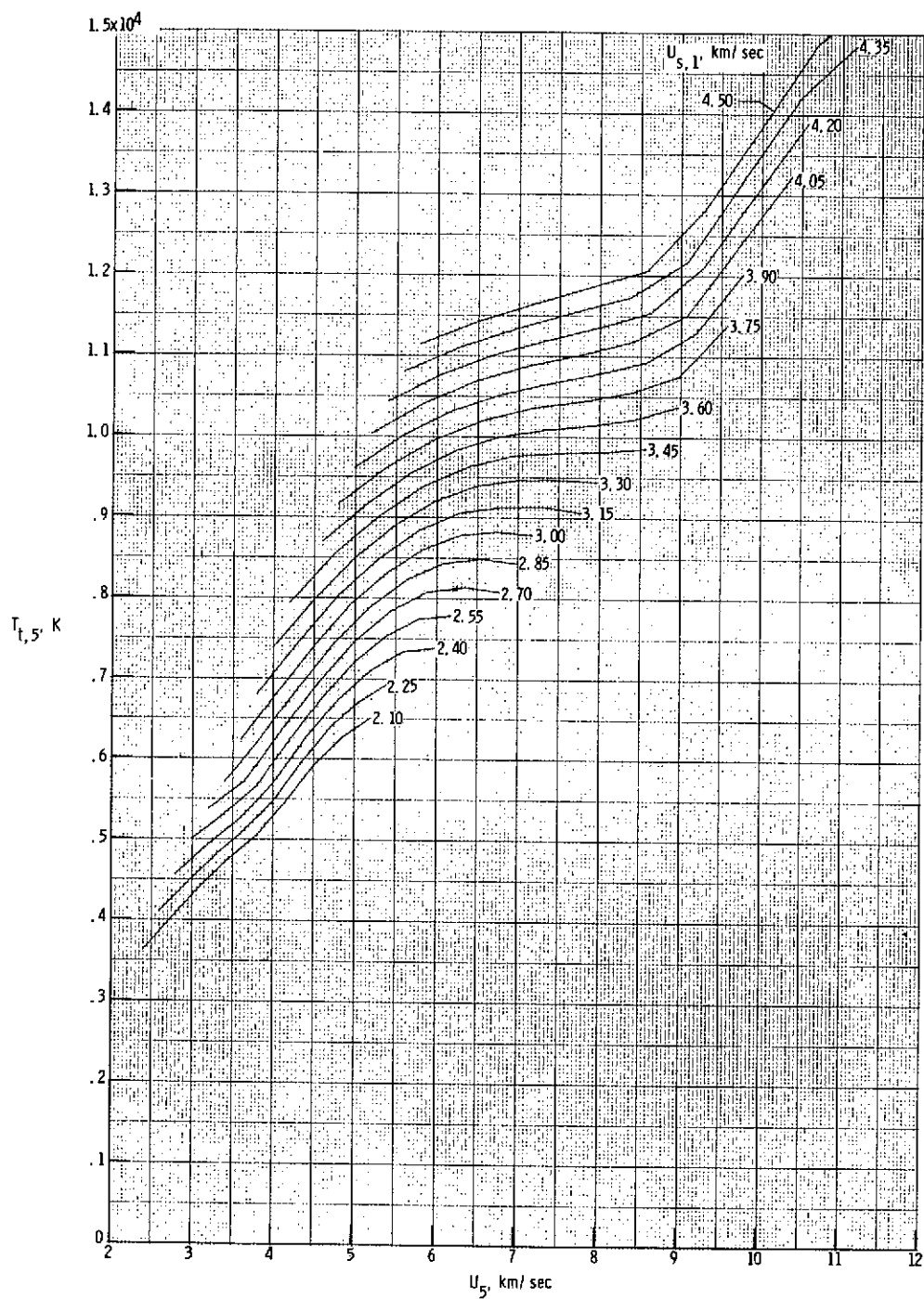
(g) Stagnation pressure behind normal bow shock.

Figure 11.- Continued.



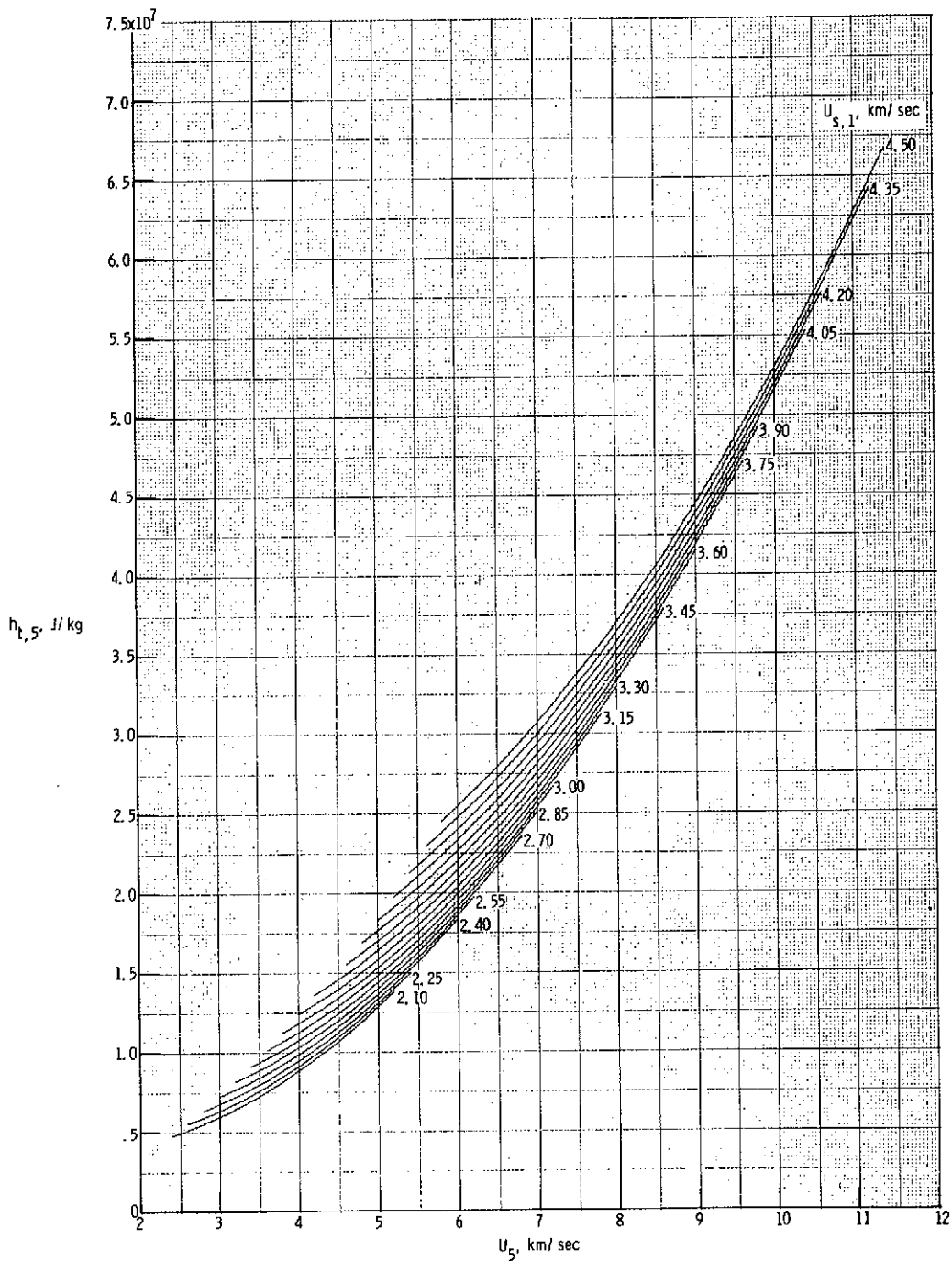
(h) Stagnation density behind normal bow shock.

Figure 11.- Continued.



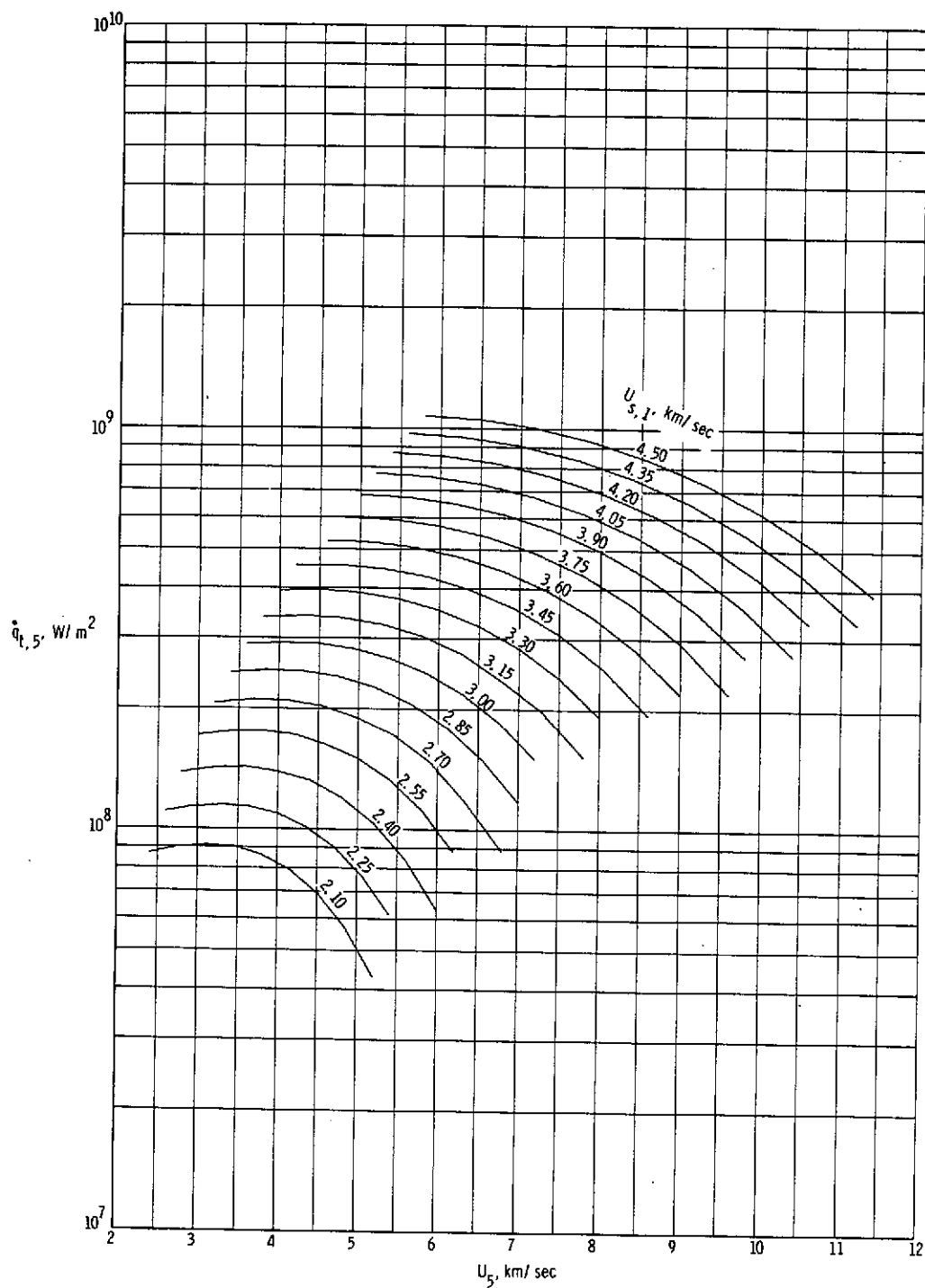
(i) Stagnation temperature behind normal bow shock.

Figure 11.- Continued.



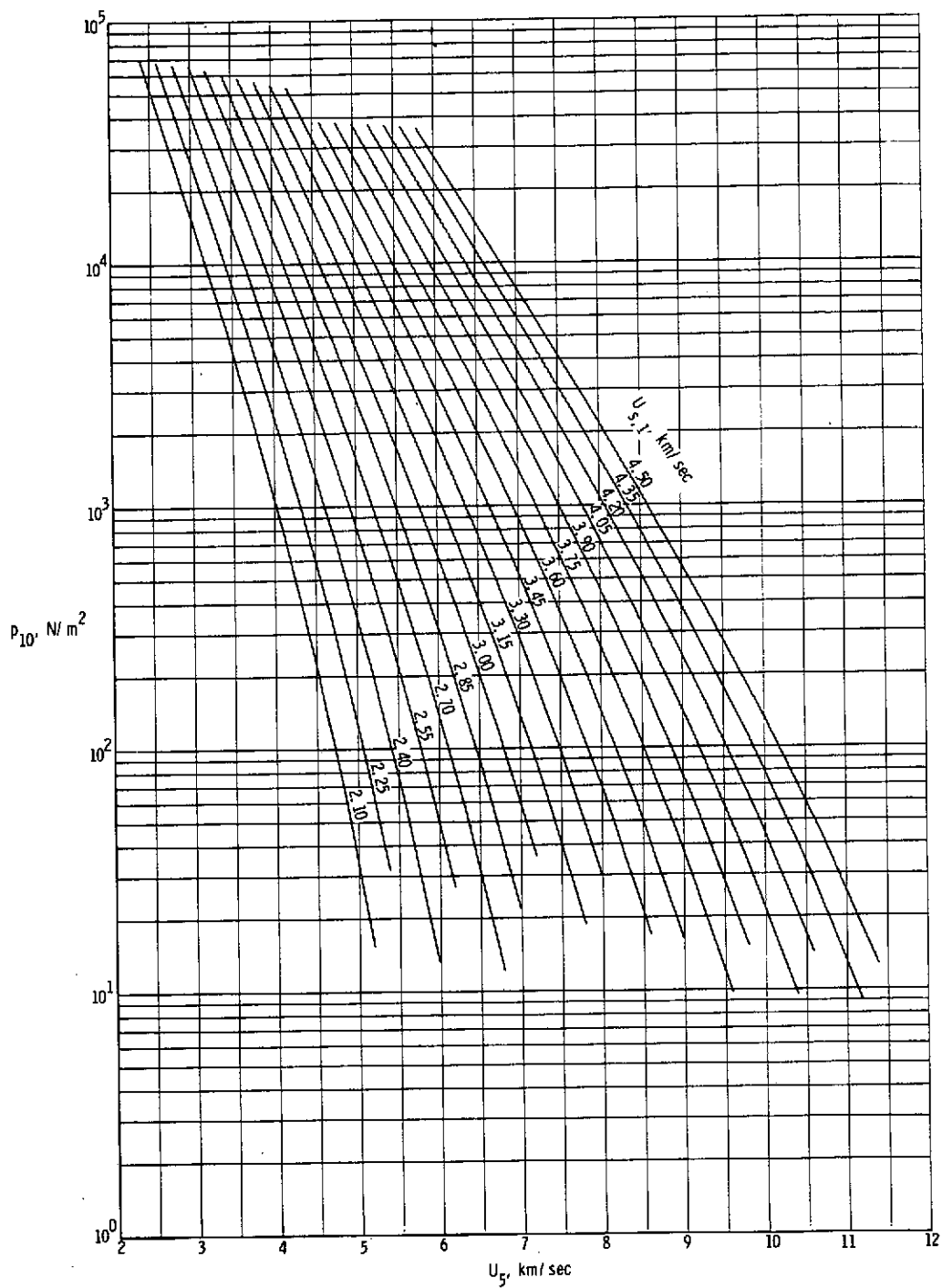
(j) Stagnation enthalpy behind normal bow shock.

Figure 11.- Continued.



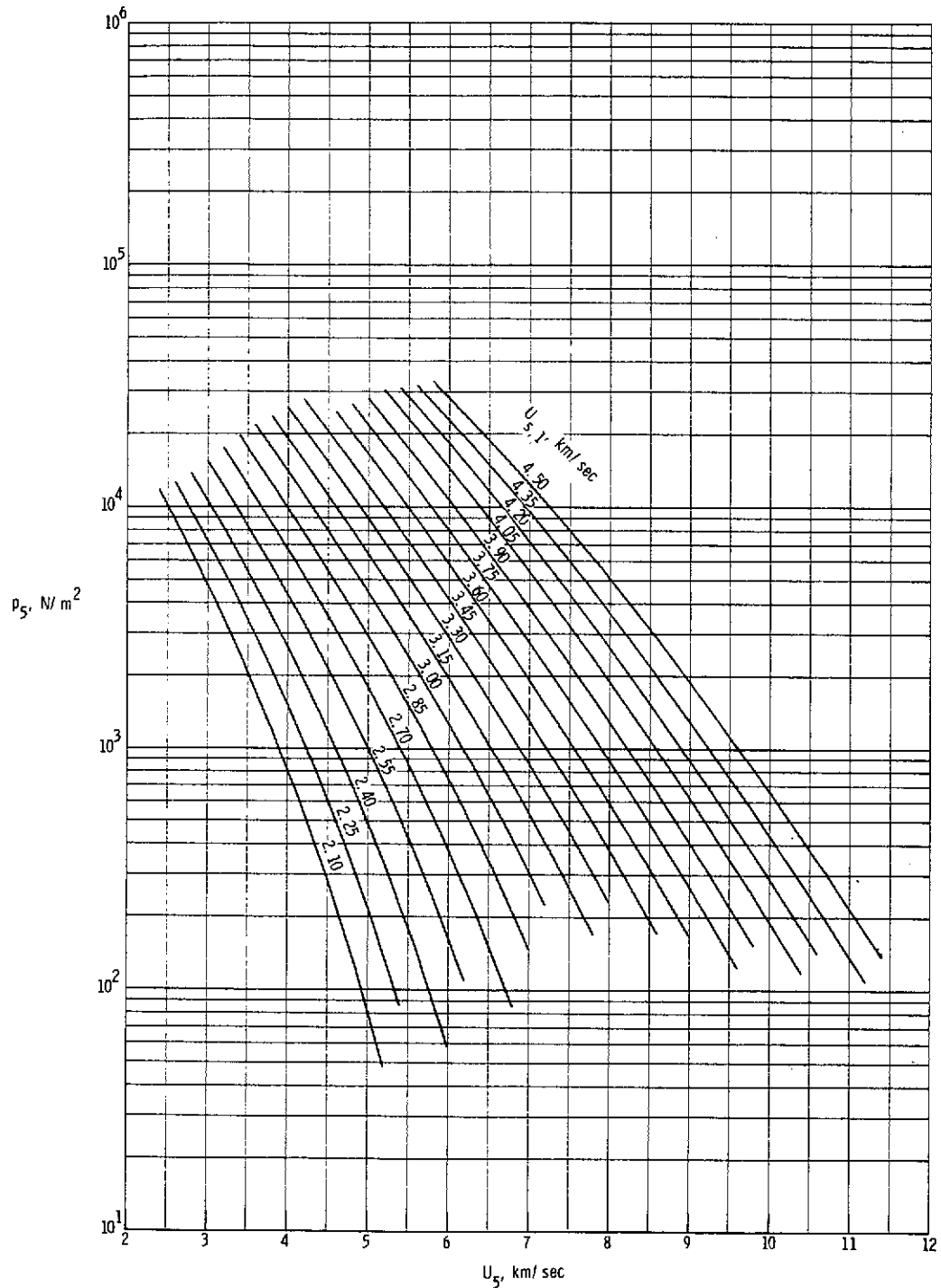
(k) Stagnation-point convective heat-transfer rate to sphere having radius of 2.54 cm.

Figure 11.- Continued.



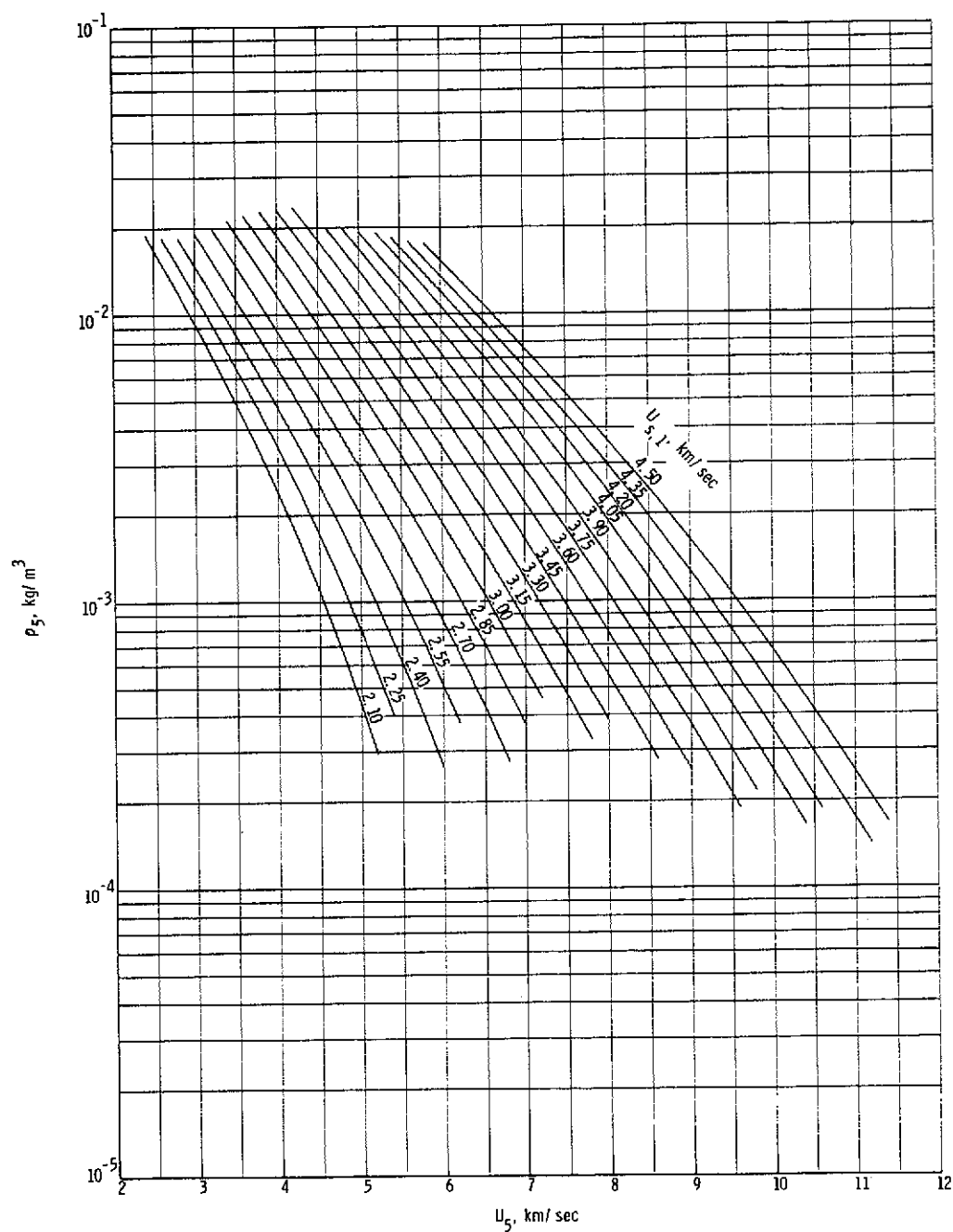
(1) Quiescent acceleration air pressure in region (10).

Figure 11.- Concluded.



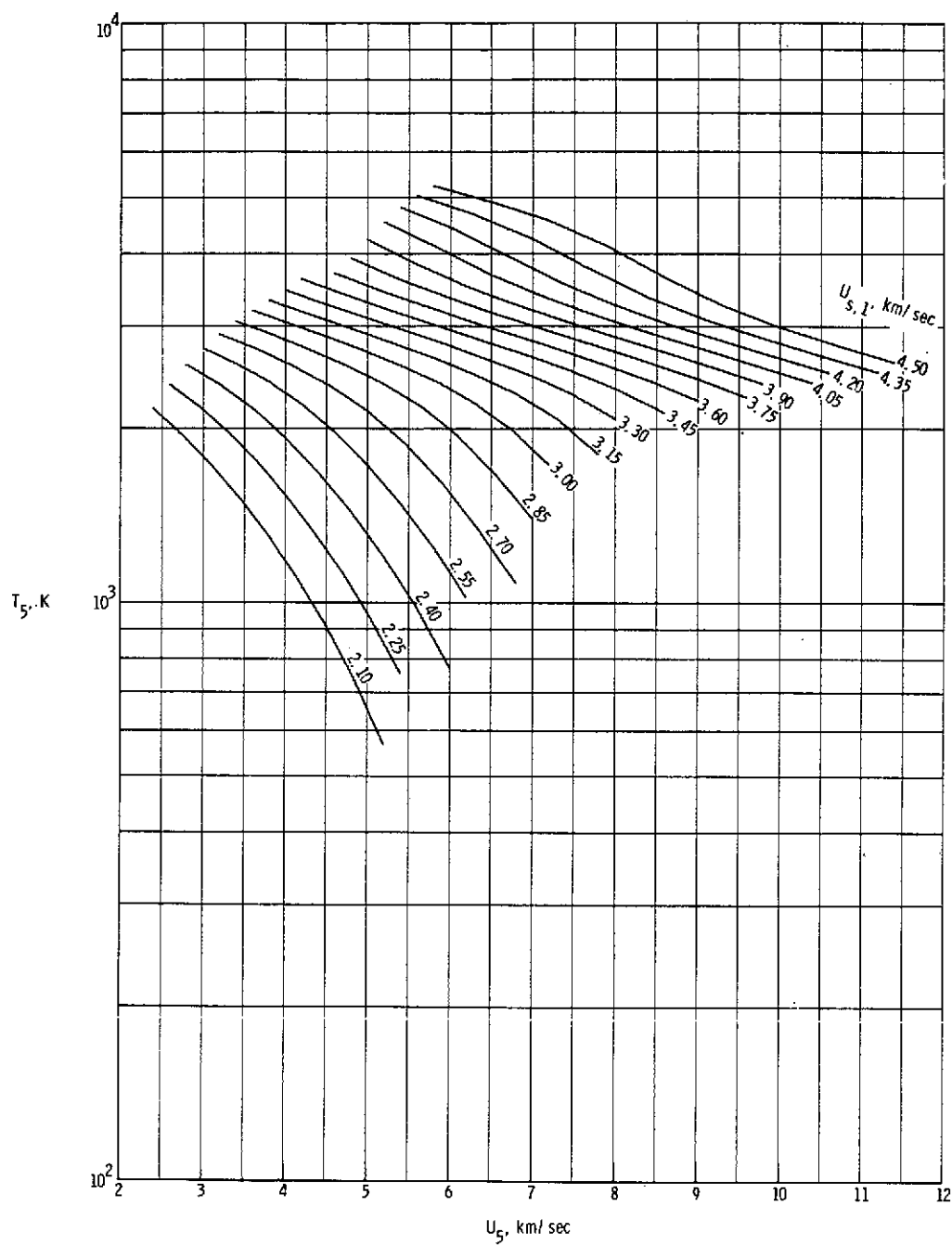
(a) Static pressure in region (5).

Figure 12.- Various expansion tube flow parameters for real air in thermochemical equilibrium as a function of flow velocity and assuming a totally reflected shock at the secondary diaphragm. $p_1 = 689.5 \text{ N/m}^2$.



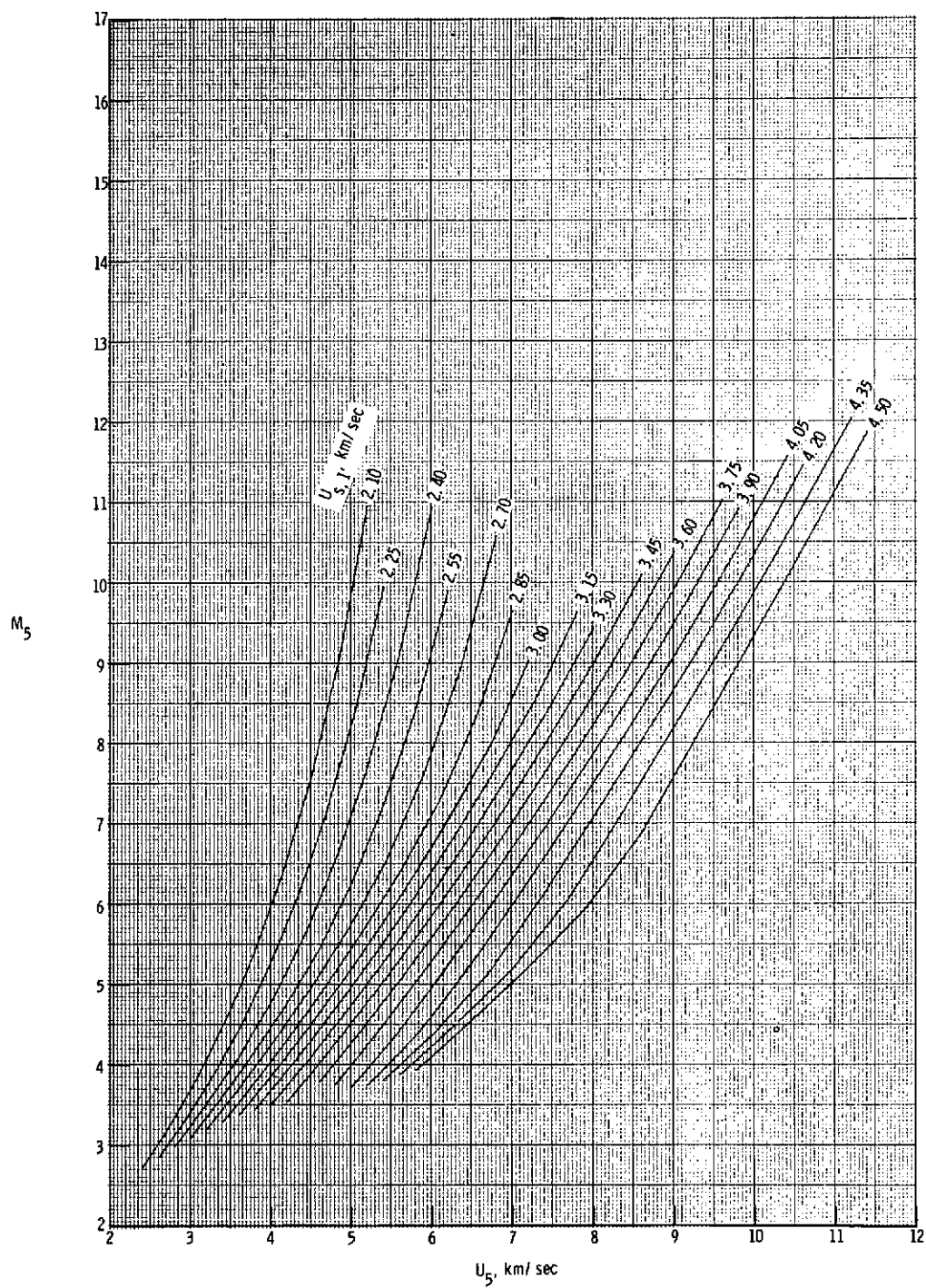
(b) Static density in region ⑤.

Figure 12.- Continued.



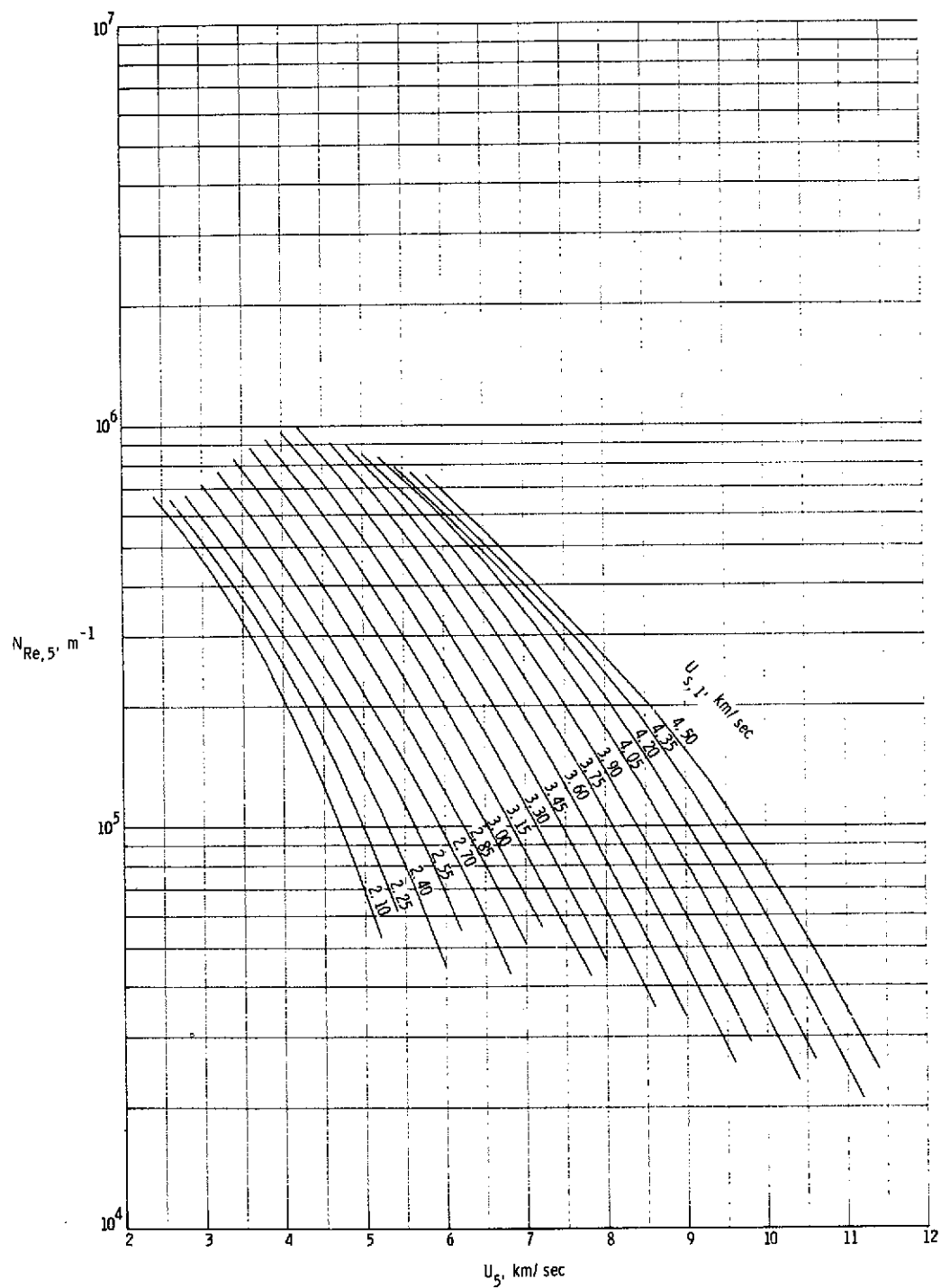
(c) Static temperature in region (5).

Figure 12.- Continued.



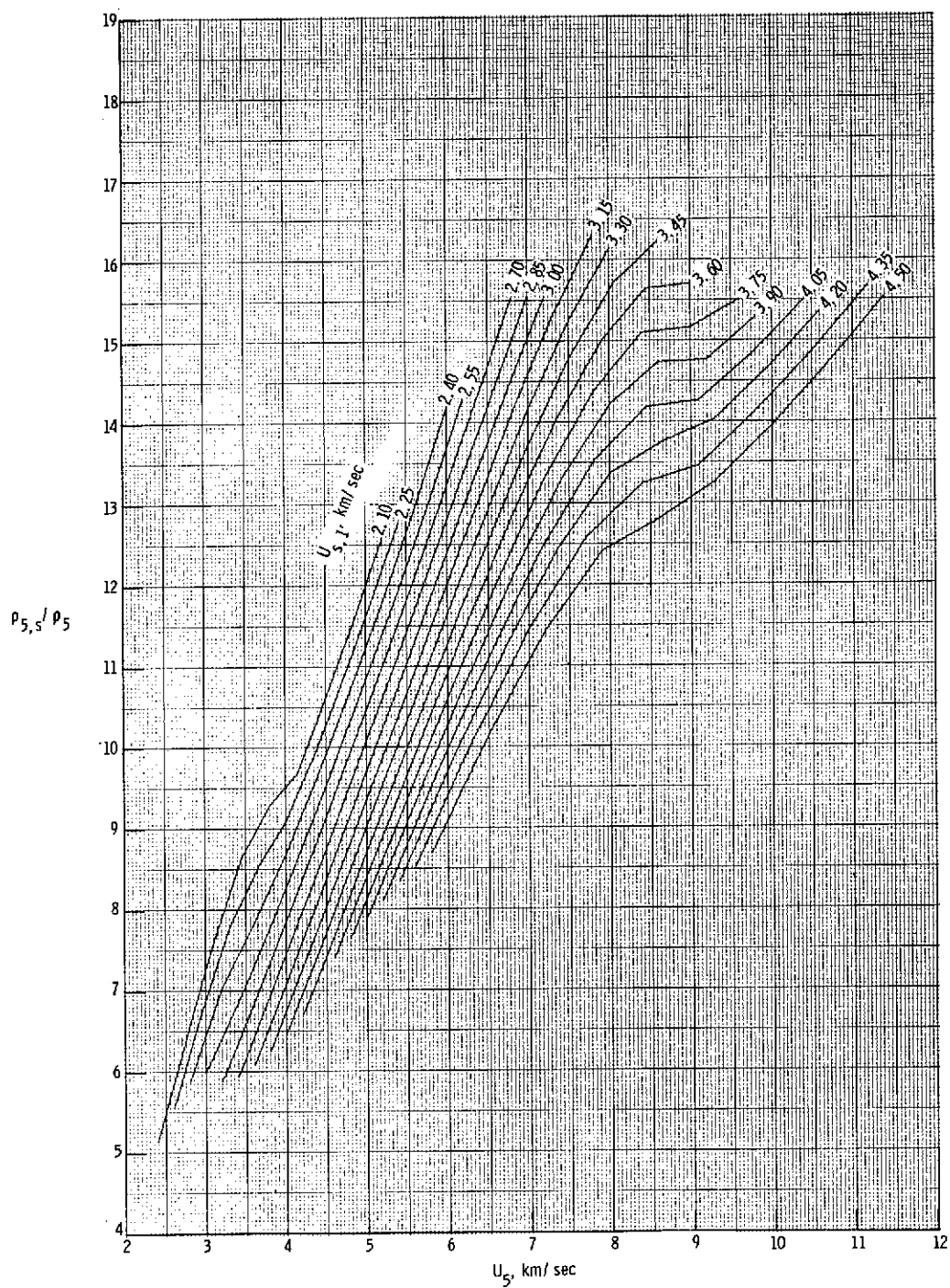
(d) Mach number in region ⑤.

Figure 12.- Continued.



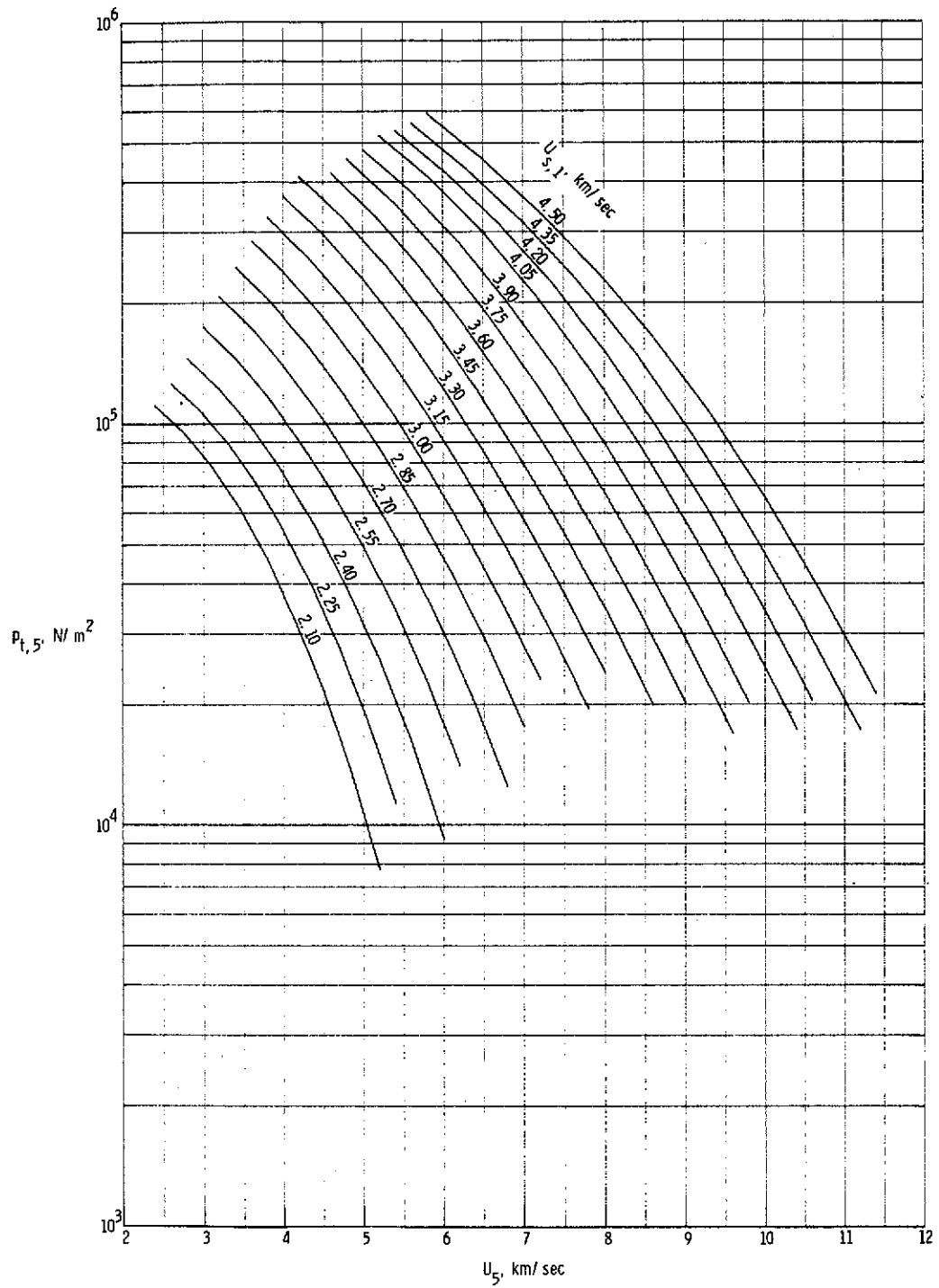
(e) Unit Reynolds number in region (5).

Figure 12.- Continued.



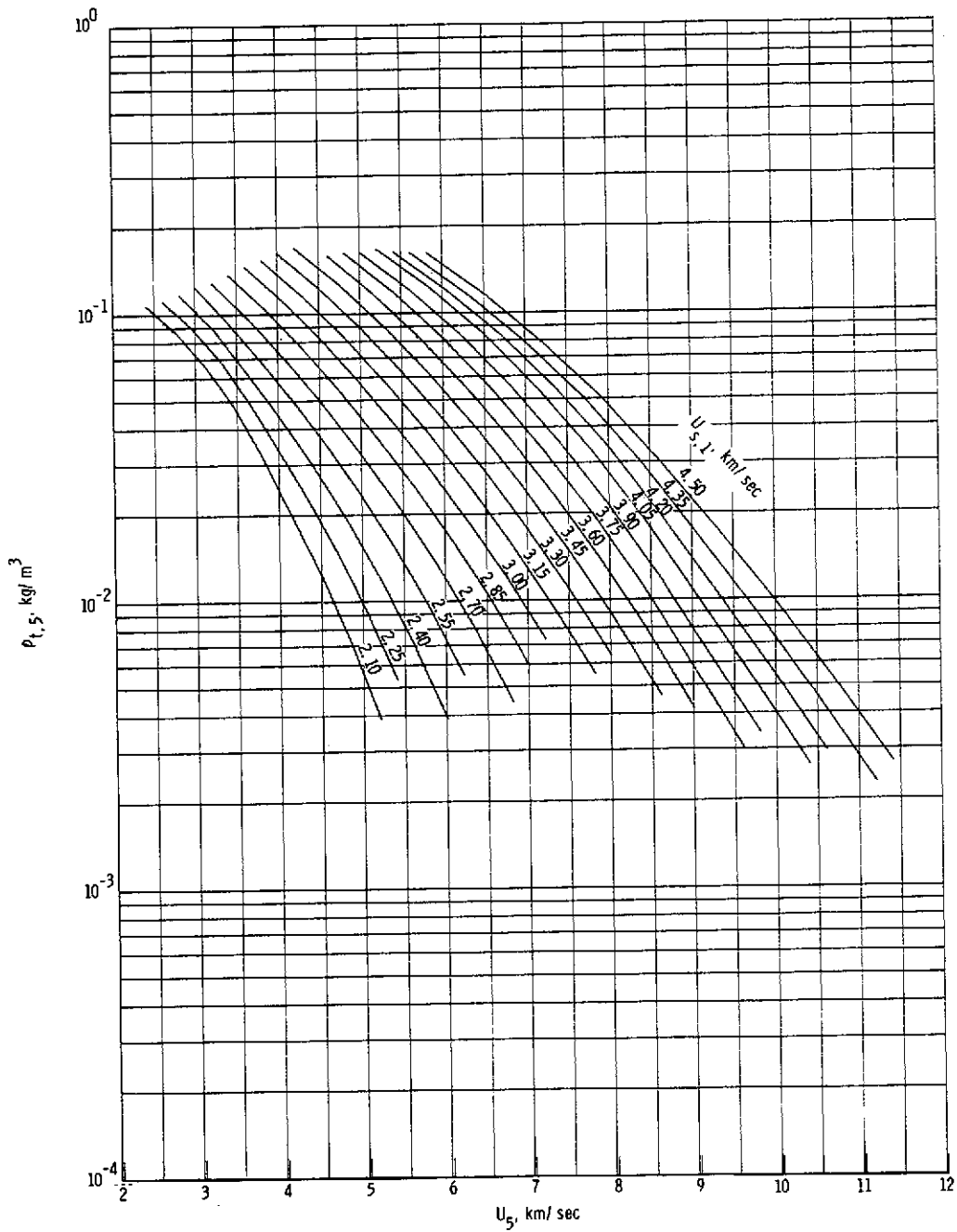
(f) Normal shock density ratio.

Figure 12.- Continued.



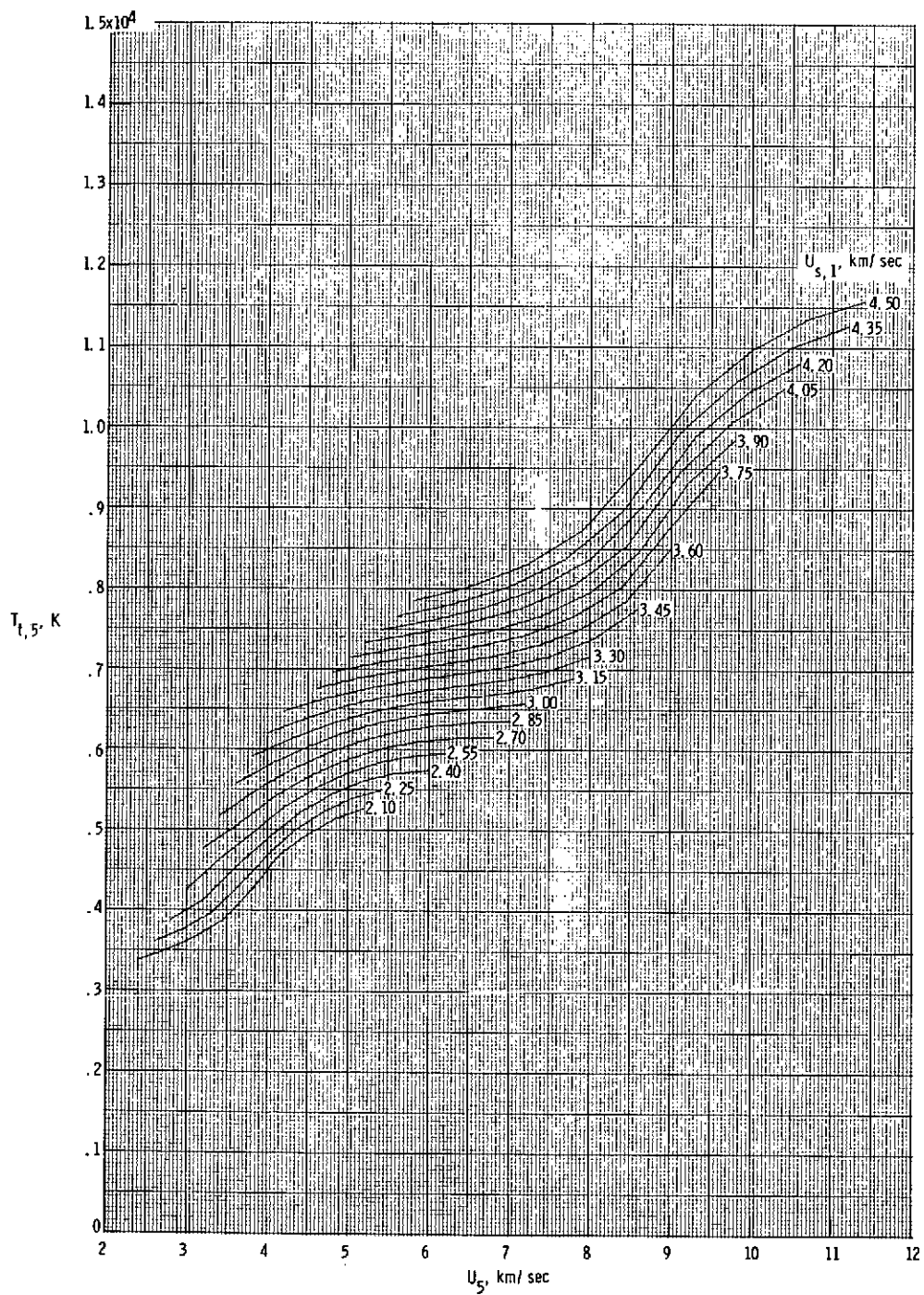
(g) Stagnation pressure behind normal bow shock.

Figure 12.- Continued.



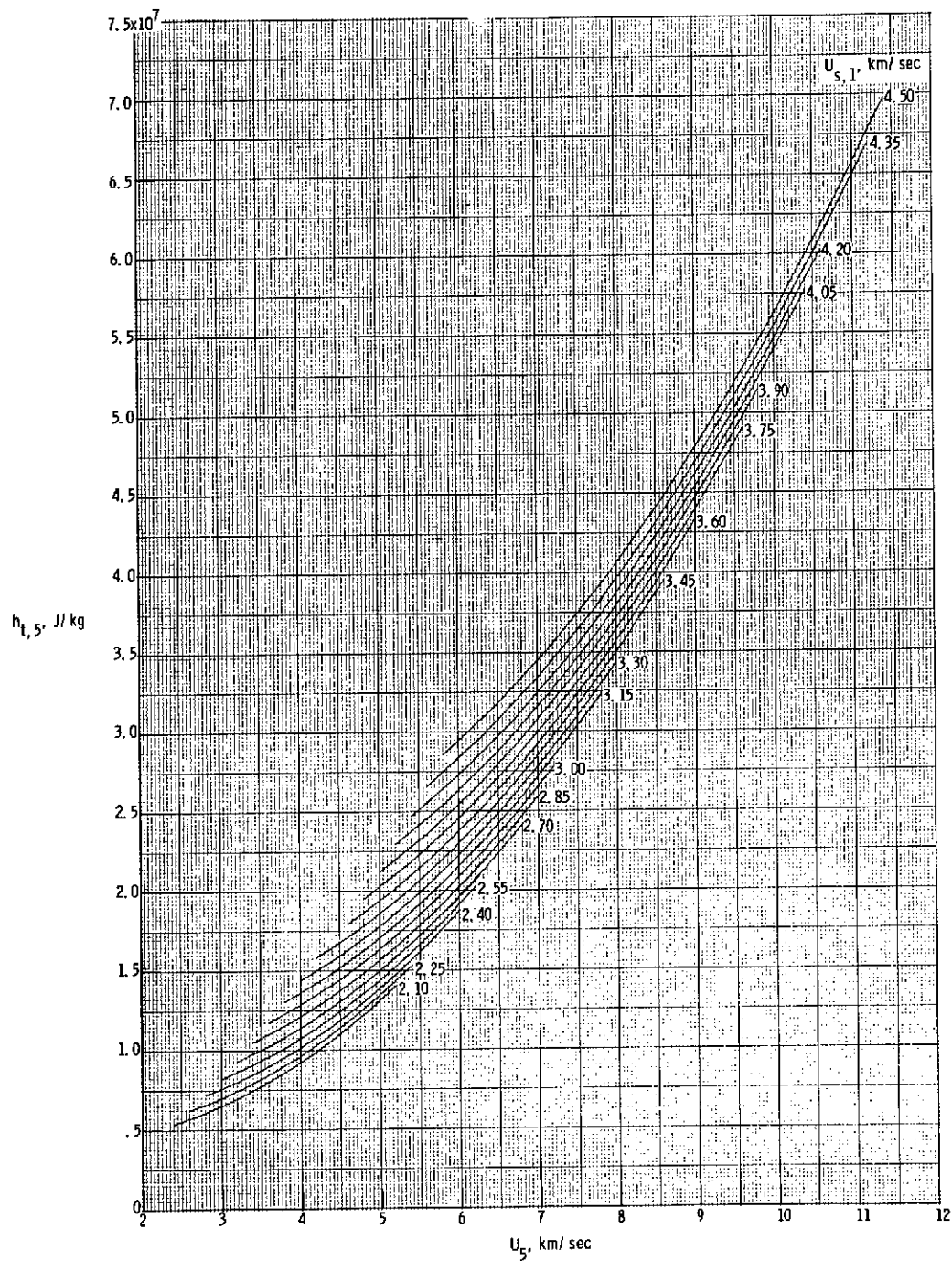
(h) Stagnation density behind normal bow shock.

Figure 12.- Continued.



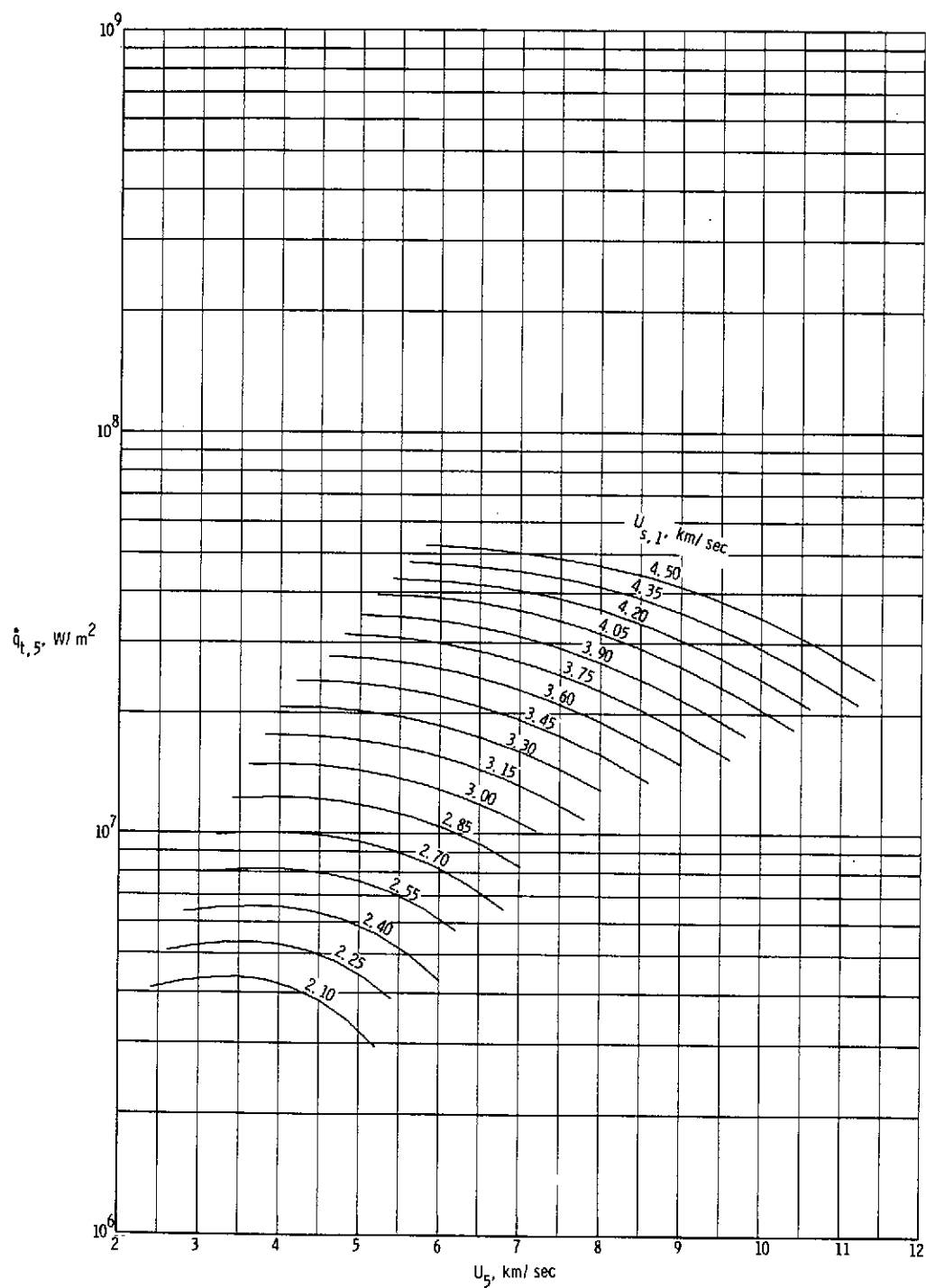
(i) Stagnation temperature behind normal bow shock.

Figure 12.- Continued.



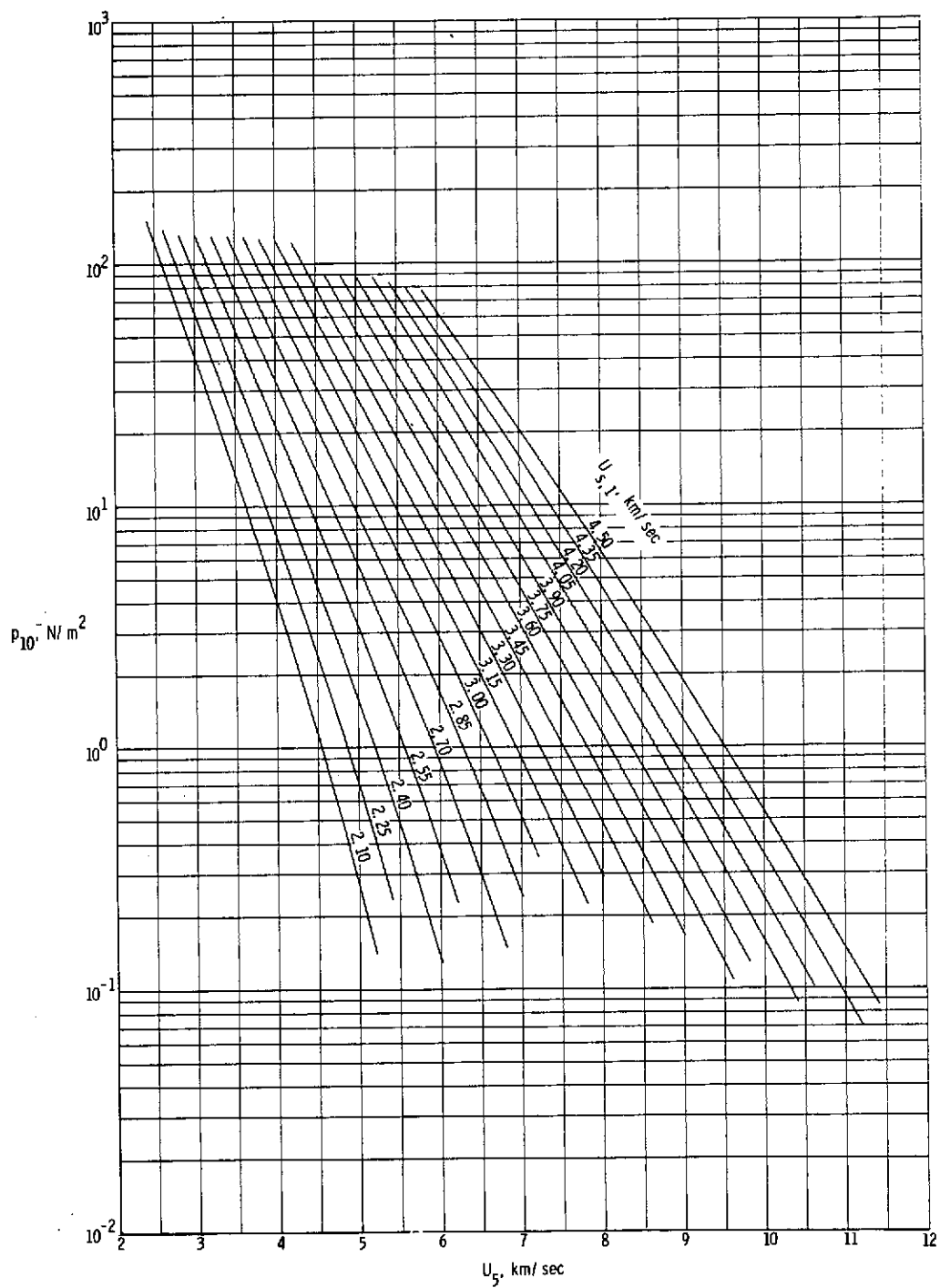
(j) Stagnation enthalpy behind normal bow shock.

Figure 12.- Continued.



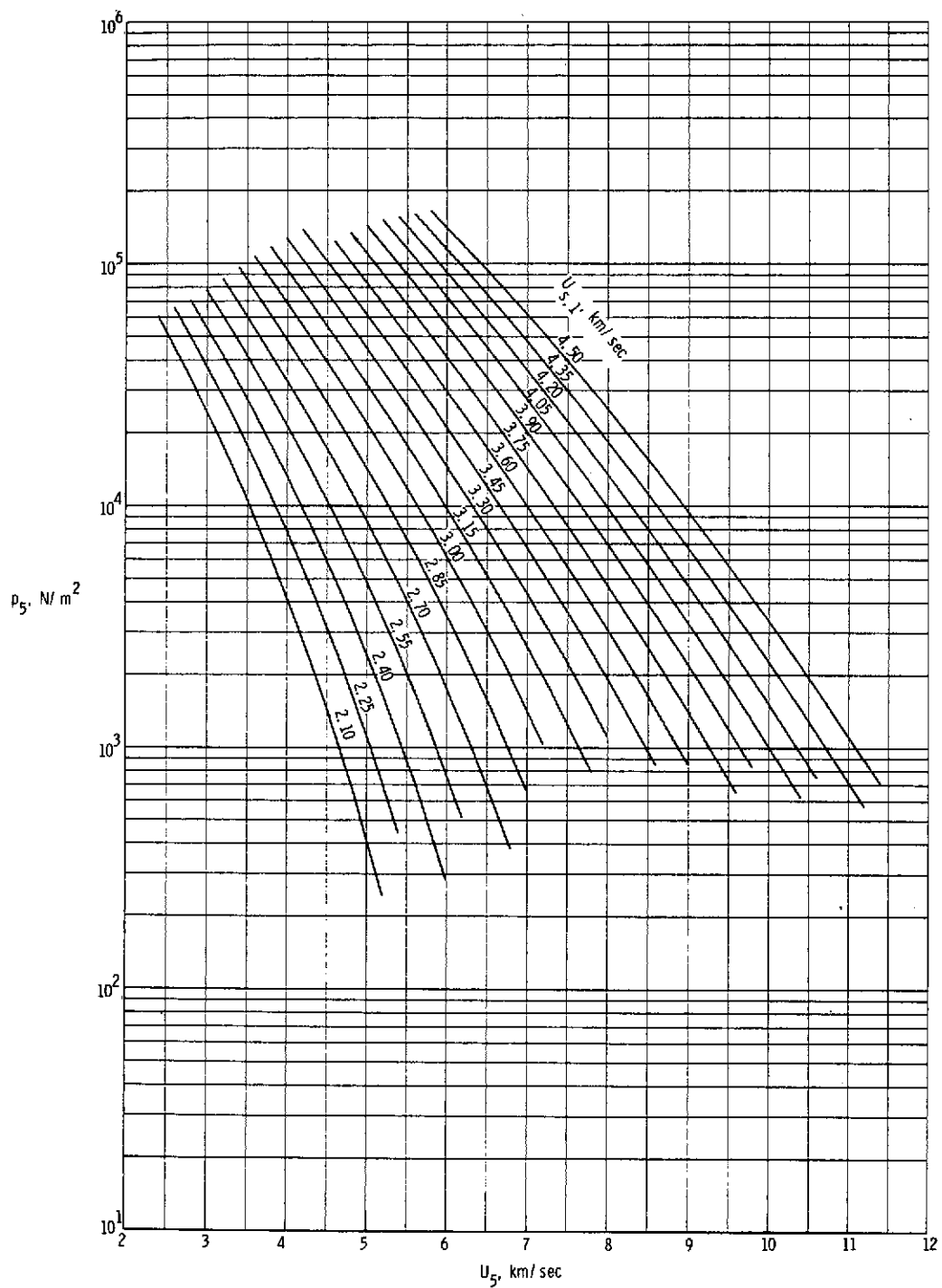
(k) Stagnation-point convective heat-transfer rate to sphere having radius of 2.54 cm.

Figure 12.- Continued.



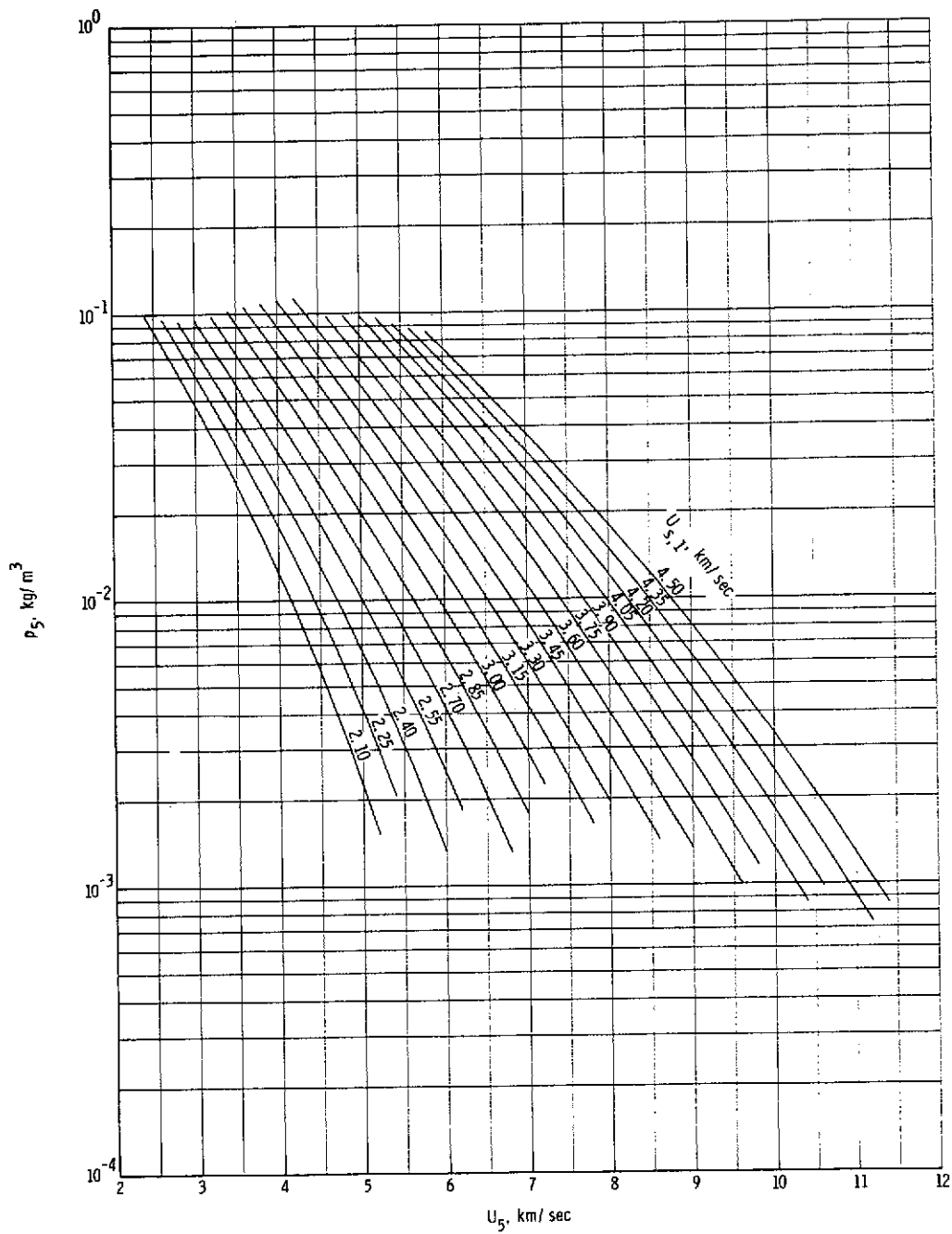
(1) Quiescent acceleration air pressure in region (10).

Figure 12.- Concluded.



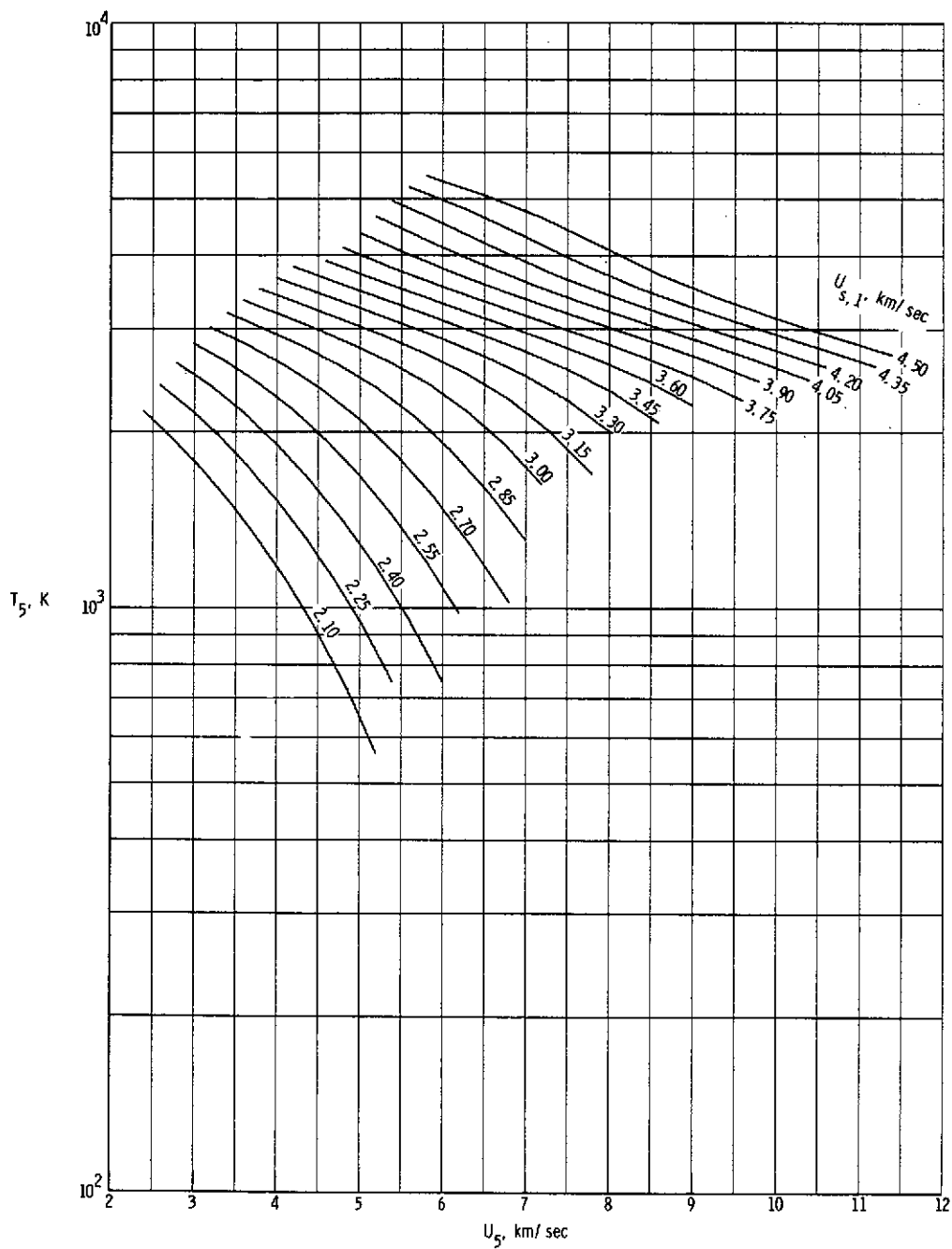
(a) Static pressure in region (5).

Figure 13.- Various expansion tube flow parameters for real air in thermochemical equilibrium as a function of flow velocity and assuming a totally reflected shock at the secondary diaphragm. $p_1 = 3.45 \text{ kN/m}^2$.



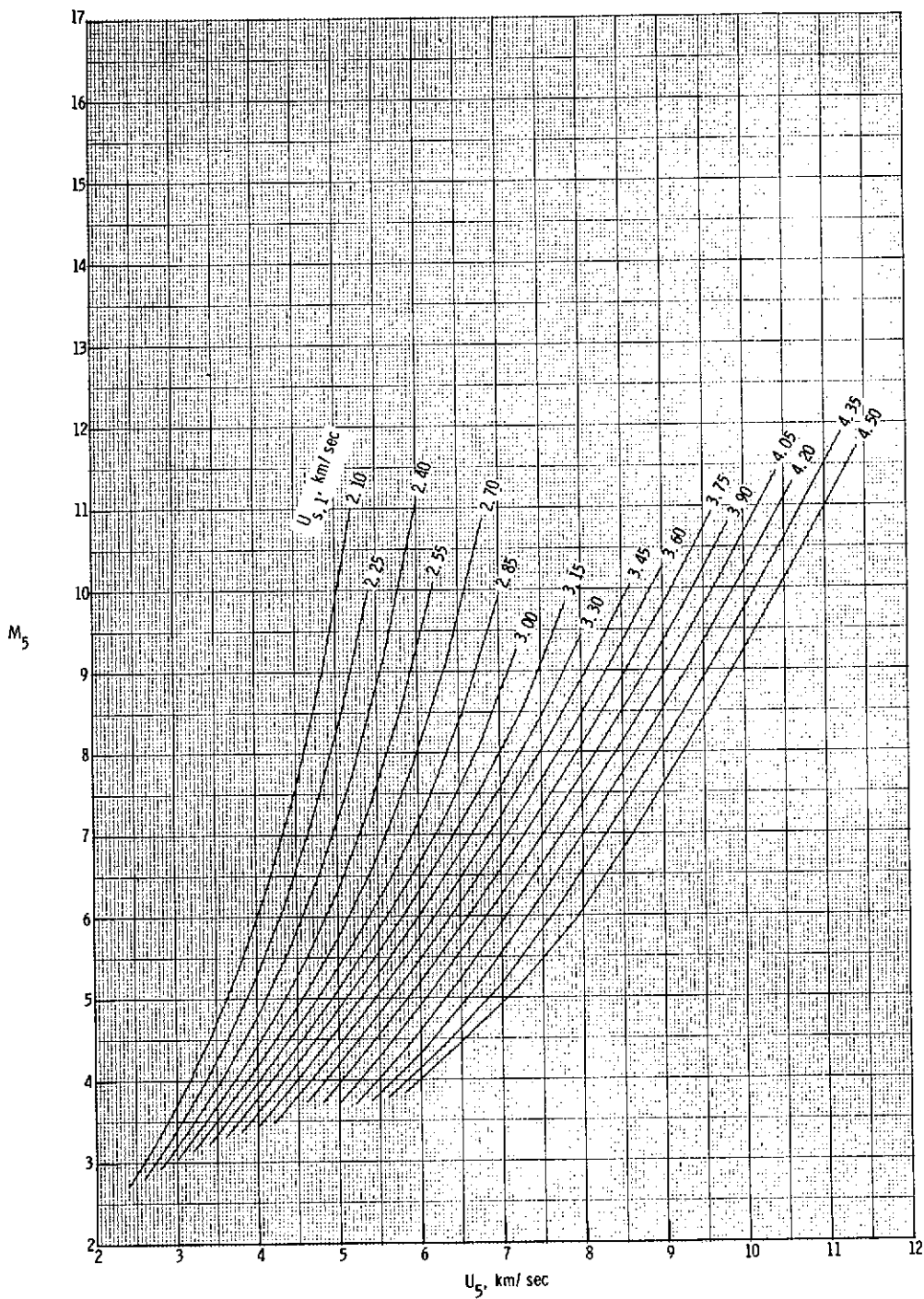
(b) Static density in region ⑤.

Figure 13.- Continued.



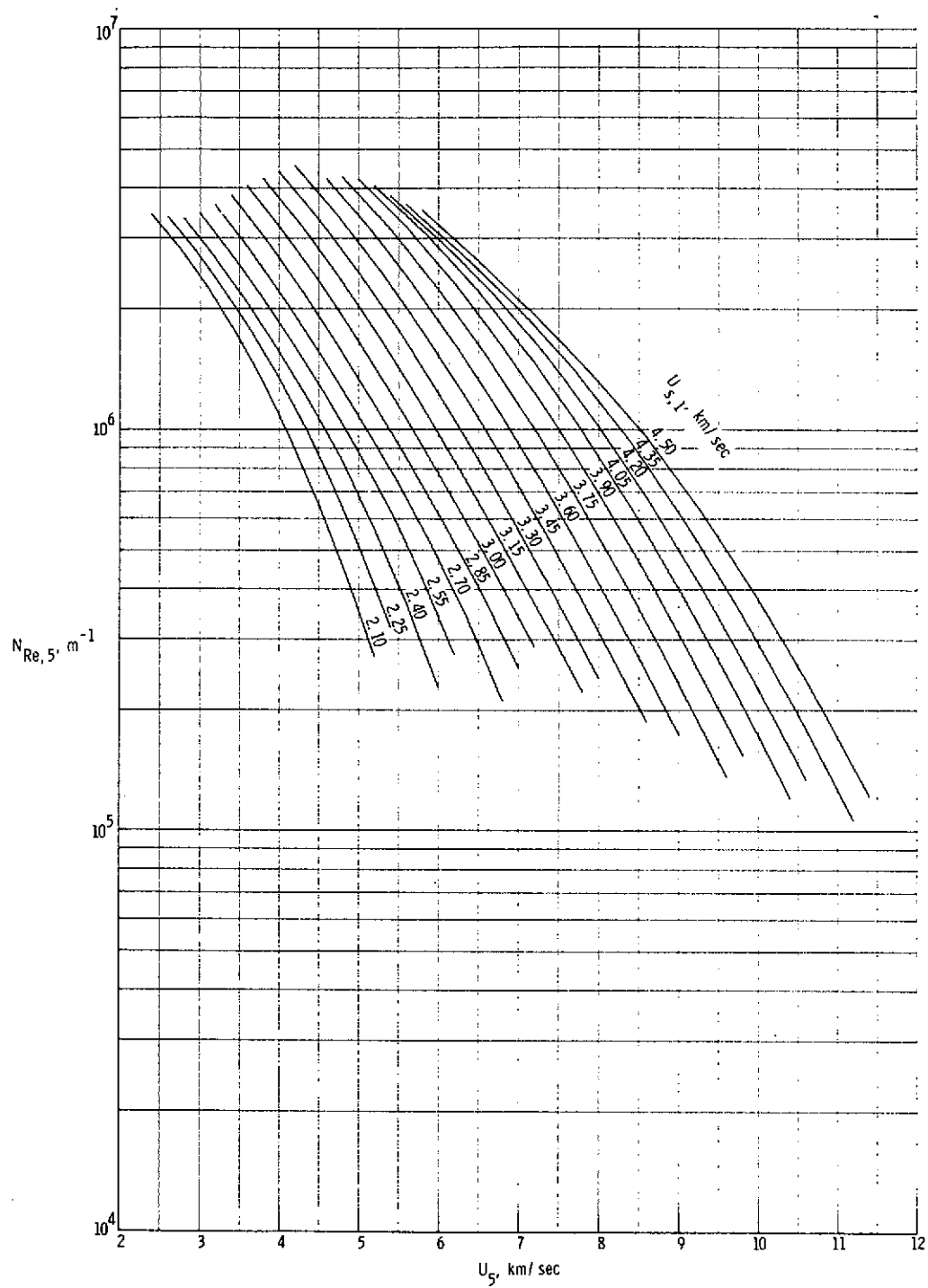
(c) Static temperature in region (5).

Figure 13.- Continued.



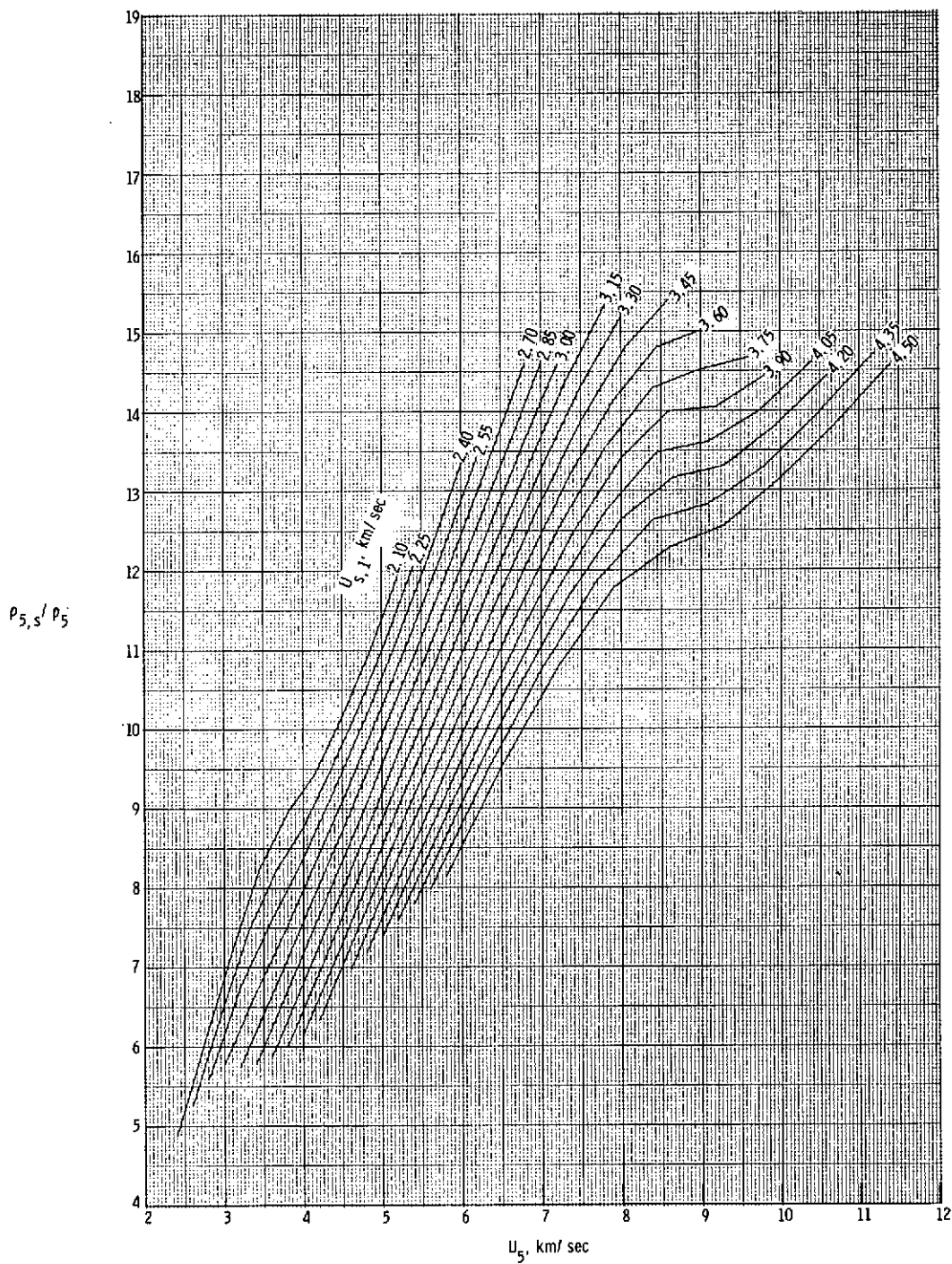
(d) Mach number in region (5).

Figure 13.- Continued.



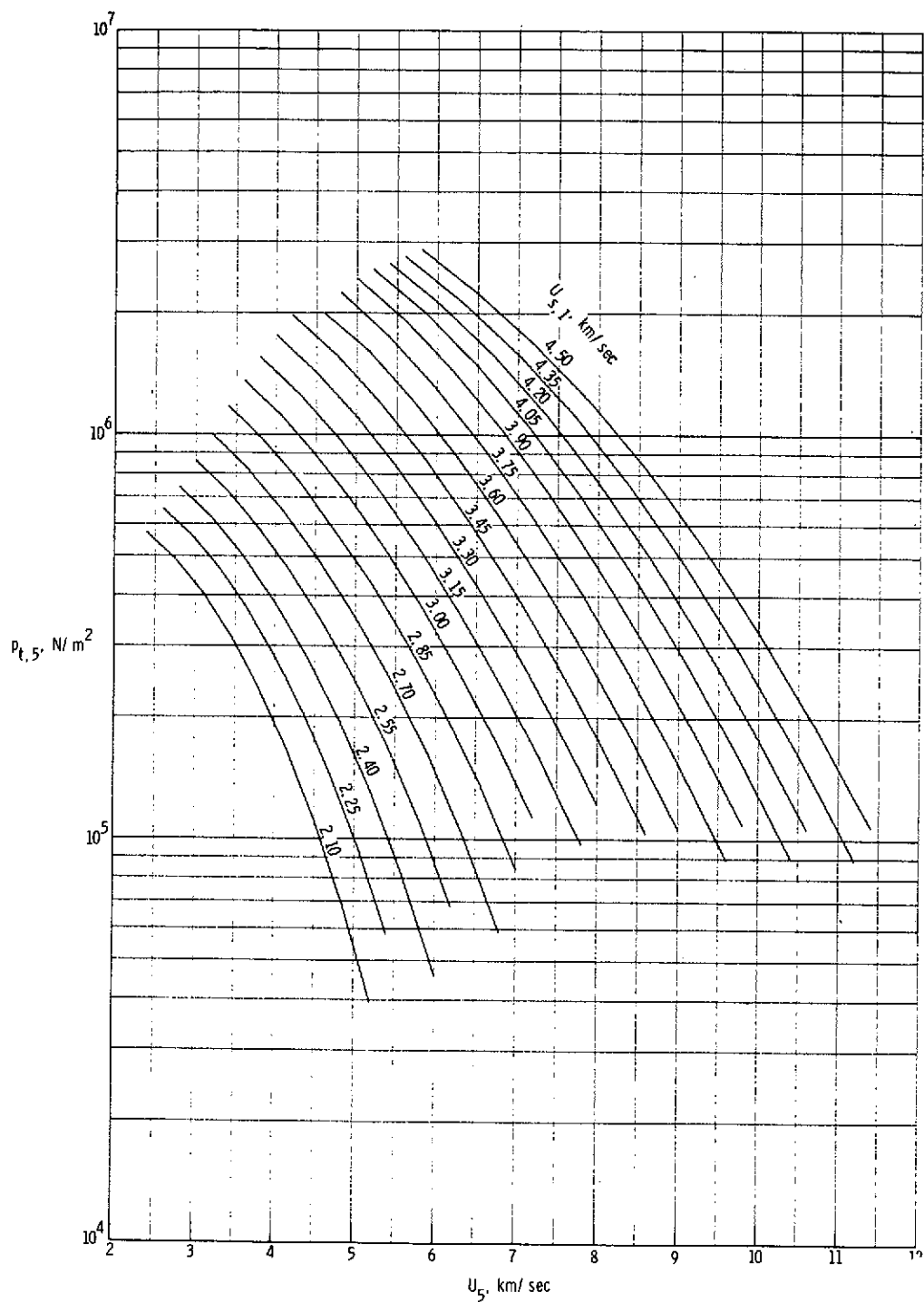
(e) Unit Reynolds number in region (5).

Figure 13.- Continued.



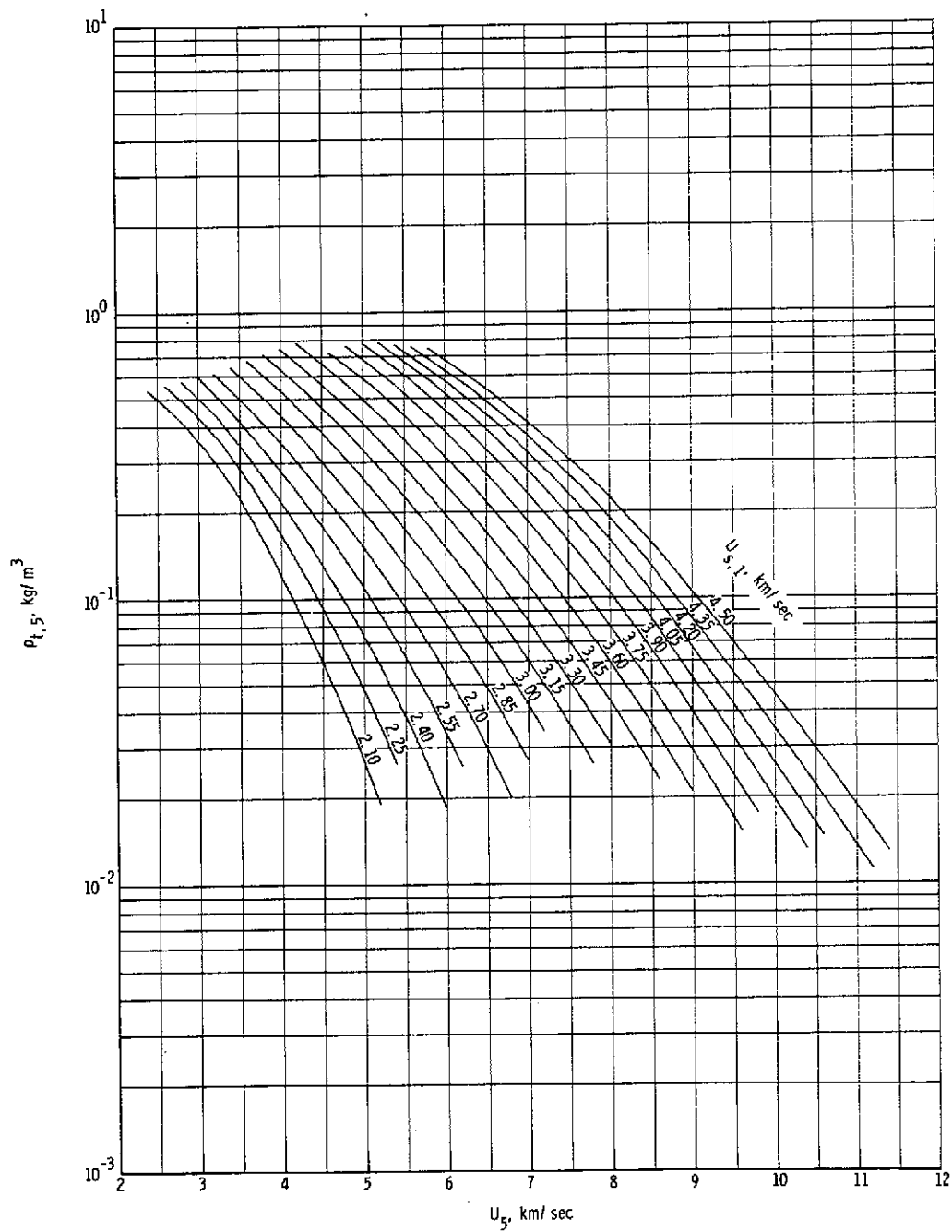
(f) Normal shock density ratio.

Figure 13.- Continued.



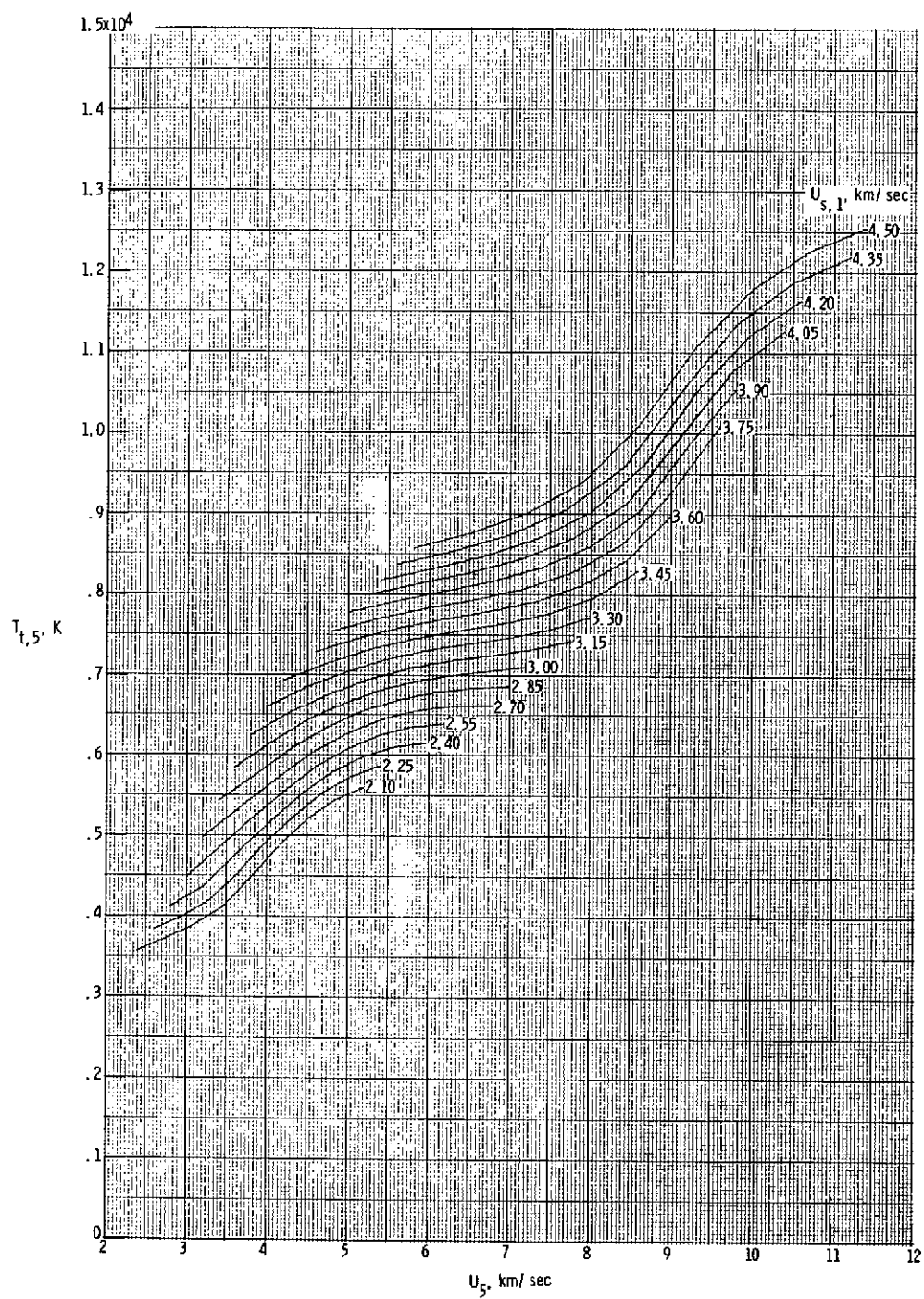
(g) Stagnation pressure behind normal bow shock.

Figure 13.- Continued.



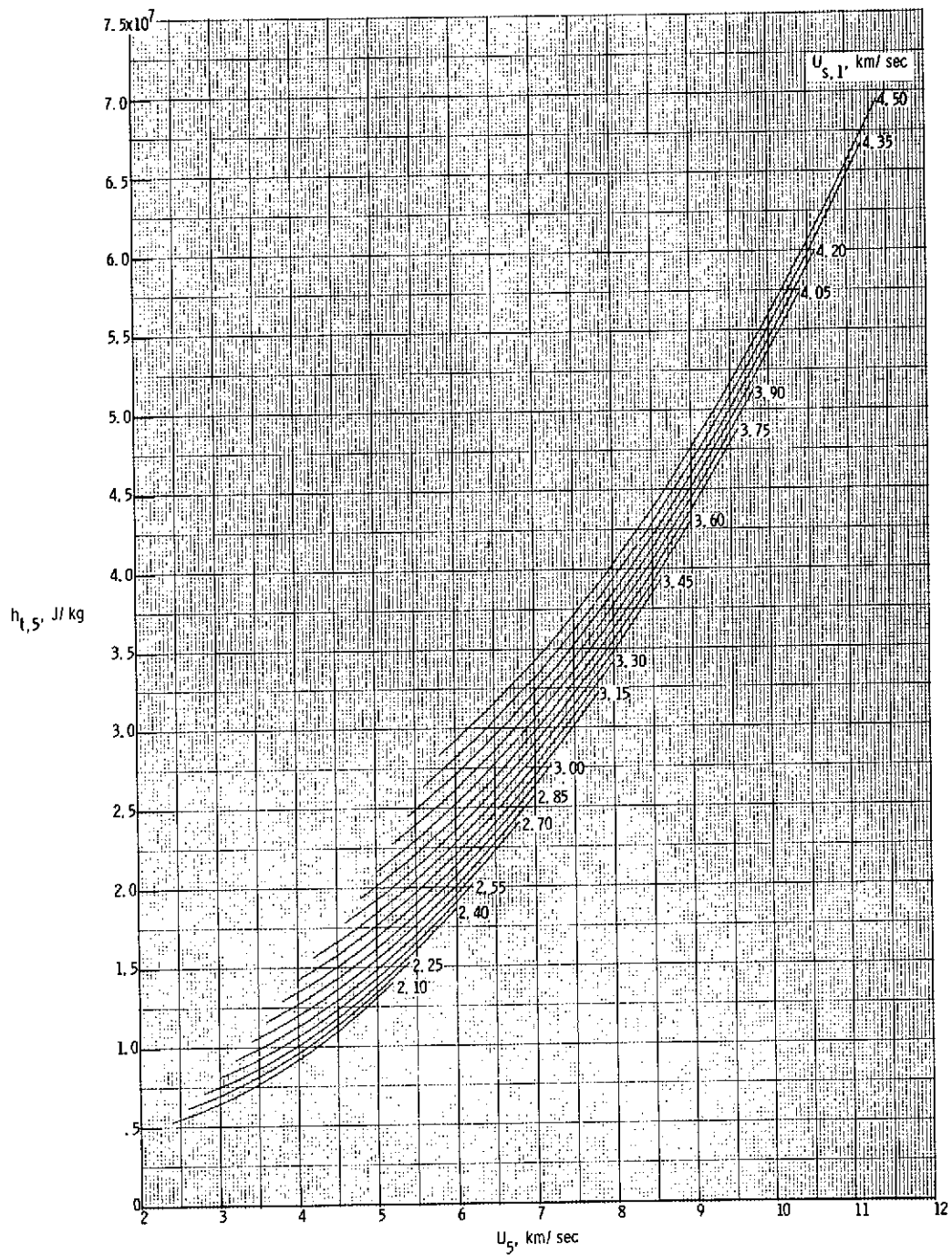
(h) Stagnation density behind normal bow shock.

Figure 13.- Continued.



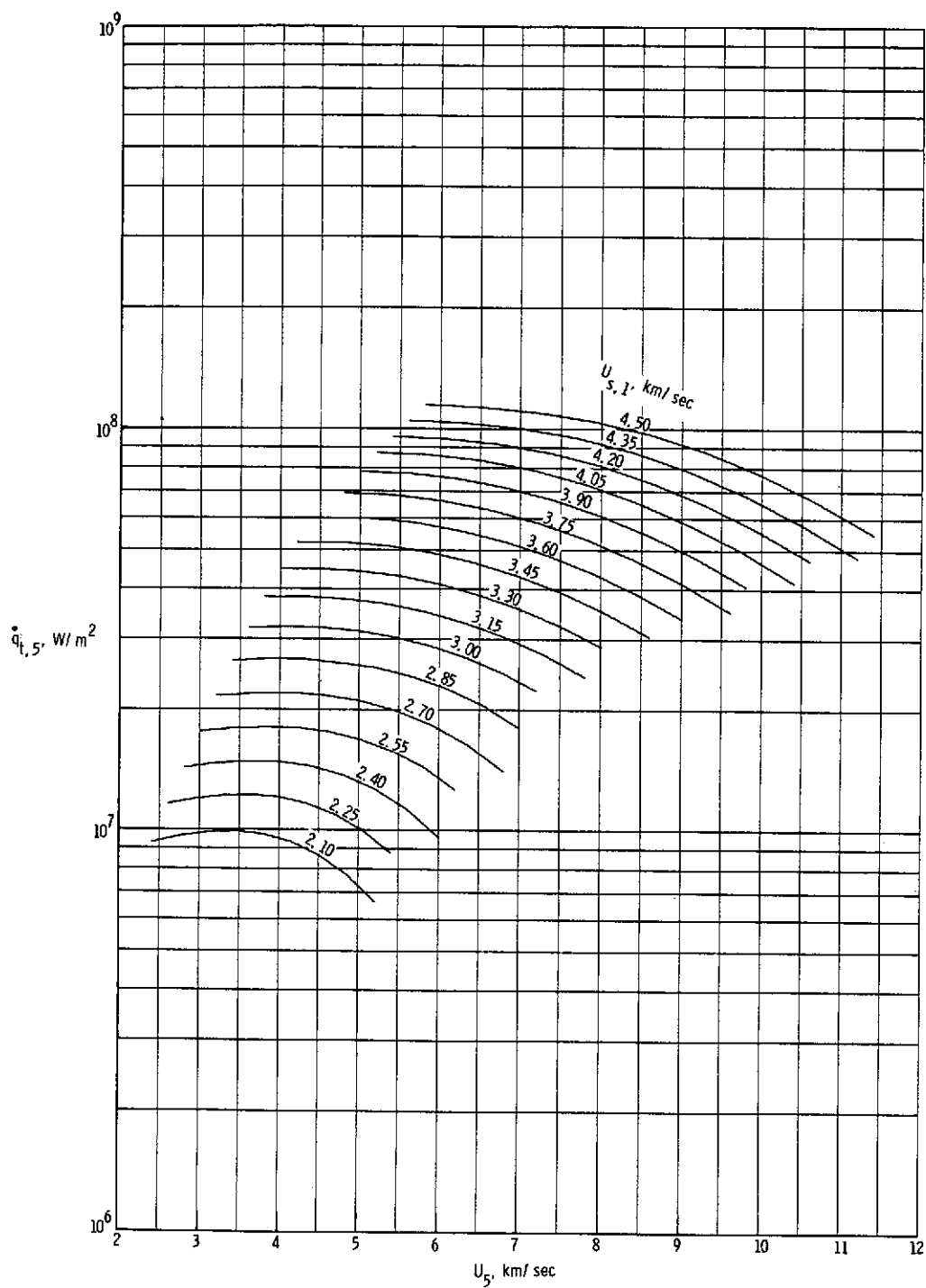
(i) Stagnation temperature behind normal bow shock.

Figure 13.- Continued.



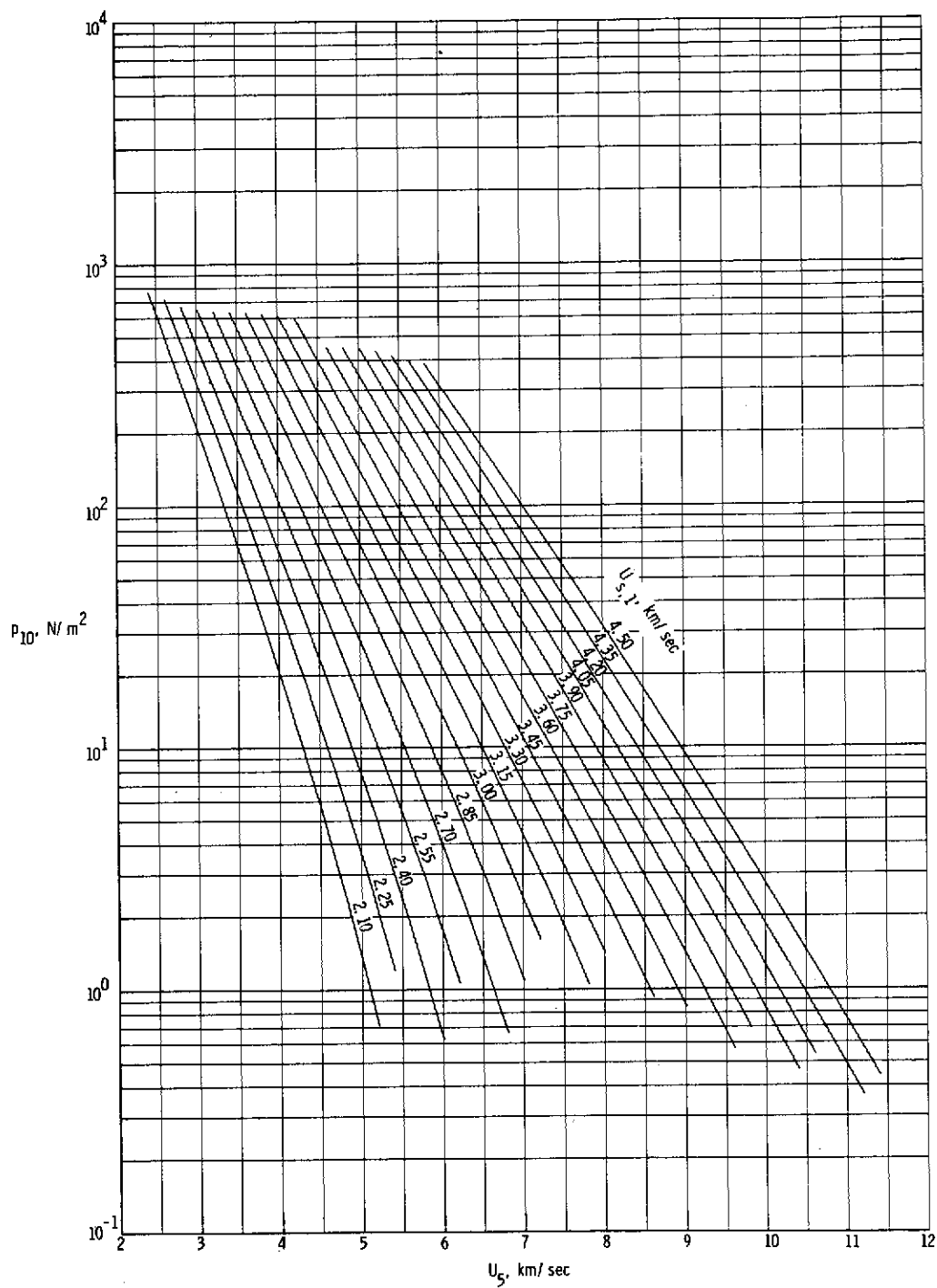
(j) Stagnation enthalpy behind normal bow shock.

Figure 13.- Continued.



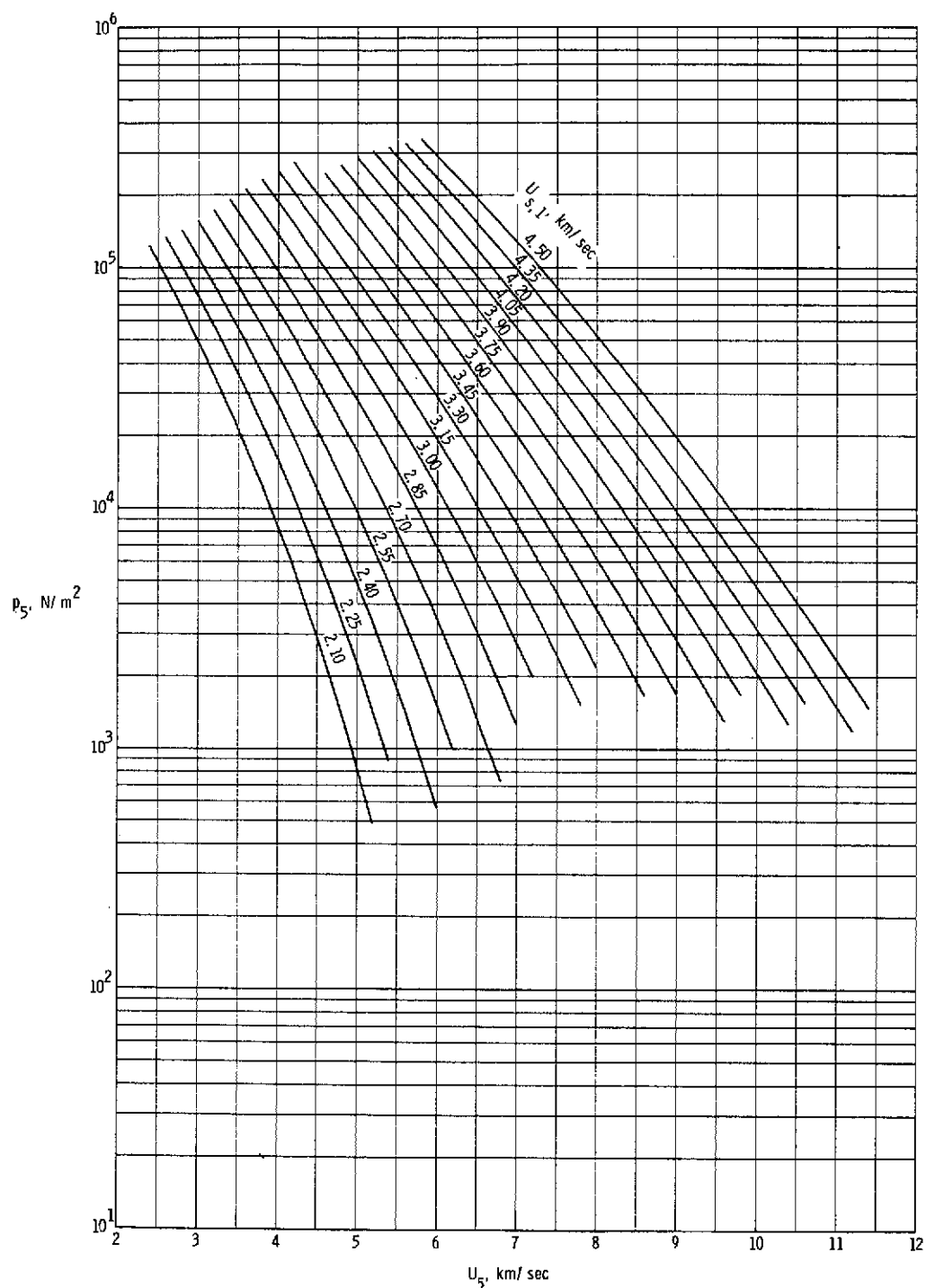
(k) Stagnation-point convective heat-transfer rate to sphere having radius of 2.54 cm.

Figure 13.- Continued.



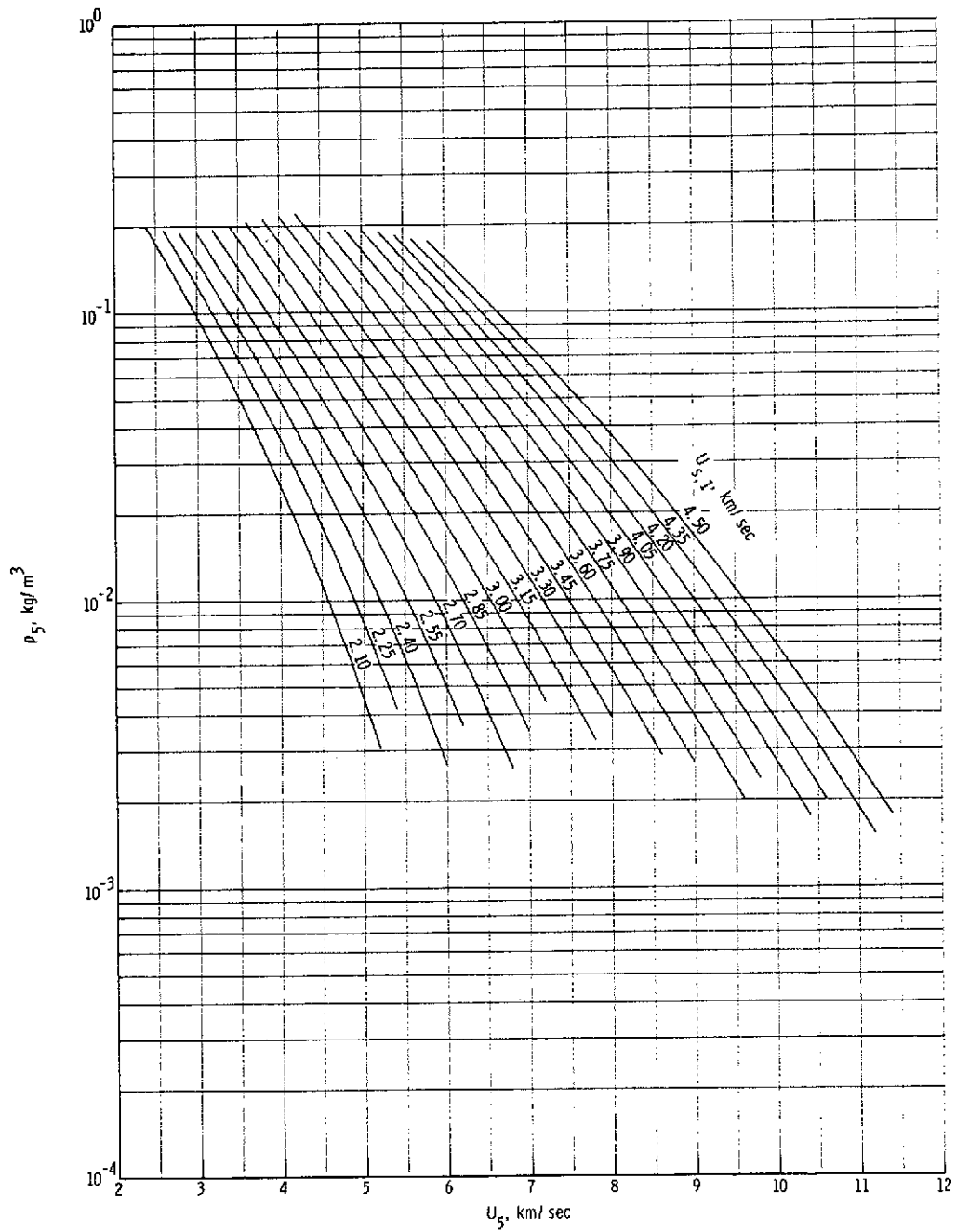
(1) Quiescent acceleration air pressure in region (10).

Figure 13.- Concluded.



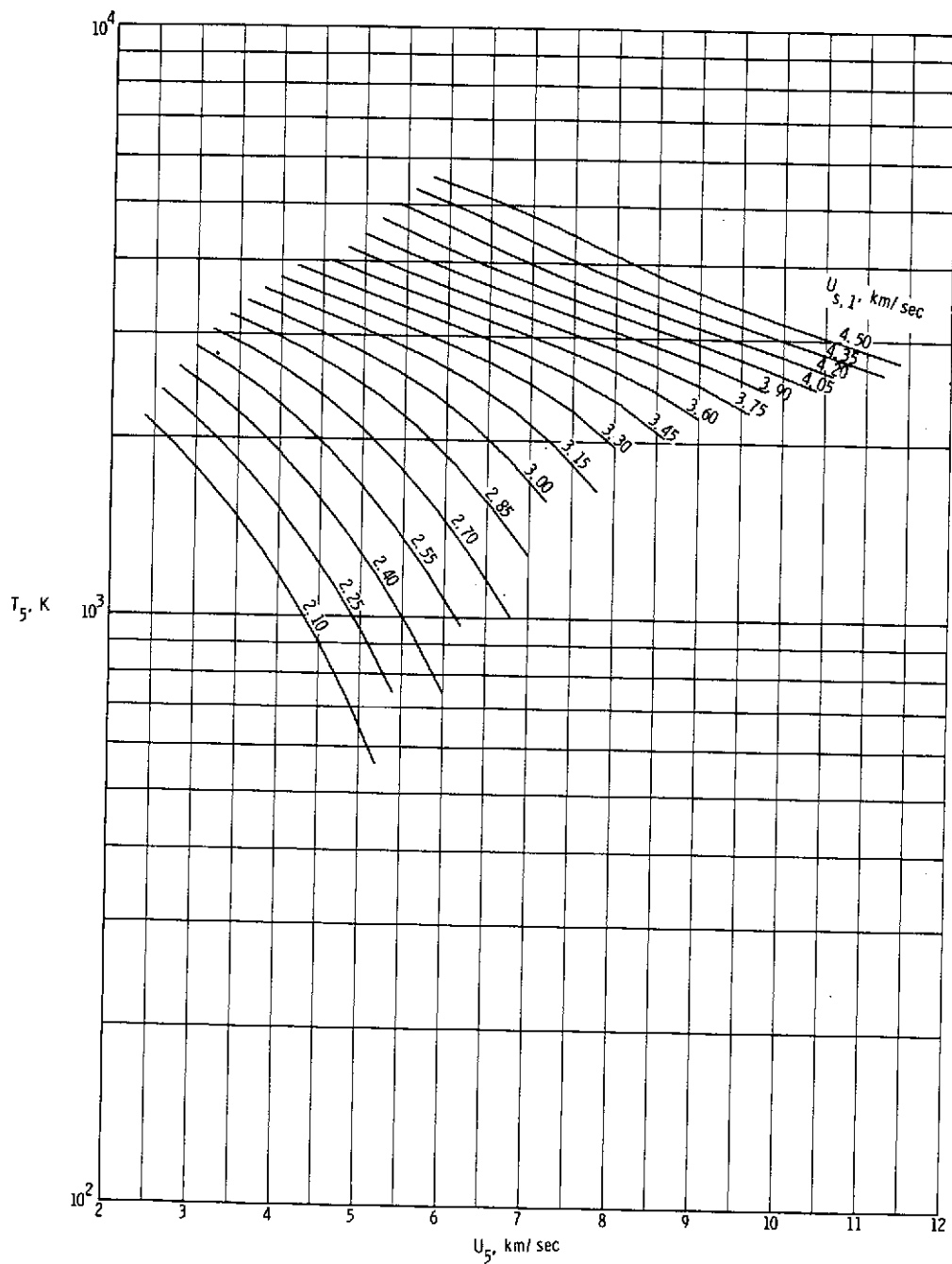
(a) Static pressure in region (5).

Figure 14.- Various expansion tube flow parameters for real air in thermochemical equilibrium as a function of flow velocity and assuming a totally reflected shock at the secondary diaphragm. $p_1 = 6.90 \text{ kN/m}^2$.



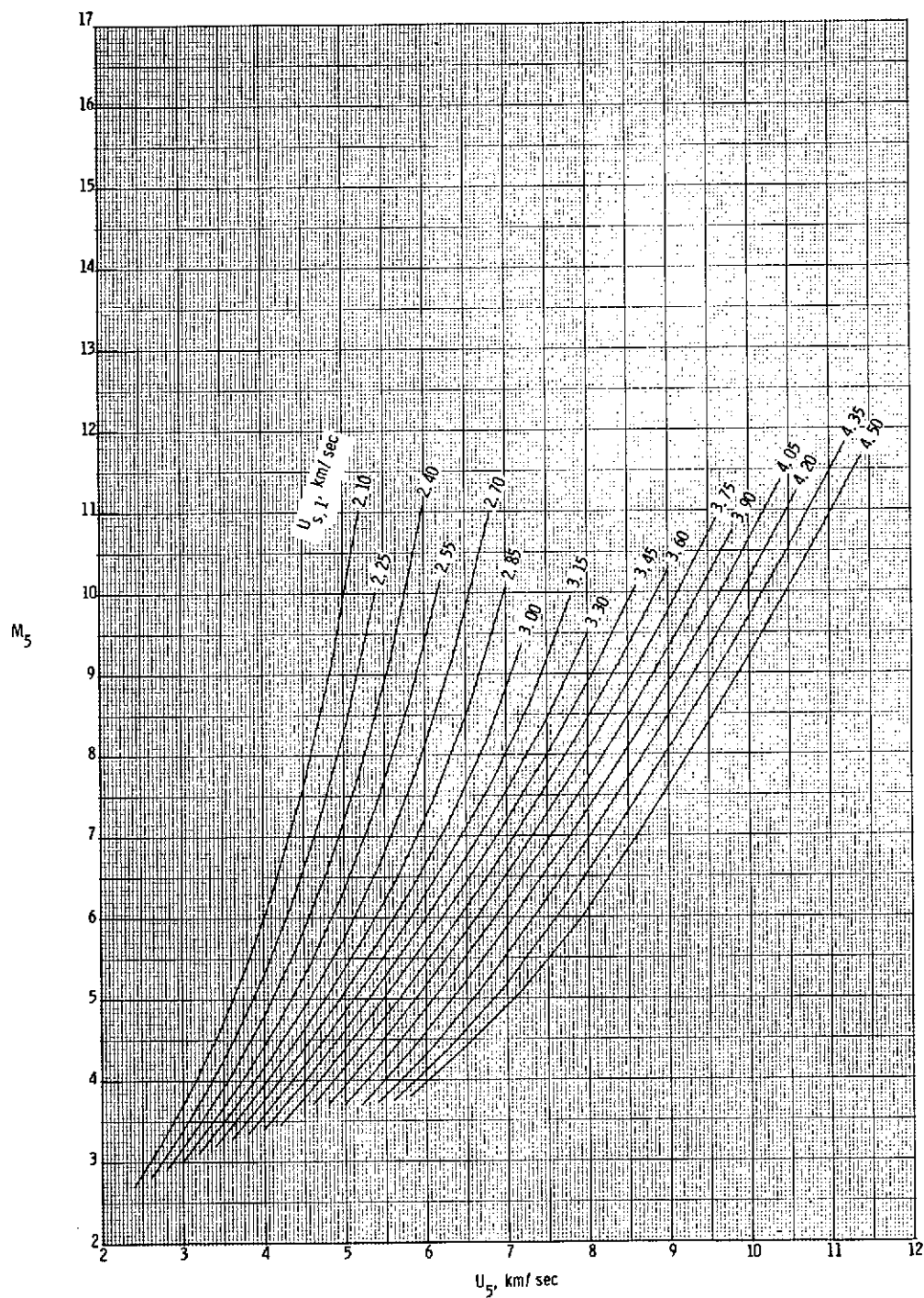
(b) Static density in region (5).

Figure 14.- Continued.



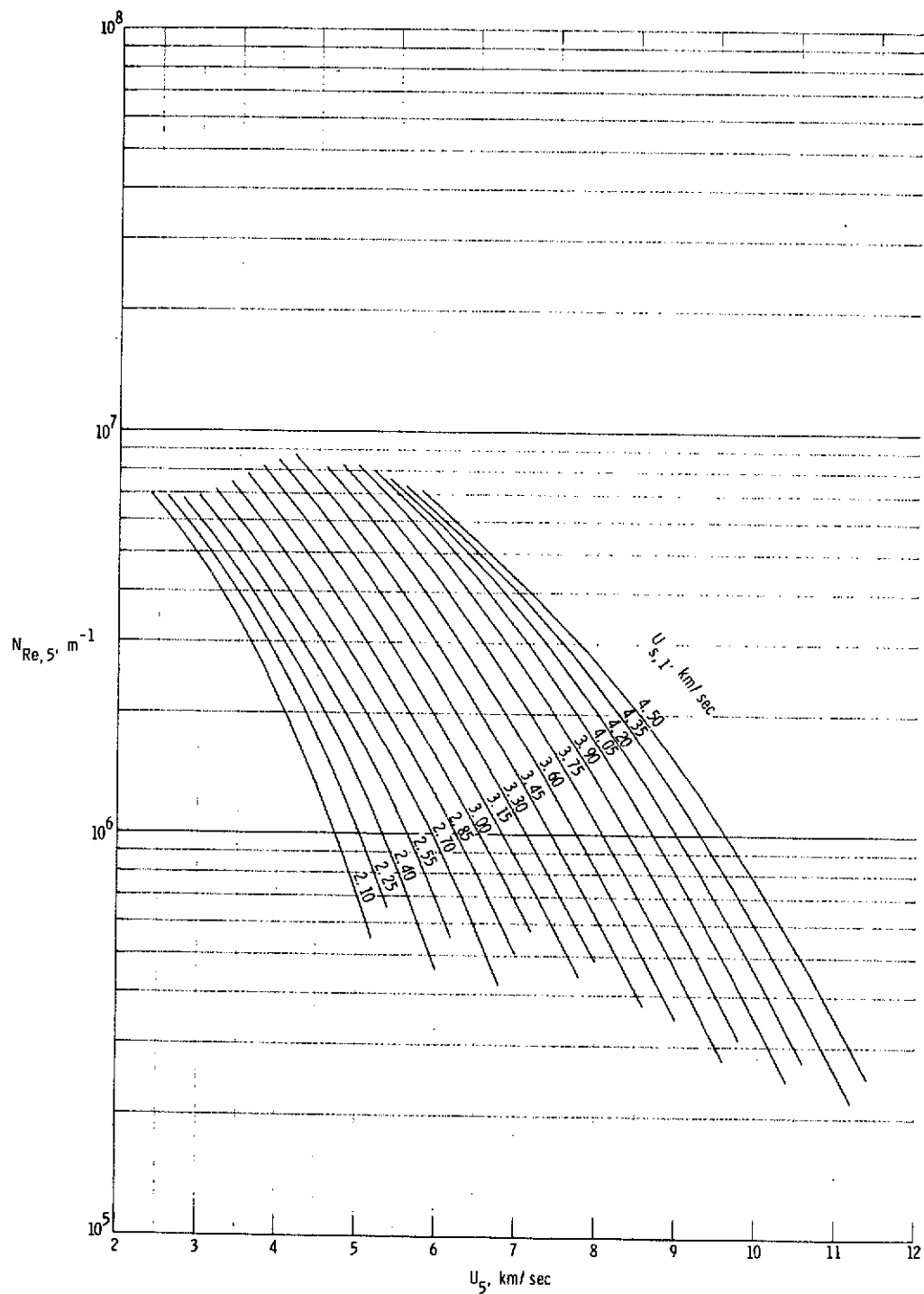
(c) Static temperature in region (5).

Figure 14.- Continued.



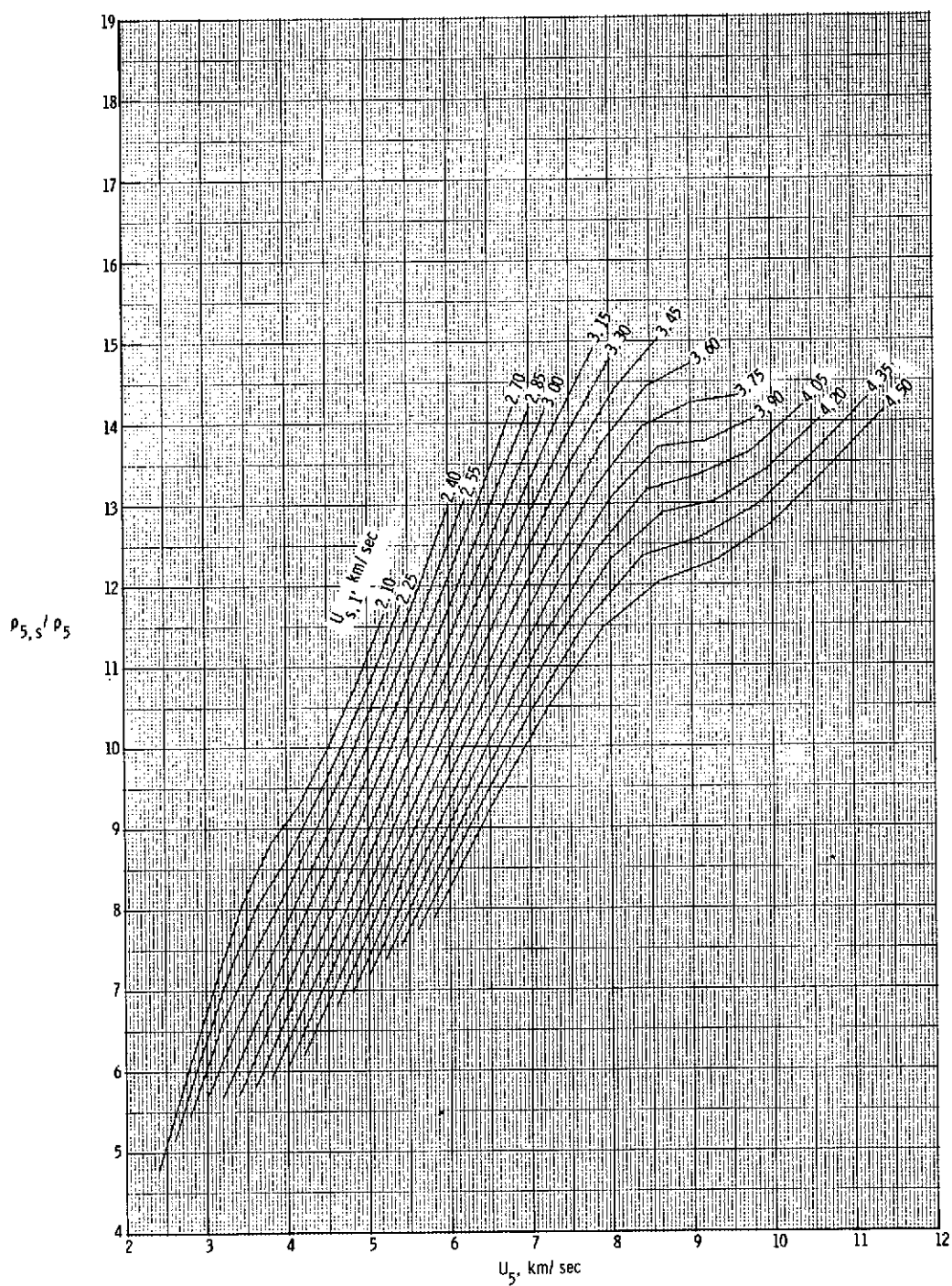
(d) Mach number in region (5).

Figure 14.- Continued.



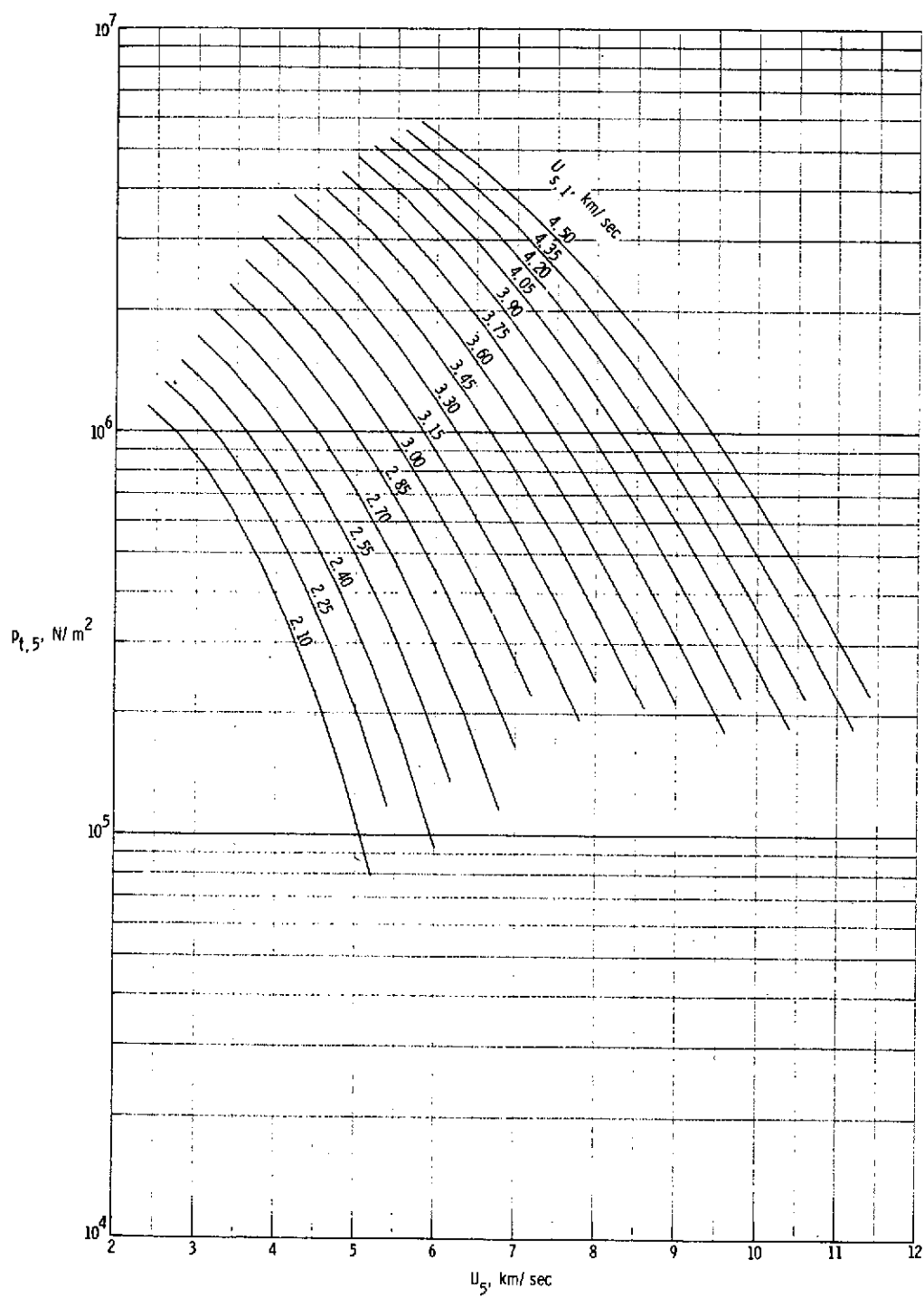
(e) Unit Reynolds number in region (5).

Figure 14.- Continued.



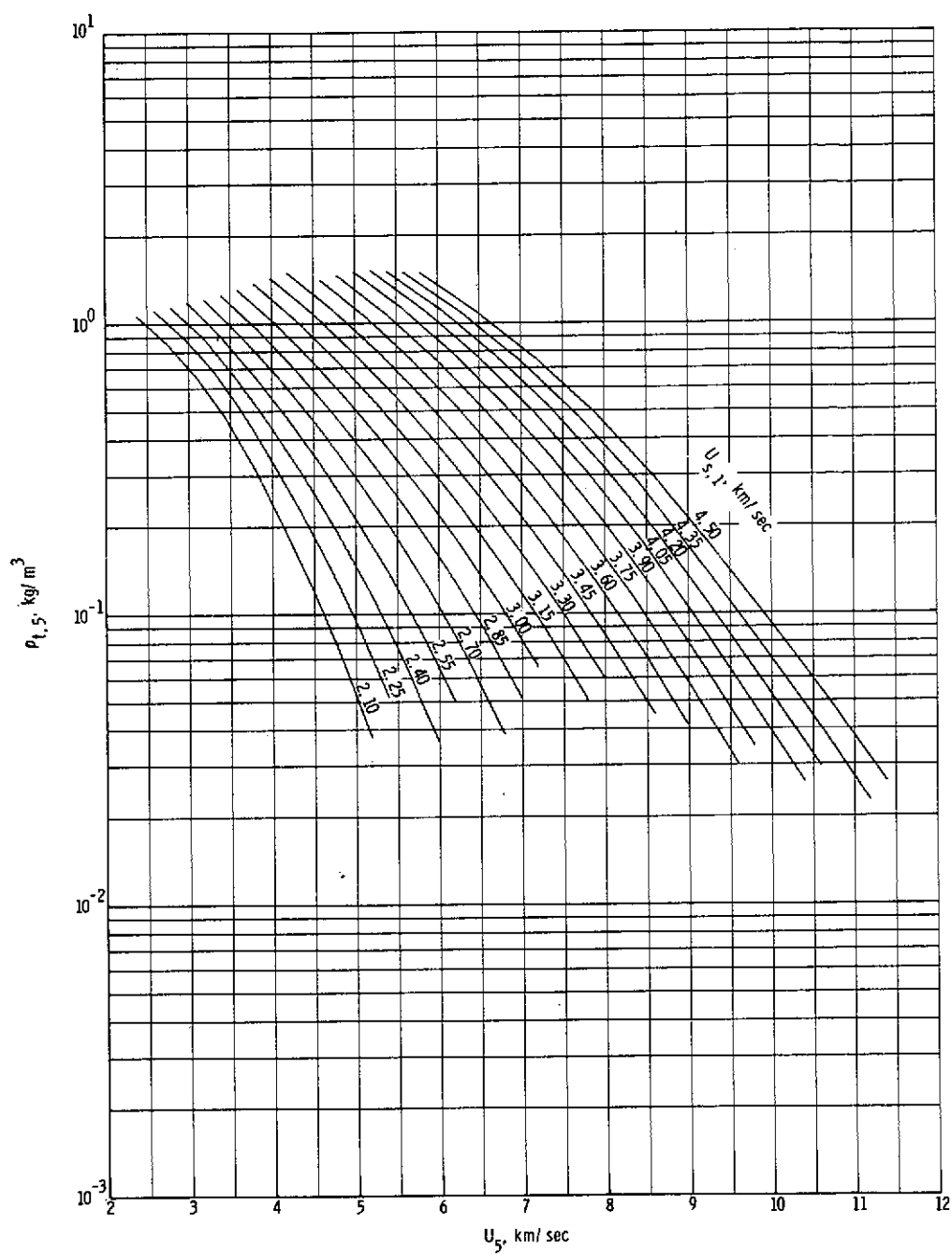
(f) Normal shock density ratio.

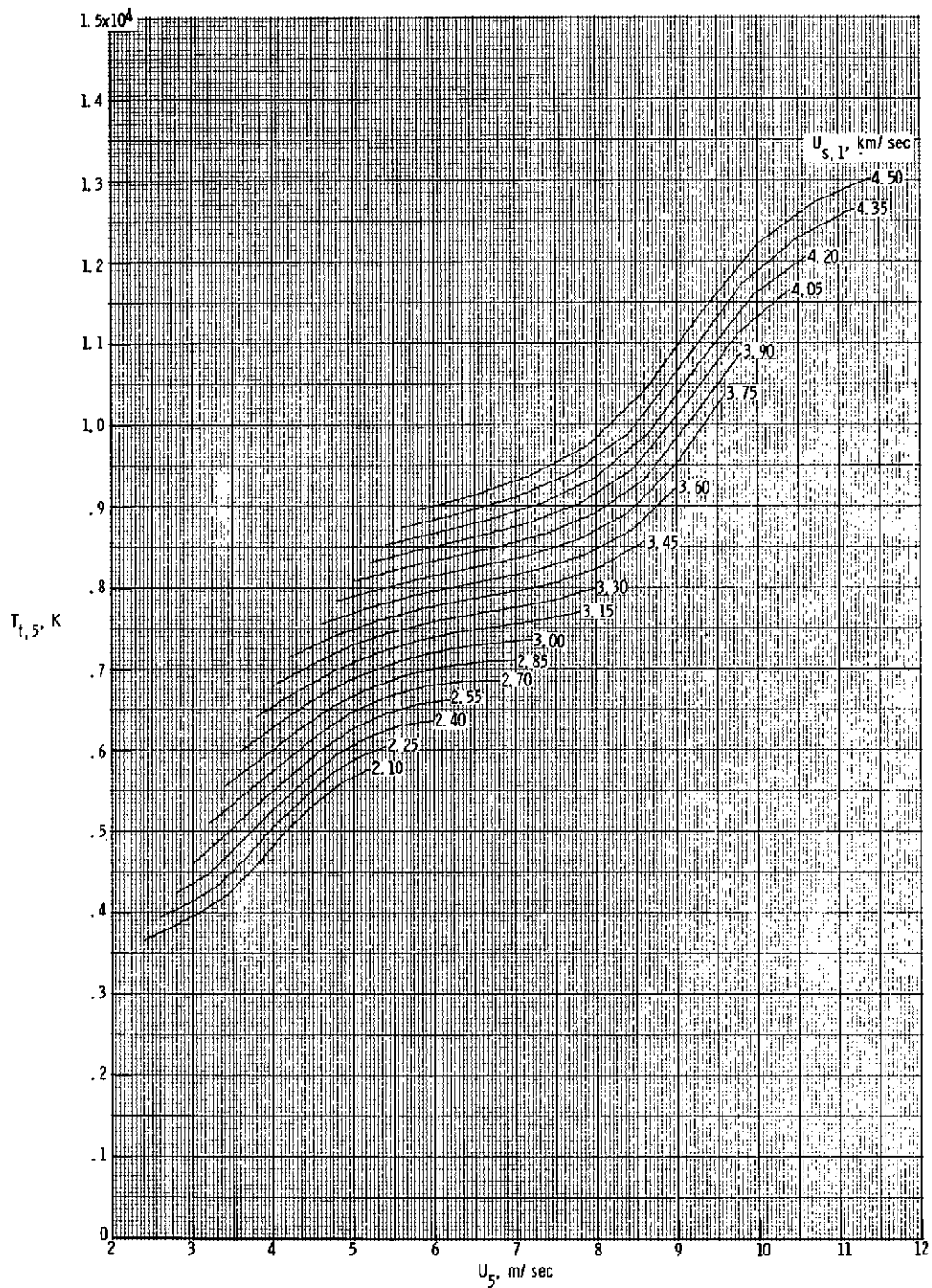
Figure 14.- Continued.



(g) Stagnation pressure behind normal bow shock.

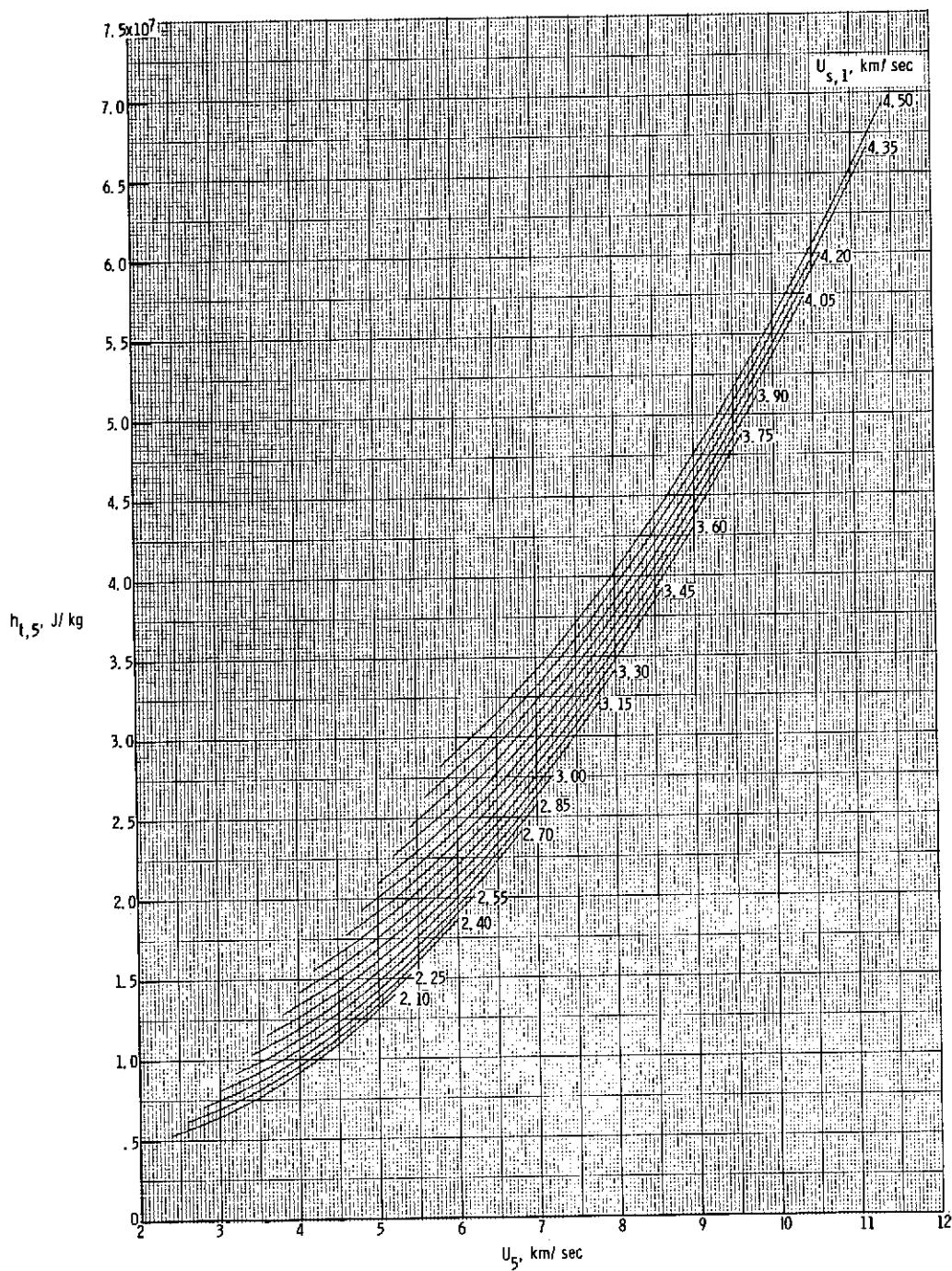
Figure 14.- Continued.





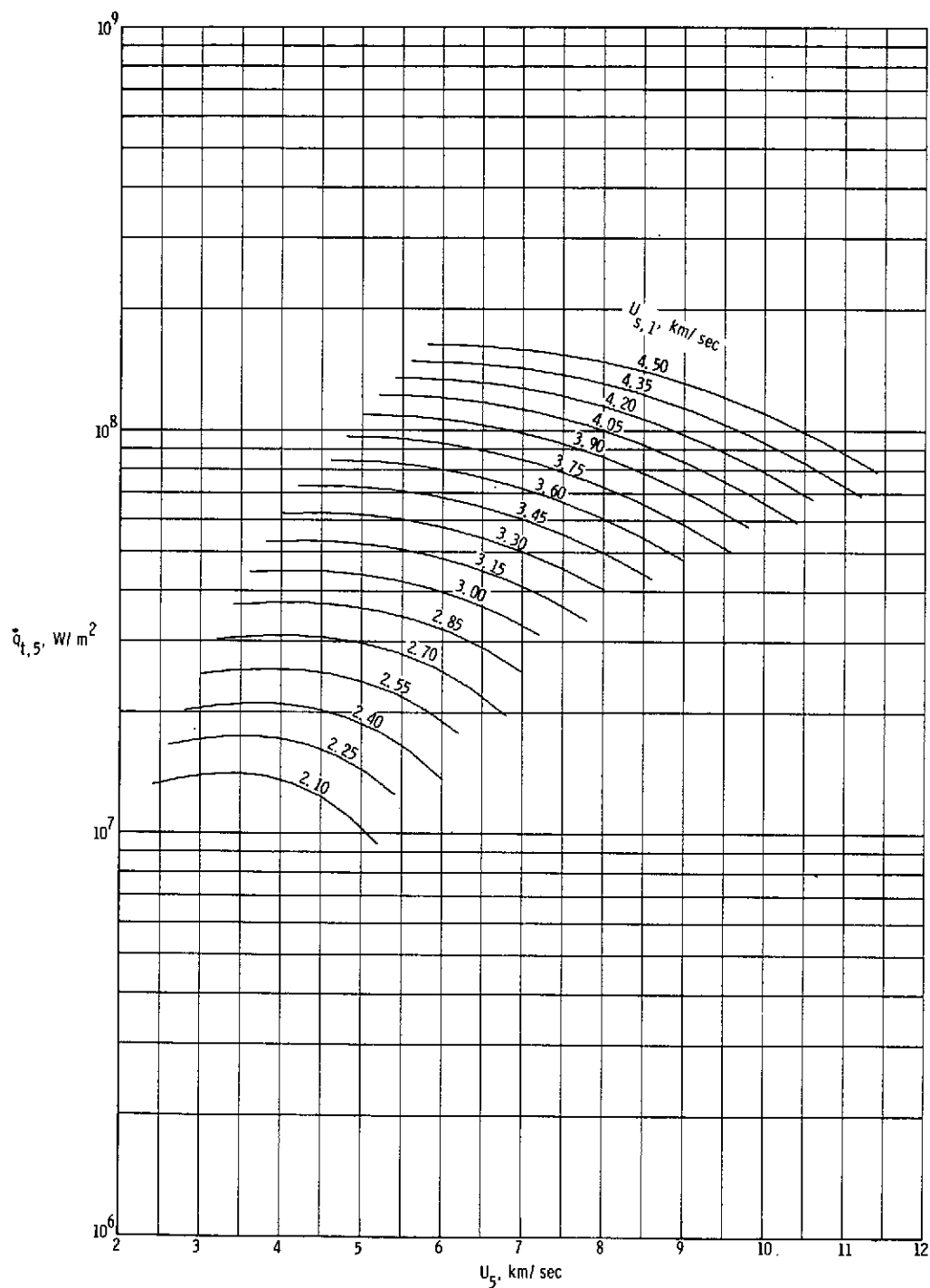
(i) Stagnation temperature behind normal bow shock.

Figure 14.- Continued.



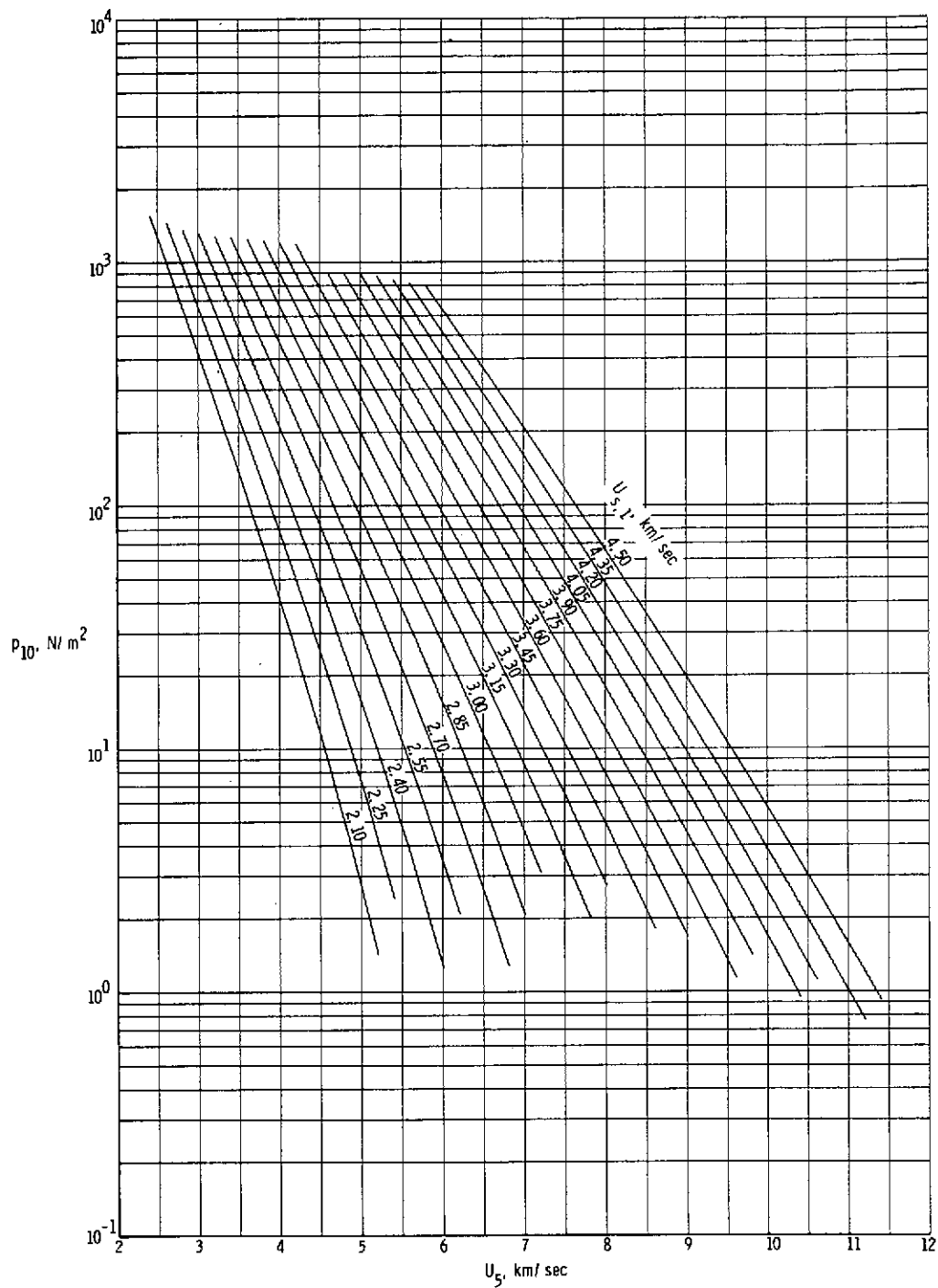
(j) Stagnation enthalpy behind normal bow shock.

Figure 14.- Continued.



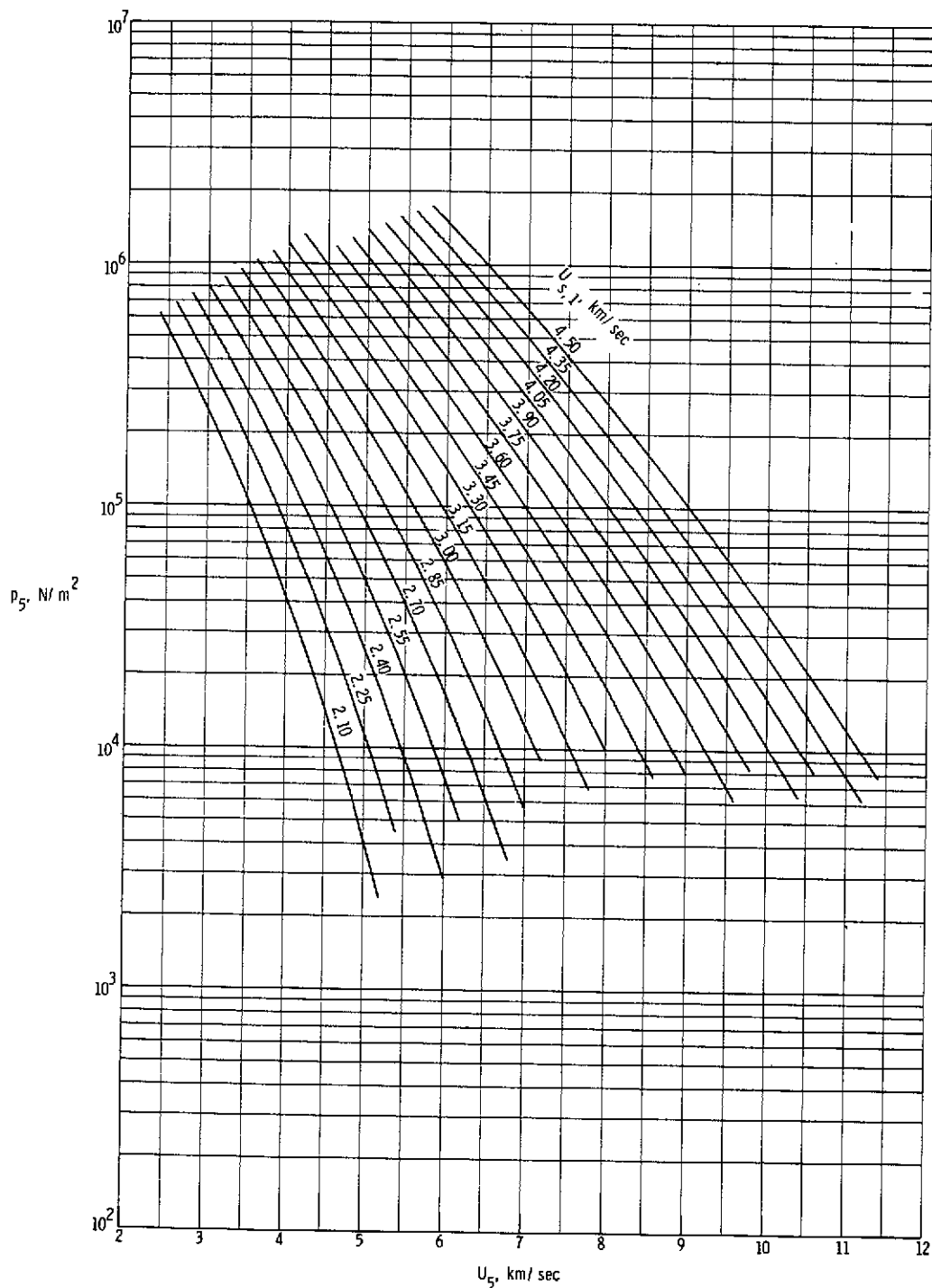
(k) Stagnation-point convective heat-transfer rate to sphere having radius of 2.54 cm.

Figure 14.- Continued.



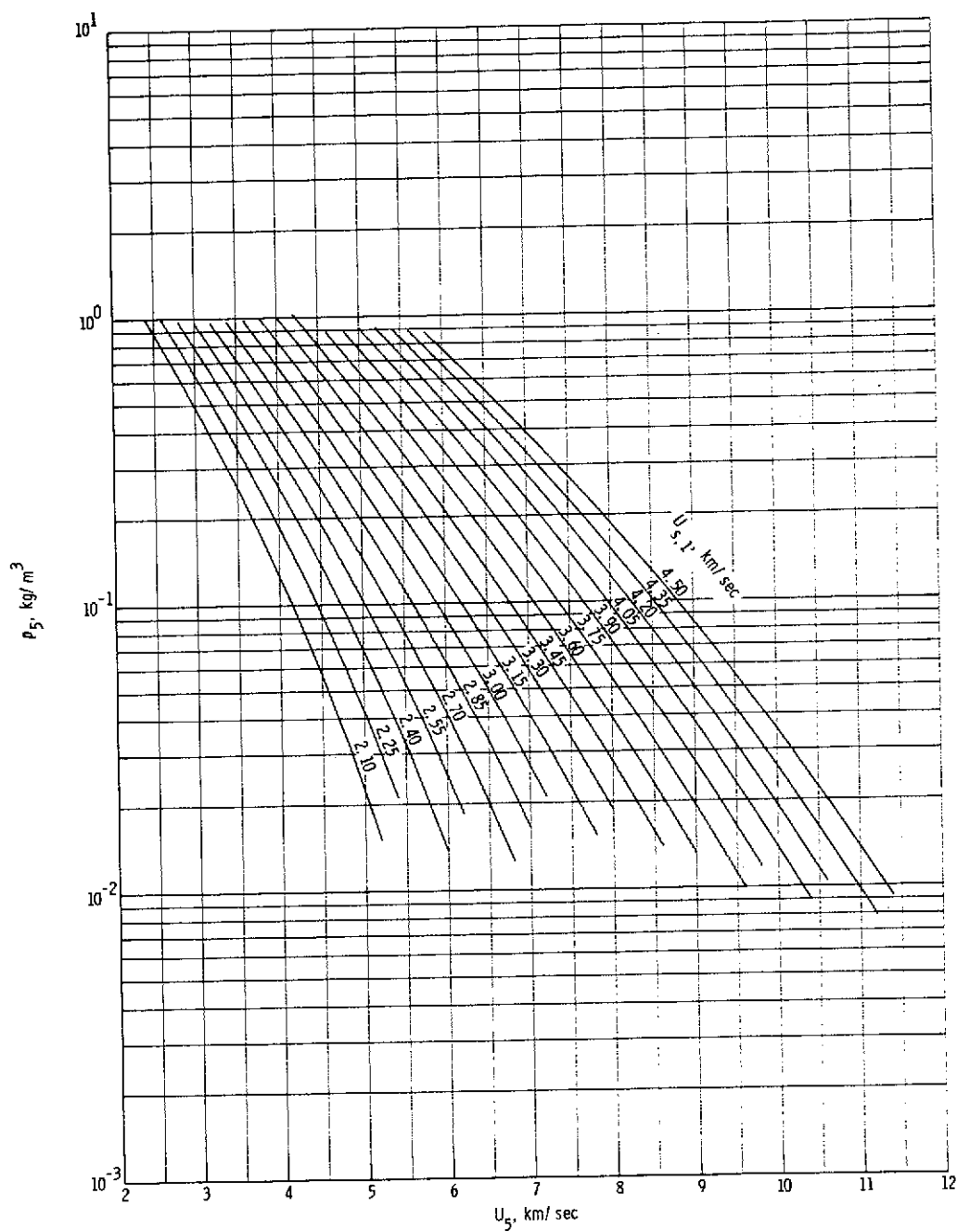
(1) Quiescent acceleration air pressure in region (10).

Figure 14.- Concluded.



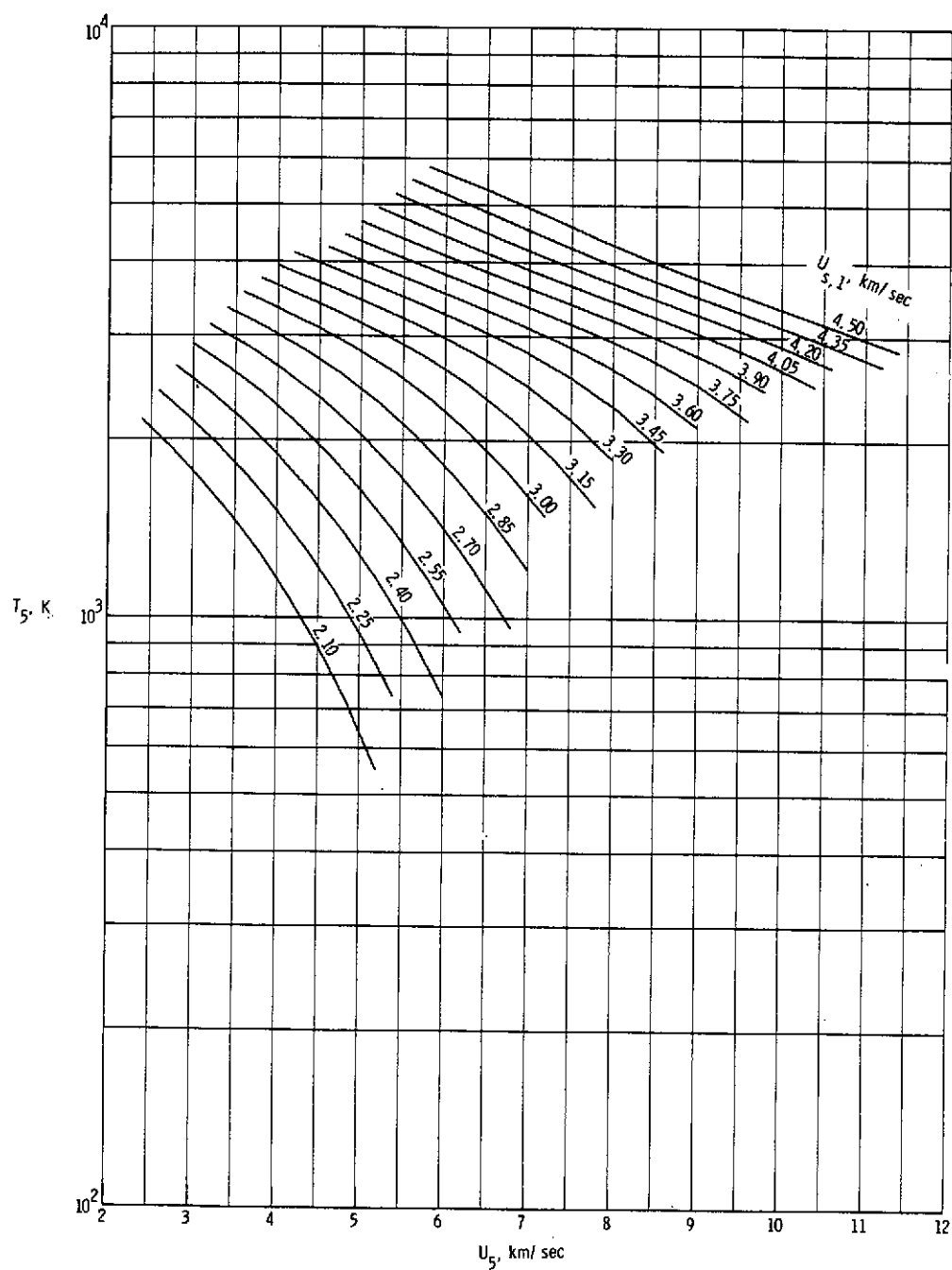
(a) Static pressure in region (5).

Figure 15.- Various expansion tube flow parameters for real air in thermochemical equilibrium as a function of flow velocity and assuming a totally reflected shock at the secondary diaphragm. $p_1 = 34.47 \text{ kN/m}^2$.



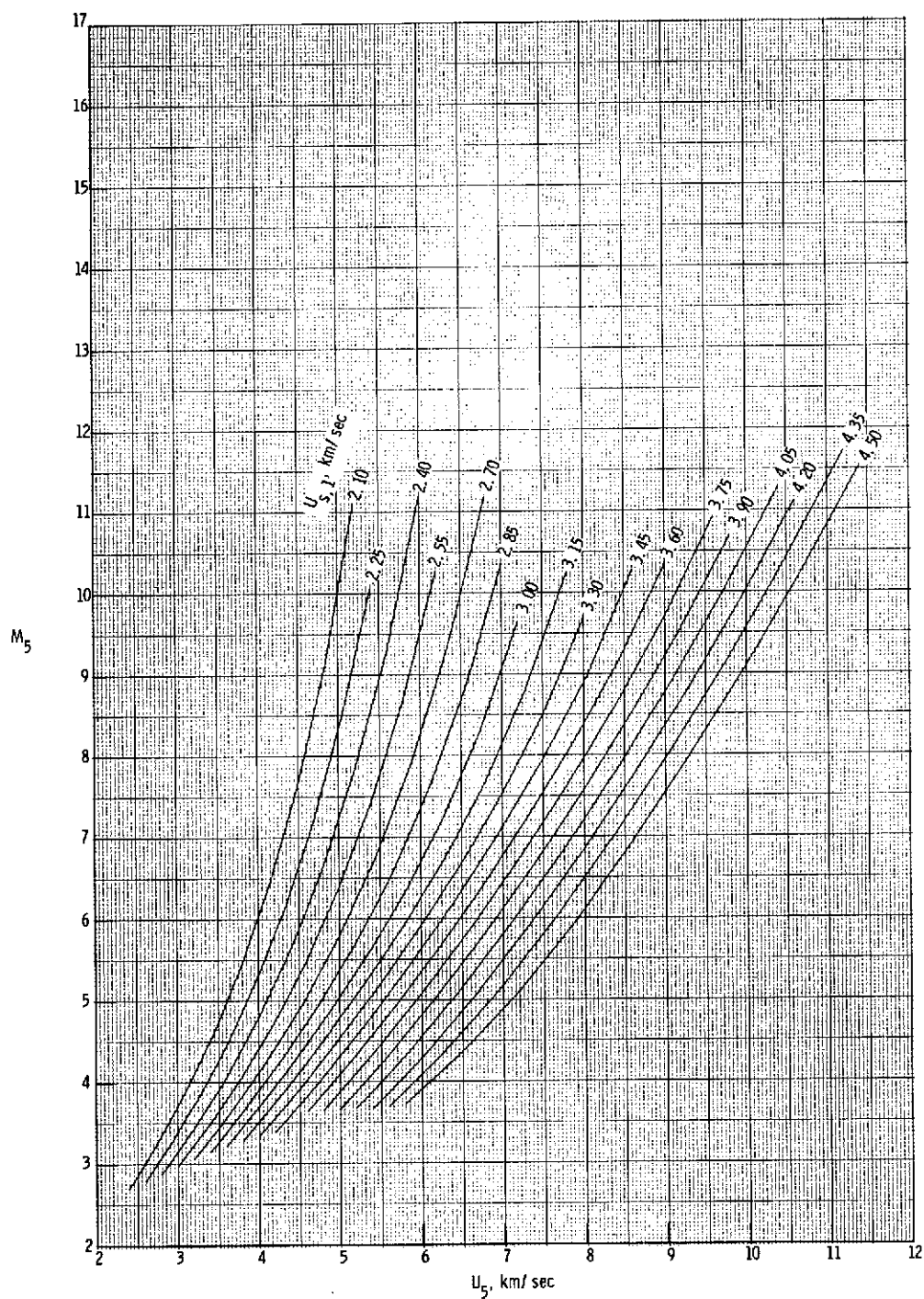
(b) Static density in region (5).

Figure 15.- Continued.



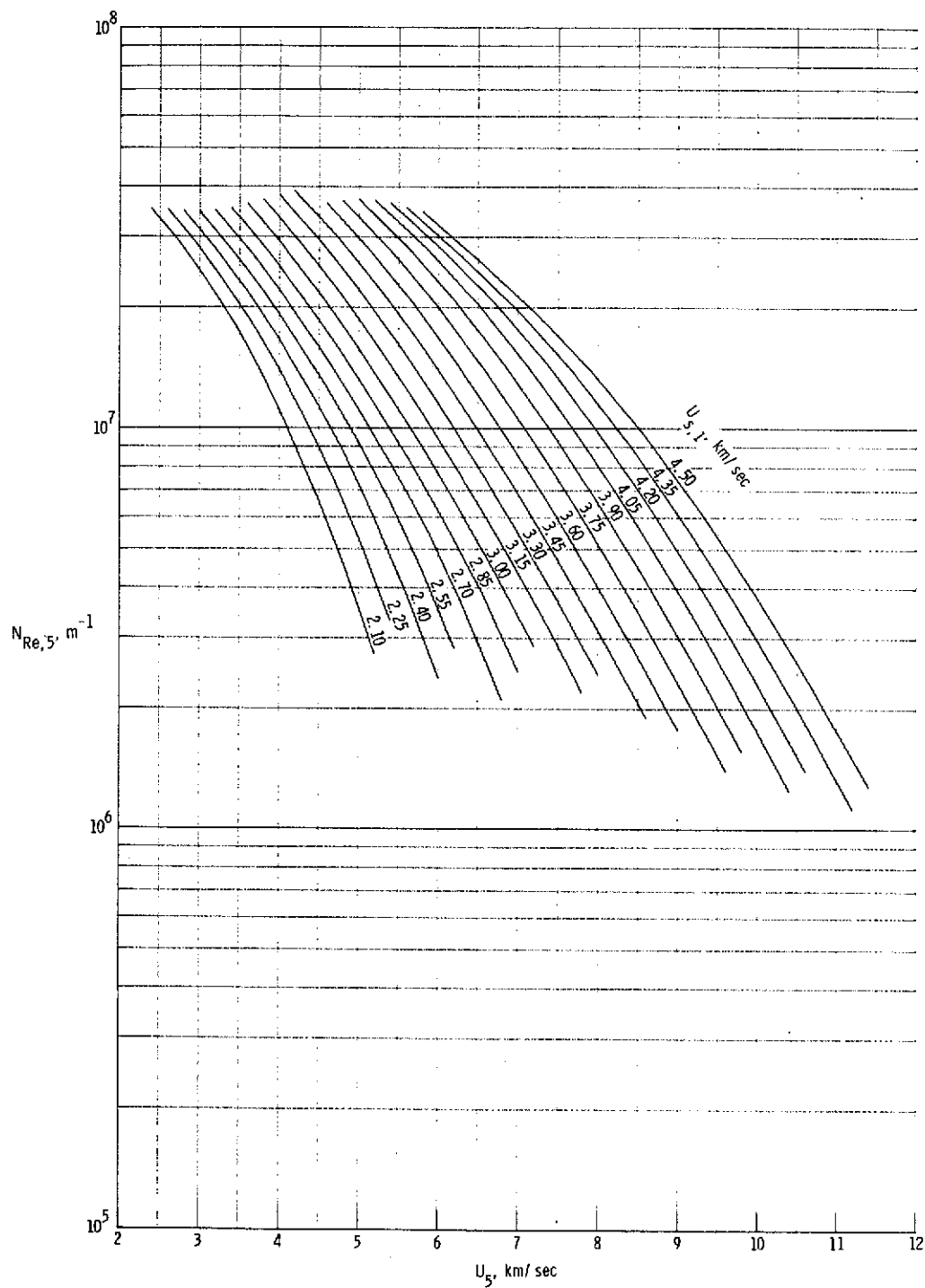
(c) Static temperature in region ⑤.

Figure 15.- Continued.



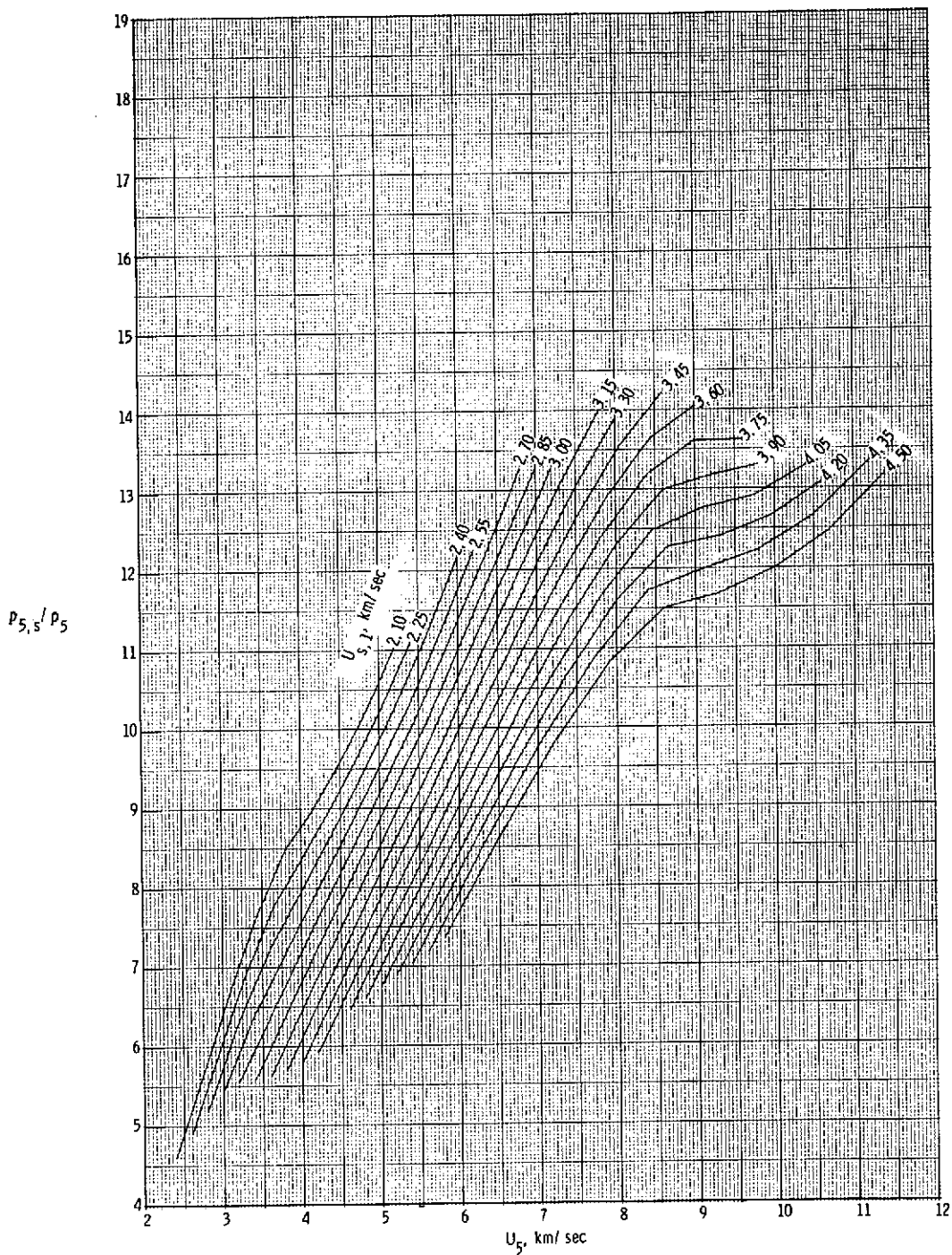
(d) Mach number in region (5).

Figure 15.- Continued.



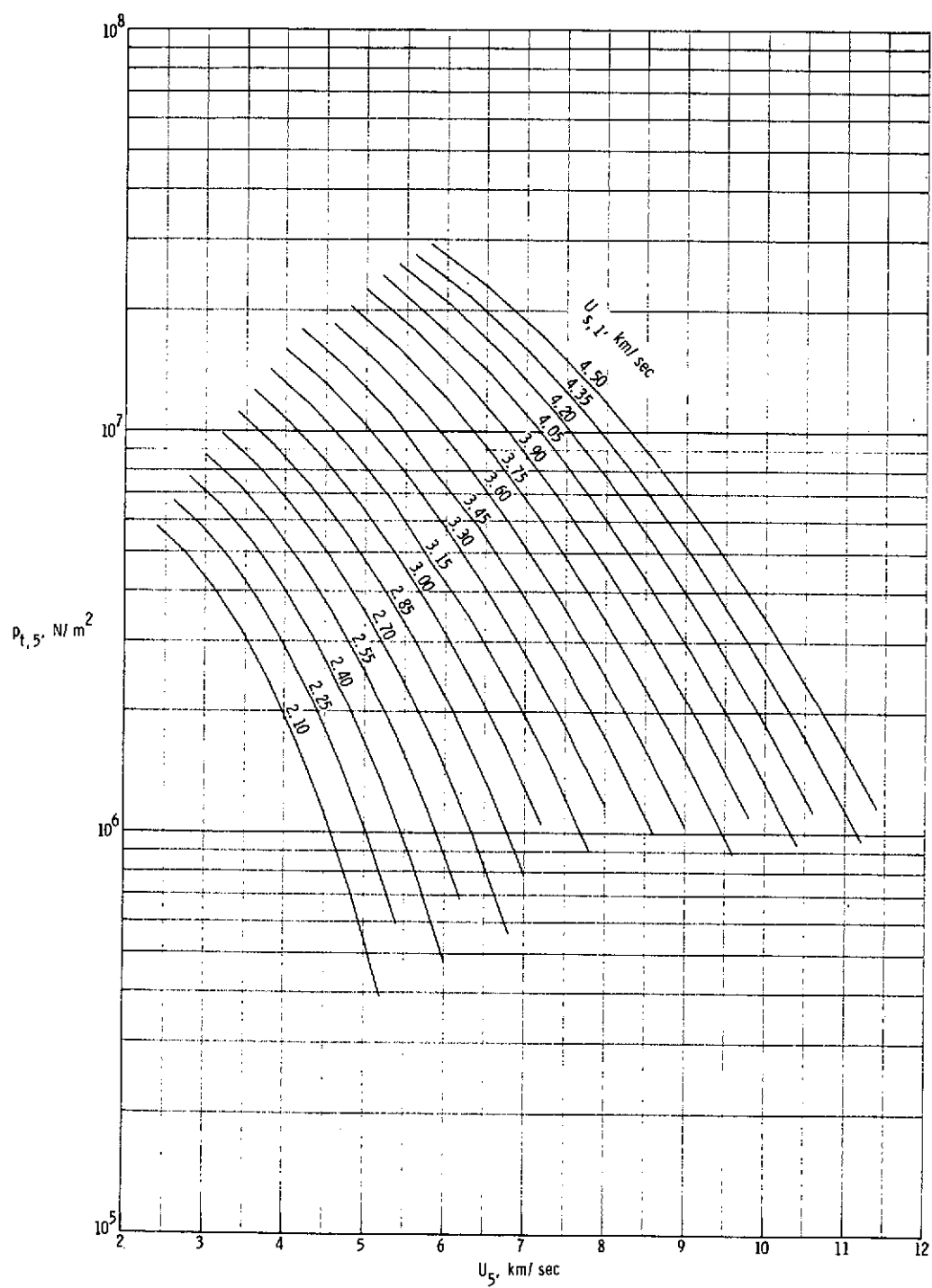
(e) Unit Reynolds number in region (5).

Figure 15.- Continued.



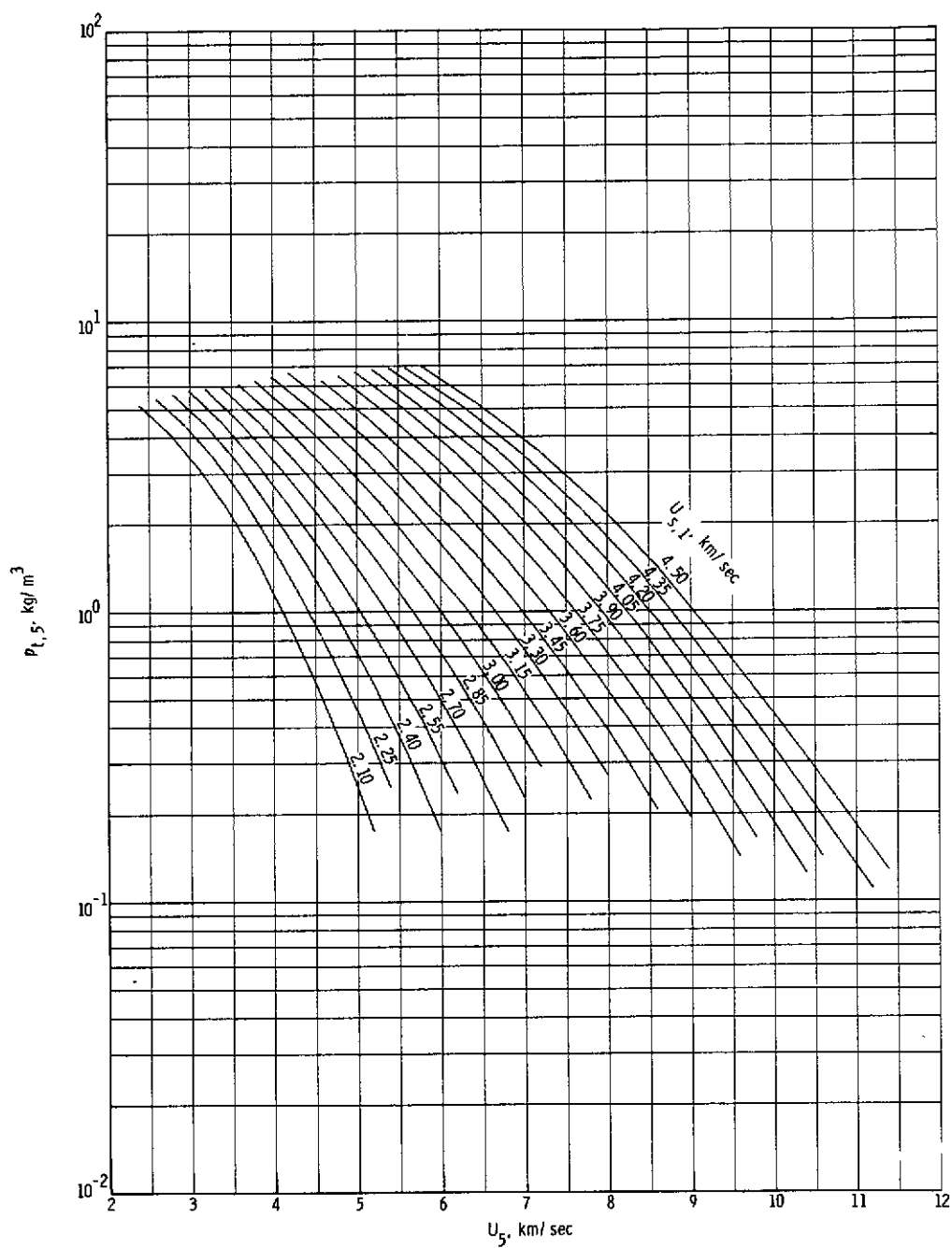
(f) Normal shock density ratio.

Figure 15.- Continued.



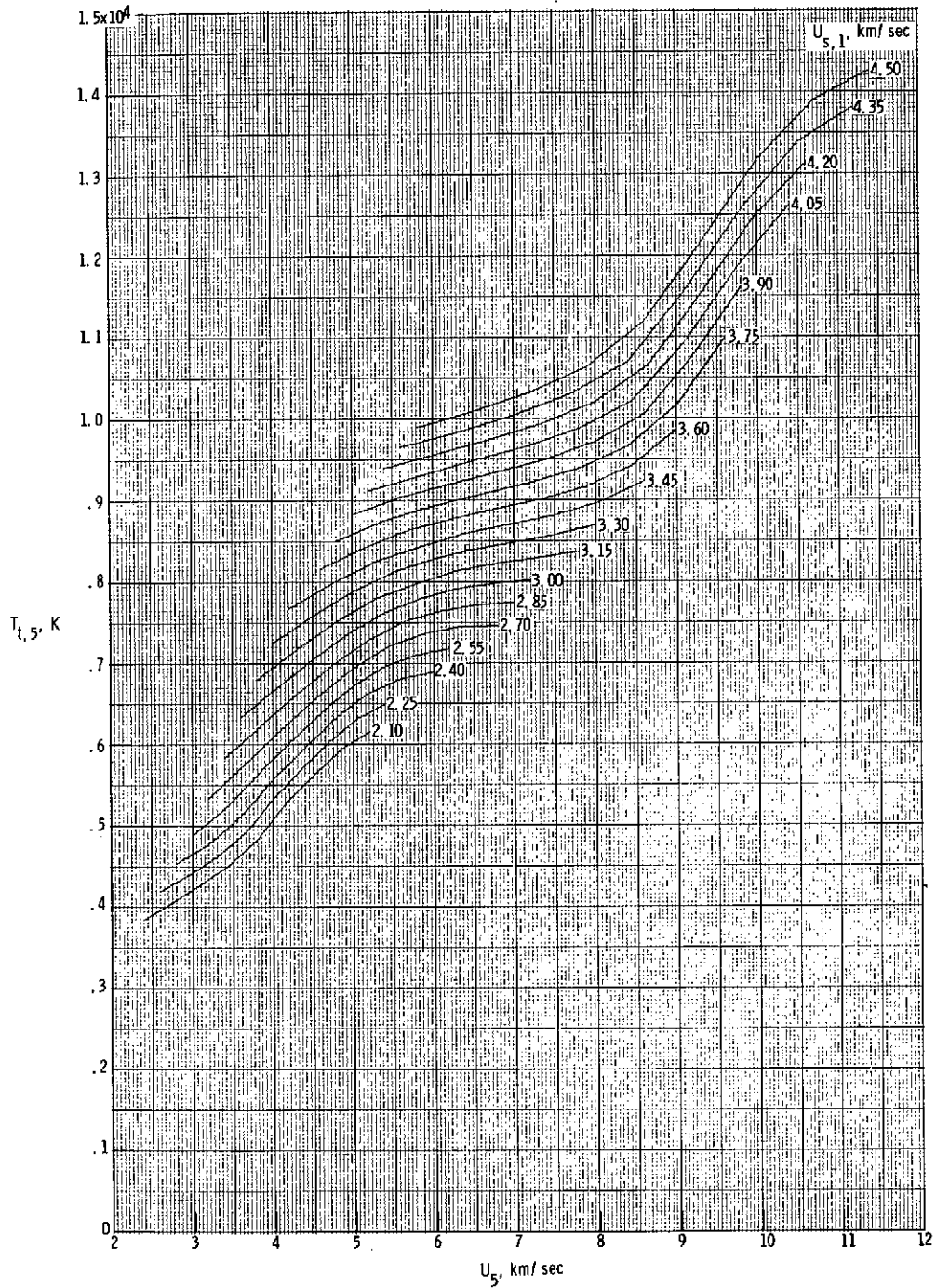
(g) Stagnation pressure behind normal bow shock.

Figure 15.- Continued.



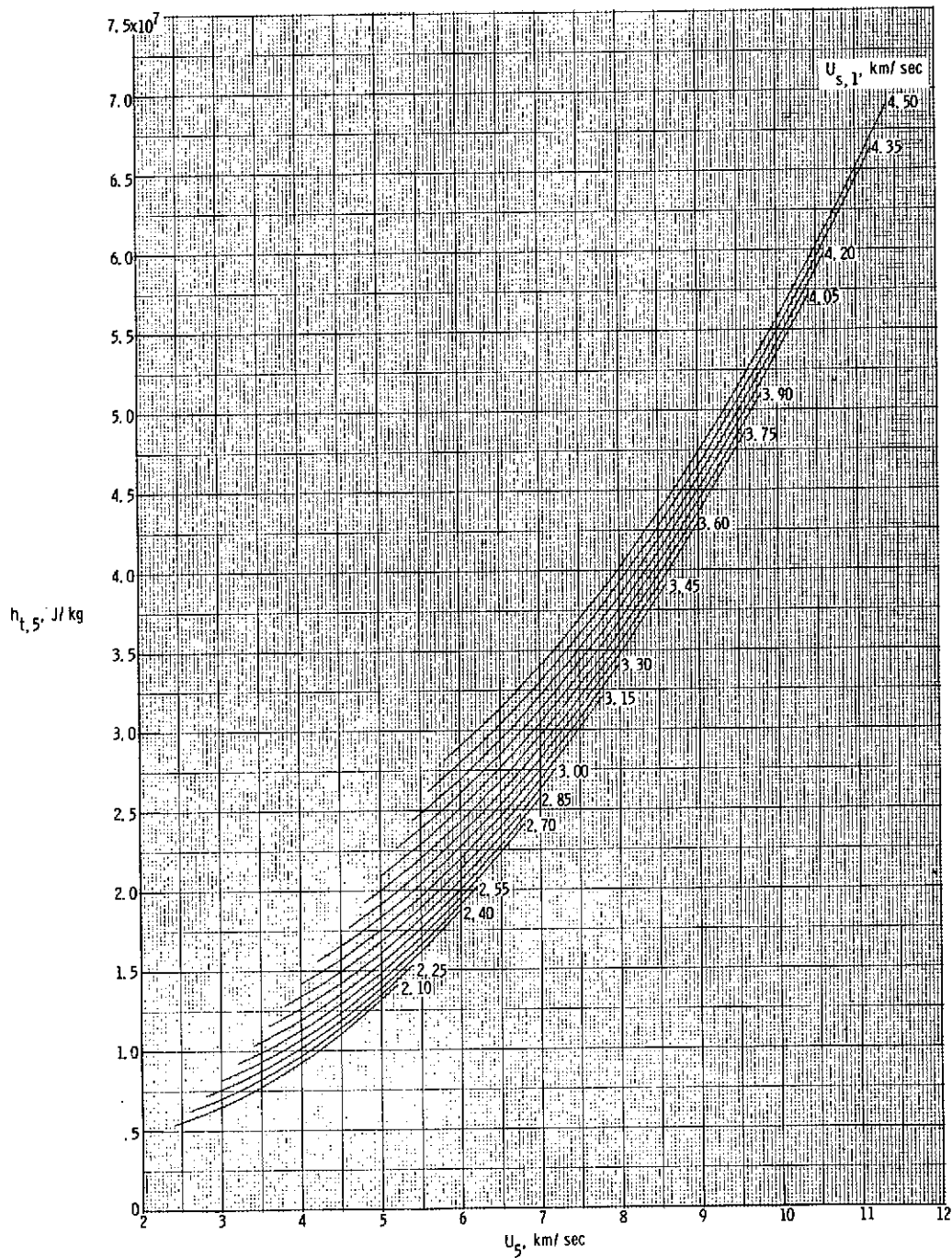
(h) Stagnation density behind normal bow shock.

Figure 15.- Continued.



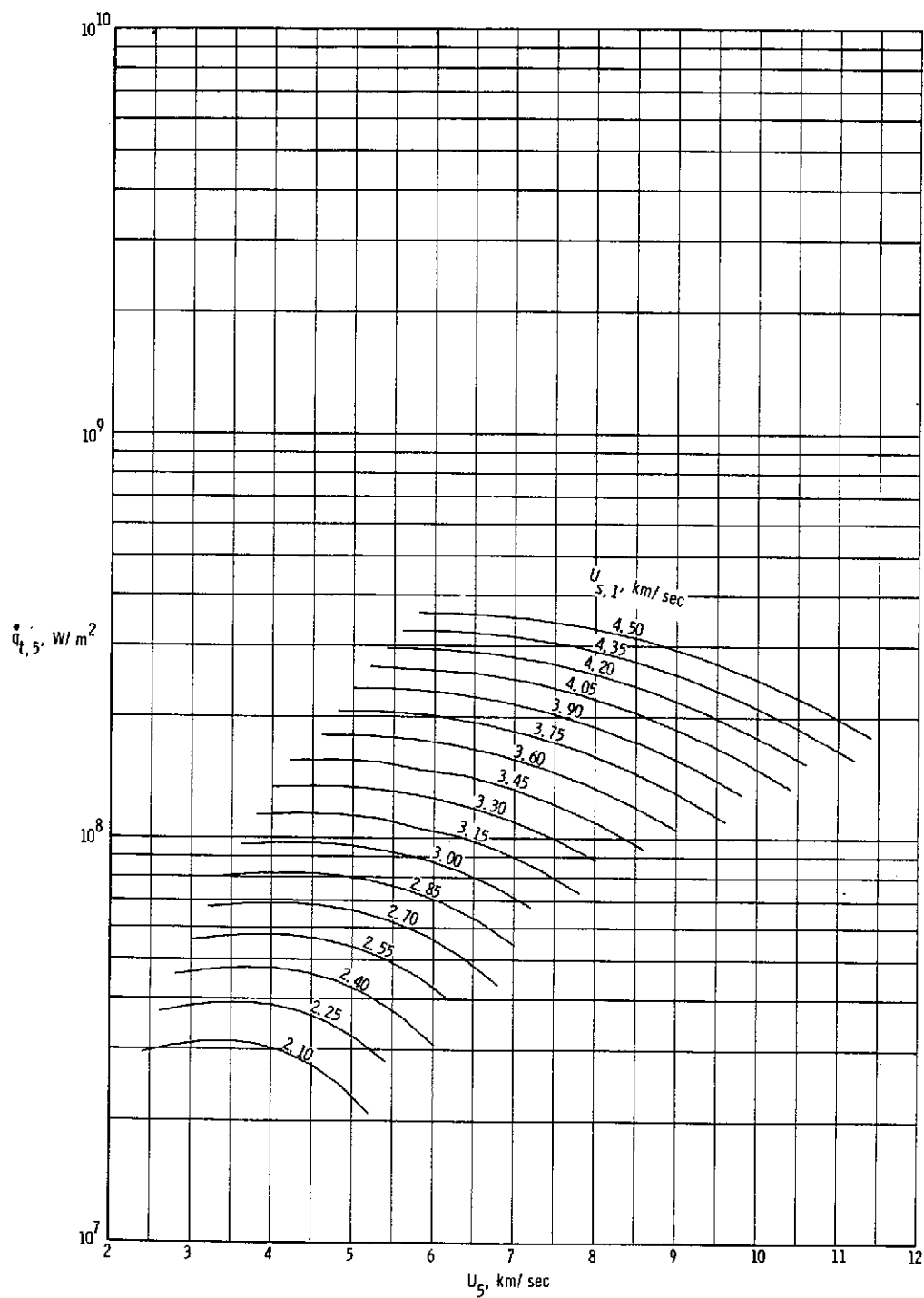
(i) Stagnation temperature behind normal bow shock.

Figure 15.- Continued.



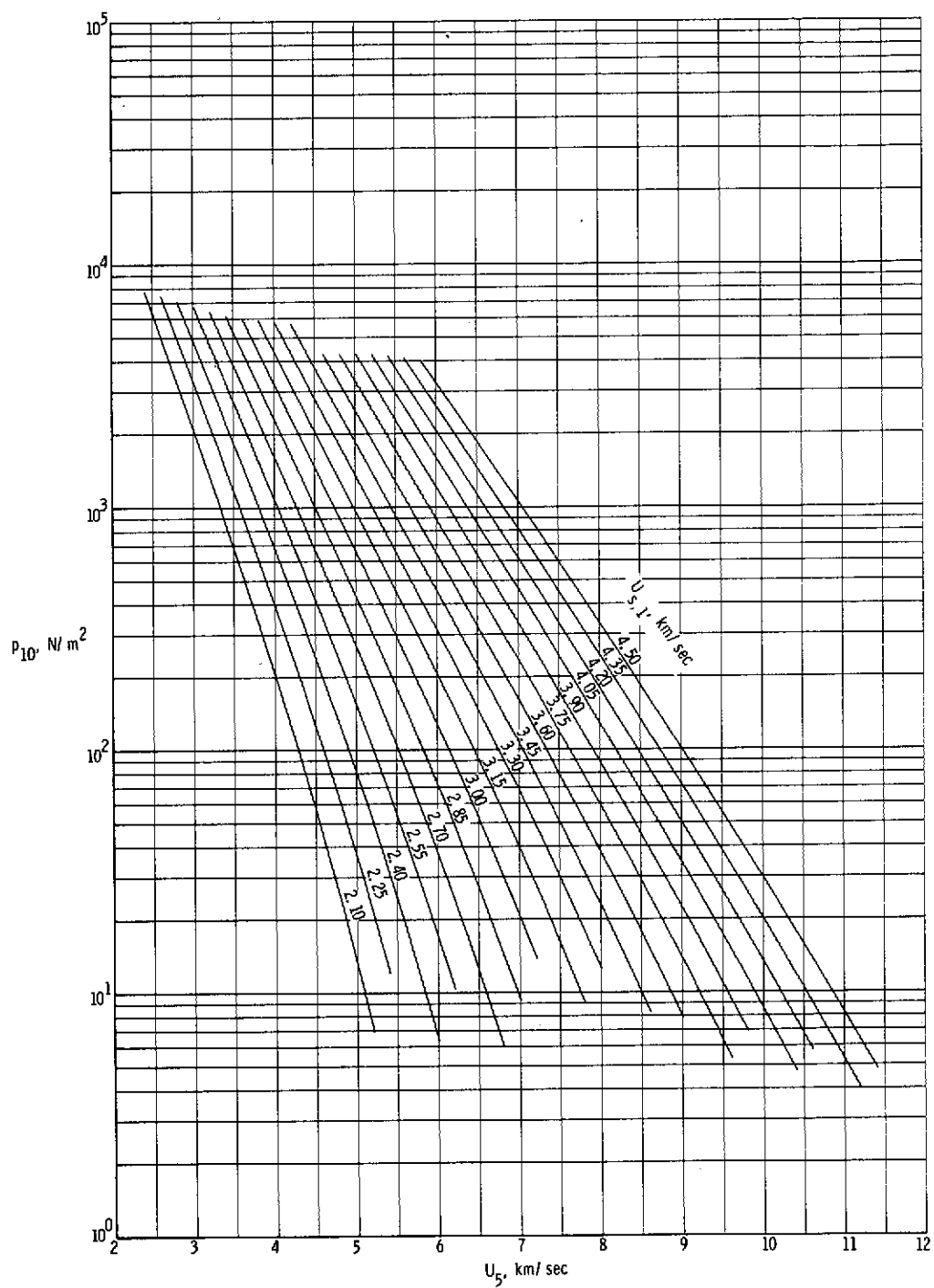
(j) Stagnation enthalpy behind normal bow shock.

Figure 15.- Continued.



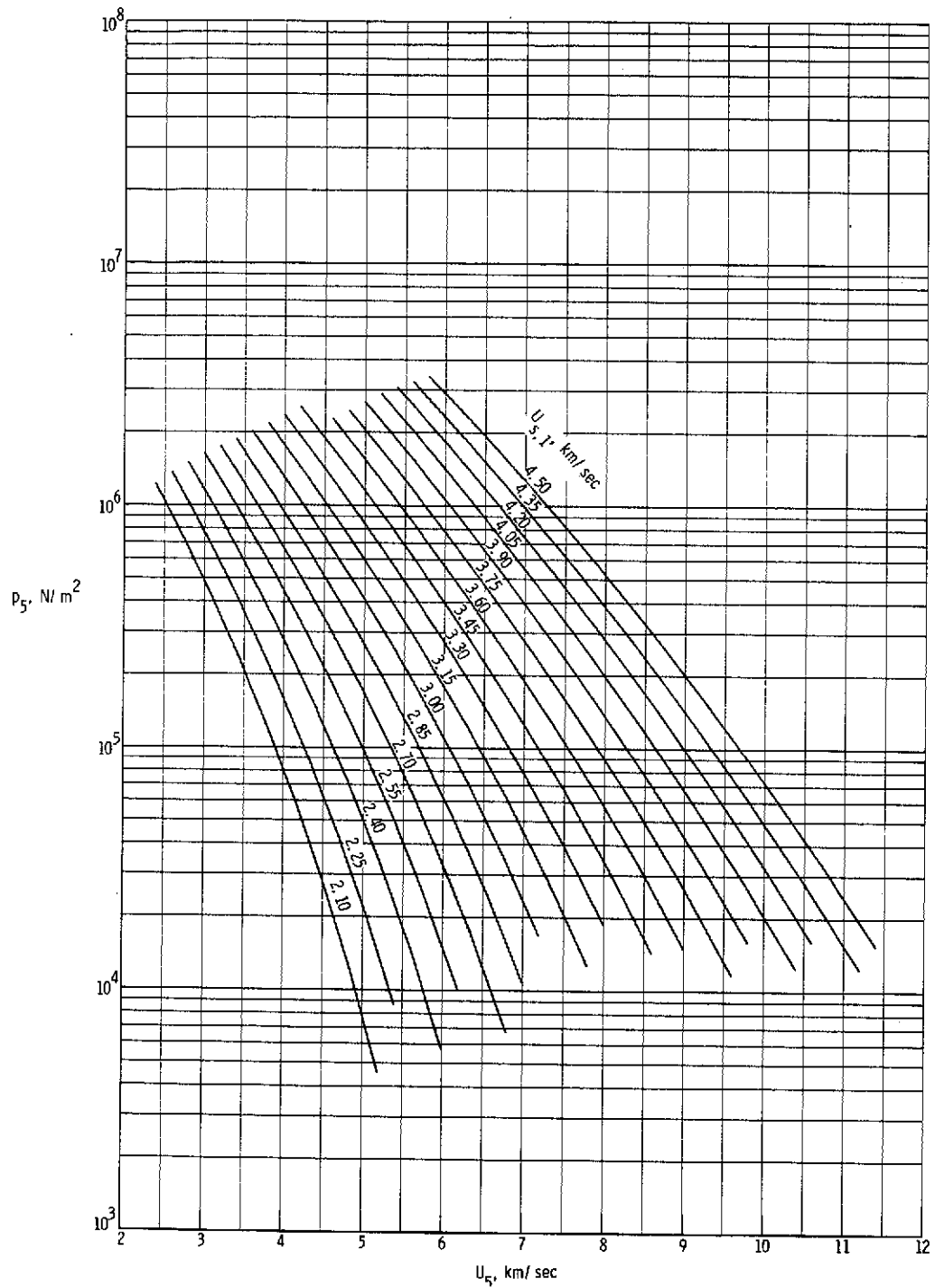
(k) Stagnation-point convective heat-transfer rate to sphere having radius of 2.54 cm.

Figure 15.- Continued.



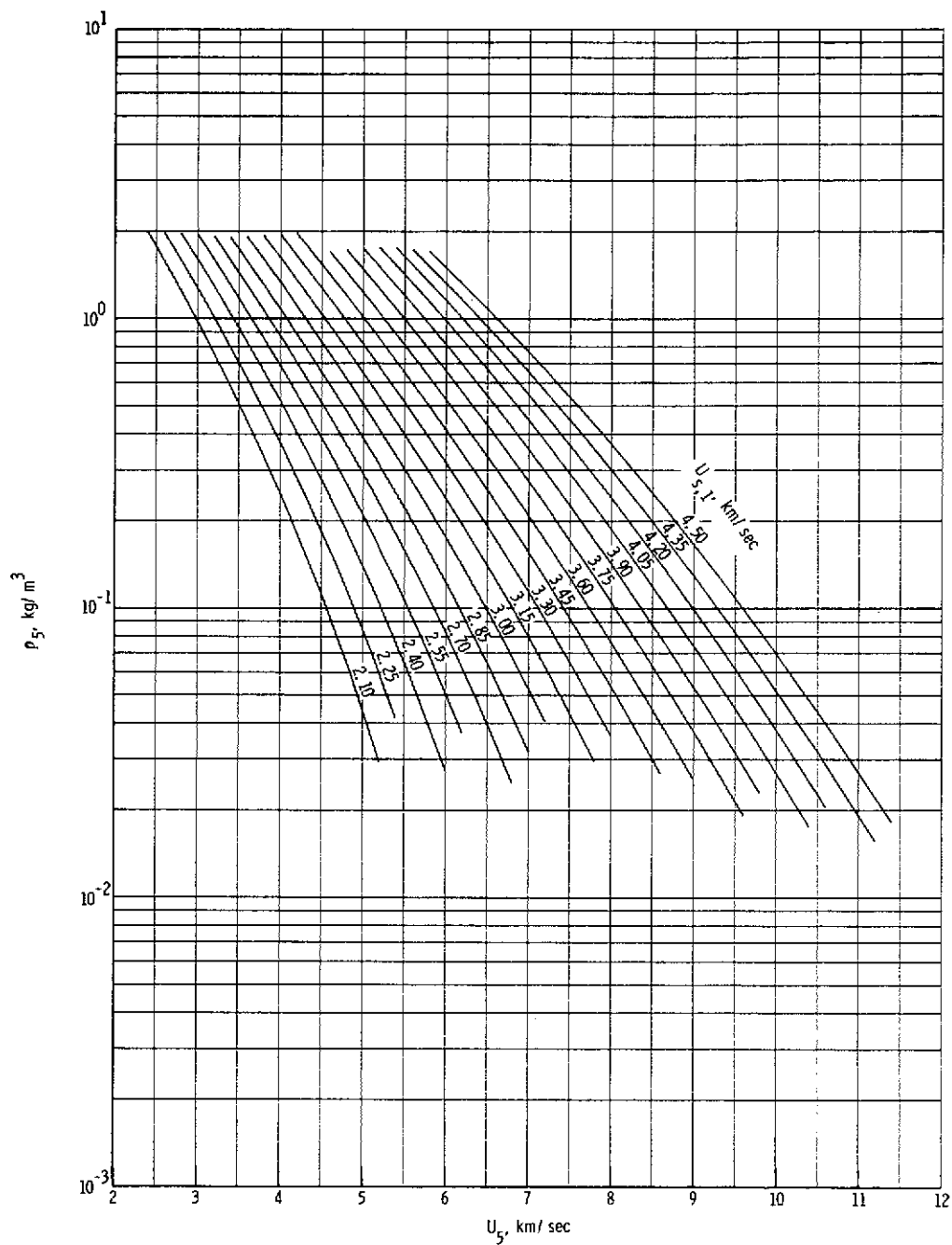
(1) Quiescent acceleration air pressure in region (10).

Figure 15.- Concluded.



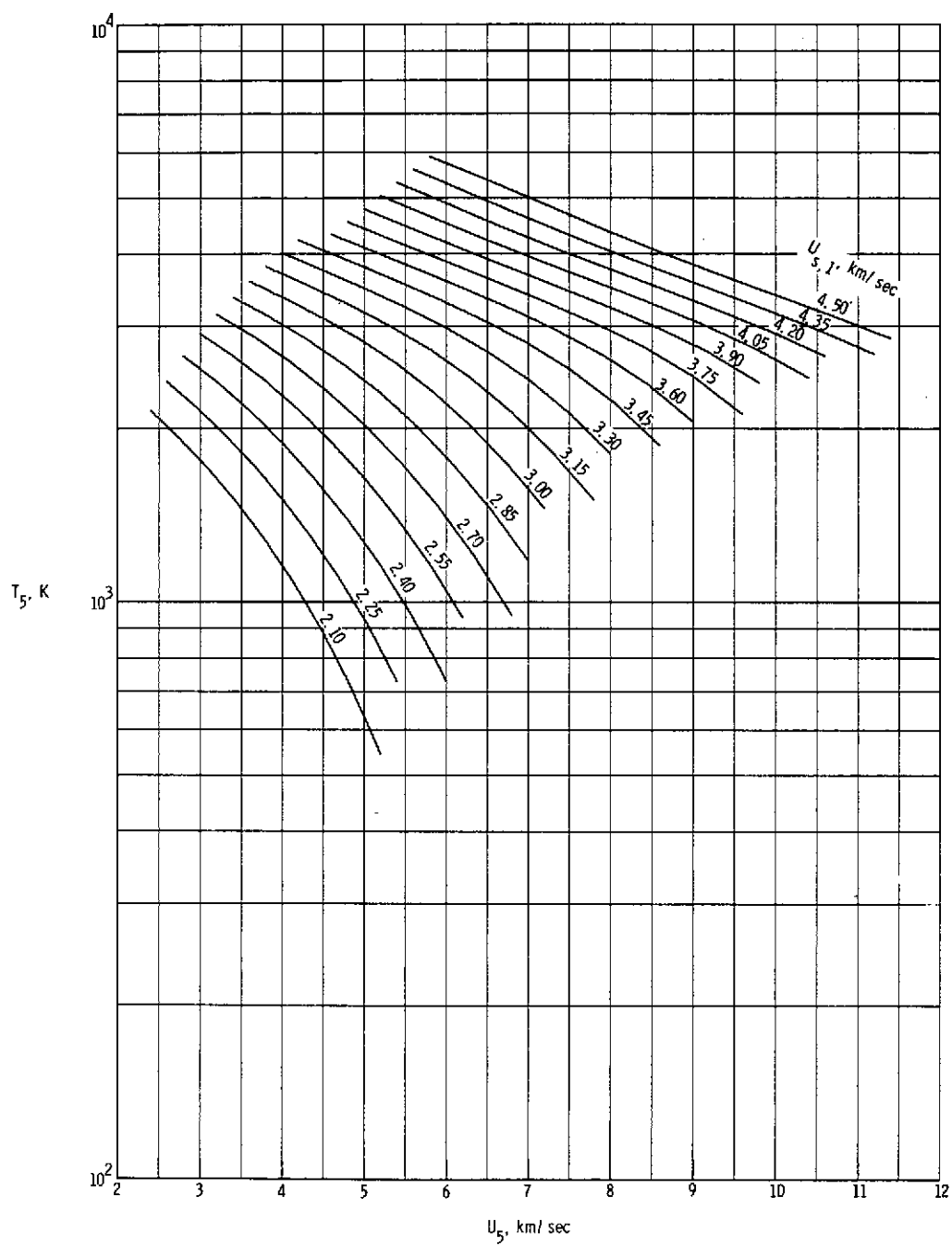
(a) Static pressure in region (5).

Figure 16.- Various expansion tube flow parameters for real air in thermochemical equilibrium as a function of flow velocity and assuming a totally reflected shock at the secondary diaphragm. $p_1 = 68.95 \text{ kN/m}^2$.



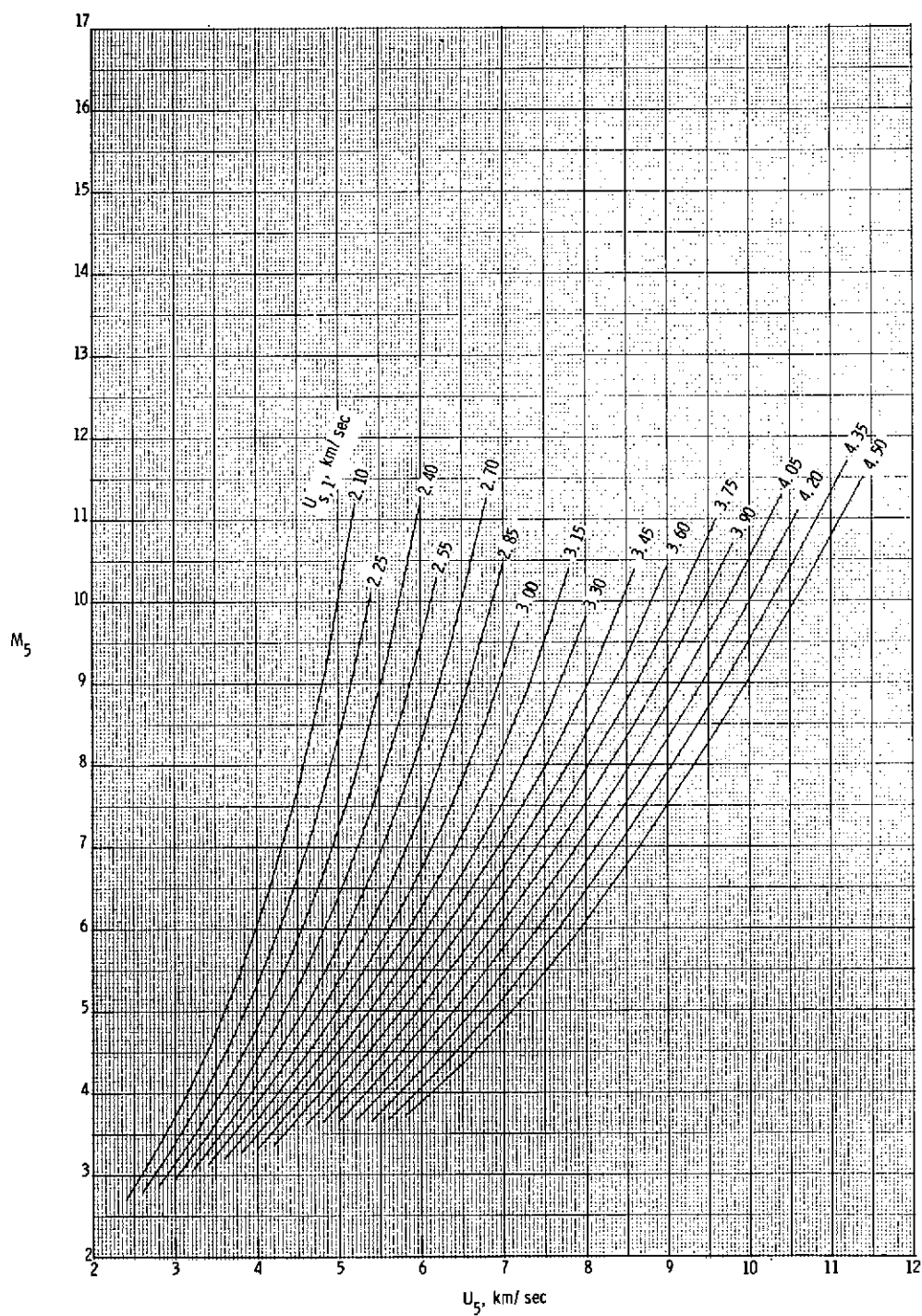
(b) Static density in region (5).

Figure 16.- Continued.



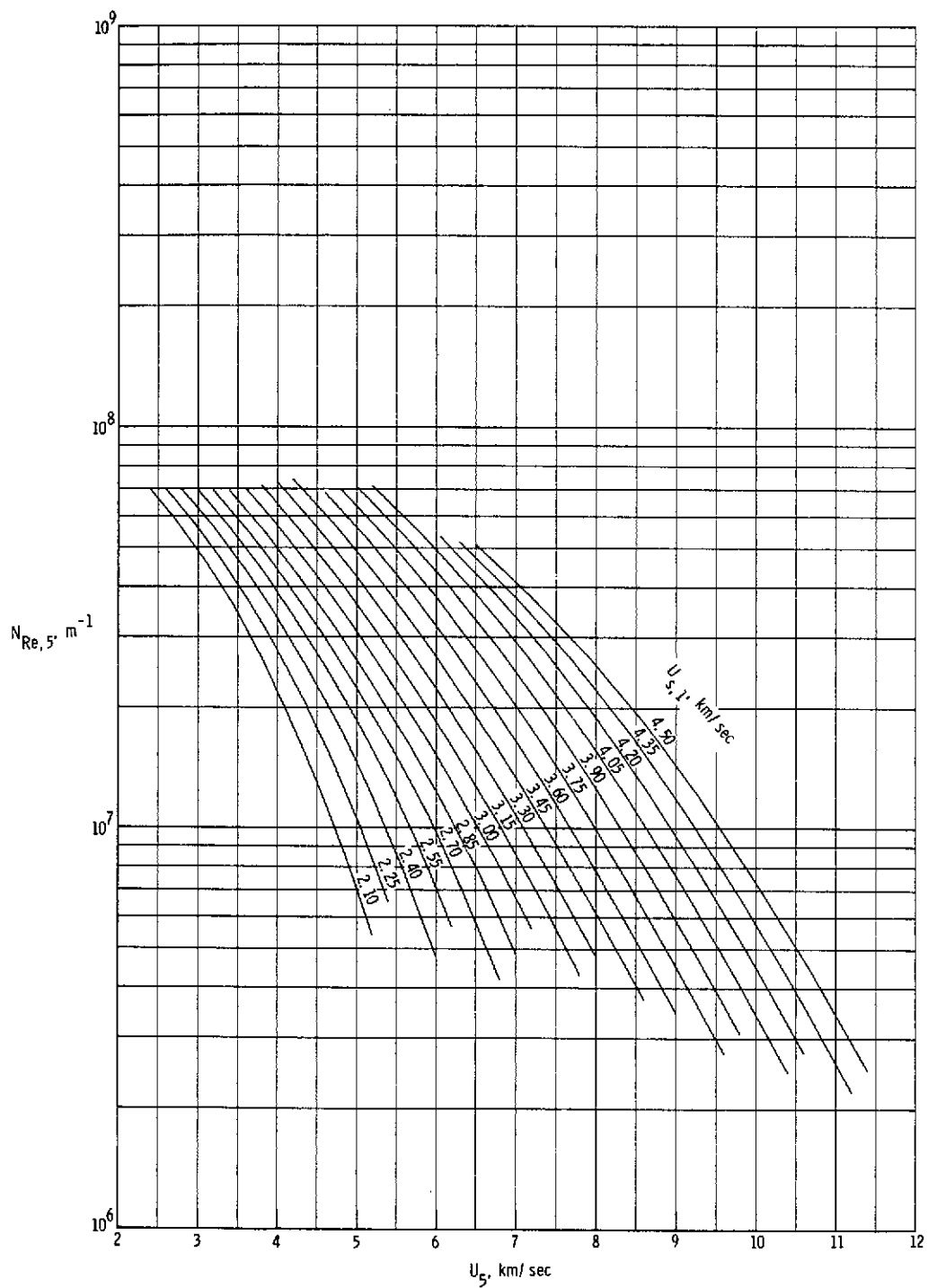
(c) Static temperature in region ⑤.

Figure 16.- Continued.



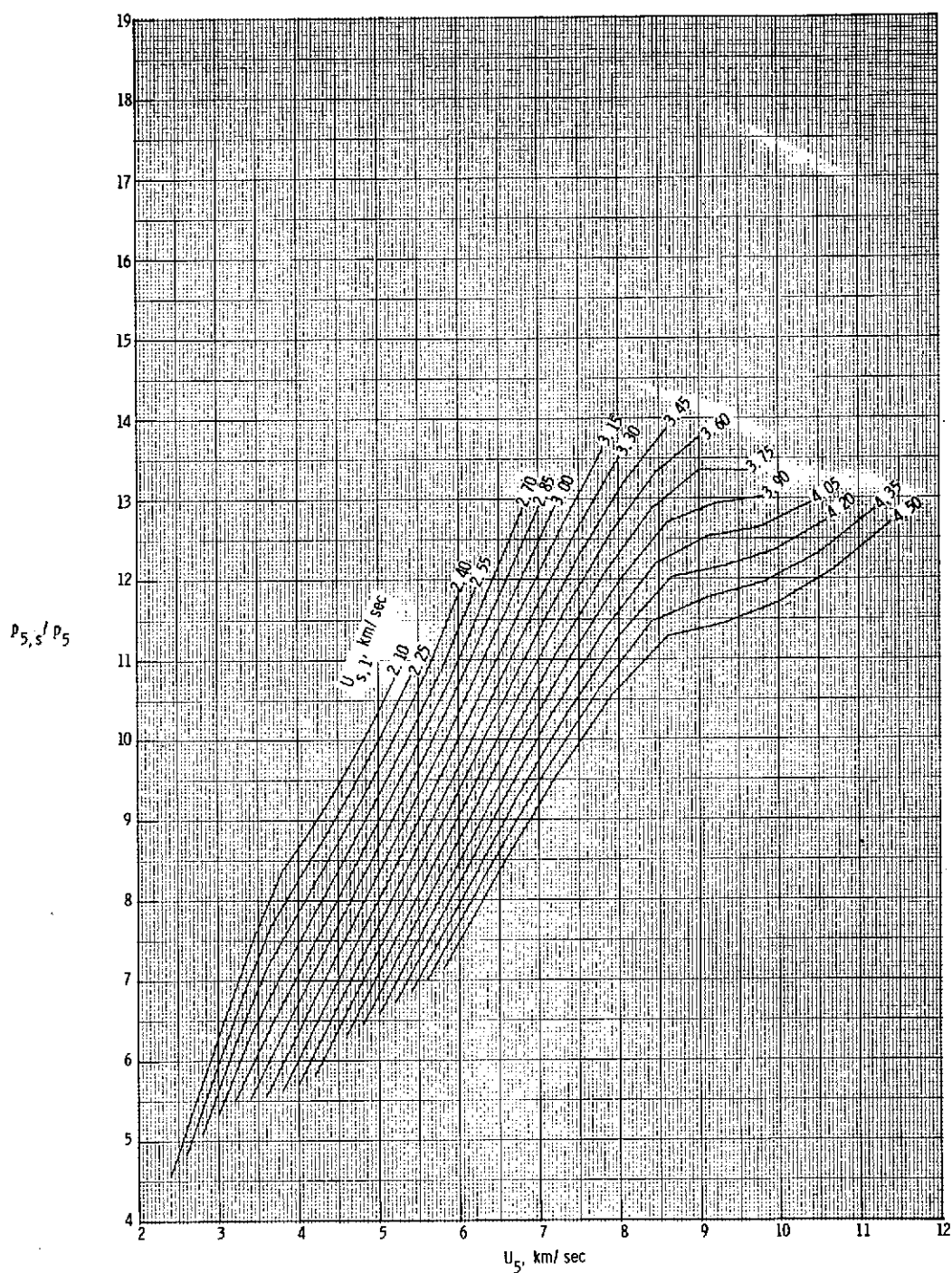
(d) Mach number in region (5).

Figure 16.- Continued.



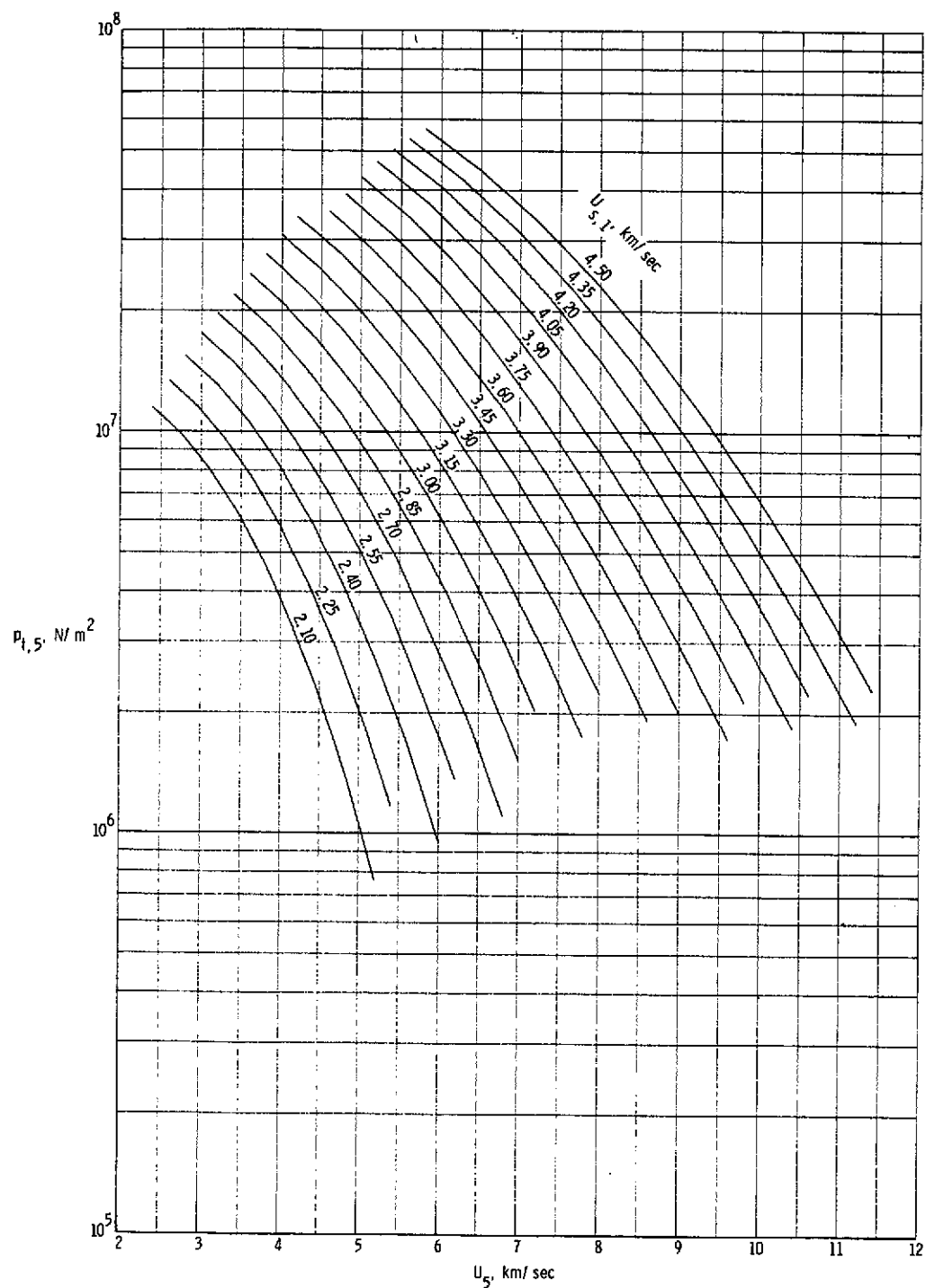
(e) Unit Reynolds number in region (5).

Figure 16.- Continued.



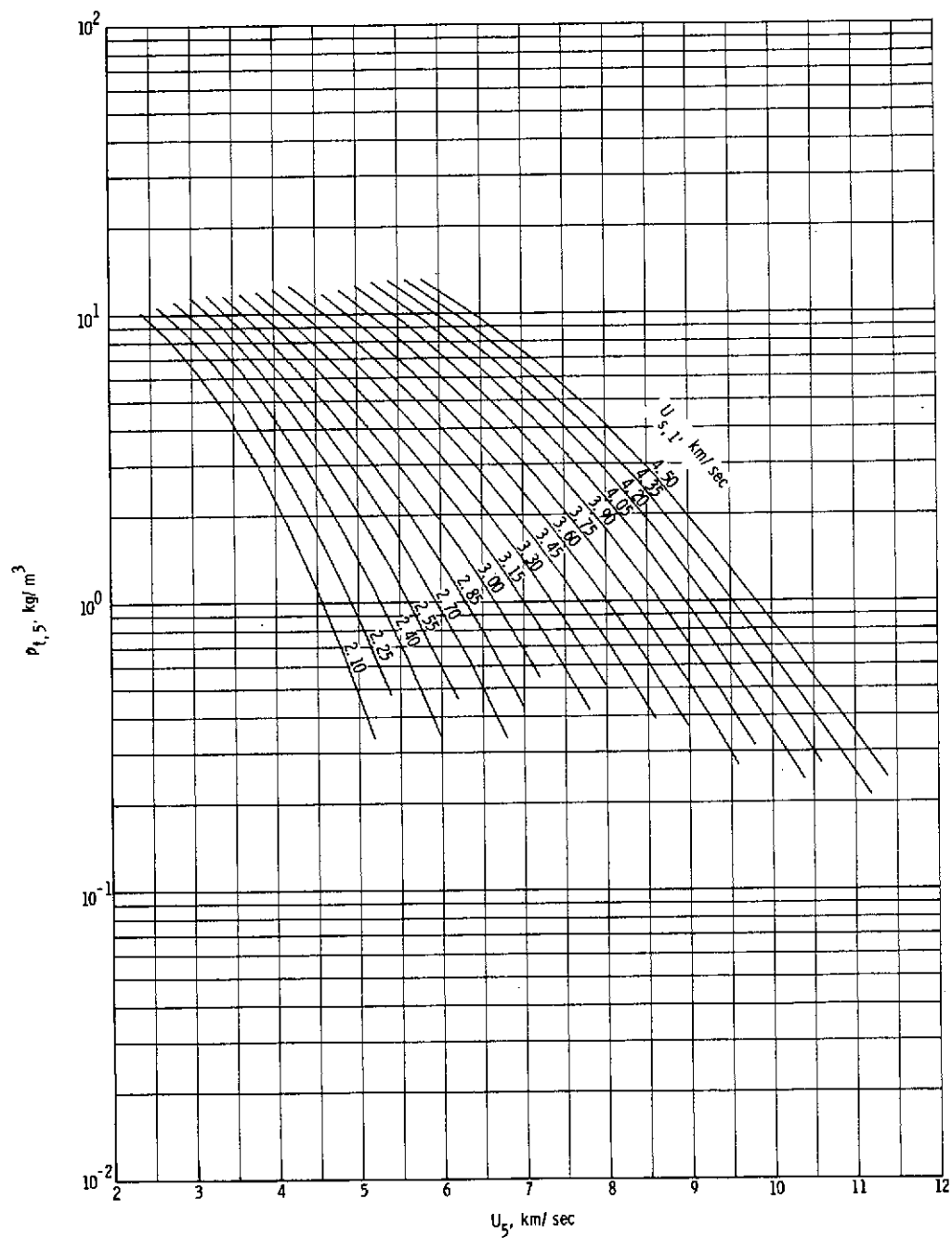
(f) Normal shock density ratio.

Figure 16.- Continued.



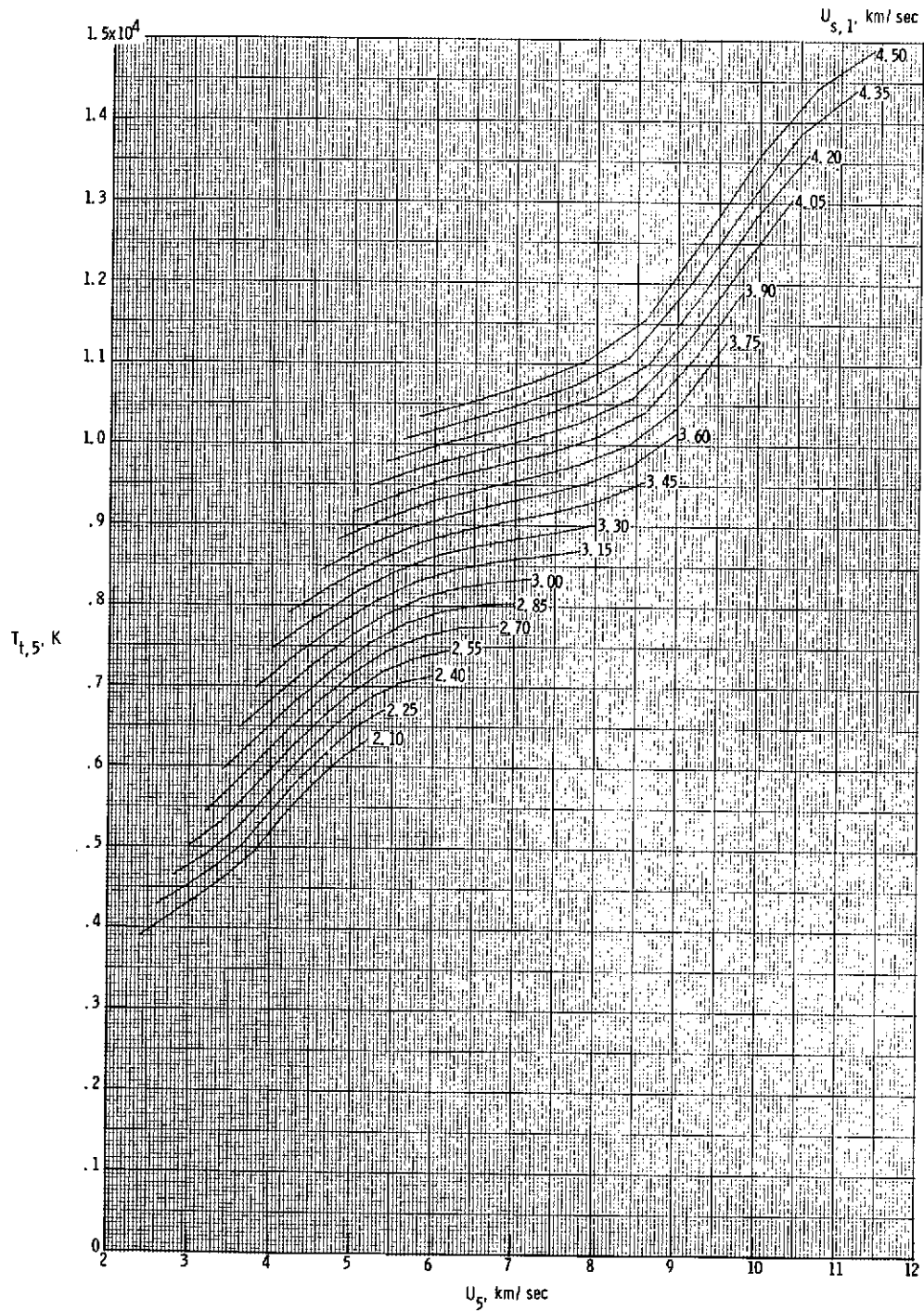
(g) Stagnation pressure behind normal bow shock.

Figure 16.- Continued.



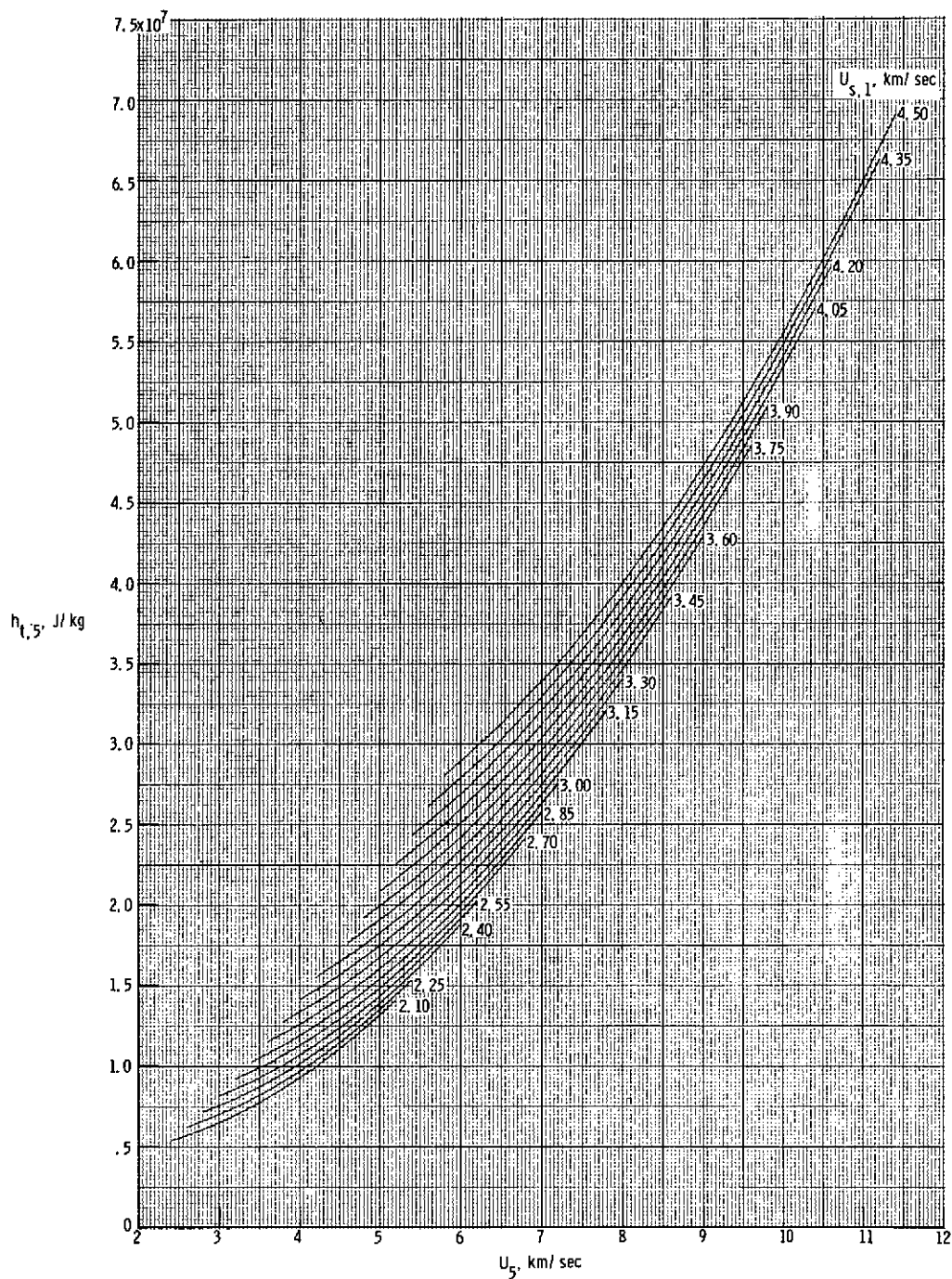
(h) Stagnation density behind normal bow shock.

Figure 16.- Continued.



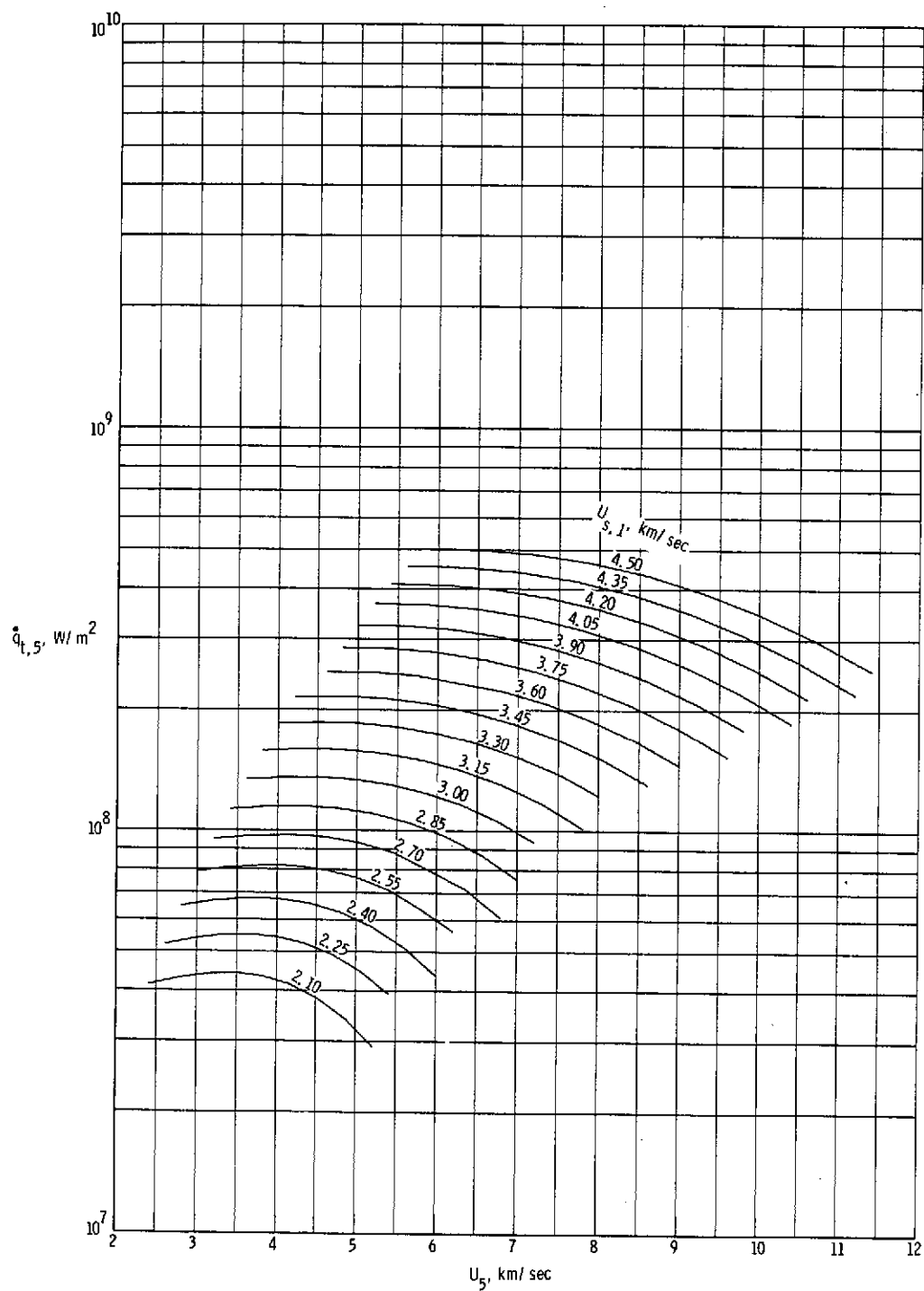
(i) Stagnation temperature behind normal bow shock.

Figure 16.- Continued.



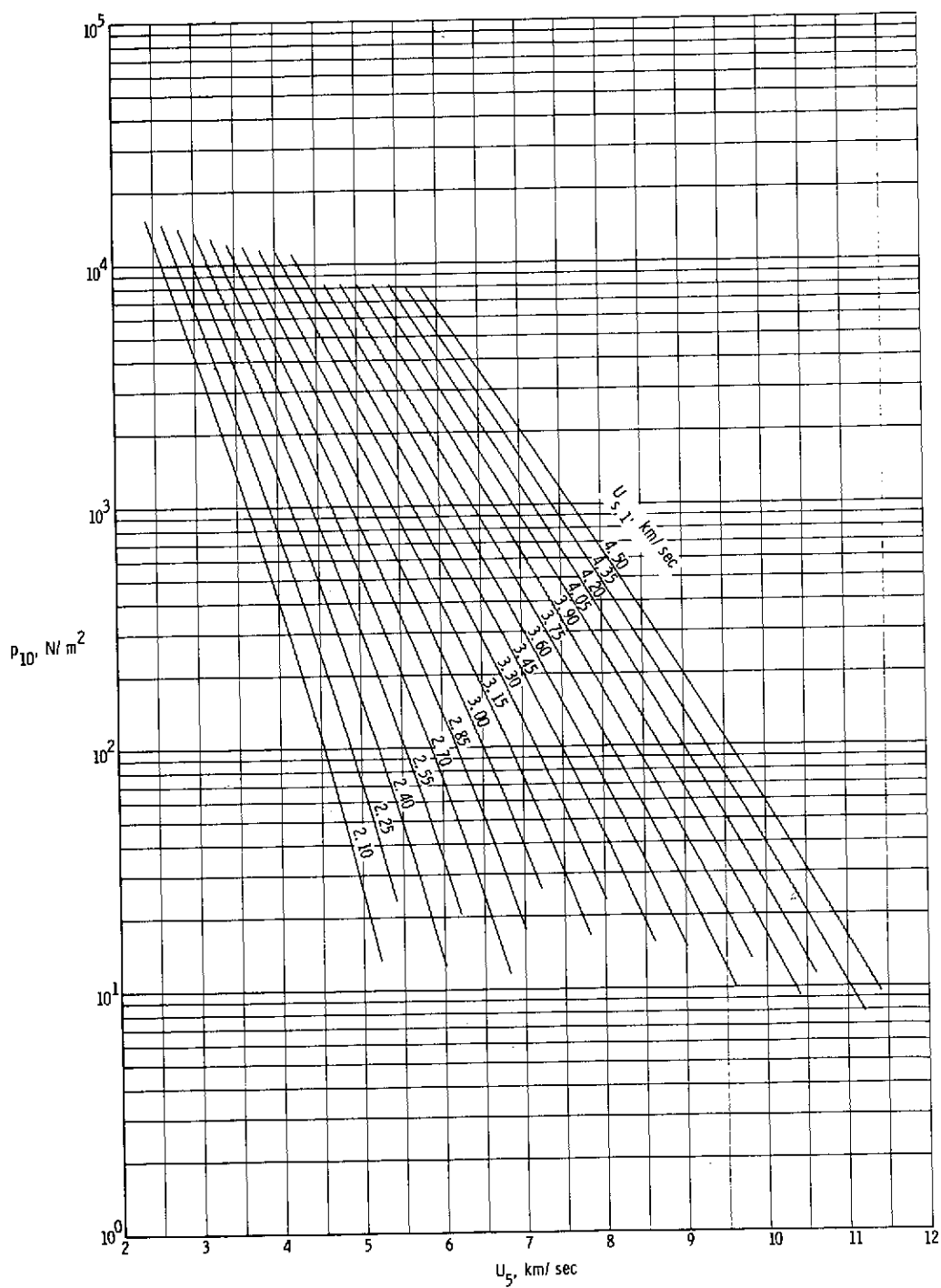
(j) Stagnation enthalpy behind normal bow shock.

Figure 16.- Continued.



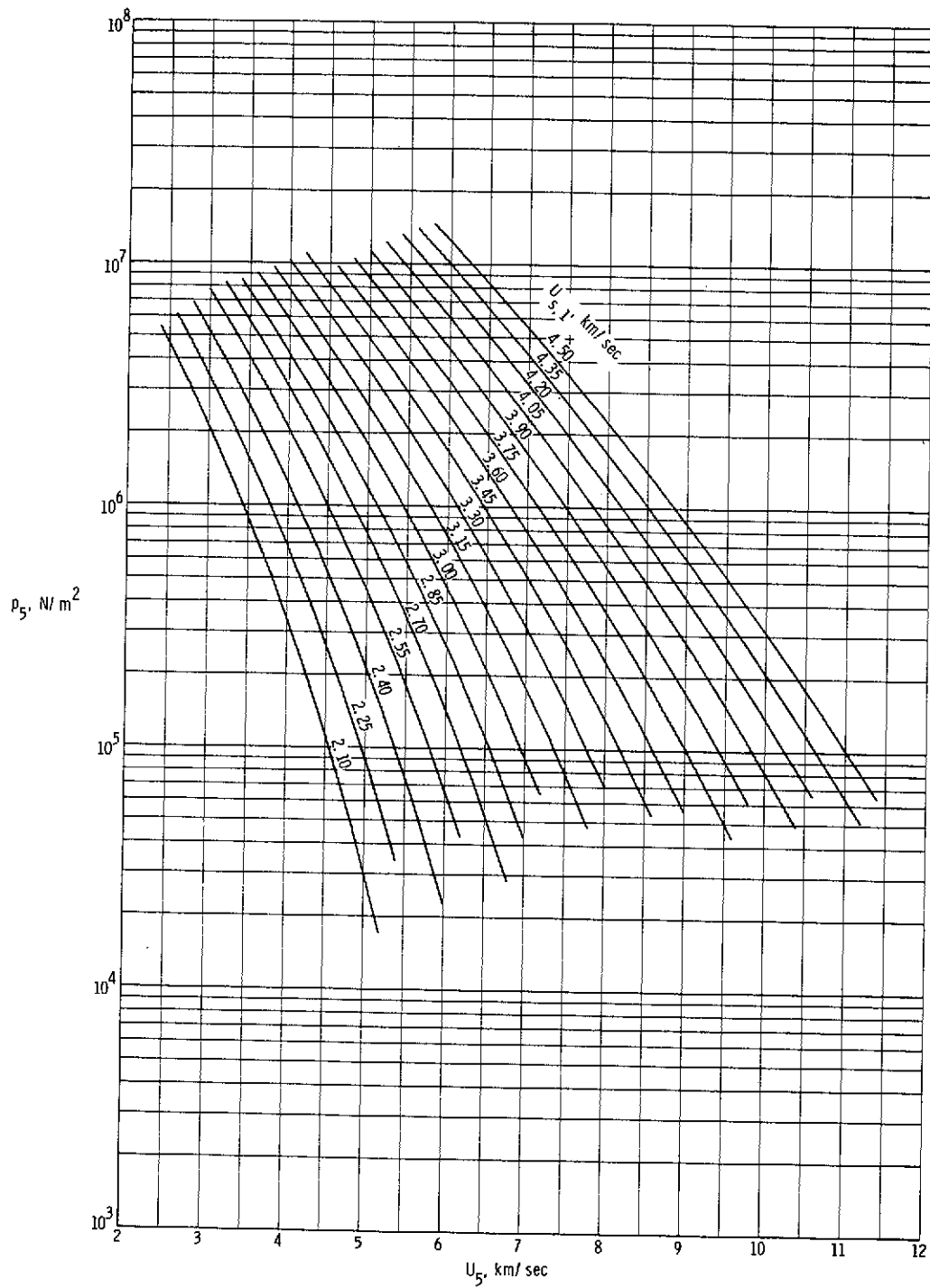
(k) Stagnation-point convective heat-transfer rate to sphere having radius of 2.54 cm.

Figure 16.- Continued.



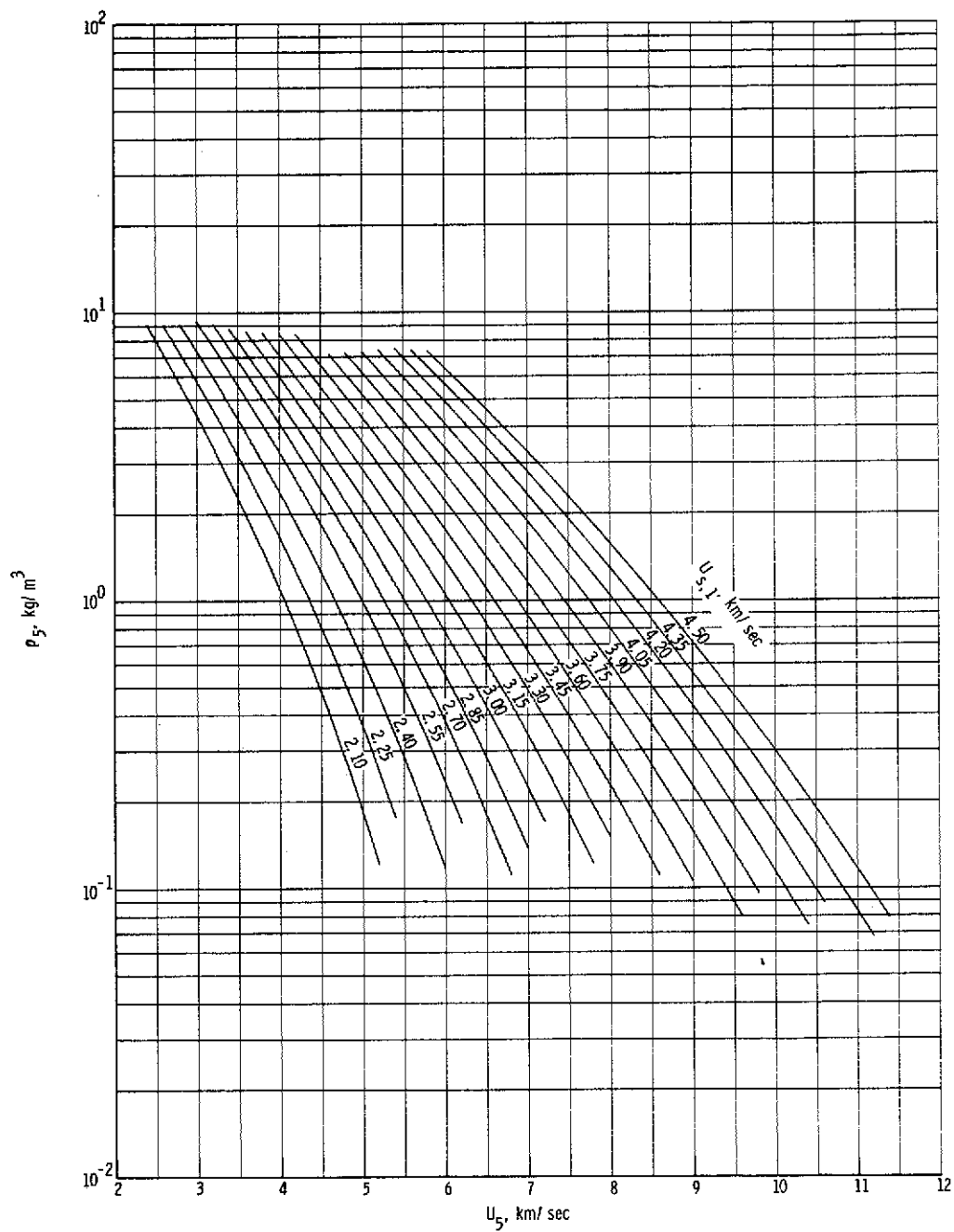
(1) Quiescent acceleration air pressure in region (10).

Figure 16.- Concluded.



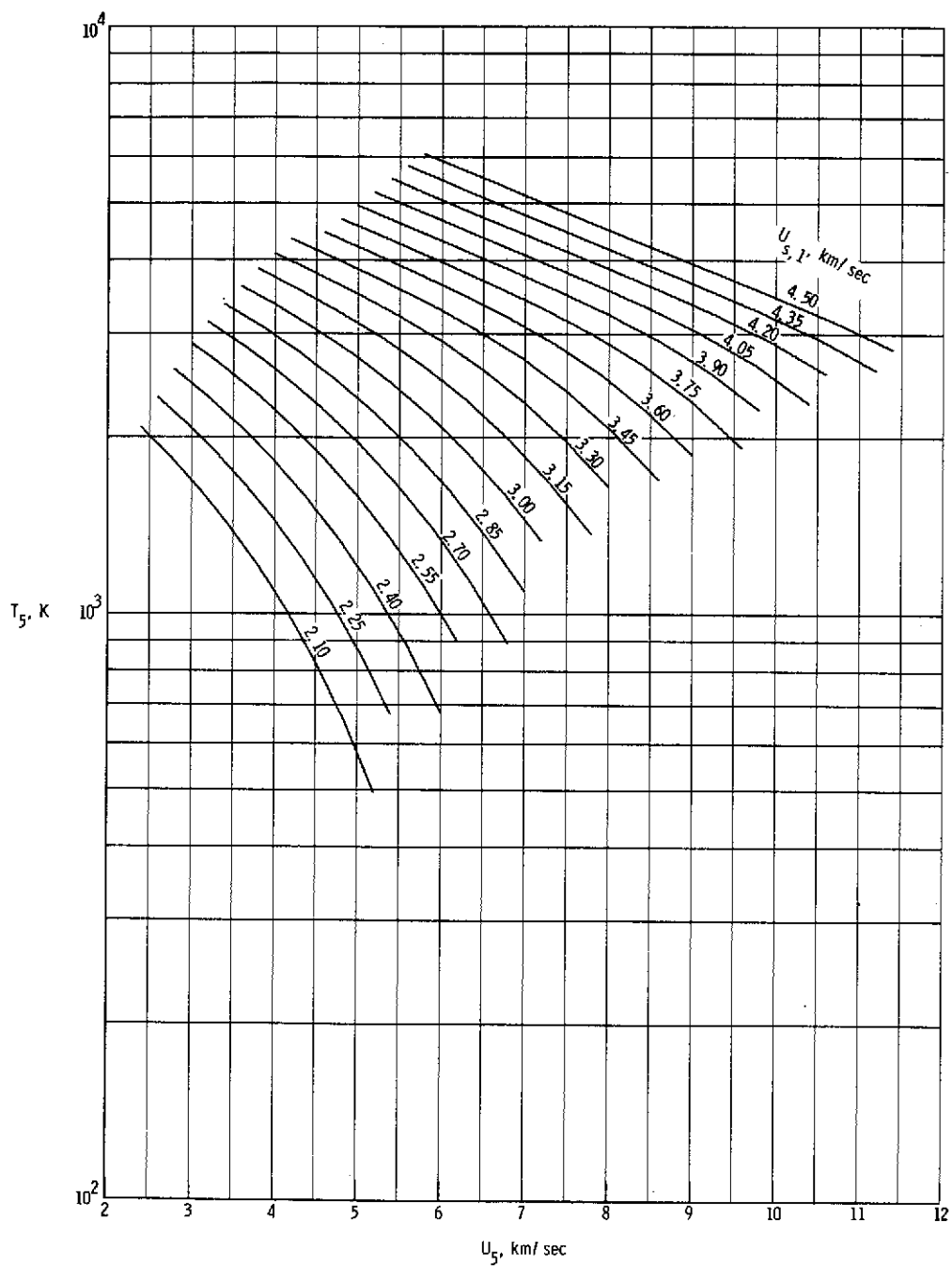
(a) Static pressure in region (5).

Figure 17.- Various expansion tube flow parameters for real air in thermochemical equilibrium as a function of flow velocity and assuming a totally reflected shock at the secondary diaphragm. $p_1 = 344.74 \text{ kN/m}^2$.



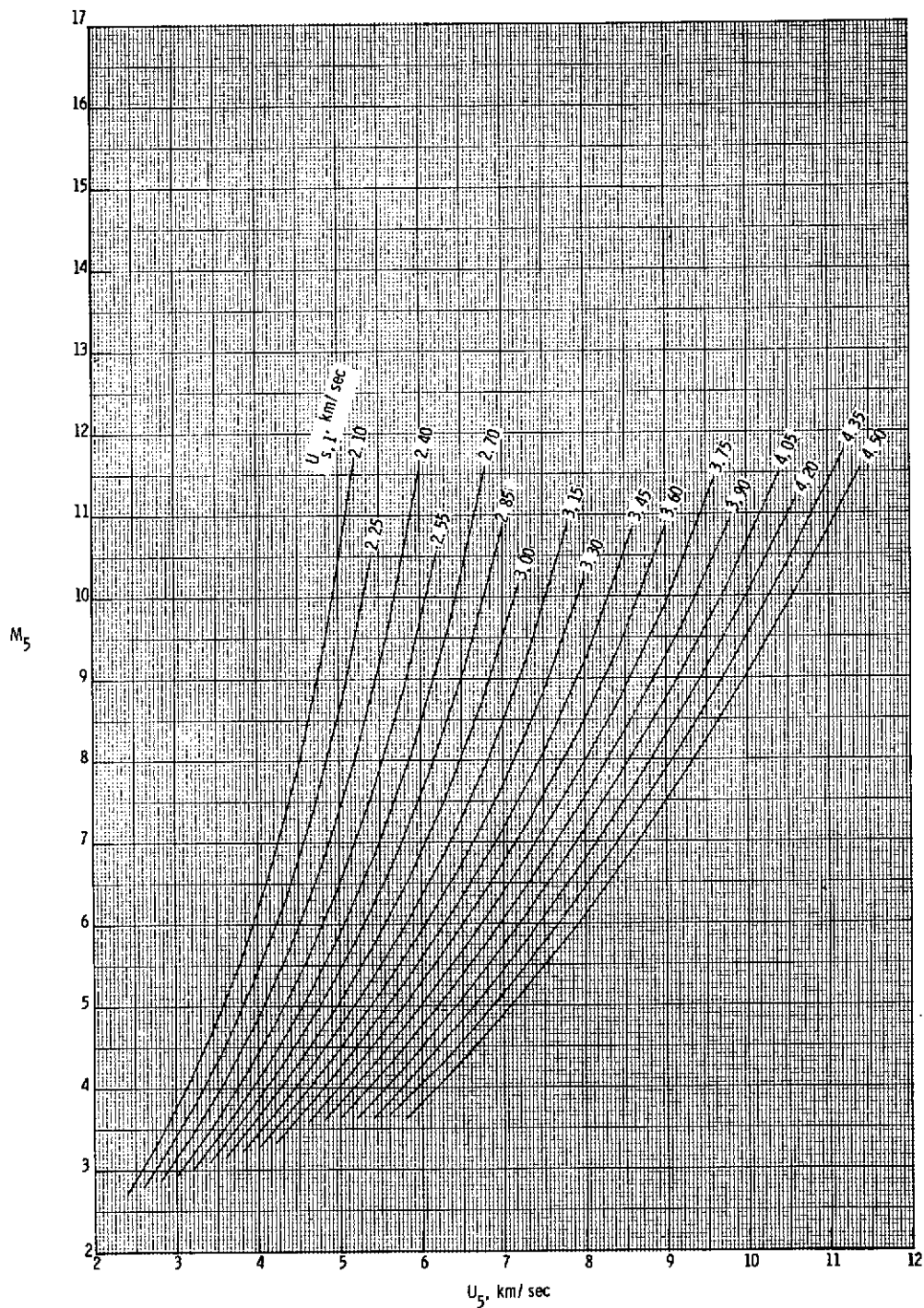
(b) Static density in region (5).

Figure 17.- Continued.



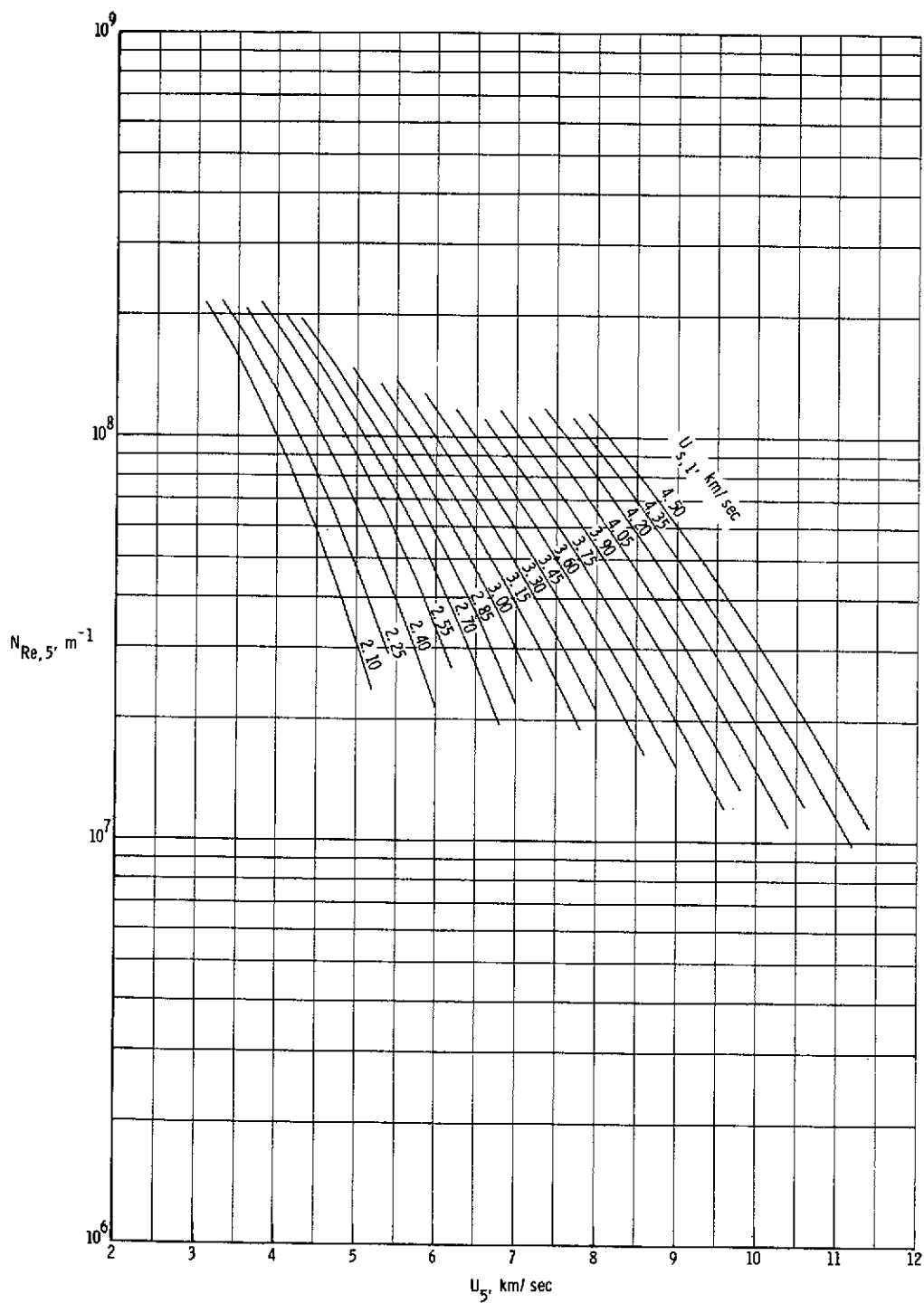
(c) Static temperature in region (5).

Figure 17.- Continued.



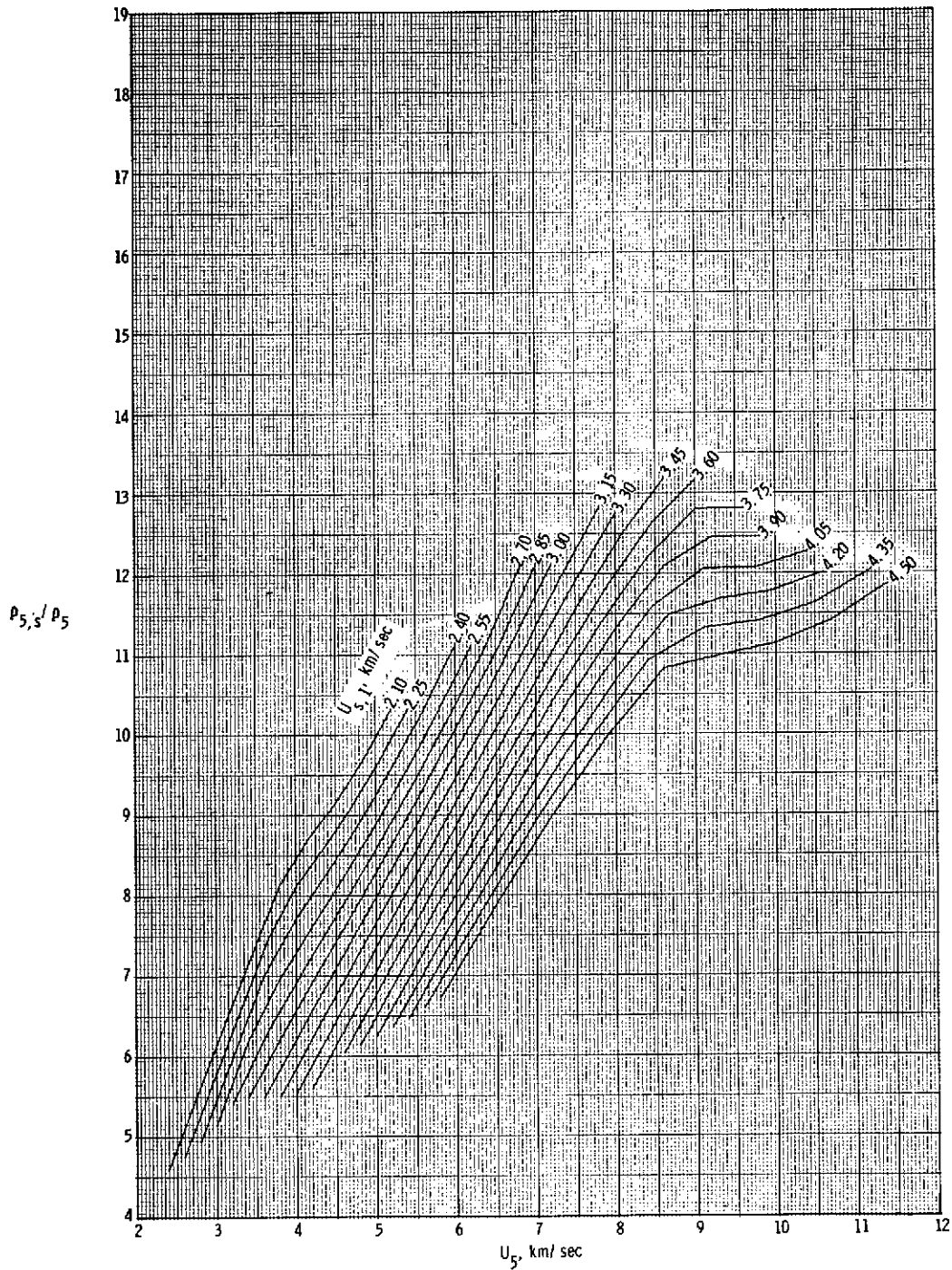
(d) Mach number in region (5).

Figure 17.- Continued.



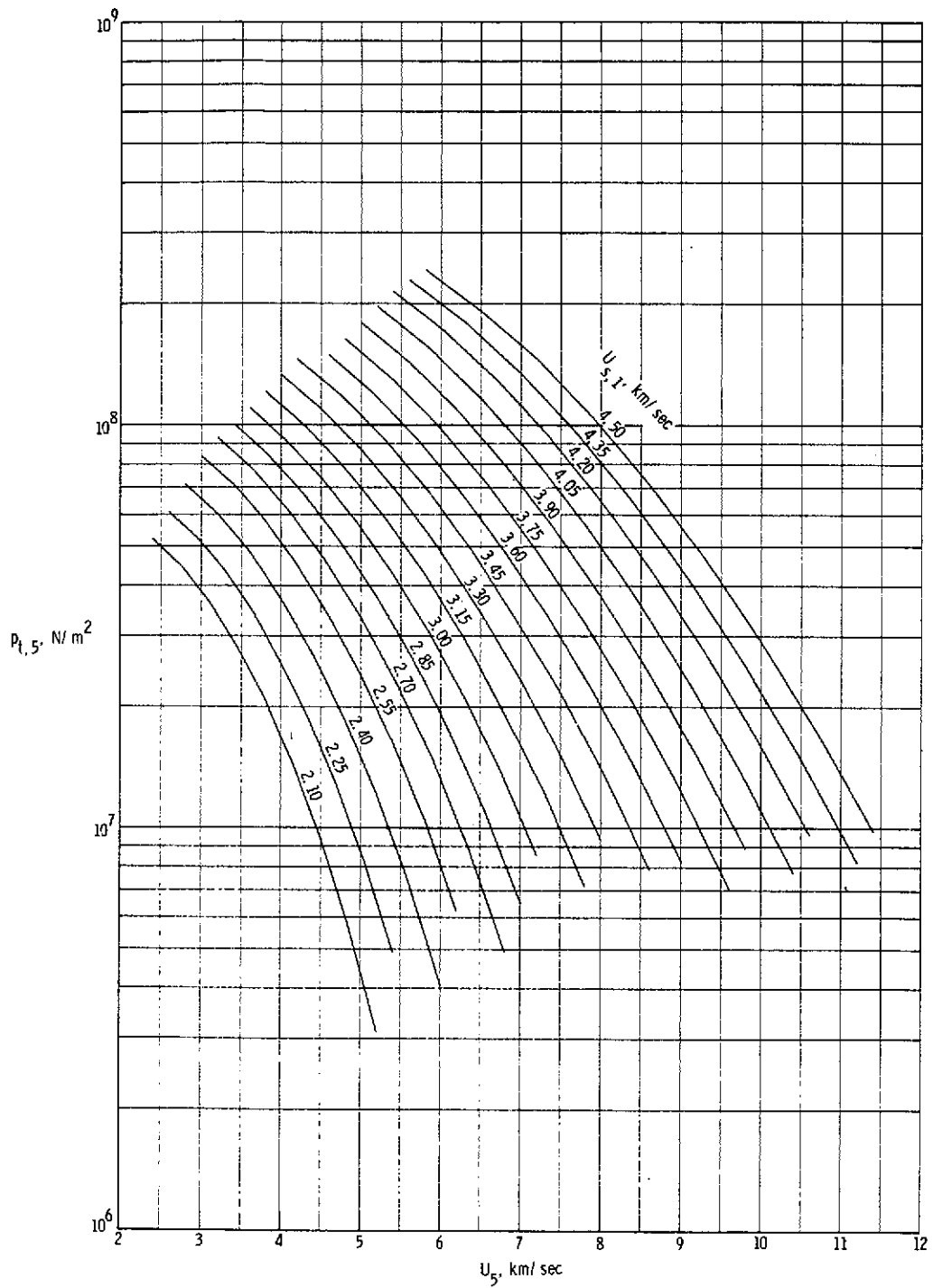
(e) Unit Reynolds number in region (5).

Figure 17.- Continued.



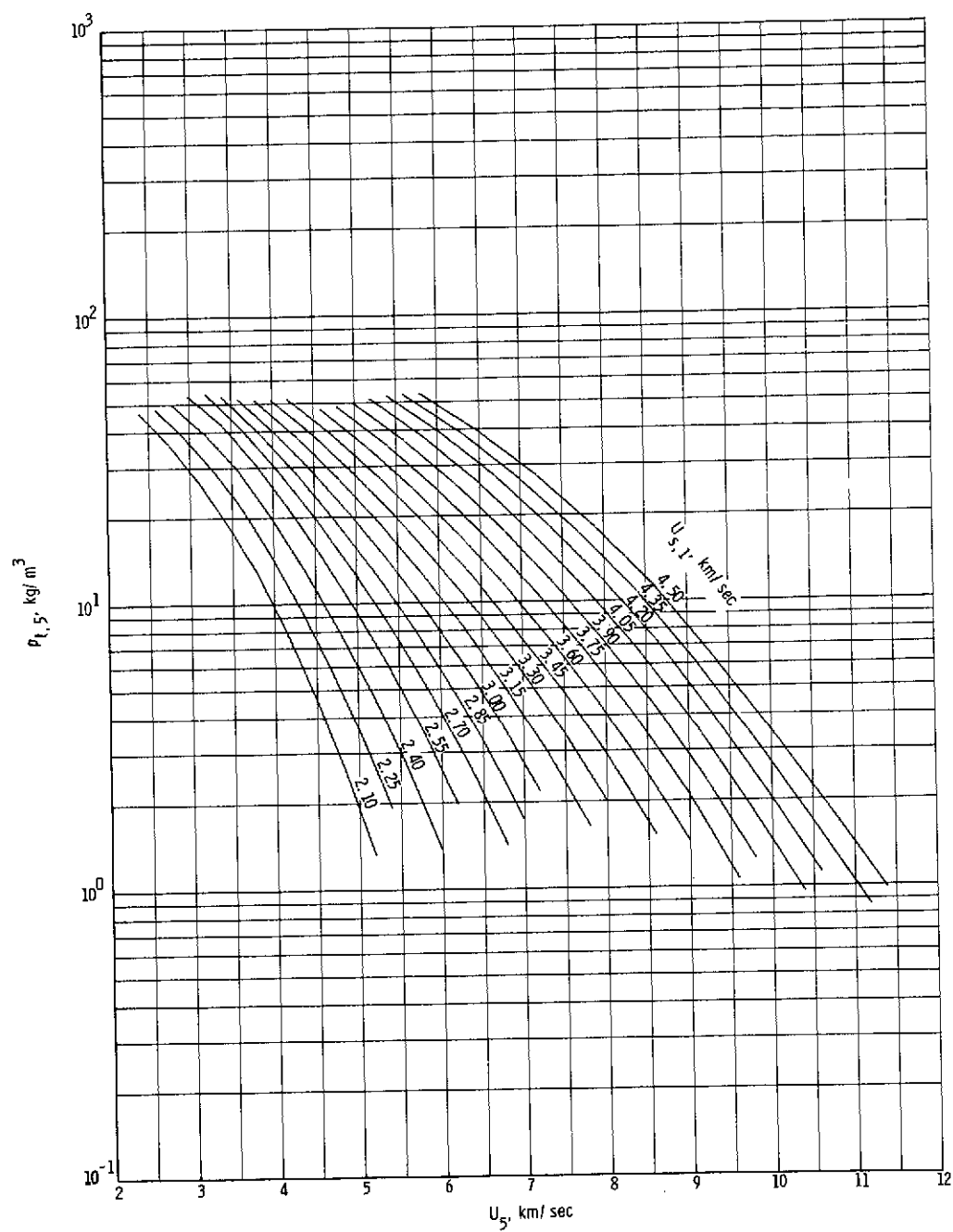
(f) Normal shock density ratio.

Figure 17.- Continued.



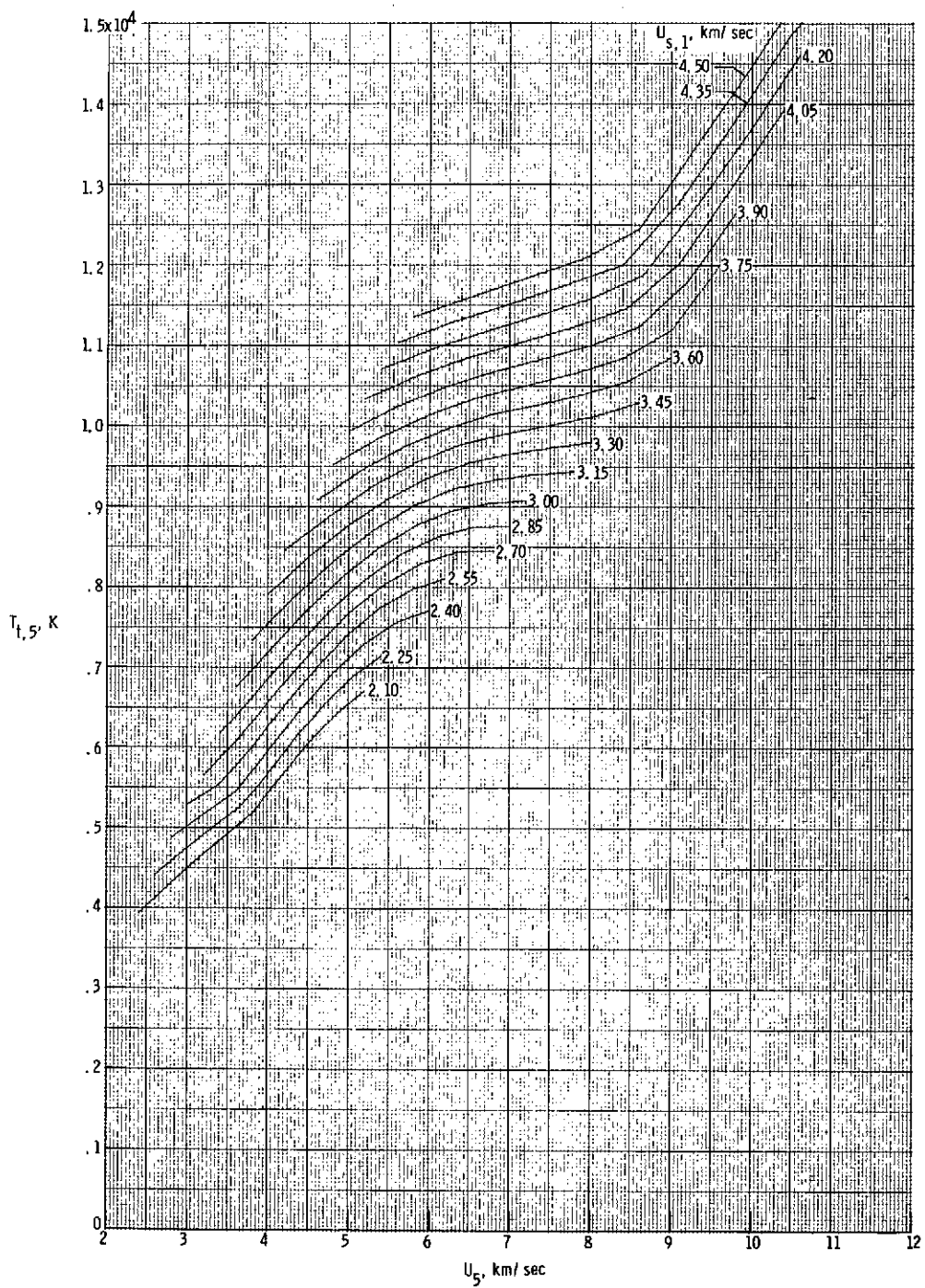
(g) Stagnation pressure behind normal bow shock.

Figure 17.- Continued.



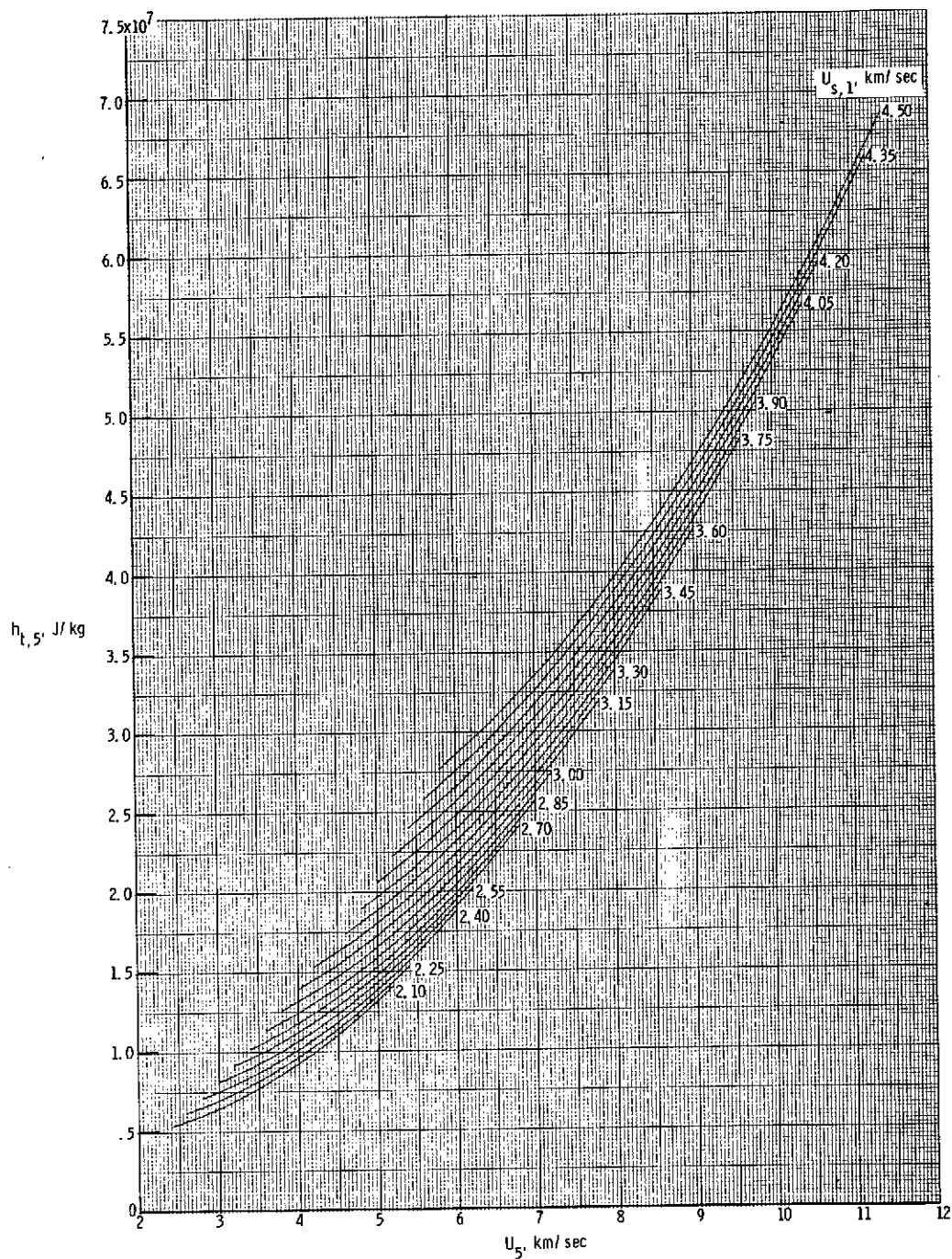
(h) Stagnation density behind normal bow shock.

Figure 17.- Continued.



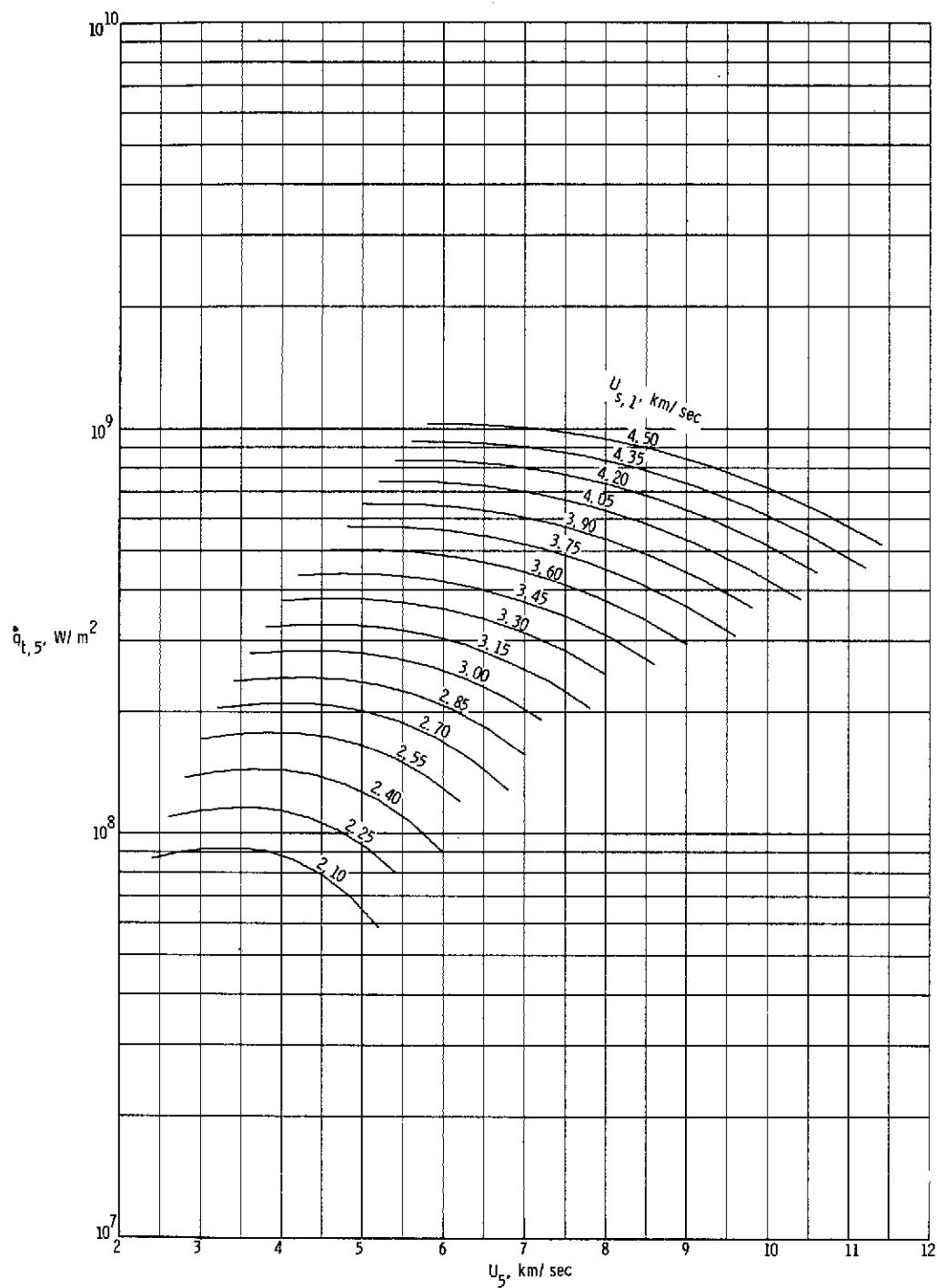
(i) Stagnation temperature behind normal bow shock.

Figure 17.- Continued.



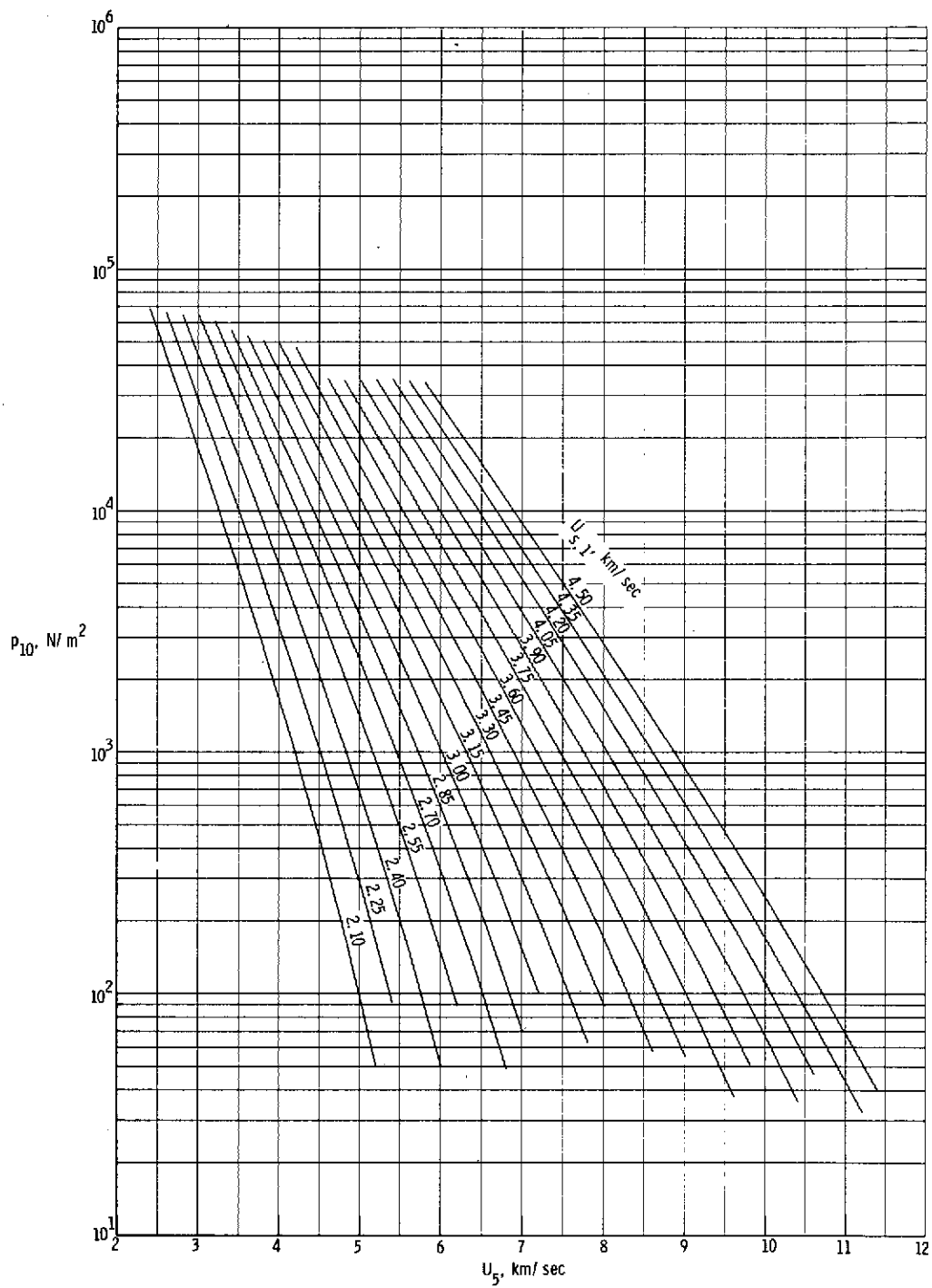
(j) Stagnation enthalpy behind normal bow shock.

Figure 17.- Continued.



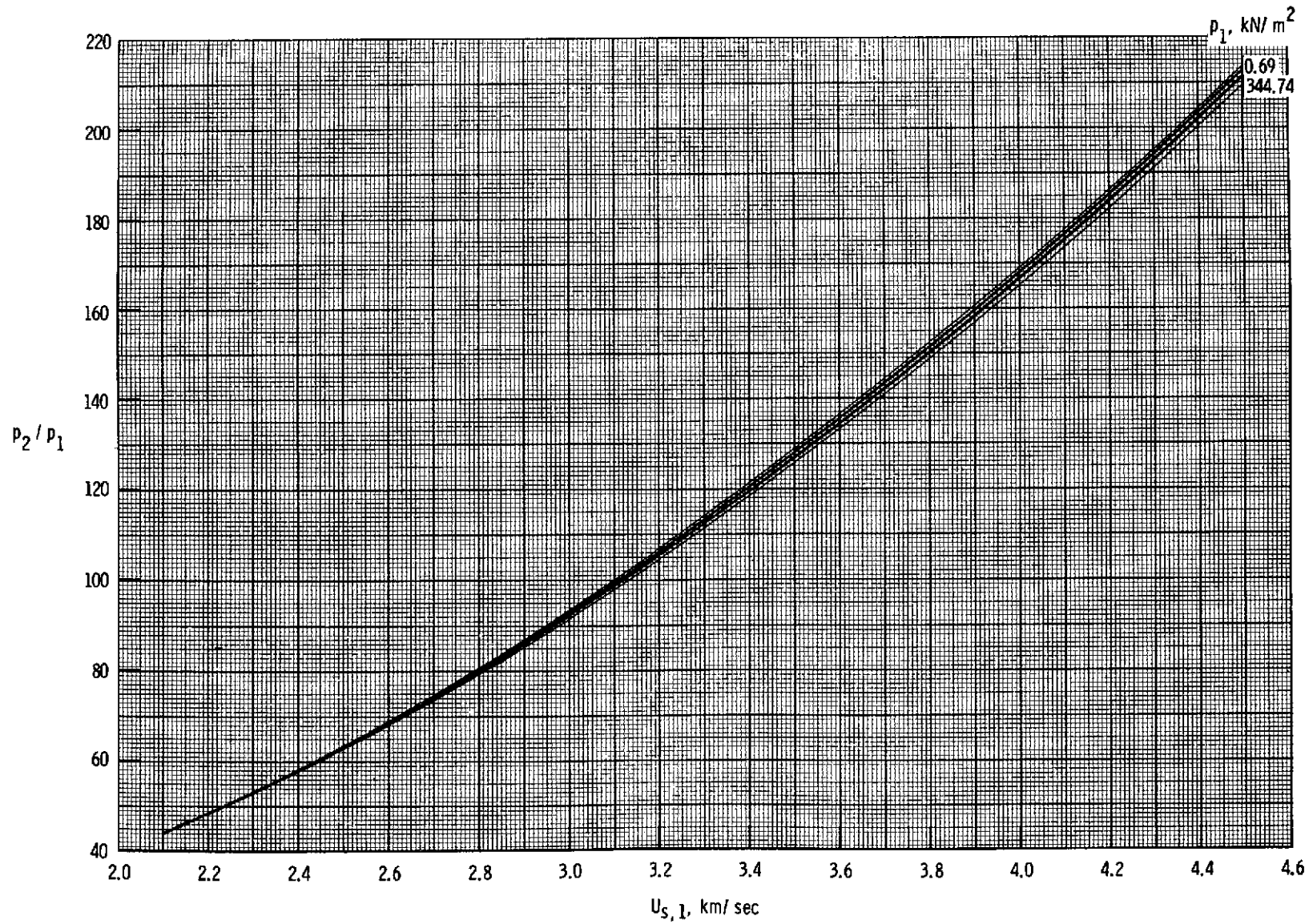
(k) Stagnation-point convective heat-transfer rate to sphere having radius of 2.54 cm.

Figure 17.- Continued.



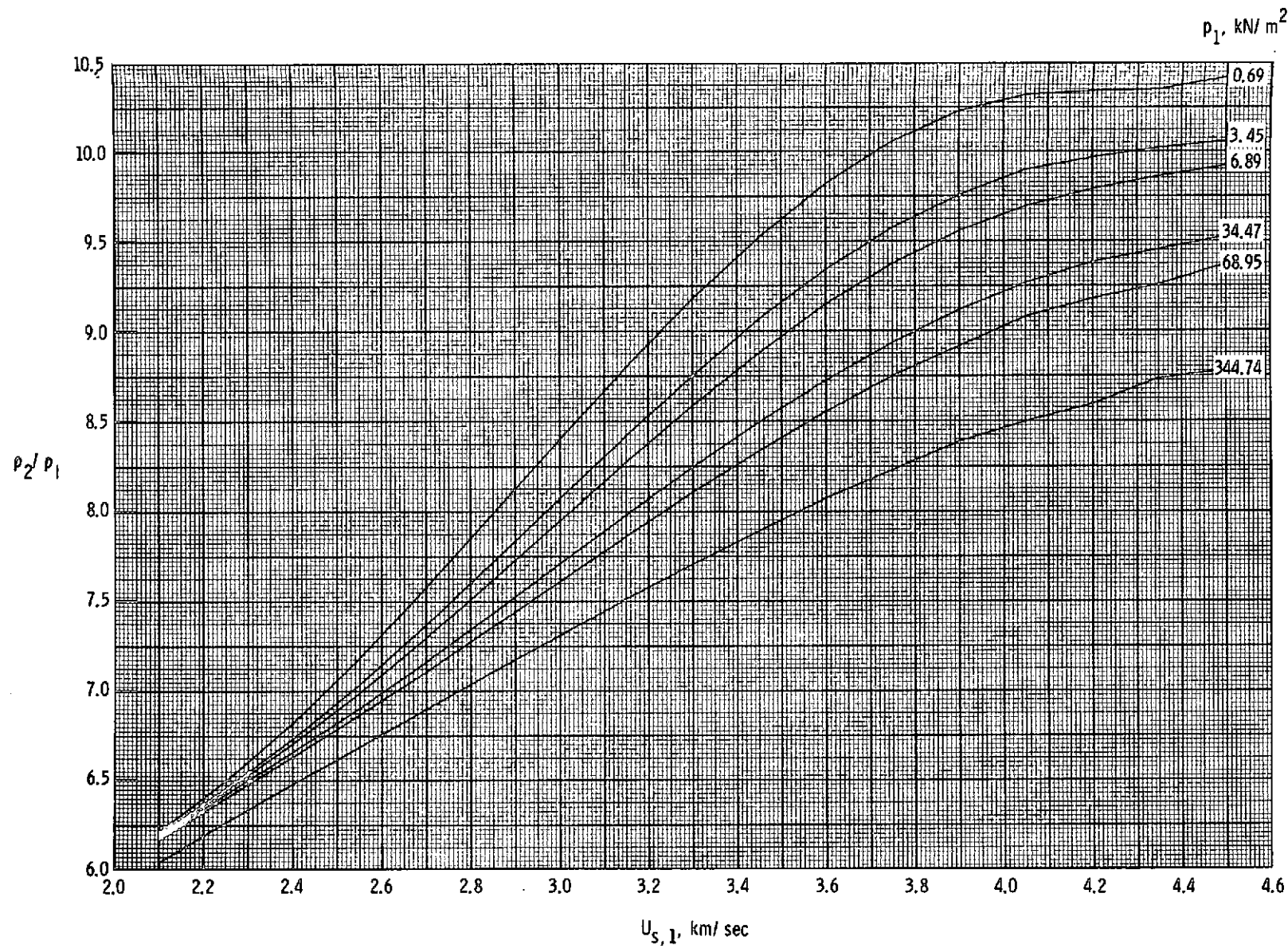
(1) Quiescent acceleration air pressure in region (10).

Figure 17.- Concluded.



(a) Static pressure, p_2/p_1 .

Figure 18.- Various nondimensionalized flow parameters in region (2) as a function of incident normal shock velocity.



(b) Static density, ρ_2/ρ_1 .

Figure 18.- Continued.

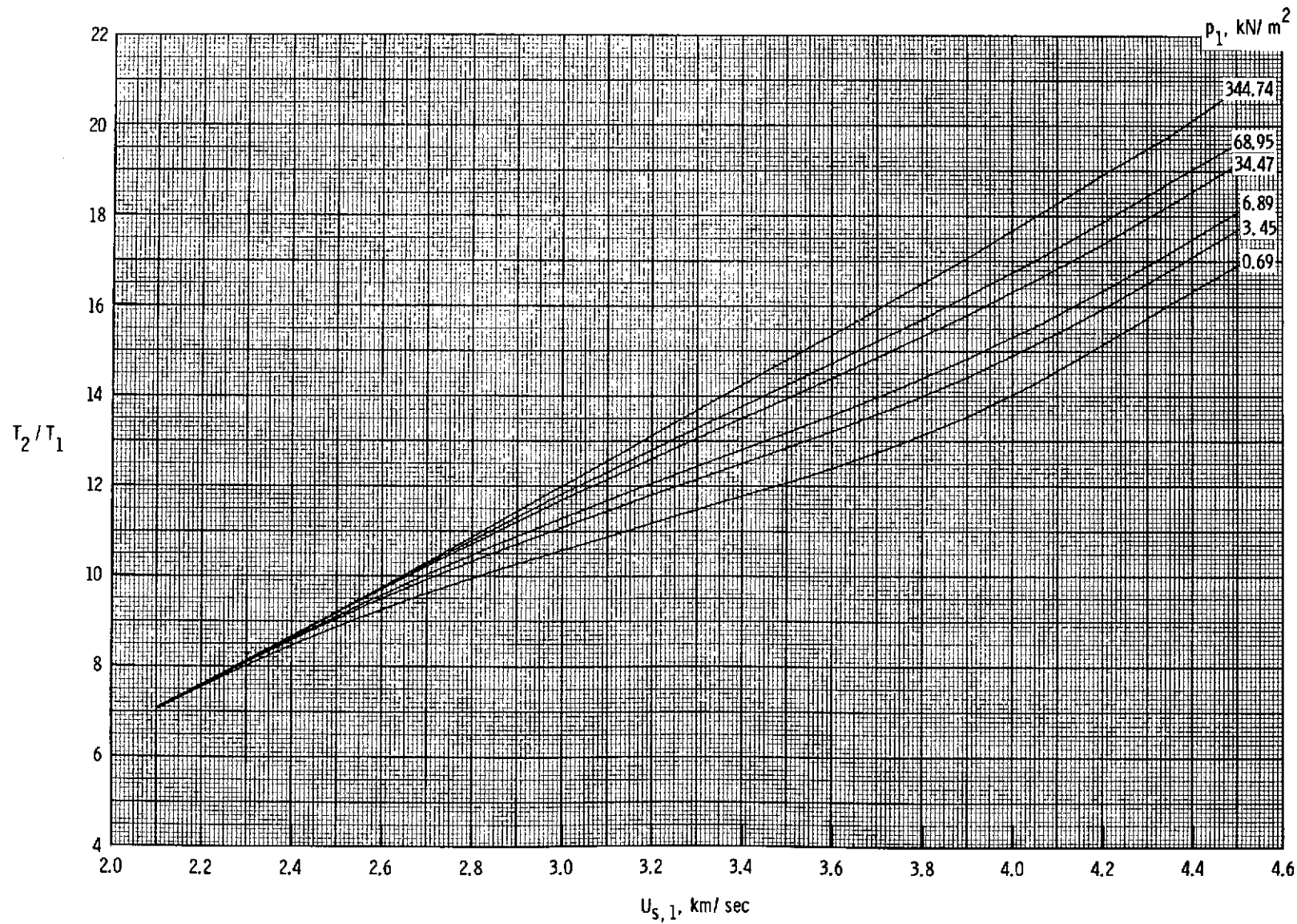
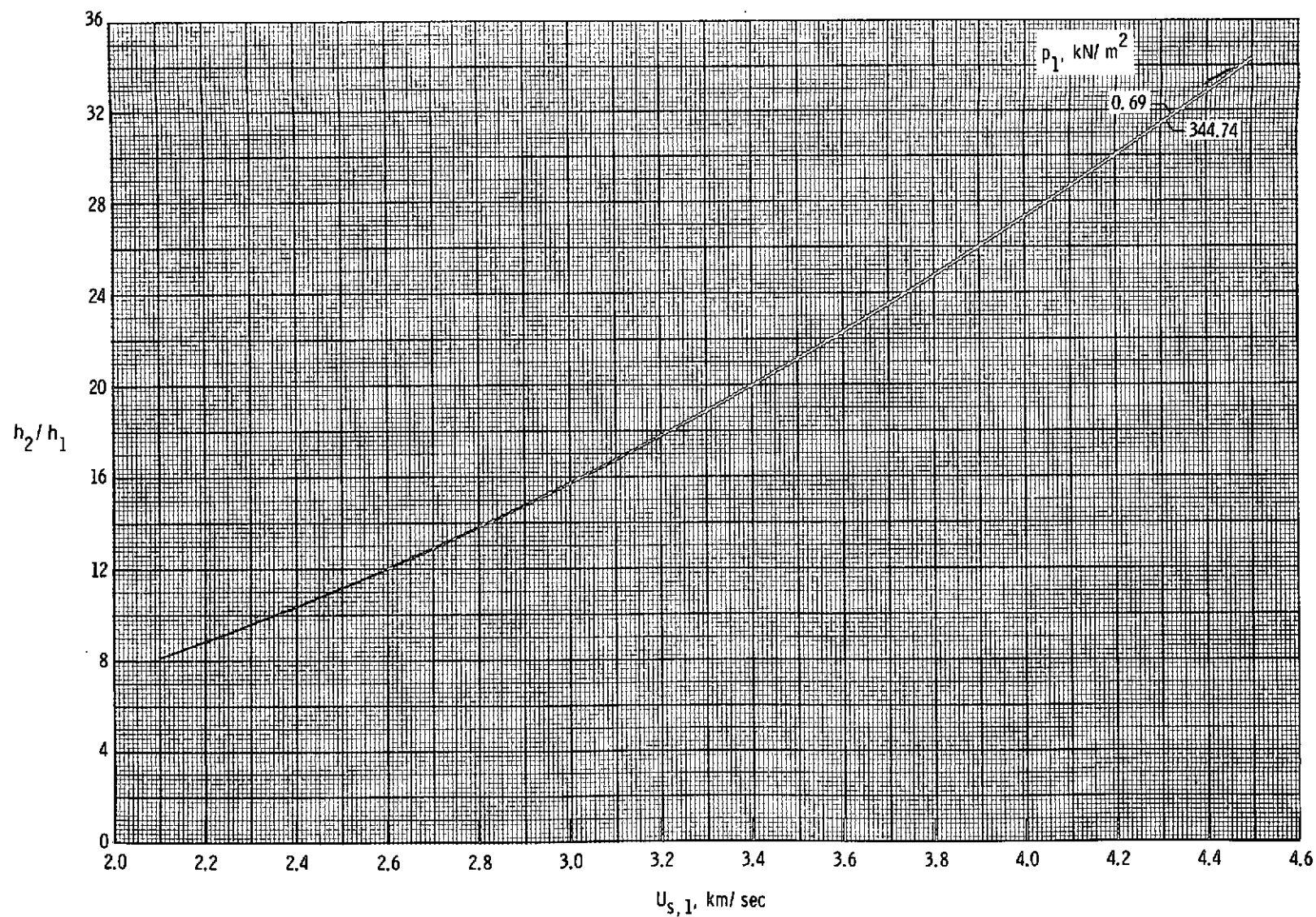
(c) Static temperature, T_2/T_1 .

Figure 18.- Continued.



(d) Static enthalpy, h_2/h_1 .

Figure 18.- Continued.

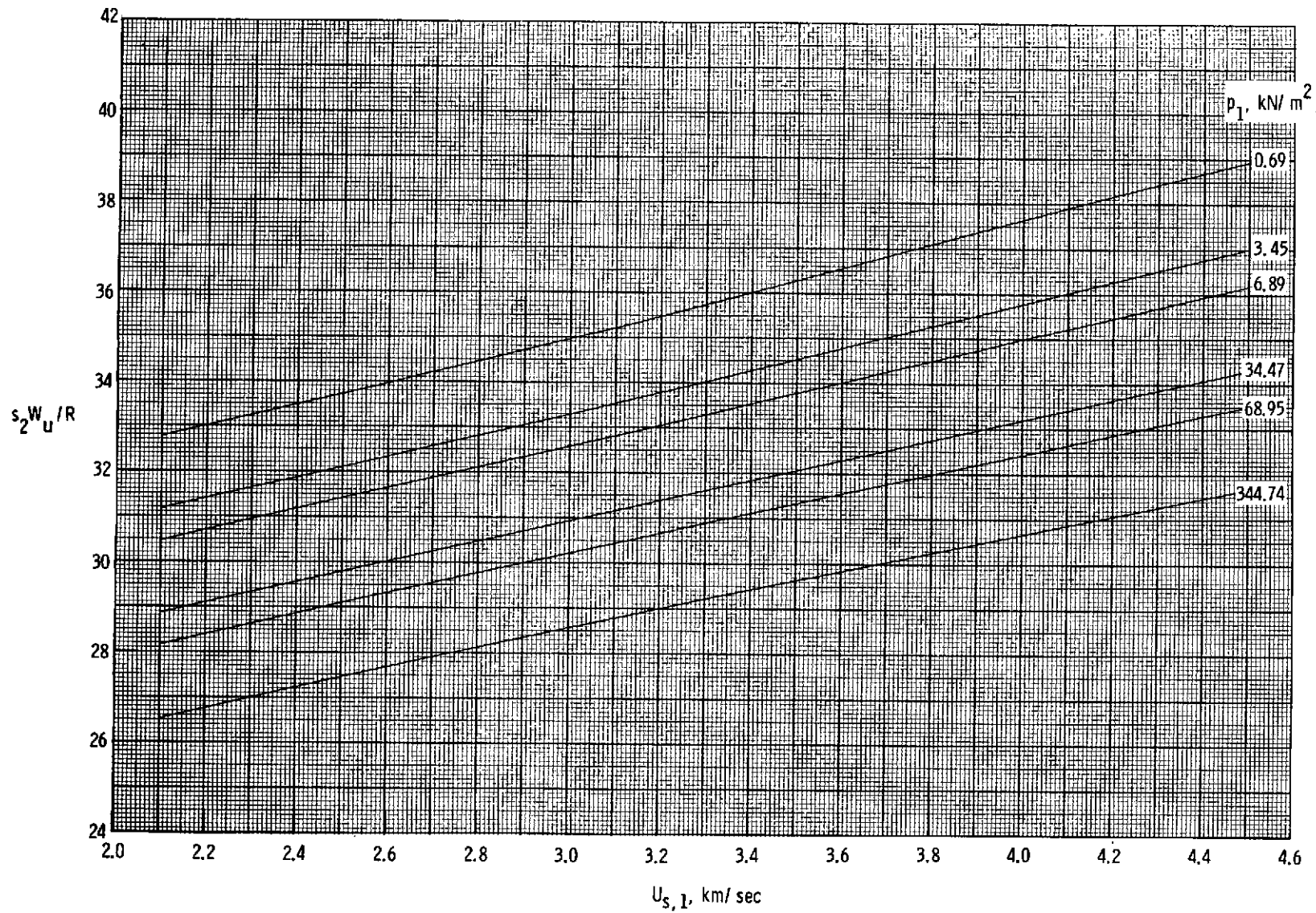
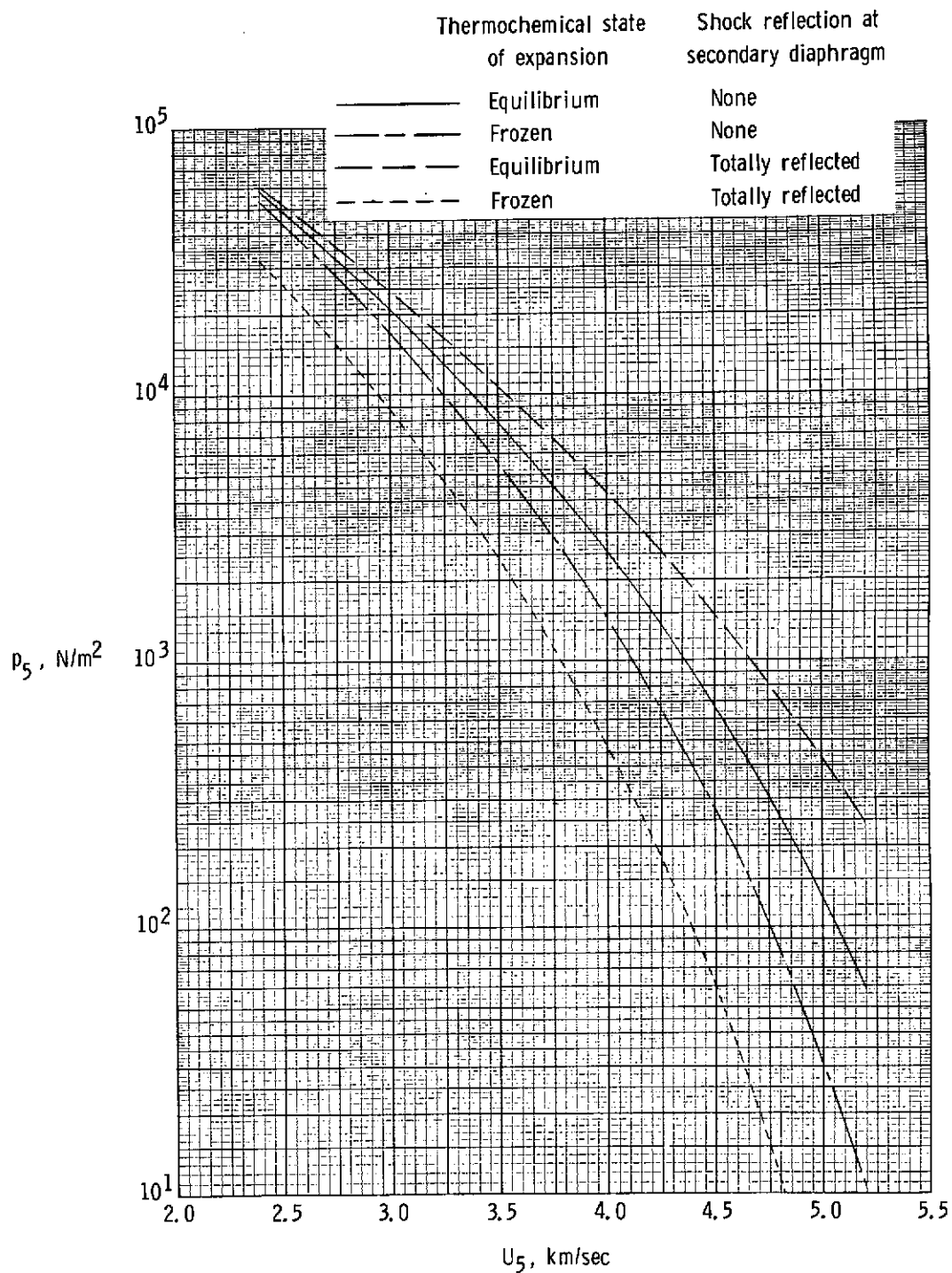
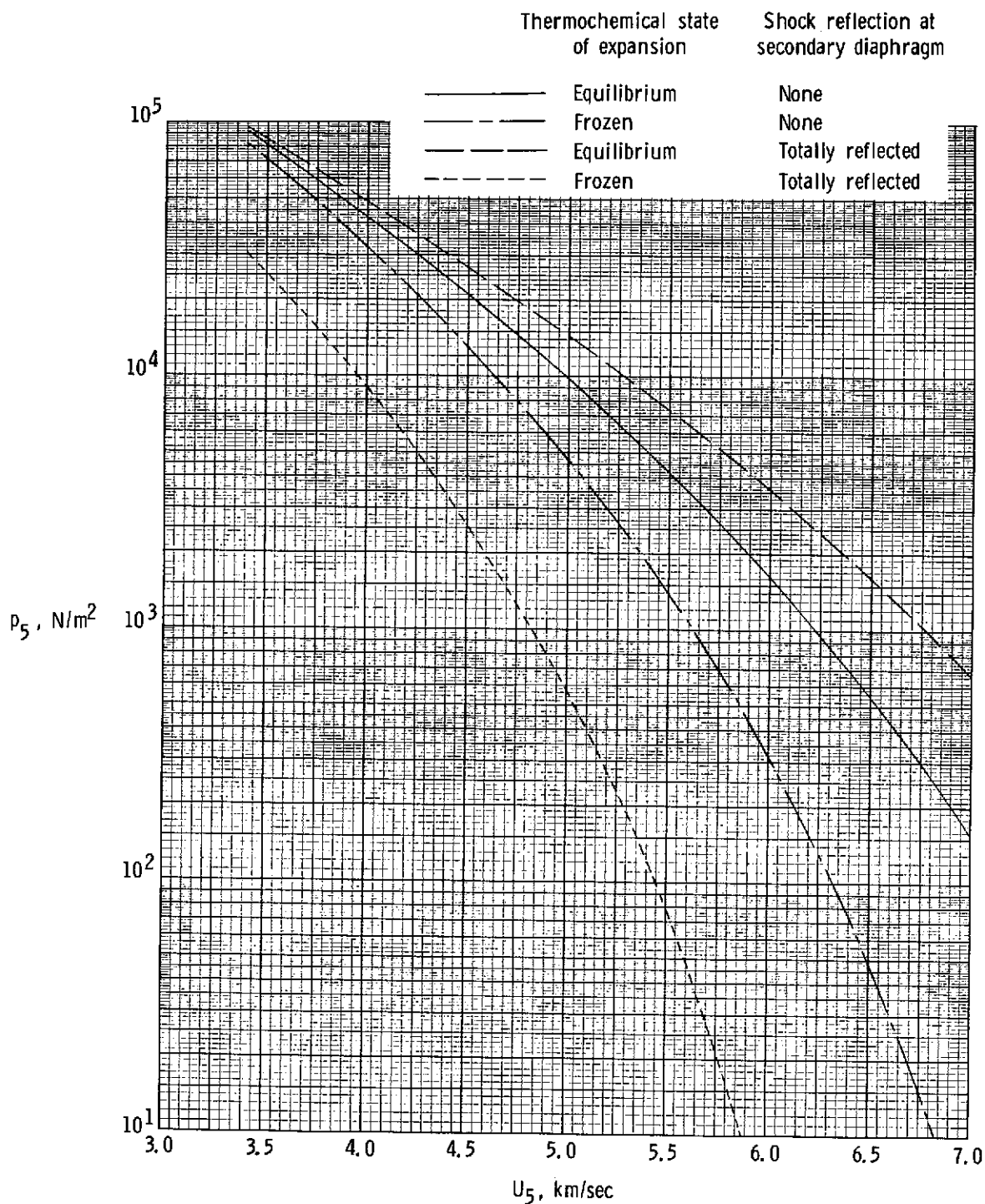
(e) Entropy, s_2W_u/R .

Figure 18.- Concluded.



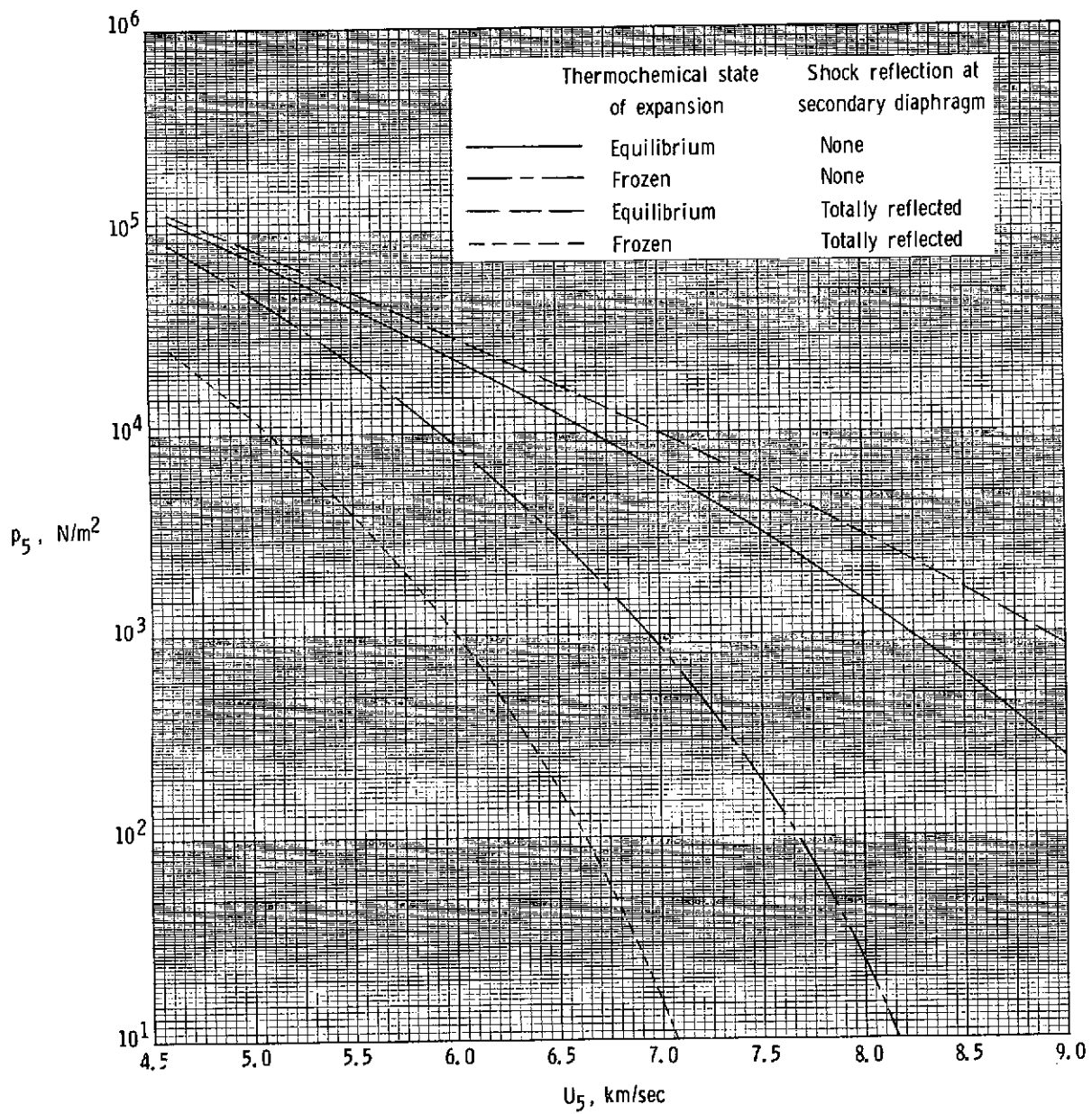
(a) $U_{s,1} = 2.1 \text{ km/sec}$.

Figure 19.- Static pressure in region (5) as a function of air flow velocity for $p_1 = 3.45 \text{ kN/m}^2$ and various incident normal-shock velocities.



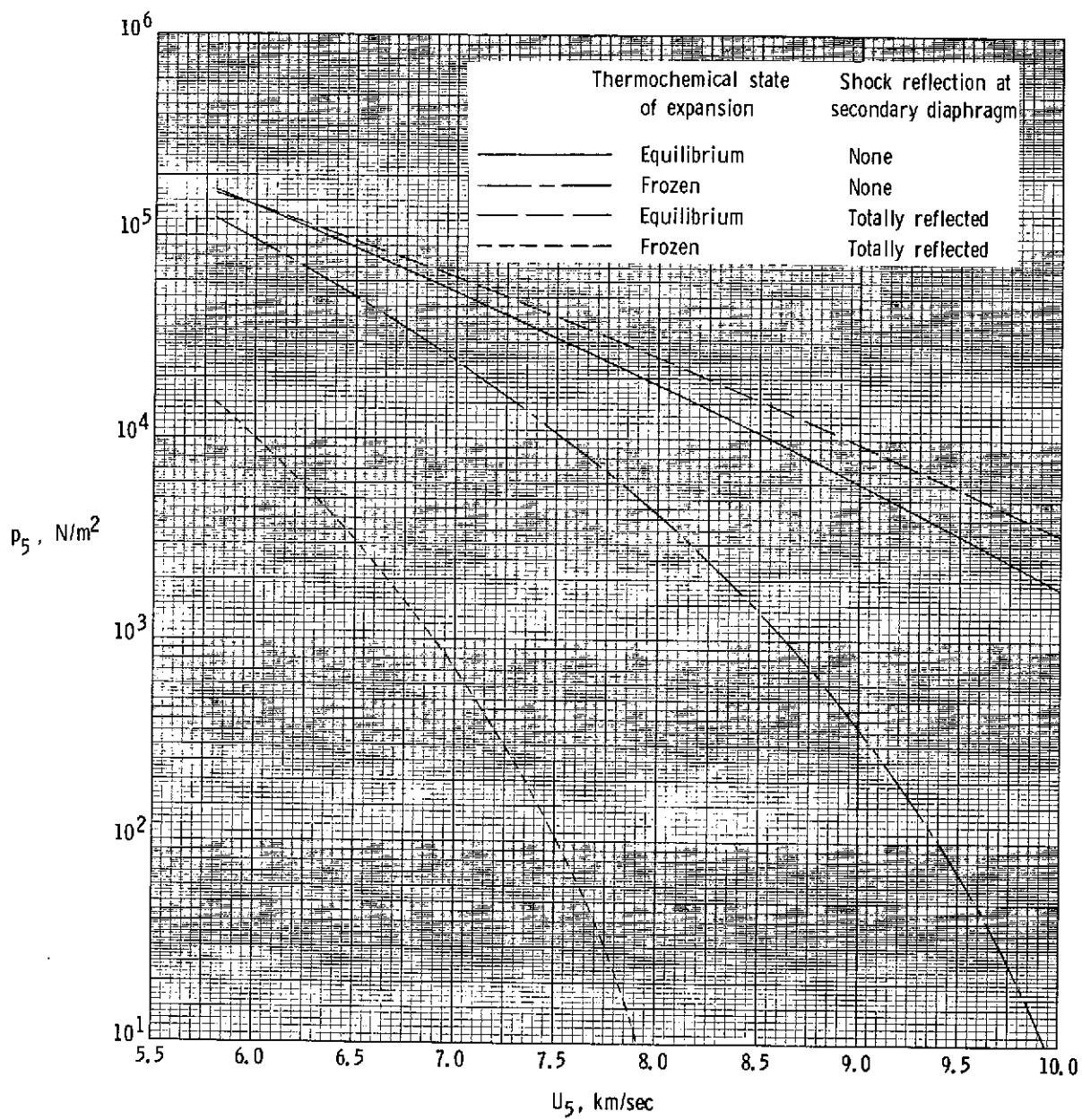
(b) $U_{s,1} = 2.85 \text{ km/sec.}$

Figure 19.- Continued.



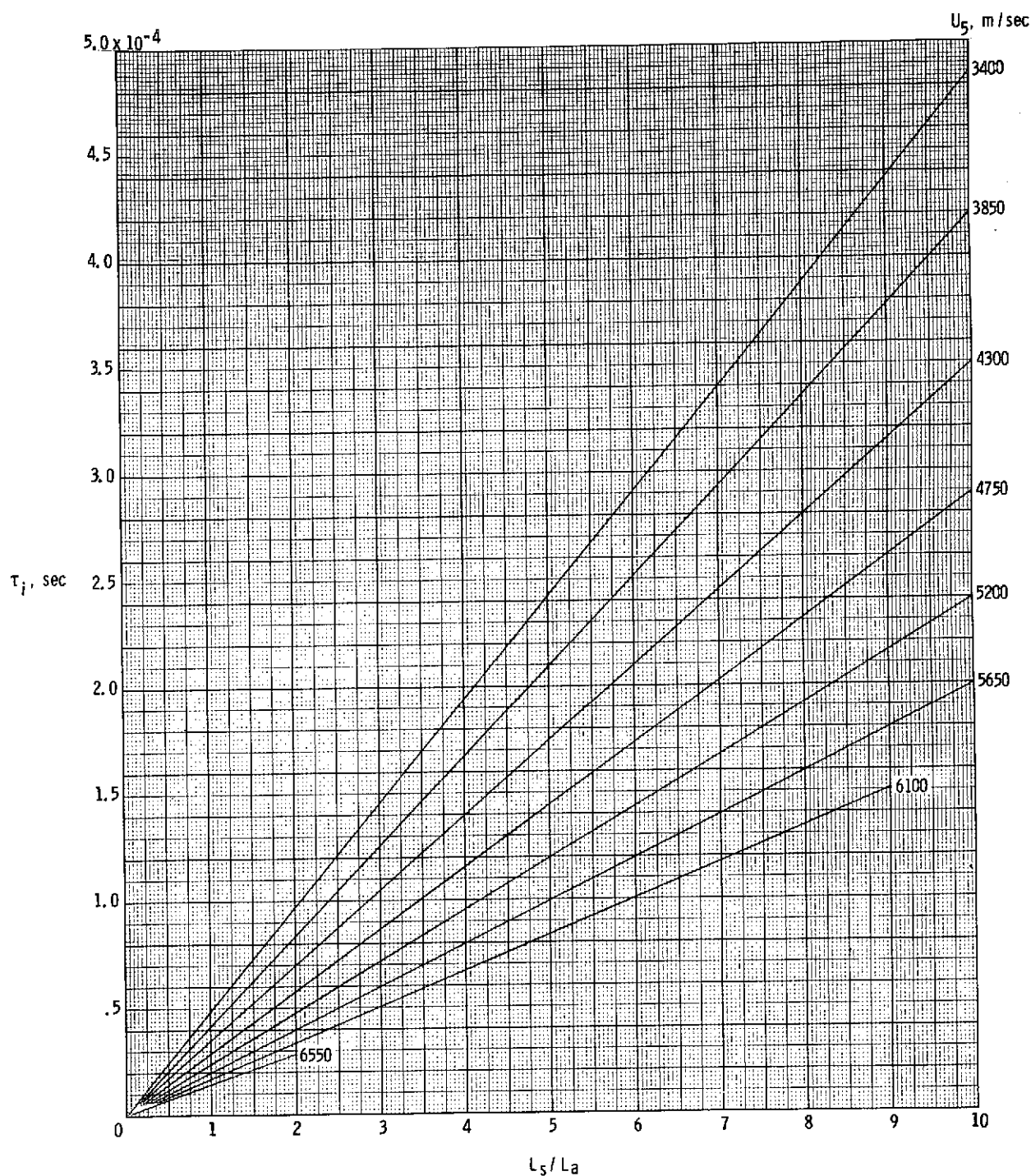
(c) $U_{s,1} = 3.6 \text{ km/sec.}$

Figure 19.- Continued.



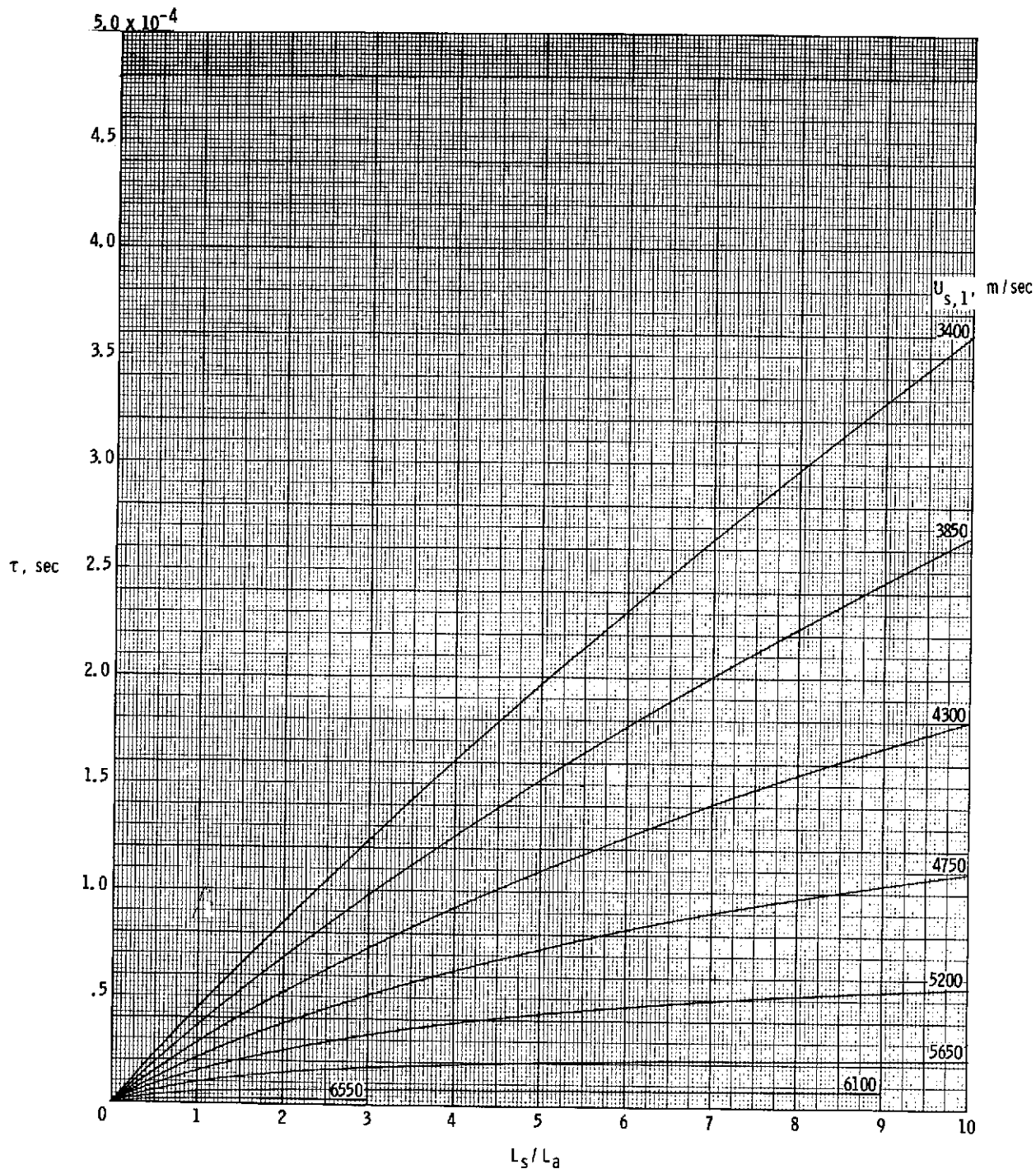
(d) $U_{s,1} = 4.5 \text{ km/sec.}$

Figure 19.- Concluded.



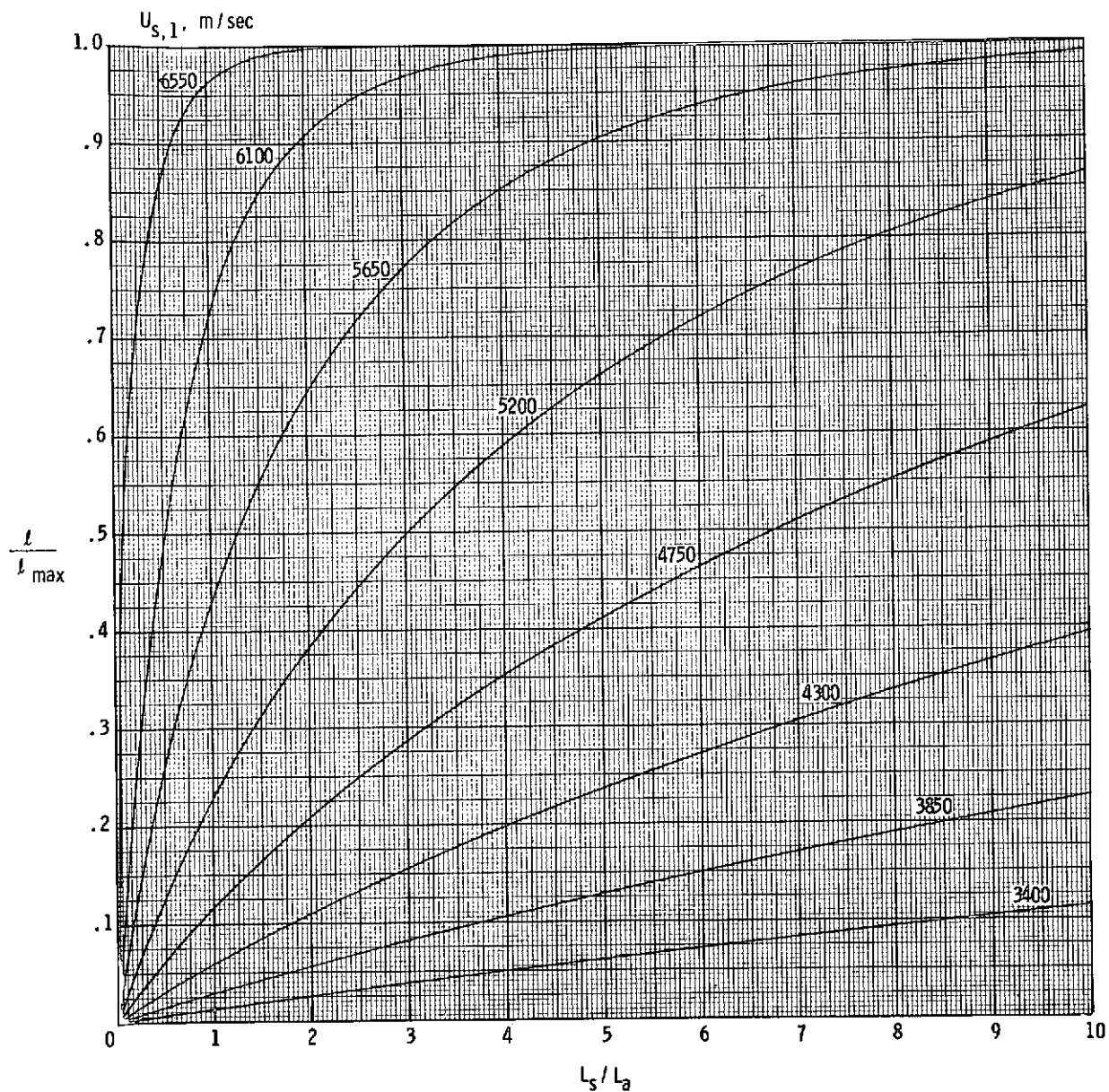
(a) Ideal time interval between arrival of incident normal shock into region (10) and acceleration-air-test-air interface.

Figure 20.- Acceleration air flow quantities as a function of distance downstream from secondary diaphragm for $p_1 = 3.45 \text{ kN/m}^2$ and $U_{s,1} = 2.85 \text{ km/sec}$.



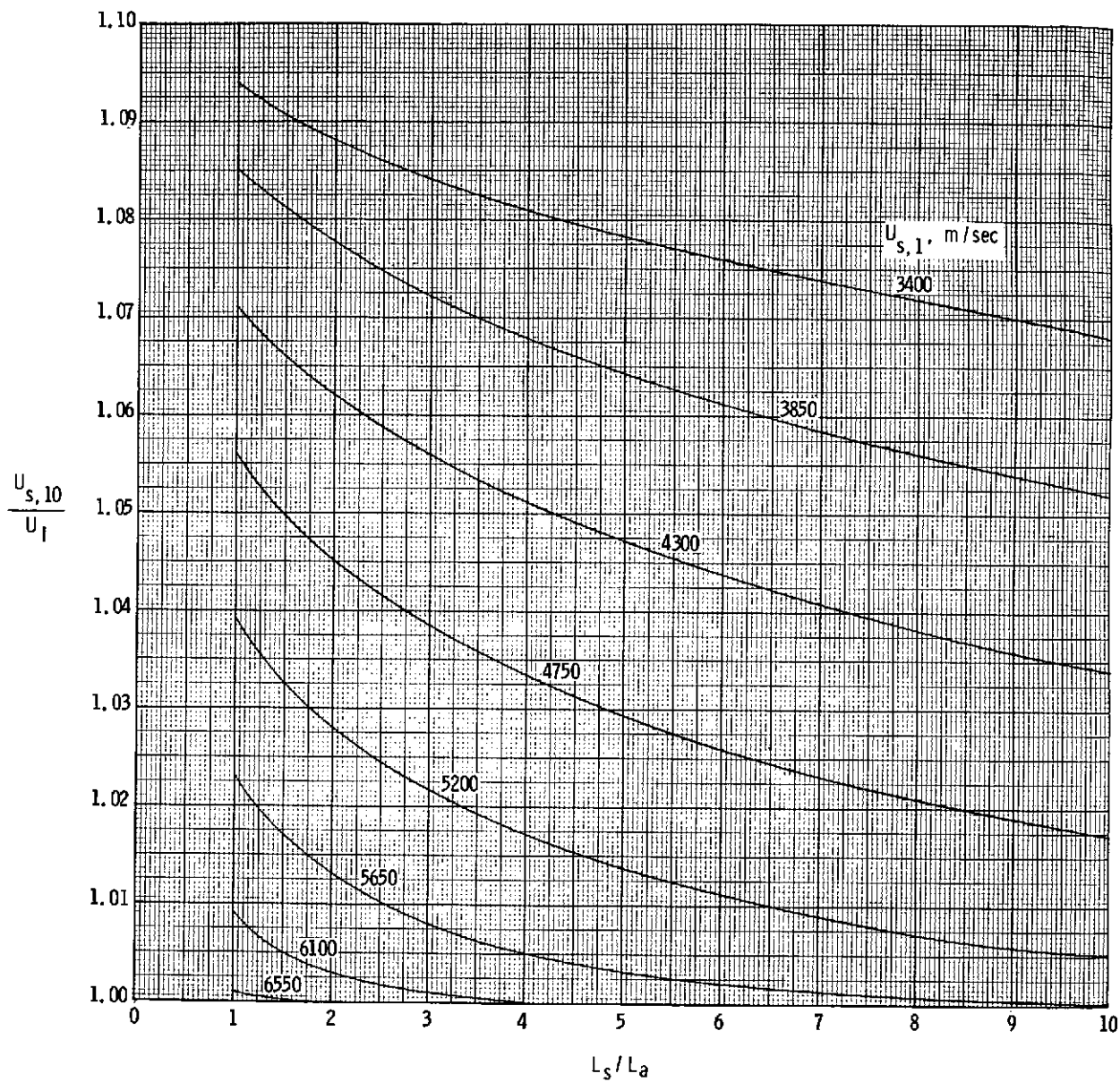
(b) Time interval between arrival of incident normal shock into region (10) and acceleration-air—test-air interface.

Figure 20.- Continued.



(c) Nondimensionalized distance between incident normal shock into region (10) and acceleration-air—test-air interface.

Figure 20.- Continued.



(d) Ratio of incident normal shock into region (10) to acceleration-air—test-air interface velocity.

Figure 20.- Concluded.

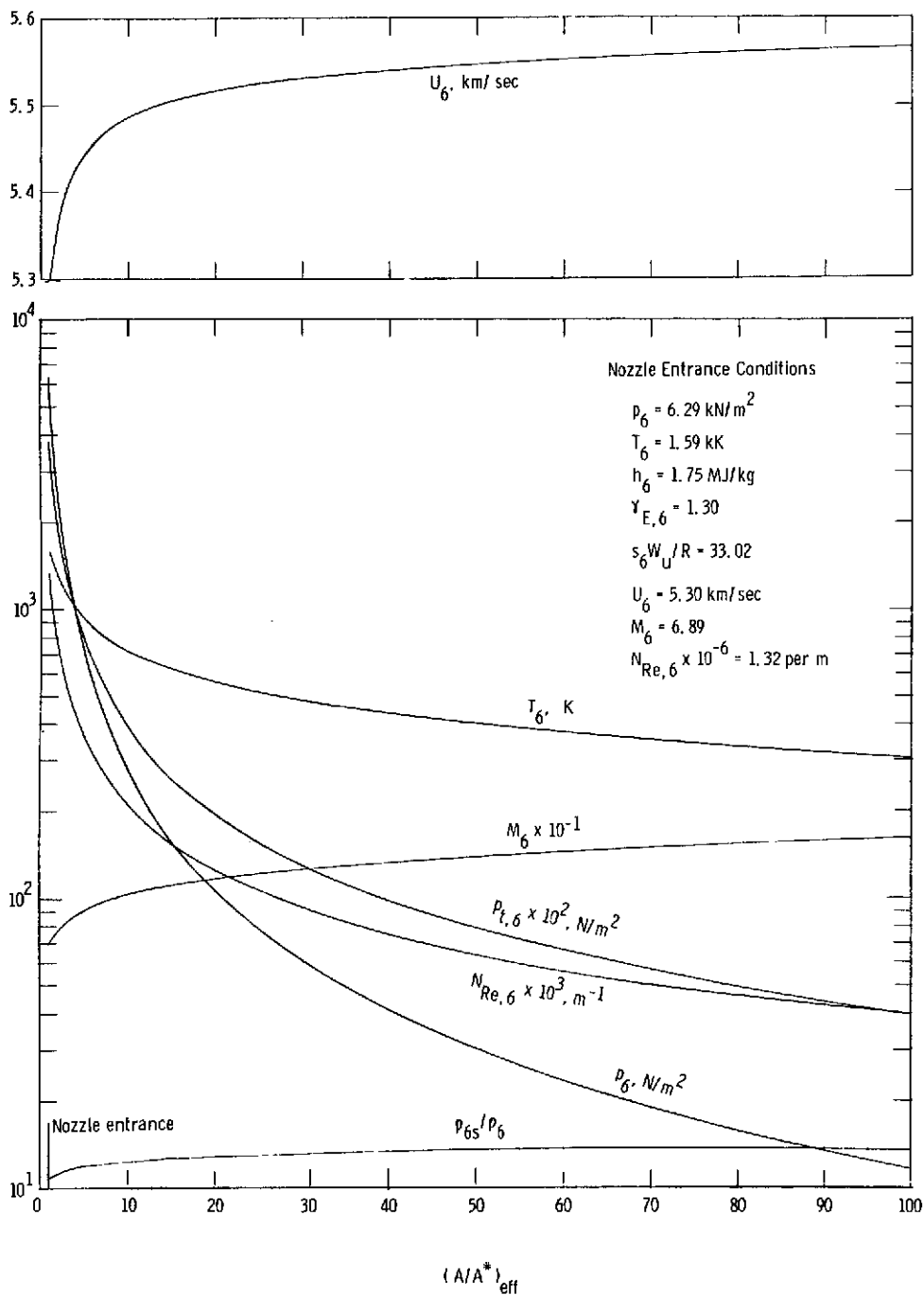
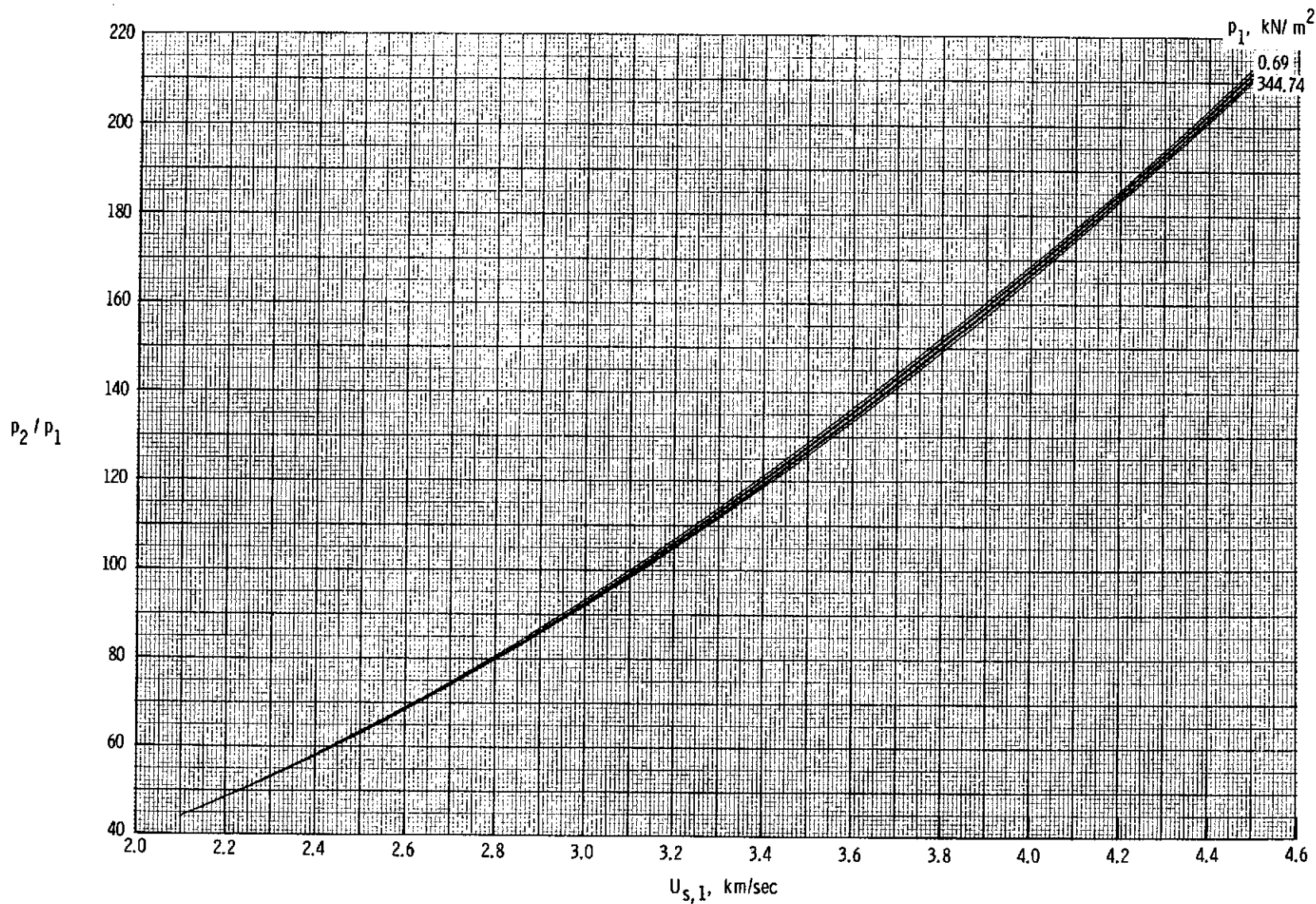
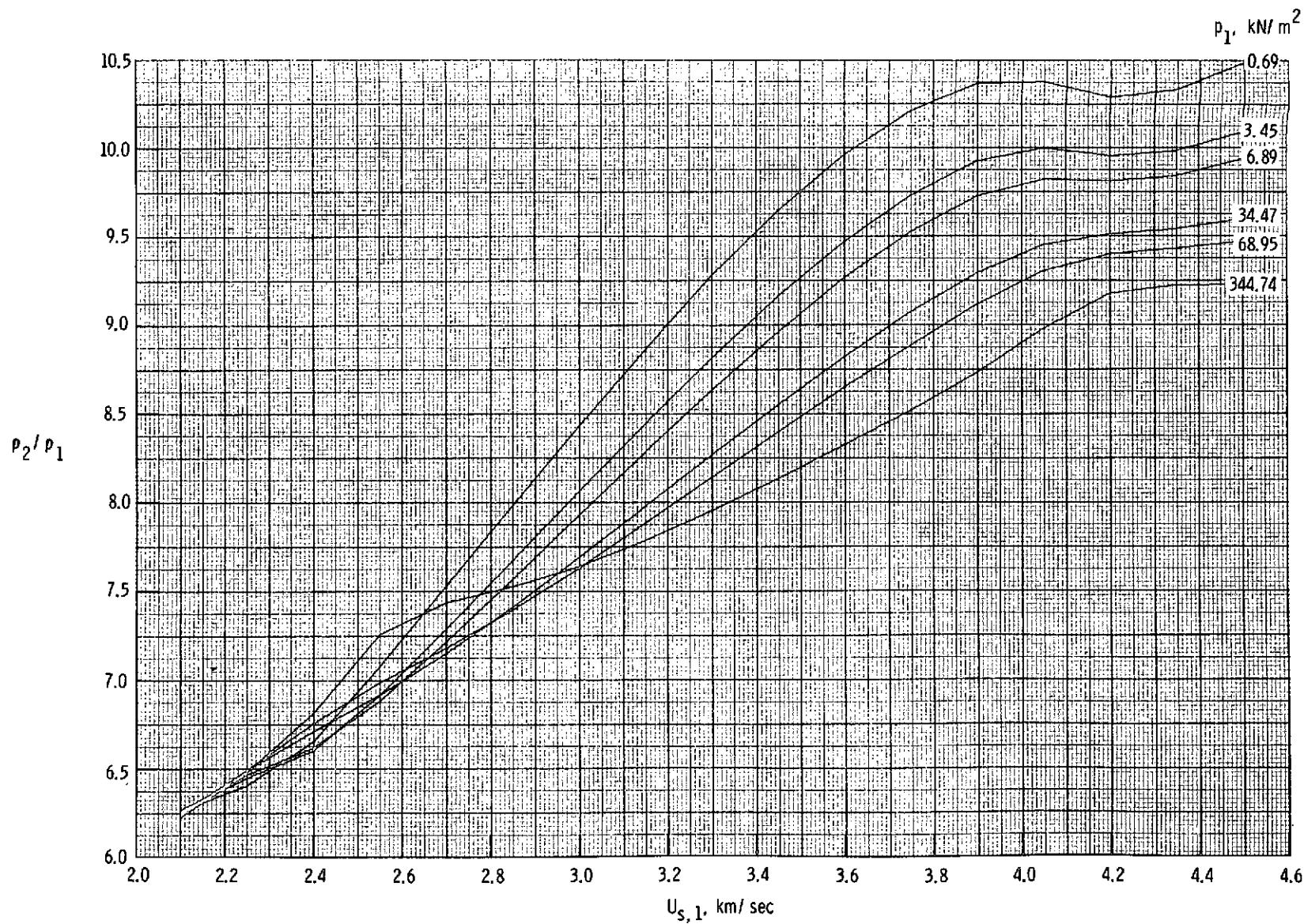


Figure 21.- Various expansion tunnel flow quantities as a function of effective area ratio.



(a) Static pressure, p_2/p_1 .

Figure 22.- Various nondimensional flow parameters in region (2) as a function of incident normal-shock velocity. (Predicted by using curve-fit expressions of ref. 11.)



(b) Static density, ρ_2/ρ_1 .

Figure 22.- Continued.

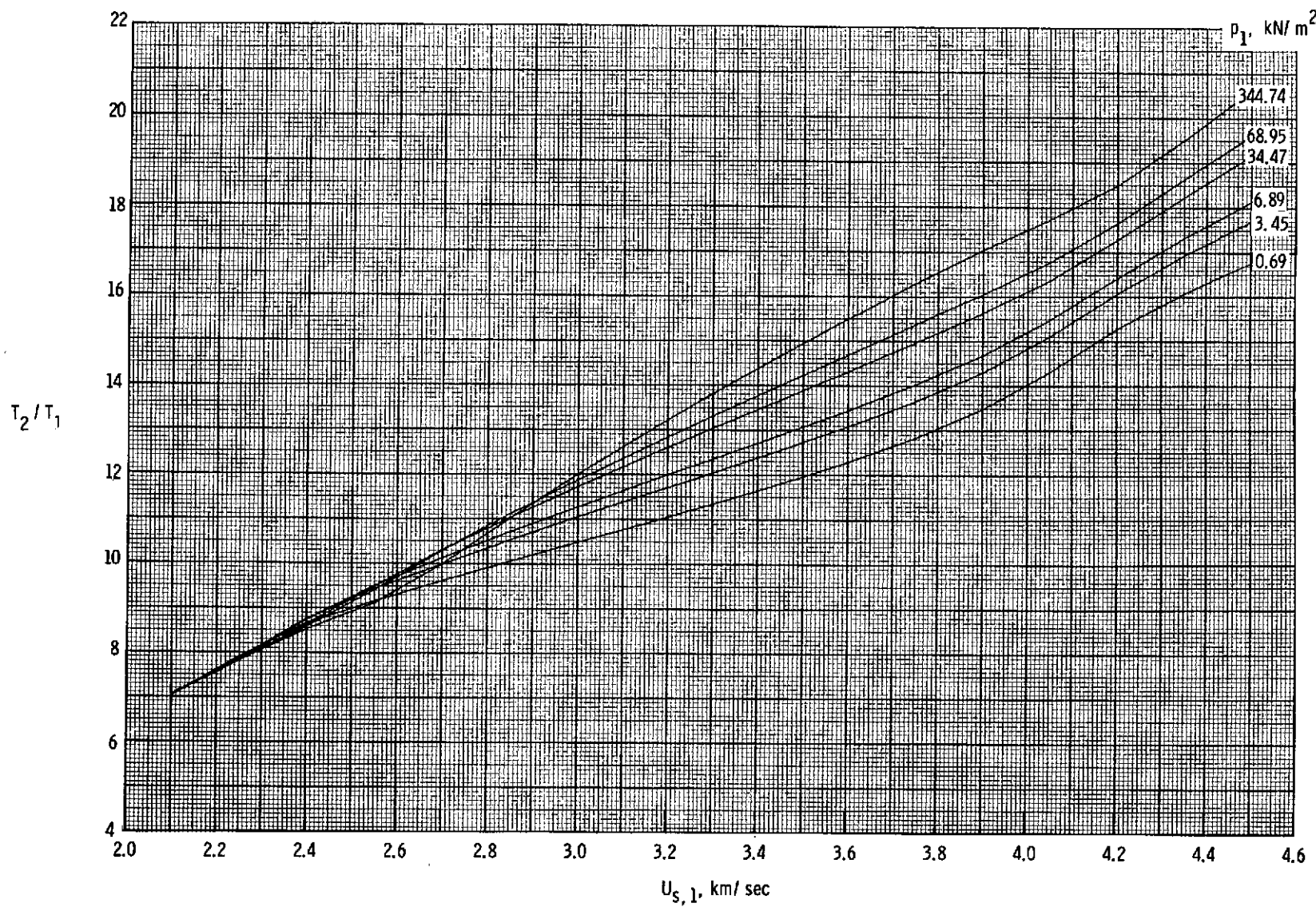
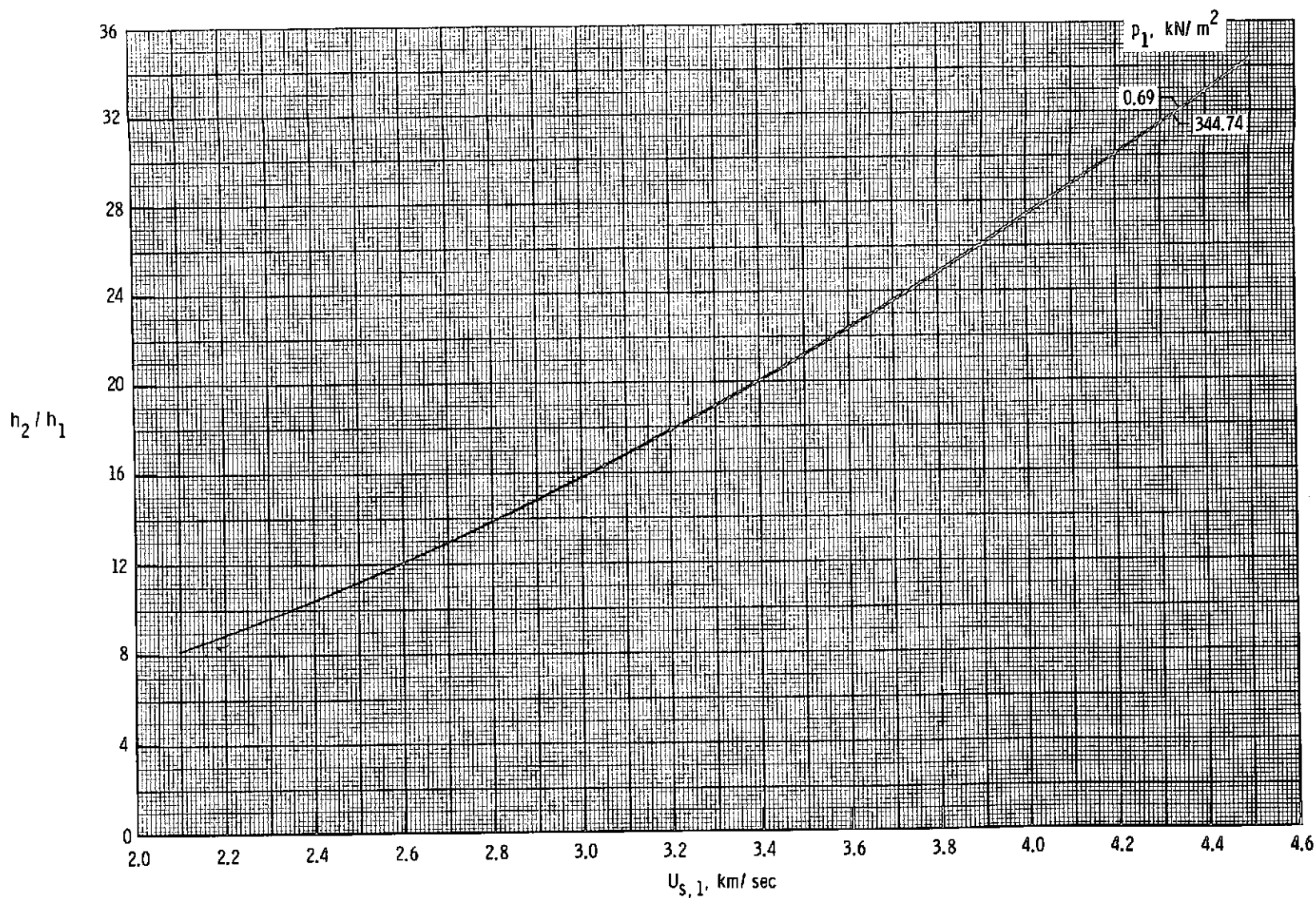
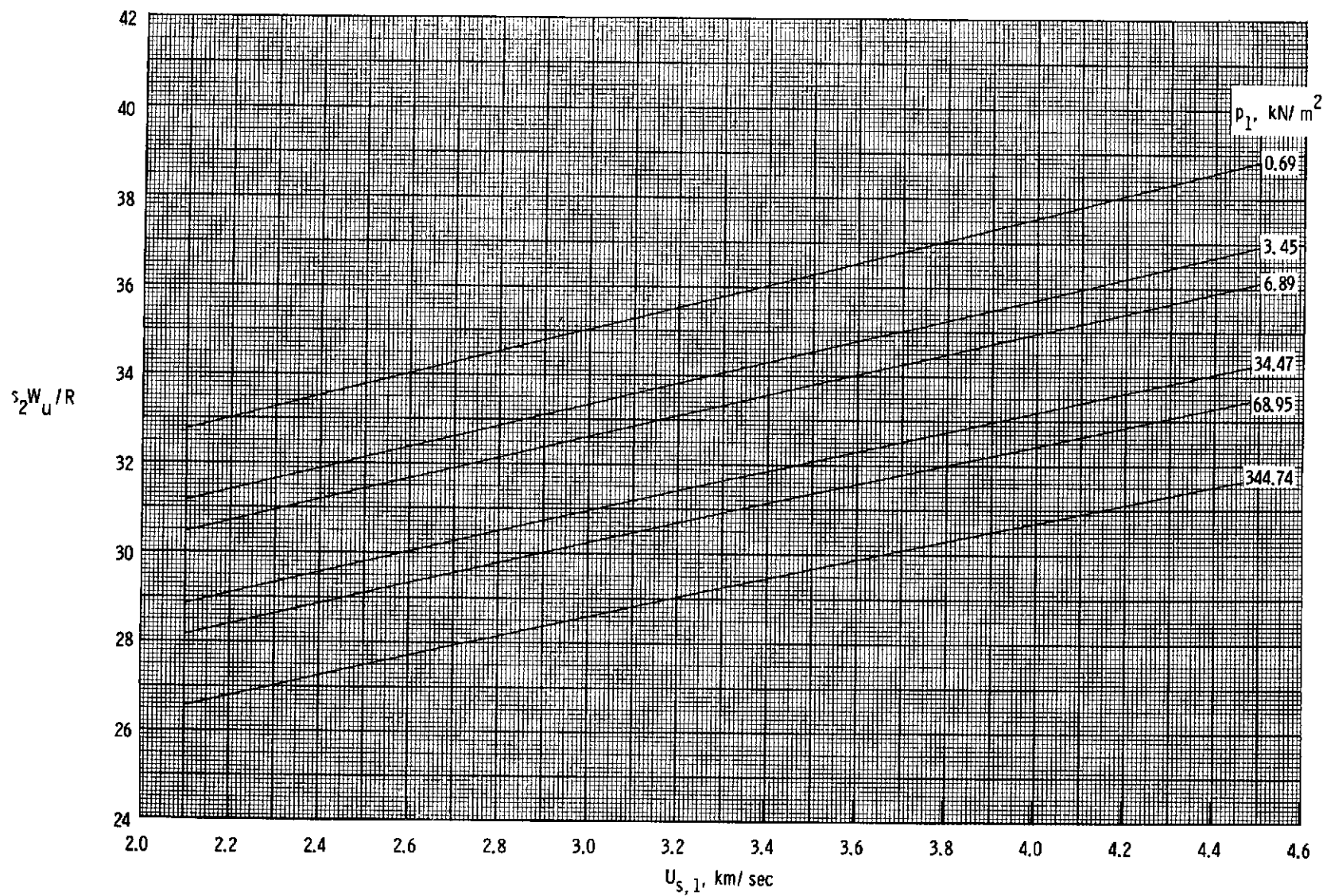
(c) Static temperature, T_2/T_1 .

Figure 22.- Continued.



(d) Static enthalpy, h_2/h_1 .

Figure 22.- Continued.



(e) Entropy, $s_2 W_u / R$.

Figure 22.- Concluded.